Topics in Organometallic Chemistry 53

Xiao-Bing Lu *Editor*

# Carbon Dioxide and Organometallics

Springer

# 53
# Topics in Organometallic Chemistry

## Aims and Scope

The series *Topics in Organometallic Chemistry* presents critical overviews of research results in organometallic chemistry. As our understanding of organometallic structure, properties and mechanisms increases, new ways are opened for the design of organometallic compounds and reactions tailored to the needs of such diverse areas as organic synthesis, medical research, biology and materials science. Thus the scope of coverage includes a broad range of topics of pure and applied organometallic chemistry, where new breakthroughs are being achieved that are of significance to a larger scientific audience.

The individual volumes of *Topics in Organometallic Chemistry* are thematic. Review articles are generally invited by the volume editors. All chapters from Topics in Organometallic Chemistry are published OnlineFirst with an individual DOI. In references, Topics in Organometallic Chemistry is abbreviated as Top Organomet Chem and cited as a journal.

More information about this series at http://www.springer.com/series/3418

Xiao-Bing Lu
Editor

# Carbon Dioxide and Organometallics

With contributions by

A. Angelini · M. Aresta · M. Beller · M. Brill · L.P. Carrodeguas · C.S.J. Cazin · L.-N. He · R. Jackstell · A.W. Kleij · S. Kraus · V. Laserna · F. Lazreg · Q. Liu · X.-B. Lu · R. Ma · S.P. Nolan · B. Rieger · J. Rintjema · C. Romain · P.K. Saini · S. Sopeña · A. Thevenon · C.K. Williams · L. Wu · S. Zhang · W.-Z. Zhang

Springer

*Editor*
Xiao-Bing Lu
State Key Laboratory of Fine Chemicals
Dalian University of Technology
Dalian
China

ISSN 1436-6002 ISSN 1616-8534 (electronic)
Topics in Organometallic Chemistry
ISBN 978-3-319-22077-2 ISBN 978-3-319-22078-9 (eBook)
DOI 10.1007/978-3-319-22078-9

Library of Congress Control Number: 2015949229

Springer Cham Heidelberg New York Dordrecht London


Printed on acid-free paper

Springer International Publishing AG Switzerland is part of Springer Science+Business Media (www.springer.com)

# Preface

Atmospheric carbon dioxide is the elixir of life. It is the primary raw material for green plants to construct their tissues through photosynthesis, which in turn are the feedstocks for animals to build theirs. The managed ecosystems maintain the quality of life and the environment for millions years. Nevertheless, human activities in the recent two centuries significantly disturb the carbon cycle of our planet, which involves dynamic carbon exchanges between the geosphere, the biosphere, the oceans and the atmosphere. It was observed that carbon dioxide concentrations in the atmosphere have been increasing significantly over the past century, especially with an average growth of 2 ppm/year in the last 10 years. Compared to the rather steady level of the pre-industrial era (about 280 ppm), the concentration of atmospheric carbon dioxide in 2013 (396 ppm) was about 40% higher than that in the mid-1800s.

Absolutely, mitigating climate change, preserving the environment, replacing fossil fuels and using renewable energy are the great challenges for our sustainable planet. The utilization of carbon dioxide as a C1 feedstock for producing fuels and chemicals is an attractive strategy to fulfill these grand challenges. Reusing $CO_2$ not only addresses the balance of $CO_2$ in the atmosphere, but also employs it as an alternative feedstock to fossil fuels, an abundant, inexpensive and non-toxic renewable carbon source. As a longer-term visionary idea, it is possible to create a $CO_2$-economy for achieving full-circle recycling of $CO_2$ as a renewable energy source, analogous to plants' converting $CO_2$ and water to sugar and $O_2$ via photosynthesis. Therefore, the development of efficient catalytic processes for carbon dioxide transformation into desirable, economically competitive products has been a long-standing goal for chemists. Up to now, more than 20 reactions involving $CO_2$ as a starting material have been developed in recent decades. Although the number remains less, several $CO_2$ reactions that include the syntheses of urea, methanol, salicylic acid, synthetic gas and organic carbonates have been successfully industrialized. It is apparent that the quantity of consumed $CO_2$ in these processes is likely a very small fraction (0.5%) of the total $CO_2$ generated from human activity (about 37 Gt). However, these strategies potentially provide

more environmentally benign routes to producing chemicals otherwise made from the reagents detrimental to the environment.

Carbon dioxide is a thermodynamically stable molecule ($\Delta G_f^\circ = -396$ kJ/mol), the end product in any carbon-based combustion process, thus relatively high-energy reagents are often used to facilitate its transformation. From the energetic point of view, the conversion of $CO_2$ will require an amount of energy that depends on the downward steps of the oxidation state of carbon from +4 in $CO_2$ to the value in the target chemical. If one converts $CO_2$ into species in which the O/C ratio is less than 2, energy is needed. Conversely, if $CO_2$ is kept in its +4 oxidation state by increasing the O:C ratio in the products derived from it, the transformation process is an exoenergic reaction (e.g. production of organic carbonates). However, whether endothermic or exoenergic reaction, the activation of carbon dioxide is pivotal for its effective transformation. In recent decades, we have witnessed the great progress in carbon dioxide activation and catalytic transformation. Among these processes, organometallics plays an important role in activating $CO_2$. This volume (Carbon Dioxide and Organometallics) is a timely overview of various reactions utilizing carbon dioxide as a starting material, focused on metal-mediated incorporation of $CO_2$. Several excellent and active research groups in this field are invited to highlight new directions and developments in the exciting field of $CO_2$ activation and transformation.

This volume is organized into nine chapters, which are independent of each other, and the authors responsible for each chapter were given sufficient freedom to organize their materials. As a consequence, the possible overlapped citation and description of some literatures are inevitable; however, these reiterations should be different based on their individual viewpoints. The first chapter by Prof. Aresta provides an introduction to the structural features of carbon dioxide molecule and its interaction with electrophiles and nucleophiles. Chapter "Metal Complexes Catalyzed Cyclization with $CO_2$" by Prof. Kleij describes organometallic/inorganic complexes catalyzed cyclization reactions that incorporate an intact $CO_2$ fragment without changing the formal oxidation state of the carbon centre. Chapter "Silver-Catalyzed Carboxylation Reaction Using Carbon Dioxide as Carboxylative Reagent" by Dr. Zhang covers silver-catalyzed carboxylation reactions using carbon dioxide as a carboxylative reagent. In this chapter, silver-catalyzed cyclization reactions of propargylic alcohols or amines, *o*-alkynylanilines and alkynyl ketones with carbon dioxide, as well as carboxylation of terminal alkynes and arylboronic esters with carbon dioxide will be documented. The copolymerization of carbon dioxide and epoxides represents an interesting method to prepare a range of aliphatic polycarbonates. In chapter "Dinuclear Metal Complex-Mediated Formation of $CO_2$-Based Polycarbonates", Prof. Williams highlights kinetic and mechanistic studies which have implicated di- or multi-metallic pathways for $CO_2$/epoxide polymerization catalysis and the subsequent development of highly active and selective di(multi-) nuclear catalysts. Chapter "Transition Metal-Free Incorporation of $CO_2$" by Prof. He features recent advances on methodologies for catalytic transformation of $CO_2$ promoted by organocatalysts (e.g. *N*-heterocyclic carbenes, frustrated Lewis pairs

and superbases), ionic liquids, main-group metals to produce value-added chemicals. Chapter "$CO_2$-Mediated Formation of Chiral Fine Chemicals" by Prof. Lu aims to principally showcase the recent progress regarding the stereochemically controlled catalytic $CO_2$ fixation/conversion processes for the production of $CO_2$-based chiral fine chemicals. Chapter "Ni-Catalyzed Synthesis of Acrylic Acid Derivatives from $CO_2$ and Ethylene" by Prof. Rieger focuses the discussion on the analysis of the reaction mechanism of Ni-catalyzed synthesis of acrylic acid derivatives from $CO_2$ and ethylene. Chapter "Transition Metal-Catalyzed Carboxylation of Organic Substrates with Carbon Dioxide" by Prof. Nolan provides a comprehensive summary on transition metal-catalyzed carboxylation reactions involving the use of $CO_2$ in organic synthesis and its incorporation into typical organic substrates such as alkenes, alkynes and various C−H and C–heteroatom bonds. In chapter "Recent Progress in Carbon Dioxide Reduction Using Homogeneous Catalysts", Prof. Beller and coworkers describe the recent developments in carbon dioxide reductions to CO, formic acid derivatives, methanol and methylamines, mainly focusing on the use of defined organometallic catalysts.

The editor believes that the authors have highlighted the most important progress with regard to carbon dioxide activation and transformation in recent decades. This volume is expected to serve as a guide for researchers with an interest in catalytic $CO_2$ fixation/conversion. The descriptive modes for carbon dioxide activation in this volume benefit for encouraging the readers more creative ideas for the development of new reactions with $CO_2$ as a C1 feedstock.

The editor is very grateful to all chapter authors for their significant contributions to the volume. Special thanks go to Dr. Elizabeth Hawkins, who originally initiated this book, and to Arun Manoj for his patience and support during the editing process.

Dalian, China Xiao-Bing Lu

# Contents

Top Organomet Chem (2016) 53: 1–38
DOI: 10.1007/3418_2015_93

Published online: 26 June 2015

# The Carbon Dioxide Molecule and the Effects of Its Interaction with Electrophiles and Nucleophiles

**Michele Aresta and Antonella Angelini**

**Abstract** This chapter discusses the $CO_2$ molecule in its ground and excited states, correlating the energy to the molecular geometry. The effect of adding or taking out an electron is illustrated, opening the way to the coordination of $CO_2$ to metal centers. Several modes of bonding of $CO_2$ are presented and the IR and multinuclear NMR spectroscopic data of transition metal complexes or adducts with Lewis acids and bases are commented. The reactivity of the coordinated heterocumulene is presented through several examples. The use of IR and NMR techniques for determining the molecular behavior of transition metal complexes in solution is exemplified.

**Keywords** $CO_2$ molecule · Ground and excited states · Interaction with Lewis acids and bases · IR · Modes of bonding · NMR · Reactivity of coordinated $CO_2$ · Spectroscopic techniques

## Contents



M. Aresta
Department of Chemical and Biomolecular Engineering, NUS, Singapore, Singapore

CIRCC, via Celso Ulpiani 27, 70126 Bari, Italy

A. Angelini (✉)
CIRCC, via Celso Ulpiani 27, 70126 Bari, Italy
e-mail: cheam@nus.edu.sg

## 1 Introduction

$CO_2$ is the waste end product of several human activities (fossil combustion, cement manufacture, fermentation, industrial processes); ca. 700 Gt/year of $CO_2$ is involved in the natural C-cycle (production of biomass by photosynthesis, carbonization processes, etc.). The actual anthropogenic emissions of $CO_2$ reach the level of more than 35 Gt/year bringing to a continuous increase of $CO_2$ concentration in the atmosphere, which is regarded to severely contribute to climate change of our planet.

Efficient strategies able to reduce the emission/accumulation of $CO_2$ in the atmosphere are under study. Among them, carbon dioxide chemical utilization (CCU), which consists in converting the $CO_2$ molecule into fuels or other valuable products, is an interesting route for reducing waste and making a better use of both fossil carbon and energy.

In order to obtain satisfactory results in the chemical conversion of $CO_2$, it is necessary to know the basic features of the reactivity of this molecule. In the present chapter, a complete description of the electronic configuration of the molecule in its ground and excited states is presented, and the correlation to the structural features and reactivity are discussed.

## 2 The Ground State of Carbon Dioxide and Its Lowest Excited States

Carbon dioxide is a linear molecule in which the distance C–O is equal to 1.1600 Å [1, 2]. In its electronic ground state, it belongs to the point group $D_{\infty h}$. The two carbon–oxygen bonds are polar, and a net partial charge is present on carbon and oxygen atoms [3–8]; however, because of the linear geometry of the molecule, being the two dipole moments opposite each other, the entire molecule is nonpolar (Fig. 1).

The molecule has a moment of electric quadrupole equal to $-4.3 \times 10^{-26}$esu/cm$^2$ [9, 10] that allows the formation of intermolecular interactions and even neutral aggregates $(CO_2)_n (2 \leq n \leq 5)$ as confirmed *by* mass spectrometry [4, 6]. If a cationic or anionic $CO_2$ molecule is present, the intermolecular interactions can become even stronger affording charged intermolecular aggregates [11, 12]. In particular, positively charged aggregates $(CO_2)_n^+ (2 \leq n \leq 10)$ are generated by interaction of neutral $CO_2$ molecules with $CO_2^+$ radical cation [13] giving

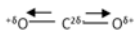

**Fig. 1** Dipole moments in the carbon dioxide molecule

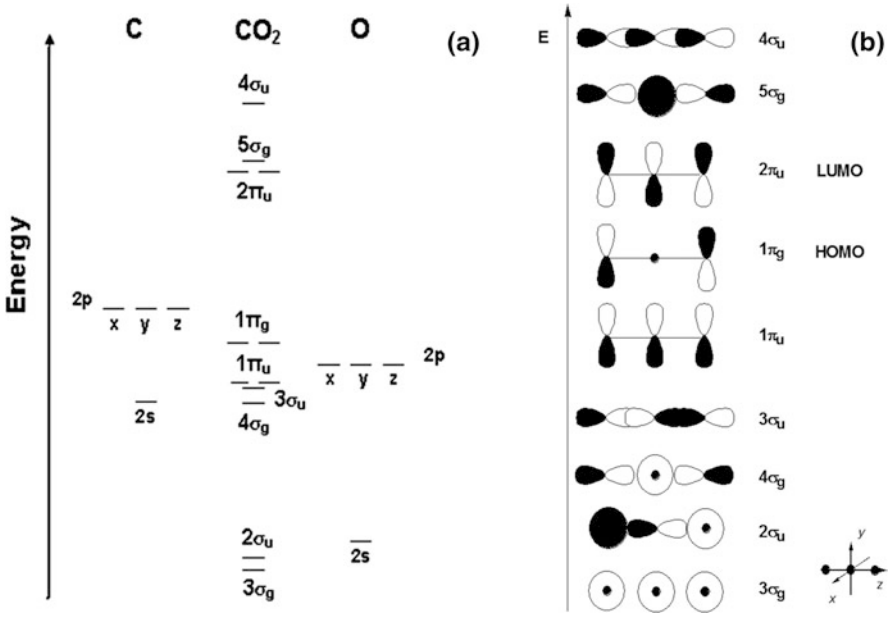


**Fig. 2** Molecular orbital diagram of carbon dioxide (**a**) Energy levels, (**b**) orbital shape

clusters more stable than neutral aggregates. On the other hand, anionic clusters are more stable than $CO_2^-$ radical anion: the dimeric species $(CO_2)_2^-$ is more stable by 0.9 eV, and the stability increases with increasing the cluster size [14].

In the linear molecule, six σ molecular orbitals are generated by combining six atomic orbitals: $2s_O$ (−32.4 eV) and $2p_O$ (−15.9 eV) for the two oxygen and $2s_C$ (−19.4 eV) and $2p_C$ (−10.7 eV) for carbon. The K-shell orbitals of oxygen and carbon remain basically unchanged in the molecule and become $1\sigma_u$, $1\sigma_g$, and $2\sigma_g$.

The six MOs are marked in Fig. 2a as $3\sigma_g$, $4\sigma_g$, $5\sigma_g$, $2\sigma_u$, $3\sigma_u$, and $4\sigma_u$. The remaining $2p_x$ and $2p_y$ orbitals form three doubly degenerate π-orbitals denoted as $1\pi_u$, $1\pi_g$, and $2\pi_u$. The electronic configuration of the linear ground state, $^1\Sigma_g^+$, of $CO_2$ is reported below, and the energy diagram is shown in Fig. 2.

$$^1\Sigma_g^+(\text{ground state}) : 1\sigma_u^2\,1\sigma_g^2(-541.1\text{ eV})\,2\sigma_g^2(-297.5\text{ eV})\,3\sigma_g^2(-37.6\text{ eV})\,2\sigma_u^2(-37.6\text{ eV})$$
$$4\sigma_g^2(-19.4\text{ eV})\,3\sigma_u^2(-18.1\text{ eV})\,1\pi_u^4(-17.6\text{ eV})\,1\pi_g^4(-13.8\text{ eV})$$

The energies of the $CO_2$ molecular orbitals (MO) in parenthesis have been evaluated by measuring the ESCA ionization energies for the molecule [15–17]. Calculations clearly indicate that $3\sigma_g$ has a lower energy than $2\sigma_u$ [3–8]. $3\sigma_u$ is slightly more stable than the $1\pi_u$.

The main contributors to the energy lowest valence molecular orbital, $3\sigma_g(3a_1)$, are the $2s_O$ and $2s_C$ atomic orbitals, with a minor contribution from the $2p_{zO}$ AOs (Fig. 2b). The $2\sigma_u(2b_2)$ MO is mainly a bonding combination of $2s_O$ AOs and the $2p_{zC}$ AO. This molecular orbital presents a nodal plane passing through the central carbon and perpendicular to the molecular axis. The $4\sigma_g(4a_1)$ and $3\sigma_u(3b_2)$ MOs contain C–O antibonding combinations of $2s_O$ with $2s_C$ and $2p_{zC}$, respectively, but they are compensated by strong admixture of bonding $2p_{zO}$ states. The doubly degenerate $1\pi_{ux}(1b_1)$ and $1\pi_{uy}(5a_1)$ orbitals are, respectively, bonding combinations of $2p_x$ and $2p_y$ states on all the three atoms. The $1\pi_{ux}(1b_1)$ MO is equivalent to the $1\pi_{uy}(5a_1)$ orbital in the linear configuration, but it is rotated by 90° about the internuclear axis. In the linear configuration also the doubly degenerate $1\pi_{gx}(1a_2)$ and $1\pi_{gy}(4b_2)$ molecular orbitals are equivalent and reciprocally rotated by 90° about the molecular axis. They have no weight on the carbon atom and play the role of lone pairs. The $1\pi_{gx}(1a_2)$ MO consists of an antibonding combination of $2p_{xO}$ AOs, whereas the $1\pi_{gy}(4b_2)$ MO is an antibonding combination of $2p_{yO}$ AOs.

The first lowest unoccupied molecular orbitals (LUMOs) are the two $2\pi_u$ MOs. Both of them are degenerated and equivalent in the linear configuration. The $2\pi_{ux}(2b_1)$ MO has mainly a $2p_{xC}$ character with a little contribution from the $2p_{xO}$ AOs. Besides a nodal plane passing through the internuclear axis, this molecular orbital has nodal planes intersecting each CO bond, since the starting atomic orbitals are combined in an antibonding manner. The $2\pi_{uy}(6a_1)$ MO is equivalent to the $1\pi_u(1b_1)$ MO in the linear configuration, but it involves the $2p_y$ AOs of all the three atoms.

Both the $5\sigma_g(7a_1)$ and $4\sigma_u(5b_2)$ MOs are strongly antibonding. The $5\sigma_g(7a_1)$ MO is made up of $2s_C$ AO and $2s_O$ and $2p_{zO}$ AOs combined in an antibonding manner and shows four nodal planes perpendicular to the internuclear axis, which intersect the two oxygen atoms and the two C–O bonds. The $4\sigma_u(5b_2)$ MO consists of $2p_z$ AO from all three atoms with a $2s_O$ AO contribution.

The 16 valence electrons of $CO_2$ are distributed over the four σ-orbitals (eight electrons) $3\sigma_g$, $2\sigma_u$, $4\sigma_g$, and $3\sigma_u$ and the four π-orbitals (eight electrons) $1\pi_u$ and $1\pi_g$. Of the eight occupied molecular orbitals, both $3\sigma_g$ and $2\sigma_u$ are responsible for the σ-bonding skeleton of the molecule, while the $1\pi_u$ orbitals account for the C–O π-bonds. By contrast, the electrons $4\sigma_g$, $3\sigma_u$, and $1\pi_g$ are, respectively, σ and π lone pairs. This interpretation agrees with a few features of the ESCA spectrum of $CO_2$. In fact, the fairly sharp nature of the bands at 13.8 ($1\pi_g$), 18.1 ($3\sigma_u$), and 19.4 eV ($4\sigma_g$) in the ESCA spectrum [15–17] is consistent with their assignment to electrons largely localized on the end oxygen atoms. Conversely, the level associated with the band at 17.6 eV ($1\pi_u$), which is broad and exhibits a fine vibrational structure, has apparently a bonding character.

In Fig. 3 the Walsh diagram correlates the MO energies with the OCO bond angle [18]. As evident, by changing the OCO bond angle, the MO energies are affected. The degeneracy of the π-orbitals is lost in the bent geometry, and each couple of formerly equivalent and degenerate π-orbitals splits in two nonequivalent orbitals with different energies, depending on the plane of bending. The splitting is relatively modest for both $1\pi_u$ and $1\pi_g$. In the case of $1\pi_u$ orbitals, the destabilization of $1\pi_u(5a_1)$ is roughly compensated by the stabilization of $1\pi_u(1b_1)$. By

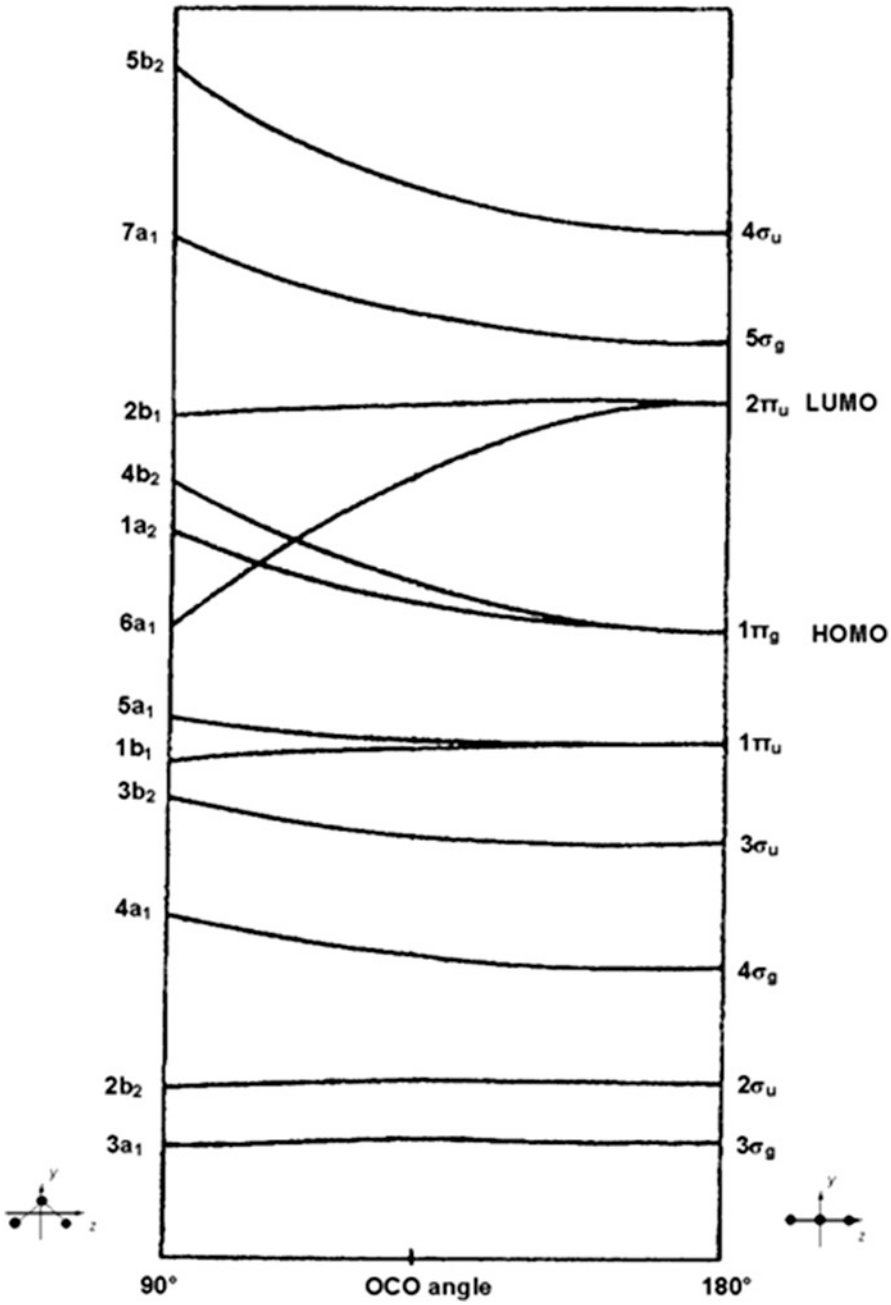


**Fig. 3** Qualitative Walsh diagram for $CO_2$: correlation energy-OCO angle

**Table 1** Correlation of electronic state representations between $D_{\infty h}$ and $C_{2v}$ point groups

| Point group | Ground state | $(1\pi_g \rightarrow 2\pi_u)$ transition states | | | |
|---|---|---|---|---|---|
| $D_{\infty h}$ | $^1\Sigma_g^+$ | $^{1,3}\Sigma_u^-$ | $^{1,3}\Delta_u$ [a] | | $^{1,3}\Sigma_u^+$ |
| $C_{2v}$ | $^1A_1$ | $^{1,3}A_2$ | $^{1,3}A_2$ | $^{1,3}B_2$ | $^{1,3}B_2$ |

[a]The doubly degenerate $\Delta_u$ state splits into two components ($A_2$ and $B_2$) in the point group of lower symmetry ($C_{2v}$)

contrast, in the case of $1\pi_g$ orbitals, the energies of both components increase with diminution of the bond angle. The energy increase upon bending is much faster for $1\pi_g(4b_2)$ than for $1\pi_g(1a_2)$. The rapid increase of the energy of $1\pi_g(4b_2)$ upon molecule bending accounts for the linearity of the $CO_2$ molecule in the ground state. As for the $2\pi_u$ MOs, the energy of the component $2\pi_u(2b_1)$ is only negligibly affected by extent of bending. However, bending causes a net decrease of the energy of the $2\pi_u(6a_1)$ MO, which may become even more stable than $1\pi_g(4b_2)$. This suggests that any event which enables the $2\pi_u(6a_1)$ level to be populated is also expected to produce a distortion of $CO_2$ molecule from linearity.

Figure 2a says that the excitation of the $CO_2$ molecule involves the promotion of one $1\pi_g$ electron into the $2\pi_u$ MO. The resulting excited electronic configuration, $1\sigma_u^2\,1\sigma_g^2\,2\sigma_g^2\,3\sigma_g^2\,2\sigma_u^2\,4\sigma_g^2\,3\sigma_u^2\,1\pi_u^4\,1\pi_g^3\,2\pi_u^1$, gives rise to six excited states in the linear configuration, $^3\Sigma_u^-$, $^3\Delta_u$, $^3\Sigma_u^+$, $^1\Sigma_u^-$, $^1\Delta_u$ and $^1\Sigma_u^+$, which correspond to $A_2$ and/or $B_2$ states in the point group of lower symmetry, $C_{2v}$, resulting from bending the molecule (Table 1).

According to the Walsh diagram, the above excited states $A_2$ and $B_2$ should strongly bend, while the remaining are expected to be slightly bent or linear [18].

Ab initio calculations demonstrate that the electronic energy and the geometric parameters of the nuclear configuration, such as the C–O bond distances and OCO bond angle, are strongly correlated [19]. Using large-scale multireference configuration interaction, the ordering of the lowest valence excited states of $CO_2$ was calculated to be $^3B_2$, $^3A_2$, $^1A_2$ followed by $^1B_2$ that presents bent equilibrium structures. The lowest $^{1,3}A_2$ and $^{1,3}B_2$ states have much longer C–O equilibrium distances (around 1.26 Å) than the electronic ground state (1.16 Å) (Table 2). Moreover, regardless of the spin multiplicity, the $B_2$ states (OCO bond angle $\approx 118°$) were found to be markedly more bent than the $A_2$ states (OCO bond angle $\approx 127°$).

Several experimental evidences that support theoretical calculation have been reported in the literature [19–24].

## 3 The Carbon Dioxide Radical Anion, $CO_2^{\bullet -}$

Carbon dioxide radical anion $CO_2^{\bullet -}$ is isoelectronic with $NO_2$. Theoretical studies [18, 25–32] predict a bent equilibrium geometry ($C_{2v}$ symmetry) with longer carbon–oxygen bonds in the $^2A_1$ ground state, which may be expressed as $(1a_1)^2\,(1b_2)^2\,(2a_1)^2\,(3a_1)^2\,(2b_2)^2\,(4a_1)^2\,(3b_2)^2\,(1b_1)^2\,(5a_1)^2\,(1a_2)^2\,(4b_2)^2\,(6a_1)^1$.

**Table 2** Structural parameters of bent valence excited states of $CO_2$

| Structural parameter | Calculated values [19] | | | | Experimental values | | |
|---|---|---|---|---|---|---|---|
| | $^3A_2$ | $^1A_2$ | $^3B_2$ | $^1B_2$ | $^1A_2$ [20] | $^3B_2$ | $^1B_2$ [21] |
| $R_e$(CO)/Å | 1.261 | 1.262 | 1.251 | 1.260 | $1.262 \pm 0.010$ | 1.249(2) [22] | $1.246 \pm 0.008$ |
| | | | | | | 1.237(2) [22] | |
| $\alpha_e$(OCO)/deg | 127.4 | 127.0 | 118.5 | 117.8 | $129 \pm 1$ | 148.2(2) [22] | $122 \pm 2$ |
| | | | | | | 152.2(2) [22] | |

According to a recent theoretical analysis at B3LYP6-31-G**//B3LYP/6-31G* level [30], the charge density distribution of $CO_2^-$, from a natural population analysis (NPA), shows a negative character for the two O atoms ($-0.76e$) and a positive charge on the C atom ($+0.52e$). Spin (densities) populations indicate a 68% electron delocalization on the C atom and 16% on each oxygen. $CO_2^{\bullet -}$ is, therefore, a radical-like species at carbon and basic at oxygen. The electronic nature of $CO_2^{\bullet -}$ affects its reactivity: calculations show that O-protonation of the radical anion, which affords the hydroxycarbonyl radical OCOH, is more favored than C-protonation, upon which the less stable formiloxy radical HCOO [25, 31] should be formed. Moreover, the *trans*-OCOH is more stable than the *cis*-isomer and barely bound with respect to the H+$CO_2$ asymptote [25, 31, 32].

Paulson [33–37] first demonstrated the existence of $CO_2^{\bullet -}$ radical anion in the gas phase, a species with a short lifetime [Eq. (1)] (vide-infra) by studying the reactions of $O^-$ ion with $CO_2$.

$$CO_2^{\bullet -} \longrightarrow CO_2 + e^- \tag{1}$$

Then, Cooper and Compton [34, 35] observed the formation of metastable, autodetaching $CO_2^{\bullet -}$ ions in collisions of electrons or Cs atoms with cyclic anhydrides (maleic anhydride, succinic anhydride), which contained nonlinear OCO units. The lifetimes of the generated species, measured with a time-of-flight spectrometer, were in the range 30–60 μs. A subsequent study gave a mean lifetime of $90 \pm 20$ μs [36].

The $CO_2^{\bullet -}$ in its equilibrium geometry is metastable, being stabilized kinetically by the barrier, calculated by Pacanski et al. to be 0.4 eV [26], risen by the change of the molecular geometry on going from the $^2A_1$ state of $CO_2^{\bullet -}$ to the ground state of $CO_2$.

In 1961 Ovenall and Whiffen [38] isolated for the first time $CO_2^{\bullet -}$ in a solid matrix. ESR experiments allowed to determine the $CO_2^{\bullet -}$ bond angle (134°), the ground state ($^2A_1$), and the coefficients (14% carbon 2 s, 66% carbon $2p_z$, and 10% for each oxygen $2p_z$) for the mixing of atomic orbitals in the half-filled $6a_1$ molecular orbital, occupied by the odd electron.

UV–VIS absorption spectrum [39] and infrared spectrum of $CO_2^{\bullet -}$ [40] allowed to clarify the electronic configuration and the geometrical features of such species. In the UV region ($\lambda > 240.0$ nm), three maxima were present at 340.0, 280.0, and 255.0 nm, the first being assigned to the $2b_1\left(^2B_1\right) \leftarrow 6a_1\left(^2A_1\right)$ transition. FTIR allowed to determine the bond angle of $127 \pm 8°$ and the CO-bond distance (1.25 Å), which is markedly longer than that measured for $CO_2$.

$CO_2^-$ was easily reacted with water, giving hydrogen carbonate and formate anions [Eq. (2)].

$$2CO_2^- + H_2O \longrightarrow HCO_3^- + HCO_2^- \tag{2}$$

Under anhydrous conditions, a bimolecular process converted the radical anion into either $CO_3^{2-}$ and CO [41] or oxalate (see below), [Eq. (3), (4)]

**Scheme 1** Mechanism of formation of $CO_2^-$ in apatites

$$2CO_2^- \longrightarrow CO_3^{2-} + CO \tag{3}$$

$$2CO_2^- \rightleftarrows C_2O_4^{2-} \tag{4}$$

$CO_2^{\bullet -}$ species detected by Callens et al. [42] by ESR in KCl single crystals doped with $Na_2{}^{13}CO_3$ after X-rays irradiation at room temperature allowed to calculate weights of $2s_C$ and $2p_{zC}$ orbitals contributing to the $6a_1$ molecular orbital of the radical anion to be 11.8% and 43.6%, respectively. The spin density on the oxygen atoms was found to be 0.45, similar to that found for the oxygen atoms of $NO_2$ in the same host lattice.

The ESR technique revealed also the formation of $CO_2^{\bullet -}$ radicals in biological apatites (tooth enamel, bone), when exposed to X-rays or UV light or thermal treatment [43] (Scheme 1). The metastable short-lived $CO_3^{3-}$ radical is formed which rapidly decays to $CO_2^-$.

Several other matrices were used for generating the radical anion, such as lithium formate monohydrate ($HCO_2Li \cdot H_2O$) [44] [Eqs. (5), (6)]. Such process was studied by using X-band EPR, ENDOR, and ENDOR-induced EPR (EIE) spectroscopy at 200 or 295 K.

$$HCOO^-Li^+ \longrightarrow HCOOLi^+ + e^- \tag{5}$$

$$HCOOLi^+ \longrightarrow COO^-Li^+ + H^+ \tag{6}$$

Alternative mechanisms for the formation of $CO_2^{\bullet -}$ have been suggested [45] based on hydrogen atoms [Eq. (8)] and a formate anion [Eq. (9)] with the intermediacy of the extremely unstable radical anion $HCO_2^{2-}$ [Eq. (10)].

$$HCOO^- \longrightarrow HCOO + e^- \tag{7}$$

$$HCOO \longrightarrow H + CO_2 \tag{8}$$

$$H + HCOO^- \longrightarrow H_2 + CO_2^- \tag{9}$$

$$HCOO^- + e^- \longrightarrow HCOO_2^{2-} \tag{10}$$

The reaction of carbon dioxide with alkali metals such as Li, Na, K, and Cs in rare gas and nitrogen matrices at low temperature leads to the formation of $M^+CO_2^-$ species [46–50] showing various geometries depending on the used metal [49]. Lithium generates two isomers of formula $Li^+CO_2^-$ [47, 48], one with rhombus-shaped $C_{2v}$ symmetry, in which the cation interacts symmetrically with both the oxygen atoms of $CO_2^-$, the second having a $C_s$ symmetry and the lithium cation bonded to only one of the two oxygen. The latter rearranges to the former upon

photolysis with a Nernst glower IR source [47]. Jordan [51] has calculated the energy of stabilization of the two isomers with respect to neutral $CO_2$ and metal atom as being 0.85 eV ($C_{2v}$) vs. 0.83 eV ($C_s$).

With metal in excess, $M_2CO_2$ species can be formed [47, 49, 50] either by reaction of $M_2$ molecules with $CO_2$ ($M_2CO_2$, $C_s$) or by sequential addition of M to $MCO_2$ ($C_{2v}$) [49].

Therefore, $CO_2^{\bullet -}$ that has a limited lifetime in gas phase can be stabilized by a metal countercation that influences the spectroscopic features of the radical anion [52–60]. The free $CO_2^-$ has been produced [53, 58–60], and FTIR measurements [53, 59, 60] show that the antisymmetric stretching frequency is located at 1,658.3 $cm^{-1}$ [53], lower than the values (1,665–1,676 $cm^{-1}$) found in pressed alkali halide pellets [40].

$CO_2^-$ anion is stabilized by interaction with the surface of solids [61–70]. Recently Chiesa et al. [63, 70] studied the interaction of $CO_2$ with excess electrons trapped at the surface of polycrystalline MgO at 77 K and generated by ionization of H atoms under UV light. Such electrons can be transferred to gaseous $CO_2$, which are converted into the radical anions [63] [Eq. (11)]. CW-ESR spectroscopy revealed a bent structure with an angle of about 126° and a putative side-on structure with the two oxygen atoms symmetrically disposed with respect to four- and three-coordinated $Mg^{2+}$ ions at MgO edges, reverse corners, and corners.

$$CO_2 + e^- \longrightarrow CO_2^- \tag{11}$$

Again the process occurs at high voltage ($E\left(CO_2/CO_2^-\right) = -1.90$ V, similar to the one electron reduction in water) as a result of the large reorganizational energy between the moieties mentioned above [71].

$CO_2^{\bullet -}$ can be generated also by ionizing radiation in aqueous solutions [72, 73] through routes shown in Eqs. (12)–(15). Under pulse radiolysis with conductometric detection, the protonated form OCOH has been identified [Eq. (15)] having a $pK_a\left(OCOH/CO_2^-\right)$ of 2.3 [73].

$$OH + HCO_2H/HCO_2^- \longrightarrow H_2O + OCOH/CO_2^- \tag{12}$$

$$H + HCO_2H/HCO_2^- \longrightarrow H_2 + OCOH/CO_2^- \tag{13}$$

$$CO + OH \longrightarrow OCOH \tag{14}$$

$$OCOH \rightleftarrows CO_2^- + H^+ \tag{15}$$

As mentioned above, $CO_2^-$ can decay according to different mechanisms depending on the pH. [73]: neutral to basic solutions favor the oxalate, acidic solutions produce $CO_2$ and $HCO_2^-$ (Scheme 2).

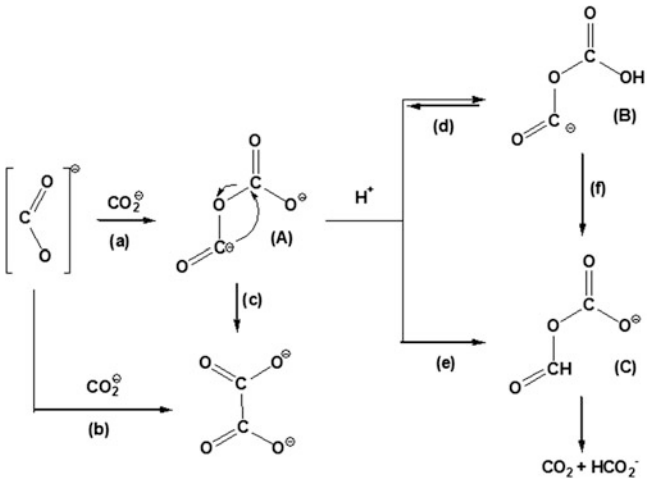


**Scheme 2** Decay of $CO_2^-$ radical anion via either head-to-tail (*a*) or head-to-head (*b*) coupling

## 4 The Carbon Dioxide Radical Cation, $CO_2^+$

$CO_2^+$, formed by extraction of a $1\pi_g$ electron from neutral $CO_2$ molecule, in its ground state $^2\Pi_g$ is linear with $D_{\infty h}$ point group symmetry: the two C–O bonds measure 1.1769 Å, only slightly longer than in the neutral molecule [74–77]. The energy required for ionization is 13.79 eV [15–17, 78], which is larger than that required for the formation of $CO_2^{\bullet -}$. Depending on the interested inner orbitals ($1\pi_u$, $3\sigma_u$, $4\sigma_g$) of $CO_2$, different excited states are generated ($^2\Pi_u$, $^2\Sigma_u^+$, and $^2\Sigma_g^+$, respectively), all linear ($D_{\infty h}$) [74–77, 79–83] with variable C–O distances: the experimental C–O bond distances for the $^2\Pi_u$ and $^2\Sigma_u^+$ excited states are 1.228 and 1.180 Å, respectively. A significant increase of the carbon–oxygen bond length takes place when the electron is removed from the $1\pi_u$, while a modest change is found when electron removal occurs from the orbitals $1\pi_g$, $3\sigma_u$, or $4\sigma_g$, due to their partial or full nonbonding character.

The non-dissociative $CO_2$ ionization affords $CO_2^+$ in an electronically and/or roto-vibrationally excited state [Eq. (16)]. The dissociative ionization of $CO_2$ reported in Eqs. (17) and (18) forms charged and neutral fragments.

$$CO_2 \longrightarrow CO_2^+ \left[\text{or } \left(CO_2^+\right)^*\right] + e^- \tag{16}$$

$$CO_2 \longrightarrow CO^+ + O + e^- \tag{17}$$

$$CO_2 \longrightarrow O^+ + CO + e^- \tag{18}$$

Collisional processes cause a multiple ionization of the molecule, in some cases followed by Coulomb explosion [Eq. (19)], i.e., by fragmentation of the molecular ion into two or three fragments [84].

$$CO_2^{n+} \longrightarrow C^{p+} + O^{q+} + O^{r+} \tag{19}$$

## 5 Carbon Dioxide Interaction with Electron-Rich and Electron-Poor Systems

On the basis of the above discussion, one can conclude that the molecular orbitals mainly involved in the chemical reactivity of $CO_2$ are the $1\pi_g$ and $2\pi_u$ orbitals, which play the role of HOMOs and LUMOs, respectively. The $1\pi_g$-occupied MOs are mainly localized on the end oxygen atoms, while the unoccupied orbitals are mostly centered on the carbon atom. $CO_2$ is, thus, an amphoteric oxide: the oxygen atoms can exhibit a Lewis base character, while the carbon atom can play the role of a Lewis acid center. As the electrophilic character of carbon is higher than the nucleophilicity of the oxygen atoms, carbon dioxide is a better acceptor than donor of electron density. However, electrons and electron-rich species (nucleophiles such as metals in a low oxidation state, bases, hydride ion, etc.) will most likely interact with $CO_2$ by binding to the C atom, while electron-poor centers (electrophiles such as the proton, metal centers in high oxidation state, electron-deficient molecules, etc.) will attack one of the O atoms.

### *5.1 The Coordination Modes of $CO_2$*

Metal centers of different properties can bind $CO_2$ in different ways as schematized in Fig. 4.

As explained by the Walsh diagram, when electron density is transferred to the LUMO, the heterocumulene molecule will minimize the energy by bending it until it reaches an OCO angle of around 125°–133°. Conversely, if electron density is transferred from the O atoms to an acceptor, the cumulene may still maintain a

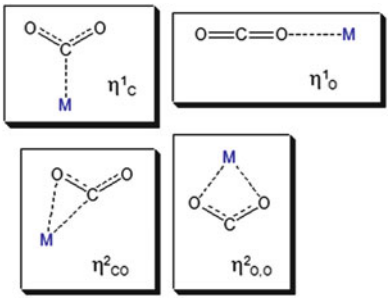


**Fig. 4** Modes of bonding of $CO_2$ to a single metal center of different nature

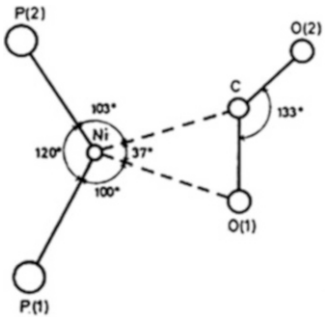


**Fig. 5** XRD structure of Ni $(CO_2)(PCy_3)_2$

quasi-linear geometry. However, some deviations from the theoretical predictions have been found experimentally.

The most popular mode of bonding of $CO_2$ is the $\eta^2$-C,O coordination, and several metal complexes having such structure [85–91] have been isolated and structurally characterized.

The first transition metal complex to be crystallized and structurally characterized was $(PCy_3)_2Ni(CO_2)$ [85] (Fig. 5). XRD spectra revealed the formation of a $\eta^2$-*C*,*O mononuclear complex* in which Ni atom shows a planar geometry and coordinated $CO_2$ has two nonequivalent CO bonds (1.17 and 1.22 Å, to be compared with 1.16 of the free molecule) and an OCO angle of 133° with a strong deviation from $D_{\infty h}$ symmetry. In such case the formation of a bent coordinated $CO_2$ molecule is well in accordance with the Walsh diagram.

Because of the similar features of coordinated $CO_2$ with "$CO_2^{\bullet-}$," it is possible to suppose that Ni has an intermediate oxidation state between 0 (considering $CO_2$ as neutral), +1 (considering $CO_2$ similar to $CO_2^-$), and +2 (if Ni–O and a Ni–C bonds are considered as real bonds since both carbon and oxygen atoms are within bonding distance from the nickel atom).

The nature of ligands on the metal strictly influences the coordination mode of $CO_2$: just replacing $PCy_3$ with $PH_3$, both the calculated OCO angle and the C–O bond lengths increase (144°, 1.204, and 1.256 Å) [86]. It has been suggested that in such case the C–O σ-bond may take part in electron donation to the metal and that the P atom of the phosphane adjacent to the C=O moiety of $CO_2$ may transfer electron density to the C atom.

An example of bis$(CO_2)$-$\eta^2$complex, namely, *trans*-$Mo(CO_2)_2HN(CH_2CH_2PMe_2)_2(PMe_3)$, was reported by Carmona et al. [87]. The complex has a distorted octahedral geometry with two staggered $CO_2$ ligands $\eta^2$-C,O coordinated to molybdenum. The $CO_2$ ligands show C–O lengths ranging from 1.199 to 1.284 Å and OCO angles of 131°. The Mo–C distance (2.08 Å), as well as the distances between the molybdenum atom and the $CO_2$ oxygen atoms bound to the metal (2.111(6) and 2.138(6) Å), demonstrate strong binding of the coordinated C–O moieties to the metal center.

The complex in which the $CO_2$ ligand is bound to a metal center through carbon and to a different metal through the oxygen atoms is also known [92]. In these cases the O,C interaction is considered as primary $\eta^1$-C coordination to a metal center

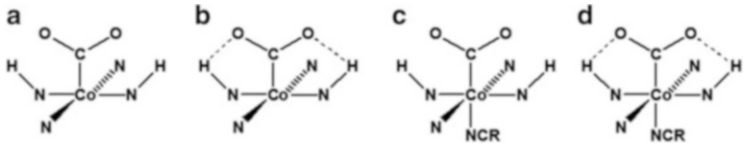


**Fig. 6** Schematic representation of the penta- and hexa-coordinated $CoLCO_2^+$ adducts (R=Me, Pr; L = 5,7,7,12,14,14-hexamethyl-1,4,8,11-tetraazacyclotetradeca-4,11-diene; see main text)

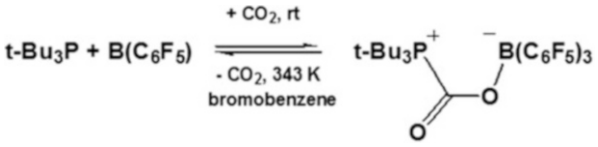


**Scheme 3** Reaction of frustrated Lewis pairs with $CO_2$

stabilized by an external O–E interaction (where E is a different center from that Binding the C atom of the cumulene).

A spectroscopic study on prim,*rac*-$CoL(CO_2)^+$ (L = 5,7,7,12,14,14-hexamethyl-1,4,8,11-tetraazacyclotetradeca-4,11-diene), a cobalt–macrocycle $CO_2$ complex in which the $CO_2$ ligand occupies the axial metal coordination site on the primary macrocycle face, has provided evidence, in solution, of a $CO_2$ ligand interacting simultaneously with the nucleophilic cobalt(I) ion, through the electrophilic carbon, and the macrocyclic ancillary ligand through the oxygen atoms via hydrogen bonds [93]. The FTIR spectra of prim,*rac*-$CoL(CO_2)^+$, measured over the range 298–198 K in $CD_3CN$ and in a $CD_3CN$/THF mixture, indicated the existence, in solution, of four $CO_2$ adducts (Fig. 6), two of which, respectively, penta (B)- and hexa-coordinated (D), showed intramolecular hydrogen bonds between bound $CO_2$ and the amine hydrogen of the macrocyclic ligand.

Analogous systems have been detected by Sauvage et al. [94, 95 and references therein] by studying the selective reduction of $CO_2$ to CO by Ni(cyclam)$Cl_2$.

Intra- and intermolecular acid–base activation of $CO_2$ gives rise to $\eta^2$-C,O coordination. For instance, the components of the couple *t*-$Bu_3P/B(C_6F_5)_3$ pair add to $CO_2$ at ambient temperature in bromobenzene with P–C and O–B bond formation, yielding the product *t*-$Bu_3P$–C(O)O–$B(C_6F_5)_3$ (Scheme 3) [96, 97]. An analogous behavior was also observed with the intramolecular frustrated Lewis pair $(C_6H_2Me_3)_2PCH_2CH_2B(C_6F_5)_2$. Other important examples of bifunctional activation of carbon dioxide are provided by carboxylation of sodium phenoxide, the key step of Kolbe–Schmitt synthesis of salicylic acid [98, 99], carboxylation of Grignard reagents [100], and carbonic anhydrase promoted hydration of carbon dioxide [101].

When $CO_2$ acts as an only C-electrophile, a $\eta^1$-C coordination is observed that is much more unstable than the $\eta^2$-C,O described above. However, examples of isolated complexes are available in the literature since some methods can be used to stabilize the "M–$CO_2$" moiety that can be in some cases isolated and characterized. In particular the solvating properties of the solvent and the donor properties of the metal are of crucial importance for the stability of the M–C bond. In some cases

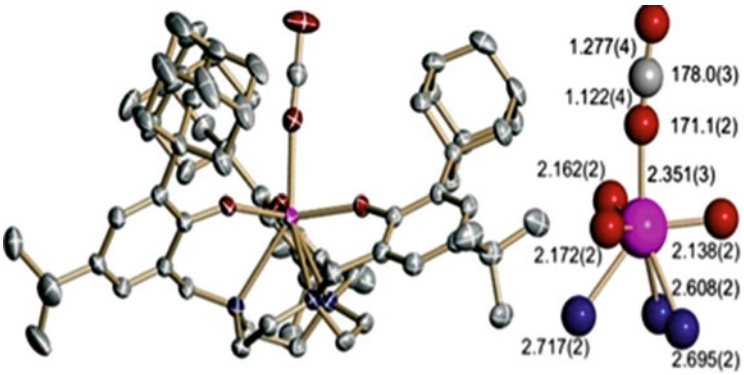


**Fig. 7** XRD structure of the $(^{Ad}ArO)_3tacnU(\eta^1\text{-}OCO)$ complex showing angles and bond lengths

the $\eta^1$-C complex is stabilized by the interaction of the O atom with an external electrophile.

The reaction of $Rh(diars)_2Cl$ (diars = *o*-phenylene-bis(dimethyl)arsine) with slightly pressurized $CO_2$ in $CH_3CN$ affords $Rh(diars)_2(Cl)(CO_2)$ in which $CO_2$ seats *trans* to chlorine and acts as a monodentate ligand, interacting with the nucleophilic metal center through the central carbon [102]. In such adduct, the C–O bond distances, 1.20(2) and 1.25(2) Å, respectively, are both elongated, although, asymmetrically, with respect to the free ligand, while the OCO angle is 126°.

The $\eta^1$-C coordination has also been claimed in a few other Rh and Ir complexes [102–104] and some Ru complexes [105].

The so-called O end-on coordination (linear $\eta^1$-O coordination) was detected for the first time by Castro-Rodriguez in 2004 [106, 107] studying the reaction of $CO_2$ with $(^{Ad}ArO)_3tacnU^{III}$ ($(^{Ad}ArO)_3tacn$ = 1,4,7-tris(adamantyl-5-*tert*-butyl-2-hydroxybenzyl)1,4,7-triazacyclononane). The sterically hindered ligands prevented the $\eta^2$-C,O bonding. XRD of the obtained $(^{Ad}ArO)_3tacnU(\eta^1\text{-}OCO)$ complex (Fig. 7) has revealed that the OCO angle is close to linear (178°), and the U–O bond length is 2.351 Å, with a short bond and a longer terminal C–O bond: the terminal C–O bond length is 1.277(4) Å, that is, longer than the internal C–O bond distance (1.122(4) Å).

The bonding model foresees an oxidized original U(III) to U(IV) with resonance structures represented by $U^{IV} = O = C - O^- \leftrightarrow U^{IV} - O \equiv C - O^-$ that justify the short and long C–O bonds. Magnetic moment ($\mu_{eff}$) measurements have clearly established that $U^{III}$ was oxidized to $U^{IV}$ with the transfer of virtually one electron to $CO_2$. This transfer does not bring the electron in the empty LUMO centered on C, and therefore, the molecule is not bent as in $\eta^1$-C or $\eta^2$-C,O complexes.

The coordination of $CO_2$ to more than one metal center is also very common. The possible coordination modes are shown in Fig. 8. Such complexes are in general quite stable.

An interesting example of a $\mu\text{–}\eta^4$ complex in which both C=O bonds of a single cumulene molecule are bonded to a metal center has been reported by Sadighi

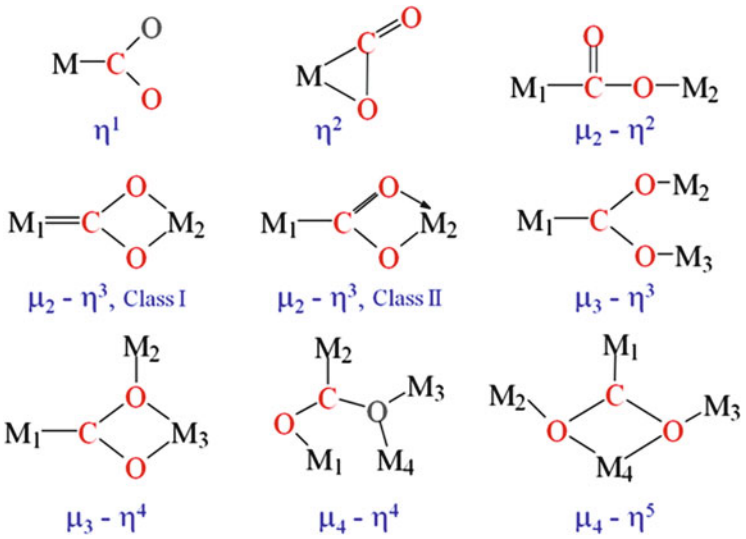


**Fig. 8** Modes of bonding of $CO_2$ in multinuclear complexes with the metal centers bonded to O and C

et al. in 2007 [108] in the complex $[(IPr)Ni]_2(\mu\text{-}CO)(\mu-\eta^2,\eta^2\text{-}CO_2)$ where IPr is 1,3-bis(2,6-diisopropylphenyl)imidazol-2-ylidene. CO and $CO_2$ ligands are bridging two nickel atoms in a side-on way (Fig. 9). The $CO_2$ ligand is bent with a COC angle equal to 133.4°, and the CO bond lengths are 1.255 and 1.257 Å.

Side-on bonded $CO_2$ has been found also in metal organic frameworks systems such as M-MOF-74 (M=Mg and Zn) [109]. On the basis of DFT calculation, metals should interact with the O atoms of $CO_2$, while the carbon atom gives strong interactions with the O atoms of the organic linkers of the MOF.

An O end-on coordination of $CO_2$ is also observed in other metal organic frameworks. This is the case of MOF $Ni_2$(dhtp), where dhtp is 2,5-dihydroxyterephtalic acid [110] in which $CO_2$ is bound to Ni(II) in a $\eta^1$-O end-on fashion and slightly bent (Fig. 10).

In 2005 Chang et al. [111] reported an example of O end-on coordination in trimeric aluminum–magnesium complexes. The structure, confirmed by X-ray diffraction (Fig. 11), shows a $C_3$ symmetry axis in which three carbon dioxide moieties are coordinated in the almost linear μ-O,O′ mode forming a 12-membered ring. The OCO angles are in the range 169.6°–175.3°, larger than the angles found in the $\eta^1$ or $\eta^2$ complexes. The C–O bond lengths are in the range 1.149 and 1.233 Å, with a longer and a shorter bond with respect to the free molecule.

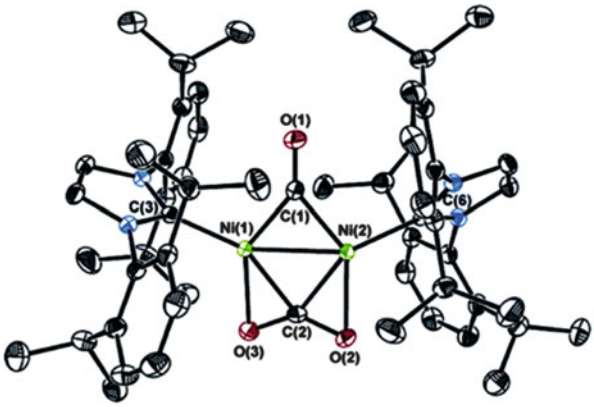


**Fig. 9** XRD structure of $[(IPr)Ni]_2(\mu-XO)(\mu-\eta^2,\eta^2-CO_2)$ where IPr is 1,3-bis (2,6-diisopropylphenyl) imidazol-2-ylidene

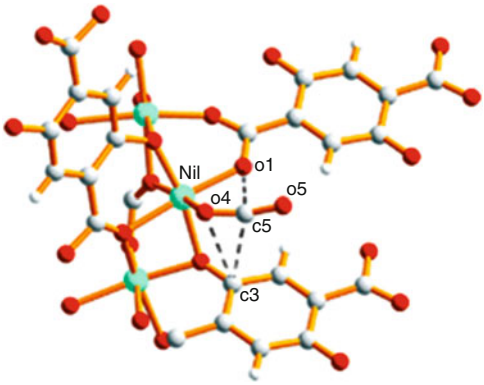


**Fig. 10** Mode of bonding of $CO_2$ adsorbed on MOF ($Ni_2$(dhtp)) (From [110])

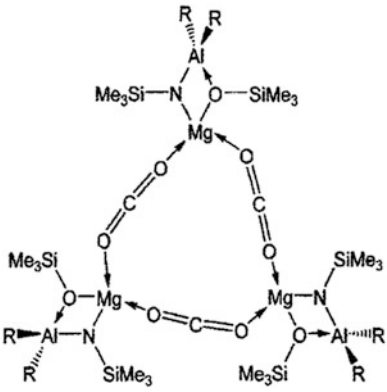


**Fig. 11** Schematic representation of trimeric aluminum–magnesium complexes (R=Me, Et)

## 5.2 *Carbon Dioxide as* O*-Nucleophile*

Experimental measurements and theoretical calculations [112–121] have been carried out in order to quantify the weak basic character of the oxygen atoms in $CO_2$. The proton affinity of the molecule ranges around $540.5 \pm 2$ kJ/mol [120], which is appreciably lower than those found for other O-containing molecules, such as $H_2O$, MeOH, $Me_2O$, $H_2CO$, MeCHO, $Me_2CO$, $HCO_2H$, and $MeCO_2H$ [115, 119, 120].

Hydroxycarbonyl cation $HOCO^+$, the simplest adduct in which $CO_2$ acts as an *O*-nucleophile, was first detected in the interstellar space by Thaddeus et al. [122]. By using different spectroscopic techniques, this molecule was shown to form in ion–molecule reactions by proton transfer between $CO_2$ and $H_3^+$, $NH_2^+$, or $HBr^+$ [123, 124]. Experimental data allow to distinguish between two possible structures: a *cis* conformation with a quasi-linear heavy-atom chain or a *trans* conformation with a small bending at the C atom [125]. However, theoretical investigations indicate as more stable a slight bent structure with a *trans* configuration and the C–O and C–OH bond distances being, respectively, shorter and longer than the non-protonated molecule [114–116, 126].

Several examples of O-coordinated $CO_2$ to metal centers or other molecules or ions show that whenever $CO_2$ behaves exclusively as an *O*-nucleophile, the coordinated $CO_2$ molecule essentially retains its original linear geometry or undergoes only slight distortion from linearity. This suggests that the interaction of $CO_2$ with an electrophilic center through one of the $1\pi_g$ lone pairs is not accompanied by any significant back donation of electron density into the $2\pi_u$ orbitals of the heterocumulene, which, therefore, are left empty. This is the case of transition metals from groups 8 to 12 binding $CO_2$ that form $M^+(CO_2)_n$ adducts with $n$ varying from 1 to 4 [127]. The major stabilizing strength is the donation O-to-metal cation as the $\pi-$back donation is close to zero. The $M^+$–$CO_2$ bond distances depend on both the size of the cation and its electronic configuration, and the binding energies follow the trend of the ion size and the repulsion between the metal cation d-orbitals and the $CO_2$ occupied orbitals, the order of repulsion being $3d\sigma > 3d\pi > 3d\delta$. The binding energies usually vary between 10 (Mn and Fe) and 25 kcal $mol^{-1}$. $CO_2$ clusters with general formula $M^+(CO_2)_n$ are also formed with V ($n$ up to 11) [128], Fe ($n = 1$–18) [129–131], and Ni ($n$ up to 14) [132].

Often in reacting $CO_2$ with early transition metal cations (Sc, Ti, Y, Zr, Nb, La, Hf, Ta, W) [133, 134], an O atom transfer takes place to afford "$MO^+$ + CO." The driving force is the high O affinity of the cations that makes stable $MO^+$ moieties. The conversion of $CO_2$ into CO upon coordination to a metal center [135] opened to great expectation as running a cycle like that represented in Fig. 12 would be of great practical interest.

The reaction of ground state copper $Cu^+$ [136] with $CO_2$ might form $CuO^+$ and CO, a reaction that is endothermic and spin limited. $Pt^+$ [137] forms an associative nonlinear end-on complex $Pt^+ \cdot OCO$, with subsequent formation of the final

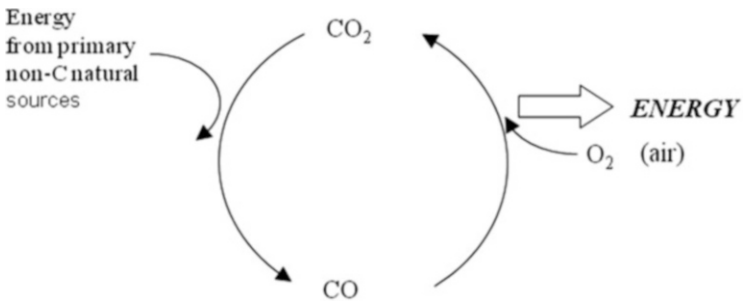


**Fig. 12** Solar-driven cyclic interconversion of $CO_2$–CO–$CO_2$ with production of thermal energy

product O–$Pt^+$–CO. $Al^+$ [138] produces $AlO^+$ + CO. Finally, $U^+$ can give $UO^+$ + CO, an exothermic reaction by 2.1 eV, which has a low cross section [139].

Group 2 metals Be [140], Mg [141–143], and Ca [144] have been studied, both experimentally and theoretically, and shown to promote the reaction $M + CO_2 \rightarrow MO + CO$, endothermic by 26, 66, and 35 kcal $mol^{-1}$ for Be, Mg, and Ca atoms, respectively. The reaction steps through the cyclic ($\eta^2$-O,O)-MOCO structures having barriers of 23, 20, and 14 kcal $mol^{-1}$, respectively. Thermal Mg atoms [141] led to the formation the $MgOCO$ $C_{2v}$ cyclic structure (calculated OCO angle of 128°) and IR bands located at 1,580, 1,385, and 866 $cm^{-1}$ with only a small number of Mg atoms being active (even in pure $CO_2$). The product of condensation of Mg atoms with a $CO_2/C_2H_4$/Ar mixture exhibits IR bands at 1,768, 1,284, and 1,256 $cm^{-1}$, assigned to the formation of a five-member cycle $MgC_2H_4CO_2$ through the formation of a C–C bond between ethylene and carbon dioxide (binding energy, 18 kcal $mol^{-1}$).

B [145, 146] promotes the $CO_2$ to CO conversion, and the reaction $B + CO_2 \rightarrow BO + CO$ is exothermic by 64 kcal $mol^{-1}$. The recombination of BO and CO leads to OBCO ($\nu_{CO} = 1{,}863$ $cm^{-1}$) and is barrier-free [146].

Al atoms react with $CO_2$ in Ar matrices [147] leading to the formation of $AlCO_2$ moieties from which two isomers originate, according to the temperature. At low temperature, the adduct presents a $C_s$ symmetry, with two nonequivalent CO bonds, whereas at higher temperature (25 K) a ring structure is formed in which Al interacts with both oxygen atoms. Above 30 K, the cluster structure yields $Al_2O$ and CO.

## *5.3 Carbon Dioxide as C-Electrophile*

The acidic center of $CO_2$ is located on the carbon atom. When a $\eta^1$-C coordination occurs, an important electron density transfers from metal d-orbitals to the empty antibonding $2\pi_u(6a1)$ orbital of $CO_2$, which weakens the C–O bonds and, as expected from the Walsh diagram, causes the bending of the molecule. Such

structural modification is observed every time the electrophilic carbon atom of $CO_2$ is involved in an interaction with electron-rich species (amines, alcohols, carbanions, etc.). Upon interaction, the nucleophilicity of the O atoms of $CO_2$ increases favoring the interaction with electrophilic species [148–150].

Reactions with nucleophiles are much less documented in the literature. In general they are promoted by a previous coordination of $CO_2$ through the oxygen atom that increases the electrophilicity of carbon. Any electron-rich species is a potential reagent: $H^-$, $OH^-$, $OR^-$, $NR_3$, $NR_2{}^-$, $RR'R''C^-$, and so on. The question is open whether coordinated $CO_2$ is necessary or free $CO_2$ may interact with the "catalyst-activated" nucleophile to afford a carboxylate that then is bound to the metal center.

Recently, in a theoretical study [151] of the hydrogenation of $CO_2$ to formic acid using $Ru^{II}$ catalysts in the presence of water, no coordination of $CO_2$ to the metal center was identified, but low-energy assemblages with the C and O atoms of $CO_2$ interacting with $H^-$ bound to the metal or the $H^+$ of $H_2O$, respectively. In the absence of water, $CO_2$ directly coordinates to the Ru center to afford $Ru(H)_2(\eta^2\text{-}CO_2)(PMe_3)_3$. The Ru-($\eta^1$-formate) intermediate is produced via $CO_2$ interaction with the M–H bond more than the attack by the $H^-$ on coordinated $CO_2$.

Using kinetic measurements, Konno et al. [152] have shown that the nucleophilic attack of the hydride ligand of $Ru(tpy)(4,4'\text{-}X_2bpy)H^+$ (X=H, MeO) to the carbon atom of $CO_2$ was the rate determining step for the formation of the formate complex $Ru(tpy)(4,4'\text{-}X_2bpy)(OCHO)^+$, while the coordination of $CO_2$ to the metal, either in a $\eta^1$-O or $\eta^2$-C,O mode, does not play any important role in the transition state.

## 5.4 *Amphoteric Reactivity of Carbon Dioxide*

The presence of both basic and acid sites in the heterocumulene molecule gives it the possibility to react as amphoteric species. Side-on ($\eta^2$-C,O) coordination of $CO_2$ to metal (Fig. 13) occurs in this case forming a three-membered oxametallacycles, thanks to a formal oxidative addition of one of the $\pi$ bonds of the cumulene to the metal center: both the metal center, which increases of two units its formal oxidation state, and $CO_2$ ligand act simultaneously as both electron acceptor and electron donor.

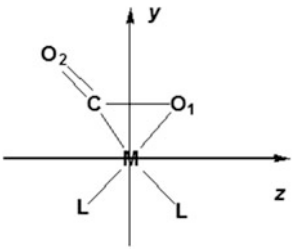


**Fig. 13** Side-on coordination of $CO_2$ to a metal center

Otherwise, ($\eta^2$-C,O) adducts could result from both electron donation from the O-centered $1\pi_{uy}(5a_1)$ and $1\pi_{gy}(4b_2)$ orbitals of $CO_2$ to empty d-orbitals of the metal center and, at a greater extent, electron back donation from a filled d-orbital of metal to the empty carbon-centered $2\pi_{uy}(6a_1)$ orbital of the ligand [153].

Such amphoteric reactivity, under very high pressures, gives rise to the formation of solid $CO_2$ hard crystalline material [154–160]. Depending on the pressure and the temperature, several phases can be formed in which the π molecular bond is replaced by an extended network of C–O single bonds. Recent results suggest that carbon dioxide polymerization does not occur via intermediate states where molecules gradually distort as pressure increases, but is most likely due to solid-state chemical reactions between $CO_2$ molecules [160].

## 6 Spectroscopic Techniques for the Characterization of $CO_2$–Metal Compounds

Spectroscopic techniques such as infrared (IR or FTIR or DRIFT) and $^{13}$C-nuclear magnetic resonance ($^{13}$C-NMR) have been used so far in order to characterize $CO_2$–metal complexes. They represent a good alternative when noncrystalline material is obtained and XRD technique cannot be used. By using simultaneously IR, NMR, and DFT calculations, a fully structural characterization can be achieved.

### *6.1 Infrared (IR) Spectroscopy*

The infrared spectra of $CO_2$ molecules are well known in the scientific world. The linear triatomic molecule exhibits four normal vibration modes (3N−5, where N is the number of atoms in the molecule) (Fig. 14).

The symmetric stretching mode ($\nu_1$) is IR inactive, as it does not generate any change of the electric dipole moment of the molecule.

The antisymmetric stretching ($\nu_3$) is found at 2,349.16 cm$^{-1}$ in the gaseous state [161] and 2,344 cm$^{-1}$ in the solid state [162]. A very slightly shift from the vapor phase is found in aqueous solution (down to 2,343 cm$^{-1}$), indicating the absence of hydrogen bonding between water molecules and dissolved $CO_2$ [163].

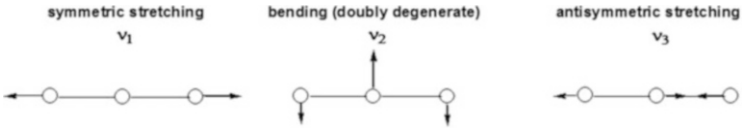


**Fig. 14** Normal vibration modes of carbon dioxide molecule in its ground state

**Table 3** Vibrational normal modes and related frequencies ($cm^{-1}$) for neutral, cationic, and anionic $CO_2$

| | $\nu_1$ ($\nu_s$(OCO)) | $\nu_2$ (δ(OCO)) | $\nu_3$ ($\nu_a$(OCO)) | Notes | Refs. |
|---|---|---|---|---|---|
| $CO_2$ | 1,333 | 667.38 | 2,349.16 | Gas state | [161–163] |
| $CO_2^+$ | 1,244.3 | 511.4 | 1,423.08 | Gas state | [164] |
| $CO_2^-$ | 1,253.8 | 714.2 | 1,658.3 | Ne matrix | [53, 60] |

The bending vibration is generally found at 667.38 $cm^{-1}$ for gaseous $CO_2$ [161] or splits into two components centered at 654.7 and 659.8 $cm^{-1}$ for pure $CO_2$ ice due to the highly ordered ice structure (Davydov splitting) [162].

Gaseous $CO_2^+$ and $CO_2^-$ show quite different absorption with respect to the neutral molecule [53, 60, 164] (Table 3).

The IR spectrum of $CO_2^-$ has been measured in a neon matrix in order to avoid any interaction of the radical anion with metal cations that could strongly influence the resultant IR spectrum. Due to the bent geometry ($C_{2v}$) of the anion, all the three normal vibration modes of $CO_2^-$ are IR active and are lower with respect to the neutral $CO_2$. This is due mainly to a reduced CO bond order, which resulted to be 1.5 in $CO_2^-$ and 2 in $CO_2$.

On the other hand, the $CO_2^+$ cation shows an anomalous low $\nu_3$ frequency [75, 165, 166]. Kawaguchi et al. [165] explained that it could depend on a vibronic interaction between the $^2\Pi_g$ ground state and the $^2\Pi_u$ excited electronic state through the $\nu_3$ vibration normal mode.

On the basis of the structural changes the $CO_2$ molecule undergoes upon coordination as described above, it is possible to predict the consequent changes in the IR spectra.

In general, upon coordination, the antisymmetric stretching mode, $\nu_a$(OCO), is lowered in the range 2,250–1,400 $cm^{-1}$; the symmetric stretching mode, $\nu_s$(OCO), becomes IR active and can absorb in the region 1,400–1,100 $cm^{-1}$; the bending mode δ(OCO) is shifted from 667 $cm^{-1}$; and additional vibrational modes, such as metal–carbon and/or metal–oxygen stretching modes, C=O out-of-plane deformation, may be observed in the low-frequency region (down to 300 $cm^{-1}$).

This means that the spectroscopic features of these absorptions can provide useful information on the bonding modes of the heterocumulene in the adduct [89, 167–169].

In particular the ν(C=O) and the δ(C=O) are of fundamental importance in the forecast of the coordination mode. In Table 4 data relevant to a number of $T_M$ complexes are collected. To summarize, since the C atom coordination gives rise to a bend molecule, a consequent low-energy replacement of ν(C=O) from 2,340 $cm^{-1}$ to ca. 1,750–1,650 $cm^{-1}$ is observed. In the case of O end-on coordination, the molecule preserves its linearity so that only a slight displacement to lower frequencies occurs (shift to ca. 2,200 $cm^{-1}$) [106].

**Table 4** IR $\nu_{OCO}$ bands ($cm^{-1}$) for several types of $CO_2$ complexes

| Compound | Type | $\nu_{asym}$ | $\nu_{sym}$ |
|---|---|---|---|
| $Rh(diars)_2(Cl)(CO_2)$ | $\eta^1$-C | 1,610 | 1,210 |
| $Ni(PCy_3)_2(CO_2)$ | $\eta^2$-C,O | 1,740 | 1,140, 1,094 |
| $[Pt(PEt_3)_2(Ph)]_2(CO_2)$ | $\mu_2$-$\eta^2$ | 1,495 | 1,290, 1,190 |
| $[Co(en)_2(CO_2)](ClO_4)\cdot H_2O$ | | 1,512 | – |
| $CpFe(CO)_2(CO_2)SnPh_3$ | | 1,499 | 1,159 |
| *cis*,*cis*-$Ru(bpy)_2(CO)(CO_2)$–$Ru(bpy)_2(CO)^+{}_2$ $2PF_6^-$ | | 1,507 | 1,176 |
| $[(PPh_3)_2(Cl)(t\text{-Bupy})Ir$–$(\mu\text{-}O)(\mu\text{-}CO_2)Os(O)_2$ $(t\text{-Bupy})_2]^+ClO_4^-$ | | 1,593 | 1,022 |
| $Cp^*Ir(\mu\text{-}t\text{-BuN})(\mu\text{-}CO_2)ZrCp_2$ | | 1,569 | 1,015 |
| $Ru_2(\mu\text{-}CO_2)(CO)_4[(\mu\text{-}OPr)_2PNEtP(OPr)_2]_2$ | | 1,710 | – |
| $Cp^*Re(CO)(NO)(CO_2)Re(CO)_3(PPh_3)$ | $\mu_2$-$\eta^3$, class I | 1,437 | 1,282 |
| $CpFe(CO)(PPh_3)(CO_2)Re(CO)_3[P(OEt)_3]$ | | 1,435 | 1,252 |
| $CpRu(CO)_2(CO_2)Zr(Cl)Cp_2$ | | 1,348 | 1,290 |
| $CpRe(NO)(PPh_3)(CO_2)SnPh_3$ | $\mu_2$-$\eta^3$, class II | 1,395 | 1,188 |
| $Cp^*Re(CO)(NO)(CO_2)SnPh_3$ | | 1,429 | 1,188 or 1,175 |
| $(AdArO)_3tacnU(\eta^1\text{-OCO})$ | $\eta^1$-O | 2,188 | |
| $\{R_2Al(\mu\text{-}NSiMe_3)(\mu\text{-}OSiMe_3)Mg$ $(THF)_2(\mu\text{-}O_2C)\}_3$ | $\mu^2$-O,O | 2,267(R=Me) | |
| | | 2,275(R=Et) | |
| $(C_3H_5N_2)_3(C_3H_4N_2)$ $(PMo_{11}CoO_{38}(CO_2))\cdot 4H_2O$ | | 2,169 | |

Very useful for the assignment of the bands is the isotopic labeling of $CO_2$ with $^{13}C$ and $^{18}O$ [167–169]. Jegat et al. [168] elaborated a general relationship to correlate FTIR data to structure of $T_M$–$CO_2$ complexes:

$$\text{side-on coordination}: \Sigma\Delta\nu\left(^{13}C\right) > \Sigma\Delta\nu\left(^{18}O\right) \text{ and } \Sigma\Delta\nu\left(^{18}O\right) < 60\,cm^{-1};$$
$$\eta^1\text{-C coordination}: \Sigma\Delta\nu\left(^{13}C\right) > \Sigma\Delta\nu\left(^{18}O\right) \text{ with } 60\,cm^{-1} < \Sigma\Delta\nu\left(^{18}O\right) < 70\,cm^{-1};$$
$$\text{end-on coordination}: \Sigma\Delta\nu\left(^{13}C\right) < \Sigma\Delta\nu\left(^{18}O\right) \text{ with } < \Sigma\Delta\nu\left(^{18}O\right) > 70\,cm^{-1}$$

It is interesting to note that in $\eta^1$-C-coordinated $CO_2$ complexes, the frequency splitting between the two $\nu$(OCO) stretching modes is often less than 400 $cm^{-1}$, and in end-on ($\eta^1$-OCO) complexes, the out-of-plane bending mode $\gamma$(C=O), absorbing in the 650–500 $cm^{-1}$ range, shows a pronounced $^{18}O$ effect, differently from the other coordination modes, where a larger $^{13}C$ effect is observed ($\Delta\gamma\left(^{13}C\right) = 10$ to 20 $cm^{-1}$ vs $\Delta\gamma\left(^{18}O\right) = 5\,cm^{-1}$) [167–169].

The IR spectra of the O end-on complexes $Mg \leftarrow O = C = O \rightarrow Mg$ [111] exhibit strong absorptions at 2,267 and 2,275 $cm^{-1}$ slightly redshifted by 73 and

65 $cm^{-1}$ relative to free $CO_2$, whereas side-on complexes usually exhibit shifts greater than 300 $cm^{-1}$.

An extensive analysis of IR spectra of $CO_2$–TM complexes can be found in [18].

## 6.2 UV Spectrum of Carbon Dioxide

Several experimental [20, 78, 113, 170, 171] and theoretical [7, 19, 22, 172–175] studies on the UV spectrum of carbon dioxide are reported in the literature.

Carbon dioxide does not show any absorption in the visible and near-to-middle ultraviolet regions [74, 176]. The first signal appears in the vacuum ultraviolet region at 147.5 (8.41 eV), 133.2 (9.31 eV), and 112.1 nm (11.08 eV). The assignment of those three absorption maxima is still under investigation. Several authors have assigned the maxima at 147.5 and 133.2 nm to transitions to $^1\Delta_u$ and $^1\Pi_g$ states, respectively. The maximum at 112.1 nm exhibits much higher intensity. This is the strongest absorption band of carbon dioxide. The intensity of the absorption indicates that this transition, identified as $^1\Sigma_u^+ \leftarrow {}^1\Sigma_g^+$, is optically allowed [177]. Above 11 eV there are several Rydberg series converging to the various states of $CO_2^+$.

The importance of the spectroscopic properties of $CO_2$ in the UV region is related to photodissociation into CO and O that the molecule undergoes upon UV irradiation [Eq. (20)] [178–183].

$$CO_2 \xrightarrow{h\nu} CO + O \tag{20}$$

The energy states of O and CO generated by $CO_2$ photodissociation depend on the energy of the absorbed UV light (Table 5). The so obtained electronically excited oxygen atoms may undergo subsequent quenching to the O($^3$P) ground state by collisions affording molecular oxygen, $O_2$.

When using UV photons of energy in the range 7.42–10.45 eV (120.0 nm $< \sigma <$ 167.2 nm), $CO_2$ can dissociate via two channels affording O($^3$P) or O($^1$D), respectively [Eqs. (21a) and (21b)].

**Table 5** Energy (eV) and wavelength (nm) thresholds for the photodissociation of $CO_2\left(^1\Sigma_g^+\right)$ to $CO\left(X^1\Sigma^+, a^3\Pi, A^1\Pi\right)$ and O ($^3$P, $^1$D, $^1$S)[a]

| $CO_2$ | CO | O | E | σ |
|---|---|---|---|---|
| $^1\Sigma_g^+$ | $X^1\Sigma^+$ | $^3$P | 5.45 | 227.5 |
| $^1\Sigma_g^+$ | $X^1\Sigma^+$ | $^1$D | 7.42 | 167.2 |
| $^1\Sigma_g^+$ | $X^1\Sigma^+$ | $^1$S | 9.65 | 128.6 |
| $^1\Sigma_g^+$ | $a^3\Pi$ | $^3$P | 11.47 | 108.2 |
| $^1\Sigma_g^+$ | $A^1\Pi$ | $^3$P | 13.50 | 92.0 |

[a]From [178]

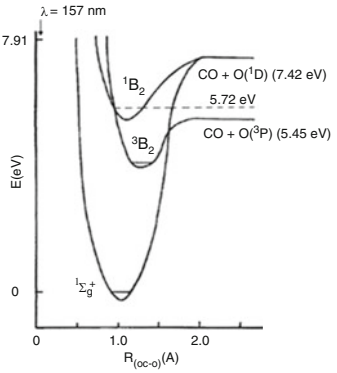


**Fig. 15** Photodissociation of $CO_2$ at 157 nm

$$CO_2 + h\nu \longrightarrow CO(^1\Sigma) + O(^3P) \tag{21a}$$

$$CO_2 + h\nu \longrightarrow CO(^1\Sigma) + O(^1D) \tag{21b}$$

The dissociation of $CO_2$ at 147.0 and 130.2–130.6 nm was studied in detail by Slanger and Black [179] who determined that quantum yield for oxygen atom production was unity. Zhu and Gordon [180] determined the branching ratio between reactions (21a) and (21b), which was 94% O($^1$D) and 6% O($^3$P) for $h\nu$ corresponding to light at 157 nm. The latter was deeper studied in order to verify the formation mechanism of O($^3$P) under operative condition [181, 182]. The 157 nm (7.91 eV) excitation should correspond to the dissociation products CO($^1\Sigma$) and O ($^1$D) (7.42 eV) (Fig. 15) since the photodissociation of $CO_2$ to $CO(^1\Sigma) + O(^3P)$ violates the spin conservation rule (the spin of $CO_2$ in the ground state ($^1\Sigma_g^+$) is zero, whereas the total spin of $CO(^1\Sigma) + O(^3P)$ is one, and therefore, reaction (21a) is a spin-forbidden process). In order to explain the formation of $CO(^1\Sigma) + O(^3P)$ products, a transition from the surface of the $^1B_2$ state to the surface of the lower $^3B_2$ state has been supposed. Figure 15 shows that the two states intersect approximately 0.27 eV above the $CO(^1\Sigma) + O(^3P)$ asymptote. In principle, the efficiency of this singlet–triplet transition will depend on the lifetime of the excited state. According to Zhu and Gordon [180], although the molecule contains energy excess (11 kcal/mol; 0.48 eV) over the $CO(^1\Sigma) + O(^1D)$ dissociation threshold, it does not dissociate readily because the bent upper state ($^1B_2$) makes it difficult to concentrate enough energy along the reaction coordinate. This increases the lifetime of the excited state and the probability of curve crossing to the triplet state.

Other authors [181, 182], instead, proposed the $^3A_2$ state rather than the $^3B_2$, as the $CO_2$ triplet state involved in the photodissociation process. Bhattacharya et al. [183] studied the formation of $O_2$ and CO produced by $CO_2$ photolysis at $185 \pm 2$ nm (≈6.7 eV; Hg lamp). In such operative conditions the mechanism for $CO_2$ dissociation implies an electronic transition of the $CO_2$ molecule from the

singlet ground state ($^1\Sigma_g^+$) to the upper (bound) singlet state $^1B_2$ that is above the crossover zone with the state $^3B_2$.

Dissociation can occur if the molecule can reach the crossover region (by collisions, for instance) and undergo a transition to the triplet state $^3B_2$.

## 6.3 Nuclear Magnetic Resonance (NMR) Spectroscopy

As for IR spectroscopy, $^{13}$C-NMR is a really useful technique to investigate structural features of compounds containing the $CO_2$ molecule, as a whole. In fact the carbon chemical shift is strongly affected by the chemical surrounding the molecule. Free $CO_2$ dissolved in a nonpolar solvent, such as benzene or toluene, exhibits only one $^{13}$C resonance around 124 ppm. In aqueous solutions the resonance is close to 125 ppm [184]. The $^{13}$C resonance of $CO_2$ shifts downfield upon fixation of the heterocumulene into organic products, such as carbamic acids or carbamates (150–160 ppm), carbonates (145–165 ppm), acids (160–180 ppm), esters (160–170 ppm), or their metallo-organic analogs (metallo-carbamates $L_nM(O_2CNR_2)$, metallo-carbonates $L_nM(O_2COR)$, metallo-carboxylates $L_nM(O_2CR)$, metallo-carboxylic acids $L_nM(CO_2H)$, metallo-esters $L_nM(CO_2R)$).

The coordination mode could also be predicted by the chemical shift: O end-on complexes show $^{13}$C resonance slightly upfield shifted (around ca. 121–110 ppm) with respect to the free $CO_2$, whereas side-on complexes usually show $^{13}$C resonances downfield shifted at around 200 ppm [89]. The shift is obviously correlated to the transfer of electron density to/from the coordinated $CO_2$ and to the molecular geometry. Table 6 reports a selection of data which can be helpful in illustrating the relation structure–NMR properties of the $CO_2$–TM complexes.

An example of end-on complexes is $\{R_2Al(\mu\text{-}NSiMe_3)(\mu\text{-}OSiMe_3)Mg(THF)_2(\mu\text{-}O_2C)\}_3$ (120.87 ppm, R=Me; 120.76 ppm, R=Et) [111] or $(C_3H_5N_2)_3(C_3H_4N_2)(PMo_{11}CoO_{38}(CO_2))\cdot 4H_2O$ (113.86 ppm) and $(C_3H_5N_2)_4(SiMo_{11}CoO_{38}(CO_2))\cdot 4H_2O$ (112.50 ppm) [185].

In the latter case some irregular behavior could be observed sometimes since the coordination geometry of the adducts and the different nature of coordinating metal

**Table 6** NMR data for selected carbon dioxide transition metal complexes with different coordination

| Complex | $\delta$M-$^{13}CO_2$ | *d* M-C (Å) |
|---|---|---|
| $(PCy_3)_2Ni(\eta^2\text{-}C,O)$ | 159.28 | 1.84 |
| $[(dppp)(CO)_3Re(\mu_2\text{-}\eta^3\text{-}CO_2)\ Re(CO)_3(dppp)]$ | 191.7 | 2.191(13) |
| $[(cp^*)(CO)(NO)Re(\mu_2\text{-}\eta^3\text{-}CO_2)W(Cp)_2][BF_4]$ | 247.4 | 2.04(4) |
| $[(cp^*)(CO)(NO)Re(\mu_2\text{-}\eta^2\text{-}CO_2)SnMe_3]$ | 196.1 | 2.103(5) |
| $[(PMe_2Ph)_3Os(\mu\text{-}H)_2(\mu_3\text{-}\eta^3\text{-}CO_2)Rh_2(cod)_2]$ | 193 | 2.062(19) |
| $[(cp^*)Ir(\mu\text{-}tBuN)(\mu_2\text{-}\eta^2\text{-}CO_2)Zr(cp)_2]$ | 164.0 | 2.098(10) |
| $[(Et_3P)_2Pt(\mu_2\text{-}\eta^2\text{-}CO_2)Ge\{N(TMS)_2\}]$ | 171.4 | 2.086(9) |

center could affect the final spectrum. For example, in the side-on complexes Ni($\eta^2$-$CO_2$)($PCy_3$)$_2$ (159.28 ppm, at 298 K) and Pd($\eta^2$-$CO_2$)($PMePh_2$)$_2$ (166.2 ppm), coordinated $CO_2$ resonates at upper fields than in the metallocene derivatives ($Cp^*$)$_2$Nb($\eta^2$-$CO_2$)($CH_2SiMe_3$) (200.5 ppm) and $Cp_2Ti(\eta^2$-$CO_2)(PMe_3)$ (212.3 ppm) or a few bis-($\eta^2$-$CO_2$) complexes of molybdenum (201–217 ppm) [87]. In such case the determination of coupling constant of the $^{13}C$ nucleus of coordinated $CO_2$ with the nuclei of the metal center or other ligands was useful to clarify the structure of the adducts. For instance, the $CO_2$ ligand in Ni(dcpp)($\eta^2$-$CO_2$) absorbs at 164.2 ppm, very close to 166.2 ppm which is the resonance of the carbonate ligand in Ni(dcpe)($CO_3$). However, the carbonate ligand in Ni(dcpe)($CO_3$) resonates as singlet, while coordinated $CO_2$ in Ni(dcpp)($\eta^2$-$CO_2$) gives a doublet with a $^2J(C\text{-}P_{trans})$ equal to 45 Hz [186, 187].

VT multinuclear NMR and solid-state CP–MAS–NMR technique have also been used to establish whether the M-coordinated $CO_2$ framework is a rigid structure or not and if it retains the same configuration in solution with respect to the solid state [188, 189].

A good example of such applications can be find in the characterization of Ni($\eta^2$-$CO_2$)($PCy_3$)$_2$ investigated by Aresta's group [188]. CP–MAS–NMR and VT–NMR experiments demonstrate that below 200 K Ni($\eta^2$-$CO_2$)($PCy_3$)$_2$ presents identical structures both in the solid state and in solution.

The $^{31}P$ CP–MAS–NMR spectrum of solid Ni($\eta^2$-$CO_2$)($PCy_3$)$_2$ showed two main peaks at 48.9 and 20.9 ppm, respectively, as expected for a planar arrangement of ligands around the Ni atom. The $^{13}C$ CP–MAS–NMR spectrum of a $^{13}CO_2$-enriched solid sample of Ni($\eta^2$-$^{13}CO_2$)($PCy_3$)$_2$ exhibited the peak of $CO_2$ ligand at 159.28 ppm. In solution, below 200 K, the same profiles were found in the $^{31}P$ spectrum without high differences in the chemical shifts of the signals (51.7 and 20.9 ppm; J(P-P) = 39.6 Hz). This suggest that, at these temperatures, $CO_2$ is rigidly anchored at the planar nickel center in the ($\eta^2$-C,O) coordination mode (Fig. 16). In accordance with the above findings, the low-temperature limiting $^{13}C$ spectrum (173 K) of Ni($\eta^2$-$^{13}CO_2$)($PCy_3$)$_2$, the resonance of the $CO_2$ ligand appeared as a doublet of doublets at 159.88 ppm with $J(C\text{-}P_{trans})$ and $J(C\text{-}P_{cis})$ of 41 and 10 Hz, respectively (Fig. 17).

Upon increasing temperature above 233 K, the two $^{31}P$ signals coalesce into a singlet, showing that the phosphane ligands became equivalents. $\Delta G^{\ddagger}$ for the exchange process was calculated to be 39.3 kJ/mol (9.4 kcal/mol). In the fast exchange regime, at 253 K, a triplet at 158.12 ppm was found for the coordinated $CO_2$, with an average value of J(P-C) equal to 14.1 Hz. The following mechanisms have been proposed (Scheme 4).

The available NMR data did not allow to differentiate between mechanisms (i)–(iii) in Scheme 4. However, additional FTIR studies and CAS-SCF calculations of Ni($CO_2$)$L_2$ isomers showed that formation of the end-on coordinated intermediate (mechanism iii) may reasonably account for the fluxional behavior Ni($\eta^2$-$CO_2$)($PCy_3$)$_2$ [169, 188].

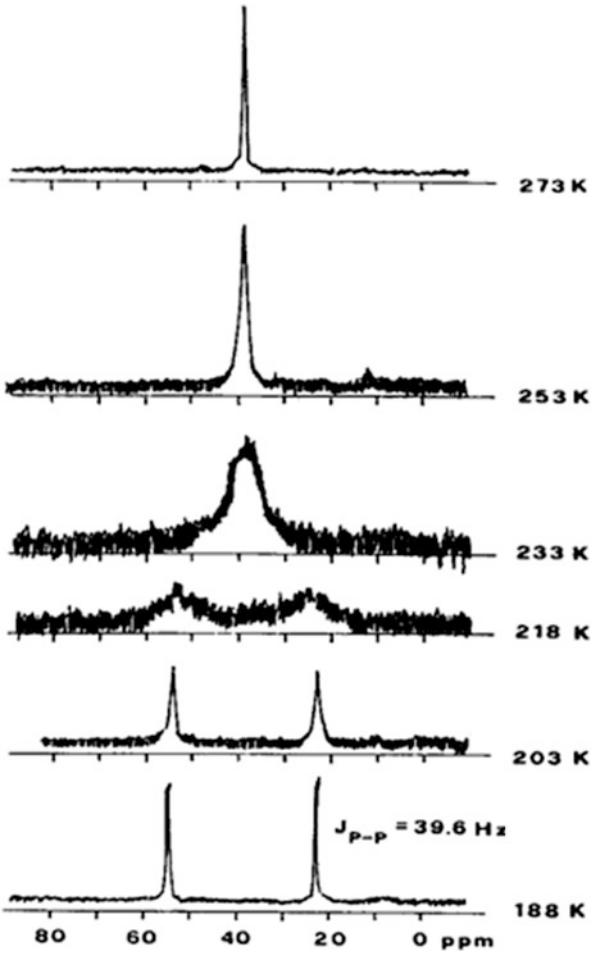


**Fig. 16** VT $^{31}P\{^{1}H\}$ spectra of $Ni(CO_2)(PCy_3)_2$

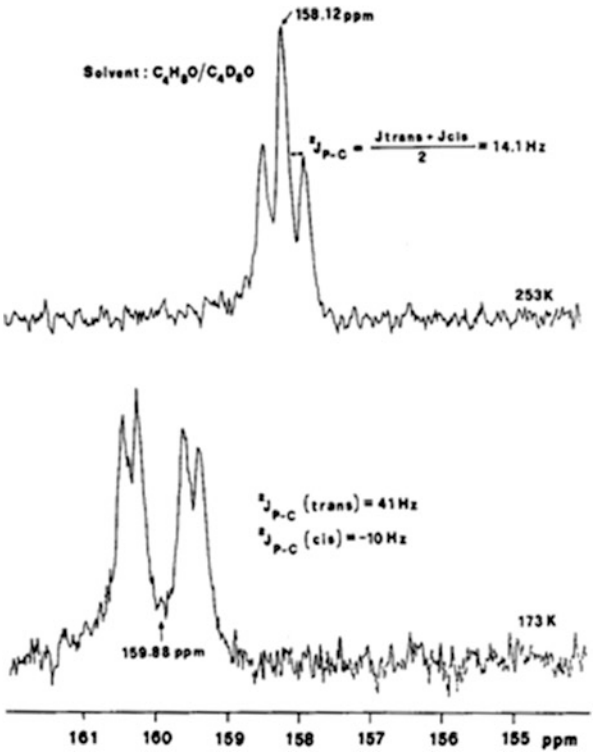


**Fig. 17** $^{13}C\{^1H\}$ spectra of $Ni(^{13}CO_2)(PCy_3)_2$ at 253 K (*top*) and 173 K (*bottom*)

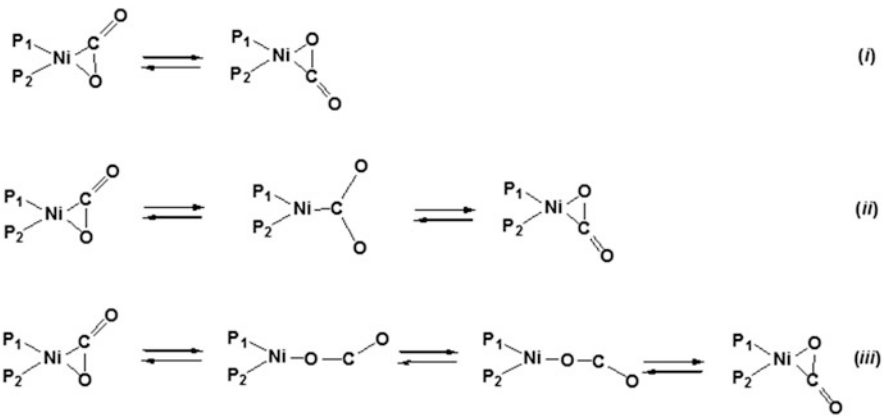


**Scheme 4** Fluxional behavior of $Ni(CO_2)(PCy_3)_2$

## References


1. Kuchitsu K (ed) (1992) Structure data of free polyatomic molecules, vol II/21, Landolt-Börnstein. Springer, Berlin, p 151
2. Kuchitsu K (ed) (1995) Structure data of free polyatomic molecules, vol II/23, Landolt-Börnstein. Springer, Berlin, p 146
3. Vučelić M, Ohrn Y, Sabin JR (1973) *Ab initio* calculation of the vibrational and electronic properties of carbon dioxide. J Chem Phys 59:3003–3007
4. Cremaschi P, Simonetta M (1974) A theoretical study of electrophilic aromatic substitution. I. The electronic structure of $NO_2^+$. Theor Chim Acta 34:175–182
5. Müller JE, Jones RO, Harris J (1983) Density functional calculations for $H_2O$, $NH_3$, and $CO_2$ using localized muffin-tin orbitals. J Chem Phys 79:1874–1884
6. Moncrieff D, Wilson S (1995) On the accuracy of the algebraic approximation in molecular electronic structure calculations: IV. An application to a polyatomic molecule: the $CO_2$ molecule in the Hartree-Fock approximation. J Phys B At Mol Opt Phys 28:4007–4013
7. Nakatsuji H (1983) Cluster expansion of the wavefunction. Valence and Rydberg excitations, ionizations, and inner-valence ionization of $CO_2$ and $N_2O$ studied by the SAC and SAC CI theories. Chem Phys 75:425–441
8. Gutsev GL, Bartlett RJ, Compton RN (1998) Electron affinities of $CO_2$, OCS, and $CS_2$. J Chem Phys 108:6756–6762
9. Maroulis G, Thakkar AJ (1990) Polarizabilities and hyperpolarizabilities of carbon dioxide. J Chem Phys 93:4164–4171
10. Buckingham AD, Disch RL, Dunmur DA (1968) Quadrupole moments of some simple molecules. J Am Chem Soc 90:3104–3107
11. Lobue JM, Rice JK, Novick SE (1984) Qualitative structure of $(CO_2)_2$ and $(OCS)_2$. Chem Phys Lett 112:376–380
12. Rossi AR, Jordan KD (1979) Comment on the structure and stability of $(CO_2)_2^-$. J Chem Phys 70:4442–4444
13. Johnson MA, Alexander ML, Lineberger WC (1984) Photodestruction cross sections for mass-selected ion clusters: $(CO_2)_n^+$. Chem Phys Lett 112:285–290
14. Bowen KH, Liesegang GW, Sanders RA, Herschbach DR (1983) Electron attachment to molecular clusters by collisional charge transfer. J Phys Chem 87:557–565
15. Allian CJ, Gelius U, Allison DA, Johansson G, Siegbahn H, Siegbahn K (1972) ESCA studies of $CO_2$, $CS_2$ and COS. J Electron Spectrosc Relat Phenom 1:131–151
16. Turner DW (1968) Molecular photoelectron spectroscopy. In: Hill HAO, Day P (eds) Physical methods in advanced inorganic chemistry. Interscience, London
17. Turner DW, May DP (1967) Frank-Condon factors in ionization: experimental measurements using molecular photoelectron spectroscopy. J Chem Phys 46:1156–1160
18. Walsh AD (1953) The electronic orbitals, shapes, and spectra of polyatomic molecules. Part II. Non-hydride $AB_2$ and BAC molecules. J Chem Soc 75(9):2266–2288
19. Spielfieldel A, Feautrier N, Cossart-Magos C, Werner H-J, Botschwina P (1992) Bent valence states of $CO_2$. J Chem Phys 97:8382–8388
20. Cossart-Magos C, Launay F, Parkin JE (1992) High resolution absorption spectrum of $CO_2$ between 1750 and 2000 Å. 1. Rotational analysis of nine perpendicular-type bands assigned to a new bent-linear electronic transition. Mol Phys 75:835–856
21. Dixon RN (1963) The carbon monoxide flame bands. Proc R Soc Lond A 275:431–446
22. Cossart-Magos C, Launay F, Parkin JE (2005) High resolution absorption spectrum of $CO_2$ between 1750 and 2000 Å. 2. Rotational analysis of two parallel-type bands assigned to the lowest electronic transition $1^3B_2 \leftarrow X^1\Sigma_g^+$. Mol Phys 103:629–641
23. Mohammed HH, Fournier J, Deson J, Vermeil C (1980) Matrix isolation study of the $CO_2$ lowest triplet state. Chem Phys Lett 73:315–318

24. Winter NW, Bender CF, Goddard WA III (1973) Theoretical assignments of the low-lying electronic states of carbon dioxide. Chem Phys Lett 20:489–492
25. Matoušek I, Fojtík A, Zahradník R (1975) A semiempirical molecular orbital study of radicals and radical ions derived from carbon oxides. Collect Czech Chem Commun 40: 1679–1685
26. Pacansky J, Wahlgren U, Bagus PS (1975) SCF *ab initio* ground state energy surface for $CO_2$ and $CO_2^-$. J Chem Phys 62:2740–2744
27. England WB, Rosemberg BJ, Fortune PJ, Wahl AC (1976) *Ab initio* vertical spectra and linear bent correlation diagrams for the valence states of $CO_2$ and its singly charged ions. J Chem Phys 65:684–691
28. England WB (1981) Accurate *ab initio* SCF energy curves for the lowest electronic states of $CO_2/CO_2^-$. Chem Phys Lett 78:607–613
29. Sommerfeld T, Meyer H-D, Cederbaum LS (2004) Potential energy surface of $CO_2^-$ anion. Phys Chem Chem Phys 6:42–45
30. Villamena FA, Locigno EJ, Rockenbauer A, Hadad CM, Zweier JL (2006) Theoretical and experimental studies of the spin trapping of inorganic radicals by 5,5-dimethyl-1-pyrroline *N*-oxide (DMPO).1. Carbon dioxide radical anion. J Phys Chem 110:13253–13258
31. Feller D, Dixon DA, Francisco JS (2003) Coupled cluster theory determination of the heats of formation of combustion-related compounds: CO, HCO, $CO_2$, $HCO_2$, HOCO, HC(O)OH, and HC(O)OOH. J Phys Chem 107:1604–1617
32. Dixon DA, Feller D, Francisco JS (2003) Molecular structure, vibrational frequencies, and energetics of the HCO, HOCO and $HCO_2$ anions. J Phys Chem A 107:186–190
33. Paulson JF (1970) Some negative-ion reactions with $CO_2$. J Chem Phys 52:963–964
34. Cooper CD, Compton RN (1972) Metastable anions of $CO_2$. Chem Phys Lett 14:29–32
35. Cooper CD, Compton RN (1973) Electron attachment to cyclic anhydrides and related compounds. J Chem Phys 59:3550–3565
36. Compton RN, Reinhardt PW, Cooper CD (1975) Collisional ionization of Na, K, and Cs by $CO_2$, COS, and $CS_2$: molecular electron affinities. J Chem Phys 63:3821–3827
37. Boness MJW, Schulz GJ (1974) Vibrational excitation in $CO_2$ *via* the 3.8-eV resonance. Phys Rev A 9:1969–1979
38. Ovenall DW, Whiffen DH (1961) Electron spin resonance and structure of the $CO_2^-$ radical anion. Mol Phys 4:135–144
39. Chantry GW, Whiffen DH (1962) Electronic absorption spectra of $CO_2^-$ trapped in γ-irradiated crystalline sodium formate. Mol Phys 5:189–194
40. Hartman KO, Hisatsune IC (1966) Infrared spectrum of carbon dioxide anion radical. J Chem Phys 44:1913–1918
41. Hisatsune IC, Adl T, Beahm EC, Kempf RJ (1970) Matrix isolation and decay kinetics of carbon dioxide and carbonate anion free radicals. J Phys Chem 74:3225–3231
42. Callens F, Matthys P, Boesman E (1989) Paramagnetic resonance spectrum of $CO_2^-$ trapped in KCl. J Phys Chem Solids 50:377–381
43. Rudko VV, Vorona JP, Baran NP, Ishchenko SS, Zatovsky IV, Chumakova LS (2010) The mechanism of $CO_2^-$ radical formation in biological and synthetic apatites. Health Phys 98:322–326
44. Vestad TA, Gustafsson H, Lund A, Hole EO, Sagstuen E (2004) Radiation-induced radicals in lithium formate monohydrate ($LiHCO_2{\cdot}H_2O$). EPR and ENDOR studies of X-irradiated crystal and polycrystalline samples. Phys Chem Chem Phys 6:3017–3022
45. Symons MCR, West DX, Wilkinson JG (1976) Radiation damage in thallous formate and acetate: charge transfer from thallous ions. Int J Radiat Phys Chem 8:375–379
46. Jacox ME, Milligan DE (1974) Vibrational spectrum of $CO_2^-$ in an argon matrix. Chem Phys Lett 28:163–168
47. Kafafi ZH, Hauge RH, Billups WE, Margrave JL (1983) Carbon dioxide activation by lithium metal. 1. Infrared spectra of $Li^+CO_2^-$, $Li^+C_2O_4^-$ and $Li_2^{2+}CO_2^{2-}$ in inert gas matrices. J Am Chem Soc 105:3886–3893

48. Manceron L, Loutellier A, Perchard JP (1985) Reduction of carbon dioxide to oxalate by lithium atoms: a matrix isolation study of the intermediate steps. J Mol Struct 129:115–124
49. Kafafi ZH, Hauge RH, Billups WE, Margrave JL (1984) Carbon dioxide activation by alkali metals. 2. Infrared spectra of $M^+CO_2^-$ and $M_2^{2+}CO_2^{2-}$ in argon and nitrogen matrices. Inorg Chem 23:177–183
50. Bencivenni L, D'Alesssio L, Raimondo F, Pelino M (1986) Vibrational spectra and structure of $M(CO_2)$ and $M_2(CO_2)_2$ molecules. Inorg Chim Acta 121:161–166
51. Jordan KD (1984) Theoretical investigation of lithium and sodium complexes with $CO_2$. J Phys Chem 88:2459–2465
52. Borel JP, Faes F, Pittel A (1981) Electron paramagnetic resonance of Li-$CO_2$ complexes in a $CO_2$ matrix at 77 K. J Chem Phys 74:2120–2123
53. Jacox ME, Thompson WE (1989) The vibrational spectra of molecular ions in solid neon. I. $CO_2^+$ and $CO_2^-$. J Chem Phys 91:1410–1416
54. Cook RJ, Whiffen DH (1967) Endor measurements in X-irradiated sodium formate. J Phys Chem 71:93–97
55. Atkins PW, Keen N, Symons MCR (1962) Oxides and oxyions of the non-metals. Part II. $CO_2^-$ and $NO_2$. J Chem Soc: 2873–2880
56. Dalal NS, McDowell CA, Park JM (1975) EPR and ENDOR studies of $CO_2^-$ centers in x- and uv-irradiated single crystals of sodium formate. J Chem Phys 63:1856–1862
57. Bentley J, Carmichael I (1985) Electron spin properties of complexes formed by Li or Na with $CO_2$. J Phys Chem 89:4040–4042
58. Knight LB Jr, Hill D, Berry K, Babb R, Feller D (1996) Electron spin resonance rare gas matrix studies of $^{12}CO_2^-$, $^{13}CO_2^-$, and $C^{17}O_2^-$: comparison with *ab initio* calculations. J Chem Phys 105:5672–5686
59. Jacox ME, Thompson WE (1999) The vibrational spectra of $CO_2^+$, $(CO_2)_2^+$, $CO_2^-$ and $(CO_2)_2^-$ trapped in solid neon. J Chem Phys 110:4487–4496
60. Zhou M, Andrews L (1999) Infrared spectra of the $CO_2^-$ and $C_2O_4^-$ anions in solid argon. J Chem Phys 110:2414–2422
61. Freund HJ, Roberts MW (1996) Surface chemistry of carbon dioxide. Surf Sci Rep 25: 225–273
62. Inoue T, Fujishima A, Konishi S, Honda K (1979) Photoelectrocatalytic reduction of carbon dioxide in aqueous suspensions of semiconductor powders. Nature 277:637–638
63. Chiesa M, Giamello E (2007) Carbon dioxide activation by surface excess electrons: an EPR study of the $CO_2^-$ radical ion adsorbed on the surface of MgO. Chem Eur J 13:1261–1267
64. Farkas AP, Solymosi F (2009) Activation and reaction of $CO_2$ on a K-promoted Au(111) surface. J Phys Chem C 113:19930–19936
65. Thampi KR, Kiwi J, Gratzel M (1987) Methanation and photo-methanation of carbon dioxide at room temperature and atmospheric pressure. Nature 327:506–508
66. Ikeue K, Yamashita H, Anpo M, Takewaki T (2001) Photocatalytic reduction of $CO_2$ with $H_2O$ on Ti−β zeolite photocatalysts: effect of the hydrophobic and hydrophilic properties. J Phys Chem B 105:8350–8355
67. Hwang JS, Chang JS, Psrk SE, Ikeue K, Anpo M (2005) Photoreduction of carbon dioxide on surface functionalized nanoporous catalysts. Top Catal 35:311–319
68. Saladin F, Alxneit I (1997) Temperature dependence of the photochemical reduction of $CO_2$ in the presence of $H_2O$ at the solid/gas interface of $TiO_2$. J Chem Soc Faraday Trans 93: 4159–4163
69. He H, Zapol P, Curtiss LA (2010) A theoretical study of $CO_2$ anions on anatase (101) surface. J Phys Chem C 114:21474–21481
70. Preda G, Pacchioni G, Chiesa M, Giamello E (2008) Formation of $CO_2^-$ radical anion from $CO_2$ adsorption on an electron-rich MgO surface: a combined *ab initio* and pulse EPR study. J Phys Chem C 112:19568–19576
71. Wardman P (1989) Reduction potentials of one-electron couples involving free radicals in aqueous solutions. J Phys Chem Ref Data 18:1637–1756

72. Von Sonntag C (1987) The chemical basis of radiation biology. Taylor and Francis, London
73. Flyunt R, Schuchmann MN, von Sonntag C (2001) A common carbanion intermediate in the recombination and proton-catalysed disproportionation of the carboxyl radical anion $CO_2$, in aqueous solution. Chem Eur J 7:796–799
74. Herzberg G (1966) Molecular spectra and molecular structure.III. Electronic spectra and electronic structure of polyatomic molecules. Van Nostrand-Reinhold, New York
75. Johnson MA, Rostas J (1995) Vibronic structure of the $CO_2$ $^+$ ion: reinvestigation of the antisymmetric stretch vibration in the X, $\tilde{A}$, and B states. Mol Phys 85:839–868
76. Gauyacq D, Larcher C, Rostas J (1979) The emission spectrum of the $CO_2^+$ ion: rovibronic analysis of the $\tilde{A}^2\Pi_u$ - $X^2\Pi_g$ band system. Can J Phys 57:1634–1649
77. Gauyacq D, Horani M, Leach S, Rostas J (1975) The emission spectrum of the $CO_2^+$ ion: $B^2\Sigma_u^+ - X^2\Pi_g$ band system. Can J Phys 53:2040–2059
78. Cossart-Magos C, Jungen M, Launay F (1987) High resolution absorption spectrum of $CO_2$ between 10 and 14 eV. Assignment of nf Rydberg series leading to a new value of the first ionization potential. Mol Phys 61:1077–1117
79. Horsley JA, Fink WH (1969) Study of the electronic structure of the ions $CO_2^+$ and $N_2O^+$ by the LCAO-MO-SCF method. J Phys B At Mol Phys 2(12):1261–1270
80. Carsky P, Kuhn J, Zahradnik R (1975) Semiempirical all-valence-electron MO calculations on the electronic spectra of linear radicals with degenerate ground states. J Mol Spectrosc 55: 120–130
81. Grimm FA, Larsson M (1984) A theoretical investigation on the low lying electronic states of $CO_2^+$ in both linear and bent configurations. Phys Scr 29:337–343
82. Chambaud G, Gabriel W, Rosmus P, Rostas J (1992) Ro-vibronic states in the electronic ground state of $CO_2^+$ ($X^2\Pi_g$). J Phys Chem 96:3285–3293
83. Gellene GI (1998) $CO_2^+$: a difficult molecule for electron correlation. Chem Phys Lett 287: 315–319
84. Siegmann B, Werner U, Lutz HO, Mann R (2002) Complete coulomb fragmentation of $CO_2$ in collisions with 5.9 MeV $u^{-1}$ $Xe^{18+}$ and $Xe^{43+}$. J Phys B At Mol Opt Phys 35:3755–3766
85. Aresta M, Nobile CF, Albano VG, Forni E, Manassero M (1975) New nickel-carbon dioxide complex: synthesis, properties, and crystallographic characterization of (carbon dioxide)bis (tricyclohexylphosphine)nickel. J Chem Soc Chem Commun 15:636–637
86. Kégl T, Ponec R, Kollar L (2011) Theoretical insights into the nature of nickel–carbon dioxide interactions in $Ni(PH_3)_2(\eta^2\text{-}CO_2)$. J Phys Chem C 115:12463–12473
87. Contreras L, Paneque M, Sellin M, Carmona E, Perez PJ, Gutierrez-Puebla E, Monge A, Ruiz C (2005) Novel carbon dioxide and carbonyl carbonate complexes of molybdenum. The X-ray structures of *trans*-$[Mo(CO_2)_2\{HN(CH_2CH_2PMe_2)_2\}(PMe_3)]$ and $[Mo_3(\mu_2\text{-}CO_3)(\mu_2\text{-}O)_2(O)_2(CO)_2(H_2O)(PMe_3)_6]\cdot H_2O$. New J Chem 29:109–115
88. Bristow GS, Hitchcock PB, Lappert DM (1981) A novel carbon dioxide complex: synthesis and crystal structure of $[Nb(\eta\text{-}C_5H_4Me)_2(CH_2SiMe_3)(\eta^2\text{-}CO_2)]$. J Chem Soc Chem Commun 21:1145–1146
89. Gibson DH (1996) The organometallic chemistry of carbon dioxide. Chem Rev 96: 2063–2095
90. Yin X, Moss JR (1999) Recent developments in the activation of carbon dioxide by metal complexes. Coord Chem Rev 181:27–59
91. Gibson DH (1999) Carbon dioxide coordination chemistry: metal complexes and surface-bound species. What relationships? Coord Chem Rev 185–186:335–355
92. Gambarotta S, Arena F, Floriani C, Zanazzi PF (1982) Carbon dioxide fixation: bifunctional complexes containing acidic and basic sites working as reversible carriers. J Am Chem Soc 104:5082–5092
93. Fujita E, Creutz C, Sutin N, Brunschwig BS (1993) Carbon dioxide activation by cobalt macrocycles: evidence of hydrogen bonding between bound $CO_2$ and the macrocycle in solution. Inorg Chem 32:2657–2662

94. Beley M, Collin JP, Ruppert R, Sauvage JP (1986) Electrocatalytic reduction of carbon dioxide by nickel cyclam$^{2+}$ in water: study of the factors affecting the efficiency and the selectivity of the process. J Am Chem Soc 108:7461–7467
95. Collin JP, Sauvage JP (1986) Electrochemical reduction of carbon dioxide mediated by molecular catalysts. Coord Chem Rev 1993:245–268
96. Stephan DW, Erker G (2010) Frustrated Lewis pairs. Angew Chem Int Ed 49:46–76
97. Appelt C, Westenberg H, Bertini F, Ehlers AW, Slootweg JC, Lammertsma K, Uhl W (2011) Geminal phosphorous/aluminum-based frustrated Lewis pairs: C-H versus C≡C activation and $CO_2$ fixation. Angew Chem Int Ed 50:3925–3928
98. Zevaco T, Dinjus E (2010) Main group element- and transition metal-promoted carboxylations of organic substrates (alkanes, alkenes, alkynes, aromatics, and others). In: Aresta M (ed) Carbon dioxide as chemical feedstock. Wiley, Weinheim
99. Haruki E (1982) Organic synthesis with carbon dioxide. In: Inoue S, Yamazaki N (eds) Organic and bioorganic chemistry of carbon dioxide. Halsted, New York
100. Takay I, Yamamoto A (1982) Organometallic reactions of carbon dioxide. In: Inoue S, Yamazaki N (eds) Organic and bioorganic chemistry of carbon dioxide. Halsted, New York
101. Bertini I, Luchinat C (1994) The reaction pathway of zinc enzymes and related biological catalysts. In: Bertini I, Gray HB, Lippard SJ, Valentine JS (eds) Bioinorganic chemistry. University Science, Mill Valley
102. Calabrese JC, Herskovitz T, Kinney JB (1983) Carbon dioxide coordination chemistry. 5. Preparation and structure of Rh($\eta^1$-$CO_2$)(Cl)(diars)$_2$. J Am Chem Soc 1983:5914–5915
103. Harlow RL, Kinney JB, Herskovitz T (1980) Carbon dioxide co-ordination chemistry: preparation and *X*-ray crystal structure of the methoxycarbonyl complex [IrCl($CO_2$Me)-($Me_2PCH_2CH_2PMe_2$)$_2$]$FSO_3$ from a $CO_2$ adduct. J Chem Soc Chem Commun 17:813–814
104. Aresta M, Nobile CF (1977) Carbon dioxide-transition metal complexes.III. Rh(I)-$CO_2$ complexes. Inorg Chim Acta 24:L49–L50
105. Tanaka K, Ooyama D (2002) Multi-electron reduction of $CO_2$ via Ru-$CO_2$, -C(O)OH, -CO, -CHO, and -$CH_2OH$ species. Coord Chem Rev 226:211–218
106. Castro-Rodriguez I, Nakai H, Zakharov LN, Rheingold AL, Meyer K (2004) A linear, O-coordinated $\eta^1$-$CO_2$ bound to uranium. Science 305:1757–1759
107. Lam OP, Anthon C, Meyer K (2009) Influence of steric pressure on the activation of carbon dioxide and related small molecules by uranium coordination complexes. Dalton Trans 44:9677–9691
108. Lee CH, Laitar DS, Mueller P, Sadighi JP (2007) Generation of a doubly bridging $CO_2$ ligand and deoxygenation of $CO_2$ by an (NHC)Ni(0) complex. J Am Chem Soc 129:13802–13803
109. Hou XJ, He P, Li H, Wang X (2013) Understanding the adsorption mechanism of $C_2H_2$, $CO_2$, and $CH_4$ in metal-organic frameworks with coordinatively unsaturated metal sites. J Phys Chem C 117:2824–2834
110. Dietzel PDC, Johnsen RE, Fjellväg H, Bordiga S, Groppo E, Chavan S, Blom R (2008) Adsorption properties and structure of $CO_2$ adsorbed on open coordination sites of metal–organic framework $Ni_2$(dhtp) from gas adsorption, IR spectroscopy and X-ray diffraction. J Chem Soc Chem Commun 41:5125–5127
111. Chang CC, Liao MC, Chang TH, Peng SM, Lee GH (2005) Aluminum-magnesium complexes with linear bridging carbon dioxide. Angew Chem Int Ed 44:7418–7420
112. Green S, Schor H, Siegbahn P, Thaddeus P (1976) Theoretical investigation of protonated carbon dioxide. Chem Phys 17:479–485
113. Seeger U, Seeger R, Pople JA, Schleyer Pvon R (1978) Isomeric structures of protonated carbon dioxide. Chem Phys Lett 55:399–403
114. Scarlett M, Taylor PR (1986) Protonation of $CO_2$, COS, $CS_2$. Proton affinities and the structure of protonated species. Chem Phys 101:17–26
115. Hartz N, Rasul G, Olah GA (1993) Role of oxonium, sulfonium, and carboxonium dications in superacid-catalyzed reactions. J Am Chem Soc 115:1277–1285

116. Gronert S, Keeffe JR (2007) The protonation of allene and some heteroallenes, a computational study. J Org Chem 72:6343–6352
117. Traeger JC, Kompe BM (1991) Determination of the proton affinity of carbon dioxide by photoionization mass spectrometry. J Mass Spectrom Org Mass Spectrom 26:209–214
118. Bohme DK, Mackay GI, Schiff HI (1980) Determination of proton affinities from the kinetics of proton transfer reactions. The proton affinities of $O_2$, $H_2$, Kr, O, $N_2$, Xe, $CO_2$, $CH_4$, $N_2O$, and CO. J Chem Phys 73:4976–4986
119. Lias SG, Liebman JF, Levin RD (1984) Evaluated gas phase basicities and proton affinities of molecules. J Phys Chem Ref Data 13:695–808
120. Hunter EP, Lias SG (1998) Evaluated gas phase basicities and proton affinities of molecules: an update. J Phys Chem Ref Data 27:413–656
121. Hayhurst AN, Taylor SG (2001) The proton affinities of CO and $CO_2$ and the first hydration energy of gaseous $H_3O^+$ from mass spectrometric investigations of ions in rich flames of $C_2H_2$. Phys Chem Chem Phys 3:4359–4370
122. Taddeus P, Guélin M, Linke RA (1981) Three new "nonterrestrial molecules". Astrophys J 246:L41–L45
123. Burt JA, Dunn JL, Mc Ewan MJ, Sutton MM, Roche AE, Schiff HI (1970) Some ion-molecule reactions of $H_3^+$ and the proton affinity of $H_2$. J Chem Phys 52:6062–6075
124. Adams NG, Smith D, Tichy M, Javahery J, Twiddy ND, Ferguson EE (1989) An absolute proton affinity scale in the 130–140 kcal $mol^{-1}$ range. J Chem Phys 91:4037–4042
125. Bogey M, Demuynek C, Destombes JL, Krupnov A (1988) Molecular structure of $HOCO^+$. J Mol Struct 190:465–474
126. Hammami K, Jaidane N, Lakhdar ZB, Spielfeldel A, Feautrier N (2004) New *ab initio* potential energy surface for the ($HOCO^+$-He) van der Waals complex. J Chem Phys 121: 1325–1330
127. Sodupe M, Branchadell V, Rosi M, Bauschlicher CW (1997) Theoretical study of $M^+$-$CO_2$ and $OM^+CO$ systems for first transition row metal atoms. J Phys Chem 101:7854–7859
128. Walker NR, Walters RS, Duncan MA (2004) Infrared photodissociation spectroscopy of $V^+(CO_2)_n$ and $V^+(CO_2)_nAr$ complexes. J Chem Phys 120:10037–10045
129. Gregoire G, Duncan MA (2002) Infrared spectroscopy to probe structure and growth dynamics in $Fe^+$-$(CO_2)$n clusters. J Chem Phys 117:2120–2130
130. Griffin JB, Armentrout PB (1997) Guided ion beam studies of the reactions of $Fe_n^+$ (n = 1–18) with $CO_2$: iron cluster oxide bond energies. J Chem Phys 107:5345–5355
131. Tjelta BL, Walter D, Armentrout PB (2001) Determination of weak $Fe^+$–L bond energies (L=Ar, Kr, Xe, $N_2$, and $CO_2$) by ligand exchange reactions and collision-induced dissociation. Int J Mass Spectrom 204:7–21
132. Walker NR, Walters RS, Grieves GA, Duncan MA (2004) Growth dynamics and intracluster reactions in $Ni^+(CO_2)_n$ complexes via infrared spectroscopy. J Chem Phys 121:10498–10507
133. Herman J, Foutch JD, Davico GE (2007) Gas-phase reactivity of selected transition metal cations with CO and $CO_2$ and the formation of metal dications using a sputter ion source. J Phys Chem A 111:2461–2468
134. Koyanagi GK, Bohme DK (2006) Gas-phase reactions of carbon dioxide with atomic transition-metal and main-group cations: room-temperature kinetics and periodicities in reactivity. J Phys Chem A 110:1232–1241
135. Albano P, Aresta M, Manassero M (1980) Interaction of carbon dioxide with coordinatively unsaturated rhodium(I) complexes with the ligand 1,2 bis(diphenylphosphino)ethane. Inorg Chem 19(4):1069–1072
136. Rodgers MT, Walker B, Armentrout PB (1999) Reactions of $Cu^+$ (1 S and 3 D) with $O_2$, CO, $CO_2$, $N_2$, NO, $N_2O$, and $NO_2$ studied by guided ion beam mass spectrometry. Int J Mass Spectrom 182(183):99–120
137. Zang XG, Armentrout PB (2003) Activation of $O_2$, CO, and $CO_2$ by $Pt^+$: the thermochemistry of $PtO^+$. J Phys Chem A 107:8904–8914

138. Clemmer DE, Weber ME, Armentrout PB (1992) Reactions of aluminum (1+)(1S) with nitrogen dioxide, nitrous oxide, and carbon dioxide: thermochemistry of aluminum monoxide and aluminum monoxide (1+). J Phys Chem 96:10888–10893
139. Armentrout PB, Beauchamp JL (1980) Reactions of $U^+$ and $UO^+$ with $O_2$, CO, $CO_2$, COS, $CS_2$ and $D_2O$. Chem Phys 50:27–36
140. Hwang DY, Mebel AM (2000) Theoretical study on reforming of $CO_2$ catalyzed with Be. Chem Phys Lett 325:639–644
141. Solov'ev VN, Polikarpov EV, Nemukhin AV, Sergeev GB (1999) Matrix isolation and ab initio study of the reactions of magnesium atoms and clusters with $CO_2$, $C_2H_4$, and $CO_2/C_2H_4$ mixtures: formation of cyclic complexes. J Phys Chem A 103:6721–6725
142. Hwang DY, Mebel AM (2000) Theoretical study on the reaction mechanism of $CO_2$ with Mg. J Phys Chem A 104:7646–7650
143. Polikarpov EV, Granovsky AA, Nemukhin AV (2001) On the potential-energy surface of the $Mg + CO_2$ ($C_{2v}$) system. Mendeleev Commun 11:150–151
144. Hwang DY, Mebel AM (2000) Reaction mechanism of $CO_2$ with Ca atom: a theoretical study. Chem Phys Lett 331:526–532
145. Burkholder TR, Andrews L, Bartlett RJ (1993) Reaction of boron atoms with carbon dioxide: matrix and ab initio calculated infrared spectra of OBCO. J Phys Chem 97:3500–3503
146. Chin CH, Mebel AM, Hwang DY (2003) Theoretical study of the reaction mechanism of boron atom with carbon dioxide. Chem Phys Lett 375:670–675
147. Lequere AM, Xu C, Manceron L (1991) Vibrational spectra, structures, and normal-coordinate analysis of aluminum-carbon dioxide complexes isolated in solid argon. J Phys Chem 95:3031–3037
148. Aresta M, Quaranta E (1997) Carbon dioxide: a substitute for phosgene. ChemTech 27:32–40
149. Ballivet-Tkatchenko D, Dibenedetto A (2010) Synthesis of linear and cyclic carbonates. In: Aresta M (ed) Carbon dioxide as chemical feedstock. Wiley, Weinheim
150. Quaranta E, Aresta M (2010) The chemistry of N-$CO_2$ bonds: synthesis of carbamic acids and their derivatives, isocyanates, and ureas. In: Aresta M (ed) Carbon dioxide as chemical feedstock. Wiley, Weinheim
151. Ohnishi YY, Nakao Y, Sato H, Sakaki S (2006) Ruthenium(II)-catalyzed hydrogenation of carbon dioxide to formic acid. Theoretical study of significant acceleration by water molecule. Organometallics 25:3352–3363
152. Konno H, Kobayashi A, Sakamoto K, Fagalde F, Katz N, Saitoh H, Ishitani O (2000) Synthesis and properties of $[Ru(tpy)(4,4'\text{-}X_2bpy)H]^+$(tpy = 2,2′:6′,2″-terpyridine, bpy = 2,2-′-bipyridine, X=H and MeO), and their reactions with $CO_2$. Inorg Chim Acta 299:155–163
153. Sakaki S (1990) Transition-metal complexes of nitrogen, carbon dioxide, and similar small molecules. *Ab-initio* MO studies of their stereochemistry and coordinate bonding nature. In: Stereochemistry of organometallic and inorganic compounds. Stereochemical Control, Bonding Steric Rearrangements, vol 4. Elservier Amsterdam, pp 95–177
154. Santoro M (2010) Non-molecular carbon dioxide at high pressure. In: Boldyreva E, Dera P (eds) High-pressure crystallography: from fundamental phenomena to technological applications. Springer, Dordrecht
155. Schettino V, Bini R, Ceppatelli M, Ciabini L, Citroni M (2005) Chemical reactions at very high pressure. Adv Chem Phys 11:105–242
156. Iota V, Yoo CS, Cynn H (1999) Quartzlike carbon dioxide: an optically nonlinear extended solid at high pressures and temperatures. Science 283:1510–1513
157. Yoo CS, Cynn H, Gygi F, Galli G, Iota V, Nicol M, Carlson S, Häusermann D, Mailhiot C (1999) Crystal structure of carbon dioxide at high pressure: "superhard" polymeric carbon dioxide. Phys Rev Lett 83:5527–5530
158. Santoro M, Gorelli FA, Bini R, Ruocco G, Scandolo S, Crichton WA (2006) Amorphous silica-like carbon dioxide. Nature 441:857–860

159. Yota V, Yoo CS, Klepeis JH, Jenei Z, Evans W, Cynn H (2007) Six-fold coordinated carbon dioxide VI. Nat Mater 6:34–38
160. Datchi F, Giordano VM, Munsch P, Saitta AM (2009) Structure of carbon dioxide phase IV: breakdown of the intermediate bonding state scenario. Phys Rev Lett 103:185701
161. Shimanouchi T (1972) Tables of molecular vibrational frequencies, consolidated volume I. NSRDS-NBS (US) 39:1–164
162. van Broekhuizen FA, Groot IMN, Fraser HJ, van Dishoeck EF, Schlemmer S (2006) Infrared spectroscopy of solid CO-$CO_2$ mixtures and layers. Astron Astrophys 451:723–731
163. Falk M, Miller AG (1992) Infrared spectrum of carbon dioxide in aqueous solution. Vib Spectrosc 4:105–108
164. Jacox ME (1990) Vibrational and electronic energy levels of polyatomic transient molecules. Supplement 1. J Phys Chem Ref Data 19:1388–1546
165. Kawaguchi K, Yamada C, Hirota E (1985) Diode laser spectroscopy of the $CO_2^+$ $\nu_3$ band using magnetic field modulation of the discharge plasma. J Chem Phys 82:1174–1177
166. Carter S, Handy NC, Rosmus P, Chambaud G (1990) A variational method for the calculation of spin-rovibronic levels of Renner-Teller triatomic molecules. Mol Phys 71:605–622
167. Jegat C, Fouassier M, Mascetti J (1991) Carbon dioxide coordination chemistry. 1. Vibrational study of *trans*-$Mo(CO_2)_2(PMe_3)_4$ and $Fe(CO_2)(PMe_3)_4$. Inorg Chem 30:1521–1529
168. Jegat C, Fouassier M, Tranquille M, Mascetti J (1991) Carbon dioxide coordination chemistry. 2. Synthesis and FTIR study of $Cp_2Ti(CO_2)(PMe_3)$. Inorg Chem 30:1529–1536
169. Jegat C, Fouassier M, Tranquille M, Mascetti J, Tommasi I, Aresta M, Ingold F, Dedieu A (1993) Carbon dioxide coordination chemistry. 3. Vibrational, NMR, and theoretical studies of $Ni(CO_2)(PCy_3)_2$. Inorg Chem 32:1279–1289
170. Rabalais JW, McDonald JM, Scherr V, McGlynn SP (1971) Electron spectroscopy of isoelectronic molecules. II. Linear triatomic groupings containing sixteen valence electrons. Chem Rev 71:73–108
171. Ogawa M (1971) Absorption cross sections of $O_2$ and $CO_2$ continua in the Schumann and Far-UV region. J Chem Phys 54:2550–2556
172. England WB, Ermler WC (1979) Theoretical studies of atmospheric triatomic molecules. New *ab initio* results for the $^1\Pi_g$-$^1\Delta_u$ vertical state ordering in $CO_2$. J Chem Phys 70: 1711–1719
173. Spielfeldel A, Feautrier N, Chambaud G, Rosmus P, Werner H-J (1993) The first dipole-allowed electronic transition of $1^1\Sigma_u^+ - X^1\Sigma_g^+$ of $CO_2$. Chem Phys Lett 216:162–166
174. Buenker RJ, Honigmann M, Liebermann H-P, Kimura M (2000) Theoretical study of the electronic structure of carbon dioxide: bending potential curves and generalized oscillator strengths. J Chem Phys 113:1046–1054
175. Wiberg KB, Wang Y-G, de Oliveira AE, Perera SA, Vaccaro PH (2005) Comparison of CIS and EOM-CCSD-calculated adiabatic excited states structures. Change in charge density on going to adiabatic excited states. J Phys Chem 109:466–477
176. Eiseman BJ Jr, Harris L (1932) The transmission of liquid carbon dioxide. J Am Chem Soc 54:1782–1784
177. Mascetti J, Tranquille M (1988) Ab initio investigation of several low-lying states of all-trans octatetraene. J Phys Chem 92:2177–2184
178. Okabe H (1978) Photochemistry of small molecules. Wiley, New York
179. Slanger TG, Black G (1978) $CO_2$ photolysis revised. J Chem Phys 68:1844–1849
180. Zhu Y-F, Gordon RJ (1990) The production of $O(^3P)$ in the 157 nm photodissociation of $CO_2$. J Chem Phys 92:2897–2901
181. Matsumi Y, Shafer N, Tonukura K, Kawasaki M, Huang Y-L, Gordon RJ (1991) Doppler profiles and fine structure branching ratios of $O(^3P_J)$ from photodissociation of carbon dioxide at 157 nm. J Chem Phys 95:7311–7316
182. Miller RL, Kable SH, Houston PL, Burak I (1992) Product distributions in the 157 nm photodissociation of $CO_2$. J Chem Phys 96:332–338

183. Mahata S, Bhattacharya SK (2009) Anomalous enrichment of $^{17}O$ and $^{13}C$ in photodissociation products of $CO_2$: possible role of nuclear spin. J Chem Phys 130:234312 (1–17)
184. Liger-Belair G, Prost R, Parmentier M, Jeandet P, Nuzillard J-M (2003) Diffusion coefficient of $CO_2$ molecules as determined by $^{13}C$ NMR in various carbonated beverages. J Agric Food Chem 51:7560–7563
185. Gao G, Li F, Xu L, Liu X, Yang Y (2008) $CO_2$ coordination by inorganic polyoxoanion in water. J Am Chem Soc 130:10838–10839
186. Leitner W (1996) The coordination chemistry of carbon dioxide and its relevance for catalysis: a critical survey. Coord Chem Rev 153:257–284
187. Mastrorilli P, Moro G, Nobile CF, Latronico M (1992) Carbon dioxide-transition metal complexes. IV. New Ni(0)-$CO_2$ complexes with chelating diphosphines: influence of P-Ni-P angle on complex stabilities. Inorg Chem Acta 192:189–193
188. Aresta M, Gobetto R, Quaranta E, Tommasi I (1992) A bonding-reactivity relationship for Ni$(PCy_3)_2(CO_2)$: a comparative solid-state-solution nuclear magnetic resonance study ($^{31}P$, $^{13}C$ as a diagnostic tool to determine the mode of bonding of $CO_2$ to a metal center). Inorg Chem 21:4286–4290
189. Carmona E, Hughes AK, Munoz MZ, O'Hare DM, Perez PJ, Poveda ML (1991) Rotational isomerism and fluxional behavior of bis(carbon dioxide) adducts of molybdenum. J Am Chem Soc 113:9210–9218

Top Organomet Chem (2016) 53: 39–72
DOI: 10.1007/3418_2015_94

Published online: 7 April 2015

# Metal Complexes Catalyzed Cyclization with $CO_2$

**Jeroen Rintjema, Leticia Peña Carrodeguas, Victor Laserna, Sergio Sopeña, and Arjan W. Kleij**

**Abstract** This chapter describes in general terms the catalytic methodology that has been made available for the use of carbon dioxide ($CO_2$) in cyclization reactions that incorporate an intact $CO_2$ fragment without changing the formal oxidation state of the carbon center. The major focus of this chapter will be on the most successful organometallic/inorganic complexes that have been used as catalyst systems throughout the last decade and the preferred ligand frameworks leading to elevated reactivity and/or selectivity behavior in $CO_2$ coupling reactions. Attention will be especially given to homogeneous catalyst systems as they have proven to be more versatile in $CO_2$ conversion catalysis and often have modular characteristics that allow for optimization of structure–activity relationships. The most important reactions that have been studied in the current context are designated $CO_2$ "addition" reactions to small molecule heterocycles such as epoxides and aziridines, though more recently other coupling partners such as diamines, dialcohols, and amino nitriles have further advanced the use of $CO_2$ in organic synthesis providing access to a wider range of structures. This chapter will serve to demonstrate the utility of $CO_2$ as a carbon reagent in the catalytic formation of the most prominent organic structures using cyclization strategies specifically.

**Keywords** Addition reactions · Carbon dioxide · Coupling reactions · Homogeneous catalysis · Organic synthesis

## Contents



J. Rintjema, L. Peña Carrodeguas, V. Laserna, S. Sopeña, and A.W. Kleij (✉)
Institute of Chemical Research of Catalonia (ICIQ), Av. Països Catalans 16, 43007 Tarragona, Spain
e-mail: akleij@iciq.es

## 1 Introduction

Carbon dioxide ($CO_2$) has recently emerged as an attractive carbon reagent that may partially substitute fossil fuels in synthetic strategies toward a wide range of organic structures [1–3]. It represents a cheap and abundant carbon building block, but its kinetic stability is a challenge that can only be addressed by devising efficient catalytic processes and ditto catalyst systems [4, 5]. Therefore, a lot of focus in the scientific communities has been on the design of suitable catalyst systems than can potentially combine modular features, high reactivity and selectivity, and amplified substrate scope that would serve to increase the synthetic application of $CO_2$ as a building block [6, 7]. The most widely studied reactions include the formation of polycarbonate polymers [8], the formation of carboxylated scaffolds [9], and the coupling between epoxides/oxetanes/aziridines [10–12] leading to various heterocyclic structures with synthetic, pharmaceutical, or solvent-derived application potential.

The latter category of organic molecules is particularly interesting for a number of reasons. Cyclic carbonates, derived from epoxide/$CO_2$ couplings, are organic compounds that possess very interesting properties such as low evaporation rates, low toxicity, and biodegradability [13]. These properties make them useful for industrial or scientific applications such as aprotic high-boiling polar solvents, electrolytes for lithium-ion batteries, precursors for polymeric materials, fine chemical intermediates, fuel additives, plastic materials, and agricultural chemicals [14, 15]. One of the most important examples in this respect is propylene carbonate which is produced at an industrial level. Apart from their industrial applications, cyclic carbonate structures also appear in various natural compounds present in fungi, bacteria, and/or plants. Some examples of such cyclic carbonate-containing natural products include Hololeucin and Cytosporin E [16] which are shown in Fig. 1.

In industry, cyclic carbonates are mostly obtained by environmentally hazardous methodologies which involve the use of phosgene. Although phosgene is a versatile reagent widely used in the production of plastics and pesticides, it is also a toxic, corrosive, and difficult to handle gas. Exposure to phosgene may have adverse consequences to health, and therefore its use is not desirable. For these reasons, its application in industrial large-scale synthesis should be avoided, and a lot of effort has been put into finding suitable alternatives. In the last decades, greener routes for the synthesis of cyclic carbonates such as those based on the use of carbon dioxide have generated great interest. This chemistry has also been amplified to similar

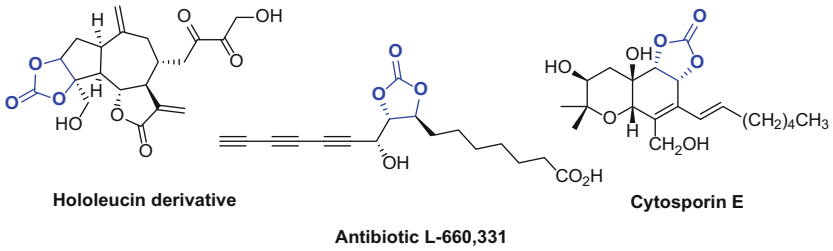


**Fig. 1** Some examples of cyclic carbonate-containing natural compounds found in plants, fungi, and bacteria. Note that the carbonate unit is highlighted in *blue*

types of coupling reactions that involve aziridines and oxetanes. In general, the development of low-toxic, cost-effective, and highly active catalytic systems has been a major milestone providing attractive solutions for the chemical fixation of $CO_2$ producing organic matter with an increased value.

With the rise of green chemistry, the number of environmentally more friendly processes toward $CO_2$-based heterocyclic structures and alike has been increasing at a rapid pace. Some of these new greener processes involve the use of ionic liquids [17], organocatalysts [18–23], supercritical $CO_2$ [24, 25], or metal-based photocatalysts [26, 27] although the most commonly used catalysis methodology for the synthesis of these compounds is the metal-catalyzed "cycloaddition" of carbon dioxide to small heterocyclic substrates better referred to as $CO_2$/substrate couplings. The use of ring-strained substrates thermodynamically favors the formation of the heterocyclic compounds. When using oxiranes (epoxides) as substrates, five-membered cyclic carbonates are obtained, and in a similar way six-membered cyclic carbonates are derived from oxetanes (Scheme 1). The conversion of oxetanes into six-membered carbonates has been much less studied probably due to their lower intrinsic reactivity and more limited accessibility compared to oxiranes. In the conversion of epoxides, the cyclic carbonates are the thermodynamic products with possible competitive formation of polycarbonates, which are the kinetic products. The selectivity toward polycarbonates or cyclic carbonates generally depends on the catalyst, additives, temperature, pressure, and epoxide concentration [28].

During the last 30 years, the homogeneously catalyzed formation of cyclic carbonates through $CO_2$ addition chemistry has been a thoroughly investigated topic, and many catalytic systems have appeared that address different process features such as chemo-selectivity, enantioselectivity, sustainability, reactivity, and substrate scope. In the next sections, a detailed description of these classes of catalyst systems will be given together with their specifics. As such, a comprehensive overview of the literature is avoided, as the intention is to showcase the most important developments in this area of $CO_2$ catalysis.

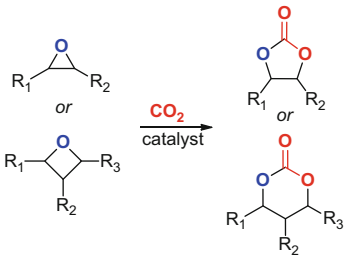


**Scheme 1** Cyclic carbonate synthesis from oxiranes and oxetanes

## 2 Binary Type Catalysts

Undoubtedly, the most popular catalyst type in the context of $CO_2$ addition catalysis is the binary catalyst system. These systems usually consist of a metal complex acting as an (Lewis acid) activator in the presence of amines or ammonium/phosphonium halides as nucleophilic cocatalysts. It is known that metal complex catalysts combining both a Lewis acidic and basic function effectively couple carbon dioxide and epoxides to afford cyclic carbonates [29]. In 2002, Caló and coworkers [30] reported on the cyclic carbonate synthesis from carbon dioxide and oxiranes using tetrabutylammonium halides as solvents and/or catalysts under atmospheric pressure of $CO_2$. Alternatively, Lau and coworkers [23] reported on the coupling of carbon dioxide and oxiranes catalyzed by bis(triphenylphosphine) iminium (PPN) salts to yield cyclic carbonates. These two contributions can be considered as milestones in the field, as these PPN and tetrabutylammonium salts are the most employed salts as cocatalysts. However, the use of metal complexes as substrate activators has resulted in far better catalyst systems enabling significantly higher reactivities and selectivities.

Important advances in this area have been obtained by using complexes based on transition/main group metals such as aluminum, cobalt, or iron with ligand frameworks such as porphyrins [26], phthalocyanines [31–33], triphenolates [34], and salens (Fig. 2) [35–40]. Metalloporphyrinates and metallophthalocyanines are compounds that have been typically used as dyes, functional materials, and oxidation catalysts. These metal complexes possess high activity towards the coupling reaction between carbon dioxide and oxiranes allowing the formation of linear or cyclic carbonates and polycarbonates in high yields. However, typically high reaction temperatures are required for efficient catalytic turnover making the systems of lesser value from a sustainability point of view (Scheme 2).

Metal–salen complexes are the most versatile and popular catalysts applied in the reactions between carbon dioxide and oxiranes [6]. One of the reasons for their popularity is the ease of synthesis in comparison with porphyrins and the fact that the condensation of the diamine and the aldehyde precursors allows for a straightforward modulation of the steric and electronic properties of the metal catalyst [41]. The large number of possible structural combinations has enabled the development of a extensive number of catalysts based on salphens, binaphthyl-derived salens, and bimetallic salen complexes (Fig. 3), among others. These metal complexes require,

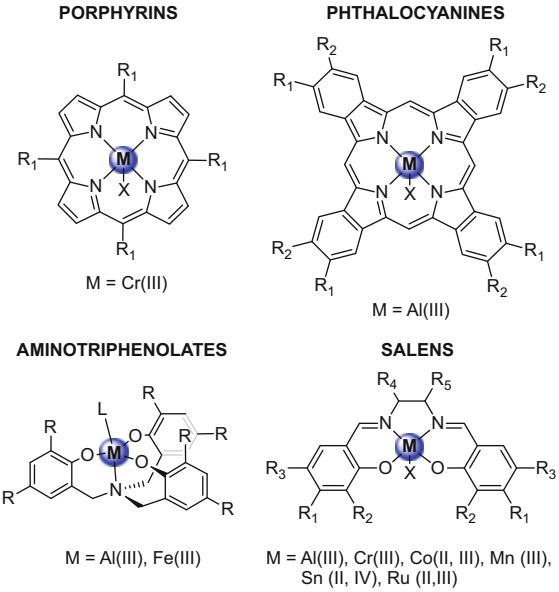


**Fig. 2** Typically used metal complexes derived from porphyrins, phthalocyanines, aminotriphenolates, and salens used as catalysts for the synthesis of cyclic carbonates from oxiranes and oxetanes. The X usually refers to a halide

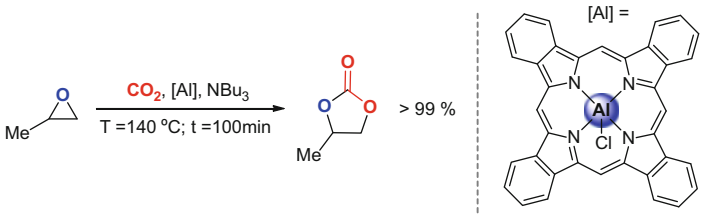


**Scheme 2** Example of a binary catalyst system formed by an Al(phthalocyanine) complex and tributylamine as nucleophilic cocatalyst in the coupling reaction between propylene oxide and carbon dioxide

as is the case for porphyrin and phthalocyanine metal-based catalysts, an additional nucleophilic cocatalyst to attain high activity (i.e., binary-type catalyst).

Jacobsen and coworkers discovered that Co(III)salens are highly efficient catalysts for the hydrolytic kinetic resolution of (*rac*)-epoxides using water as the nucleophile [42]. The formation of cyclic carbonates shows large resemblance with this seminal work of Jacobsen as the ring opening of an oxirane by a nucleophile/Lewis base is requisite to react it with $CO_2$. In the absence of any cocatalytic nucleophile, high activity cannot be obtained, and only trace amounts of the cyclic carbonate are formed. Generally, the activity of a binary catalytic system can be increased with increasing basicity of the Lewis base. In the case of halide

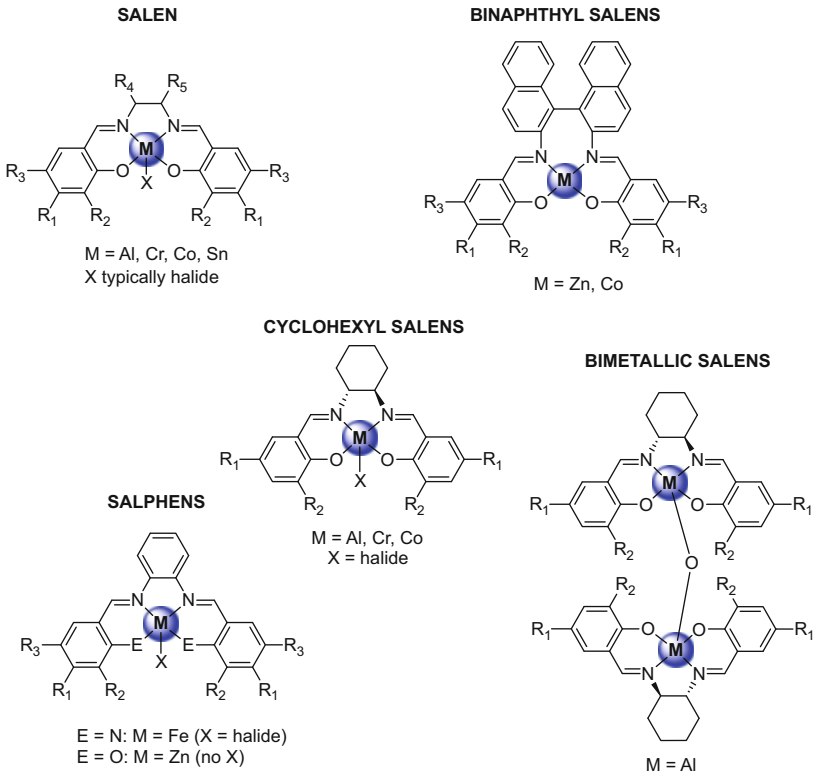


**Fig. 3** Most commonly used metal–salen structures derived from salen, salphen, and binaphthyl-based ligand scaffolds

nucleophiles, also the leaving group ability and size features are important parameters controlling the reactivity.

A clear example that illustrates the easy fine-tuning of salen complexes with respect to chemo-selectivity was provided by the work from Darensbourg and coworkers [8]. The presence of electron-donating or electron-withdrawing groups on the backbone of the metal–salen complex can be used to favor the preferred formation of the cyclic or polycarbonate product [43–46].

Although there are various contributions that focus on the conversion of terminal epoxides into their respective carbonates in high yields and under relatively mild reaction conditions [47–49], further improvement of the substrate scope is still warranted. Both chemo-selectivity and higher reactivity are required to achieve high catalytic efficiency with less reactive substrates such as internal epoxides and oxetanes. As a potential solution for these challenges, other types of catalysts have to be considered. Kleij et al. [34] developed a binary catalytic system (Scheme 3) that consists of a triphenolate complex acting as Lewis acid and tetrabutylammonium bromide (TBAB) as cocatalyst. In this case, the choice of cocatalyst and also the ratio between the iron catalyst and the nucleophilic cocatalyst are of high importance as this controls the activity and selectivity [50] of the reaction,

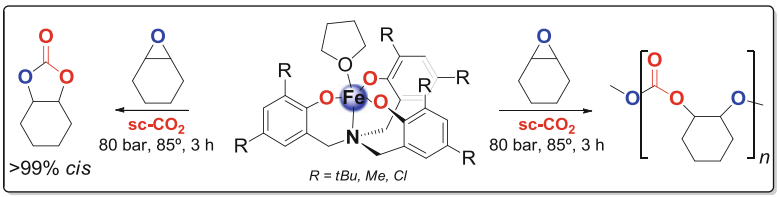


**Scheme 3** Reaction of cyclohexene oxide with carbon dioxide under supercritical conditions in the presence of a binary catalyst system comprising of a Fe(III) aminotriphenolate complex

allowing, for instance, the selective conversion of cyclohexene oxide into either the cyclic carbonate or the polycarbonate depending on the catalyst/nucleophile ratio.

The stereo-controlled preparation of value-added commodities from $CO_2$ has recently emerged as one of the future challenges [51]. Optically active substances, in particular the ones which contribute to biological activity, are key substances in different areas such as the pharmaceutical industry and agriculture. Traditional extraction from natural sources cannot always satisfy the current demand for these types of compounds. This situation has resulted in the development of new alternative synthetic drugs that are obtained through asymmetric synthesis from racemic precursors. Taking advantage of the ease of modulation of salen ligands in general, groundbreaking approaches toward chiral epoxidation [52, 53] and hydrolytic kinetic resolution of (*rac*)-epoxides [54] have been developed by Jacobsen and Katsuki. These previous developments have been and still are of significant importance to the field of (poly)carbonate formation.

The simplest way to produce enantiopure cyclic carbonates is from enantiopure epoxides and carbon dioxide using catalytic procedures that favor a high level of retention of configuration at the chiral carbon center of the oxirane unit. DiBenedetto and Aresta [55] used Nb (IV) and Nb (V) complexes based on chelating diphosphine, pyrrolidine, or oxazoline ligands to convert (*R*)- or (*S*)-configured terminal epoxides, hereby achieving retentions higher than 98%. Kinetic resolution of racemic oxiranes is more attractive in this respect as it creates new chiral centers from cheaper precursors. The most widely studied substrate has been propylene oxide, and chiral catalysts have been used that are able to convert one of the epoxide enantiomers with a significantly higher rate providing thus a basis for epoxide resolution. Lu and coworkers reported on an elegant and efficient chiral Co (III)salen/quaternary ammonium halide binary-type catalyst (Scheme 4) that allows the direct synthesis of optically active cyclic carbonates from racemic epoxides under mild and solvent-free conditions. This study demonstrated clearly the influence of the anion of the quaternary ammonium salt in the binary catalyst systems, as it directs the enantiomeric purity and reaction rate [56].

Other studies concerning the asymmetric coupling reaction between $CO_2$ and oxiranes were carried out by Jing and coworkers, who developed chiral binaphthyl-based Co(III)salen complexes. In this case, the use of the binaphthyl-based salen ligands (see Fig. 4) provided access to two different types of catalysts being either mono- or dinuclear. In both cases, the catalysts retained the chiral information in the bridging cyclohexyl fragment [57]. The structural variety and success in catalytic

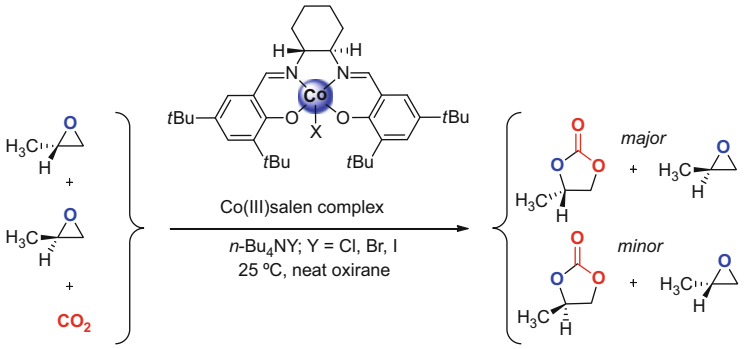


**Scheme 4** Kinetic resolution of a racemic epoxide mixture using a Co(III)salen type (spatial) catalyst

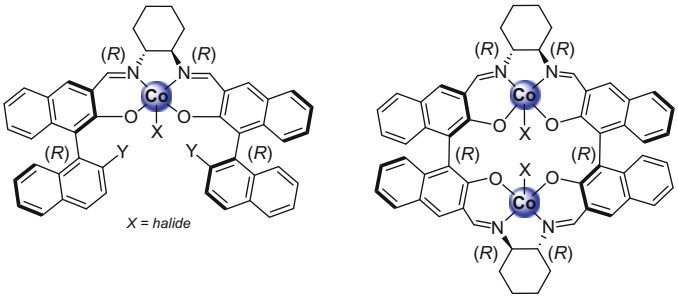


**Fig. 4** Example of BINAP-based Co(III)salen structures used as chiral catalysts in $CO_2$/epoxide couplings

operations are obviously an attractive feature, and for this reason it is not surprising that the vast majority of the catalysts developed for $CO_2$/epoxide couplings are based on Co(salen) structures.

Due to the ease of synthesis of these chiral M(salen) catalysts, other systems have also been studied including their Al(III) derivatives. The first studies reporting on this type of Al catalyst focused on the polymerization of epoxides [58], but in 2002, He et al. developed a binary catalyst system that mediated the formation of cyclic carbonate from propylene oxide in supercritical carbon dioxide in the presence of quaternary ammonium or phosphonium salts [36, 59]. A complementary study developed by Lu and coworkers showed how the coupling of $CO_2$ and oxiranes is altered by changing the substitution on the aromatic rings of the salen ligands and by using various crown ethers as cocatalysts [60]. North and coworkers demonstrated that bimetallic Al(salen) complexes display a much higher catalytic conversion than their monometallic analogues. In this case, the reaction, which gave no conversion in the absence of either the catalyst or cocatalyst, took place under very mild conditions (25°C, 1 atm), aspects that may be of interest for commercial applications [61].

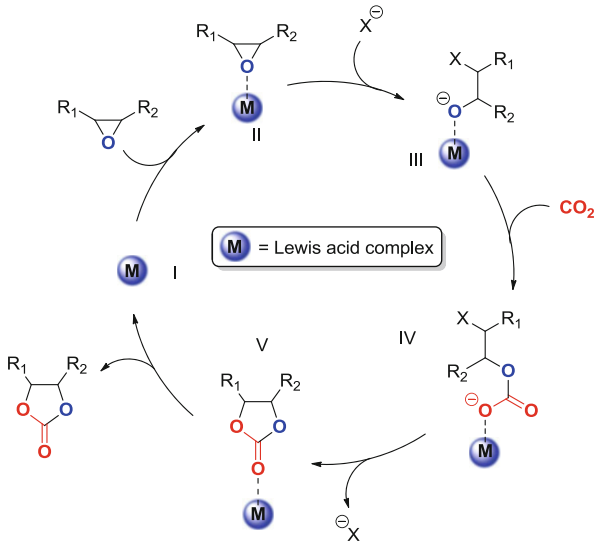


**Scheme 5** Generally proposed mechanism for the coupling of $CO_2$ to oxiranes catalyzed by a Lewis acid (M) in combination with a suitable nucleophile X

Other coordination/organometallic compounds such as $[M(PR_3)X_2]$ (M = Ni [62], M = Zn), [(dppp)$Mn(CO)_3$X] [38], various copper complexes embedded in macrocyclic ligands [63], [(OC)CpRu(μ-dppm)$Mn(CO)_4$] [64], and $[VO(acac)_2]$ [65] are also active in the synthesis of cyclic carbonates from $CO_2$ and epoxides. However, when compared to the previously mentioned Co(salen) complexes, the scope, reactivity, and/or selectivity features are generally less appealing.

The widely accepted mechanistic proposal that involves binary systems in the synthesis of organic carbonates is explained in Scheme 5. First, the oxirane/epoxide coordinates to the metal center through a coordinative M–O bond (stage II) resulting in the activation of the epoxide. The anion X here acts as a nucleophile, usually attacking the less hindered side of the oxirane furnishing a metal alkoxide intermediate species (III). Then, insertion of $CO_2$ into the metal alkoxide occurs to form a linear hemi-carbonate (IV) that undergoes a ring closure leading to the formation of the cyclic carbonate (V) that is released by the metal complex to allow for further turnover. Some of these elementary steps have been supported by X-ray crystallographic analysis (in the case of the resting state of some of the catalysts reported) [66] and computational studies [67].

## 3 Bifunctional Catalysts

In the last decades, the concept of green chemistry has turned out to be an important aspect in designing new catalytic systems. Using less toxic or nontoxic metals, increasing energy efficiency, and minimizing the amount of waste are key issues to be dealt with in synthetic chemistry. To address this problem, bifunctional catalysts

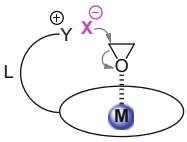


**Scheme 6** Conceptual approach toward cooperative activation of an epoxide by a bifunctional type catalyst [70]

have gained increased attention as they may offer more efficient strategies towards the conversion of organic substrates by means of cooperative and/or synergistic effects [68]. Bifunctional catalysis in the context of $CO_2$ conversion has also conquered a prominent position, and the catalysts that are generally used differ from binary type catalysts having complementary built-in functions (i.e., basic sites or nucleophiles) that entropically favor catalytic turnover. Also, these bifunctional systems often allow for catalyst immobilization and do not require the presence of additional (external) cocatalytic additives thereby increasing the overall efficiency. Most known bifunctional catalysts have a counteranion (= nucleophile) implemented in the catalytic structure in the form of an ammonium/phosphonium halide unit. The metal ion, counteranion, and substrate are all arranged in close proximity, which enhances the reaction rate and/or selectivity. Usually the cocatalyst unit used for ring opening of the substrate (in the case of cyclic carbonate formation) is attached to the catalyst via a linker unit (L), and the rigidity and linker length are crucial for optimal catalyst performance [69].

The proposed reaction mechanism for cyclic carbonate formation from $CO_2$/epoxide couplings mediated by bifunctional catalyst systems is rather similar to that reported for the binary systems (Scheme 5). Initial coordination of the epoxide to a metal complex is followed by ring opening by intramolecular, nucleophilic attack from the anion. The anion is ion paired to a (flexible) cationic linker group of the catalyst structure and therefore already in close proximity to facilitate the ring-opening step (Scheme 6). Subsequent steps proceed in a similar way as for the binary system, which finally leads to the formation of the cyclic carbonate and regeneration of the catalyst.

An example of an effective bifunctional catalytic system was reported in 2009 by North et al. [71]. They reported on a bimetallic Al(salen) complex where the cocatalyst is implemented in the catalytic system by modifying the salen units with ammonium salts having bromide counteranions. In terms of catalyst reactivity and stability, the bifunctional catalyst gives similar or even better results than the binary system [72], leading to high yields under very mild conditions (atmospheric $CO_2$ pressure, room temperature). The main advantage in comparison to the binary system is that this bifunctional catalyst can be immobilized on a solid support which opens the possibilities for use in flow reactors, and the same authors demonstrated at a later stage that this is indeed feasible [73]. Although this bifunctional catalyst can be reused for multiple runs, the catalytic activity gradually decreases over the consecutive cycles probably due to *retro*-Menshutkin or Hofmann elimination like chemistry. Similar strategies to create a bifunctional Al catalyst having built-in

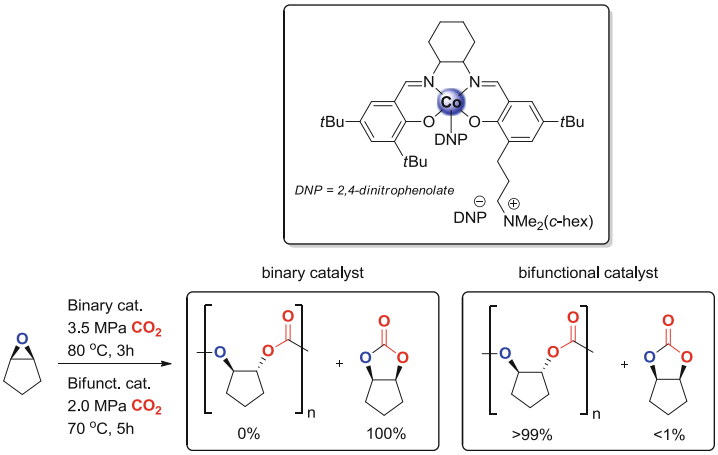


**Scheme 7** Improved selectivity toward polycarbonate formation from CPO/$CO_2$ using a bifunctional Co(salen) catalyst

quaternary ammonium salts led to a variety of one-component catalytic systems for cyclic carbonate formation. Whereas the first catalytic systems showed a considerable decrease in catalytic activity in subsequent cycles, the Al(salen) catalyst reported by Darensbourg in 2012 showed higher stability towards moisture and heat; it tolerates process impurities and shows only a minor loss in activity over five catalytic cycles [74].

Facilitating the immobilization of catalysts for flow reactors is not the only potential advantage of using a bifunctional catalyst. The selectivity for cyclic carbonate formation toward exclusive polymer formation in the coupling between an epoxide and $CO_2$ can be achieved by replacing the binary system for a bifunctional analogue. This feature was demonstrated by Lu and coworkers using Co(salen) derived catalyst, and its binary and bifunctional derivative were evaluated in terms of chemo-selectivity behavior in the asymmetric copolymerization of $CO_2$ and epoxides [75].

A similar comparison was done by Darensbourg et al. employing bifunctional (*R*,*R*)–(salen)M(III) catalysts with M being Cr or Co [76]. In the latter case, the performance of a binary and a bifunctional catalyst was compared in the copolymerization of $CO_2$ with either cyclopentene (CPO) or cyclohexene oxide (CHO). The binary catalyst system gives an excellent selectivity for polycarbonate formation when CHO is used as substrate, while in the case of CPO, only cyclic carbonate is observed. The bifunctional catalyst (see Scheme 7), however, is able to form selectively the polycarbonate product from CPO with virtual perfect selectivity. The specific conformation of the bifunctional catalyst system promotes polymer chain growth instead of ring closure that leads to cyclic carbonate formation.

Another interesting catalytic system was developed by Sakai and Ema, a bifunctional porphyrin-based catalyst modified with peripheral quaternary ammonium bromide groups (Scheme 8) [70]. This system exhibited an extremely high activity

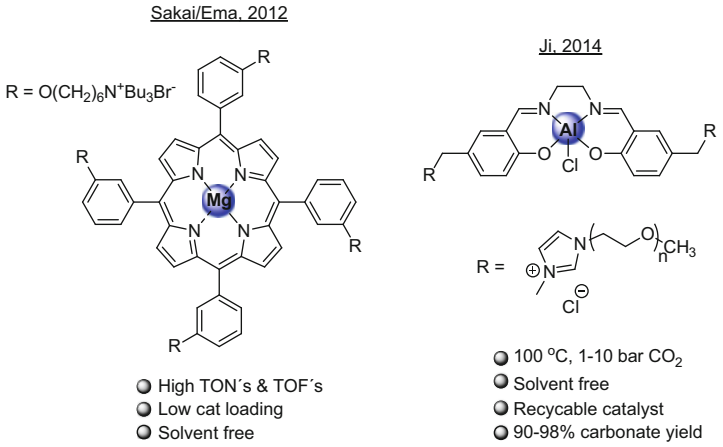


**Scheme 8** Examples of successful bifunctional catalyst designs in cyclic carbonate formation

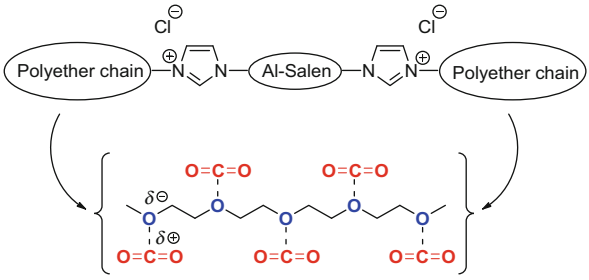


**Scheme 9** Proposed "$CO_2$ capture effect" by polyether chains

in the reaction of $CO_2$ with epoxides, leading to one of the highest reported turnover numbers (TONs, 103,000) and turnover frequencies (TOFs, 12,000 $h^{-1}$). The cooperative effect of the catalyst and cocatalyst induced by the bifunctional catalyst turned out to be highly important, as a binary-type system comprising of a Mg (porphyrin) and tetrabutylammonium bromide (TBAB) gave only 4% yield (TON, 5,000) under similar conditions. Differently substituted epoxides could be converted with high yield (81–99%) with no observable by-product formation.

Ji and coworkers recently reported on an Al(III)–salen complex functionalized by imidazolium groups (Scheme 8) [77]. These bifunctional Al(salen) complexes do catalyze the formation of cyclic carbonates from epoxides although in moderate yield. A significant enhancement in the yield of the carbonate product was obtained upon employing a *trifunctional* catalyst system having additional polyether chains incorporated. These polyether chains are proposed to increase the local density of $CO_2$ by assumed weak interactions between the oxygen atoms of the ether fragments and $CO_2$ as depicted in Scheme 9. As such, the reaction shows a significantly reduced diffusion-dependent kinetic behavior and thus increased reactivity and product yields.

Various epoxides were converted in excellent yields (94–99%) by the trifunctional catalyst. In comparison, the catalyst without polyether groups only provides moderate conversion or no reaction at all under similar conditions. Comparable effects of increasing the local concentration of $CO_2$ by a judicious choice of the solvent medium have also been reported [48]. Another advantage of these modified Al(salen) complexes is the facile catalyst separation and recyclability. The catalyst can be separated from the reaction mixture by addition of ether which causes the Al-complex to precipitate. The catalyst can be used in subsequent catalytic cycles with virtually no loss in reaction rate and only a minor decrease in selectivity to 98% after six consecutive runs. Since the advent of bifunctional catalysis as an alternative to binary catalysis, various research groups have reported bifunctional catalysts of which the noteworthy ones include a bimetallic macrocyclic Fe(III) complex [78], a trinuclear bis-salphen metalloligand [79], and other chiral Co(salen)-based systems [80].

## 4 Addition of Carbon Dioxide to Double and Triple Bonds

Chemical fixation processes with $CO_2$ should preferably rely on low-energy processes to minimize the net output of $CO_2$ during the reaction. Ideally, cyclic carbonates could be obtained from a reaction between $CO_2$ and an unsaturated alcohol, leading to the formation of an elusive carbonic acid mono-alkyl ester, though these compounds are too unstable to be observed and isolated [81]. An interesting strategy to overcome this problem was reported by Minakata et al. in 2010 [82]. They reported on the formation of carbonic acid intermediates from unsaturated alcohols and $CO_2$. Despite the unfavorable thermodynamic equilibrium, the carbonic acid derivative can be conveniently trapped by *tert*-butyl hypoiodite (*t*-BuOI) to form a carbonic acid iodide intermediate (Scheme 10). In the presence of an alkene/alkyne group in the substrate, fast ring closure toward a cyclic carbonate product is observed that drives the equilibrium toward the targeted product through an intramolecular addition onto the double bond. A variety of unsaturated alcohols with either alkene- or alkyne-accepting groups can be easily converted by this innovative reaction with good to excellent yields under very mild conditions using only 1 bar of $CO_2$ at temperatures as low as −20 °C.

Another recent example of $CO_2$ addition to unsaturated carbon–carbon bonds is the conversion of $CO_2$ and olefins to form cyclic carbonates, a process reported by Hatton and Jamison in 2014 [83]. They used a flow system containing a

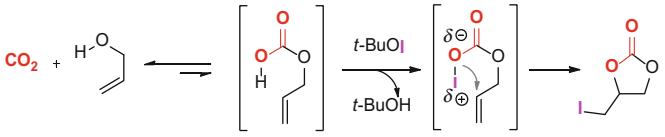


**Scheme 10** Trapping of a carbonic acid intermediate with *tert*-butyl hypoiodite

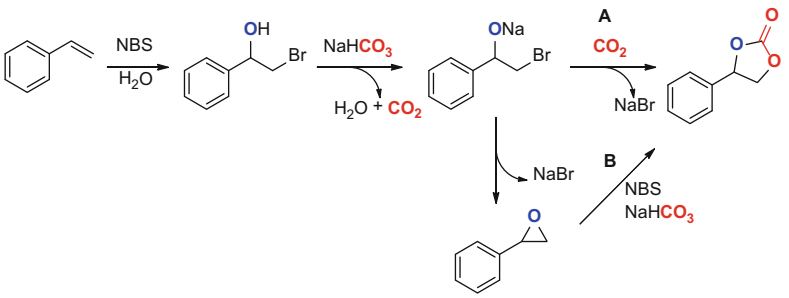


**Scheme 11** Proposed mechanism for the formation of cyclic carbonates from olefins using a NBS/$NaHCO_3$/water medium

combination of *N*-bromo-succinimide (NBS), 1,8-diazabicycloundec-7-ene (DBU) as a base, water, and $CO_2$. The optimal temperature for this reaction turned out to be 100 °C, as at lower temperatures the main product is the epoxide and at higher reaction temperatures, the formation of the diol (through carbonate hydrolysis) is favored. Under these optimized reaction conditions, styrene could be fully converted into styrene carbonate in up to 85% isolated yield without the formation of by-products.

The proposed mechanism [84] of this reaction most likely follows one of the two pathways described in Scheme 11 using sodium bicarbonate as the $CO_2$ source. The first step is the reaction of the olefin with NBS and water to form a reactive bromohydrin, which can be deprotonated by sodium bicarbonate to release $CO_2$ and water. The anionic intermediate of the halohydrin can then react directly with $CO_2$ to produce the cyclic carbonate (path A) or via the epoxide (path B). As the reaction that forms the epoxide proceeds faster than the coupling with $CO_2$, a substantial amount of cyclic carbonate is supposed to form through the latter pathway. Although the approaches from Minakata et al. and Jamison/Hatton do not make use of metal catalysis, they serve as inspiring examples of efficient $CO_2$ conversion catalysis examples.

Compared to carbon–carbon double bonds, the carbon–carbon triple bond is more reactive and thus generally does not require elevated temperatures for its reaction with carbon dioxide. The addition of a strong base or in some cases an organocatalyst is sufficient to convert propargylic alcohols [85] and propargylic amines [86] to cyclic carbonates and oxazolidinones [87, 88], respectively. Although there are various reported examples that concern the use of bases, this work will focus on metal-catalyzed addition reactions that involve $CO_2$ as a reagent. Significant contribution to this field was made by Yamada and coworkers; they reported on the Ag-catalyzed $CO_2$ incorporation into propargylic alcohols [85]. The $CO_2$ reacts with the alcohol group of the substrate, after which ring closure occurs through activation of the alkyne group by the Ag complex to give a cyclic carbonate with an exo-cyclic double bond. In subsequent work, the same authors showed that cyclic carbonates can be formed from bis-propargylic alcohols at low temperatures allowing for practical enantioselective reactions (Scheme 12) [89]. The combination of AgOAc and a chiral Schiff base ligand gave access to a

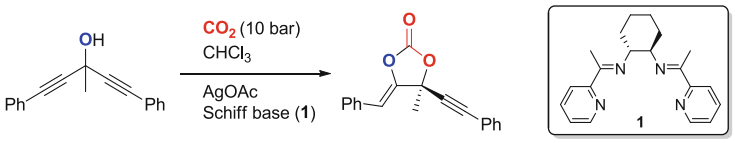


**Scheme 12** Addition of $CO_2$ to a bis-propargylic alcohol catalyzed by a chiral silver complex based on Schiff base (1)

variety of cyclic carbonates in high yields (90–98%) and with *ee*'s of up to 93%. These reactions can be performed under mild conditions using 10 bars of $CO_2$ at 5 °C. At this temperature, there is excellent enantio-control though at the expense of the reaction rate: under low-temperature conditions, the reactions require 2–7 days to reach complete conversion of the substrates.

An interesting contribution to this field was made by the group of Jiang that reported on *N*-heterocyclic carbene–Ag complexes immobilized on a polystyrene support [90]. Various terminal secondary and tertiary propargylic alcohols were conveniently converted to their cyclic carbonate products by this supported catalyst with excellent selectivity and yield. These reactions could be performed under relatively mild conditions at 40 °C using 50 bars of $CO_2$ pressure. For some of the more sterically hindered substrates, a slightly higher temperature was required to give high yields. An additional benefit of this system is its recyclability; after 15 catalytic cycles, no significant change in the activity was observed.

## 5 Synthesis of Oxazolidinones Using $CO_2$ and Metal Catalysts

Oxazolidinones (also known as five-membered cyclic carbamates) are an important class of heterocyclic compounds widely present in pharmaceutically relevant organic structures. Particularly, 5-substituted oxazolidin-2-ones have shown extensive antibacterial and antimicrobial activity, and these structures are represented in several (commercially available) synthetic drugs (Fig. 5) [91–94]. Furthermore, these cyclic carbamates are frequently used in synthetic organic chemistry [51, 95] since Evans [96] reported in 1981 on the use of enantiomerically pure 4-substituted oxazolidinones as chiral auxiliaries in asymmetric synthesis (i.e., the use of a polymer-supported chiral Evans' auxiliary in diastereoselective *syn*-aldol reactions) [97]. Finally, the commercialization of linezolid, an oxazolidinone-based antibacterial drug, raised the interest of the scientific community toward developing new synthetic routes for oxazolidinones especially those that are based on the use of $CO_2$ as a reagent [98].

The conventional preparation of oxazolidinones includes the use of environmentally harmful/toxic reagents such as phosgene, isocyanates, or carbon monoxide. Most popular routes which lead to oxazolidinones include the carboxylation of

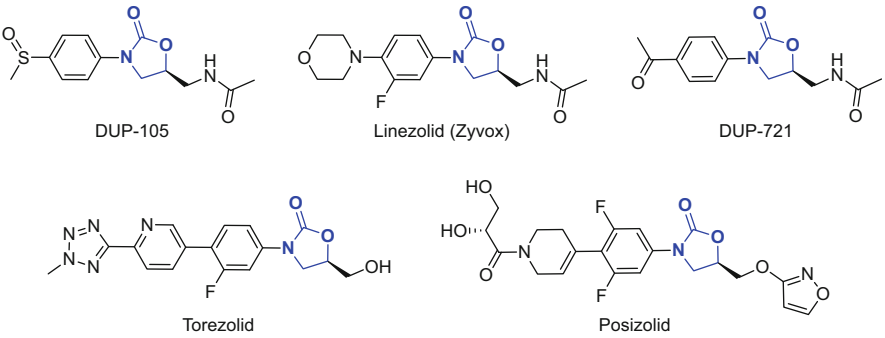


**Fig. 5** Schematic structures of some oxazolidinone-based biologically relevant compounds. All are industrially produced as antibiotic against Gram-positive bacteria

1,2-amino alcohols using phosgene [99] as a carbonyl source, coupling between epoxides and isocyanates [100], or a two-step process involving the carboxylation of $\beta$-amino alcohols with CO followed by an oxidative cyclization with molecular oxygen [101]. As the oxazolidinone building block has gained extensive synthetic and medical applications over the last years, the development of greener chemical methodologies has attracted considerable attention. In order to avoid the use of phosgene or isocyanates, great effort has been devoted to incorporate $CO_2$ as an alternative C1 carbon source [102]. There are three main synthetic strategies using $CO_2$ as C1 building block depending on the starting material employed: (1) insertion/addition of $CO_2$ (in)to an aziridine moiety, (2) reaction of 1,2-amino alcohols with $CO_2$, and (3) reaction of propargylic amines with $CO_2$. These methods will be discussed in more detail in the sections below.

## 5.1 *Insertion of $CO_2$ into an Aziridine Moiety*

Aziridines are important three-membered, small-sized heterocyclic compounds. Structurally, they are analogous to epoxides with the nitrogen group replacing the oxygen. The chemistry of aziridines has been studied extensively over the last few decades, and their applications have been greatly expanded. Since aziridines are highly ring-strained compounds, they are promising candidates to react with relatively inert $CO_2$ without the need for extreme reaction conditions. The direct coupling reaction between $CO_2$ and aziridines represents obviously an attractive route to oxazolidinones compared to the processes based on phosgene or CO. An efficient aziridine/$CO_2$ coupling reaction is 100% atom efficient, which is an important factor for sustainable development. As a result, different research groups have developed relatively green approaches toward the synthesis of oxazolidinones through catalytic and non-catalytic routes. The reaction of aziridines with $CO_2$ usually affords two regio-isomeric structures: the 4- and 5-substituted isomer

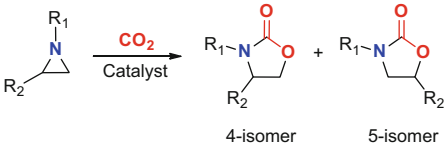


**Scheme 13** Reaction scheme of the insertion of carbon dioxide into an aziridine group

**Table 1** Influence of the aziridine substituents on the oxazolidinone isomer ratio using different catalytic systems

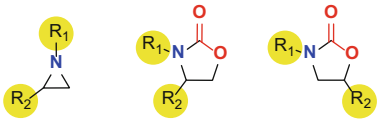


aziridine 4-isomer 5-isomer

| | | Preferred oxazolidinone | | |
|---|---|---|---|---|
| $R_1$ aziridine | $R_2$ aziridine | $MX_n$ (Pinhas) | Co(salen)/DMAP (Nguyen) | $ZrOCl_2 \cdot 8H_2O$ (Wu) |
| Alkyl | Alkyl | 67% (4) | 5-Isomer | 4-Isomer |
| Alkyl | Phenyl | 5-Isomer | 5-Isomer | 5-Isomer |
| Phenyl | Phenyl | No reaction | 5-Isomer | No reaction |

(Scheme 13). The ratio between these two isomers is mostly dependent on the aziridine substituents ($R^1$ and $R^2$, Table 1).

The main drawback in the synthesis of oxazolidinones from $CO_2$ is the relative inertness of the latter combined with the lower reactivity of aziridines compared to epoxides. These limitations can be (partially) overcome by using a high $CO_2$ pressure and/or electrolysis methods [103]. Good results for the insertion of $CO_2$ into the C–N bond of aziridines have been obtained by electrosynthesis using stable and readily available complexes of Ni(II) incorporating a cyclam ligand (1,4,8,11-tetra-azacyclo-tetradecane) or using a bipyridine ligand. The reaction takes place under extremely mild reaction conditions (ambient pressure and temperature) which provides a green chemical approach compared with existing methodologies. Both types of Ni(II) complexes led to the corresponding oxazolidinones in good yields (50–99%) depending on the substituents present in the starting aziridine and displayed moderate to good regioselectivities for the 4-isomer product (50–84%).

Endo et al. reported in 2003 on the first selective synthesis of 2-oxazolidinones by coupling of $CO_2$ with an aziridine [104]. The conversion of 2-methylaziridine and 2-phenylaziridine into their corresponding oxazolidinones was studied using simple and cheap metal halides as catalysts such as LiBr and NaBr. In both cases, the reaction shows an excellent regioselectivity and provides exclusively the 4-substituted oxazolidinone (Scheme 13). Whereas ambient conditions ($pCO_2 = 1$ bar and room temperature) were used for the coupling of 2-methylaziridine with $CO_2$, an increase in the reaction temperature (up to 100 °C) was required for the conversion of 2-phenylaziridine probably as a result of an increasing steric effect at the ring-opening stage of the reaction.

Simultaneously, Pinhas and coworkers reported on the use of an identical metal halide catalyst for the conversion of *N*-substituted aziridines under similar conditions as those reported by Endo (i.e., ambient conditions) [105]. A dramatic effect of the aziridine substitution on the regio-isomer distribution was observed. When the $R^1$ and $R^2$ groups (Table 1) are both alkyl groups, a 2:1 mixture of 4- and 5-isomer is obtained. On the other hand, if $R^2$ is a phenyl group, the mixture product is almost quantitatively enriched in the 5-isomer. However, if $R^1$ is a phenyl group (Table 1) or any electron-withdrawing group, no reaction is observed at all.

This problem was solved by Nguyen in 2004, who reported on a highly active and selective catalyst [106] based on a binary complex comprising of a Cr(III)–salen complex and 4-dimethylaminopyridine (DMAP) for the coupling reaction between $CO_2$ and *N*-substituted aziridines under mild reaction conditions. The Nguyen method proved to be successful with *N*-phenyl-substituted aziridines (Table 1, Scheme 14) which is highly important as all oxazolidinone-based biologically relevant compounds have *N*-aryl substitutions. In addition, for the first time this catalytic system showed a general and clear preference for the formation of the 5-isomer. The excellent regioselectivity is of high importance as only the 5-substituted oxazolidinones have shown to exhibit biological activity. Furthermore, this binary complex shows high catalytic activity for a wide range of substrates, and the oxazolidinone products were generally obtained in excellent yields and regioselectivities.

The proposed mechanism is shown in Scheme 14. The aziridine is first activated by coordination to the metal center replacing the labile chloride atom. As a result of

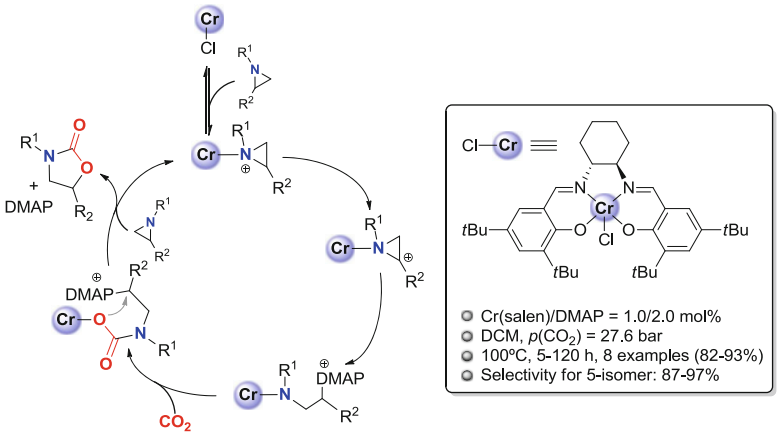


**Scheme 14** Proposed mechanism for the coupling of $CO_2$ and aziridines by a Cr(III)–salen/DMAP binary catalyst system

this coordinative interaction, a partially positive charge is delocalized over the aziridine ring allowing nucleophilic attack by the Lewis base cocatalyst DMAP at the most substituted carbon. The regioselectivity of the reaction is controlled by this step affording predominantly the 5-isomer.

A different method to obtain 5-substituted oxazolidinones in excellent yields and regioselectivities was reported by Wu and coworkers [107]. Zirconyl chloride ($ZrOCl_2{\cdot}8H_2O$) was used as an effective solid catalyst for the coupling between $CO_2$ and aziridines under mild conditions without the need of any additives or solvent. This methodology was successfully applied to the synthesis of a variety of *N*-alkyl-2-phenyl aziridines to obtain *N*-alkyl-5-phenyl-based oxazolidinones. The 4-substituted product is the predominant one when $CO_2$ is coupled to 2-alkyl aziridines (Table 1). The activity of the $ZrOCl_2{\cdot}8H_2O$ catalyst, which is regarded to be an ionic cluster of $[Zr_4(OH)_8(H_2O)_{16}]Cl_8$, can be explained by the coexistence of Lewis acidic zirconium (IV) and Lewis basic chloride. The bifunctional catalyst can be easily recovered from the reaction mixture by filtration and reused for at least five times without significant loss in catalytic activity, rendering the process economically and potentially viable for commercial applications.

In addition to these methods, other catalytic systems have been developed to get 4,5-disubstituted oxazolidinones. Pinhas [105] studied the formation and stereochemistry of oxazolidinones starting with 2,3-disubstituted aziridines. Using LiI as catalyst, high yields (85–90%) were obtained for dialkyl-substituted aziridines with retention of the starting *cis*/*trans* stereochemistry. At a later stage, a binary catalytic system composed of palladium-dibenzylideneacetone $[Pd_2(dba)_3]$ and tetrabutylammonium difluorotriphenylsilicate (TBAT) was reported by Aggarwal and coworkers [108] to effectively convert 2-allyl-3-substituted aziridines to the corresponding oxazolidinones in mild conditions (0 °C and 1 bar of $CO_2$); see Scheme 15. This Pd-mediated reaction proceeds with overall retention of configuration although the palladium intermediate can possibly isomerize to yield the product with opposite configuration. The effect of this isomerization process could almost be fully suppressed under the reaction conditions (0 °C) but becomes a significant competitive pathway at room temperature or in the absence of a halide

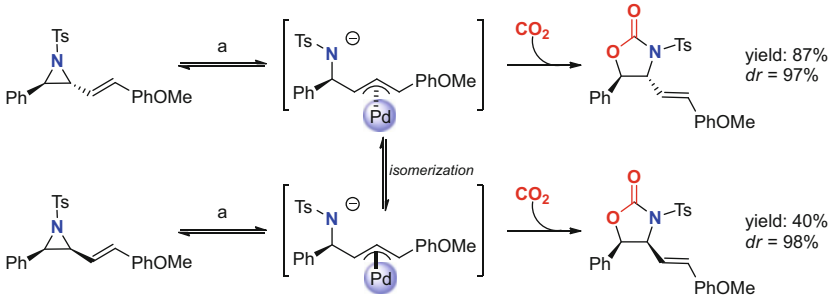


**Scheme 15** Stereoselective palladium-catalyzed oxazolidinone synthesis from aziridines and $CO_2$. (a) Reaction conditions: $Pd_2(dba)_3$, $CHCl_3$, $PPh_3$, TBAT, $p(CO_2) = 1$ bar, toluene

salt. A Pd(0) complex acts as catalyst for the ring-opening "cyclization" reaction forming a π-allyl palladium intermediate. Trapping of this intermediate by $CO_2$ gives the vinyl oxazolidinone after ring closure by attack of the carbamate group onto the activated Pd–allyl fragment.

Other methods for the coupling reaction between $CO_2$ and aziridines comprise the use of $I_2$ [109, 110], organocatalysts such as *N*-heterocyclic carbenes [111], or recyclable systems based on a polyethylene glycol support containing quaternary $NBu_3Br$ groups [112] and polymer-supported amino acids [21]. Interestingly, Pinhas et al. demonstrated that the coupling of aziridines and $CO_2$ could also be performed without catalyst using 2-aryl- and 2-alkylaziridines as substrates affording selectively the 5-oxazolidinones in good yields making use of high-speed ball milling as a mechanical stimulus [113]. However, this section focuses on metal-mediated processes; thus, these latter examples fall out of the primary scope of this chapter.

## 5.2 *$CO_2$ Coupling Reactions with Amino Alcohols and Propargylic Reagents*

Alternative ways to obtain oxazolidinones include the coupling of $CO_2$ with 2-amino alcohols or propargylic amines (Scheme 16). However, these processes are not (always) atom efficient; considerably harsh conditions may be required for efficient turnover and produce significant amounts of waste. Therefore, they are considered less sustainable than those based on aziridines and $CO_2$ couplings, and these methods will therefore only be briefly discussed in this chapter.

Since 2-amino alcohols are readily available derivatives of amino acids, they have been frequently used in the synthesis of oxazolidinones using $CO_2$ as the carbonyl source. The main drawback of the reaction is finding a suitable dehydrating pathway after the insertion of $CO_2$ in the 2-amino alcohol moiety as the reaction is thermodynamically not favored. Nomura and coworkers reported the first organometallic catalyst for this reaction ($Ph_3SbO$) [114], which was able to

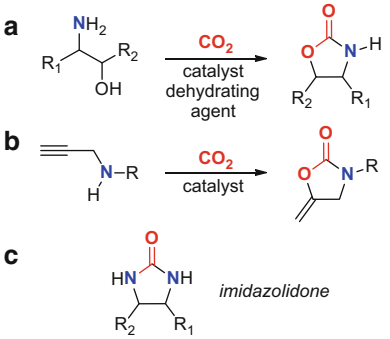


**Scheme 16** Synthesis of oxazolidinones from 1,2-amino alcohols (**a**) and *N*-substituted propargylamines (**b**). Under (**c**) an example of an imidazolidinone product observed by Shi et al.

perform the conversion to 2-oxazolidinones in good yield (over 94%) but under harsh temperature conditions (160°C, 24 h) using molecular sieves (3 Å) as dehydrating additive. After this initial report, other catalysts were used in this transformation such as chlorostannoxanes reported by Ghosh [115]. In the presence of 1,3-dichloro-1,1,3,3-tetraalkyldistannoxanes, retention of chirality (up to 99%) of the starting amino alcohols and high turnover numbers (up to 138) were observed under the reaction conditions. Other catalytic systems that were studied for this reaction are based on the use of carbodiimides and phosphines [116, 117].

The reaction between propargylamines and carbon dioxide is one of the most common approaches toward the formation of unsaturated oxazolidinones. An important example of a binary catalyst system for the formation of these types of oxazolidinones was reported by Mitsudo [118] in 1987 using a Ru catalyst [i.e., (4-1,5-cyclooctadiene) (6-1,3, 5-cyclooctatriene)ruthenium] and a tertiary phosphine to give the 5-methylene-2-oxazolidinone products from *N*-substituted propargylamines and $CO_2$ in high yield and good regio- and stereoselectivity. In this context, Costa reported some interesting examples of unsaturated oxazolidinone formation in 1996 and 1999. First, the use of strong organic bases as catalysts for the synthesis of 5-substituted oxazolidinones was probed using propargylamines [87], and hereafter oxazolidinone synthesis was investigated using $PdI_2$ as catalyst [119]. With this methodology, 3-substituted oxazolidinones were obtained in good yields and with a 1:3 *E*/*Z* ratio after optimization of the reaction conditions. Shi and coworkers also studied various palladium-based catalysts such as $Pd(OAc)_2$ and $Pd(PPh_3)_4$ for the reaction between propargylamines and $CO_2$ under mild reaction (20 °C) conditions [120]. The latter example demonstrates that the chemo-selectivity can be an issue when propargylic amines are used as substrates. The combination of a suitable Pd salt with an appropriate counteranion can drive the selectivity toward the desired oxazolidinone or alternatively toward the imidazolidinone product (Scheme 16c). The use of a basic phosphine [$P(t\text{Bu})_3$] fully suppressed the formation of the imidazolidinone and gave the highest yield of the desired oxazolidinone (90%).

## 6 Synthesis of Ureas and Quinazolines

Ureas and their derivatives are an important type of organic compounds where two amine groups are connected by a carbonyl group. They are important end products or intermediates for pharmaceuticals, agricultural pesticides, antioxidants in gasoline, dyes, and resin precursors [121]. Many cyclic derivatives can be synthesized using $CO_2$ as a reactant. Substituted 2,4-dihydroxyquinazolines have been interesting for their biological activities. For example, 7-chloro-1-carboxymethyl-3-(4-bromo-20-fluorophenylmethyl)-2,4(1*H*,3*H*)quinazolinone was developed as an aldol reductase inhibitor as a remedy for complications of diabetes mellitus.

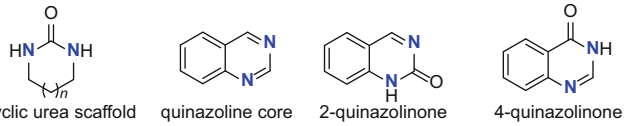


**Fig. 6** Structures of some urea/urea-like scaffolds

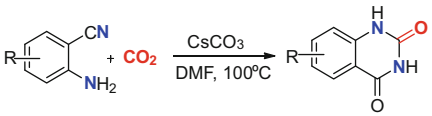


**Scheme 17** Bhanage's quinazoline-2,4(1H,3H)-dione synthesis from 2-aminobenzonitriles

Quinazolinones are also a class of drugs which function as hypnotic/sedative drugs that contain a 4-quinazoline core (Fig. 6).

Generally, their synthesis is carried out by treatment of anthranilic acid with urea, anthranilamide with phosgene, carbon monoxide with sulfur, or anthranilic acid with potassium cyanate. Obviously, these methods are considerably limited because of the high toxicity of the reagents employed and/or the drastic reaction conditions applied. Mizuno et al. [122] reported in 2000 the first synthesis of these types of compounds using $CO_2$ as a reactant. 2,4-Dihydroxyquinazolines were prepared in high yield starting from 2-aminobenzonitriles and $CO_2$ under mild conditions (1 atm, 20 °C) in the presence of DBU. The use of DBU is disadvantageous due to problems associated with its handling including its hygroscopic nature, high viscosity, and tedious rework procedures. Following the need for simpler and more practical methods for the synthesis of these compounds, Bhanage et al. proposed [123] an alternative method using cesium salts for the synthesis of quinazoline-2,4(1*H*,3*H*)-diones using $CO_2$ and 2-aminobenzonitriles (Scheme 17).

The proposed mechanism starts with deprotonation of the Ar-$NH_2$ that reacts with $CO_2$ to afford a Cs-amide intermediate. This amide then attacks the nitrile group in an intramolecular process giving rise to a cyclized species that rearranges into an isocyanate intermediate followed by another intramolecular process where a hydroxyl-imine group attacks the carbon center of the isocyanate yielding a new cyclized compound that finally stabilizes/rearranges into the desired dihydroxyquinazoline. Improvements of the method are still required as the process needs high pressures ($\geq$13 bar) and temperatures (100 °C).

Other basic catalysts which have proved to be very efficient in $CO_2$ fixation (TON up to 938) into urea derivatives are polyoxometalates such as the mononuclear and simplest tungstate $[WO_4]^{-2}$. $TBA_2[WO_4]$ (TBA = $[(n\text{-}C_4H_9)_4N]^+$) can act as a highly efficient homogeneous catalyst for the conversion of $CO_2$ with amines, 2-aminobenzonitriles, and propargylic alcohols to give urea derivatives, quinazoline-2,4(1*H*,3*H*)-diones, and unsaturated cyclic carbonates, respectively [124, 125]. Interestingly, the tungstate used in this latter work seems to be able to activate both types of substrates, and NMR investigations have supported that the

(bifunctional) catalyst species is involved in binding of a $CO_2$ molecule thus activating it for catalytic turnover. Mechanistic investigation [125] showed unambiguously that the formation of a carbamic acid intermediate and its subsequent conversion by $TBA_2[WO_4]$ plays a key role in the synthesis of the heterocyclic products. Other methods towards quinazoline derivatives using $CO_2$ as reagent have also recently been disclosed but will not be discussed in detail here [126].

## 7 Formation of Lactones

A lactone is defined as a cyclic ester, and it may be regarded as the condensation product of an alcohol and an acid group within the same molecule. It consists of a cycle of at least 2 carbon atoms and a single *endo*-cyclic oxygen atom with an adjacent carbonyl group. In this section, we will focus on the importance of this type of molecules and the different synthetic routes that have been reported utilizing $CO_2$ as a key reagent. The kinetic stability of $CO_2$ towards its conversion represents a huge challenge, and therefore the development of catalytic methods for its activation is crucial. Cyclic structures containing ester functions require complex synthetic routes, and their formation can be formally achieved through the insertion of $CO_2$ into C–H, C–C, E–C, or C–O–C bonds (E represents other elements than H, C, or O). These reactions are expected to have favorable thermodynamics associated to adverse kinetics. The main $CO_2$ activation strategy has been the direct interaction of the $CO_2$ molecule with a metal center. The first structurally characterized metal complex capable of binding $CO_2$ was reported in 1975 by Aresta and coworkers [127], and since then, the insertion of $CO_2$ into M–E bonds has been intensively investigated with the aim of discovering new catalysts for (direct) $CO_2$ conversion.

In essence, there are two principal routes considering $CO_2$ insertion into organic molecules leading to lactone-based structures: (1) reactions of $CO_2$ with olefins or alkynes and (2) the insertion of $CO_2$ into metal–element bonds, which, depending on the co-reactants, leads to different transformation products such as carboxylates, esters, or carbonates. First, the focus will be on the first route which leads to the production of lactones and metallo-lactones. In nearly all reported cases, late transition metals have been used including Fe(0), Rh(I), Ni(0), Pd(0), and Pd (II) as they are highly basic and capable of binding weak σ-donor ligands such as olefins through π-back bonding. Many recent reports are still based on the initial research from the 1970s and 1980s, published by the groups of Inoue, Musco, Hoberg, Walther, and Behr, who focused their research in the field of catalytic $CO_2$ activation. The pioneering examples of lactone formation using $CO_2$ were provided by Inoue et al. and Musco et al. in the late 1970s [128–132]. Using $Pd(dppe)_2$ as a catalyst [131], 1,3-dienes could be activated towards coupling with $CO_2$ to afford five- and six-membered lactones (Scheme 15a) although resulting in a (complex) mixture of products. Another interesting contribution in the field of lactone formation describes the coupling between $CO_2$ and (substituted) methylenecyclopropanes

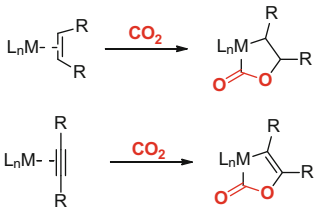


**Scheme 18** Reaction of $CO_2$ with olefins and alkynes giving metallo-lactones

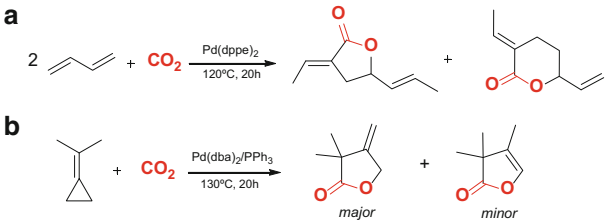


**Scheme 19** Inoue's contributions in the field of lactone formation using $CO_2$: (**a**) dppe = $Ph_2P(CH_2)_2PPh_2$ and (**b**) dba = dibenzylideneacetone

[130] using a Pd(0) complex based on $Pd(dba)_2$ and $PPh_3$ (ratio 1:4) as catalyst (Scheme 19b). The main issues of these reactions were the high $CO_2$ pressures needed (40 bar) combined with low chemo-selectivity. Two types of lactones were observed, one with an *exo*-cyclic and one with an *endo*-cyclic double bond, and a challenge is the combination of high conversion and high selectivity for either lactone while maintaining high isolated yields (Scheme 18).

The reaction involving the telomerization of butadiene with $CO_2$ (Scheme 19a) to form a functional lactone has been a topic of intensive research after the first contributions from Inoue and coworkers as these lactones potentially have multiple applications as an organic intermediate. Over the years, the yields and selectivity have been successfully increased (up to 48% and 95%, respectively), and the process was optimized to mini-plant scale [133–135]. Several investigations were conducted to explain in more detail the reaction/mechanistic pathway (Scheme 20).

The proposed reaction mechanism involves the formation of a Pd(0)–phosphine complex ($PdL_n$) from a palladium(II) precursor and a tertiary phosphine. The second step is the coordination of two butadiene molecules forming a bis-$\eta^3$-allyl–Pd complex **A**. This species is in equilibrium and can either react to form 1,3,7-octatriene **B** or give rise to an allylic carbonate **D** by insertion of $CO_2$ in one of the allyl–Pd bonds in **C**. Through ring closure of this intermediate **D,** various cyclic lactones can be obtained, although there are side reactions which can produce other aliphatic cyclic esters **F** and **G**. Another important side reaction that has to be taken into account is that the Pd catalyst can also promote the coupling of a different number of molecules of butadiene before the carboxylation step, which leads to linear open-chain ester products of different lengths/sizes (cf., formation of **H** and

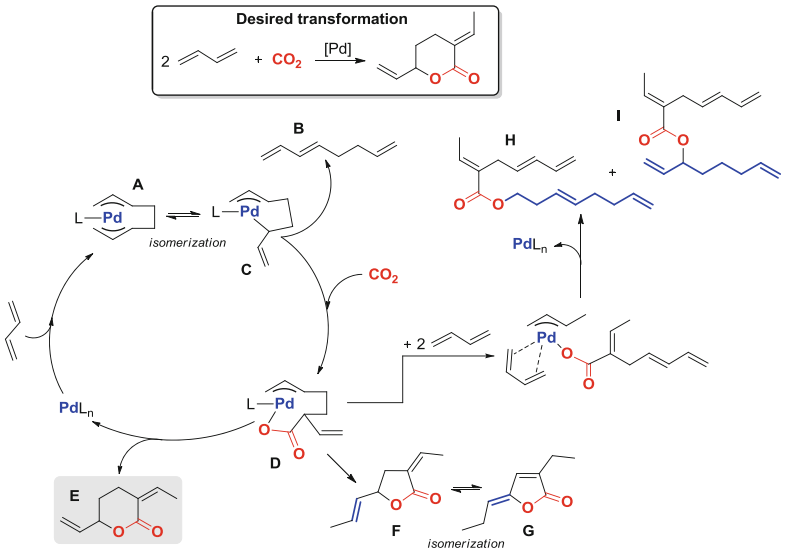


**Scheme 20** The reaction mechanism for the telomerization of $CO_2$ and butadiene proposed by Behr et al.

**I**). This detailed mechanism therefore explains the low yield and poor selectivity of the reaction in the first seminal reports, but clearly optimization based on by-product recycling drastically increased the selectivity towards the *δ*-lactone **E**.

The resulting lactone is highly functional allowing for various post-synthetic manipulations. Through further conversion with different bulk reagents, several relevant industrial products may be prepared, and the lactone could be regarded as an ideal chemical platform molecule amenable toward hydrogenation, hydroformylation, hydroamination, oxidation, and polymerization among other valuable conversions (Scheme 21).

In 2014, Nozaki [136] and coworkers were able to develop a strategy to create a polymer from dienes and $CO_2$ in which $CO_2$ represented 29% of the weight of the product. The key feature to make this process feasible was to employ the *meta*-stable *δ*-lactone **E** to overcome the thermodynamic barrier. Copolymerization of $CO_2$ and dienes to form polylactones has always been an appealing research topic as it would allow for the preparation of new materials from inexpensive feed stocks such as $CO_2$ and dienes. This has generally not been possible due to the inertness of $CO_2$ combined with the high kinetic barrier associated with the alternating copolymerization of ethylene/polyene and $CO_2$.

Nozaki et al. made clever use of the optimized synthetic methodology developed by Behr for *δ*-lactone **E** which could easily undergo thermally initiated radical polymerization under aerobic conditions in the presence of an appropriate thermally activated radical initiator [i.e., ABCN = 1,1′-azo-bis(cyclohexane-1-carbonitrile)]. The system was optimized to obtain high molecular weights (62–85 kDa) with narrow molecular weight distributions (PDIs around 1.3) and polymer yields around 48%. As depicted in Scheme 22, the copolymerization results in the

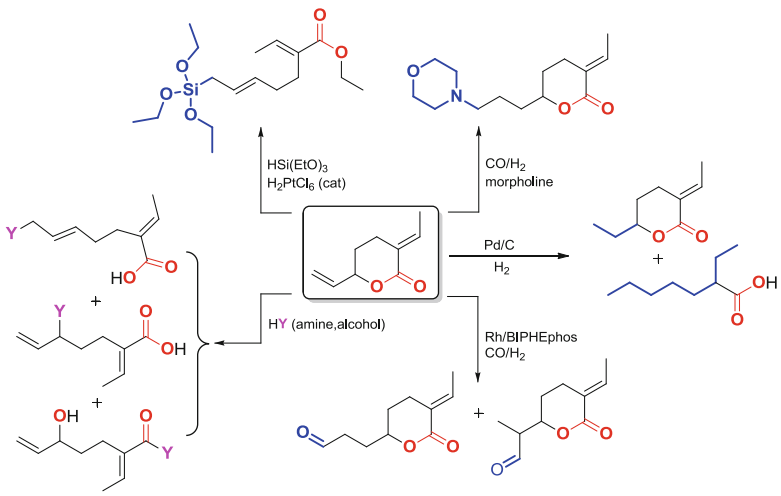


**Scheme 21** Functionalization reactions of the $\delta$-lactone E from Scheme 20 towards several products with potential industrial applications

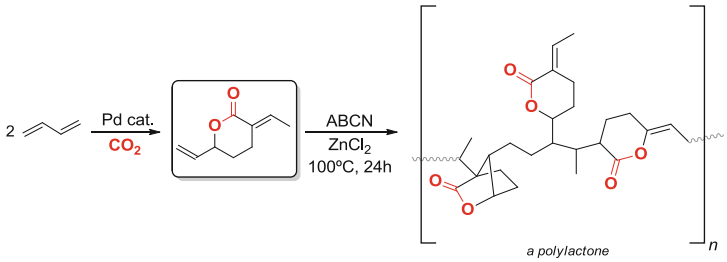


**Scheme 22** Nozaki's strategy to create a novel lactone copolymer based on $CO_2$

formation of several isomeric subunits in the polymer. The scope of polymerization reactions was extended to the incorporation of more complex diene structures (e.g., 1,3-pentadiene and isoprene) within the polymeric chain.

Revisiting Inoue's work in the 1970s, the same group also discovered that by using Ni(COD)$_2$–dppb as a catalyst (COD = 1,5-cyclooctadiene), it is possible to combine two alkyne molecules with $CO_2$ affording six-membered lactones [128]; using internal alkynes they were able to obtain more reasonable yields of the lactone products. First, $CO_2$ coordinates to electron-rich metal centers in a $\eta^2$-form (see Fig. 7). Alkenes or alkynes in the presence of stoichiometric amounts of the metal–$CO_2$ complex form metallocycles, which are important intermediates in the lactone synthesis. The most widely studied metallocycles are the ones formed with Ni(0) precursors, the so-called oxa-nickelacycles.

Hoberg et al. [137] published in the 1980s a series of air-stable complexes where $CO_2$, a suitable Ni precursor and an unsaturated substrate, forms a series of metallocyclic complexes incorporating a carboxylate (O = C–O) moiety. As

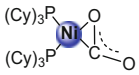


**Fig. 7** A $\eta^2$-(C,O) chelating $CO_2$ complex reported by Aresta et al.

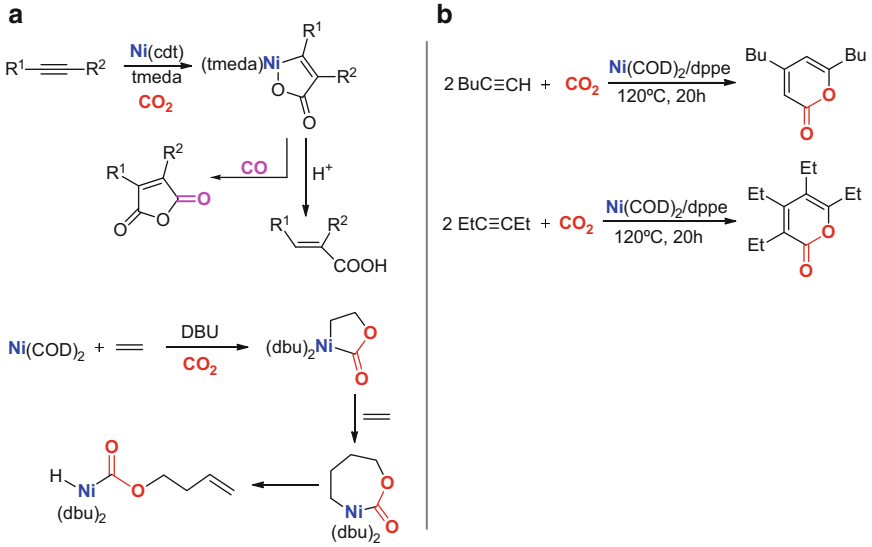


**Scheme 23** (**a**) Hoberg's work on oxa-nickelacycles (cdt = cyclododeca-1,5,9-triene; COD = 1,5-cyclooctadiene; tmeda = tetramethylethylenediamine; dbu = 1,8-diazabicyclo[5.4.0] undec-7-ene) and (**b**) Inoue's work on quinone synthesis from alkynes

illustrated in Scheme 23a, these metallocycles can be useful precursors for other compounds by expanding the ring through incorporation of more ethene molecules or through ring opening to form unsaturated carboxylic structures. A clear disadvantage is the lack of true catalytic turnover, an aspect that has recently regained the attention of the scientific communities focusing on the direct coupling of alkenes and $CO_2$ [138–140]. An oxa-nickelacycle is also an important intermediate in the quinone synthesis from alkynes and $CO_2$ described by Inoue (Scheme 23b) [128].

Strained rings can be easily carboxylated [141], and the final product can vary in structural nature, but all reactions are formally $CO_2$ insertion reactions into C–C bonds. A major drawback, however, is that generally the reaction intermediate is a highly stable metallocycle. The lactone formation reaction is promoted by transition metals such as Ni or Rh, but the chemistry has little practical use as it requires stoichiometric amounts of metal with TONs rarely exceeding 1 making these processes far from economically acceptable. Recent work [138–140] has indicated that a delicate catalyst design may help to overcome these limitations in the (near) future.

The ability of Ni(0) to bind both unsaturated species (i.e., alkenes and alkynes) and $CO_2$ was further demonstrated by Tsuda et al. who prepared bicyclic $\alpha$-pyrones

by treating $\alpha$-,$\omega$-diynes under high $CO_2$ pressure (~50 bar) and in the presence of a Ni(COD)-bis-trialkylphosphine pre-catalyst (10 mol%) [142]. Tailoring the ligand further, i.e., by using a *N*-heterocyclic carbene ligand (IPr) [143], led to significant improvement in catalyst efficiency and yields (>80%) of the $\alpha$-pyrone products and allowed lowering of the metal loading (typically 5 mol%) needed for fast enough turnover and the pressure of $CO_2$ to 1 bar. This process can be considered a formal [2 + 2 + 2] cycloaddition reaction between diynes and $CO_2$. In Scheme 24a, the proposed mechanism for this reaction shows both a Ni(0)-bis-alkyne-$CO_2$ adduct and an oxa-nickelacycle intermediate.

Coupling between two alkynes has found useful applications in synthetic chemistry; it has been applied to the preparation of arylnaphthalene lignan lactones which are valuable natural products (Scheme 24b) with promising anticancer and antiviral properties. In this case, the alkynes were present in different precursor molecules, and the catalyst used was based on AgI. Anastas et al. [144] envisioned that the cross-coupling reaction between phenylacetylene, $CO_2$, and 3-bromo-1-

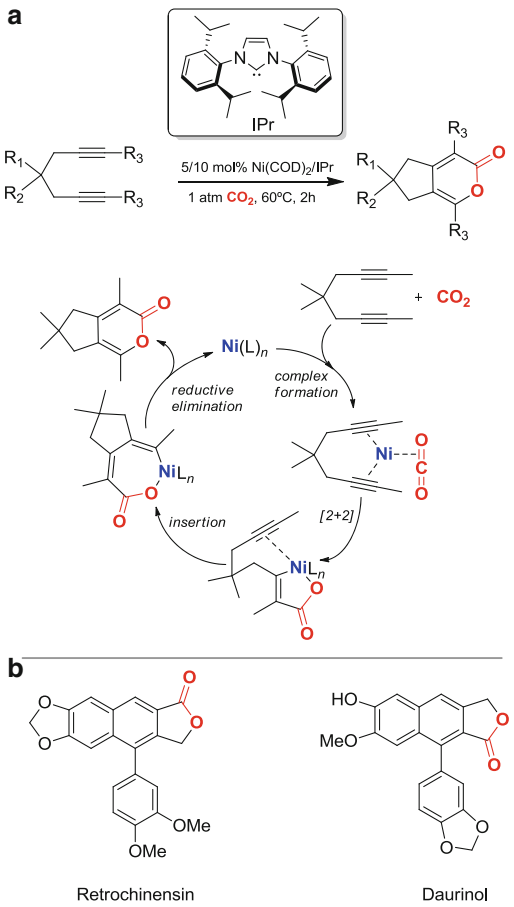


**Scheme 24** (**a**) Reaction mechanism proposed by Tekavec et al. for the formation of bicyclic $\alpha$-pyrones from diynes and $CO_2$. (**b**) Examples of natural products based on the $\alpha$-pyrone core

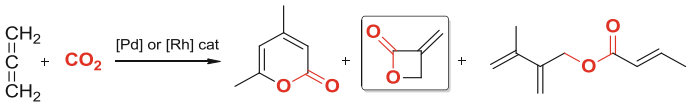


**Scheme 25** Possible products derived from the reaction of allenes and $CO_2$

phenyl-1-propyne would generate the corresponding 1,6-diyne which could then subsequently cyclize to the naphthalene core through a formal [2 + 2 + 2] cycloaddition.

Allenes can also be transformed into pyrones (Scheme 25) [145] albeit in lower yields to 4-membered lactones, which is the result of a formal [2 + 2] addition of both cumulenes, $CO_2$ and the allene. In both cases, the catalysts employed were based on noble metals such as Pd and Rh. This [2 + 2] addition represents the first example of this type of coupling reaction obtained by using $CO_2$ as a reagent. Allenes and $CO_2$ are *iso*electronic, but the energy gap between the HOMO (highest occupied molecular orbital) and LUMO (lowest occupied molecular orbital) is large; therefore, *homo*-coupling is energetically favored. In order to make the hetero-coupling reaction possible, optimization of the reaction conditions is essential to control the chemo-selectivity of the reaction. In order to stir the chemo-selectivity toward the 4-membered lactone product, high $CO_2$ pressures combined with low $H_2$ pressures and room temperature conditions are necessary. Despite all the efforts made, only limited yields of the lactone products were obtained, and therefore more sophisticated catalysts are required to make this process more attractive.

## 8 Outlook

This book chapter intends to give an overview of the most recent developments of the catalytic coupling of $CO_2$ with various reaction partners to give cyclized products while maintaining the formal oxidation state of the carbon center. Thus, these reactions are regarded as non-reductive couplings. Rather than giving a comprehensive overview of all the literature that has appeared over the years, typical examples of each class of coupling reaction involving $CO_2$ as a key reagent have been discussed emphasizing the synthetic merits and challenges that (still) need to be overcome. These coupling reactions involve the formation of saturated and unsaturated cyclic carbonates, oxazolidinones, imidazolidinones, cyclic ureas, quinazoline derivatives, and various lactone-based molecules. Despite this wealth of distinct and useful methodology yet developed, there still exists a need to expand the use of $CO_2$ as a coupling partner to get access to other types of (functional) molecules where the formal oxidation state of the $CO_2$ coupling partner may change through the catalytic event making the process a formal reductive coupling step [146]. It is not likely that the efforts to develop new and improved catalytic processes will lead to a net reduction of the global $CO_2$ emissions that we are currently facing, but its use as a carbon feedstock that is cheap, renewable, basically

nontoxic, and readily available in large quantities may help to present a viable carbon feedstock alternative for our fossil fuel-based economies. In this respect, research devoted to the design and implementation of modular, selective, and highly active catalysts can be regarded as a key strategy toward the increase of sustainable chemical processing. In the near future, this may help to preserve our standard of living and improving (where necessary) problems associated with raw material usage, energy consumption, and waste management. Undoubtedly, organometallic chemistry will continue to be an important discipline that can contribute both from a fundamental and application point of view providing the knowledge to create our future catalysts required in fine chemical and bulk chemical synthesis.

## References

1. Aresta M (2010) Carbon dioxide as chemical feedstock. Wiley-VCH, Weinheim
2. Peters M, Köhler B, Kuckshinrichs W, Leitner W, Markewitz P, Müller TE (2011) ChemSusChem 4:1216–1240
3. Cokoja M, Bruckmeier C, Rieger B, Herrmann WA, Kühn FE (2011) Angew Chem Int Ed 50:8510–8537
4. Martín R, Kleij AW (2011) ChemSusChem 4:1259–1263
5. Sakakura T, Choi J-C, Yasuda H (2007) Chem Rev 107:2365–2387
6. Decortes A, Castilla AM, Kleij AW (2010) Angew Chem Int Ed 49:9822–9837
7. Mikkelsen M, Jørgensen M, Krebs FC (2010) Energy Environ Sci 3:43–81
8. Darensbourg DJ (2007) Chem Rev 107:2388–2410
9. Boogaerts IIF, Nolan SP (2011) Chem Commun 47:3021–3024
10. North M, Pasquale R, Young C (2010) Green Chem 12:1514–1539
11. Pescarmona PP, Taherimehr M (2012) Catal Sci Technol 2:2169–2187
12. Maeda C, Miyazaki Y, Ema T (2014) Catal Sci Technol 4:1482–1497
13. Yoshida M, Ihara M (2004) Chem Eur J 10:2886–2893
14. Sakakura T, Kohno K (2009) Chem Commun: 1312–1330
15. Schäffner B, Schäffner F, Verevkin SP, Börner A (2010) Chem Rev 110:4554–4581
16. Zhang H, Liu H-B, Yue J-M (2013) Chem Rev 114:883–898
17. He Q, O'Brien JW, Kitselman KA, Tompkins LE, Curtis GCT, Kerton FM (2014) Catal Sci Technol 4:1513–1528
18. Whiteoak CJ, Nova A, Maseras F, Kleij AW (2012) ChemSusChem 5:2032–2038
19. Chatelet B, Joucla L, Dutasta J-P, Martinez A, Szeto KC, Dufaud V (2013) J Am Chem Soc 135:5348–5351
20. Tsutsumi Y, Yamakawa K, Yoshida M, Ema T, Sakai T (2010) Org Lett 12:5728–5731
21. Qi C, Ye J, Zeng W, Jiang H (2010) Adv Synth Catal 352:1925–1933
22. Zhou H, Zhang W-Z, Liu C-H, Qu J-P, Lu X-B (2008) J Org Chem 73:8039–8044
23. Sit WN, Ng SM, Kwong KY, Lau CP (2005) J Org Chem 70:8583–8586
24. Doll KM, Erhan SZ (2005) Green Chem 7:849–854
25. Kawanami H, Ikushima Y (2000) Chem Commun: 2089–2090
26. Sugimoto H, Inoue S (1998) Pure Appl Chem 70:2365–2369
27. Ishida N, Shimamoto Y, Murakami M (2012) Angew Chem Int Ed 51:11750–11752
28. Coates GW, Moore DR (2004) Angew Chem Int Ed 43:6618–6639
29. Ratzenhofer M, Kisch H (1980) Angew Chem Int Ed Engl 19:317–318
30. Caló V, Nacci A, Monopoli A, Fanizzi A (2002) Org Lett 4:2561–2563

31. Kasuga K, Kabata N, Kato T, Sugimori T, Handa M (1998) Inorg Chim Acta 278:223–225
32. Kasuga K, Nagao S, Fukumoto T, Handa M (1996) Polyhedron 15:69–72
33. Ji D, Lu X, He R (2000) Appl Cat A Gen 203:329–333
34. Taherimehr M, Al-Amsyar SM, Whiteoak CJ, Kleij AW, Pescarmona PP (2013) Green Chem 15:3083–3090
35. Paddock RL, Nguyen ST (2001) J Am Chem Soc 123:11498–11499
36. Lu X-B, Feng X-J, He R (2002) Appl Cat A Gen 234:25–33
37. Shen Y-M, Duan W-L, Shi M (2003) J Org Chem 68:1559–1562
38. Darensbourg DJ, Fang CC, Rodgers JL (2004) Organometallics 23:924–927
39. Jing H, Edulji SK, Gibbs JM, Stern CL, Zhou H, Nguyen ST (2004) Inorg Chem 43: 4315–4327
40. Lu X-B, Zhang Y-J, Jin K, Luo L-M, Wang H (2004) J Catal 227:537–541
41. Whiteoak CJ, Salassa G, Kleij AW (2012) Chem Soc Rev 41:622–631
42. Tokunaga M, Larrow JF, Kakiuchi F, Jacobsen EN (1997) Science 277:936–938
43. Darensbourg DJ, Phelps AL (2005) Inorg Chem 44:4622–4629
44. Darensbourg DJ, Bottarelli P, Andreatta JR (2007) Macromolecules 40:7727–7729
45. Darensbourg DJ, Yarbrough JC (2002) J Am Chem Soc 124:6335–6342
46. Darensbourg DJ, Yarbrough JC, Ortiz C, Fang CC (2003) J Am Chem Soc 125:7586–7591
47. Monassier A, D'Elia V, Cokoja M, Dong H, Pelletier JDA, Basset J-M, Kühn FE (2013) ChemCatChem 5:1321–1324
48. Decortes A, Kleij AW (2011) ChemCatChem 3:831–834
49. Clegg W, Harrington RW, North M, Pasquale R (2010) Chem Eur J 16:6828–6843
50. Whiteoak CJ, Martin E, Escudero-Adán EC, Kleij AW (2013) Adv Synth Catal 355: 2233–2239
51. Kielland N, Whiteoak CJ, Kleij AW (2013) Adv Synth Catal 355:2115–2138
52. Zhang W, Loebach JL, Wilson SR, Jacobsen EN (1990) J Am Chem Soc 112:2801–2803
53. Irie R, Noda K, Ito Y, Matsumoto N, Katsuki T (1990) Tetrahedron Asymmetry 2:481–494
54. Jacobsen EN (2000) Acc Chem Res 33:421–431
55. Aresta M, DiBenedetto A, Gianfrate L, Pastore C (2003) Appl Catal A Gen 255:5–11
56. Lu X-B, Liang B, Zhang Y-J, Tian Y-Z, Wang Y-M, Bai C-X, Wang H, Zhang R (2004) J Am Chem Soc 126:3732–3733
57. Jin L, Huang Y, Jing H, Chang T, Yan P (2008) Tetrahedron Asymmetry 19:1947–1953
58. Vincens V, Borgne AL, Spassky N (1989) Makromol Chem Rapid 10:623–628
59. Lu X-B, He R, Bai C-X (2002) J Mol Catal A Chem 186:1–11
60. Lu X-B, Zhang YJ, Liang B, Wang H (2004) J Mol Catal A Chem 210:31–34
61. Achard TRJ, Clutterbuck LA, North M (2005) Synlett: 1828–1847
62. Li F, Xia C, Xu L, Sun W, Chen G (2003) Chem Commun: 2042–2043
63. Srivastava R, Bennur TH, Srinivas D (2005) J Mol Catal A Chem 226:199–205
64. Man ML, Lam KC, Sit WN, Ng SM, Zhou Z, Lin Z, Lau CP (2006) Chem Eur J 12: 1004–1015
65. Darensbourg DJ, Horn A Jr, Moncada AI (2010) Green Chem 12:1376–1379
66. Decortes A, Martínez Belmonte M, Benet-Buchholz J, Kleij AW (2010) Chem Commun 46: 4580–4582
67. Castro-Gómez F, Salassa G, Kleij AW, Bo C (2013) Chem Eur J 19:6289–6298
68. Haak RM, Wezenberg SJ, Kleij AW (2010) Chem Commun 46:2713–2723
69. Ren W-M, Liu Z-W, Wen Y-Q, Zhang R, Lu X-B (2009) J Am Chem Soc 131:11509–11518
70. For a recent example see: Ema T, Miyazaki Y, Koyama S, Yano Y, Sakai T (2012) Chem Commun 48:4489–4491
71. Melendez J, North M, Villuendas P (2009) Chem Commun:2577–2579
72. Meléndez J, North M, Pasquale R (2007) Eur J Inorg Chem 21:3323–3326
73. North M, Wang B, Young C (2011) Energy Environ Sci 4:4163–4170
74. Tian D, Liu B, Gan Q, Li H, Darensbourg DJ (2012) ACS Catal 2:2029–2035
75. Liu Y, Ren W-M, Liu J, Lu X-B (2013) Angew Chem Int Ed 52:11594–11598

76. Darensbourg DJ, Chung W-C, Wilson SJ (2013) ACS Catal 3:3050–3057
77. Luo R, Zhou X, Chen S, Li Y, Zhou L, Ji H (2014) Green Chem 16:1496–1506
78. Buchard A, Kember MR, Sandeman KG, Williams CK (2011) Chem Commun 47:212–214
79. Escárcega-Bobadilla MV, Martínez Belmonte M, Martin E, Escudero-Adán EC, Kleij AW (2013) Chem Eur J 19:2641–2648
80. Chang T, Jin L, Jing H (2009) ChemCatChem 1:379–383
81. Jessop PG, Subramaniam B (2007) Chem Rev 107:2666–2694
82. Minakata S, Sasaki I, Ide T (2010) Angew Chem Int Ed 49:1309–1311
83. Wu J, Kozak JA, Simeon F, Hatton TA, Jamison TF (2014) Chem Sci 5:1227–1231
84. Yang X, Wu J, Mao X, Jamison TF, Hatton TA (2014) Chem Commun 50:3245–3248
85. Yamada W, Sugawara Y, Cheng HM, Ikeno T, Yamada T (2007) Eur J Org Chem 2604–2607
86. Yoshida S, Fukui K, Kikuchi S, Yamada T (2009) Chem Lett 38:786–787
87. Costa M, Chiusoli GP, Rizzardi M (1996) Chem Commun:1699–1700
88. Ca ND, Gabriele B, Ruffolo G, Veltri L, Zanetta T, Costa M (2011) Adv Synth Catal 353: 133–146
89. Yoshida S, Fukui K, Kikuchi S, Yamada T (2010) J Am Chem Soc 132:4072–4073
90. Tang X, Qi C, He H, Jiang H, Ren Y, Yuan G (2013) Adv Synth Catal 355:2019–2028
91. Diekema D, Jones R (2000) Drugs 59:7–16
92. Pandit N, Singla RK, Shrivastava B (2012) Indo Global J Pharm Sci 2:245–249
93. Shaw KJ, Barbachyn MR (2011) Ann NY Acad Sci 1241:48–70
94. Michalska K, Karpiuk I, Król M, Tyski S (2013) Bioorg Med Chem 21:577–591
95. Zappia G, Cancelliere G, Gacs-Baitz E, Delle Monache G, Misiti D, Nevola L, Botta B (2007) Curr Org Synth 4:238–309
96. Evans DA, Takacs JM, McGee LR, Ennis MD, Mathre DJ, Bartroli J (1981) Pure Appl Chem 53:1109–1127
97. Green R, Peed J, Taylor JE, Blackburn RAR, Bull SD (2013) Nat Protoc 8:1890–1906
98. For a recent example see: Nale DB, Rana S, Parida K, Bhanage BM (2014) Appl Catal A Gen 469:340–349
99. Sibi MP, Deshpande PK, Ji J (1995) Tetrahedron Lett 36:8965–8968
100. Buchstaller H-P (2003) J Comb Chem 5:789–793
101. Mizuno T, Takahashi J, Ogawa A (2002) Tetrahedron 58:7805–7808
102. Pulla S, Felton CM, Ramidi P, Gartia Y, Ali N, Nasini UB, Ghosh A (2013) J CO2 Utiliz 2:49–57
103. Tascedda P, Dunach E (2000) Chem Commun:449–450
104. Sudo A, Morioka Y, Koizumi E, Sanda F, Endo T (2003) Tetrahedron Lett 44:7889–7891
105. Hancock MT, Pinhas AR (2003) Tetrahedron Lett 44:5457–5460
106. Miller AW, Nguyen ST (2004) Org Lett 6:2301–2304
107. Wu Y, He L-N, Du Y, Wang J-Q, Miao C-X, Li W (2009) Tetrahedron 65:6204–6210
108. Fontana F, Chen CC, Aggarwal VK (2011) Org Lett 13:3454–3457
109. Soga K, Hosoda S, Nakamura H, Ikeda S (1976) J Chem Soc Chem Commun 16:617
110. Kawanami H, Ikushima Y (2002) Tetrahedron Lett 43:3841–3844
111. Seayad J, Seayad AM, Ng JKP, Chai CLL (2012) ChemCatChem 4:774–777
112. Du Y, Wu Y, Liu A-H, He L-N (2008) J Org Chem 73:4709–4712
113. Phung C, Ulrich RM, Ibrahim M, Tighe NTG, Lieberman DL, Pinhas AR (2011) Green Chem 13:3224–3229
114. Nomura R, Matsuda H, Baba A, Kori M, Ogawa S (1985) Ind Eng Chem Prod Res Dev 24: 239–242
115. Pulla S, Felton CM, Gartia Y, Ramidi P, Ghosh A (2013) ACS Sust Chem Eng 1:309–312
116. Dinsmore CJ, Mercer SP (2004) Org Lett 6:2885–2888
117. Kodaka M, Tomohiro T, Okuno H (1993) J Chem Soc Chem Commun 81–82
118. Mitsudo T-A, Hori Y, Yamakawa Y, Watanabe Y (1987) Tetrahedron Lett 28:4417–4418
119. Chiusoli GP, Costa M, Gabriele B, Salerno G (1999) J Mol Catal Chem 143:297–310
120. Shi M, Shen Y-M (2002) J Org Chem 67:16–21

121. Meessen JH (2005) "Urea", Ullmann's encyclopedia of industrial chemistry. Wiley-VCH, Weinheim, pp 657–693
122. Mizuno T, Okamoto N, Ito T, Miyata T (2000) Tetrahedron Lett 41:1051–1053
123. Patil YP, Tambade PJ, Jagtap SR, Bhanage BM (2008) Green Chem Lett Rev 1:127–132
124. Kimura T, Kamata K, Mizuno N (2012) Angew Chem Int Ed 51:6700–6703
125. Kimura T, Sunaba H, Kamata K, Mizuno N (2012) Inorg Chem 51:13001–13008
126. Fujita S-I, Tanaka M, Arai M (2014) Catal Sci Technol 4:1563–1569
127. Aresta M, Nobile CF, Albano VG, Forni E, Manassero M (1975) J Chem Soc Chem Commun 636–637
128. Inoue Y, Itoh Y, Hashimoto H (1977) Chem Lett 855–856
129. Inoue Y, Itoh Y, Hashimoto H (1978) Chem Lett 633–634
130. Inoue Y, Hibi T, Satake M, Hashimoto H (1979) J Chem Soc Chem Commun:982–982
131. Sasaki Y, Inoue Y, Hashimoto H (1976) J Chem Soc Chem Commun:605–606
132. Musco A, Perego C, Tartiari V (1978) Inorg Chim Acta 28:L147–L148
133. Behr A, He R, Juszak KD, Krueger C, Tsay YH (1986) Chem Ber 119:991–1015
134. Behr A, Bahke P, Becker M (2004) Chem Ing Tech 76:1828–1832
135. Behr A, Heite M (2000) Chem Ing Tech 72:58–61
136. Nakano R, Ito S, Nozaki K (2014) Nat Chem 6:325–331
137. Hoberg H, Peres Y, Krueger C, Tsay YH (1987) Angew Chem 99:799–800
138. Huguet N, Jevtovikj I, Gordillo A, Lejkowski ML, Lindner R, Bru M, Khalimon AY, Rominger F, Schunk SA, Hofmann P, Limbach M (2014) Chem Eur J 51:16858–16862
139. Hendriksen C, Pidko EA, Yang G, Schäffner B, Vogt D (2014) Chem Eur J 51:12037–12040
140. Lejkowski ML, Lindner R, Kageyama T, Bódizs GÉ, Plessow PN, Müller IB, Schäfer A, Rominger F, Hofmann P, Futter C, Schunk SA, Limbach M (2012) Chem Eur J 18: 14017–14025
141. Behr A, Thelen G (1984) C1 Mol Chem 1:137–153
142. Tsuda T, Morikawa S, Sumiya R, Saegusa T (1988) J Org Chem 53:3140–3145
143. Louie J, Gibby JE, Farnworth MV, Tekavec TN (2002) J Am Chem Soc 124:15188–15189
144. Foley P, Eghbali N, Anastas PT (2010) J Nat Prod 73:811–813
145. Doehring A, Jolly PW (1980) Tetrahedron Lett 21:3021–3024
146. See for a recent example: Das Neves Gomes C, Jacquet O, Villiers C, Thuéry P, Ephritikhine M, Cantat T (2012) Angew Chem Int Ed 51:187–190

Top Organomet Chem (2016) 53: 73–100
DOI: 10.1007/3418_2015_96

Published online: 29 March 2015

# Silver-Catalyzed Carboxylation Reaction Using Carbon Dioxide as Carboxylative Reagent

**Wen-Zhen Zhang**

**Abstract** The transformation of carbon dioxide into value-added fine chemicals via homogeneous catalysis has gained much attention since carbon dioxide is an abundant, nontoxic, and inexpensive C1 feedstock. Silver catalysis has emerged as important synthetic methods for a wide range of organic transformations in the last two decades. In silver-catalyzed carboxylation reactions using carbon dioxide as a carboxylative reagent, silver(I) salts or complexes generally serve as a π-Lewis acid catalyst to activate unsaturated systems, especially alkynes, or in situ generate silver acetylides or arylsilver intermediates as reactive carbon nucleophiles. In this chapter, silver-catalyzed cyclization reactions of propargylic alcohols or amines, *o*-alkynylanilines, and alkynyl ketones with carbon dioxide are reviewed. Also, silver-catalyzed carboxylation of terminal alkynes and arylboronic esters with carbon dioxide is documented.

**Keywords** Alkynyl ketone · Arylboronic esters · Carbon dioxide · Carboxylation · Cyclization reaction · *o*-Alkynylaniline · Propargylic alcohol · Propargylic amine · Rearrangement · Silver · Terminal alkyne

## Contents



W.-Z. Zhang (✉)
State Key Laboratory of Fine Chemicals, Dalian University of Technology, Dalian 116024, China
e-mail: zhangwz@dlut.edu.cn

## 1 Introduction

In the past decades, the rapid increase of carbon dioxide concentration in the atmosphere and its significant impact on the environment has become an important issue in the world. This has prompted great efforts to reduce carbon dioxide emission and, more importantly, to develop efficient catalytic processes to transform this main greenhouse gas into value-added chemicals, since for chemist, carbon dioxide is an abundant, nontoxic, and inexpensive C1 feedstock [1–16].

From a structural point of view, carbon dioxide can be considered to be an electrophile, which can be used in carboxylation reaction with various nucleophiles [3, 5, 11]. Attack at its weakly electrophilic carbon center by an oxygen, nitrogen, or carbon nucleophile affords carbonates, carbamates, or carboxylic acids and their derivatives, respectively. Due to the thermodynamic and kinetic stability of carbon dioxide, high-energy molecules are often used as substrates, and in most cases, transition-metal catalysts play an important role and allow efficient and selective reactions under mild conditions. Depending on the structural properties of substrates, nickel-, copper-, rhodium-, palladium-, and silver-catalyzed carboxylation reactions of various nucleophiles with carbon dioxide have been developed recently [1–16]. In this chapter, we focus on silver-catalyzed carboxylation reactions of various substrates to yield various synthetically important compounds.

As a precious metal, silver has been known and used extensively since ancient times. In organic chemistry, silver(I) compounds are usually used as halogen scavengers or oxidants and used in stoichiometric amounts. Silver(I)-catalyzed organic transformations have not been gained much chemists' attentions until two decades ago. At present, silver catalysis covers a variety of chemical reaction including cycloaddition, cycloisomerization, allylation, aldol reactions, carbene-transfer reactions, and C–H bond activation [17–25]. Generally, silver(I) salts serve as a σ-Lewis acid and/or π-Lewis acid in homogeneous catalysis. The $d^{10}$ electronic configuration makes silver(I) cation prefers interacting with unsaturated systems, especially alkynes. This alkynophilicity makes silver(I) salts an effective catalyst for alkyne activation. Upon coordination to silver(I) salts, alkyne moiety is prone to nucleophilic attack by a relatively weak nucleophile, for example, carboxylate group in situ generated by reaction of carbon dioxide with oxygen, nitrogen, or carbon nucleophiles. For terminal alkynes, silver acetylides can be formed in the presence of a suitable base and react with carbon dioxide as a carbon nucleophile. On the basis of the above characteristics of silver(I) catalysis, in this chapter, silver-catalyzed cyclization reactions of propargylic alcohols or amines, *o*-alkynylanilines, and alkynyl ketones with carbon dioxide are reviewed.

Also, silver-catalyzed carboxylation of terminal alkynes and arylboronic esters with carbon dioxide is documented.

## 2 Silver-Catalyzed Cyclization Reactions of Propargylic Alcohols and Amines with Carbon Dioxide

Cyclic carbonates and carbamates are versatile intermediates in organic synthesis. They have found wide applications in the syntheses of many biologically active compounds such as pharmaceuticals and agrochemicals. The cyclization reactions of propargylic alcohols and amines with carbon dioxide provide an attractive method to synthesize α-alkylidene cyclic carbonates and carbamates. Besides silver, this reaction can be catalyzed by transition metals such as copper [26–29], gold [30], cobalt [31], palladium [32–37], ruthenium [38, 39] catalyst, or phosphine [40–42], *N*-heterocycle carbene [43], superbase [44–47], and other reagents [48–51] under much harsher reaction conditions. With respect to the mechanism of transition-metal-catalyzed reactions, the carbonate or carbamate intermediates were generally thought to be first formed by the reaction of the propargylic alcohols or amines with carbon dioxide in the presence of a suitable base, which then conduct intramolecular nucleophilic attack on the activated alkyne moiety, yielding 5-*exo* cyclization products (Scheme 1). In this catalytic cycle, the transition-metal catalyst plays a crucial role to activate the triple bond upon π-coordination. Compared with other transition metals, silver catalysis shows many notable features including broad substrate scope, mild reaction condition (low temperature and pressure), high efficiency and selectivity, and operational simplicity.

In 2007, Yamada and coworker reported the first silver(I)-catalyzed cyclization reaction of propargylic alcohols with carbon dioxide [52]. Although other catalytic systems were previously reported, they suffered from a substrate scope limited to terminal alkynes or harsh reaction conditions. It is found that 10 mol% of silver perchlorate or silver *p*-toluenesulfonate efficiently catalyzed cyclization reaction of phenyl-substituted internal alkyne substrate **1a** with 2.0 MPa of carbon dioxide to give quantitatively α-alkylidene cyclic carbonate product **2a** in the presence of 1 equiv. of 1,8-diazabicyclo[5.4.0]undec-7-ene (DBU). Other π-Lewis acidic catalysts such as rhodium(III) acetylacetonate, platinum(II) chloride, palladium (II) chloride, copper(I) chloride, and gold(I) chloride gave no product. The counter anion of silver(I) salts had a notable effect on the catalytic activity. Further screening with alkyl-substituted internal alkyne substrate, which had not been reported as substrated for this class of transformation, reveals that the optimal conditions for this reaction include the use of silver(I) acetate as catalyst, toluene as the solvent, and 1.0 MPa of carbon dioxide pressure.

The optimized catalytic system proved to show a wide substrate scope with respect to the propargylic alcohols and convert terminal alkynes and aryl- or alkyl-substituted internal alkynes into corresponding α-alkylidene cyclic carbonates in

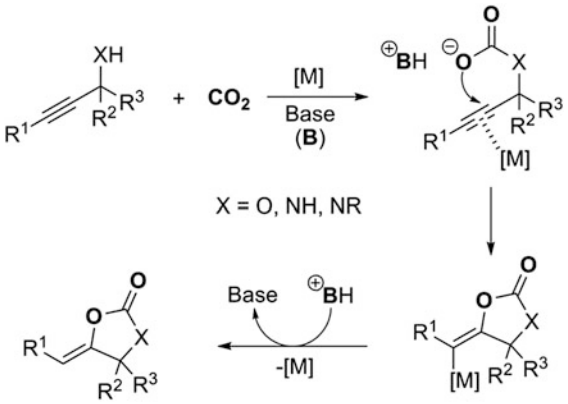


**Scheme 1** General mechanism for transition-metal-catalyzed cyclization reactions of propargylic alcohols and amines with carbon dioxide

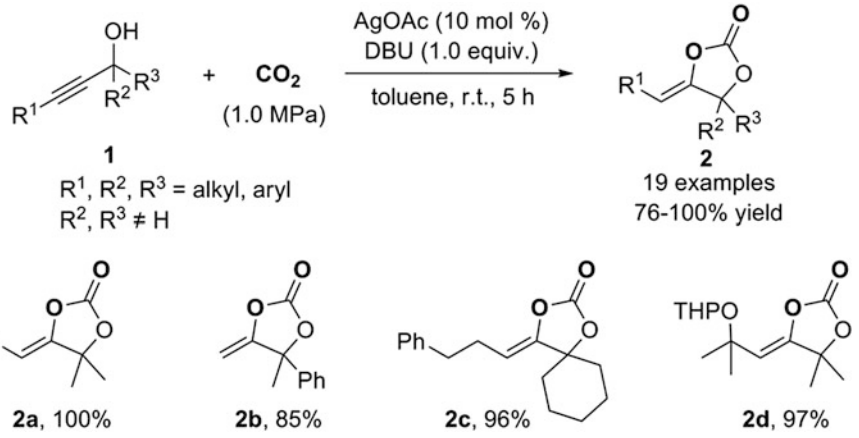


**Scheme 2** Silver-catalyzed cyclization reaction of propargylic alcohols with carbon dioxide

good to excellent yield (Scheme 2). By X-ray analysis and NOE experiments, the olefins in all products from internal alkynes have a *Z* configuration. The reaction can also be carried out with a lower catalyst loading (1 mol%) or under 0.1 MPa carbon dioxide pressure. It is noteworthy that propargylic position has to be fully substituted. Primary or secondary propargylic alcohols afford no α-alkylidene cyclic carbonate product with this catalytic system.

Later, Yamada and coworker found that the silver(I) catalytic system was efficient for cyclization reaction of propargylic amines with carbon dioxide under milder reaction conditions and a wider substrate scope (Scheme 3) [53]. Since the primary or secondary amines readily form relatively stable carbamate intermediate with carbon dioxide [54], the reaction of propargylic amines with carbon dioxide can be carried out at lower carbon dioxide pressure and in the absence of an external

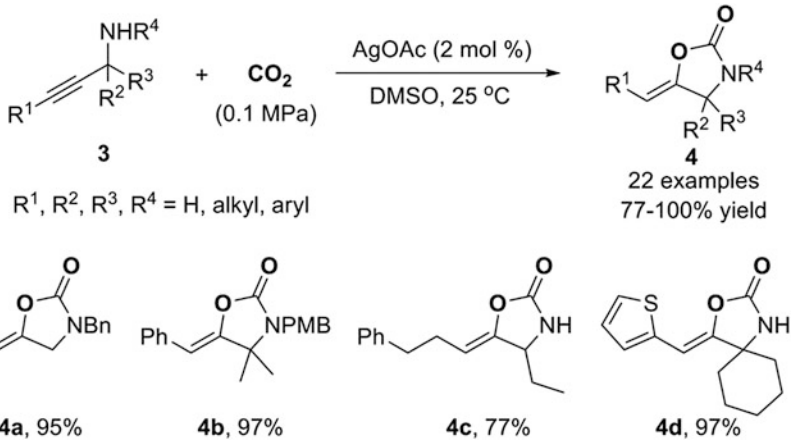


**Scheme 3** Silver-catalyzed cyclization reaction of propargylic amines with carbon dioxide

base such as DBU. In view of the stability of the carbamate intermediate, aprotic polar solvents, such as acetonitrile, *N*,*N*-dimethylformamide (DMF), *N*,*N*-dimethylacetamide (DMAc), and dimethyl sulfoxide (DMSO), were chosen as solvents for this reaction.

Using the optimized catalytic system (2 mol% silver acetate, 0.1 MPa carbon dioxide, DMSO as solvent, 25°C), a wide range of propargylic amines were converted into oxazolidinones in good to excellent yield. Similar to propargylic alcohols' reactions, aryl- or alkyl-substituted internal alkynes substrate which had not been accomplished using other catalytic system proved to be suitable substrate. Differing from propargylic alcohols' reaction system, primary or secondary propargylic amines reacted smoothly with carbon dioxide to furnish corresponding cyclic product in good yield. Likewise, *Z* isomer was found to be the sole product according to the X-ray analysis and NOE experiment.

At present, the concentration of carbon dioxide in air is about 0.04% (v/v). The direct use of air as a source of carbon dioxide and capturing and transforming atmospheric carbon dioxide into valuable products has become an important issue. In 2013, based on the DBU-mediated atmospheric carbon dioxide fixation using 4-(benzylamino)-2-butynyl carbonates and benzoates as substrates [46], Yoshida and coworker reported a more efficient system using silver nitrate/DBU dual catalyst for the reaction of propargylic amines with atmospheric carbon dioxide (Scheme 4) [55]. In the presence of silver nitrate and DBU in DMSO at 60°C, various propargylic amines reacted with carbon dioxide from air to afford the corresponding oxazolidinones in good yield. When alkyl-substituted internal alkyne substrates such as **3g** and **3h** are used, a little amount of 6-*endo* cyclization products are observed as by-products. The author proposed that DBU helped to trap carbon dioxide from air [56–58].

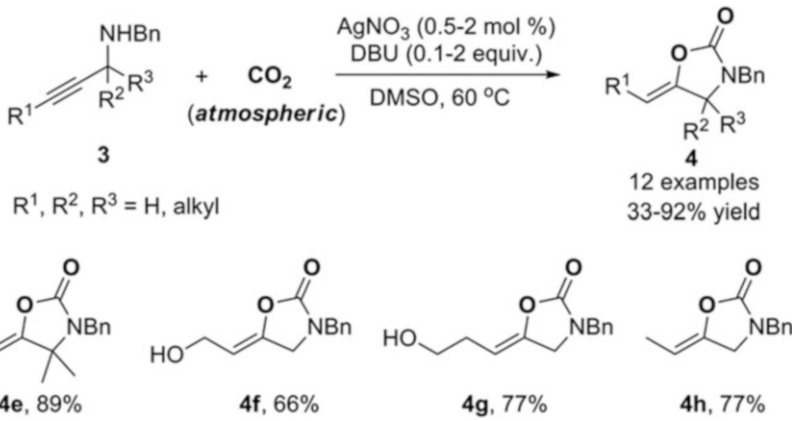


**Scheme 4** Silver-catalyzed cyclization reaction of propargylic amine with atmospheric carbon dioxide

On the basis of cyclization mechanism for the reaction of propargylic alcohol with carbon dioxide (Scheme 1), the reaction of bispropargylic alcohols substrate would give the enantiomerically enriched alkynyl-substituted α-alkylidene cyclic carbonate products with the use of chiral silver(I) catalyst. In 2010, Yamada and coworker reported an enantioselective silver-catalyzed reaction of bispropargylic alcohols with carbon dioxide (Scheme 5) [59, 60]. At the beginning of the study, the combination of silver acetate with many chiral ligands such as ferrocene derivatives, BINAP, BOX, and Py-BOX was used as catalysts for the reaction of substrate **5a** and carbon dioxide in the presence of a stoichiometric or catalytic amount of DBU. The reactions give high yields of product **6a**, but no enantioselectivity is observed presumably due to the strong affinity between silver cation and DBU. When the chiral Schiff base ligand synthesized from 1,2-diaminocyclohexane and 2-pyridinecarboxyaldehyde is used without DBU, moderate enantioselectivity is obtained. Further modification of the ligand backbone revealed that ketimine ligand **7** is optimal. It is proposed that ligand **7** coordinates 2 equiv. of silver acetate to form the active catalyst. Using this catalyst in chloroform at 5°C, a variety of aryl-substituted bispropargylic alcohols, regardless of the electron nature of the substituents, are converted into the corresponding cyclic carbonate products in excellent yield and good enantioselectivity. The alkyl-substituted bispropargylic alcohol **5d** gave high yield of product **6d** with moderate enantioselectivity (Scheme 5).

The chiral cyclic carbonate product obtained can be readily hydrolyzed to α-hydroxyketone in good yield with no erosion of ee using aqueous NaOH. Also, convenient aminolysis of those products with primary, secondary, or allyl amines affords the corresponding chiral carbamates in good yield without the change of their optical purity [61]. It should be mentioned that a silver acetate/DBU-catalyzed one-pot synthesis of α-oxoalkyl carbamates from propargylic alcohols, secondary amines, and carbon dioxide in 1,4-dioxane at 90°C was also reported by Jiang and coworkers [62]. When this reaction system was carried out in supercritical carbon

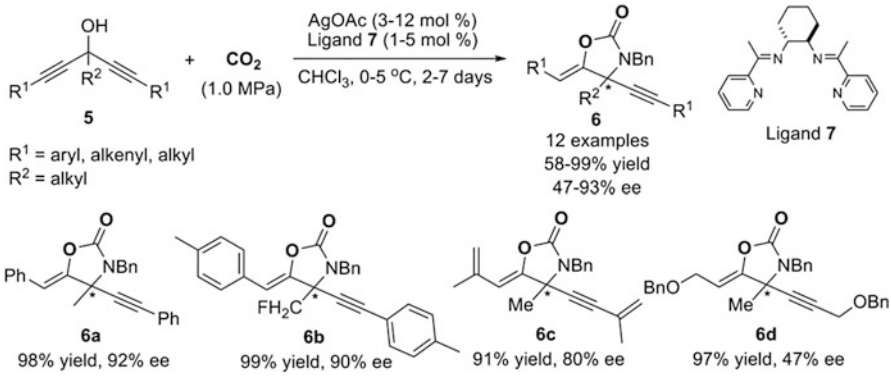


**Scheme 5** Enantioselective silver-catalyzed cyclization reaction of bispropargylic alcohols with carbon dioxide

dioxide without the use of organic solvent, 4-alkylidene-1,3-oxazolidin-2-ones are formed as main products [63].

In 2013, Jiang and coworker successfully prepared a polystyrene-supported *N*-heterocyclic carbene silver complex (PS-NHC-Ag **8**), a stable and efficient catalyst for the cyclization reaction of propargylic alcohol with carbon dioxide (Scheme 6) [64]. The supported silver catalyst can promote the reaction in the absence of an organic base such as DBU. Compared to the supported copper catalyst counterpart, the silver catalyst shows much higher catalytic activity and stability at lower carbon dioxide pressure. Although the substrate scope is limited to terminal tertiary and secondary propargylic alcohols, the supported silver catalyst offers significant advantages, such as simple workup procedures and ease of recycle and reuse. After the reaction, this supported catalyst can be readily separated from the products by filtration and reused 15 times without loss of its catalytic activity.

As mentioned above, the silver-catalyzed cyclization reaction of propargylic amines with carbon dioxide can be realized in the absence of an external base (Scheme 3). Inspired by silver-catalyzed intramolecular carboxylative addition of *o*-alkynylanilines with carbon dioxide and rearrangement (see next part, Scheme 12), Yamada and coworkers revealed that the silver-catalyzed cyclization reaction of propargylic amines with carbon dioxide in the presence of DBU at relatively high temperature does not give oxazolidinones but tetramic acid from intramolecular rearrangement (Scheme 7) [65], which is frequently found as basic structural element in many natural products and biologically active compounds [66].

Using 10 mol% silver nitrate as the catalyst and DMSO or acetonitrile as the solvent at 60°C, the reaction of internal tertiary propargylic amines with carbon dioxide in the presence of 1 equiv. of potassium carbonate, potassium hydroxide, potassium *tert*-butoxide, triethylamine or *N*,*N*-diisopropylethylamine affords oxazolidinone products exclusively, while using strong organic bases such as DBU gives tetramic acid as the predominant product. It is found that reaction

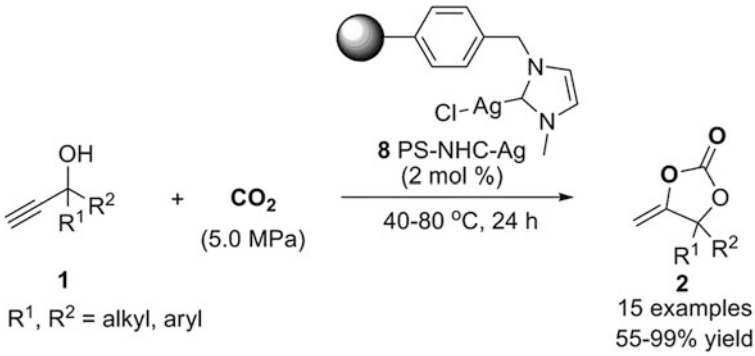


**Scheme 6** Polystyrene-supported silver catalysts for cyclization reaction of propargylic alcohol with carbon dioxide

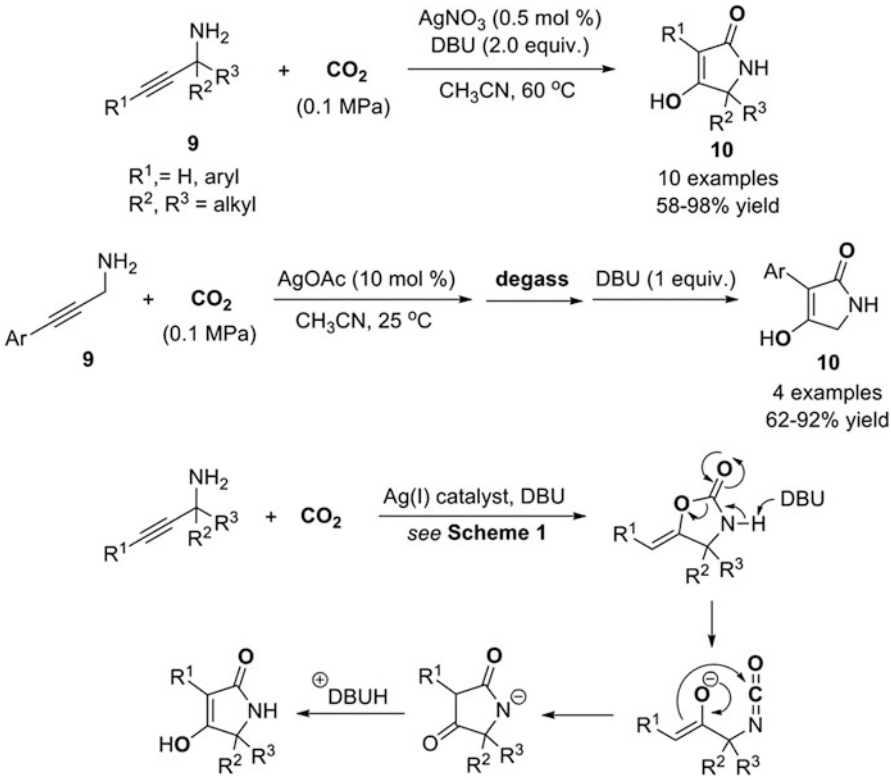


**Scheme 7** Silver-catalyzed cyclization reaction of propargylic amines with carbon dioxide and intramolecular rearrangement to afford tetramic acid

temperature has a profound effect on the product selectivity. At 10 or 20°C, the reaction still gives oxazolidinone product exclusively even in the presence of 2 equiv. of DBU. With the gradual elevation of the reaction temperature, the selectivity for the tetramic acid increases.

The silver nitrate/DBU system shows a broad substrate scope, and tertiary and secondary propargylic amines bearing different substituents are smoothly converted into corresponding tetramic acid products in good to excellent yield (Scheme 7). For the aryl-substituted internal primary propargylic amines, the stepwise procedures were carried out to avoid the formation of a complex mixture of products. Firstly the silver-catalyzed cyclization of primary propargylic amines with carbon dioxide generated oxazolidinone in the absence of DBU. Then the reaction system was degassed, and finally 1 equiv. of DBU was added to induce the rearrangement reaction to produce corresponding tetramic acid (Scheme 7).

A possible mechanism is that the silver-catalyzed cyclization of the propargylic amine with carbon dioxide forms the oxazolidinone, which is then deprotonated by DBU to generate an intermediate containing an isocyanate and an enolate moiety upon cleavage of the carbon–oxygen bond. Nucleophilic attack of the isocyanate by enolate finally affords the rearrangement product tetramic acid (Scheme 7).

It is abovementioned that the silver acetate/DBU catalytic system is not applicable to primary and secondary propargylic alcohols to give corresponding α-alkylidene cyclic carbonates. Recently, Yamada and coworker reported that in the presence of 10 mol% of silver acetate and 40 mol% of DBU, a series of 1-aryl-3-alkyl-substituted propargylic alcohol reacted with carbon dioxide in toluene at 30°C afford thermodynamically more stable vinylene carbonates [67]. They are thought to be produced by rapid double-bond isomerization of the initially formed α-alkylidene cyclic carbonates (Scheme 8).

During the study of the silver-catalyzed cyclization reaction of alkyl-substituted internal propargylic alcohols with carbon dioxide, Yamada and coworkers found that α,β-unsaturated carbonyl compounds, which might be formed by Meyer–Schuster rearrangement [68] of propargylic alcohol, are the main product when switching the solvent from toluene to dichloromethane or chlorobenzene [69]. It turned out that the solvent has an important effect on the product selectivity, and polar solvent formamide is found to be the best solvent for the formation of enones in high selectivity. In the presence of 10 mol% silver methanesulfonate and 1 equiv.

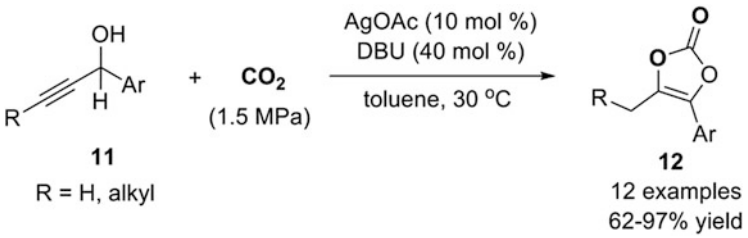


**Scheme 8** Silver-catalyzed cyclization reaction of 1-aryl-3-alkyl-substituted propargylic alcohols with carbon dioxide to give vinylene carbonates

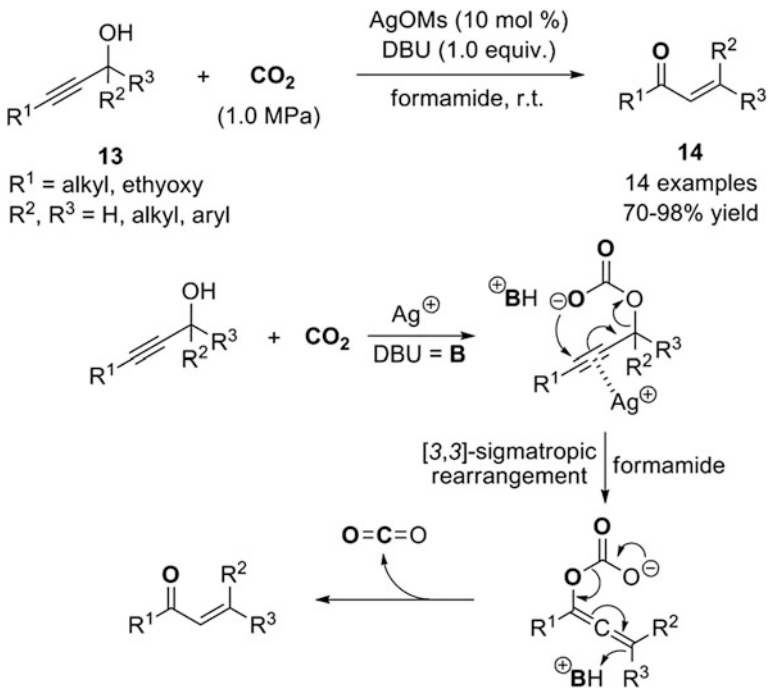


**Scheme 9** Silver-catalyzed carbon dioxide-mediated rearrangement of propargyl alcohols into α,β-unsaturated ketones

of DBU in formamide at room temperature, a variety of alkyl-substituted internal primary, secondary, and tertiary propargylic alcohols are converted into α,-β-unsaturated carbonyl compounds in good to excellent yields (Scheme 9).

In the proposed mechanism, the propargylic carbonate intermediate is first generated by the reaction of the propargylic alcohol with carbon dioxide in the presence of a base, and then β-carbon of the propargylic group is attacked by the carbonate in formamide solvent, which is different from the process of cyclic carbonate formation; to give allene carbonate intermediate via [3,3]-sigmatropic rearrangement, the release of carbon dioxide finally affords the enone product (Scheme 9). It should be noted that no reaction proceeds when the reaction is conducted in the nitrogen atmosphere instead of carbon dioxide. A labeling experiment using $C^{18}O_2$ shows that the oxygen atom in the enone product has totally come from carbon dioxide. The above experiments clearly demonstrate that this reaction is promoted by carbon dioxide, although there is no $CO_2$ moiety in the molecular structure of the product formally.

Recently, during the study of carbon dioxide-triggered and copper-catalyzed synthesis of highly substituted 3(2*H*)-furanones from propargylic alcohols and nitriles [70], Jiang and coworkers found that α-hydroxy ketones are formed in high yield and selectivity when silver acetate is used as a catalyst in the presence

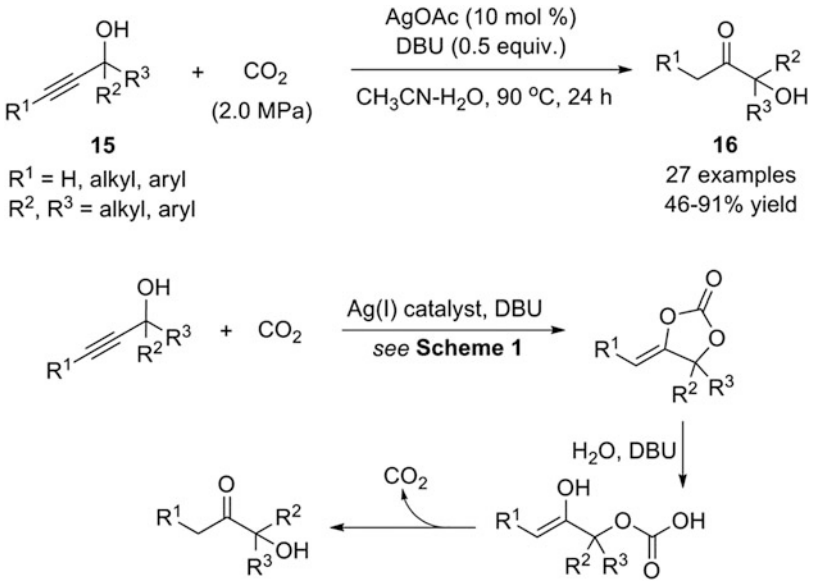


**Scheme 10** Silver-catalyzed carbon dioxide-mediated hydration of propargylic alcohols to synthesize tertiary α-hydroxy ketones

of 0.5 equiv. DBU at 70°C [71]. Further investigation shows that the yield of α-hydroxy ketones product increases when the reaction is conducted in acetonitrile/water mixed solvent at 90°C. Under the optimized reaction conditions, a wide range of tertiary propargylic alcohols are converted into synthetically important α-hydroxy ketones in moderate to good yields (Scheme 10). No reaction occurs under a nitrogen atmosphere rather than carbon dioxide. This indicates that carbon dioxide is involved in the catalytic cycle. Also, a stepwise experiment shows that the α-hydroxy ketone product probably is derived from the hydration of the initially formed α-alkylidene cyclic carbonate. Based on these observations, the author proposed that a silver-catalyzed cyclization reaction of the propargylic alcohol with carbon dioxide gives α-alkylidene cyclic carbonate firstly. Then the nucleophilic attack of a water molecule at the carbonyl group affords the alkylcarbonic acid intermediate. This is followed by keto-enol tautomerization, and the release of carbon dioxide finally forms the α-hydroxy ketone product (Scheme 10).

## 3 Silver-Catalyzed Reaction of *o*-Alkynylanilines with Carbon Dioxide

In 2013, Yamada and coworker reported a silver-catalyzed intramolecular carboxylative addition reaction of *o*-alkynylanilines with carbon dioxide to synthesize benzoxazine-2-ones via 6-*exo*-dig cyclization (Scheme 11) [72]. This

represents a highly attractive alternative to general approach to access this building block. Among the various metal salts investigated, palladium acetate, platinum chloride, copper(I) bromide, gold(I) chloride, and gold(III) chloride show no catalytic activity for this reaction. Silver nitrate or silver acetate proved to be an excellent π-Lewis acid catalyst for this reaction. Using 1 equiv. of DBU as the base and DMSO as the solvent, the conversion of a series of *N*-alkyl *o*-alkynylaniline into the corresponding benzoxazine-2-ones is catalyzed by 10 mol% silver nitrate in excellent yields. Terminal alkynes and alkyl-, aryl-, or heterocyclic-substituted alkynes are all suitable substrates for this reaction. Similar to the silver-catalyzed cyclization reaction of propargylic alcohols or amines with carbon dioxide to give α-alkylidene cyclic carbonate and carbamate, the *Z* isomer is found to be the sole product by X-ray analysis and NOE experiments. No 7-*endo*-dig cyclization product is observed in this reaction system. For primary *o*-alkynylanilines, the combination of 10 mol% silver acetate and 20 mol% 1,4-diazabicyclo[2.2.2]octane (DABCO) is employed as the catalytic system, and the corresponding benzoxazine-2-ones are also obtained in good yield (Scheme 11).

A possible mechanism is also similar to the silver-catalyzed cyclization reaction of propargylic alcohols or amines with carbon dioxide. The carbamate intermediate is first formed by the reaction of *o*-alkynylaniline with carbon dioxide in the presence of a base, followed by intramolecular nucleophilic attack on the alkyne, which is activated by silver(I) catalyst to give benzoxazine-2-one through 6-*exo* cyclization.

When the reaction of *primary o*-alkynylaniline and carbon dioxide is performed in the presence of 10 mol% silver nitrate and 1 equiv. of DBU, no benzoxazine-2-one is detected. Instead, 4-hydroxyquinolin-2(1*H*)-one, which is a structural motif in a vast array of natural products and biologically important compounds [73], is

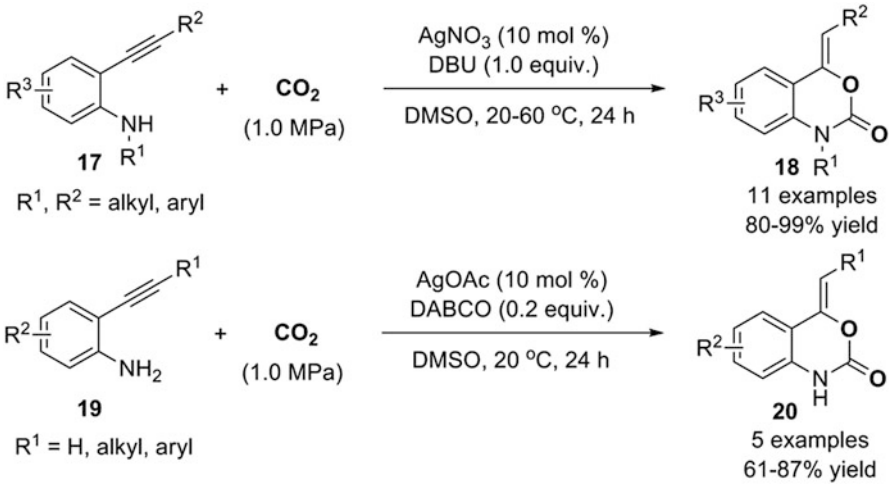


**Scheme 11** Silver-catalyzed intramolecular carboxylative addition reaction of *o*-alkynylanilines with carbon dioxide to synthesize benzoxazine-2-ones

isolated as the sole product in high yield. Further examination of the reaction conditions shows that the reaction can be carried out under 0.1 MPa of carbon dioxide at 60°C. A wide range of terminal alkynes and alkyl-, aryl-, or heterocyclic-substituted alkynes are successfully transformed into functionalized 4-hydroxyquinolin-2(1*H*)-ones in excellent yields (Scheme 12) [74].

An isotopic labeling experiment using $C^{18}O_2$ revealed that carbon dioxide was totally incorporated into the 4-hydroxyquinolin-2(1*H*)-one product. The reaction of benzoxazin-2-one with DBU was monitored by in situ IR, and absorption of isocyanate group was detected. Based on this experiment, the author proposed a silver-catalyzed intramolecular carboxylative addition of *o*-alkynylaniline with carbon dioxide and a DBU-mediated rearrangement of benzoxazin-2-one to produce 4-hydroxyquinolin-2(1*H*)-one (Scheme 12). The silver-catalyzed reaction of *o*-alkynylaniline with carbon dioxide gives benzoxazin-2-one, which is deprotonated by DBU and undergoes a carbon–oxygen bond cleavage to generate an intermediate containing an isocyanate and an enolate moiety. The nucleophilic attack of the enolate on the isocyanate affords 1,3-diketone, which tautomerizes to furnish 4-hydroxyquinolin-2(1H)-one.

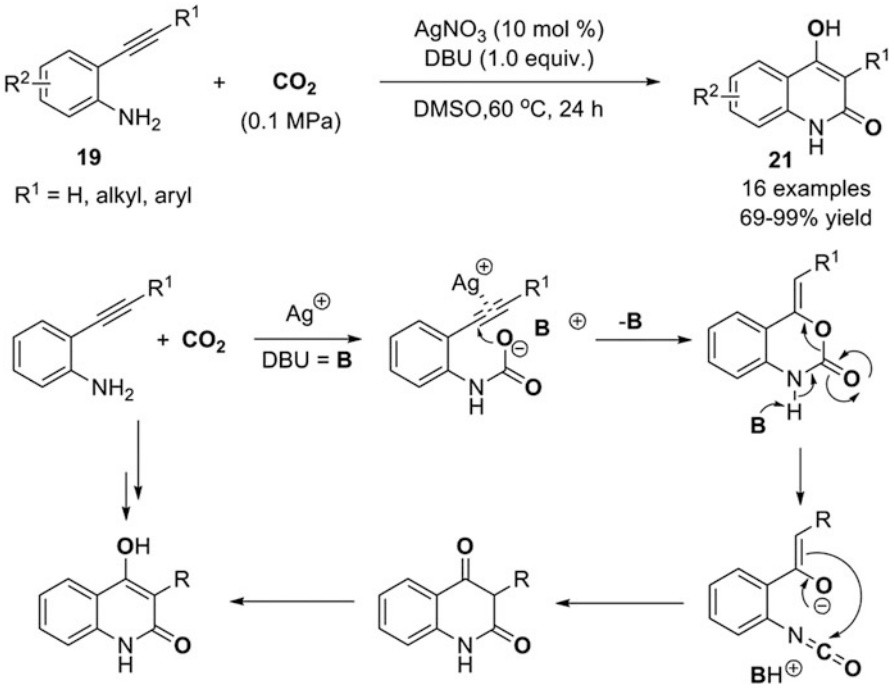


**Scheme 12** Silver-catalyzed intramolecular carboxylative addition of *o*-alkynylanilines with carbon dioxide and rearrangement to synthesize 4-hydroxyquinolin-2(1*H*)-ones

## 4 Silver-Catalyzed Reaction of Alkynyl Ketones with Carbon Dioxide

It is well known that the α C–H bonds in some ketones, especially aromatic ketones, can undergo carboxylation reactions with carbon dioxide in the presence of a suitable organic or inorganic base to produce β-ketocarboxylates [75–82]. This could be trapped by silver(I)-activated alkynes, as in the silver-catalyzed cyclization reaction of propargylic alcohols or amines with carbon dioxide.

In 2012, Yamada and coworker found that in the presence of 20 mol% silver (I) benzoate and 2 equiv. of DBU, 3,3-dimethyl-1,5-diphenyl-4-pentyne-1-one (**22a**) undergoes carboxylative addition with carbon dioxide to give 40% yield of γ-lactone product **23a** in DMSO [83], in which in situ formed alkynyl β-ketocarboxylate conducts 5-*exo*-dig cyclization reaction under silver catalysis (Scheme 13). Other metal salts, such as palladium acetate, copper(II) trifluoromethanesulfonate, gold(I) chloride, gold(III) chloride, and gold(I) benzoate, show no catalytic activity for the formation of γ-lactones. Further investigation of the reaction conditions showed that the yield of γ-lactone sharply increases when using 4 equiv. of 7-methyl-1,5,7-triazabicyclo[4.4.0]dec-1-ene (MTBD) as the base and DMF as the solvent. The substrate scope of this silver catalytic system proved to be very broad, and various alkyl- or aryl-substituted alkynes and aliphatic or aromatic

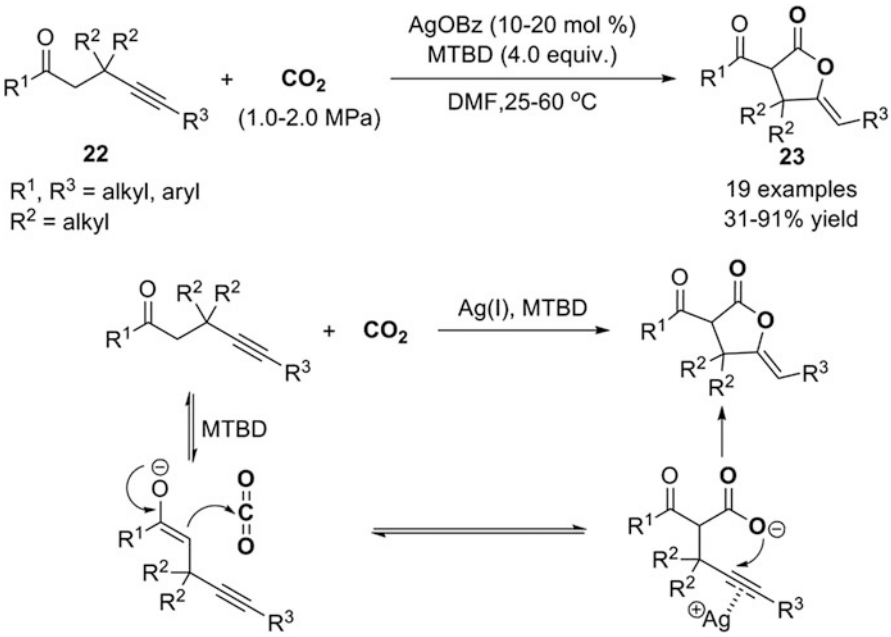


**Scheme 13** Silver-catalyzed intramolecular carboxylative addition of alkynyl ketones with carbon dioxide

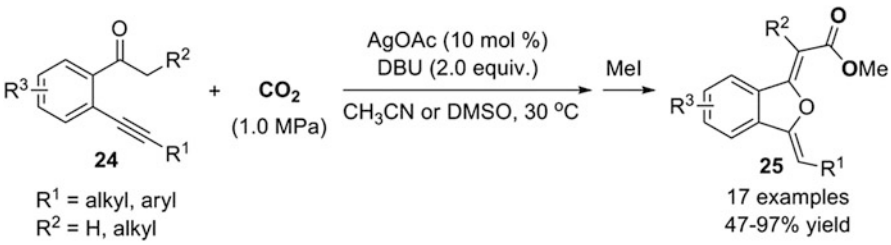


**Scheme 14** AgOAc-catalyzed sequential carboxylation/intramolecular cyclization reaction of *o*-alkynyl acetophenones with carbon dioxide

ketones are competent substrates for this reaction. For the aliphatic ketones, there are two possible carboxylation sites. Therefore, at least two lactones should be formed. However, γ-lactone products are observed exclusively in this reaction. It should be noted that full substituent at the propargylic position is also essential. The geometry of the C–C double bond is determined to be *Z* by X-ray analysis and NOE experiments.

Since carboxylates are considered to be a relatively weak nucleophile, the ketone moiety in a β-ketocarboxylate is more reactive toward electrophiles than the carboxylate. The nucleophilicity of the ketone moiety is also enhanced by the presence of the carboxylate partly due to keto-enol tautomerization. Therefore, after carboxylation of a ketone to form a β-ketocarboxylate, the ketone can become nucleophilic enough to undergo a cyclization reaction with a tethered activated alkyne to afford a more stable carboxylated product.

In 2013, Yamada and coworker reported a silver-catalyzed sequential carboxylation/intramolecular cyclization reaction of *o*-alkynyl acetophenones with carbon dioxide to synthesize 1(*3*H)-isobenzofuranylidene acetic acids and the corresponding esters (Scheme 14) [84]. The reaction is conducted in the presence of 10 mol% silver(I) acetate and 2 equiv. of DBU under 1.0 MPa carbon dioxide pressure in acetonitrile or DMSO at 30°C. A wide range of *o*-alkynyl acetophenone substrates are converted into 1(*3*H)-isobenzofuranylidene acetates in moderate to excellent yield, with a high selectivity for 5-*exo* cyclization.

Later, Zhang and Lu also realized the same reaction under very mild reaction conditions (low catalyst loading, carbon dioxide balloon, and room temperature) (Scheme 15) [85]. The reaction is conducted in the presence of 2 mol% silver (I) tetrafluoroborate and 2 equiv. of MTBD under 0.1 MPa carbon dioxide pressure in DMF at 25°C. This silver(I) catalyst system also shows wide substrate scope and various functional groups ranging from electron-rich aryl ethers to electron-withdrawn aryltrifluoromethyl, and arylfluoro functionalities are tolerated. The reaction gives 1(*3*H)-isobenzofuranylidene acetates in high yield and exclusively forms 5-*exo*-cyclizaion products.

Deuterium-labeling experiments showed that the α-H of the carboxylate and phenyl group in the product come from the methyl hydrogen in the substrate. The obvious deuterium-content difference existed between the two α-H and substrate,

which might indicate that the hydrogen shift is probably involved during the reaction.

A possible reaction mechanism is shown in Scheme 15. In the presence of MTBD, *o*-alkynyl acetophenone is firstly carboxylated with $CO_2$ to produce β-ketocarboxylate **I**. There are two possible pathways for the following cyclization reaction. In Path 1, β-ketocarboxylate **I** undergoes keto-enol tautomerism and the nucleophilic enol oxygen of **II** attacks the silver(I)-activated alkyne moiety, and forms 1(3*H*)-isobenzofuranylidene acetate **IV** was formed. Path 2 involves the direct attack of the keto oxygen atom of intermediate **I** at the silver(I)-activated

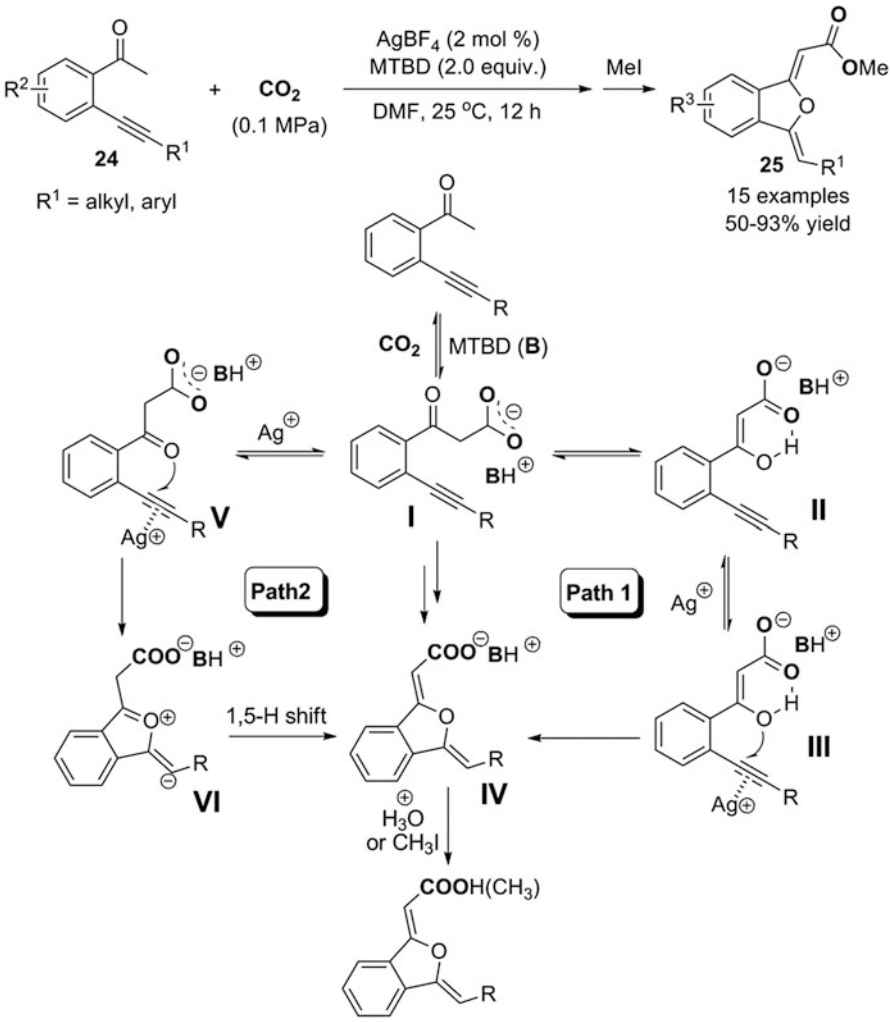


**Scheme 15** $AgBF_4$-catalyzed sequential carboxylation/intramolecular cyclization reaction of *o*-alkynyl acetophenones with carbon dioxide

alkyne moiety to generate intermediate **V**. The following 1,5-hydrogen shift gives acetate **IV**. Finally, the acidification or esterification of the resulting carboxylate **IV** releases the carboxylic acid or ester. Computational studies revealed that intermediate **III** is more stable than intermediate **V**, and the energy barrier of the cyclization step through intermediate **V** is much higher than that through intermediate **III**, indicating that Path 1 might be more favorable for this reaction. Also, DFT studies successfully explain the exclusive formation of the product from 5-*exo* oxygen cyclization.

## 5 Silver-Catalyzed Carboxylation of Terminal Alkynes with Carbon Dioxide

From a general mechanistic viewpoint, in the silver(I)-catalyzed carboxylation of terminal alkynes with carbon dioxide, a silver cation first coordinates to the terminal alkyne as a carbophilic π-Lewis acid, enhancing the acidity of the alkyne C–H bond. A deprotonation reaction of the silver-coordinated terminal alkyne by suitable base follows to form a silver(I) acetylide. The insertion of carbon dioxide into the carbon–silver bond gives silver(I) propiolate, and subsequent acidification or esterification reactions afford propiolic acid or ester, which are important and versatile building blocks in organic synthesis [86].

In 1974, Saegusa and coworkers reported that copper or silver phenylacetylide can be obtained by the reaction of phenylacetylene with copper(I) or silver(I) *tert*-butoxide at room temperature [87]. In the presence of a stoichiometric amount of tributyl phosphine or *tert*-butyl isocyanide in THF at 80°C, the formed copper (I) and silver(I) phenylacetylide that react smoothly with carbon dioxide gave copper(I) and silver(I) phenylpropiolate, which are then converted into methyl phenylpropiolate by alkylation with methyl iodide (Scheme 16).

In 1994, Inoue and coworkers reported copper(I)- and silver(I)-catalyzed carboxylative coupling reaction of terminal alkynes, carbon dioxide, and alkyl bromides (Scheme 17) [88]. Using 4 mol% of copper(I) bromide or silver(I) iodide as the catalyst, 6 equiv. of potassium carbonate or phosphate as the base, a limited number of aryl- and alkyl-substituted terminal alkynes undergo carboxylative coupling reaction with carbon dioxide and *n*-hexyl bromide in aprotic polar solvents, such as DMF, DMAc, or NMP at 100°C, producing the corresponding *n*-hexyl propiolates in good yield. When benzyl bromide is used, 55% yield of

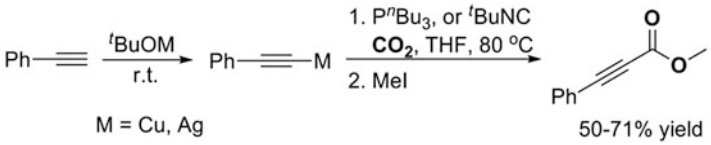


**Scheme 16** Insertion of carbon dioxide into silver(I) acetylide

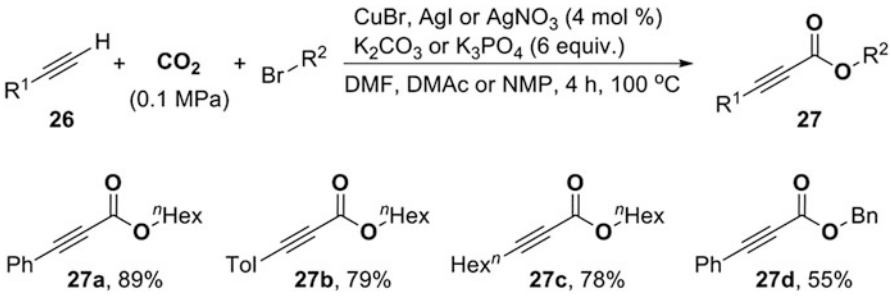


**Scheme 17** Copper- or silver-catalyzed carboxylative coupling reaction of the terminal alkynes, carbon dioxide, and alkyl bromides

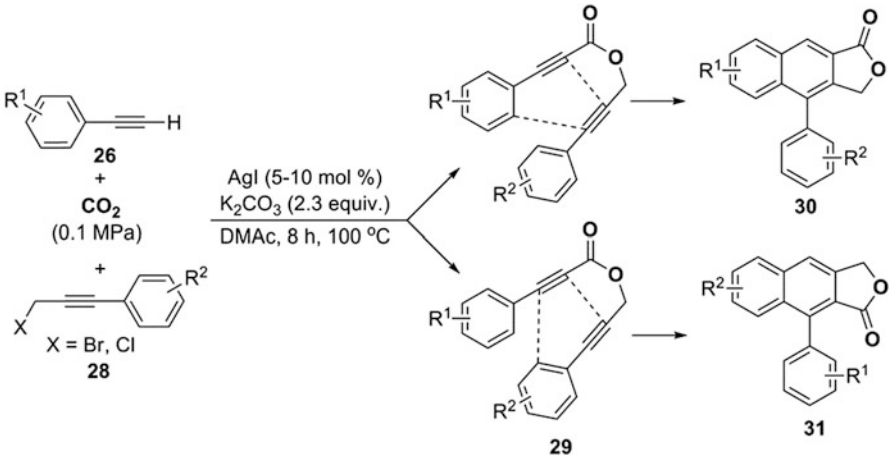


**Scheme 18** Silver-catalyzed carboxylative coupling reaction of phenylacetylene, carbon dioxide, and phenylpropargylic halides for the synthesis of arylnaphthalene lactones

alkynoate is obtained together with 43% yield of dibenzyl carbonate forming from the reaction of potassium carbonate and benzyl bromide.

In 2008, Anastas and coworker reported a silver(I)-catalyzed carboxylative coupling reaction of phenylacetylene, carbon dioxide, and phenylpropargylic halides for direct synthesis of arylnaphthalene lactones [89], which are valuable natural products and biologically important compounds (Scheme 18). In the presence of 10 mol% silver(I) iodide and 2.3 equiv. of potassium carbonate, the reaction of phenylacetylene, carbon dioxide and phenylpropargylic bromide produces phenylpropargyl phenylpropiolate **29**, which then undergoes slow thermal cyclization to furnish arylnaphthalene lactones **30** and **31** in moderate yield. When copper (I) iodide is used as catalyst, no desired product is observed, only non-carboxylative product from direct coupling of phenylacetylene and phenylpropargylic bromide is obtained. When $R^1$ is electron donating, the reaction favors the formation of

compounds **30,** while electron-withdrawing groups favor the formation of lactone **31**. Using this silver(I) catalytic system and a phase transfer catalyst 18-crown-6, the author also realized the direct synthesis of six arylnaphthalene lactone natural products through the reaction of corresponding phenylacetylenes, carbon dioxide, and phenylpropargylic chlorides [90].

Compared to traditional approaches to the synthesis of propiolic acids such as carboxylation of air- and moisture-sensitive alkynyl–magnesium or alkynyl–lithium, oxidation of propargylic alcohols or aldehydes, and hydrolysis of corresponding derivatives [91–94], direct carboxylation of terminal alkynes with carbon dioxide represents a straightforward and convenient method. Goossen [95] and Zhang [96] reported nitrogen or *N*-heterocyclic carbene ligand-assisted copper-catalyzed direct carboxylation of terminal alkynes with carbon dioxide. Based on the previously reported highly selective copper(I)-catalyzed carboxylative coupling reaction of terminal alkynes, allylic chlorides, and carbon dioxide [97], Zhang and Lu developed a convenient ligand-free silver(I)-catalyzed direct carboxylation of terminal alkynes using carbon dioxide as a carboxylative agent affording a variety of functionalized propiolic acids (Scheme 19) [98].

The established optimal reaction conditions include the use of 1 mol% of silver (I) iodide as the catalyst, 1.5 equiv. of cesium carbonate as the base, 0.2 MPa of carbon dioxide pressure, DMF as the solvent, at 50°C. Using copper(I) salt as a catalyst or potassium carbonate as a base leads to decreased yield. It is noteworthy that the reaction carried out with 1.5 equiv. cesium carbonate without any transition-metal catalyst affords a very low yield of the product, which clearly demonstrates the catalytic role of silver(I) salt. The addition of a ligand has a negative effect on the catalyst activity. The presence of 1 mol% tricyclohexyl phosphine results in an obvious decrease of the yield. No carboxylation product is observed when the reaction is carried out in the absence of carbon dioxide. When

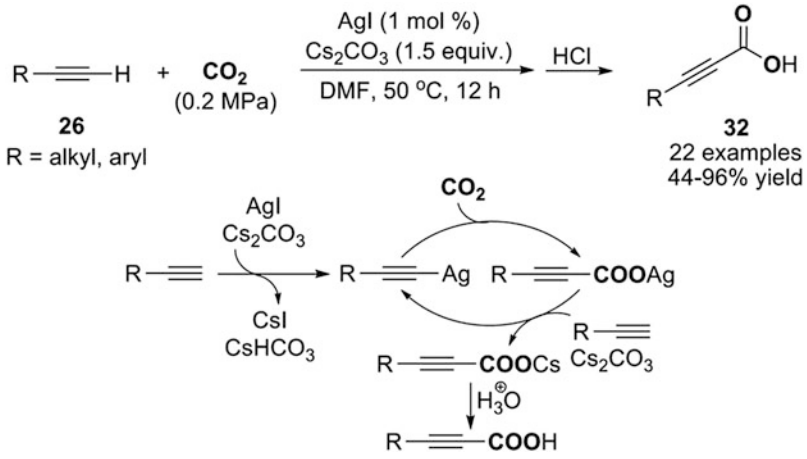


**Scheme 19** Silver-catalyzed direct carboxylation of terminal alkynes with carbon dioxide to synthesize propiolic acids

phenylacetylene reacts with $^{13}$C-labeled carbon dioxide, $^{13}C_{carbonyl}$-labeled phenylpropiolic acid is obtained in excellent yield. These results demonstrate that the CO2 unit in the carboxylation product comes from free carbon dioxide, rather than the carbonate salts.

This ligand-free silver(I)-catalyzed direct carboxylative approach shows generality for the synthesis of functionalized propiolic acids. Various aryl- and alkyl-substituted terminal alkynes smoothly undergo the carboxylation reaction and are converted into the corresponding propiolic acids in moderate to excellent yield. Both electron-donating and electron-withdrawing group substituted phenylacetylenes are successfully carboxylated with carbon dioxide. The reactions are compatible with aryl-OMe, OH, F, $CF_3$, Br, Cl, and $NO_2$ groups.

In the proposed catalytic cycle (Scheme 19), the terminal alkyne first coordinates to the silver(I) salt, and the acidity of the alkyne C–H bond is enhanced. Then the deprotonation reaction of the terminal alkyne by cesium carbonate affords silver (I) acetylide. The insertion of carbon dioxide into the sp-hybridized carbon–silver bond forms the silver propiolate intermediate, which subsequently reacts with another terminal alkyne and cesium carbonate releasing cesium propiolate and simultaneously regenerating silver(I) acetylide. Acidic workup affords the propiolic acid.

Based on systematic DFT calculations, Luo and coworker proposed that the catalytically active species in this reaction is silver compound **A** bearing a $CsCO_3$ anionic ligand rather than silver(I) acetylide or silver(I) propiolate (Scheme 20) [99]. The cesium carbonate does not only function as a base to abstract a proton from the terminal alkyne but also participates in the generation of the catalytically active species. It is also found that carbon dioxide insertion is the rate-determining step in the catalytic cycle.

Silver-catalyzed direct carboxylation of terminal alkynes with carbon dioxide using cesium carbonate as a base was employed by Hong and coworker to test

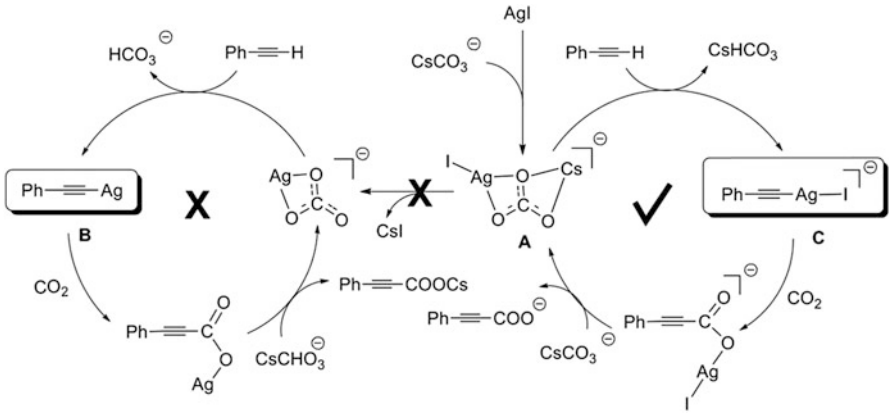


**Scheme 20** Mechanism for silver-catalyzed direct carboxylation of terminal alkynes with carbon dioxide based on DFT studies

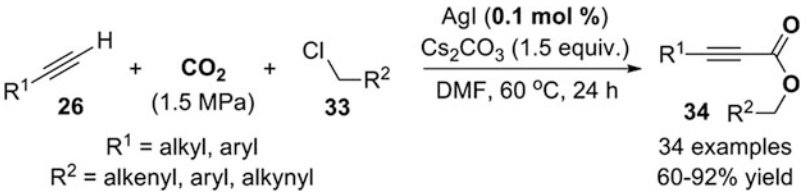


**Scheme 21** Silver-catalyzed carboxylative coupling reaction of the terminal alkynes, carbon dioxide, and chloride compounds

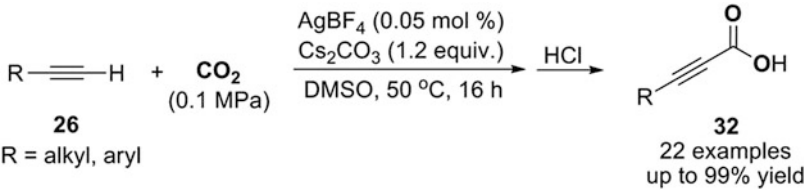


**Scheme 22** $AgBF_4$-catalyzed direct carboxylation of terminal alkynes with carbon dioxide in DMSO

efficiencies of carbon dioxide capturing solutions [100]. It was found that the carboxylation reaction gave comparable yields using carbon dioxide captured by ethanolamine solution directly from exhaust gas.

The ligand-free and simple silver(I) iodide/cesium carbonate system is also found to be highly efficient and selective for carboxylative coupling of aryl- or alkyl-substituted terminal alkynes, carbon dioxide, and various allylic, propargylic, or benzylic chloride, exclusively yielding functionalized 2-alkynoates (Scheme 21) [101]. Compared to the previously reported *N*-heterocyclic carbene copper (I) catalytic system, the ligand-free silver(I) catalytic system shows greatly enhanced activity (more than 300 times) and selectivity at much lower catalyst loading. The ligand-free silver(I) catalytic system shows a general substrate scope, tolerating both functionalized terminal alkynes and chlorides.

In 2012, Goosen and coworker reported carboxylation of terminal alkynes catalyzed by low loadings of silver(I) salts in DMSO at ambient carbon dioxide pressure (Scheme 22) [102]. Using cesium carbonate as the base in DMSO at 50°C, 0.05 mol% of silver(I) tetrafluoroborate catalyst is enough to ensure the excellent yield of most terminal alkyne substrate. The author argued that the remarkable efficiency of this catalytic system might be ascribed to DMSO-ligated silver (I) carbonate as the actual catalytic species and excellent solubility of carbon dioxide and cesium carbonate in DMSO.

Following their poly-*N*-heterocyclic carbene and copper(I) catalytic system [96], Zhang and coworker developed a *N*-heterocyclic carbene polymer-supported silver nanoparticle catalyst system for the carboxylation of terminal alkynes with carbon dioxide under ambient conditions (Scheme 23) [103]. The catalyst P-NHC-Ag was prepared by the reaction of the poly-imidazolium with silver nitrate in hot DMSO.

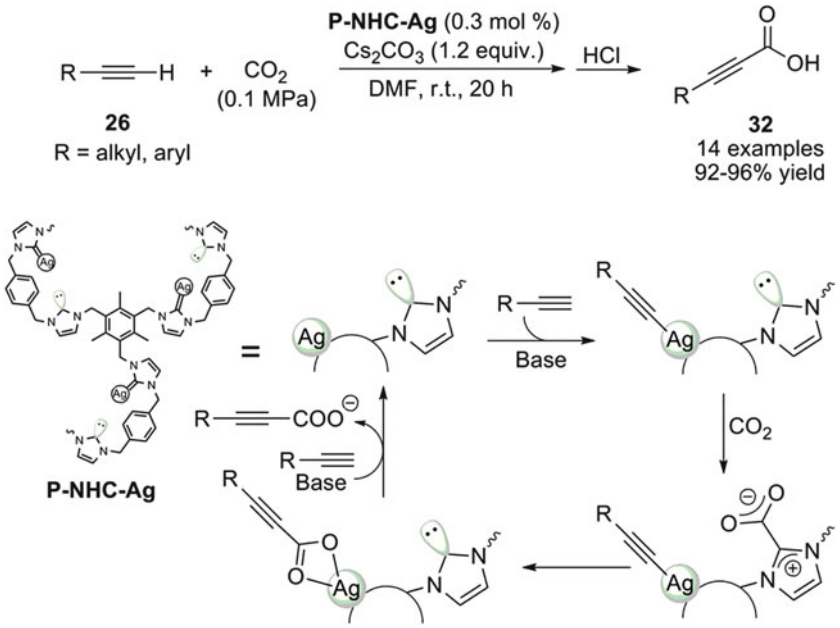


**Scheme 23** Direct carboxylation of terminal alkynes with carbon dioxide catalyzed by poly(*N*-heterocyclic carbene)-supported silver nanoparticles

Transmission electron microscopy showed that silver nanoparticles are deposited on the poly-NHC polymer material. P-NHC-Ag exhibited highly catalytic activity comparable to Goosen's silver(I) tetrafluoroborate/DMSO system [102] and superior to that of silver on carbon, silver iodide, or *N*-heterocyclic carbene silver iodide complex [104]. Similar to the previous poly-*N*-heterocyclic carbene and copper (I) catalytic system, the author believed that the synergistic effect of the organocatalyst NHC and the silver nanoparticle catalyst accounted for its high catalytic activity. The terminal alkyne is activated by the silver nanoparticle and converted to silver acetylide in the presence of the base, and carbon dioxide is activated by NHC and transformed into a NHC-$CO_2$ adduct. The silver acetylide is carboxylated with the NHC-$CO_2$ adduct to afford silver propiolate, and a metathesis reaction regenerates the catalyst and releases the propiolate salt in the presence of the base (Scheme 23). The reaction with P-NHC-Ag catalyst shows wide substrate scope and tolerates various functional groups. Importantly, the catalyst is stable to air and can be easily recovered by simple centrifugation and filtration and reused for several times without significant loss of catalytic activity.

## 6 Silver-Catalyzed Carboxylation of Arylboronic Esters with Carbon Dioxide

Using carbon dioxide as a carboxylative reagent, transition-metal catalyzed carboxylation reaction of various carbon nucleophiles including organotin [105], organoboron [106–110] and organozinc reagents [111, 112], terminal alkynes, and activated C–H bonds [113–118] represent an effective method to synthesize functionalized carboxylic acids and derivatives. Among these nucleophiles, organoboronic acids and their derivatives are particularly attractive due to their ease of handling, broad availability, and functional group compatibility. A rhodium-catalyzed carboxylation of aryl- and alkenylboronic esters was first reported by Iwasawa and coworker in 2006 [106]. However, the rhodium catalytic system proved to be inert toward bromo-, nitro-, alkynyl-, and vinyl-substituted organoboronic esters. This limitation was subsequently overcome by using CuI/bisoxazoline ligands catalytic system discovered by Iwasawa group [107] or *N*-heterocyclic carbene copper(I) catalysts developed by Hou group [108]. These copper(I) catalytic systems show a much higher chemoselectivity and a wider substrate scope.

With regard to the mechanism of rhodium- or copper-catalyzed carboxylation of organoboronic esters with carbon dioxide (Scheme 24), active species bearing a new metal–carbon bond is initially formed by transmetalation reaction of metal catalyst with organoboronic ester, the subsequent insertion of carbon dioxide into the metal–carbon bond affords metal carboxylate, which further undergoes one or two transmetalation reaction regenerating catalytically active species and simultaneously forming the new carboxylate product. It is well known that besides rhodium

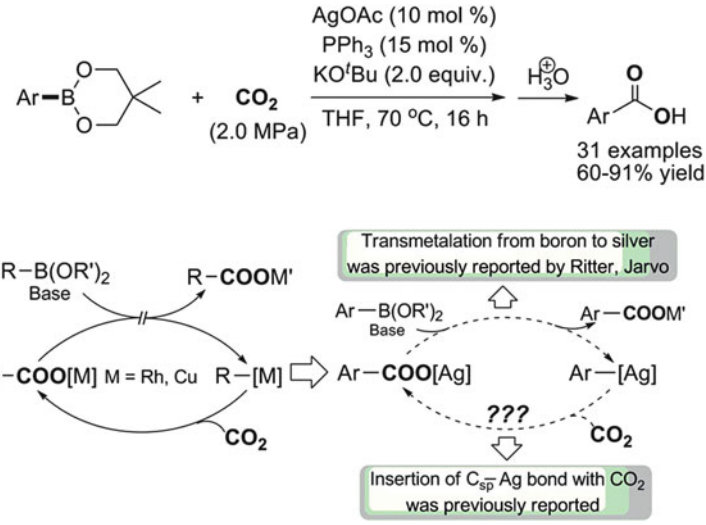


**Scheme 24** Silver(I)-catalyzed carboxylation of arylboronic esters with carbon dioxide

and copper catalysts, silver complexes can also serve as effective catalysts for the reaction using allenyl and arylboronic acids or esters as nucleophiles [119–123]. In those reactions, transmetalation from boron to silver can easily proceed in the presence of a suitable base; thus, highly reactive species bearing a $sp^2$-hybridized carbon–silver bond is thought to be formed. Given that carbon dioxide could insert into the $sp^2$-hybridized carbon–silver bond to afford silver carboxylate, silver would be another metal candidate that shows expectant activity toward the carboxylation of arylboronic reagents with carbon dioxide. On the basis of above mechanistic insights, Zhang and Lu developed a simple and efficient silver(I)-catalyzed carboxylation reaction of a variety of arylboronic esters with carbon dioxide (Scheme 24) [124].

A combination of 10 mol% of silver(I) acetate with 15 mol% of triphenyl phosphine can serve as an effective catalyst for the carboxylation reaction of various arylboronic esters in the presence of 2 equiv. of potassium *tert*-butoxide in THF at 70°C. Compared to the readily available triphenyl phosphine ligand, *N*-heterocyclic carbene ligands, which are obtained by multistep synthesis, give lower yield. Notably, 1 mol% loading of silver catalyst at 100°C in 1,4-dioxane also gives a good yield of the desired product in a shorter time. The silver(I) catalytic system proved to be sensitive to the carbon dioxide pressure, and relatively high carbon dioxide pressure enhances the reaction rate.

This silver(I) catalytic systems show wide substrate scopes, and a wide range of functional groups are tolerated, from electron-rich aryl ethers to electron-withdrawn aryltrifluoromethyl, arylnitro, arylcyano, arylaldehyde, arylketone, and arylester functionalities. Boronic esters with heteroaromatic derivatives are also found to be suitable substrates. Notably, similar to the copper catalytic systems, the silver(I) catalytic system proved applicable for bromo-, iodo-, nitro-, vinyl-, and alkynyl-substituted organoboronic esters which are inactive toward rhodium catalytic systems. The advantage of the silver(I) catalytic system is that silver(I) acetate and triphenyl phosphine are inexpensive and commercially available, making it more attractive for the potentially practical applications.

## 7 Conclusion

In the last decades, there has been an increasing interest in applying homogeneous silver catalysis for the transformation of carbon dioxide since silver catalysis shows many notable advantages over other transition-metal catalysis including easy accessibility of catalysts, broad substrate scopes, mild reaction conditions (low temperature and carbon dioxide pressure), high efficiency and selectivity, and operational simplicity. Acting as effective π-Lewis acid catalysts, various propargylic alcohols or amines, *o*-alkynylanilines, and alkynyl ketones are converted into synthetically important cyclic carbonates, cyclic carbamates, and lactones, respectively, using carbon dioxide as a carboxylative reagent. The silver-catalyzed carbon dioxide incorporation/rearrangement sequence offers convenient

methods to synthesize tetramic acid and 4-hydroxyquinolin-2(*1*H)-one that cannot be easily obtained by other approaches. By the formation of silver acetylides or arylsilver intermediates as reactive carbon nucleophiles, silver-catalyzed carboxylation of terminal alkynes and arylboronic esters with carbon dioxide provide a straightforward and attractive access to functionalized carboxylic acids and esters. With the further mechanistic understanding of silver catalysis and development of reactions with carbon dioxide, more and more new silver-catalyzed carboxylation reactions using carbon dioxide as a carboxylative reagent will be emerged in near future.

**Acknowledgments** Our research in the field of carbon dioxide transformation is supported by National Natural Science Foundation of China (21172026). Thanks to John Chu from Colorado State University for the proofreading of this chapter's manuscript.

## References

1. Louie J (2005) Curr Org Chem 9:605
2. Mori M (2007) Eur J Org Chem 4981
3. Sakakura T, Choi JC, Yasuda H (2007) Chem Rev 107:2365
4. Aresta M, Dibenedetto A (2007) Dalton Trans 2975
5. Correa A, Martin R (2009) Angew Chem Int Ed 48:6201
6. Riduan SN, Zhang Y (2010) Dalton Trans 39:3347
7. Behr A, Henze G (2011) Green Chem 13:25
8. Huang K, Sun CL, Shi ZJ (2011) Chem Soc Rev 40:2435
9. Cokoja M, Bruckmeier C, Rieger B, Herrmann WA, Kuhn FE (2011) Angew Chem Int Ed 50:8510
10. Lu XB, Darensbourg DJ (2012) Chem Soc Rev 41:1462
11. Zhang WZ, Lu XB (2012) Chin J Catal 33:745
12. Tsuji Y, Fujihara T (2012) Chem Commun 48:9956
13. Zhang L, Hou Z (2013) Chem Sci 4:3395
14. Cai X, Xie B (2013) Synthesis 45:3305
15. Kielland N, Whiteoak CJ, Kleij AW (2013) Adv Synth Catal 355:2115
16. Aresta M, Dibenedetto A, Angelini A (2014) Chem Rev 114:1709
17. Harmata M (2010) Silver in Organic Chemistry. John Wiley & Sons, Inc
18. Naodovic M, Yamamoto H (2008) Chem Rev 108:3132
19. Weibel JM, Blanc A, Pale P (2008) Chem Rev 108:3149
20. Alvarez-Corral M, Munoz-Dorado M, Rodriguez-Garcia I (2008) Chem Rev 108:3174
21. Yamamoto Y (2008) Chem Rev 108:3199
22. Rasika Dias HV, Lovely CJ (2008) Chem Rev 108:3223
23. Chen QA, Wang DS, Zhou YG (2010) Chem Commun 46:4043
24. Hafner A, Jung N, Brase S (2014) Synthesis 46:1440
25. Munoz MP (2014) Chem Soc Rev 43:3164
26. Laas H, Nissen A, Nurrenbach A (1981) Synthesis 958
27. Kim HS, Kim JW, Kwon SC, Shim SC, Kim TJ (1997) J Organomet Chem 545–546:337
28. Gu Y, Shi F, Deng Y (2004) J Org Chem 69:391
29. Jiang HF, Wang AZ, Liu HL, Qi CR (2008) Eur J Org Chem 2309
30. Hase S, Kayaki Y, Ikariya T (2013) Organometallics 32:5285
31. Inoue Y, Ishikawa J, Taniguchi M, Hashimoto H (1987) Bull Chem Soc Jpn 60:1204

32. Iritani K, Yanagihara N, Utimoto K (1986) J Org Chem 51:5499
33. Inoue Y, Itoh Y, Yen IF, Imaizumi S (1990) J Mol Catal 60:L1
34. Bacchi A, Chiusoli GP, Costa M, Gabriele B, Righi C, Salerno G (1997) Chem Commun 1209
35. Uemura K, Kawaguchi T, Takayama H, Nakamura A, Inoue Y (1999) J Mol Catal A Chem 139:1
36. Chiusoli GP, Costa M, Gabriele B, Salerno G (1999) J Mol Catal A Chem 143:297
37. Shi M, Shen YM (2002) J Org Chem 67:16
38. Sasaki Y (1986) Tetrahedron Lett 27:1573
39. Mitsudo T, Hori Y, Yamakawa Y, Watanabe Y (1987) Tetrahedron Lett 28:4417
40. Fournier J, Bruneau C, Dixneuf PH (1989) Tetrahedron Lett 30:3981
41. Joumier JM, Fournier J, Bruneau C, Dixneuf PH (1991) J Chem Soc Perkin Trans 1:3271
42. Kayaki Y, Yamamoto M, Ikariya T (2007) J Org Chem 72:647
43. Kayaki Y, Yamamoto M, Ikariya T (2009) Angew Chem Int Ed 48:4194
44. Costa M, Chiusoli GP, Rizzardi M (1996) Chem Commun 1699
45. Costa M, Chiusoli GP, Taffurelli D, Dalmonego G (1998) J Chem Soc Perkin Trans 1:1541
46. Yoshida M, Komatsuzaki Y, Ihara M (2008) Org Lett 10:2083
47. Della Ca' N, Gabriele B, Ruffolo G, Veltri L, Zanetta T, Costa M (2011) Adv Synth Catal 353:133
48. Minakata S, Sasaki I, Ide T (2010) Angew Chem Int Ed 49:1309
49. Takeda Y, Okumura S, Tone S, Sasaki I, Minakata S (2012) Org Lett 14:4874
50. Kayaki Y, Yamamoto M, Suzuki T, Ikariya T (2006) Green Chem 8:1019
51. Maggi R, Bertolotti C, Orlandini E, Oro C, Sartori G, Selva M (2007) Tetrahedron Lett 48:2131
52. Yamada W, Sugawara Y, Cheng HM, Ikeno T, Yamada T (2007) Eur J Org Chem 2604
53. Yoshida S, Fukui K, Kikuchi S, Yamada T (2009) Chem Lett 38:786
54. DellAmico DB, Calderazzo F, Labella L, Marchetti F, Pampaloni G (2003) Chem Rev 103:3857
55. Yoshida M, Mizuguchi T, Shishido K (2012) Chem Eur J 18:15578
56. Perez ER, da Silva MO, Costa VC, Rodrigues-Filho UP, Franco DW (2002) Tetrahedron Lett 43:4091
57. Perez ER, Santos RHA, Gambardella MTP, de Macedo LGM, Rodrigues-Filho UP, Launay JC, Franco DW (2004) J Org Chem 69:8005
58. Heldebrant DJ, Jessop PG, Thomas CA, Eckert CA, Liotta CL (2005) J Org Chem 70:5335
59. Yoshida S, Fukui K, Kikuchi K, Yamada T (2010) J Am Chem Soc 132:4072
60. Kikuchi S, Yamada T (2014) Chem Rec 14:62
61. Kikuchi S, Yoshida S, Sugawara Y, Yamada W, Cheng HM, Fukui K, Sekine K, Iwakura I, Ikeno T, Yamada T (2011) Bull Chem Soc Jpn 84:698
62. Qi CR, Huang LB, Jiang HF (2010) Synthesis 9:1433
63. Jiang HF, Zhao JW (2009) Tetrahedron Lett 50:60
64. Tang XD, Qi CR, He HT, Jiang HF, Ren YW, Yuan GQ (2013) Adv Synth Catal 355:2019
65. Ishida T, Kobayashi R, Yamada T (2014) Org Lett 16:2430
66. Royles BJL (1995) Chem Rev 95:1981
67. Ugajin R, Kikuchi S, Yamada T (2014) Synlett 25:1178
68. Meyer KH, Schuster K (1922) Chem Ber 55:819
69. Sugawara Y, Yamada W, Yoshida S, Ikeno T, Yamada T (2007) J Am Chem Soc 129:12902
70. Qi CR, Jiang HF, Huang LB, Yuan GQ, Ren YW (2011) Org Lett 13:5520
71. He HT, Qi CR, Hu XH, Guana YQ, Jiang HF (2014) Green Chem 16:3729
72. Ishida T, Kikuchi S, Tsubo T, Yamada T (2013) Org Lett 15:848
73. McCormick JL, McKee TC, Cardellina JH II, Boyd MR (1996) J Nat Prod 59:469
74. Ishida T, Kikuchi S, Yamada T (2013) Org Lett 15:3710
75. Corey EJ, Chen RHK (1973) J Org Chem 38:4086
76. Haruki E, Arakawa M, Matsumura N, Otsuji Y, Imoto E (1974) Chem Lett 427

77. Sakurai H, Shirahata A, Hosomi A (1980) Tetrahedron Lett 21:1967
78. Hirai Y, Aida T, Inoue S (1989) J Am Chem Soc 111:3062
79. Chiba K, Tagaya H, Miura S, Karasu M (1992) Chem Lett 923
80. Flowers BJ, Gautreau-Service R, Jessop PG (2008) Adv Synth Catal 350:2947
81. Beckmana EJ, Munshi P (2011) Green Chem 13:376
82. Van Ausdall BR, Poth NF, Kincaid VA, Arif AM, Louie J (2011) J Org Chem 76:8413
83. Sekine K, Ishida T, Yamada T (2012) Angew Chem Int Ed 51:6989
84. Sekine K, Takayanagi A, Kikuchi S, Yamada T (2013) Chem Commun 49:11320
85. Zhang WZ, Shi LL, Liu C, Yang XT, Wang YB, Luo Y, Lu XB (2014) Org Chem Front 1:275
86. Manjolinho F, Arndt M, Goosen K, Goosen LJ (2012) ACS Catal 2:2014
87. Tsuda T, Ueda K, Saegusa T (1974) J Chem Soc Chem Commun 380
88. Fukue Y, Oi S, Inoue Y (1994) J Chem Soc Chem Commun 2091
89. Eghbali N, Eddy J, Anastas PT (2008) J Org Chem 73:6932
90. Foley P, Eghbali N, Anastas PT (2010) J Nat Prod 73:811
91. Lyons TW, Sanford MS (2009) Tetrahedron 65:3211
92. Zhao M, Li J, Mano E, Song Z, Tschaen DM, Grabowski EJJ, Reider PJ (1999) J Org Chem 64:2564
93. Lee ASY, Hu YJ, Chu SF (2001) Tetrahedron 57:2121
94. Koster F, Dinjus E, Dunach E (2001) Eur J Org Chem 2507
95. Goosen LJ, Rodriguez N, Manjolinho F, Lange PP (2010) Adv Synth Catal 352:2913
96. Yu D, Zhang Y (2010) Proc Natl Acad Sci USA 107:20184
97. Zhang WZ, Li WJ, Zhang X, Zhou H, Lu XB (2010) Org Lett 12:4748
98. Zhang X, Zhang WZ, Ren X, Zhang LL, Lu XB (2011) Org Lett 13:2402
99. Liu C, Luo Y, Zhang WZ, Qu JP, Lu XB (2014) Organometallics 33:2984
100. Kim SH, Kim KH, Hong SH (2014) Angew Chem Int Ed 53:771
101. Zhang X, Zhang WZ, Shi LL, Zhu C, Jiang JL, Lu XB (2012) Tetrahedron 68:9085
102. Arndt M, Risto E, Krause T, Goosen LJ (2012) ChemCatChem 4:484
103. Yu D, Tan MX, Zhang Y (2012) Adv Synth Catal 354:969
104. Wang WL, Zhang GD, Lang R, Xia CG, Li FW (2013) Green Chem 15:635
105. Shi M, Nicholas KM (1997) J Am Chem Soc 119:5057
106. Ukai K, Aoki M, Takaya J, Iwasawa N (2006) J Am Chem Soc 128:8706
107. Takaya J, Tadami S, Ukai K, Iwasawa N (2008) Org Lett 10:2697
108. Ohishi T, Nishiura M, Hou Z (2008) Angew Chem Int Ed 47:5792
109. Ohmiya H, Tanabe M, Sawamura M (2011) Org Lett 13:1086
110. Ohishi T, Zhang L, Nishiura M, Hou Z (2011) Angew Chem Int Ed 50:8114
111. Ochiai H, Jang M, Hirano K, Yorimitsu H, Oshima K (2008) Org Lett 10:2681
112. Yeung CS, Dong VM (2008) J Am Chem Soc 130:7826
113. Boogaerts IIF, Nolan SP (2010) J Am Chem Soc 132:8858
114. Zhang L, Cheng J, Ohishi T, Hou Z (2010) Angew Chem Int Ed 49:8670
115. Boogaerts IIF, Fortman GC, Catherine MRL, Nolan SP (2010) Angew Chem Int Ed 49:8674
116. Mizuno H, Takaya J, Iwasawa N (2011) J Am Chem Soc 133:1251
117. Dalton DM, Rovis T (2010) Nat Chem 2:710
118. Sasano K, Takaya J, Iwasawa N (2013) J Am Chem Soc 135:10954
119. Furuya T, Ritter T (2009) Org Lett 11:2860
120. Seiple IB, Su S, Rodriguez RA, Gianatassio R, Fujiwara Y, Sobel AL, Baran PS (2010) J Am Chem Soc 132:13194
121. Wisniewska HM, Jarvo ER (2011) Chem Sci 2:807
122. Fujiwara Y, Domingo V, Seiple IB, Gianatassio R, Del Bel M, Baran PS (2011) J Am Chem Soc 133:3292
123. Huang C, Liang T, Harada S, Lee E, Ritter T (2011) J Am Chem Soc 133:13308
124. Zhang X, Zhang WZ, Shi LL, Guo CX, Zhang LL, Lu XB (2012) Chem Commun 48:6292

Top Organomet Chem (2016) 53: 101–142
DOI: 10.1007/3418_2015_95

Published online: 28 May 2015

# Dinuclear Metal Complex-Mediated Formation of $CO_2$-Based Polycarbonates

**Charles Romain, Arnaud Thevenon, Prabhjot K. Saini, and Charlotte K. Williams**

**Abstract** This review describes selected metal catalysts for the copolymerisation of epoxides and carbon dioxide to produce polycarbonates. It highlights kinetic and mechanistic studies which have implicated di- or (multi-) metallic pathways for this catalysis and the subsequent development of highly active and selective di-/(multi-) nuclear catalysts. The emphasis is on homogeneous di-/bimetallic catalysts.

**Keywords** Bimetallic · Carbon dioxide chemistry · Catalysis · Dinuclear catalysts · Homogeneous catalysis · Polycarbonates · Polymerisation · Polymerisation catalysis

## Contents



C. Romain, A. Thevenon, P.K. Saini, and C.K. Williams (✉)
Department of Chemistry, Imperial College London, London SW7 2AZ, UK
e-mail: c.k.williams@imperial.ac.uk

## Abbreviations

| | |
|---|---|
| BDI | β-Diiminate |
| BOXDIPY | 1,9-bis(2-oxidophenyl)dipyrrinate |
| CHC | Cyclohexylene carbonate |
| CHO | Cyclohexene oxide |
| CPO | Cyclopentene oxide |
| dipp | 2,5-diisopropylphenyl |
| DMAP | 4-Dimethylaminopyridine |
| DMC | Double Metal Cyanide |
| GPE | Glycidyl phenyl ether |
| HH | Head to head |
| *N*-MeIm | *N*-MethylImidazole |
| PC | Propylene carbonate |
| PCHC | P(cyclohexylene carbonate) |
| PO | Propylene oxide |
| PPC | Poly(propylene carbonate) |
| PPN | Bis(triphenylphosphine)iminium |
| PSC | Poly(styrene carbonate) |
| SO | Styrene oxide |
| TH | Tail to head |
| TOF | Turn over frequency |
| TON | Turn over number (mol/mol in this review) |
| TT | Tail to tail |

## 1 Introduction

### *1.1 Polycarbonates from $CO_2$*

The copolymerisation of carbon dioxide and epoxides represents an interesting method to prepare a range of aliphatic polycarbonates (Fig. 1). The reaction is attracting considerable attention due to the potential to add value to waste carbon dioxide and to replace expensive petrochemical raw materials (epoxides) with lower-cost, renewable $CO_2$ [1–3]. In this regard, commercialisation efforts are particularly focussed towards the preparation of low molecular weight polycarbonate polyols which may be used in place of petrochemical polyols in the

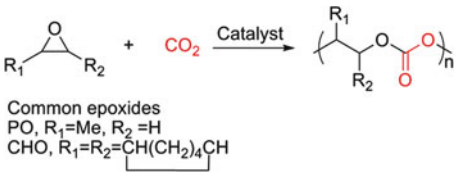


**Fig. 1** An illustration of the copolymerisation of $CO_2$ and epoxide to generate polycarbonate

manufacture of polyurethanes [4, 5]. An alternative commercial opportunity for the aliphatic polycarbonates lies in the application of higher molecular weight polymers for applications spanning films and rigid plastics [6, 7]. There have been interesting recent reports from Bayer, Novomer and Econic Technologies, amongst others, describing opportunities and applications for such $CO_2$-derived polycarbonates [8]. Furthermore, a recent life cycle analysis of the reaction, performed with partial $CO_2$ uptake and at high pressures, shows that there can be clear advantages to using these materials compared to petrochemicals, including reductions of ~20% in fossil fuels and carbon dioxide emissions [9]. Additionally, it has been established that carbon dioxide contaminated with compounds commonly found in flue gases/off-gases can be applied in the polymerisation [10]. Indeed, one recent report establishes the potential to use $CO_2$ captured from a power station, without any purification, for the successful preparation of polyols. Considering the epoxide comonomer, it has already proven possible to prepare fully renewable polycarbonates by applying epoxides derived from biomass [11–13]. Two examples include studies from Coates and co-workers using limonene oxide, which is derived from citrus fruits, and, very recently, our group and that of Meier reported a series of cyclohexene oxides derived from fatty acids [11, 12]. Whilst the opportunities, both commercial and environmental, for this class of polymer appear promising, the science underpinning their production is also of fundamental academic interest. One area of considerable growth is in the production of catalysts to facilitate the copolymerisation, the topic for the current review. In this field of catalysis, the activities and productivities have dramatically increased over the decades since the first reported catalysts which took two weeks to reach completion through to highly active catalysts which undergo >10,000 turnovers per hour [14, 15]. Furthermore, the selection of the catalyst is critical to influence the molecular weight of the polymer (chain length/degree of polymerisation), the distribution of chain lengths (polydispersity), chain end group functionality and any regio- or stereochemical control. These factors affect macroscopic properties such as crystallinity, thermal resistance, elasticity/mechanical strength and degradability of the resulting polymers. Both heterogeneous and homogeneous catalysts are known, with the latter generally showing significantly faster rates and much finer control compared to the solid-state materials. This review only briefly describes heterogeneous or surface catalysis; for more insights into this topic, the reader is referred to previous reports and reviews [16–32]. It is also important to draw the reader's attention to various comprehensive reviews in the area of homogeneous catalysis [6, 33–46]. This particular review focusses on the successes achieved using homogeneous di- or (multi-) nuclear metal complexes as catalysts.

## 1.2 Catalyst Classes and Scope of the Review

The copolymerisation of epoxides/$CO_2$ has been known for more than 40 years [47], with some excellent homogeneous catalysts having been developed. The initial reports focussed on complexes prepared by the hydrolysis/alcoholysis of dialkyl zincs; such species are almost certainly aggregated under the conditions of the catalysis [47–49]. Subsequently, research has focussed on well-defined single-site catalysts of the stoichiometry (LMX), where L is an ancillary ligand, M is the Lewis acidic metal centre and X is the co-ligand or initiating group. Metal centres (M) with a strong precedent in this field include Zn(II), Co(III) and Cr(III), although successful complexes of metals including Ti(IV) [50, 51], Zr(IV) [50], Sn(IV) [50], Ge(IV) [50], Mn(II) [52], Mn(III) [52–54], Fe(III) [55, 56], Lu(III) [57], Y(III) [57, 58], Sc(III) [58], Dy(III) [57, 58], Lu(III) [57, 58], Al(III) [59–62], Mg(II) [63, 64], Co(II) [38, 65], Cu(II) [66] and Ni(II) [67] have all been reported and will be highlighted herein. Whilst a range of ancillary ligands (L) have been explored and will be the described in more detail subsequently, it is possible to identify some common and successful ligand classes (Fig. 2). These include porphyrins and the closely related corroles [55, 59, 68–74]; Schiff base ligands, most commonly salens/salans [40, 46, 75]; β-diiminates [76–82]; and (macrocyclic) phenoxy-

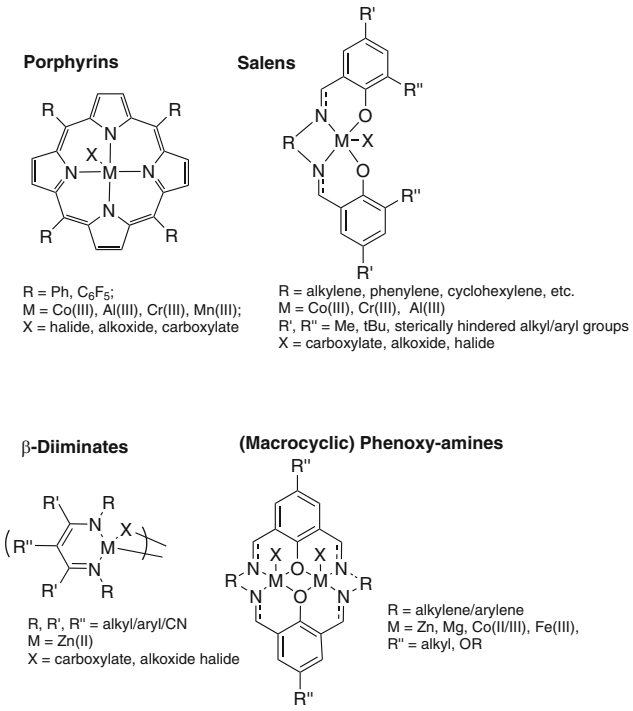


**Fig. 2** An illustration of the general structures for selected catalysts which have been applied successfully in $CO_2$/epoxide copolymerisations

amine ligands, including deliberately dinucleating macrocycles [63, 65, 83–88]. The first two classes are dianionic and are largely targeted towards M(III) oxidation states, whereas the latter two are often used to prepare M(II) catalysts.

The co-ligand (X) is the initiating group during catalysis and becomes the site at which the growing polymer chain is proposed to propagate. It is often a halide, carboxylate or alkoxide group, although any nucleophilic group may be applied. Furthermore, for salen and porphyrin complexes and their related derivatives, a cocatalyst may usually be required. Such cocatalysts either are ionic groups, including ammonium or phosphonium salts, or are nucleophiles, including *N*-containing bases such as DMAP/pyridine/*N*-methylimidazole. They are added to enhance activity, which is proposed to occur via coordination of the anion/Lewis base to the octahedral metal centre at a position *trans*- to the initiating group (X). This coordination is proposed to weaken/labilise the group X and accelerate both initiation and propagation [40, 49]. In contrast, some of the β-diiminate Zn complexes and macrocyclic complexes do not require, or benefit from, the addition of such cocatalysts [63, 65, 76, 77, 85].

The catalysts described in this review can be separated into three distinct types, as illustrated schematically in Fig. 3, according to their structures and mode of action. Much attention has focussed on Type I systems, particularly for the metal porphyrin/salen and cocatalyst systems, and these are not the focus for extensive discussion herein as they have been well reviewed previously [6, 33–45]. However, recently, it has been revealed in a number of studies that some improved performances can be observed using bimetallic (Type II) or two-component catalysts (Type III). The bimetallic catalysts can be further classified into structures which form into single-ligand bimetallic complexes, i.e. complexes which apply ligands which are deliberately dinucleating (Type IIa), dimeric catalysts which form under the conditions of the catalysis by monometallic complex dimerisation (Type IIb) or

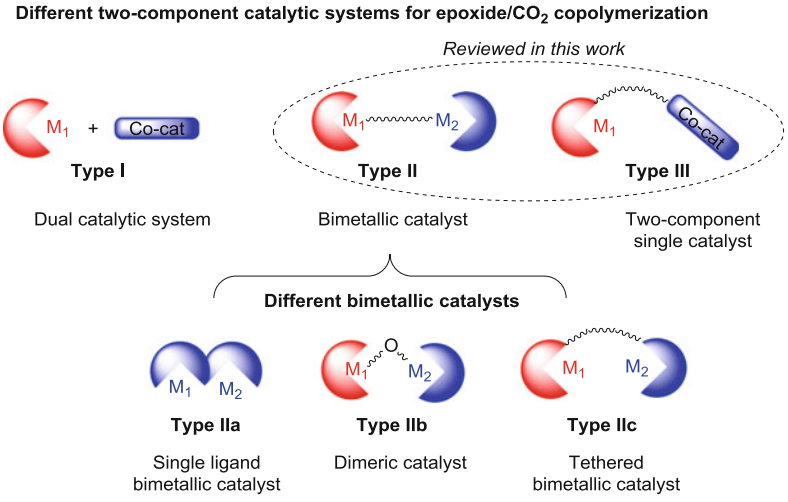


**Fig. 3** Different classes of catalysts and the subdivisions for bimetallic or two-component systems which are the subject of this review

tethered bimetallic catalysts, whereby previously successful monometallic complexes are covalently linked to one another to produce more active and selective bimetallic complexes (Type IIc). The two-component single catalysts (Type III) include systems where a metal catalyst and its cocatalyst (either an ionic species or a Lewis base) are connected together to provide a more active/selective system; most commonly they are improved versions of salen ligands.

## *1.3 Polymerisation Pathways and Selectivities*

In $CO_2$/epoxide copolymerisation, the elementary catalytic steps can be separated into initiation, propagation, chain transfer and termination (Scheme 1).

The *initiation* regime refers to the insertion of the first monomers (epoxide and/or $CO_2$) at the metal centre, leading to the initiating group (X) being

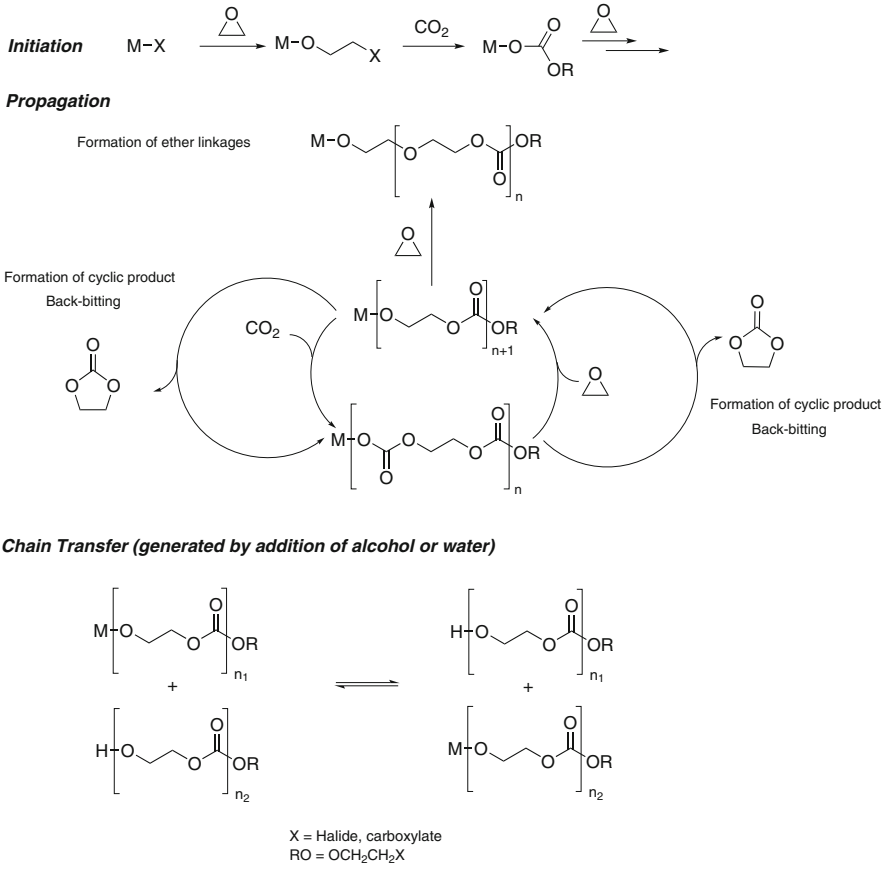


**Scheme 1** An illustration of the elementary steps occurring during copolymerisation, including initiation, propagation and chain transfer processes

incorporated as a chain end group. This is followed by the propagation phase, during which the two monomers are sequentially enchained.

During *propagation*, the catalyst alternates between metal alkoxide and metal carbonate intermediates, with the two species being interconverted via the reaction of the alkoxide with carbon dioxide to (re-)generate the carbonate and the reaction of the carbonate with the epoxide, via ring opening, to (re-)generate the alkoxide. Catalysts exhibiting controlled behaviour typically enable the chain length, and molecular weights, to be predicted and controlled. Experimental features of such control include an inverse relationship between catalyst concentration and molecular weight (at constant monomer conversion) and a linear increase in molecular weight as the polymerisation conversion increases.

In many cases, the polymerisations are also operating under immortal conditions [89], whereby very rapid exchange between the growing polymer chain (alkoxide group) and protic compounds leads to *chain transfer*. It is rather common that such chain transfer processes occur more rapidly than propagation, thereby leading to narrow molecular weight distributions (polydispersities) and molecular weights which depend on the quantity of protic compound(s), as well as the catalyst concentration. Chain transfer reactions with protic compounds can lead to bimodal molecular weight distributions, particularly if a mixture of telechelic and monofunctional chains is concurrently propagating [85]. It can also result in mixtures of chain end groups.

The polymerisations are typically terminated by exposure of the mixture to acids/aqueous conditions which hydrolyse the growing chains from the residual catalyst and prevent any further propagation.

In addition to the sequence of reactions leading to polymerisation, there are two common side reactions which are relevant to all polymerisation cycles: the sequential enchainment of epoxides which leads to ether linkages in the polycarbonates and the formation of a cyclic carbonate by-product. The five-membered-ring cyclic carbonates are the thermodynamically favoured product of carbon dioxide/epoxide couplings. Thus, selectivity for the kinetic product, the polymer, is frequently achieved either by selection of the catalyst or by control over the conditions (most commonly the temperature). It should be noted that the five-membered-ring cyclic carbonates generally cannot re-enter into polymerisation cycles as their ring-opening polymerisation is thermodynamically unfavourable. This year, the first example of the polymerisation of five-membered cyclic carbonate was reported by Carpentier and Guillaume and co-workers [90]. In that case, the polymerisation is thermodynamically possible because a highly strained *trans*-cyclohexene carbonate was applied as the monomer.

For pro-chiral and mono-substituted epoxides, such as propylene oxide, there are also different regio- and stereochemical outcomes. Control of regio-chemistry for mono-substituted epoxides (including propylene oxide) results in three possible dyads, depending on whether ring opening occurs at the methylene or methine group: head–head, head–tail and tail–tail. The regio-regular (HT) structures may be desirable for some applications, although for others regio-random material may be quite acceptable. One interesting example of propylene oxide (PO) stereoselectivity was reported by Nozaki and co-workers whereby stereogradient polycarbonate was

isolated, which was proposed to form a stereocomplex or co-crystallites between the two enantiomers, showing superior thermal properties which was proposed due to the stereogradient material exhibiting a higher thermal decomposition temperature [91]. For cyclohexene oxide (CHO), catalysts able to exert stereocontrol enable the production of iso- and syndiotactic polymers. Recently, several catalysts, most notably metal salen and β-diiminate complexes, have proved capable of exerting excellent control over both the regio- and stereochemistry [34, 55, 72, 76, 91–104].

It also may be instructive to briefly note the abbreviations used in this review. The abbreviations applied to the commonly used epoxides are propylene oxide or epoxypropane (PO), cyclohexene oxide (CHO) and ethylene oxide (EO). The abbreviations used for the common polycarbonates are poly(propylene carbonate) (PPC), poly(cyclohexylene carbonate) (PCHC) and poly(ethylene carbonate) (PEC).

## 2 Early Developments in the Field and Heterogeneous Catalysts

### *2.1 Early Discoveries and Heterogeneous Systems*

The first report of the copolymerisation of $CO_2$ and epoxide was published by Inoue et al., in 1969 [47]. A system comprising mixtures of $ZnEt_2$–$H_2O$, in propylene oxide at 80°C and at high $CO_2$ pressure (50–60 bar), was reported. This catalytic system showed a turnover frequency (TOF) of just 0.12 $h^{-1}$ (mol of epoxide converted to copolymer per mol of metal per hour) [47].

Since this discovery, several groups have studied the copolymerisation of $CO_2$/PO with mixtures of dialkyl zinc reagents ($ZnR_2$) and hydric sources (water, methanol, amine) [105–113]. The systems containing monohydric sources (methanol or a secondary amine) were usually of lower activity than multi-hydric sources ($H_2O$ or dihydric phenol) [114]. Heterogeneous mixtures of carboxylic acids and Zn $(OH)_2$ also showed promising activities [107].

These studies of zinc carboxylates led, several years later, to reports of a new type of heterogeneous catalyst: zinc glutarate $[Zn(O_2C(CH_2)_3CO_2)]_n$. This species was easily prepared by reaction between zinc oxide and glutaric acid, although several other synthetic methods are also possible [30, 32, 115, 116]. It can also be formed as either a crystalline or amorphous material, with the crystalline structures showing higher activity (~300 g PPC/g Zn) and producing polymers with high molecular weight [117]. Characterisation studies, by X-ray diffraction, showed that each zinc atom adopts a tetrahedral configuration and is coordinated by four oxygen atoms belonging to different glutarate molecules (Fig. 4) [26].

The other class of heterogeneous catalysts are the double metal cyanides (DMCs), species with the stoichiometry $Zn_3[M(CN)_6]_2$, where M = Fe(III) or Co (III) [22, 118]. These catalysts are widely applied in the homopolymerisation of epoxides to produce polyethers. Many reports of their synthesis and application are in the patent literature [119–125]. They are usually prepared by the reaction of an

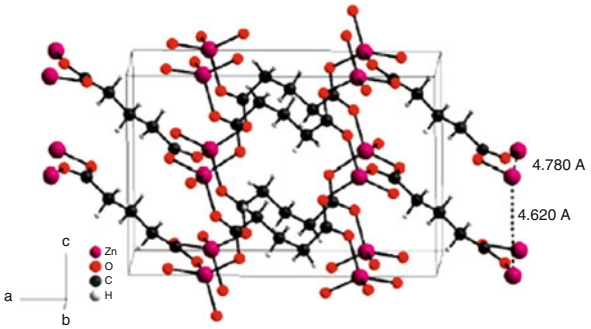


**Fig. 4** Representation of part of the repeat unit in zinc glutarate, determined by X-ray diffraction. Reprinted (adapted) with permission from Klaus et al. [25] (Copyright (2011), American Chemical Society) [25]

aqueous solution of a metal salt with an aqueous solution of a metal cyanide salt, in the presence of various additives, including organic "ligands" and salts. The DMCs can adopt either an amorphous or a crystalline structure depending on the reaction conditions [20–22, 118, 126, 127]. Amorphous DMC appears to have higher activity and productivity in polycarbonate synthesis, with typical activities being reported as 500–1,000 g polymer/g Zn produced when M = Co(III) is used [20–22, 118, 126, 127]. Nevertheless, a crystalline $Zn_3[Co(CN)_6]_2$ material was reported with an activity of ~2,500 g PPC/g Zn [128]. The drawback of these heterogeneous catalysts is their lower reactivity towards $CO_2$ [24]. Typical values for carbonate linkages in PPC are in the range of 20–40%, whilst those for PCHC can reach 90% [22, 118, 126]. Moreover, the copolymerisation conditions require high pressures of $CO_2$ (50–100 atm) [21, 22, 118, 126]. Finally, the copolymer molecular weights were moderate (10,000–30,000 g/mol), with large dispersities as would be expected from multisite initiators.

Several groups have attempted to prepare well-defined homogeneous analogues of the DMC structures. Darensbourg et al. reported $[CpFe(PPh_3)(i\text{-}CN)_2Zn/2,6\text{-}OC_6H_3(tert\text{-butyl})/_2(THF)]_2$ which catalysed CHO copolymerisation leading to PCHC with >85% carbonate linkages (Fig. 5) [23, 24]. The main drawbacks of these homogeneous catalysts are their lower activities (TONs <20 g of polymer/g of Zn). Coates and co-workers developed two-dimensional $Co[Ni(CN)_4]$ catalysts which showed good productivity for PO copolymerisation (TON, ~1,860 g PO/g Co, at 130°C and 54.4 atm $CO_2$), albeit with rather lower $CO_2$ incorporation [20].

There are very few reports concerning the possible mechanisms for the heterogeneous catalysts [26, 30]. In 2011, Rieger and co-workers reported a study of four zinc dicarboxylate catalysts [25]. All the species showed similar surface areas, particle sizes and morphologies. However, the most active compounds showed a larger proportion of Zn–Zn surface couples with 4.6–4.8 Å separation; coincidentally various homogenous di-zinc catalysts also showed such intermetallic separations. Calculations were used to propose an "ideal" Zn–Zn distance of 4.3–5.0 Å, and it was hypothesised that such a separation provided an optimised balance between reducing activation energy and increasing copolymerisation selectivity. The combined experimental and theoretical study indicated that, for heterogeneous zinc dicarboxylates, a bimetallic mechanism may be operative (a representation of such a pathway is provided in Scheme 2) [25].

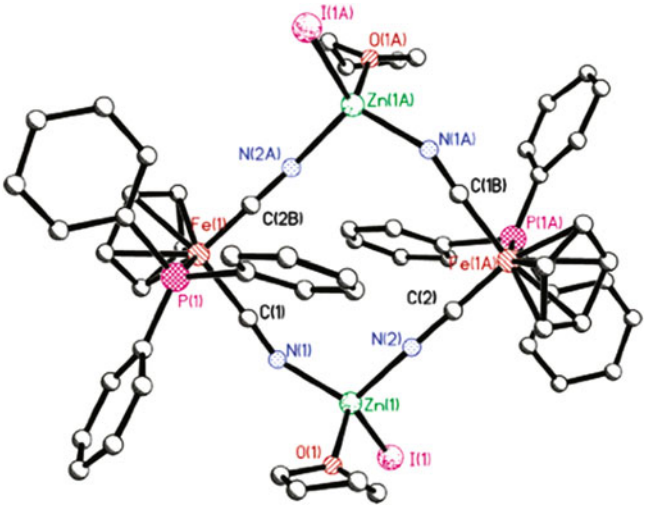


**Fig. 5** Representation of the structure of a well-defined molecular analogue of the DMC catalyst. Reprinted (adapted) with permission from Darensbourg et al. [23] (Copyright (2003), American Chemical Society) [23]

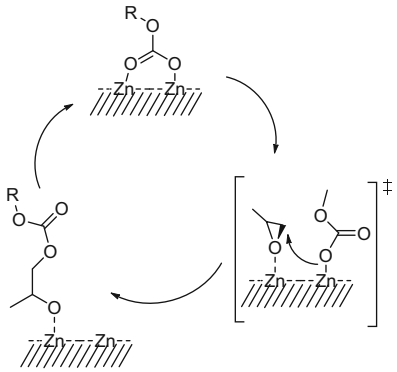


**Scheme 2** An illustration of the proposed bimetallic catalytic cycle operating on the surface of heterogeneous zinc dicarboxylate catalysts. Reprinted (adapted) with permission from Klaus et al. [25] (Copyright (2011), American Chemical Society)

## 2.2 *Homogeneous Catalysis: Uncovering Bicomponent Mechanisms*

Although heterogeneous catalysts have shown promise and have a number of advantages, they are also limited by lower rates/productivities, lower selectivities and a number of inherent problems with catalyst characterisation. For example, for these catalysts, it is very difficult to precisely define and characterise the active

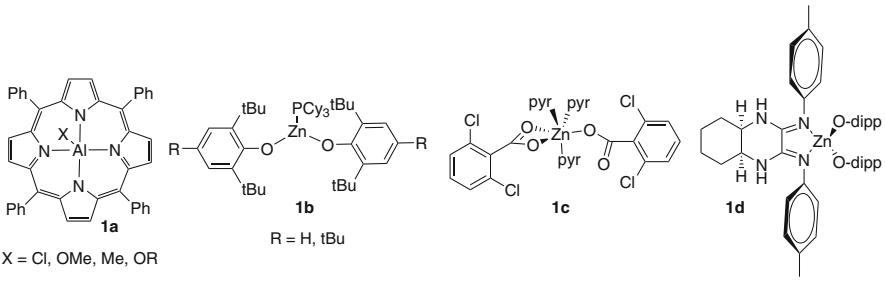


**Fig. 6** Examples of some of the early homogeneous catalysts [59, 129–133]

site(s), challenging to study the reaction kinetics and mechanism and not yet feasible to rationally improve performance (productivities/activities/selectivities). Therefore, a significant volume of research has focussed on homogeneous catalysts. Initially the community focussed on deliberate mononuclear catalysts; however, some of these were subsequently revealed to operate by bicomponent or bimetallic mechanisms.

Inoue was also the first to report a homogeneous copolymerisation catalyst: an aluminium tetraphenylporphyrin complex **1a** (Fig. 6). The complex was active for CHO/$CO_2$ and PO/$CO_2$ polymerisation, when $EtPh_3PBr$ was used as a cocatalyst [134].

Since 1995, Darensbourg and co-workers have developed a series of zinc bis (phenoxides), including complex **1b**, which were good catalysts (Fig. 6) [131–133]. Although they showed good activity, the selectivity and control were reduced leading to polydisperse polymers. The influence of bulky substituents on the phenoxides was investigated, and the major findings were that (1) the *ortho*-substituents did not affect the activity significantly and (2) having electron-donating substituents at the *para*-position on the phenoxide increased activity [131]. Darensbourg later prepared a zinc benzoate complex, **1c**, which had a TOF of 7.7 $h^{-1}$ when used in CHO/$CO_2$ copolymerisations [129]. The same group also demonstrated similar activities with bis(salicyl aldiminato)zinc and (dialkylamino) ethyltetramethylcyclopentadienyl zinc catalysts [129, 130]. In contrast, a quinoxaline-derived zinc alkoxide complex, **1d**, developed by Hampel et al. showed lower activity for CHO copolymerisation (TOF, 3–4 $h^{-1}$, at 80°C and 80 atm of $CO_2$ pressure) [135]. An important aspect of this earlier work was that some of the successful zinc catalysts were shown to exhibit di- or multimetallic structures, providing early pointers towards bimetallic polymerisation pathways.

## *2.3 Zinc β-Diiminate Catalysts: Dimeric Catalysts*

In 1998, Coates and co-workers reported a ground-breaking series of zinc catalysts which showed significantly higher activities and selectivities [136]. These

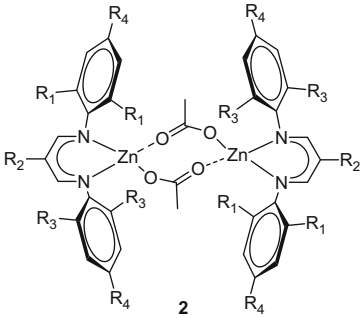


**Fig. 7** The proposed structure of the most active Zinc BDI catalysts, first reported by Coates et al. [39–41]

β-diiminate BDIZn catalysts zinc complexes, e.g. **2** (Fig. 7), enabled efficient copolymerisation to occur at 50°C and only 7 atm of $CO_2$ pressure. Under these conditions, the BDIZn catalysts showed excellent productivities and activities (TOF = 917 $h^{-1}$) and produced polymers with >99% carbonate linkages. The catalysts were extensively studied, and structure–activity studies revealed the importance of the substituents on the phenyl rings in the BDI ligand (positions $R_1$ and $R_3$ in Fig. 7) and of the initiating group (X). Furthermore, these structure–activity studies revealed the subtleties of "catalyst design" and strongly implicated a bimetallic mechanism. It was discovered that if the phenyl rings in the ligand were substituted with sterically hindered groups, the complexes formed monomeric structures which were inactive/of low activity. On the other hand, if substituents with low steric hindrance were applied, the resulting complexes formed tightly bound dimers which were also of lower activity/inactive. The best catalysts were formed from ligands with medium steric hindrance ($R_1 = R_3 = Et$, $R_4 = H$) which resulted in the formation of loosely associated dimeric structures. Electron-withdrawing substituents attached to the backbone of the BDI zinc complexes (e.g. $R_2 = CN$) also improved activities [77, 78, 136].

Kinetic and mechanistic studies strongly implicated two zinc metal centres in the copolymerisation catalytic cycle. It was proposed that the epoxide coordinates to one zinc metal centre, whilst the other metal centre provides the nucleophile to attack and ring-opens the epoxide (Scheme 3).

Coates et al. recently designed $C_1$ symmetric BDIZn catalysts for the enantioselective controlled synthesis of isotactic PCHC. These catalysts show good TOFs, up to 190 $h^{-1}$ at 22°C and 8 atm of $CO_2$, and produced polymers with high iso-selectivity (*ee* >90%). Variation of the amino substitution with the (*S*,*S*)-cyclohexyl-triiso-propylsilyl ether group increased the enantioselectivity to achieve a *ee* of 94% at 0 °C [76].

**Scheme 3** Transition state proposed by Coates involving bimetallic complexes for the ring opening of the CHO [77]

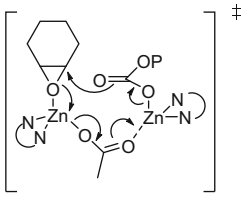


## 2.4 *Metal Salen Complexes: The Rise of Bifunctional Catalytic Systems*

One of the most widely researched classes of catalyst for this copolymerisation is the metal salen complexes (Fig. 8).

The first detailed report of metal salen catalysts came from Darensbourg and co-workers who showed that the Cr(III) salen complex **3a**, in conjunction with various Lewis bases (*N*-MeIm or DMAP), was a good catalyst for CHO/$CO_2$ copolymerisation (TOF, 32 $h^{-1}$, 80°C, 58.5 bar of $CO_2$) [137]. Shortly afterwards, Rieger and co-workers reported a very closely related Cr(III) salphen complex **3d**, in conjunction with DMAP, as a PPC catalyst [138]. Coates and co-workers established that Co(III) salen complexes, such as **3b**, were effective for PO/$CO_2$ copolymerisation [93, 139], without requiring any cocatalysts [139], at room temperature and under 55 bar of $CO_2$. Catalyst **3b** selectively afforded PPC with >95% carbonate linkages and a TOF up to 81 $h^{-1}$. It was noted that either increasing the temperature (e.g. to 40°C) or decreasing the pressure (e.g. to 40 bar) leads to a reduction in activity (TOF < 20 $h^{-1}$). Lu et al. were able to overcome this limitation, showing that the addition of ammonium salts ($nBu_4Y$, Y = Cl, Br, I, OAc) to Co(III) salen complex **3c** improved the activity (TOF > 160 $h^{-1}$), at lower $CO_2$ pressure (20 bar) [140].

Since then, a significant volume of research has been carried out on metal salen complexes, including studies of the influence of the metals, ligands, cocatalysts and reaction conditions, as well as expanding the application of these catalysts to various different epoxides. These investigations, which have been recently and extensively reviewed [38, 40, 46, 75, 99], led to the development of optimised bifunctional catalytic systems, comprising a discrete metal salen complex and a cocatalyst. However, such bifunctional systems have now been superseded by two-component single catalysts of type III (Fig. 3) featuring a cocatalyst tethered to the metal salen moiety; these latter systems will be discussed later. Furthermore, investigations of the bifunctional salen systems have implicated the formation of dimeric species in the catalytic cycles, as evidenced by kinetic studies showing orders in salen catalyst concentration of 1.2–1.8, depending on the conditions and catalysts [38, 46, 68, 69, 93].

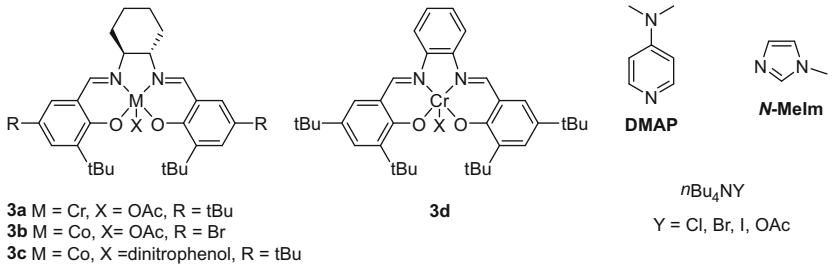


**Fig. 8** An illustration of the structures of various metal salen complexes, and cocatalysts, which are applied together in a bifunctional catalytic system

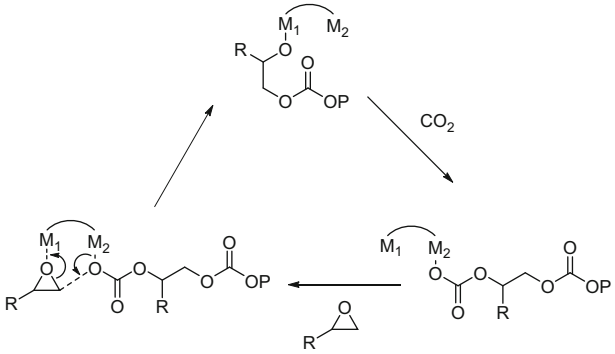


**Fig. 9** Proposed bimetallic mechanism for the alternating copolymerisation of $CO_2$ and epoxide

# 3 Bimetallic Complexes

## *3.1 Polymer Chain Shuttling Mechanism*

The results from kinetic and mechanistic studies performed on both homogeneous and heterogeneous catalysts have encouraged the development of bimetallic complexes. As discussed earlier, in many cases, the rationale for these studies is that two metal centres held in close proximity to one another have shown better activity than monometallic counterparts [33, 63, 77, 79, 84, 85, 141–143].

Typically such bimetallic systems are proposed to operate through a mechanism where one metal centre activates the epoxide via its coordination, whilst the other metal centre provides the nucleophile and facilitates the ring opening of the epoxide (Fig. 9). Within this class of catalyst, there are three commonly occurring structures; this review examines them separately. The first type of bimetallic complexes (IIa) applies deliberately dinucleating ligands, the second type (IIb) is bimetallic as a result of dimerisation of the monometallic complexes (e.g. the BDIZn catalysts, already described), and the third class (IIc) is bimetallic by tethering two monometallic complexes together (Fig. 10).

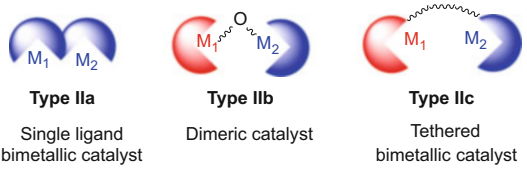


**Fig. 10** Different types of bimetallic complexes reviewed in this chapter

## *3.2 Single-Ligand Bimetallic Catalysts (IIa)*

One of the first successful deliberately bimetallic catalysts, reported by Lee and co-workers, **4**, consisted of an anilido–aldimine ligand bound to two zinc atoms (Fig. 11) [141, 142]. These catalysts showed very high activities (TON, 2,980 mol/mol) and high selectivities for carbonate linkages (85–96%) and produced very high molecular weight polymer ($M_n = 90$–$280$ kg/mol), albeit with a broader PDI. Structure–activity studies revealed that the substituents on the aryl rings as well as the addition of electron-withdrawing groups on the anildo-amidinate moieties increased the activity [141].

Xiao and co-workers reported a series of di-zinc and di-magnesium phenolate catalysts which showed significant potential [64]. Catalyst **5** polymerises CHO/$CO_2$ even at 1 atm of $CO_2$ (Fig. 12). However, the catalyst loading was high (5 mol%) particularly compared to the zinc anilido–aldimine complexes (0.006 mol%) [144].

Since 2009, our group have reported a series of bimetallic catalysts, where the two metals are coordinated by a diphenolate macrocyclic ligand (Fig. 13) [12, 43, 44, 56, 63, 65, 83–88]. These catalysts show very good activities in CHO copolymerisation, operating successfully at only 1 atm of $CO_2$ pressure, conditions under which many other catalysts are inactive. The first catalyst reported was a di-zinc complex, **6a**, which showed a TOF of 9.2 $h^{-1}$, at 80°C (Table 1, Fig. 13) [12, 43, 44, 56, 58, 76–81, 141]. Structure–activity studies revealed that variation of the *para*-phenyl substituent resulted in higher activity with the *tert*-butyl substituent, whereas a more electron-donating methoxy substituent appeared to reduce the activity slightly (TOF, 6.0 $h^{-1}$) [87].

The high activity of these complexes was attributed to the macrocyclic ligand as well as the bimetallic structure. Analogous compounds with "open" monometallic structures (i.e. coordinated by a phenolate tetraamine) were not active, despite showing good activity for lactide polymerisation [145, 146]. Trimetallic complexes, obtained by exogenous coordination of a third metal to the macrocyclic complexes, showed reasonable activity; analysis of the activity per metal centre revealed that the bimetallic catalysts were superior. This decrease in activity was attributed to the external metal centre hindering epoxide coordination [87]. The donor groups attached to the ligand are also important; Sugimoto and co-workers reported only low activities when imine instead of amine donors were applied [147].

The selection of the metals is of key importance in controlling the catalytic performance; using cobalt complexes has enabled the production of efficient

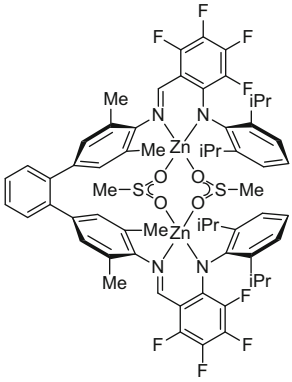


4

**Fig. 11** An illustration of one of the zinc anilido–aldimine catalyst structures, as reported by Lee and co-workers [141, 142]

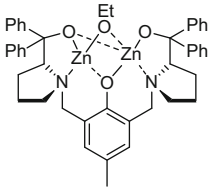


5

**Fig. 12** An illustration of the proposed structure of a di-zinc phenolate complex, as reported by Xiao and co-workers [64]

**Table 1** Copolymerisation of CHO/$CO_2$, catalysed by macrocyclic bimetallic catalysts

| Cat | T (°C) | TON[a] | TOF[b] ($h^{-1}$) | % PCHC[c] | % carbonate[c] | $M_n$[d] (g/mol) | PDI[e] | Reference |
|---|---|---|---|---|---|---|---|---|
| **6a** | 80 | 220 | 9.2 | 96 | >99 | 6,200 | 1.19 | [88] |
| **6a** | 100 | 264 | 13 | 94 | >99 | 7,360 | 1.21 | [88] |
| **6b** | 80 | 170 | 86 | >99 | >99 | 5,100 | 1.26 | [86] |
| **6c** | 80 | 145 | 47[f] | >99 | >99 | 11,400 | 1.13 | [56] |
| **6d** | 80 | 261 | 18 | >99 | >99 | 13,300 | 1.03 | [63] |
| **6d** | 100 | 229 | 76 | >99 | >99 | 11,800 | 1.03 | [63] |
| **6e** | 80 | 476 | 79 | >99 | >99 | 5,200 | 1.12 | [83] |

All copolymerisations carried out at 1 atm $CO_2$ at a loading of catalyst/CHO of 1:1,000, except entry for **6d** which is at 10 bar pressure

[a]TON = moles CHO consumed per mole of metal

[b]TOF = TON per hour

[c]Determined by $^1$H-NMR spectroscopy

[d,e]Determined by SEC in THF, using narrow polystyrene standards

[f]10 bar $CO_2$ pressure

catalysts either where both metals are in the same (II) oxidation state or where there is a mixed oxidation state (II/III) [86]. The activity of the cobalt(II) complex (Fig. 13) **6b** was approximately nine times higher (TOF = 86 $h^{-1}$) than the zinc

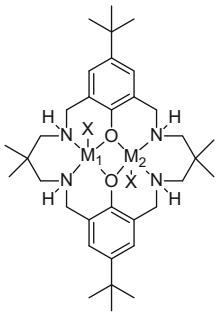


**Fig. 13** An illustration of the structures of a series of bimetallic complexes supported by a macrocyclic diphenolate ligand, as reported by Williams and co-workers [56, 63, 83, 86–88]

analogue, under the same conditions. Furthermore, the cobalt catalyst shows >99% selectivity towards copolymer, whereas the zinc catalyst (Fig. 13) produces ~4% cyclic carbonate at 80°C, 1 bar $CO_2$ pressure.

Our group have also reported some of the first examples of high-activity iron and magnesium catalysts, desirable due to the abundance, low cost and low toxicity of these metals (Fig. 13) [56, 63]. The di-iron catalyst, **6c**, shows good activity (TOF, 100 $h^{-1}$) producing PCHC with >99% carbonate linkages and <1% of cyclic by-product [56]. The addition of an ionic cocatalyst, bis(triphenylphosphino) iminium chloride (PPNCl), to the di-iron complex led to a switch in selectivity resulting in quantitative formation of *cis*-cyclohexene carbonate. The di-magnesium catalyst, **6d**, showed excellent activities (TOF >750 $h^{-1}$) and high selectivities (>99% carbonate, <1% cyclic carbonate) and produced polymers with narrow polydispersity indices [63].

Copolymerisation kinetic studies were undertaken using in situ, attenuated total reflectance infrared spectroscopy (ATR-IR) [85]. These studies, using catalyst **6a**, revealed an overall second-order rate law, which depended to the first order on both the concentrations of catalyst and of epoxide (CHO). In contrast, the dependence on carbon dioxide pressure, over the range 1–40 bar, was zero order. It was proposed that the rate-limiting step was epoxide ring opening by metal-bound carbonate, in line with structure–activity studies, spectroscopy and DFT calculations. The temperature dependence of the rate constants for both polymer and cyclic carbonate formation was studied; the rate of polymerisation increases up to around 80°C, after which point it decreases proposed to be due to decreased carbon dioxide solubility (at 1 bar pressure) in the reaction medium. In contrast, the rate of cyclic carbonate formation increases linearly with temperature.

In 2011, our group reported detailed theoretical studies of the polymerisation (density functional theory calculations) together with detailed ATR-IR studies of the elementary steps involved in polymerisation [84, 85]. As part of the calculations, a complete cycle of two sets of monomer additions was examined, with identification of the relevant transition states and intermediates [84]. This theoretical study revealed that the rate-limiting step was likely to be metal carbonate attack on the coordinated alkoxide. It was possible to compare the theoretical and

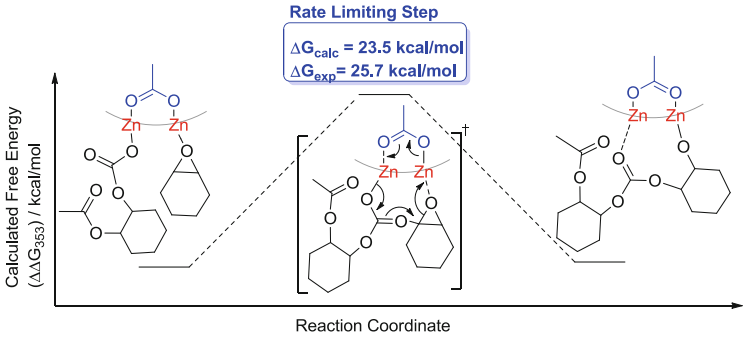


**Fig. 14** An illustration of the proposed rate-determining step for the macrocyclic bimetallic catalysts and the value for ΔG determined either by DFT calculations or from the temperature dependence of the rate constant (Eyring analysis) [84, 85]. The macrocyclic ligand is omitted for clarity and represented by the grey line. Reprinted (adapted) with permission from Buchard et al. [84] (Copyright (2012), American Chemical Society) [84].

experimental Gibbs free energy changes for this transition state, and the close agreement of the values gives confidence in the theoretical model (Fig. 14) [84].

Furthermore, the detailed spectroscopic investigation of the reaction of **6a** with the monomers showed that although two carboxylate groups (acetate) are present in the pre-catalyst, only one appears to react with the CHO. This leads to an unusual propagation pathway in which one carboxylate group serves as an initiating group and the other as a spectator co-ligand (Fig. 14 illustrates the rate-determining step). Furthermore, X-ray diffraction experiments were used to study the catalyst conformation [84]; these studies, together with a series of structure–activity studies on di-cobalt catalysts [65], indicated that the catalysts exhibit a facial selectivity, whereby the carboxylate bound on the convex face of the molecule is the site of initiation and propagation.

The proposed mechanism for these bimetallic macrocyclic catalysts, based on all the experimental and theoretical evidence, is illustrated in Scheme 4. It begins with coordination of an epoxide to the di-zinc catalyst. The epoxide is attacked and ring-opened by an acetate group coordinated at the other zinc centre. The initiation step leads to the formation of a zinc-bound alkoxide species. According to the DFT calculations, a $CO_2$ molecule approaches the di-zinc intermediate but is not directly coordinated by the zinc centres. Rather a zwitterionic intermediate forms by attack of the zinc alkoxide on the carbon dioxide molecule. This intermediate rapidly forms a zinc carbonate intermediate, bound at the other zinc site. The polymerisation propagates by the alternation of these steps. The rate-limiting step appears to be zinc carbonate attack on the zinc-bound epoxide molecule, as discussed already.

During polymerisation, it is proposed that the growing chain "shuttles" or switches its formal coordination site, between the two zinc centres. It changes its coordination site with both epoxide ring-opening and $CO_2$ insertion steps. In total, therefore, it switches twice with every propagation cycle (Scheme 4). According to this mechanism, the carboxylate (acetate) ligand plays a dual role in catalysis: one

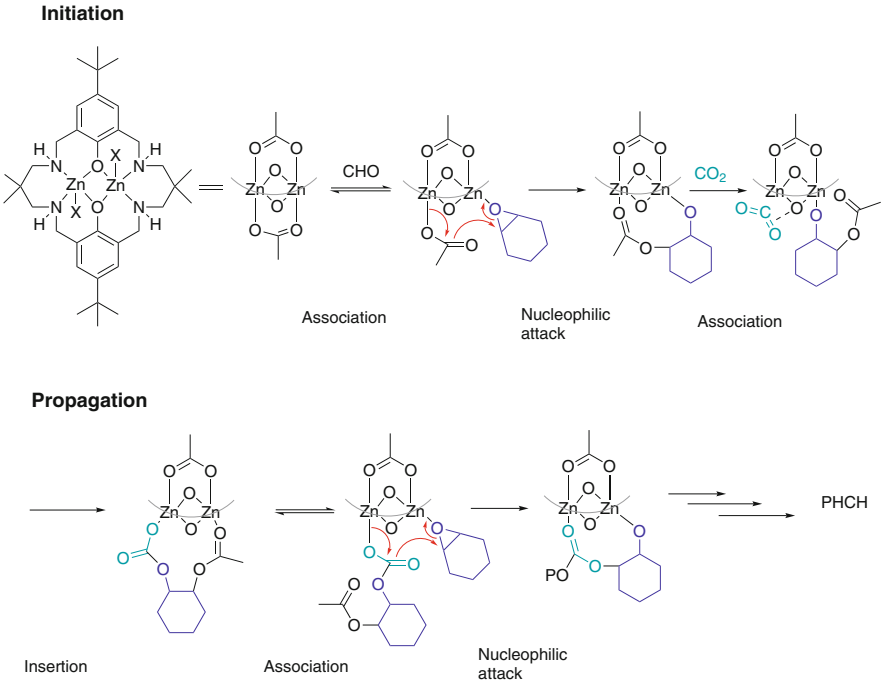


**Scheme 4** Proposed elementary steps occurring during copolymerisation catalysed by **6a**. The macrocyclic ligand is abbreviated with the *grey line* [84]

acetate group is an initiating/propagating site, whilst the other is retained during catalysis as a spectator co-ligand. The spectator acetate ligand serves to counterbalance the polymer chain "shuttling" by balancing the charge and coordination number at alternating zinc sites as the polymer chain grows. This unusual feature for the carboxylate ligand is supported by experimental results which reveal a dependence of the catalyst activity (TOF) depending on the co-ligand. Such an effect should not occur if the carboxylate ligand only serves as an initiating group (assuming initiation is relatively fast) [84, 85].

The next development was the preparation of an improved activity heterobimetallic catalyst, i.e. one containing two different metals, Zn(II) and Mg(II), **6e** [83]. The synthesis resulted in the formation of a mixture of compounds, including **6a**, **6d** and **6e**. This catalyst mixture is more efficient than either homodinuclear catalyst (**6a** or **6d**), either alone or mixed together, and shows activity which is greater than the sum of its parts (TOF, $79 \pm 5\ h^{-1}$, at 80°C and 1 atm of $CO_2$).

Very recently, Lin and co-workers have reported multidendate bis(benzotriazole iminophenol) bimetallic complexes zinc, nickel(II) and cobalt(II) (Fig. 15) [67]. Whereas the di-Zn complex **7a** mainly yields cyclic carbonate (66% vs. polymer), the di-nickel and di-cobalt complexes, **7b–c**, show good selectivity for polymer formation (94, >99% for **7c**, **7b**, respectively) and carbonate linkages

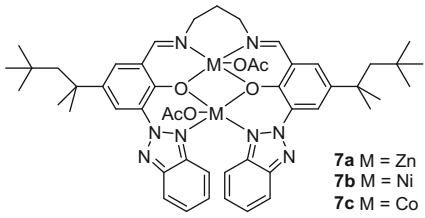


**Fig. 15** A representation of the structure of the bimetallic Zn, Co and Ni catalysts, as reported by Lin and co-workers [66]

(>99%). Under optimal conditions (T = 120°C, $pCO_2{}^\circ$ = 21 bar, 0.0625 mol% catalyst), **7b** and **7c** exhibit TOFs of 40 $h^{-1}$ and 53 $h^{-1}$, respectively.

## *3.3 Dimeric and Multimeric Structures (IIb)*

Various dimeric, and even trimeric, structures have been reported for epoxide/$CO_2$ catalysts. Most of these structures feature Schiff base ligands or multi-*N*,*O* donor ligands that dimerise via formation of *oxo* bridge, either as part of the ligand scaffold or from exogenous co-ligands (e.g. alkoxides or carboxylates).

Nozaki and co-workers reported the stereocontrolled copolymerisation of CHO/$CO_2$ using various chiral dimeric zinc complexes such as **8** (Fig. 16) [103, 148]. Catalyst **8** showed ~70% *ee*. The mechanism proposed invoked a bimetallic pathway, where initiation occurs by insertion of $CO_2$ into the amino ligand creating a monomeric zinc species which is the chiral propagating species.

In 2005, a series of dimeric rare-earth metal complexes for CHO/$CO_2$ copolymerisation were reported [57, 58]. Hou and co-workers showed that half-sandwich bis(alkyl) lutetium complexes underwent $CO_2$ insertion leading to dimeric compounds, as depicted in Fig. 17. Complex **9**, the most active of the series, affords polycarbonate ($M_n$ = 23,000 g/mol, PDI = 4.0) with 92% carbonate linkages, at 12 atm of $CO_2$ and 70°C.

Recently, Sugimoto and co-workers investigated various dimeric β-diketiminate (Fig. 18) and Schiff base aluminium complexes, including **10a–b** [149]. Complexes **10a–b**, in the presence of $Et_4NOAc$, showed good selectivity (carbonate linkages >98%) and moderate activity (TOF < 13 $h^{-1}$) and low enantioselectivity (*ee* ~25%). The *ee* was improved (*ee* ~62%) by adding various Lewis bases, most especially with bis-*N*-MeIm or bis-*N*-MeBzIm. The influence of the cocatalysts may suggest a two-component mechanism, in line with aluminium porphyrin catalysts, instead of a polymer "shuttling" mechanism.

In 2013, Nozaki and co-workers reported a dimeric iron-corrole complex, **11a**, for copolymerisation of CHO, PO and glycidyl phenyl ether (GPE) with $CO_2$ (Fig. 19) [55]. Dimeric **11a** requires the addition of a cocatalyst (e.g. PPNCl) and shows excellent selectivity for polymer formation (>99% vs cyclic carbonate) with a good activity in the case of PO (TOF > 1,000 $h^{-1}$). However, the polymers have

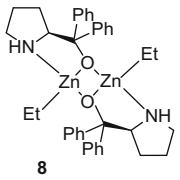


8

**Fig. 16** An illustration of the structure of one of the first dimeric catalysts, reported by Nozaki and co-workers [103]

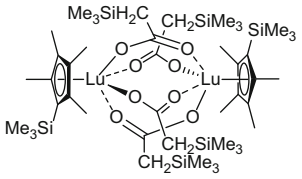


9

**Fig. 17** An illustration of the structure of a dimeric rare earth metal complex [58]

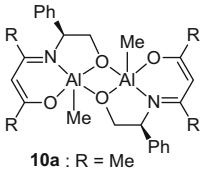


**10a** : R = Me
**10b** : R = Ph

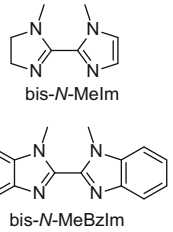


**Fig. 18** Schiff base dimeric aluminium complexes, reported by Sugimoto and co-workers [149]

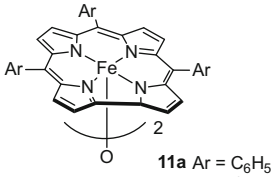


**11a** Ar = $C_6H_5$
**11b** Ar = $C_6F_5$

**Fig. 19** An illustration of the structures of various metal corrole complexes, as reported by Nozaki and co-workers [55]

low contents of carbonate linkages, up to 29% and 22% for PO and GPE, respectively.

This year, Lin and co-workers reported various well-defined copper complexes, **12**, for CHO/$CO_2$ copolymerisation (Fig. 20) [66]. The bimetallic complexes, **12c–d**, showed higher activity than the mono- and trimetallic counterparts, **12a–b**,**d**. Under optimal conditions (T = 120°C, $pCO_2$ = 21 bar, 0.2 mol% catalyst), **12c–d** show good selectivity for polymer formation (>71% vs. cyclic carbonate) with TOFs up to 18 $h^{-1}$ leading to low molecular weight polymers ($3{,}000 < M_n < 7{,}000$ g/mol).

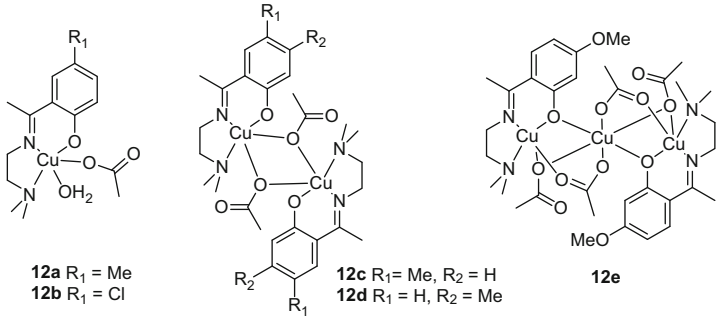


**Fig. 20** An illustration of the structures of various mono-, bi- and trimetallic copper complexes bearing Schiff base ligands, reported by Lin and co-workers [66]

## *3.4 Tethered Bimetallic Catalysts (IIc)*

As part of the ongoing investigations and opportunities for bimetallic catalysts, various groups have investigated the tethering of successful "monometallic" catalysts, including BDIZn, metal salen and porphyrin complexes [68–72, 150]. The strategies have generally been to link together two ligands, using covalent bonds, and then to coordinate two metal centres to produce homobimetallic catalysts.

### 3.4.1 Linked Bimetallic BDI Catalysts

Given the excellent performance of BDIZn catalysts and the mechanistic findings from Coates and co-workers, it was a natural next step to investigate tethered BDIZn catalysts. Ziemer et al. reported one such structure **13a**, which placed the two zinc sites parallel to each other (Fig. 21) [81]. The reported distance between the two zinc atoms was 4.92 Å, but the resulting catalyst showed a worse performance than conventional BDIZn dimers (TOF, 9 $h^{-1}$), possibly due to steric factors. An improved catalyst was obtained by bridging two BDI ligands via *para*- and *meta*-substituted phenyl groups, **13b**, as reported by Harder and co-workers (Fig. 21) [82]. Complex **13b** showed a reduced Zn–Zn distance (3.79 Å) and showed a good activity (TOF, 262 $h^{-1}$), at 10 atm of $CO_2$ and 60°C. The selectivity was excellent (>99% carbonate linkages), yielding PCHC of high molecular weights ($M_n$, 45–100 kg/mol).

In 2013, Rieger et al. reported flexibly tethered di-zinc complexes featuring BDI moieties linked through the phenyl rings (Fig. 22) [79]. Whereas the complex **14b** featuring the more rigid spacer showed only low activity for CHO/$CO_2$ copolymerisation, complex **14a** showed high activities (TOF, 9,130 $h^{-1}$, 40 bar). The kinetic and DFT studies suggested a change in the rate-determining step, depending on the $CO_2$ pressure. Below 25 bar pressure, the rate law was proposed to be first order dependent on $CO_2$ pressure and zero order in epoxide concentration,

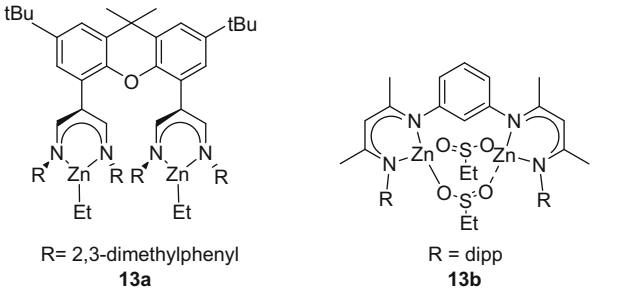


**Fig. 21** An illustration of the structures of various tethered bimetallic BDIZn catalysts, as reported by the groups of Ziemer (**13a**) and Harder (**13b**), respectively [81, 82]

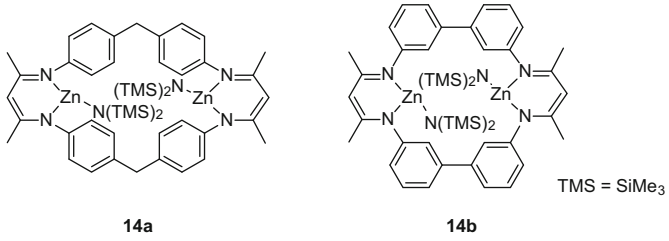


**Fig. 22** An illustration of the flexibly tethered bimetallic BDIZn catalysts, as reported by Rieger and co-workers [79]

suggesting $CO_2$ insertion is rate limiting. In contrast, above 25 bar pressure, the rate law was interpreted as first order in epoxide and zero order in $CO_2$, suggesting epoxide ring opening is rate limiting.

### 3.4.2 Linked Bimetallic Salen Complexes

As highlighted by the pioneering work of Jacobsen and co-workers using bimetallic chromium and cobalt salen complexes for the enantioselective ring opening of epoxides [151, 152] and, more recently, with the work of Coates on bimetallic cobalt salen complexes for stereoselective epoxide polymerisation [153, 154], linked bimetallic salen complexes appear promising candidates for epoxide/$CO_2$ copolymerisation.

In 2010, Nozaki and co-workers reported various linked bimetallic cobalt(III) salen complexes for the PO/$CO_2$ copolymerisation and highlighted that, in the absence of a cocatalyst, the polymerisation occurs by a bimetallic mechanism (Fig. 23) [155]. The bimetallic catalyst **15a** shows superior activities than its monometallic analogue **15d**, especially at low catalyst loadings (for [PO]/[Co] = 3,000, TOF = 120 $h^{-1}$ and 20 $h^{-1}$ for **15a** and **15d**, respectively). In addition, the relative configurations of the two metal salen units influenced the activity. Thus, the

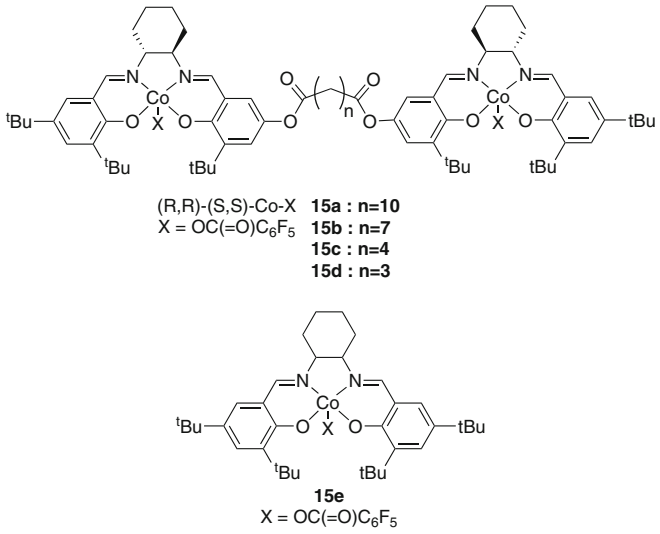


**Fig. 23** An illustration of the structures of some linked bimetallic cobalt salen complexes, as reported by Nozaki [155]

(*R*,*R*)-(*S*,*S*)-**15a** was more active than (*R*,*R*)-(*R*,*R*)-**15a** (TOF = 120 $h^{-1}$ vs. 40 $h^{-1}$, respectively). Furthermore, the length of the spacer group also affected the activity and selectivity. Thus, **15c** is the most active catalyst (TOF, 180 $h^{-1}$ at [PO]/[Co] = 3,000). These important results provide further support for a bimetallic mechanism. However, in the presence of onium salts, the polymerisation appears to occur via more complex and even monometallic mechanisms, even in the case of the linked bimetallic catalysts.

Shortly afterwards, Rieger and co-workers reported a tethered chromium salphen complex for PO/$CO_2$ copolymerisation (Fig. 24) [156]. As observed by Nozaki and co-workers, in the absence of a cocatalyst and at low catalyst loadings ([PO]/[Cr] = 20,000), the bimetallic complex **16a** shows significantly higher activity than the monometallic analogue **16b** (TOF = 7 $h^{-1}$ and 82 $h^{-1}$ for **16a** and **16b**, respectively), whereas they have comparable activity (TOF = 67 $h^{-1}$ and 49 $h^{-1}$ for **16a** and **16b**, respectively) at higher catalyst loading ([PO]/[Cr] = 2,000). Further kinetic studies suggest that reaction occurs via a bimetallic mechanism with both catalysts [157]. In the presence of onium salts as cocatalysts, the mechanism is likely to switch to a bicomponent monometallic mechanism for both complexes **16a**–**b**.

In 2013, Lu and co-workers reported the use of various dinuclear cobalt(III) complexes, **17a**–**c**, for the enantioselective copolymerisation of CHO or cyclopentene oxide (CPO) with $CO_2$ (Fig. 25) [94]. For CPO/$CO_2$ copolymerisation (25°C, 20 bar $CO_2$), in the presence of PPNX (X = 2,4-dinitrophenoxide), complexes **17a**–**b** were highly enantioselective (*ee* >99%) and highly active (TOF, ~200 $h^{-1}$). At only 1 atm of $CO_2$ pressure, complex **17b** was also able to afford

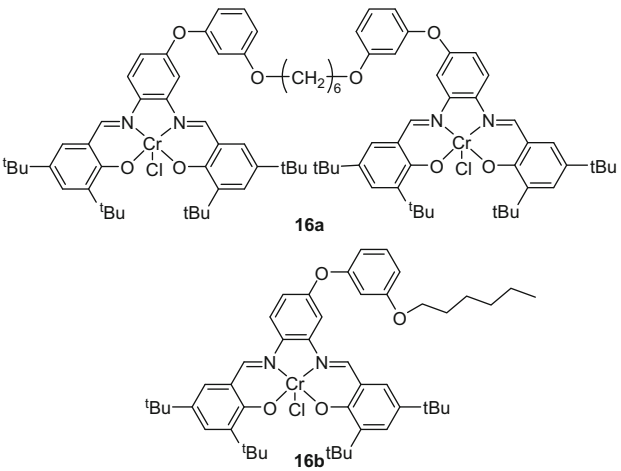


**Fig. 24** An illustration of the structures of the linked bimetallic chromium salphen complexes for $PO/CO_2$ copolymerisation, as reported by Rieger and co-workers [156]

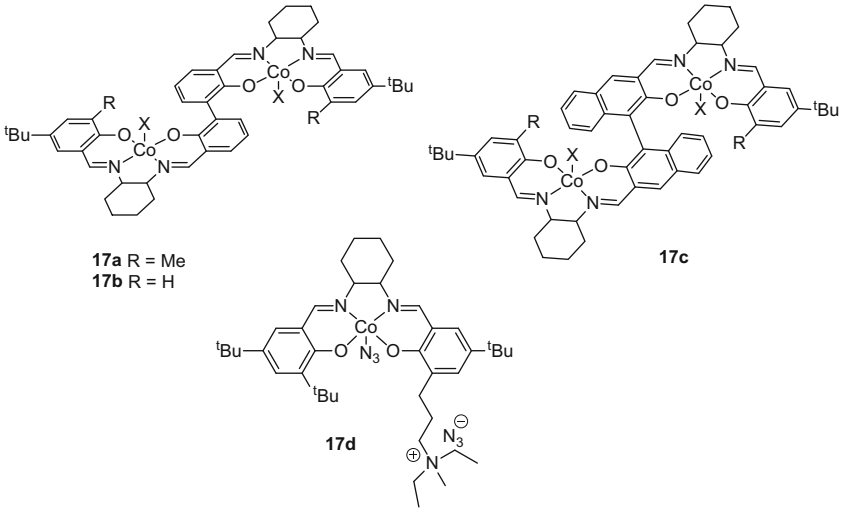


**Fig. 25** An illustration of the structures of various dinuclear cobalt(III) salen catalysts, reported by Lu and co-workers [94]

polycarbonate with good activity (TOF = 40 $h^{-1}$) whilst retaining excellent enantioselectivity (*ee* = 96%). It is interesting that the bicomponent complex **17d** shows low enantioselectivity (*ee* <30) and favours the opposite enantiomer. Under similar conditions (20 bar, 25°C), the same catalysts **17a–b**, in the presence of PPNX (X = 2,4-dinitrophenoxide), catalysed PCHC formation with high activities (TOF, 1,400 $h^{-1}$) and good enantioselectivity (*ee* ~80%). However, under optimal

conditions (0°C, in the presence of toluene), catalyst **17b** afforded highly isotactic semi-crystalline PCHC ($M_n = 35.6$ kg/mol, PDI = 1.35, *ee* = 98%) with a very high melting temperature of 272°C. Interestingly, in the absence of a cocatalyst, **17a–b** showed only very low activities and enantioselectivities for either CHO/$CO_2$ or CPO/$CO_2$ copolymerisation.

Finally, bimetallic cobalt complex **17c**, which is an effective catalyst for the enantioselective homopolymerisation of epoxide [153, 158], showed a low activity (TOF < 10 $h^{-1}$) and a poor enantioselectivity (*ee* <33%) for CPO/$CO_2$ copolymerisation, highlighting the importance of the linker on the complex geometry and the metal–metal distance.

## *3.5 Linked Bimetallic Porphyrin Catalysts*

In analogy to the success of the linked bimetallic salen catalyst, it was also possible to link together porphyrin complexes. Indeed, Rieger and co-workers studied a series of linked bis-porphyrin complexes, **18**, comparing them to a monometallic cobalt porphyrin (Fig. 26). The dinuclear complex showed lower productivities (TON = 300–696, depending on the linker position) than the monometallic counterparts (TON = 983). These findings suggest that a monometallic mechanism may operate for metal porphyrins. Moreover, the utilisation of a cocatalyst was found to be essential. One explanation for the poor performance of the bimetallic catalyst is that catalyst deactivation, by reduction of cobalt(III) to cobalt(II), appears faster in the case **18** [143, 159].

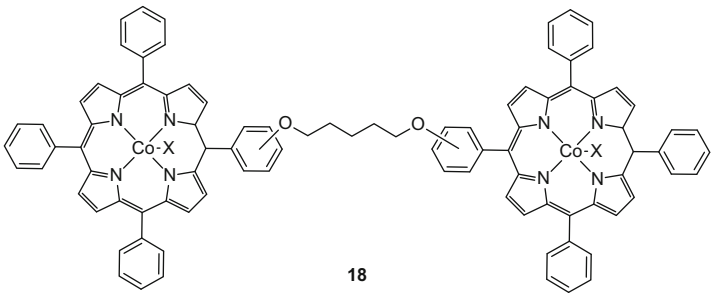


18

**Fig. 26** An illustration of the structures of a tethered bimetallic porphyrin catalyst, as reported by Rieger and co-workers [143]

## 4 Two-Component Single Catalysts (III)

The final section of the review examines the Type III catalysts, which are two-component single catalysts. These are metal salen catalysts, whereby the cocatalyst group is covalently attached to the ligand scaffold. Some of these catalysts show best performances in the metal salen class.

### *4.1 Mechanistic Considerations for Catalyst/Cocatalyst Systems*

Although most of the deliberately bimetallic catalysts, particularly those of zinc and magnesium, are able to operate without a cocatalyst, there are particular classes of catalyst for which the addition of a cocatalyst is vital for performance. The classes which require cocatalysts are metal porphyrin and metal salen complexes. Addition of cocatalysts presents some difficulties in unpicking the precise mechanisms and structures for the propagating species, and it seems that the mechanisms are rather dependent on both the conditions and catalysts selected. Both Coates and Darensbourg, and their co-workers, have reported, independently, that metal salen catalysts operate by bimetallic initiation mechanisms followed by monometallic propagation processes [93, 137]. Furthermore, recent kinetic studies from the Nozaki group have shown that for a Co(salen)Cl/PPNCl system, an order in catalyst concentration of 1.57 was obtained indicative of complex propagating processes [160]. Related fractional orders in catalyst concentration were also reported by Rieger and co-workers, using a chromium salen complex, in the absence of a cocatalyst [156]. Nozaki and co-workers also reported novel titanium and germanium BOXDIPY catalysts which [50], in the presence of a cocatalyst, showed fractional (1.57, 1.75) orders in catalyst concentrations consistent with various different mechanisms being operative [160]. Indeed, it is immediately possible to propose at least three different initiation pathways for such catalyst/cocatalyst systems (Fig. 27) including those involving two metal complexes or monometallic pathways involving metal-bound initiating group and epoxide or metal-bound epoxide being attacked by an exogenous initiating group (anion). Given the complexities of such initiation steps, it should be understood that related complex propagation pathways can be proposed. Furthermore, the nature (nuclearity) of the propagating species and whether it is a neutral or charged complex remains unknown for this class of catalyst. A very interesting recent theoretical study by Nozaki and co-workers proposes some generic methods to select highly active catalyst/cocatalyst combinations by estimation of the energies of epoxide binding/opening [160].

Given the complexities of the catalyst/cocatalyst systems, a series of two-component catalysts were designed where the cocatalyst is tethered to the

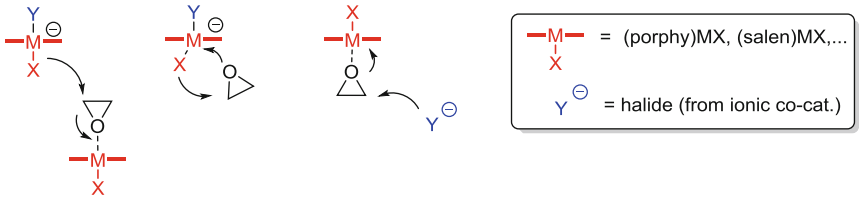


**Fig. 27** An illustration of some example of initiation pathways for catalyst/cocatalyst systems

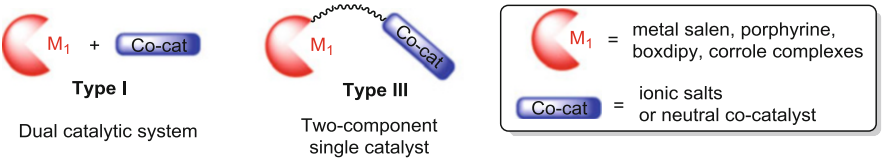


**Fig. 28** An illustration of the generic structures of two-component catalysts (Type III)

metal complex moiety (Fig. 28). This review focusses on bimetallic catalysts and such bicomponent systems are considered an important subclass.

## *4.2 Cocatalyst Tethered to Metal Salen Complex*

### 4.2.1 Metal Salen Complexes Bearing Tethered Ionic Cocatalyst(s)

Inspired by the high activity and selectivity of bifunctional catalytic systems (metal salen complex/onium salt), Nozaki and co-workers reported, as early as 2006, a novel two-component catalyst, **19a** (Fig. 29) [161]. The cobalt(III) salen complex featured a piperidinium moiety tethered to the ligand. Thus, without addition of exogenous cocatalyst, complex **19a** showed high selectivity (>99%) and activity (TOF, 250 $h^{-1}$) for PPC formation at 14 bar $CO_2$ and 25°C. The tethered piperidinium moiety efficiently suppressed the formation of cyclic carbonate, allowing the reaction to be heated to 60°C (TOF = 680 $h^{-1}$) whilst retaining high polymer selectivity (~90%).

In 2007, Lee and co-workers reported a cobalt(III) metal salen complex featuring to tethered ammonium arm, **19b**, for PO/$CO_2$ copolymerisation (Fig. 29) [162]. The complex was thermally robust and showed high activity (3,500 $h^{-1}$), at 90°C whilst retaining good polymer selectivity (~90%). Under the same conditions, an analogous catalyst/cocatalyst combination showed low activity and poor selectivity for polymer. Shortly after, Lee reported a series of cobalt(III) metal salen complexes bearing tethered ammonium groups for PO/$CO_2$ copolymerisation [163]. Thus, complex **19c**, bearing four onium substituents, was the most active and afforded PPC, at 70°C, with excellent polymer selectivity (>99%) and with very impressive productivities (TON >20,000) and activities (TOF > 20,000 $h^{-1}$). In addition, the catalyst could be separated from the polymer (by column

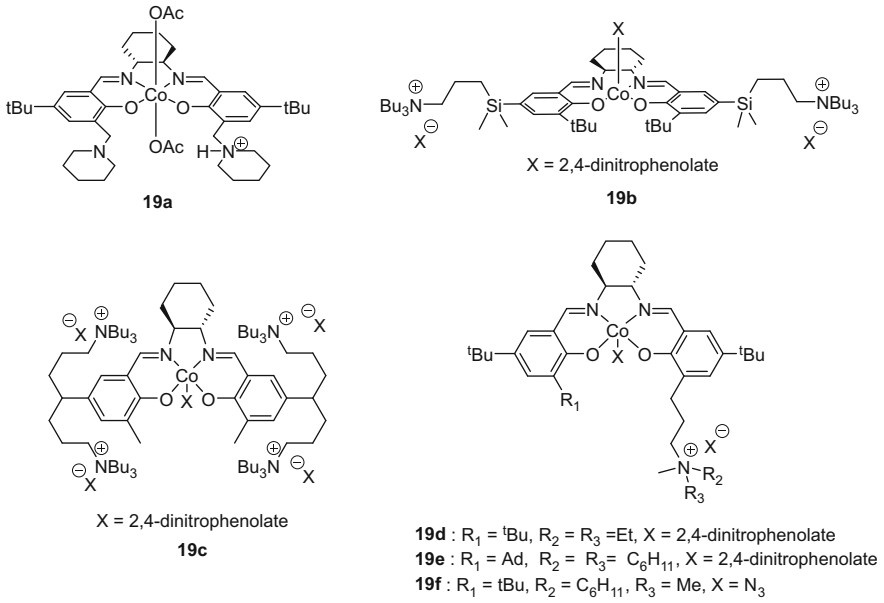


**Fig. 29** An illustration of the structure of successful two-component catalysts, as reported by Nozaki, Lu and Lee and co-workers [15, 161]

chromatography on a small scale) and reused, without significant loss of catalytic performance [163]. Further kinetic and mechanistic investigations have implicated cobaltate intermediates and various coordination geometries as important for good activity [164–166]. Additionally, the catalysts have been applied to prepare various polymers, with variable composition and architectures [167–169]. Thus, telechelic PPC has been synthetised and used to prepare block copolymers and polyurethanes [170, 171].

Lu and co-workers synthesised various cobalt(III) metal salen complexes bearing tethered ammonium salts, **19d–f**, or neutral Lewis bases, **20** (Fig. 29) [15]. The bifunctional complexes showed enhanced activity over their binary counterparts in both PO and CHO/$CO_2$ copolymerisations [172]. This was proposed to be due to the ammonium salt, tethered to the salen backbone, ensuring that any dissociated polycarbonate chains remain in "close proximity" to the metal. Moreover, the enhanced selectivities of the bifunctional catalyst over the binary systems are likely due to higher activation energy barriers to cyclic by-products. In addition, catalyst **19b**, featuring a bulky substituent, afforded isotactic poly(chloropropylene carbonate) [96]. As part of the development of this class of catalysts, Darensbourg and co-workers also applied them to the copolymerisation of other epoxides, including cyclopropene oxide and indene oxide; such monomers had previously proven very difficult to copolymerise (low selectivities/catalysts), and thus the bifunctional catalysts showed significant promise with recalcitrant monomers [173, 174]. An

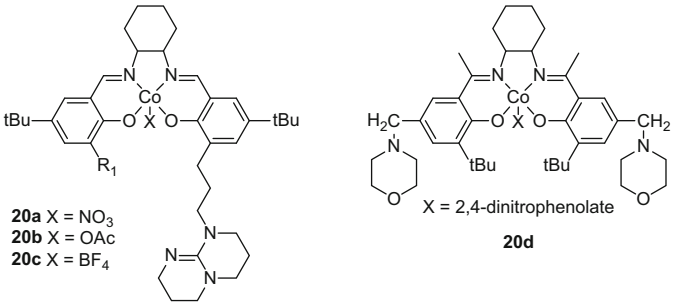


**Fig. 30** An illustration of the structures of various bicomponent cobalt(III) salen complexes bearing Lewis bases [15, 38, 93, 179]

added benefit was that poly(cyclopentene carbonate) was shown to undergo facile depolymerisation to regenerate epoxide/$CO_2$, a very unusual finding as most polycarbonates depolymerise to cyclic carbonates [175].

### 4.2.2 Metal Salen Complexes Bearing Tethered Neutral Lewis Base

Lu and co-workers also designed various new salen ligands with tethered neutral Lewis bases (Fig. 30) [15, 38, 99]. The catalyst with an anchored TBD group, **20a**, was highly active (TOF up to 10,000 $h^{-1}$) and selective (>97%), even at high temperatures (up to 100°C), for CHO/$CO_2$ and PO/$CO_2$ copolymerisations [172, 176] as well as for SO/$CO_2$ copolymerisation [177]. In addition, the catalyst afforded epichlorohydrin/$CO_2$ copolymers (>99% carbonate linkages). A decrease in the reaction temperature, from 25 to 0°C, enabled a high selectivity for polymer formation (>99% vs. cyclic carbonate), whereas under the same conditions, a binary cobalt salen/PPNX system led to only 66% selectivity for polymer [178].

In 2011, Niu reported a tetradentate Schiff base cobalt complex with two Lewis base units **20d**. It showed a high activity (TOF, 633 $h^{-1}$) and selectivity (>99% carbonate linkages) and was applied in various terpolymerisations.

## 5 Conclusions and Outlook

The field of carbon dioxide/epoxide copolymerisation is one attracting considerable attention as a means to add value to carbon dioxide and produce useful polymeric materials. Continued catalyst development is central to successful implementation of the technology. The area of catalyst development brings together the fields of organometallic and polymer chemistry. This review has highlighted the development of catalysts from the early days of the field, when zinc alkoxide and carboxylate clusters were the mainstay of research, through the development of successful single-site metal complexes, and beyond to the study of kinetics and mechanism to

inform the preparation of the current bimetallic catalysts. These mechanistic studies have implicated bimetallic active sites in many cases, although there do remain other examples where monometallic mechanisms appear dominant, most notably for metal porphyrins used with cocatalysts. There are interesting links with the mechanisms of many of the homogeneous catalysts and the heterogeneous catalysts, the zinc glutarates and double metal cyanide materials, for which multimetallic active surface sites have been predicted.

In this review, we have focussed deliberately on catalysts which are proposed or "designed" to operate by bimetallic processes. In particular, there are three subclasses of bimetallic catalyst which have been examined:

1. Catalysts which contain a single ligand which is deliberately dinucleating
2. Dimeric catalysts
3. Bimetallic catalysts prepared by tethering "monometallic" complexes

Many of these bimetallic catalysts show promising performances, including high activities, selectivities and good polymerisation control. A particular advantage for the future applications of these catalysts appears to lie in the ability to apply them successfully at low loadings. In the area of bicomponent catalysts, we have also highlighted porphyrin and salen metal complexes which require the addition of a cocatalyst for successful operation. In this area, it is now accepted that improved performance results from tethering, or covalent attachment, of the catalyst and cocatalyst. This has resulted in some very impressive performances, including high activities at higher temperatures, the ability to operate at low loadings with excellent selectivities. There are recent reports which show that such species are also capable of exerting stereochemical control so as to access new polymer tacticities and microstructures.

In conclusion, the overall goal of the review has been to highlight the emerging importance of bimetallic mechanisms and catalysts in this important area of polymerisation catalysis and carbon dioxide utilisation chemistry. There remain, however, clear priority areas for future development, fundamental challenges to understand, a need for improved theories of polymerisation catalysis and outstanding materials science challenges. Despite the successes achieved so far, it is remarkable how limited the range of catalysts for this process remains. There are clearly some excellent opportunities for new catalysts in this field, including the development of new ligands, metals and combinations so as to improve performance. An area of considerable potential could be the development of heterobimetallic catalysts, given the successes of some heterobimetallic heterogeneous catalysts (DMCs) and the first report of a highly active homogeneous catalyst earlier this year. There is also a need for fine control of polymerisation, specifically to control the regio-chemistry and stereochemistry of polymerisation, so as to enable new polymer tacticities and microstructures. The intriguing report of improved thermal properties for stereoblock polycarbonate presents an inspiring starting point, as do recent successes in achieving very high degrees of iso-selectivity in cyclohexene/propene oxide enchainment. Thus, although the

field of copolymerisation catalysis was discovered some decades ago, there remain exciting future opportunities and significant new challenges to be overcome.

## References


1. Mikkelsen M, Jorgensen M, Krebs FC (2010) The teraton challenge. A review of fixation and transformation of carbon dioxide. Energy Environ Sci 3(1):43–81
2. MacDowell N, Florin N, Buchard A, Hallett J, Galindo A, Jackson G, Adjiman CS, Williams CK, Shah N, Fennell P (2010) An overview of $CO_2$ capture technologies. Energy Environ Sci 3(11):1645–1669
3. Darensbourg DJ (2010) Chemistry of carbon dioxide relevant to its utilization: a personal perspective. Inorg Chem 49(23):10765–10780
4. von der Assen N, Voll P, Peters M, Bardow A (2014) Life cycle assessment of $CO_2$ capture and utilization: a tutorial review. Chem Soc Rev 43(23):7982–7994
5. Langanke J, Wolf A, Hofmann J, Bohm K, Subhani MA, Muller TE, Leitner W, Gurtler C (2014) Carbon dioxide ($CO_2$) as sustainable feedstock for polyurethane production. Green Chem 16(4):1865–1870
6. Luinstra GA (2008) Poly(propylene carbonate), old copolymers of propylene oxide and carbon dioxide with new interests: catalysis and material properties. Polym Rev 48(1): 192–219
7. Korashvili R, Noernberg B, Bornholdt N, Borchardt E, Luinstra GA (2013) Poly(propylene carbonate) from carbon dioxide: challenges for large-scale application. Chem Ing Tech 85(4):437–446
8. http://www.empowermaterials.com/, http://www.novomer.com/, http://www.materialscience.bayer.de/Projects-and-Cooperations/CO2-Project.aspx, http://www.econic-technologies.com/. Accessed 23 Sept 2014
9. von der Assen N, Bardow A (2014) Life cycle assessment of polyols for polyurethane production using $CO_2$ as feedstock: insights from an industrial case study. Green Chem 16(6):3272–3280
10. Darensbourg DJ, Chung W-C, Wang K, Zhou H-C (2014) Sequestering $CO_2$ for short-term storage in MOFs: copolymer synthesis with oxiranes. ACS Catal 4(5):1511–1515
11. Byrne CM, Allen SD, Lobkovsky EB, Coates GW (2004) Alternating copolymerization of limonene oxide and carbon dioxide. J Am Chem Soc 126(37):11404–11405
12. Winkler M, Romain C, Meier MAR, Williams CK (2015) Renewable polycarbonates and polyesters from 1,4-cyclohexadiene. Green Chem 17(1):300–306
13. Hu Y, Qiao L, Qin Y, Zhao X, Chen X, Wang X, Wang F (2009) Synthesis and stabilization of novel aliphatic polycarbonate from renewable resource. Macromolecules 42(23): 9251–9254
14. Jeon JY, Lee JJ, Varghese JK, Na SJ, Sujith S, Go MJ, Lee J, Ok M-A, Lee BY (2013) $CO_2$/ethylene oxide copolymerization and ligand variation for a highly active salen-cobalt(III) complex tethering 4 quaternary ammonium salts. Dalton Trans 42(25):9245–9254
15. Ren W-M, Liu Z-W, Wen Y-Q, Zhang R, Lu X-B (2009) Mechanistic aspects of the copolymerization of $CO_2$ with epoxides using a thermally stable single-site cobalt(III) catalyst. J Am Chem Soc 131(32):11509–11518
16. Varghese JK, Park DS, Jeon JY, Lee BY (2013) Double metal cyanide catalyst prepared using $H_3Co(CN)_{(6)}$ for high carbonate fraction and molecular weight control in carbon dioxide/propylene oxide copolymerization. J Polym Sci A Polym Chem 51(22):4811–4818
17. Dong Y, Wang X, Zhao X, Wang F (2012) Facile synthesis of poly(ether carbonate)s via copolymerization of $CO_2$ and propylene oxide under combinatorial catalyst of rare earth

ternary complex and double metal cyanide complex. J Polym Sci A Polym Chem 50(2): 362–370
18. Zhang X-H, Wei R-J, Sun X-K, Zhang J-F, Du B-Y, Fan Z-Q, Qi G-R (2011) Selective copolymerization of carbon dioxide with propylene oxide catalyzed by a nanolamellar double metal cyanide complex catalyst at low polymerization temperatures. Polymer 52(24): 5494–5502
19. Sun XK, Zhang XH, Liu F, Chen S, Du BY, Wang Q, Fan ZQ, Qi GR (2008) Alternating copolymerization of carbon dioxide and cyclohexene oxide catalyzed by silicon dioxide/Zn-Co-III double metal cyanide complex hybrid catalysts with a nanolamellar structure. J Polym Sci A Polym Chem 46(9):3128–3139
20. Robertson NJ, Qin ZQ, Dallinger GC, Lobkovsky EB, Lee S, Coates GW (2006) Two-dimensional double metal cyanide complexes: highly active catalysts for the homo-polymerization of propylene oxide and copolymerization of propylene oxide and carbon dioxide. Dalton Trans 45:5390–5395
21. Kim I, Yi MJ, Lee KJ, Park D-W, Kim BU, Ha C-S (2006) Aliphatic polycarbonate synthesis by copolymerization of carbon dioxide with epoxides over double metal cyanide catalysts prepared by using ZnX2 (X = F, Cl, Br, I). Catal Today 111(3–4):292–296
22. Chen S, Qi G-R, Hua Z-J, Yan H-Q (2004) Double metal cyanide complex based on Zn3[Co (CN)6]2 as highly active catalyst for copolymerization of carbon dioxide and cyclohexene oxide. J Polym Chem A Polym Chem 42(20):5284–5291
23. Darensbourg DJ, Adams MJ, Yarbrough JC, Phelps AL (2003) Synthesis and structural characterization of double metal cyanides of iron and zinc: catalyst precursors for the copolymerization of carbon dioxide and epoxides. Inorg Chem 42(24):7809–7818
24. Darensbourg DJ, Adams MJ, Yarbrough JC (2001) Toward the design of double metal cyanides for the copolymerization of $CO_2$ and epoxides. Inorg Chem 40(26):6543–6544
25. Klaus S, Lehenmeier MW, Herdtweck E, Deglmann P, Ott AK, Rieger B (2011) Mechanistic insights into heterogeneous zinc dicarboxylates and theoretical considerations for $CO_2$-epoxide copolymerization. J Am Chem Soc 133(33):13151–13161
26. Ree M, Hwang Y, Kim JS, Kim H, Kim G (2006) New findings in the catalytic activity of zinc glutarate and its application in the chemical fixation of $CO_2$ into polycarbonates and their derivatives. Catal Today 115(1–4):134–145
27. Hwang Y, Kim H, Ree M (2005) Zinc glutarate catalyzed synthesis and biodegradability of poly(carbonate-co-ester)s from $CO_2$, propylene oxide, and epsilon-caprolactone. Macromol Symp 224:227–237
28. Kim JS, Kim H, Ree M (2004) Hydrothermal synthesis of single-crystalline zinc glutarate and its structural determination. Chem Mater 16(16):2981–2983
29. Kim JS, Ree M, Shin TJ, Han OH, Cho SJ, Hwang YT, Bae JY, Lee JM, Ryoo R, Kim H (2003) X-ray absorption and NMR spectroscopic investigations of zinc glutarates prepared from various zinc sources and their catalytic activities in the copolymerization of carbon dioxide and propylene oxide. J Catal 218(1):209–219
30. Kim JS, Ree M, Lee SW, Oh W, Baek S, Lee B, Shin TJ, Kim KJ, Kim B, Lüning J (2003) NEXAFS spectroscopy study of the surface properties of zinc glutarate and its reactivity with carbon dioxide and propylene oxide. J Catal 218(2):386–395
31. Hwang Y, Jung J, Ree M, Kim H (2003) Terpolymerization of $CO_2$ with propylene oxide and ε-caprolactone using zinc glutarate catalyst. Macromolecules 36(22):8210–8212
32. Meng YZ, Du LC, Tiong SC, Zhu Q, Hay AS (2002) Effects of the structure and morphology of zinc glutarate on the fixation of carbon dioxide into polymer. J Polym Chem A Polym Chem 40(21):3579–3591
33. Klaus S, Lehenmeier MW, Anderson CE, Rieger B (2011) Recent advances in $CO_2$/epoxide copolymerization-New strategies and cooperative mechanisms. Coord Chem Rev 255 (13–14):1460–1479
34. Nozaki K (2004) Asymmetric catalytic synthesis of polyketones and polycarbonates. Pure Appl Chem 76(3):541–546

35. Kuran W (1998) Coordination polymerization of heterocyclic and heterounsaturated monomers. Prog Polym Sci 23(6):919–992
36. Darensbourg DJ, Holtcamp MW (1996) Catalysts for the reactions of epoxides and carbon dioxide. Coord Chem Rev 153:155–174
37. Darensbourg DJ, Yeung AD (2013) Thermodynamics of the carbon dioxide-epoxide copolymerization and kinetics of the metal-free degradation: a computational study. Macromolecules 46(1):83–95
38. Lu X-B, Darensbourg DJ (2012) Cobalt catalysts for the coupling of $CO_2$ and epoxides to provide polycarbonates and cyclic carbonates. Chem Soc Rev 41(4):1462–1484
39. Darensbourg DJ, Wilson SJ (2012) What's new with $CO_2$? Recent advances in its copolymerization with oxiranes. Green Chem 14(10):2665–2671
40. Darensbourg DJ (2007) Making plastics from carbon dioxide: salen metal complexes as catalysts for the production of polycarbonates from epoxides and $CO_2$. Chem Rev 107(6): 2388–2410
41. Childers MI, Longo JM, Van Zee NJ, LaPointe AM, Coates GW (2014) Stereoselective epoxide polymerization and copolymerization. Chem Rev 114(16):8129–8152
42. Darensbourg DJ, Yeung AD (2014) A concise review of computational studies of the carbon dioxide-epoxide copolymerization reactions. Polym Chem 5(13):3949–3962
43. Kember MR, Buchard A, Williams CK (2011) Catalysts for $CO_2$/epoxide copolymerisation. Chem Commun 47(1):141–163
44. Buchard A, Bakewell CM, Weiner J, Williams CK (2012) Recent developments in catalytic activation of renewable resources for polymer synthesis. In: Meier MAR, Weckhuysen BM, Bruijnincx PCA (eds) Organometallics and renewables, vol 39, Topics in organometallic chemistry. Springer, Berlin, pp 175–224. doi:10.1007/978-3-642-28288-1_5
45. Coates GW, Moore DR (2004) Discrete metal-based catalysts for the copolymerization of $CO_2$ and epoxides: discovery, reactivity, optimization, and mechanism. Angew Chem Int Ed 43(48):6618–6639
46. Darensbourg DJ (2014) Personal adventures in the synthesis of copolymers from carbon dioxide and cyclic ethers. In: Michele A, van Rudi E (eds) Advances in inorganic chemistry, vol 66. Academic, Burlington, pp 1–23. doi:10.1016/B978-0-12-420221-4.00001-9
47. Inoue S, Koinuma H, Tsuruta T (1969) Copolymerization of carbon dioxide and epoxide. J Polym Sci B Polym Lett 7:287–292
48. Inoue S (1979) Copolymerization of carbon dioxide and epoxide: functionality of the copolymer. J Macromol Sci A 13(5):651–664
49. Sugimoto H, Inoue S (2004) Copolymerization of carbon dioxide and epoxide. J Polym Chem A Polym Chem 42(22):5561–5573
50. Nakano K, Kobayashi K, Nozaki K (2011) Tetravalent metal complexes as a new family of catalysts for copolymerization of epoxides with carbon dioxide. J Am Chem Soc 133(28): 10720–10723
51. Quadri CC, Le Roux E (2014) Copolymerization of cyclohexene oxide with $CO_2$ catalyzed by tridentate N-heterocyclic carbene titanium(iv) complexes. Dalton Trans 43(11): 4242–4246
52. Robert C, Ohkawara T, Nozaki K (2014) Manganese-corrole complexes as versatile catalysts for the ring-opening homo- and Co-polymerization of epoxide. Chem Eur J 20(16): 4789–4795
53. Darensbourg DJ, Frantz EB (2007) Manganese(III) Schiff base complexes: chemistry relevant to the copolymerization of epoxides and carbon dioxide. Inorg Chem 46(15):5967–5978
54. Kuroki M, Aida T, Inoue S (1988) (5,10,15,20-Tetraphenylporphyrinato)manganese acetate as a novel initiator for the ring-opening polymerization of 1,2-epoxypropane. Makromol Chem 189(6):1305–1313
55. Nakano K, Kobayashi K, Ohkawara T, Imoto H, Nozaki K (2013) Copolymerization of epoxides with carbon dioxide catalyzed by iron–corrole complexes: synthesis of a crystalline copolymer. J Am Chem Soc 135(23):8456–8459

56. Buchard A, Kember MR, Sandeman KG, Williams CK (2011) A bimetallic iron(iii) catalyst for $CO_2$/epoxide coupling. Chem Commun 47(1):212–214
57. Cui D, Nishiura M, Tardif O, Hou Z (2008) Rare-earth-metal mixed hydride/aryloxide complexes bearing mono(cyclopentadienyl) ligands. Synthesis, $CO_2$ fixation, and catalysis on copolymerization of $CO_2$ with cyclohexene oxide. Organometallics 27(11):2428–2435
58. Cui D, Nishiura M, Hou Z (2005) Alternating copolymerization of cyclohexene oxide and carbon dioxide catalyzed by organo rare earth metal complexes. Macromolecules 38(10): 4089–4095
59. Aida T, Ishikawa M, Inoue S (1986) Alternating copolymerization of carbon dioxide and epoxide catalyzed by the aluminum porphyrin-quaternary organic salt or -triphenylphosphine system. Synthesis of polycarbonate with well-controlled molecular weight. Macromolecules 19(1):8–13
60. Sârbu T, Beckman EJ (1999) Homopolymerization and copolymerization of cyclohexene oxide with carbon dioxide using zinc and aluminum catalysts. Macromolecules 32(21): 6904–6912
61. Sarbu T, Styranec T, Beckman EJ (2000) Non-fluorous polymers with very high solubility in supercritical $CO_2$ down to low pressures. Nature 405(6783):165–168
62. Sugimoto H, Ohtsuka H, Inoue S (2005) Alternating copolymerization of carbon dioxide and epoxide catalyzed by an aluminum Schiff base–ammonium salt system. J Polym Chem A Polym Chem 43(18):4172–4186
63. Kember MR, Williams CK (2012) Efficient magnesium catalysts for the copolymerization of epoxides and $CO_2$; using water to synthesize polycarbonate polyols. J Am Chem Soc 134(38): 15676–15679
64. Xiao Y, Wang Z, Ding K (2005) Intramolecularly dinuclear magnesium complex catalyzed copolymerization of cyclohexene oxide with CO2 under ambient CO2 pressure: kinetics and mechanism. Macromolecules 39(1):128–137
65. Kember MR, Jutz F, Buchard A, White AJP, Williams CK (2012) Di-cobalt(ii) catalysts for the copolymerisation of $CO_2$ and cyclohexene oxide: support for a dinuclear mechanism? Chem Sci 3(4):1245–1255
66. Tsai C-Y, Huang B-H, Hsiao M-W, Lin C-C, Ko B-T (2014) Structurally diverse copper complexes bearing NNO-tridentate Schiff-base derivatives as efficient catalysts for copolymerization of carbon dioxide and cyclohexene oxide. Inorg Chem 53(10):5109–5116
67. Li C-H, Chuang H-J, Li C-Y, Ko B-T, Lin C-H (2014) Bimetallic nickel and cobalt complexes as high-performance catalysts for copolymerization of carbon dioxide with cyclohexene oxide. Polym Chem 5(17):4875–4878
68. Chisholm MH, Zhou Z (2004) Concerning the mechanism of the ring opening of propylene oxide in the copolymerization of propylene oxide and carbon dioxide to give poly(propylene carbonate). J Am Chem Soc 126(35):11030–11039
69. Chatterjee C, Chisholm MH (2011) The influence of the metal (Al, Cr, and Co) and the substituents of the porphyrin in controlling the reactions involved in the copolymerization of propylene oxide and carbon dioxide by porphyrin metal(III) complexes. 1. Aluminum chemistry. Inorg Chem 50(10):4481–4492
70. Chatterjee C, Chisholm MH (2012) Influence of the metal (Al, Cr, and Co) and the substituents of the porphyrin in controlling the reactions involved in the copolymerization of propylene oxide and carbon dioxide by porphyrin metal(III) complexes. 2. Chromium chemistry. Inorg Chem 51(21):12041–12052
71. Chatterjee C, Chisholm MH, El-Khaldy A, McIntosh RD, Miller JT, Wu T (2013) Influence of the metal (Al, Cr, and Co) and substituents of the porphyrin in controlling reactions involved in copolymerization of propylene oxide and carbon dioxide by porphyrin metal (III) complexes. 3. Cobalt chemistry. Inorg Chem 52(8):4547–4553
72. Harrold ND, Li Y, Chisholm MH (2013) Studies of ring-opening reactions of styrene oxide by chromium tetraphenylporphyrin initiators. Mechanistic and stereochemical considerations. Macromolecules 46(3):692–698

73. Mang S, Cooper AI, Colclough ME, Chauhan N, Holmes AB (1999) Copolymerization of $CO_2$ and 1,2-cyclohexene oxide using a $CO_2$-soluble chromium porphyrin catalyst. Macromolecules 33(2):303–308
74. Sugimoto H, Ohshima H, Inoue S (2003) Alternating copolymerization of carbon dioxide and epoxide by manganese porphyrin: the first example of polycarbonate synthesis from 1-atm carbon dioxide. J Polym Chem A Polym Chem 41(22):3549–3555
75. Darensbourg DJ, Mackiewicz RM, Phelps AL, Billodeaux DR (2004) Copolymerization of $CO_2$ and epoxides catalyzed by metal salen complexes. Acc Chem Res 37(11):836–844
76. Ellis WC, Jung Y, Mulzer M, Di Girolamo R, Lobkovsky EB, Coates GW (2014) Copolymerization of $CO_2$ and meso epoxides using enantioselective β-diiminate catalysts: a route to highly isotactic polycarbonates. Chem Sci 5(10):4004–4011
77. Moore DR, Cheng M, Lobkovsky EB, Coates GW (2003) Mechanism of the alternating copolymerization of epoxides and CO2 using β-diiminate zinc catalysts: evidence for a bimetallic epoxide enchainment. J Am Chem Soc 125(39):11911–11924
78. Cheng M, Moore DR, Reczek JJ, Chamberlain BM, Lobkovsky EB, Coates GW (2001) Single-site β-diiminate zinc catalysts for the alternating copolymerization of CO2 and epoxides: catalyst synthesis and unprecedented polymerization activity. J Am Chem Soc 123(36):8738–8749
79. Lehenmeier MW, Kissling S, Altenbuchner PT, Bruckmeier C, Deglmann P, Brym A-K, Rieger B (2013) Flexibly tethered dinuclear zinc complexes: a solution to the entropy problem in CO2/epoxide copolymerization catalysis? Angew Chem Int Ed 52(37): 9821–9826
80. Rajendran NM, Haleel A, Reddy ND (2013) Copolymerization of $CO_2$ and cyclohexene oxide: β-diketiminate-supported Zn(II)OMe and Zn(II)Et complexes as initiators. Organometallics 33(1):217–224
81. Pilz MF, Limberg C, Lazarov BB, Hultzsch KC, Ziemer B (2007) Dinuclear zinc complexes based on parallel beta-diiminato binding sites: syntheses, structures, and properties as $CO_2$/epoxide copolymerization catalysts. Organometallics 26(15):3668–3676
82. Piesik DFJ, Range S, Harder S (2008) Bimetallic calcium and zinc complexes with bridged $\hat{I}^2$-diketiminate ligands: investigations on epoxide/$CO_2$ copolymerization. Organometallics 27(23):6178–6187
83. Saini PK, Romain C, Williams CK (2014) Dinuclear metal catalysts: improved performance of heterodinuclear mixed catalysts for $CO_2$-epoxide copolymerization. Chem Commun 50(32):4164–4167
84. Buchard A, Jutz F, Kember MR, White AJP, Rzepa HS, Williams CK (2012) Experimental and computational investigation of the mechanism of carbon dioxide/cyclohexene oxide copolymerization using a dizinc catalyst. Macromolecules 45(17):6781–6795
85. Jutz F, Buchard A, Kember MR, Fredriksen SB, Williams CK (2011) Mechanistic investigation and reaction kinetics of the low-pressure copolymerization of cyclohexene oxide and carbon dioxide catalyzed by a dizinc complex. J Am Chem Soc 133(43):17395–17405
86. Kember MR, White AJP, Williams CK (2010) Highly active Di- and trimetallic cobalt catalysts for the copolymerization of CHO and $CO_2$ at atmospheric pressure. Macromolecules 43(5):2291–2298
87. Kember MR, White AJP, Williams CK (2009) Di- and Tri-zinc catalysts for the Low-pressure copolymerization of $CO_2$ and cyclohexene oxide. Inorg Chem 48(19):9535–9542
88. Kember MR, Knight PD, Reung PTR, Williams CK (2009) Highly active dizinc catalyst for the copolymerization of carbon dioxide and cyclohexene oxide at one atmosphere pressure. Angew Chem Int Ed 48(5):931–933
89. Inoue S (2000) Immortal polymerization: the outset, development, and application. J Polym Chem A Polym Chem 38(16):2861–2871
90. Guerin W, Diallo AK, Kirilov E, Helou M, Slawinski M, Brusson J-M, Carpentier J-F, Guillaume SM (2014) Enantiopure isotactic PCHC synthesized by ring-opening polymerization of cyclohexene carbonate. Macromolecules 47(13):4230–4235

91. Nakano K, Hashimoto S, Nakamura M, Kamada T, Nozaki K (2011) Stereocomplex of poly (propylene carbonate): synthesis of stereogradient poly(propylene carbonate) by regio- and enantioselective copolymerization of propylene oxide with carbon dioxide. Angew Chem Int Ed 50(21):4868–4871
92. Cheng M, Darling NA, Lobkovsky EB, Coates GW (2000) Enantiomerically-enriched organic reagents via polymer synthesis: enantioselective copolymerization of cycloalkene oxides and $CO_2$ using homogeneous, zinc-based catalysts. Chem Commun 20:2007–2008
93. Cohen CT, Chu T, Coates GW (2005) Cobalt catalysts for the alternating copolymerization of propylene oxide and carbon dioxide: combining high activity and selectivity. J Am Chem Soc 127(31):10869–10878
94. Liu Y, Ren W-M, Liu J, Lu X-B (2013) Asymmetric copolymerization of $CO_2$ with meso-epoxides mediated by dinuclear cobalt(III) complexes: unprecedented enantioselectivity and activity. Angew Chem Int Ed 52(44):11594–11598
95. Wu G-P, Zu Y-P, Xu P-X, Ren W-M, Lu X-B (2013) Microstructure analysis of a $CO_2$ copolymer from styrene oxide at the diad level. Chem Asian J 8(8):1854–1862
96. Wu G-P, Xu P-X, Lu X-B, Zu Y-P, Wei S-H, Ren W-M, Darensbourg DJ (2013) Crystalline $CO_2$ copolymer from epichlorohydrin via Co(III)-complex-mediated stereospecific polymerization. Macromolecules 46(6):2128–2133
97. Wu G-P, Ren W-M, Luo Y, Li B, Zhang W-Z, Lu X-B (2012) Enhanced asymmetric induction for the copolymerization of $CO_2$ and cyclohexene oxide with unsymmetric enantiopure SalenCo(III) complexes: synthesis of crystalline $CO_2$-based polycarbonate. J Am Chem Soc 134(12):5682–5688
98. Ren W-M, Wu G-P, Lin F, Jiang J-Y, Liu C, Luo Y, Lu X-B (2012) Role of the co-catalyst in the asymmetric coupling of racemic epoxides with $CO_2$ using multichiral Co(III) complexes: product selectivity and enantioselectivity. Chem Sci 3(6):2094–2102
99. Lu X-B, Ren W-M, Wu G-P (2012) $CO_2$ copolymers from epoxides: catalyst activity, product selectivity, and stereochemistry control. Acc Chem Res 45(10):1721–1735
100. Li B, Wu G-P, Ren W-M, Wang Y-M, Rao D-Y, Lu X-B (2008) Asymmetric, regio- and stereo-selective alternating copolymerization of $CO_2$ and propylene oxide catalyzed by chiral chromium Salan complexes. J Polym Chem A Polym Chem 46(18):6102–6113
101. Li B, Zhang R, Lu X-B (2007) Stereochemistry control of the alternating copolymerization of $CO_2$ and propylene oxide catalyzed by SalenCrX complexes. Macromolecules 40(7): 2303–2307
102. Lu XB, Shi L, Wang YM, Zhang R, Zhang YJ, Peng XJ, Zhang ZC, Li B (2006) Design of highly active binary catalyst systems for $CO_2$/epoxide copolymerization: polymer selectivity, enantioselectivity, and stereochemistry control. J Am Chem Soc 128(5):1664–1674
103. Nakano K, Hiyama T, Nozaki K (2005) Asymmetric amplification in asymmetric alternating copolymerization of cyclohexene oxide and carbon dioxide. Chem Commun 14:1871–1873
104. Nozaki K, Nakano K, Hiyama T (1999) Optically active polycarbonates: asymmetric alternating copolymerization of cyclohexene oxide and carbon dioxide. J Am Chem Soc 121(47): 11008–11009
105. Kobayashi M, Tang Y-L, Tsuruta T, Inoue S (1973) Copolymerization of carbon dioxide and epoxide using dialkylzinc/dihydric phenol system as catalyst. Makromol Chem 169(1):69–81
106. Inoue S, Koinuma H, Yokoo Y, Tsuruta T (1971) Stereochemistry of copolymerization of carbon dioxide with epoxycyclohexane. Makromol Chem 143(1):97–104
107. Kobayashi M, Inoue S, Tsuruta T (1973) Copolymerization of carbon dioxide and epoxide by the dialkylzinc–carboxylic acid system. J Polym Chem A Polym Chem 11(9):2383–2385
108. Hirano T, Inoue S, Tsuruta T (1975) Stereochemistry of the copolymerization of carbon dioxide with optically active phenylepoxyethane. Makromol Chem 176(7):1913–1917
109. Hirano T, Inoue S, Tsuruta T (1976) Stereochemistry of copolymerization of optically active cyclohexylepoxyethane with carbon dioxide. Makromol Chem 177(11):3237–3243
110. Hasebe Y, Tsuruta T (1987) Structural studies of poly(1,2-cyclohexene oxide) prepared with well-defined organozinc compounds. Makromol Chem 188(6):1403–1414

111. Hasebe Y, Tsuruta T (1988) Mechanism of stereoselective polymerization of propylene oxide with [{MeOCH2CH(Me)OZnOCH(Me)CH2OMe}2 · {EtZnOCH(Me)CH2OMe}2] as initiator. Makromol Chem 189(8):1915–1926
112. Yoshino N, Suzuki C, Kobayashi H, Tsuruta T (1988) Some features of a novel organozinc complex, [{MeOCH2CH(Me)OZnOCH(Me)CH2OMe}2 · {EtZnOCH(Me)CH2OMe}2], as an enantiomorphic catalyst for stereoselective polymerization of propylene oxide. Makromol Chem 189(8):1903–1913
113. Ishimori M, Hagiwara T, Tsuruta T, Kai Y, Yasuoka N, Kasai N (1976) The structure and reactivity of [Zn(OMe)2. (EtZnOMe)6]. Bull Chem Soc Jpn 49(4):1165–1166
114. Kuran W, Pasynkiewicz S, Skupińska J, Rokicki A (1976) Alternating copolymerization of carbon dioxide and propylene oxide in the presence of organometallic catalysts. Makromol Chem 177(1):11–20
115. Eberhardt R, Allmendinger M, Zintl M, Troll C, Luinstra GA, Rieger B (2004) New zinc dicarboxylate catalysts for the $CO_2$/propylene oxide copolymerization reaction: activity enhancement through Zn(II)-ethylsulfinate initiating groups. Macromol Chem Phys 205(1): 42–47
116. Wang SJ, Du LC, Zhao XS, Meng YZ, Tjong SC (2002) Synthesis and characterization of alternating copolymer from carbon dioxide and propylene oxide. J Appl Polym Sci 85(11): 2327–2334
117. Ree M, Bae JY, Jung JH, Shin TJ (1999) A new copolymerization process leading to poly (propylene carbonate) with a highly enhanced yield from carbon dioxide and propylene oxide. J Polym Chem A Polym Chem 37(12):1863–1876
118. Kim I, Yi MJ, Byun SH, Park DW, Kim BU, Ha CS (2005) Biodegradable polycarbonate synthesis by copolymerization of carbon dioxide with epoxides using a heterogeneous zinc complex. Macromol Symp 224(1):181–192
119. Hinz W, Dexheimer EM, Bohres E, Grosch GH (2004) Process for the copolymerization of alkylene oxides and carbon dioxide using suspensions of multi-metal cyanide compounds
120. Hinz W, Wildeson J, Dexheimer EM (2007) Reacting an H-functional initiator, an alkylene oxide, and $CO_2$ in the presence of the modified multimetal cyanide compound to form the polyethercarbonate polyol
121. Hinz W, Wildeson J, Dexheimer EM, Neff R (2004) Formation of polymer polyols with a narrow polydispersity using double metal cyanide (DMC) catalysts
122. Kruper WJ, Swart DJ (1985) Carbon dioxide oxirane copolymers prepared using double metal cyanide complexes
123. Kuyper J, Lednor PW, Pogany GA (1989) Double metal cyanide catalyst
124. Kuyper J, Lednor PW, Pogany GA (1989) Process for the preparation of polycarbonates
125. Kuyper J, Lednor PW, Pogany GA (1989) Process for the preparation of polycarbonates from epoxy compound and carbon dioxide
126. Chen S, Hua Z, Fang Z, Qi G (2004) Copolymerization of carbon dioxide and propylene oxide with highly effective zinc hexacyanocobaltate(III)-based coordination catalyst. Polymer 45(19):6519–6524
127. Sun X-K, Zhang X-H, Liu F, Chen S, Du B-Y, Wang Q, Fan Z-Q, Qi G-R (2008) Alternating copolymerization of carbon dioxide and cyclohexene oxide catalyzed by silicon dioxide/Zn-CoIII double metal cyanide complex hybrid catalysts with a nanolamellar structure. J Polym Chem A Polym Chem 46(9):3128–3139
128. Zhou T, Zou Z, Gan J, Chen L, Zhang M (2011) Copolymerization of epoxides and carbon dioxide by using double metal cyanide complex (DMC) with high crystallinity. J Polym Res 18(6):2071–2076
129. Darensbourg DJ, Wildeson JR, Yarbrough JC (2002) Solid-state structures of zinc (II) benzoate complexes. Catalyst precursors for the coupling of carbon dioxide and epoxides. Inorg Chem 41(4):973–980
130. Darensbourg DJ, Wildeson JR, Yarbrough JC (2001) Synthesis and structures of (dialkylamino)ethylcyclopentadienyl derivatives of zinc. Organometallics 20(21):4413–4417

131. Darensbourg DJ, Wildeson JR, Yarbrough JC, Reibenspies JH (2000) Bis 2,6-difluorophenoxide dimeric complexes of zinc and cadmium and their phosphine adducts: lessons learned relative to carbon dioxide/cyclohexene oxide alternating copolymerization processes catalyzed by zinc phenoxides. J Am Chem Soc 122(50):12487–12496
132. Darensbourg DJ, Holtcamp MW, Struck GE, Zimmer MS, Niezgoda SA, Rainey P, Robertson JB, Draper JD, Reibenspies JH (1998) Catalytic activity of a series of Zn(II) phenoxides for the copolymerization of epoxides and carbon dioxide. J Am Chem Soc 121(1):107–116
133. Darensbourg DJ, Holtcamp MW (1995) Catalytic activity of zinc(II) phenoxides which possess readily accessible coordination sites. Copolymerization and terpolymerization of epoxides and carbon dioxide. Macromolecules 28(22):7577–7579
134. Takeda N, Inoue S (1978) Polymerization of 1,2 epoxypropane and co-polymerization with carbon-dioxide catalysed by metalloporphyrins. Makromol Chem 179(5):1377–1381
135. Hampel O, Rode C, Walther D, Beckert R, Görls H (2002) New derivatives of quinoxaline Ð syntheses, complex formation and their application as controlling ligands for zinc catalyzed epoxide-$CO_2$ÐCopolymerization. Naturforsch B 57:946–956
136. Cheng M, Lobkovsky EB, Coates GW (1998) Catalytic reactions involving C1 feedstocks: new high-activity Zn(II)-based catalysts for the alternating copolymerization of carbon dioxide and epoxides. J Am Chem Soc 120(42):11018–11019
137. Darensbourg DJ, Yarbrough JC (2002) Mechanistic aspects of the copolymerization reaction of carbon dioxide and epoxides, using a chiral salen chromium chloride catalyst. J Am Chem Soc 124(22):6335–6342
138. Eberhardt R, Allmendinger M, Rieger B (2003) DMAP/Cr(III) catalyst ratio: the decisive factor for poly(propylene carbonate) formation in the coupling of $CO_2$ and propylene oxide. Macromol Rapid Commun 24(2):194–196
139. Qin Z, Thomas CM, Lee S, Coates GW (2003) Cobalt-based complexes for the copolymerization of propylene oxide and $CO_2$: active and selective catalysts for polycarbonate synthesis. Angew Chem Int Ed 42(44):5484–5487
140. Lu X-B, Wang Y (2004) Highly active, binary catalyst systems for the alternating copolymerization of $CO_2$ and epoxides under mild conditions. Angew Chem Int Ed 43(27):3574–3577
141. Bok T, Yun H, Lee BY (2006) Bimetallic fluorine-substituted anilido-aldimine zinc complexes for $CO_2$/(cyclohexene oxide) copolymerization. Inorg Chem 45(10):4228–4237
142. Lee BY, Kwon HY, Lee SY, Na SJ, Han S-I, Yun H, Lee H, Park Y-W (2005) Bimetallic anilido-aldimine zinc complexes for epoxide/$CO_2$ copolymerization. J Am Chem Soc 127(9): 3031–3037
143. Anderson CE, Vagin SI, Hammann M, Zimmermann L, Rieger B (2013) Copolymerisation of propylene oxide and carbon dioxide by dinuclear cobalt porphyrins. ChemCatChem 5(11): 3269–3280
144. Xiao YL, Wang Z, Ding KL (2005) Copolymerization of cyclohexene oxide with $CO_2$ by using intramolecular dinuclear zinc catalysts. Chem Eur J 11(12):3668–3678
145. Williams CK, Breyfogle LE, Choi SK, Nam W, Young VG, Hillmyer MA, Tolman WB (2003) A highly active zinc catalyst for the controlled polymerization of lactide. J Am Chem Soc 125(37):11350–11359
146. Williams CK, Brooks NR, Hillmyer MA, Tolman WB (2002) Metalloenzyme inspired dizinc catalyst for the polymerization of lactide. Chem Commun 18:2132–2133
147. Sugimoto H, Ogawa A (2007) Alternating copolymerization of carbon dioxide and epoxide by dinuclear zinc Schiff base complex. React Funct Polym 67(11):1277–1283
148. Nakano K, Nozaki K, Hiyama T (2003) Asymmetric alternating copolymerization of cyclohexene oxide and $CO_2$ with dimeric zinc complexes. J Am Chem Soc 125(18): 5501–5510
149. Nishioka K, Goto H, Sugimoto H (2012) Dual catalyst system for asymmetric alternating copolymerization of carbon dioxide and cyclohexene oxide with chiral aluminum complexes: Lewis base as catalyst activator and Lewis acid as monomer activator. Macromolecules 45(20):8172–8192

150. Bernard A, Chatterjee C, Chisholm MH (2013) The influence of the metal (Al, Cr and Co) and the substituents of the porphyrin in controlling the reactions involved in the copolymerization of propylene oxide and cyclic anhydrides by porphyrin metal(III) complexes. Polymer 54(11):2639–2646
151. Konsler RG, Karl J, Jacobsen EN (1998) Cooperative asymmetric catalysis with dimeric salen complexes. J Am Chem Soc 120(41):10780–10781
152. Ready JM, Jacobsen EN (2002) A practical oligomeric [(salen)Co] catalyst for asymmetric epoxide ring-opening reactions. Angew Chem Int Ed 41(8):1374–1377
153. Hirahata W, Thomas RM, Lobkovsky EB, Coates GW (2008) Enantioselective polymerization of epoxides: a highly active and selective catalyst for the preparation of stereoregular polyethers and enantiopure epoxides. J Am Chem Soc 130(52):17658–17659
154. Widger PCB, Ahmed SM, Coates GW (2011) Exploration of cocatalyst effects on a bimetallic cobalt catalyst system: enhanced activity and enantioselectivity in epoxide polymerization. Macromolecules 44(14):5666–5670
155. Nakano K, Hashimoto S, Nozaki K (2010) Bimetallic mechanism operating in the copolymerization of propylene oxide with carbon dioxide catalyzed by cobalt-salen complexes. Chem Sci 1:369–373
156. Vagin SI, Reichardt R, Klaus S, Rieger B (2010) Conformationally flexible dimeric salphen complexes for bifunctional catalysis. J Am Chem Soc 132(41):14367–14369
157. Lehenmeier MW, Bruckmeier C, Klaus S, Dengler JE, Deglmann P, Ott A-K, Rieger B (2011) Differences in reactivity of epoxides in the copolymerisation with carbon dioxide by zinc-based catalysts: propylene oxide versus cyclohexene oxide. Chem Eur J 17(32): 8858–8869
158. Thomas RM, Widger PCB, Ahmed SM, Jeske RC, Hirahata W, Lobkovsky EB, Coates GW (2010) Enantioselective epoxide polymerization using a bimetallic cobalt catalyst. J Am Chem Soc 132(46):16520–16525
159. Klaus S, Vagin SI, Lehenmeier MW, Deglmann P, Brym AK, Rieger B (2011) Kinetic and mechanistic investigation of mononuclear and flexibly linked dinuclear complexes for copolymerization of $CO_2$ and epoxides. Macromolecules 44(24):9508–9516
160. Ohkawara T, Suzuki K, Nakano K, Mori S, Nozaki K (2014) Facile estimation of catalytic activity and selectivities in copolymerization of propylene oxide with carbon dioxide mediated by metal complexes with planar tetradentate ligand. J Am Chem Soc 136(30): 10728–10735
161. Nakano K, Kamada T, Nozaki K (2006) Selective formation of polycarbonate over cyclic carbonate: copolymerization of epoxides with carbon dioxide catalyzed by a cobalt(III) complex with a piperidinium end-capping arm. Angew Chem Int Ed 45(43):7274–7277
162. Noh EK, Na SJ, Sujith S, Kim S-W, Lee BY (2007) Two components in a molecule: highly efficient and thermally robust catalytic system for CO2/epoxide copolymerization. J Am Chem Soc 129(26):8082–8083
163. Sujith S, Min JK, Seong JE, Na SJ, Lee BY (2008) A highly active and recyclable catalytic system for $CO_2$/propylene oxide copolymerization. Angew Chem Int Ed 47(38):7306–7309
164. Yoo J, Na SJ, Park HC, Cyriac A, Lee BY (2010) Anion variation on a cobalt(iii) complex of salen-type ligand tethered by four quaternary ammonium salts for $CO_2$/epoxide copolymerization. Dalton Trans 39(10):2622–2630
165. Na SJ, Sujith S, Cyriac A, Kim BE, Yoo J, Kang YK, Han SJ, Lee C, Lee BY (2009) Elucidation of the structure of a highly active catalytic system for $CO_2$/epoxide copolymerization: a salen-cobaltate complex of an unusual binding mode. Inorg Chem 48(21): 10455–10465
166. Cyriac A, Jeon JY, Varghese JK, Park JH, Choi SY, Chung YK, Lee BY (2012) Unusual coordination mode of tetradentate Schiff base cobalt(iii) complexes. Dalton Trans 41(5): 1444–1447

167. Seong JE, Na SJ, Cyriac A, Kim B-W, Lee BY (2009) Terpolymerizations of $CO_2$, propylene oxide, and various epoxides using a cobalt(III) complex of salen-type ligand tethered by four quaternary ammonium salts. Macromolecules 43(2):903–908
168. Cyriac A, Lee SH, Lee BY (2011) Connection of polymer chains using diepoxide in $CO_2$/propylene oxide copolymerizations. Polym Chem 2(4):950–956
169. Cyriac A, Lee SH, Varghese JK, Park JH, Jeon JY, Kim SJ, Lee BY (2011) Preparation of flame-retarding poly(propylene carbonate). Green Chem 13(12):3469–3475
170. Cyriac A, Lee SH, Varghese JK, Park ES, Park JH, Lee BY (2010) Immortal $CO_2$/propylene oxide copolymerization: precise control of molecular weight and architecture of various block copolymers. Macromolecules 43(18):7398–7401
171. Lee SH, Cyriac A, Jeon JY, Lee BY (2012) Preparation of thermoplastic polyurethanes using in situ generated poly(propylene carbonate)-diols. Polym Chem 3(5):1215–1220
172. Ren W-M, Zhang X, Liu Y, Li J-F, Wang H, Lu X-B (2010) Highly active, bifunctional Co (III)-salen catalyst for alternating copolymerization of $CO_2$ with cyclohexene oxide and terpolymerization with aliphatic epoxides. Macromolecules 43(3):1396–1402
173. Darensbourg DJ, Chung W-C, Wilson SJ (2013) Catalytic coupling of cyclopentene oxide and $CO_2$ utilizing bifunctional (salen)Co(III) and (salen)Cr(III) catalysts: comparative processes involving binary (salen)Cr(III) analogs. ACS Catal 3(12):3050–3057
174. Darensbourg DJ, Wilson SJ (2013) Synthesis of $CO_2$-derived poly(indene carbonate) from indene oxide utilizing bifunctional cobalt(III) catalysts. Macromolecules 46(15):5929–5934
175. Darensbourg DJ, Wei S-H, Yeung AD, Ellis WC (2013) An efficient method of depolymerization of poly(cyclopentene carbonate) to its comonomers: cyclopentene oxide and carbon dioxide. Macromolecules 46(15):5850–5855
176. Ren W-M, Liu Y, Wu G-P, Liu J, Lu X-B (2011) Stereoregular polycarbonate synthesis: alternating copolymerization of $CO_2$ with aliphatic terminal epoxides catalyzed by multichiral cobalt(III) complexes. J Polym Chem A Polym Chem 49(22):4894–4901
177. Wu G-P, Wei S-H, Lu X-B, Ren W-M, Darensbourg DJ (2010) Highly selective synthesis of $CO_2$ copolymer from styrene oxide. Macromolecules 43(21):9202–9204
178. Wu G-P, Wei S-H, Ren W-M, Lu X-B, Xu T-Q, Darensbourg DJ (2011) Perfectly alternating copolymerization of $CO_2$ and epichlorohydrin using cobalt(III)-based catalyst systems. J Am Chem Soc 133(38):15191–15199
179. Li H, Niu Y (2011) Alternating copolymerization of $CO_2$ with propylene oxide and terpolymerization with aliphatic epoxides by bifunctional cobalt Salen complex. Polym J 43(2):121–125

Top Organomet Chem (2016) 53: 143–170
DOI: 10.1007/3418_2015_97

Published online: 7 April 2015

# Transition Metal-Free Incorporation of $CO_2$

**Shuai Zhang, Ran Ma, and Liang-Nian He**

**Abstract** Carbon dioxide can be regarded as an ideal $C_1$ chemical feedstock in both academic and pharmaceutical laboratories owing to its abundance, low cost, non-toxicity, and nonflammability. However, due to $CO_2$ inherent thermodynamic stability and kinetic inertness, it is difficult to convert $CO_2$ to value-added chemicals under mild conditions. In order to overcome such barriers, numerous useful synthetic methodologies by strategically using highly active catalysts have been developed for the incorporation of $CO_2$ to organic compounds. Transition metal-free compounds are proved to be promising efficacious catalysts able to activate $CO_2$ molecule for efficient transformation of $CO_2$ on the basis of mechanistic understanding at the molecular level. This chapter features recent advances at methodologies for catalytic transformation of $CO_2$ promoted by organocatalysts (e.g., *N*-heterocyclic carbenes, frustrated Lewis pairs and superbases), ionic liquids, and main group metal to produce value-added chemicals such as linear or cyclic carbonates, quinazoline-2,4(1*H*,3*H*)-diones, alkylidene cyclic carbonates, amino acids, and so on.

**Keywords** Carbon dioxide · Catalysis · Ionic liquid · Organocatalyst · Sustainable chemistry · Transition metal-free process

## Contents



S. Zhang, R. Ma, and L.-N. He (✉)
State Key Laboratory of Elemento-Organic Chemistry, Collaborative Innovation Center of Chemical Science and Engineering (Tianjin), Nankai University, Weijin Rd. 94, Tianjin 300071, P. R. China
e-mail: heln@nankai.edu.cn

## 1 Introduction

From a standpoint of $C_1$ chemistry and green chemistry, incorporation of $CO_2$ has become one of the most important subjects for the synthesis of valuable organic chemicals/materials in synthetic organic chemistry [1–3]. Much effort has been devoted to this promising subject, and numerous reactions and catalytic systems have been developed for $CO_2$ utilization. However, the inherent thermodynamic stability and kinetic inertness of $CO_2$ hinder $CO_2$ conversion under mild conditions. Accordingly, practical transformation of $CO_2$ would inevitably rely on its activation via either metal coordination or weak interaction between the active species and $CO_2$ molecule. Various transition metal complexes have been developed as efficient catalysts, which are usually applied in the carboxylation reactions and hydrogenations reactions. $CO_2$ as a ligand is able to coordinate with a transition metal center and is thus activated and subsequently converted into carboxylic acids, esters, formic acid, and methanol. On the other hand, transition metal-free compounds are also promising catalysts capable of activating $CO_2$ for upgrading $CO_2$ into organics with the advantages of low cost, easy preparation, non-sensitivity to air or moisture, and relative hypotoxicity to the environment. Furthermore, the characteristics of transition metal-free catalysts, such as nucleophilicity, basicity, ease of introducing functionalized groups, and so on, could be applied to activate both $CO_2$ and substrates, furnishing further transformation of $CO_2$. In this chapter, efficient transition metal-free catalysts for the transformation of $CO_2$ including organocatalysts, ionic liquids, and main group metals are summarized. Various valuable chemicals such as carbonates, carbamates, quinazoline-diones, amino acids, etc., could be synthesized with transition metal-free catalysis under mild conditions.

## 2 Organocatalysts

### *2.1* N-*Heterocyclic Carbenes and* N-*Heterocyclic Olefins*

*N*-Heterocyclic carbenes (NHCs) are usually generated through deprotonation of the corresponding imidazolium salts by strong bases and have been extensively employed as versatile ligands for the formation of a large variety of organometallic complexes [4–7]. Inspiringly, NHCs are able to react with $CO_2$ to form NHC-$CO_2$ adducts (*N*,*N*′-disubstituted imidazolinium-2-carboxylates), in which a bent geometry with a O–C–O angle of 129–131° has been determined by X-ray single-crystal study [8, 9]. From a structural point of view, NHC-$CO_2$ adducts are considered to be zwitterionic compounds formed via NHC's nucleophilic attack at the weak electrophilic carbon center of the $CO_2$ molecule. Furthermore, NHC-$CO_2$ adducts show high catalytic activity for carboxylative cyclization with $CO_2$ because of the strong nucleophilic nature [9–11]. As depicted in Scheme 1, IPr-$CO_2$ adduct **2a** exhibits the highest catalytic activity for the coupling reaction of $CO_2$ and epoxides; 100% yield of propylene carbonate is attained from propylene oxide and $CO_2$ at 120°C, 2 MPa $CO_2$ pressure. The mechanism of the NHC-$CO_2$-catalyzed cycloaddition reaction is shown in Scheme 2. The zwitterionic compounds NHC-$CO_2$ adducts (**2**) are able to go through nucleophilic attack at the epoxide, leading to generation of the zwitterion (**3**). Then, the intramolecular cyclization produces cyclic carbonate along with the release of free NHC. The formation of NHC-$CO_2$ adduct **2** allows next catalytic cycle to begin. Indeed, the $CO_2$ adducts (MCM-41-IPr-$CO_2$) from mesoporous material-supported NHC (MCM-41-IPr) and $CO_2$ are efficient heterogeneous catalysts for the cycloaddition of $CO_2$ with epoxides or aziridines under 2.0 MPa $CO_2$ pressure at 120°C (Scheme 3) [12]. Moreover, the catalyst could easily be recovered by a simple filtration and reused multiple times without obvious loss in activity.

Furthermore, the isolable NHC-$CO_2$ catalyst provides access to a variety of five-membered α-alkylidene cyclic carbonates from propargyl alcohols [10, 11]. 73% yield of 4-methyl-5-methylene-4-phenyl-1,3-dioxolan-2-one is obtained from the corresponding propargyl alcohol and $CO_2$ with **2b** as the catalyst (catalyst loading 7.7%) under 6 MPa $CO_2$, 100°C. The cyclic carbonate formation can be explained by the mechanism involving the nucleophilic addition of the imidazolium-2-carboxylate at either the C–C bond and subsequent intramolecular cyclization of the alkoxide intermediate as depicted in Scheme 4.

*N*-Heterocyclic olefins (NHOs) with high electronegativity at the terminal carbon atom are found to show a strong tendency for $CO_2$ sequestration, affording the NHO-$CO_2$ adducts. Notably, the NHO-$CO_2$ adducts are found to be highly active in promoting the carboxylative cyclization of propargylic alcohols with $CO_2$ at 60°C, 2 MPa $CO_2$ pressure (even at ambient temperature and 1 atm $CO_2$ pressure), giving α-alkylidene cyclic carbonates in excellent yields [13]. Based on deuterium-labeling experiments, two reaction paths regarding the hydrogen at the alkenyl position of cyclic carbonates coming from substrate (path A) or both substrate and

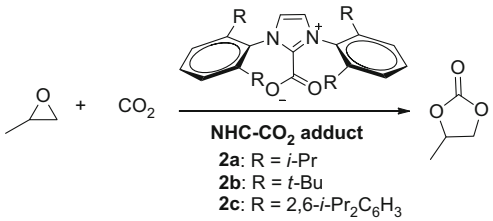


**Scheme 1** The NHC-$CO_2$ adduct-catalyzed cycloaddition reaction of epoxide and $CO_2$ [9, 10]

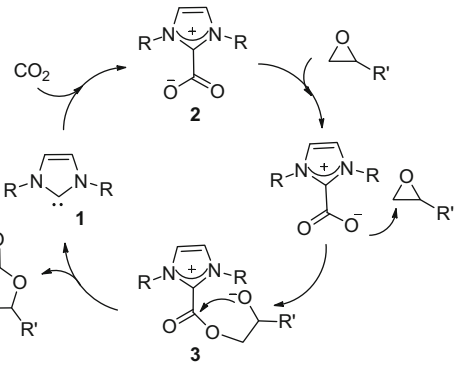


**Scheme 2** Possible mechanism for the coupling reaction of $CO_2$ with epoxides catalyzed by NHC-$CO_2$ adduct [9, 10]

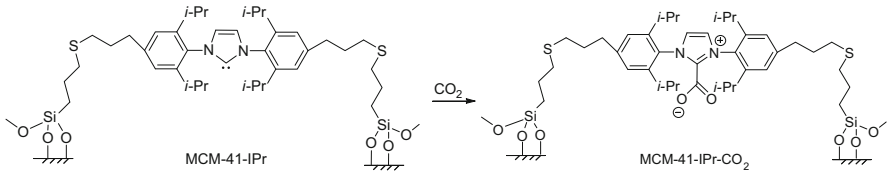


**Scheme 3** The formation of MCM-41-IPr-$CO_2$ [12]

catalyst (path B) are proposed as shown in Scheme 5. At the identical reaction conditions, NHO-$CO_2$ adducts show much higher catalytic activity than that of the corresponding NHC-$CO_2$ adducts. The high activity of the NHO-$CO_2$ adducts is tentatively ascribed to its low stability for easily releasing $CO_2$ moiety and/or the desired product, a possible rate-determining step in the catalytic cycle.

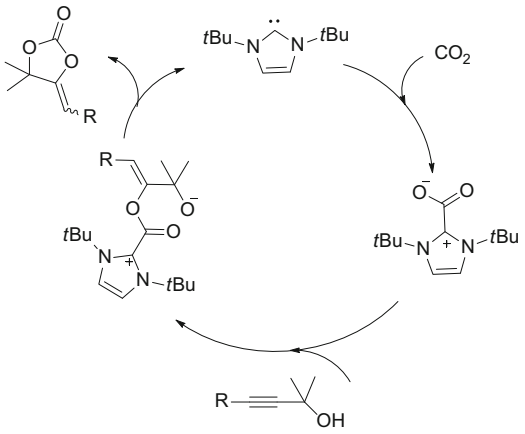

**Scheme 4** Plausible mechanism for the NHC-$CO_2$ adduct-catalyzed carboxylative cyclization of propargylic alcohol with $CO_2$ [10, 11]

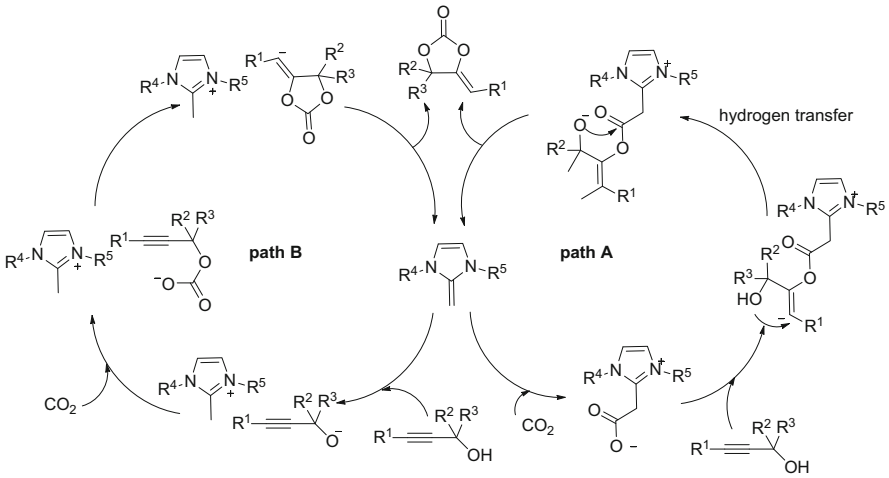


**Scheme 5** Plausible mechanism for carboxylative cyclization of propargyl alcohols with $CO_2$ catalyzed by the NHO-$CO_2$ adduct [13]

## 2.2 Superbase

Superbases, such as amidines and guanidines, have been found in many applications in $CO_2$ capture and conversion because of their characteristic of nucleophilicity and basicity. For example, a mixture of superbase and alcohol could effectively capture equimolar $CO_2$ and has been proven to be efficient catalysts in the synthesis of organic carbonates and urethanes via the respective reactions of

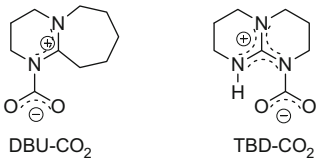


**Scheme 6** The structure of DBU-$CO_2$ and TBD-$CO_2$ adducts [16–21]

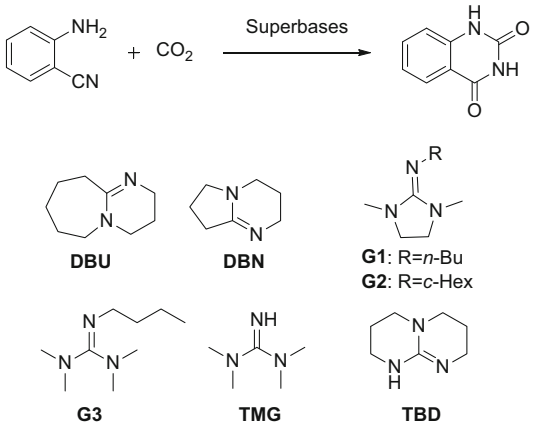


**Scheme 7** Guanidine-catalyzed cyclization reaction of 2-aminobenzonitrile and $CO_2$ [23]

$CO_2$ with epoxides and amines, respectively [14–18]. 1,8-Diazabicyclo[5.4.0] undec-7-ene (DBU) or 1,5,7-triazabicyclo[4.4.0]dec-5-ene (TBD) performs nucleophilic attack at the weakly electrophilic carbon center of $CO_2$ molecule leading to the formation of zwitterionic adducts DBU-$CO_2$ and TBD-$CO_2$, respectively (Scheme 6), just like NHC and NHO [16–21]. Recently, the existence of such adducts has been clearly confirmed by X-ray single-crystal diffraction [22] and $^{11}C$-labeling [14]. In addition, these DBU-$CO_2$ and TBD-$CO_2$ adducts could promote cycloaddition reaction of epoxides and $CO_2$ through nucleophilic attack at the ring of the epoxide.

The strong basicity enables those superbases to find application in the base-catalyzed $CO_2$ conversion. For example, superbases are efficient catalysts for the chemical fixation of $CO_2$ with 2-aminobenzonitriles for the synthesis of quinazoline-2,4(1*H*,3*H*)-diones under solvent-free conditions as depicted in Scheme 7 [23, 24]. A variety of 2-aminobenzonitriles bearing electron-withdrawing or electron-donating substitutes give the corresponding quinazoline-2,4(1*H*,3*H*)-diones in moderate to excellent isolated yields (60–95%) catalyzed by low-loading TMG under 10 MPa $CO_2$ pressure at 120°C within 4 h. As shown in Scheme 8, superbases could also catalyze the carboxylative cyclization reactions of propargylamines or propargyl alcohols with $CO_2$, affording α-methylene cyclic carbonates and oxazolidinones, respectively [25, 26].

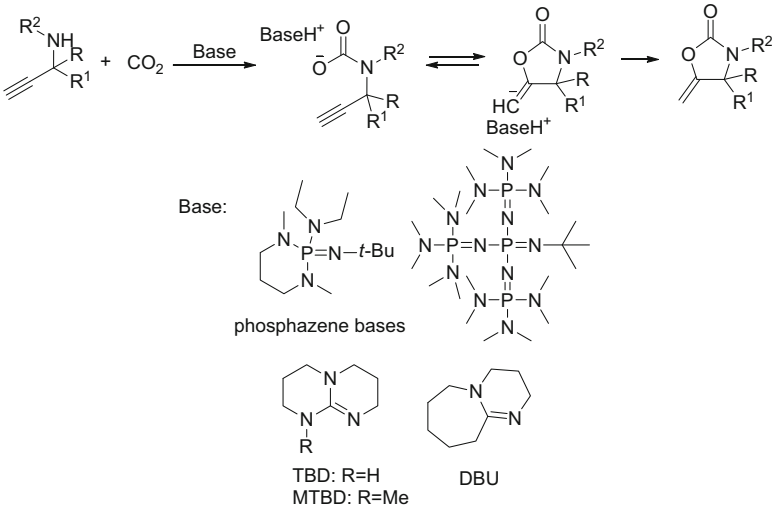


**Scheme 8** Superbase-catalyzed carboxylative cyclization of propargylamines with $CO_2$ [25, 26]

## *2.3 Frustrated Lewis Pair*

Frustrated Lewis pairs (FLPs) consist of sterically hindered Lewis donors and acceptors. The steric demands preclude the formation of simple Lewis acid–base adducts, allowing for subsequent reactions of both Lewis acids and bases with other potential molecules. Recently, FLPs have become a fundamentally unique strategy for activating a variety of small molecules [27, 28]. Especially, FLP amido-phosphoranes [29] could rapidly capture one equivalent of $CO_2$ with simultaneous activation as shown in Scheme 9. Furthermore, B/P-, B/N-, P/N-, and Al/P-based FLPs have been shown to have the ability to convert $CO_2$ into carbonic acid derivatives, methanol, methane, or CO by the groups of Stephan [30–32], O'Hare [33], and Piers [34]. For example, Al/P-based FLPs $Mes_3P(AlX_3)$ (Mes = 2,4,6-$C_6H_2Me_3$ X = Cl **4**; Br **5**), a 1:2 mixture of $PMes_3$ with $AlX_3$, could irreversibly capture $CO_2$ with the formation of species **6** and **7** ($Mes_3P(CO_2)(AlX_3)_2$ X = Cl **6**; Br **7**) (Scheme 10). Furthermore, the species **6** and **7** could react rapidly with excess ammonia borane at room temperature to give $CH_3OH$ upon quenching with water [30]. The structure of species **6** or **7** has been identified by X-ray single-crystal diffraction, in which phosphine is bound to the C atom of $CO_2$, while $AlX_3$ units are bonded to each of the O atoms. The P–C bond lengths in **6** and **7** are found to be 1.927(8) and 1.918(5) Å, respectively, while the O–Al distances are 1.807(5) and 1.808(6) Å in **6** and 1.829(4) and 1.803(3) Å in **7**. The C–O bond lengths are determined to be 1.233(8) and 1.251(8) Å in **6** and equivalent at 1.248(6) Å in **7**. The O–C–O angles are 126.6(7)°and 125.8(4)° in **6** and **7**, respectively, while the C–O–Al angles differ substantially from each other being 141.3(5)° and 165.2(6)° and 140.0(3)° and 178.7(4)° in **6** and **7**, respectively.

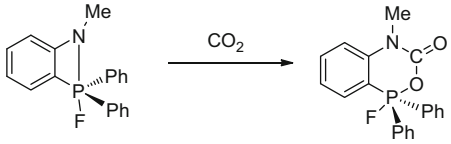


**Scheme 9** Equimolar $CO_2$ capture by amidophosphoranes [29]

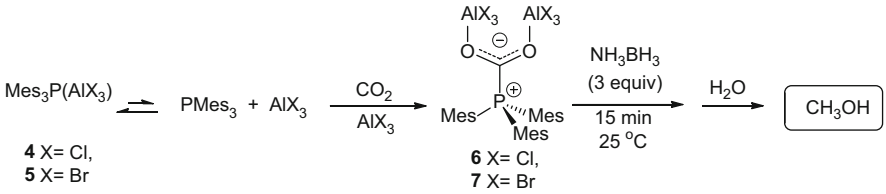


**Scheme 10** Stoichiometric reduction of $CO_2$ to $CH_3OH$ promoted by Al/P-based FLPs [30]

## 3 Ionic Liquid

Ionic liquids (ILs) being composed of organic cations and inorganic/organic anions have some very attractive properties, such as nonvolatile, nonflammable, high thermal stability, and excellent solubility. In addition, the functions of ILs can be designed for different processes by changing the structures of their cations or anions. ILs, especially task-specific ILs (TSILs) with various functionalized groups, have great potential applications in chemical reactions, material synthesis, separation, and fractionation [35, 36]. Encouragingly, by introducing corresponding functionalized groups, TSILs could activate $CO_2$ molecule or substrates for further transformation. Therefore, TSILs display superior performance for $CO_2$ capture and conversion such as hydrogenation of $CO_2$ to formic acid [37], preparation of 5-aryl-2-oxazolidinones from aziridines and $CO_2$ [38], synthesis of disubstituted urea from amines and $CO_2$ [39], synthesis of quinazoline-2,4(1*H*,3*H*)-diones from $CO_2$ and 2-aminobenzonitrile, and so on.

### *3.1 Homogeneous Ionic Liquid*

One of the most attractive synthetic protocols utilizing $CO_2$ is the coupling reaction of epoxides and $CO_2$ to afford the five-membered cyclic carbonates such as ethylene carbonate (EC) and propylene carbonate (PC) which could serve as excellent polar aprotic solvents, intermediates in the production of pharmaceuticals, and electrolytic elements of lithium secondary batteries [40–42]. ILs, for instance, tetrabutylammonium bromide (TBAB) or tetrabutylammonium iodide (TBAI) [43], 1-octyl-3-methylimidazolium tetrafluoroborate ($[C_8MIm][BF_4]$) [44], and Lewis

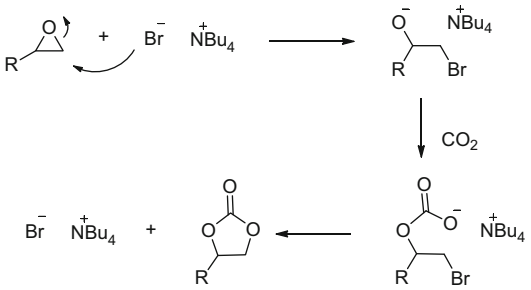


**Scheme 11** Proposed mechanism of propylene carbonate synthesis catalyzed by TBAB [43]

basic ILs [45] are effective catalysts for the cycloaddition reaction of epoxide and $CO_2$. Taking TBAB as an example, a plausible mechanism for the cycloaddition reaction is shown in Scheme 11. The epoxide ring is opened by nucleophilic attack of the bromide anion, which could lead to generation of an oxy anion species, then affording the corresponding cyclic carbonate after $CO_2$ insertion.

Under supercritical $CO_2$ ($scCO_2$) conditions, ILs usually show relatively high activity for the cycloaddition reaction due to complete miscibility of $CO_2$ in the ILs under high pressure conditions. With 1-octyl-3-methylimidazolium tetrafluoroborate ($[C_8MIm][BF_4]$) as the catalyst under supercritical conditions (14 MPa $CO_2$) at 110°C, the cycloaddition of $CO_2$ and propylene oxide could complete within 5 min with TOF of 516 $h^{-1}$ [44].

The introduction of hydroxyl group or carboxylic acid group could highly increase the catalytic activity of ILs. As depicted in Scheme 12, the interaction of the H atom with the O atom of epoxide through a hydrogen bond results in the polarization of C–O bond, so the ring of the epoxide could be opened easily. A series of hydroxyl-functionalized ILs [46, 47] and carboxyl-functionalized ILs [48–50] have been proven to be efficient catalysts for the coupling of epoxide and $CO_2$ (Scheme 13). In the presence of 1-(2-hydroxyl-ethyl)-3-methylimidazolium bromide (HEMIMB), 99% yield of propylene carbonate with >99% selectivity is obtained. The excellent catalytic activity is obtained because of the synergistic interaction of the hydrogen-bonding groups with the nucleophile in these ILs as shown in Scheme 12. Even the existence of water in ILs could also accelerate the reaction due to the formation of hydrogen bonds [51], which is quite similar to the role of hydroxyl group.

Poly(ethylene glycol)s (PEGs) are a family of water-soluble linear polymers which could be regarded as a kind of $CO_2$-philic materials. In other words, "$CO_2$-expansion" effect could lead to changes in the physical properties of the liquid phase mixture including lowered viscosity and increased gas/liquid diffusion rates [52]. PEG-functionalized ILs, $BrBu_3NPEG_{6000}NBu_3Br$ [53, 54], $BrBu_3PPEG_{6000}PBu_3Br$ [55], $PEG_{6000}(GBr)_2$ [56], and $BrTBDPEG_{150}TBDBr$ [57] as listed in Scheme 14, could be utilized as highly active homogeneous catalysts for $CO_2$ transformation. For example, the cycloaddition reaction of PO with $CO_2$ in the presence of 0.5 mol% $BrBu_3NPEG_{6000}NBu_3Br$ affords PC in 98% yield together with 99% selectivity at 120°C, 8 MPa $CO_2$, in 6 h. Furthermore, the

**Scheme 12** Proposed mechanism for the cycloaddition reaction promoted by hydrogen bonding

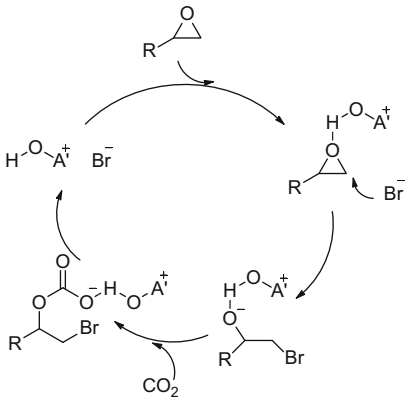


**Scheme 13** Several kinds of hydroxyl-functionalized and carboxyl-functionalized ILs [46–50]

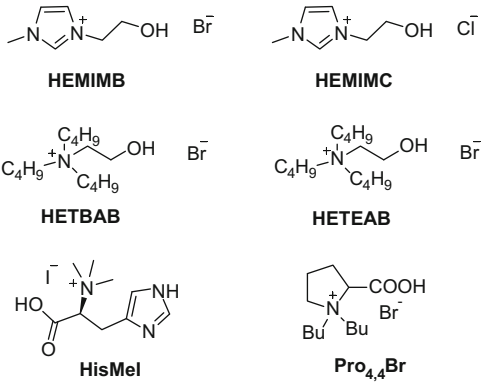


$PEG_{6000}$-supported catalyst can be readily recovered by simple filtration and reused without appreciable loss of activity.

Attachment of fluorinated chains to chelating agents and surfactants could generally enhances the solubility of such compounds in $scCO_2$. Fluorine-containing ILs and polymer [58–60] as illustrated in Scheme 15 have been proven to be efficient and recyclable homogeneous $CO_2$-soluble catalysts for solvent-free synthesis of cyclic carbonates from epoxides and $CO_2$ under $scCO_2$ conditions. Furthermore, these catalysts can be easily recovered after reaction and reused with retention of high activity and selectivity. For example, the catalyst F-PIL-Br is easily recovered through centrifugation, dried, and then used directly for the next run without any further purification. As for catalyst **8**, simple filtration can get the catalyst recovered because it precipitates upon venting $CO_2$.

Zwitterionic compounds have been used as halogen-free bifunctional catalysts for the cycloaddition of epoxides with $CO_2$. A range of aromatic zwitterions bearing an ammonium betaine able to activate $CO_2$ molecule proved to be efficient catalysts for the production of cyclic carbonates under metal-free, solvent-free

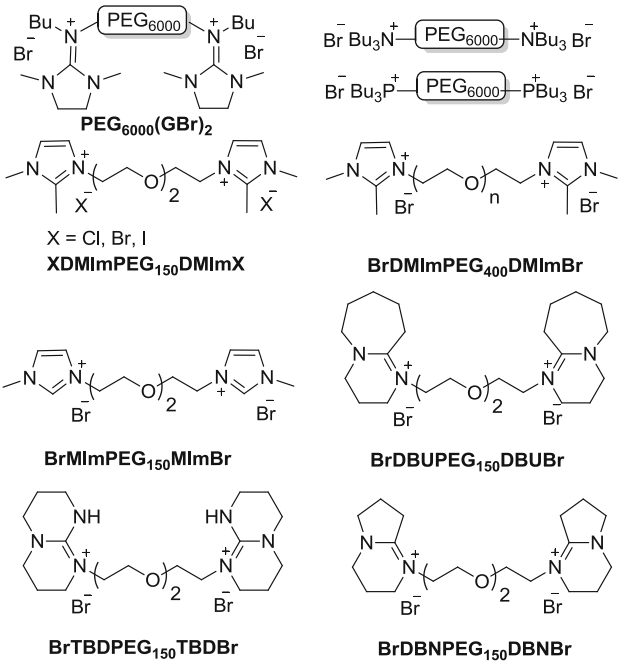


**Scheme 14** PEG-functionalized ionic liquids for the synthesis of cyclic carbonates [53–57]

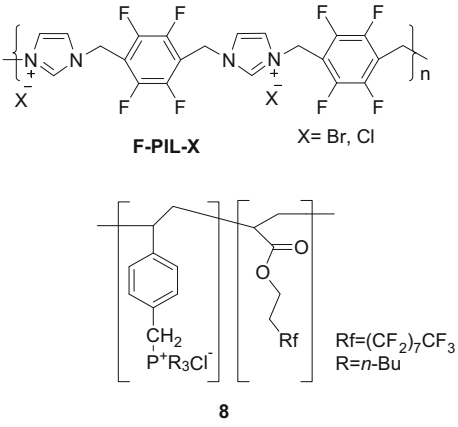


**Scheme 15** Fluoro-functionalized polymeric ionic liquids [58–60]

conditions [61]. Interestingly, the **9**-$CO_2$ adduct as shown in Scheme 16 was characterized and used as a synthon to prepare cyclic carbonates. Very recently, Lu and his coworkers reported that the alkoxide-functionalized imidazolium betaines (AFIBs) bearing an alkoxide anion and an imidazolium cation show strong tendencies for $CO_2$ capture, affording a $CO_2$ adduct (AFIB-$CO_2$) [62]. Furthermore,

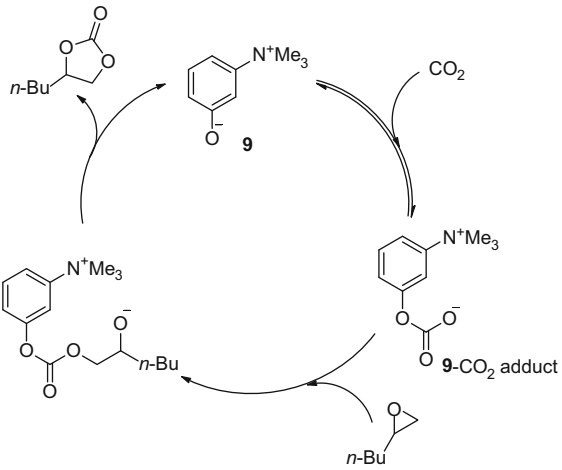


**Scheme 16** The synthesis of cyclic carbonates catalyzed by aromatic zwitterions [61]

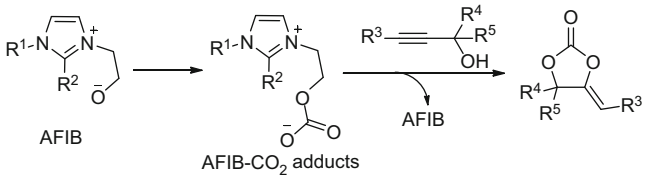


**Scheme 17** AFIB-$CO_2$ adducts catalyzed carboxylative cyclization of propargylic alcohols with $CO_2$ [62]

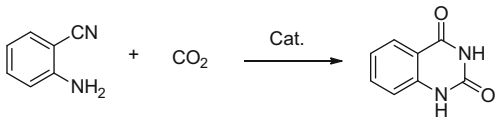


**Scheme 18** Reaction of $CO_2$ and 2-aminobenzonitrile to quinazoline-2,4(1*H*,3*H*)-dione

AFIB-$CO_2$ adducts could effectively catalyze the coupling reaction of propargylic alcohols with $CO_2$ under solvent-free reaction conditions, selectively affording alkylene cyclic carbonates, as depicted in Scheme 17.

ILs could act as both solvent and catalyst for the synthesis of quinazoline-2,4(1*H*,3*H*)-dione derivatives through incorporation of $CO_2$ into aminobenzonitriles as delineated in Scheme 18. Excellent results are attained by using 1-butyl-3-methyl imidazolium hydroxide ([Bmim]OH) [63] and 1-butyl-3-methylimidazolium acetate ([Bmim]Ac) [64]. With [Bmim]Ac as catalysts, 92% yield of quinazoline-2,4(1*H*,3*H*)-dione is attained at 1 atm $CO_2$, 90°C in 10 h. Moreover,

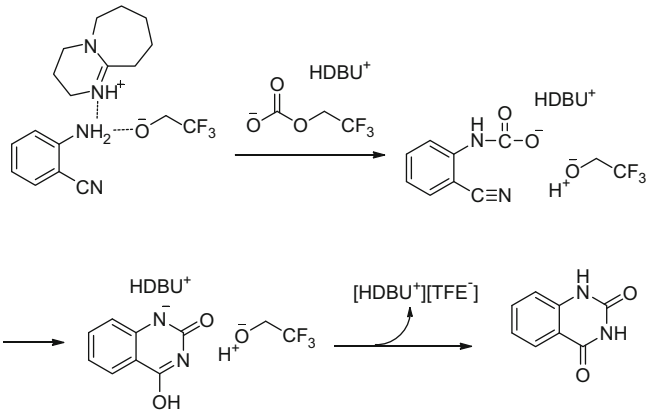


**Scheme 19** Possible dual-activation role of [$HDBU^+$][$TFE^-$] [66]

recovery of such ILs is easily performed by simple filtration. The catalyst could be reused at least five times without considerable loss in catalytic activity.

The synthesis of quinazoline-2,4(1*H*,3*H*)-dione could be regarded as a kind of base-catalyzed reactions; superbases, such as TMG, could be applied as catalysts for this transformation [65]. Furthermore, superbase-derived protic IL, e.g., [$HDBU^+$][$TFE^-$], has been found to activate $CO_2$ and 2-aminobenzonitriles simultaneously to produce quinazoline-2,4(1*H*,3*H*)-diones under 1 atm $CO_2$ and room temperature as shown in Scheme 19 [66]. 97% yield of quinazoline-2,4(1*H*,3*H*)-dione is attained with [$HDBU^+$][$TFE^-$] (3% catalyst loading) at 30°C, 1 atm $CO_2$ in 24 h. A new signal that appears at $\delta = 167.7$ ppm in the $^{13}$C-NMR spectrum of [$HDBU^+$][$TFE^-$]/$CO_2$ mixture is attributed to the carbonyl carbon atom of the carbonate, suggesting that $CO_2$ is activated by the anion [$TFE^-$], thus forming a carbonate intermediate. Simultaneously, 2-aminobenzonitriles could form hydrogen bonds with both the cation and anion of the IL, resulting in weakening the N–H bond in $NH_2$ group of 2-aminobenzonitrile.

## *3.2 Supported Ionic Liquid*

Although ILs have been reported to be one of the most efficient catalysts for $CO_2$ fixation, application of homogeneous catalysts in industry could be limited due to the complicated separation procedure. On the other hand, proper use of heterogeneous catalysis for $CO_2$ conversion may offer enhancement of the reaction rate and control of selectivity, increasing catalyst lifetime and facilitating separation.

One way is to immobilize the IL onto silica. A series of silica-supported ILs including phosphonium salts [67, 68], imidazolium ILs [69–73], 4-pyrrolidinopyridinium iodide [74], aluminum(salen) complexes [75, 76], and hexa-alkylguanidinium chloride [77] exhibit high catalytic activity, selectivity,

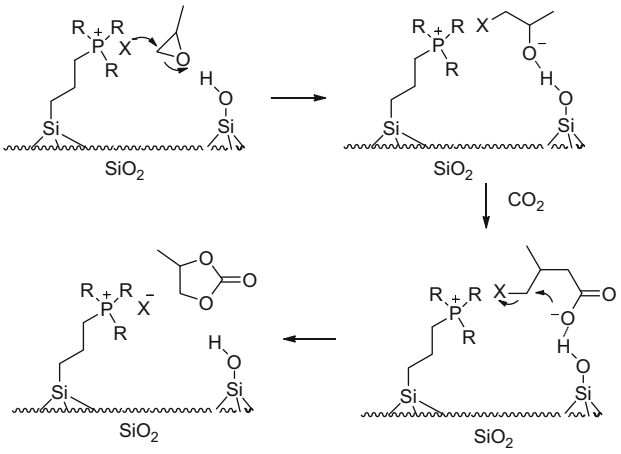


**Scheme 20** Possible acceleration mechanism for the cycloaddition reaction catalyzed by silica-supported phosphonium salts [67, 68]

and reusability in the cycloaddition of $CO_2$ to epoxides. An almost quantitative amount of propylene carbonate is produced using $SiO_2$-$C_3H_6$-P(*n*-Bu)$_3$I as catalyst at 100°C, 10 MPa of $CO_2$ in 1 h. Interestingly, the silica-supported ILs dramatically increase the catalytic activities compared to the corresponding homogeneous ILs. The cooperative catalysis originating from the silica surface and the onium part may result in the enhanced activity. In other words, the acidic surface silanol groups are able to activate epoxides, and then the ring opens via subsequent nucleophilic attack. A proposed mechanism of the coupling reaction catalyzed by silica-supported phosphonium salts [67, 68] has been proposed as shown in Scheme 20. Furthermore, these heterogeneous ILs could easily be separated and reused without considerable loss of the activity.

Besides silica, mesoporous sieves and polymeric materials are other kinds of promising supports, which could immobilize ILs. ILs immobilized on mesoporous sieves (SBA-15 [78, 79] and MCM-41 [80–82]) and polymeric materials [83, 84] could act as efficient catalysts for the transformation of $CO_2$ into cyclic carbonates with high yield and excellent selectivity under relatively mild conditions. High activity is displayed when ILs immobilized on carboxymethyl cellulose (CMC) and chitosan (CS) are applied as heterogeneous catalysts for cycloaddition of epoxides with $CO_2$, since CMC or CS is rich in hydroxyl and carboxyl groups [85–87]. CMC and CS not only act as the supporting materials for ILs but also serve as carriers of functional groups capable of activating the nucleophilic attack via the hydroxyl and the carboxyl moieties. The synergistic function originating from the hydroxyl and carboxyl moieties in the supporter could activate epoxides through formation of hydrogen bonds, thus facilitating the ring opening of epoxides.

# 4 Main Group Metal

Main group metal compounds are an important kind of effective catalysts for $CO_2$ incorporation to form value-added chemicals. Unlike transition metal catalysts, which usually coordinate with $CO_2$ molecule leading to simultaneously activate $CO_2$, main group metal catalysts usually react with substrates, in situ generating nucleophiles to go through nucleophilic attack at $CO_2$. For example, cesium carbonate could react with 2-aminobenzonitrile, providing a nitrogen anion to perform a nucleophilic attack at $CO_2$. The Lewis basic cation of aluminum(III) (salen) complex could active the epoxide through interaction with the oxygen, furnishing a nucleophilic oxygen anion to react with $CO_2$. Fluorine salts usually react with silicon compounds, affording a carbon anion to attack at $CO_2$. Stannum compounds have a strong tendency to react with alcohols with the formation of Sn–O bonds, furnishing $CO_2$ insertion. By applying these characteristics of main metal catalysts, various valuable products are obtained in high yield and selectivity.

## *4.1 Main Group Metal Salts*

Cesium carbonate shows remarkable activity for the base-catalyzed reaction of $CO_2$ with 2-aminobenzonitriles [88]. $Cs_2CO_3$ could react with 2-aminobenzonitrile, providing a nitrogen anion due to its strong basicity. As shown in Scheme 21, the nitrogen anion could attack to $CO_2$, furnishing further conversion of $CO_2$. In the presence of 0.25 equivalent $Cs_2CO_3$, 94% of quinazoline-2,4(*1H*,*3H*)-diones is obtained at 1.3 MPa $CO_2$, 100°C in 4 h. Notably, this catalytic system is applicable to a wide variety of substituted 2-aminobenzonitriles with different steric and electronic properties. Interestingly, the reaction temperature has a pronounced positive effect on the synthesis of quinazoline-2,4(*1H*,*3H*)-diones. The reaction does not occur at 80°C, while the yield increases to 94–95% with an increase in the reaction temperature from 100 to 120°C.

Inexpensive $K_2CO_3$ could catalyze the formation of carbamates in $scCO_2$ with a catalytic amount of $Bu_4NBr$ as cocatalyst [89]. The reaction efficiency in $scCO_2$ is 50–100 times higher than that attained in heptane. The amine readily forms the

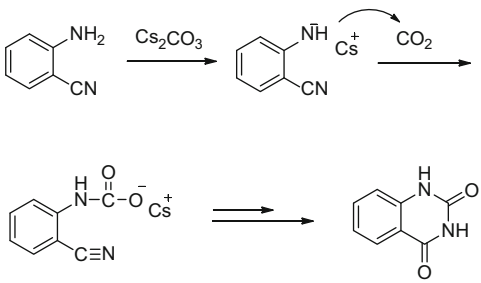


**Scheme 21** $Cs_2CO_3$-catalyzed synthesis of quinazoline-2,4(*1H*,*3H*)-diones [88]

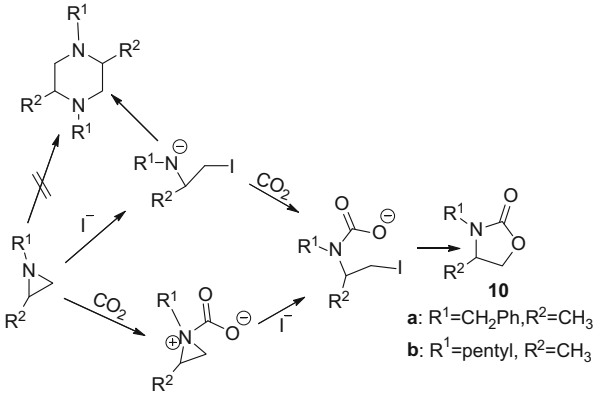


**Scheme 22** Possible mechanisms for the LiI-catalyzed cycloaddition of $CO_2$ with aziridine [91]

carbamic acid ammonium salt upon the introduction of liquid $CO_2$. As for catalytic activity among alkali metal carbonate, $Cs_2CO_3$ is much higher than $K_2CO_3$ and $Na_2CO_3$. $Cs_2CO_3$ together with tetrabutylammonium iodide (TBAI) is proven to be an efficient catalyst for the synthesis of carbamates in which $Cs_2CO_3$, TBAI, and alkyl halides are excessive [90]. Aliphatic, aromatic, and heterocyclic amines and reactive, unreactive, and secondary halides can be converted to the corresponding carbamates using DMF as solvent.

The conversion of the aziridine to the corresponding oxazolidinone can be performed by employing LiI as the catalyst in THF with hexamethylphosphoramide (HMPA, a lithium-complexing agent) as a cosolvent which is used to facilitate the ion pair separation of the LiI and strengthen the $S_N2$ character of the reaction (Scheme 22) [91]. Only one isomer oxazolidinone (**10a** 97% yield or **10b** 95% yield) can be obtained. Nucleophilic attack of the $I^-$ at the less substituted carbon leads to the ring-opened structure of aziridine, which then reacts with $CO_2$ to further form oxazolidinones by intramolecular ring closure, and the catalyst is regenerated.

Mg–Al-mixed oxide and magnesium oxide possess both acid and base surface sites and could activate both epoxides and $CO_2$. With magnesium oxide or Mg–Al-mixed oxide as catalysts, the reaction of $CO_2$ with epoxides gives organic carbonates in excellent yields [92, 93]. As depicted in Scheme 23, the basic and acidic sites located in Mg–Al-mixed oxide could activate $CO_2$ molecule and substrates, respectively, which greatly increases the catalytic activity. Especially, the Lewis basic sites could absorb $CO_2$ onto the surfaces to form the carbonate species, which promotes the ring opening of epoxides by a nucleophilic attack. Besides Mg–Al oxide, basic zeolites [94–96] are also effective catalysts for the cycloaddition of $CO_2$ with epoxides.

## *4.2 Aluminum(Salen) Complex*

Salen ligands are commonly prepared through the condensation of a salicylaldehyde and a diamine. The ease of synthesis and modification has promoted more and more interest in using salen as a ligand for many different catalytic

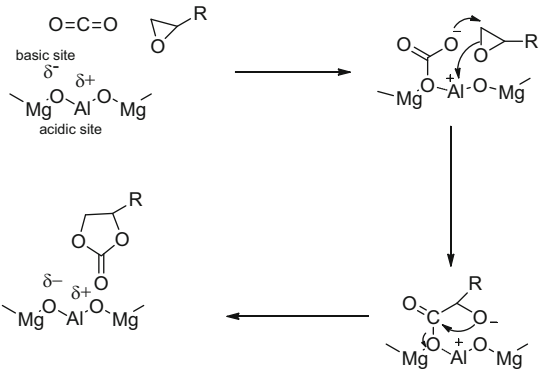


**Scheme 23** The interaction of Mg–Al-mixed oxide with epoxide and $CO_2$ [93]

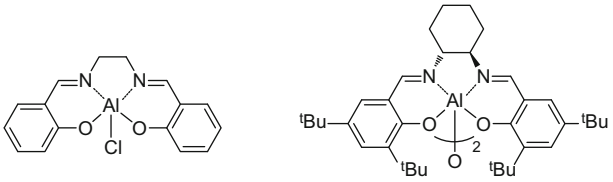


**Scheme 24** Al(III)(salen)Cl complex **11** [97] and dimeric Al(salen) complex **12** [98]

reactions. Salen complexes with a number of transition metals and main group metals have been found to catalyze the cycloaddition of $CO_2$ to epoxides. Aluminum(III)(salen) complexes are promising main group metal catalysts for the cycloaddition reaction. For example, Al(III)(salen)Cl complex **11** (Scheme 24) is reported to be effective catalysts for the synthesis of ethylene carbonate in the presence of TBAB as cocatalyst [97–101]. Quantitative yield is obtained under 16 MPa $CO_2$, 110°C, with a TOF of 2,200 $h^{-1}$. In the absence of onium cocatalysts, complex **11** shows a more moderate activity (TOF 174 $h^{-1}$) under the otherwise identical reaction conditions.

Dimeric aluminum(salen) complexes (**12**, Scheme 25) with TBAB as cocatalyst have shown exceptionally high catalytic activity for the synthesis of cyclic carbonates at ambient temperature and pressure [98]. 3-Phenylpropylene oxide, 1,2-hexene oxide, and 1,2-decene oxide are transformed into the corresponding cyclic carbonates with the yields of 99% (after 24 h), 88% (after 3 h), and 64% (after 3 h), respectively. As depicted in Scheme 19, both aluminum ions of the complex play a role in activating the epoxide and $CO_2$, resulting in the excellent catalytic activity. Furthermore, the catalyst **12** could be reused over 60 times without loss of catalytic activity, although periodic addition of TBAB is necessary.

An aluminum complex based on an amino triphenolate ligand scaffold as shown in Scheme 26 has been demonstrated to be a highly active and versatile catalyst for

**Scheme 25** Possible mechanism to explain the catalytic activity of dimeric Al(salen) complex **12** [98]

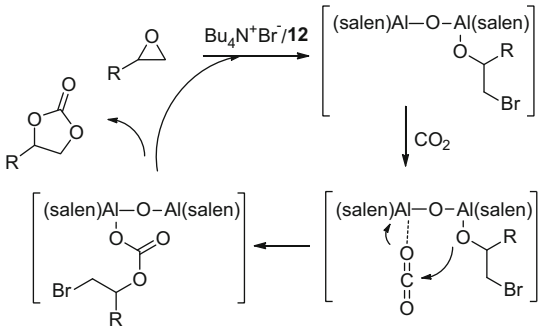


**Scheme 26** Synthesis of aluminum complex based on an amino triphenolate [99]

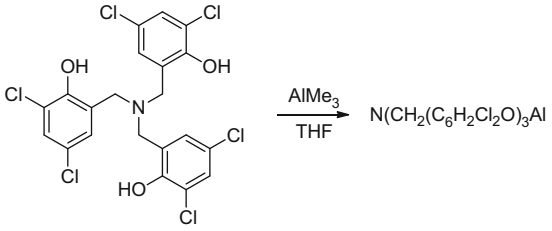


organic carbonate formation [99]. Unprecedented activity (initial TOFs up to 36,000 $h^{-1}$ and TONs exceeding 118,000) is attained during catalysis for the cycloaddition of $CO_2$ to epoxides, with a wide substrate scope and functionality tolerance [102].

## *4.3 Fluorine Salts*

Fluorine anion has a strong tendency to react with compounds containing silicon atoms, affording silicon fluoride compounds and a carbon anion. This unique characteristic is applicable to the synthesis of amino acids by using gaseous $CO_2$ as carboxylating reagent. Arylglycine derivatives are prepared from the imine equivalents (*N*-Boc-R-amido sulfones **13**) using a combination of TMS-$SnBu_3$ and CsF under $CO_2$ atmosphere as illustrated in Scheme 27 [103–106]. Reversal of polarity on the imino carbon atom is a key to the success of the proposed transformation, which could be accessed via α-metalation of alkylamine derivatives. A plausible pathway of the reaction is proposed as shown in Scheme 27. Firstly, by treatment with CsF, imine **14** could be generated in situ from a readily available synthetic precursor of imines, amino sulfone **13**. Subsequently, imine **14** is converted into amino stannane **15** by attack of tributylstannyl anion. Finally, the fluoride ion further activates α-amino stannane **15** by attack at the tin atom to improve nucleophilicity of the carbon atom, thus leading to $CO_2$ insertion into the C–Sn bond and affording α-amino acid derivative **16**.

Arynes are highly unstable species with salient electrophilic nature that could undergo nucleophilic addition with a variety of neutral nucleophiles, and the

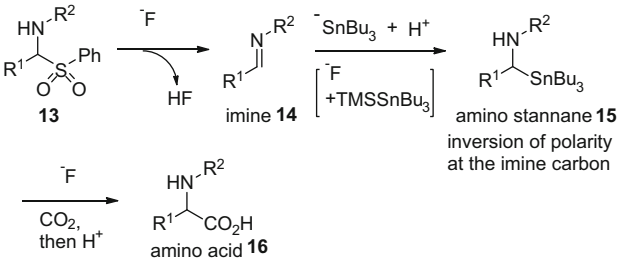


**Scheme 27** One-pot synthesis of α-amino acids with the aid of fluorine anion [103]

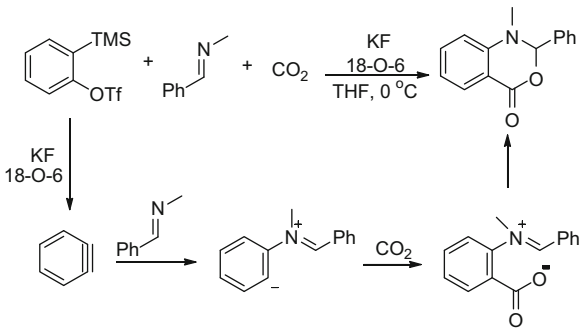


**Scheme 28** Three-component coupling of benzyne, imine, and $CO_2$ [107]

resulting reactive zwitterions are readily trapped by various carbon electrophiles such as aldehydes or sulfonylimines. In 2006, Yoshida and coworkers disclosed that $CO_2$ could be used as a carbon electrophile for the aryl anion intermediate which is generated from nucleophilic attack of imines at arynes [107]. A plausible mechanism is proposed as depicted in Scheme 28. Benzyne, which is formed by fluoride-induced 1,2-elimination of *o*-trimethylsilylphenyl triflate, undergoes nucleophilic addition with an imine. The resulting zwitterion is readily trapped by $CO_2$, and a subsequent intramolecular cyclization affords six-membered heterocycles, benzoxazinone derivatives. After that, amines or isocyanides have been used as nucleophilic partners for $CO_2$ incorporation into arynes, giving anthranilic acid derivatives and *N*-substituted phthalimides, respectively, under mild reaction conditions [108, 109].

## *4.4 Stannum Compounds*

Sn compounds are remarkable catalysts for the synthesis of organic carbonates, such as dimethyl carbonate (DMC), and cyclic carbonates from methanol, glycol, and glycerol with $CO_2$ as raw materials as depicted in Scheme 29.

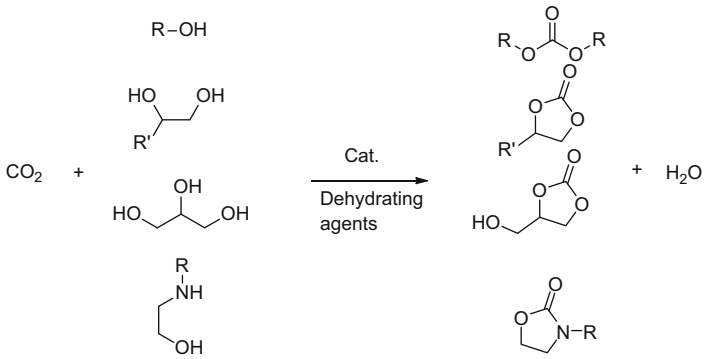


**Scheme 29** Incorporation of $CO_2$ promoted by dehydrating agents

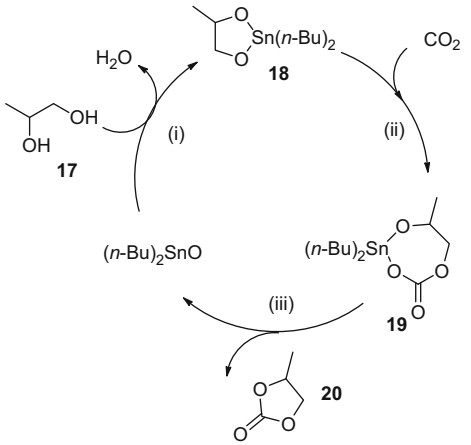


**Scheme 30** A postulated mechanism for PC synthesis from PG and $CO_2$ catalyzed by $Bu_2SnO$ [112]

Sn compounds, such as dibutyltin oxide ($Bu_2SnO$) and dibutyltin dimethoxide ($Bu_2Sn(OMe)_2$), have been reported to be efficient catalysts for the carboxylation of methanol [110, 111], glycol [112], glycerol [113], and 1,2-aminoalcohols into carbonates and 2-oxazolidinones, respectively. Taking the carboxylation of propylene glycol with $CO_2$ as an example, a plausible catalytic cycle is proposed as illustrated in Scheme 30. It involves three steps: (1) the reaction of $Bu_2SnO$ and propylene glycol gives 2,2-dibutyl-1,3,2-dioxastannolan **18** [114]; (2) since Sn–O bond is known to be susceptible to $CO_2$ insertion [115], a cyclic tin carbonate **19** is formed through the insertion of $CO_2$ to **17**; (3) subsequent intramolecular nucleophilic attack of alkoxy group at the carbonyl group may cause the production of propylene carbonate along with regenerating dibutyltin oxide. The removal of water is a crucial issue for the reaction by shifting the equilibrium to carbonates. In the presence of a catalytic amount of $Bu_2SnO$ or $Bu_2Sn(OMe)_2$ with molecular

sieve as the dehydrating agent, the yield of propylene carbonate reaches nearly 50% at 180°C for 72 h.

## 5 Conclusion and Prospective

Over the past decade, $CO_2$ chemistry has been developed greatly. Catalytic $CO_2$ incorporation into valuable organic molecules has become an essential subject in synthetic organic chemistry. This chapter highlights many promising transition metal-free catalysts, including organocatalysts, ionic liquids, and main group metal, which are proven to be efficient catalysts for the transformation of $CO_2$. Compared to transition metal-based catalysts, catalysts outlined in this chapter possess many significant advantages of low cost, easy preparation, non-sensitivity to air or moisture, and relative hypotoxicity to the environment. Many important progresses on transition metal-free incorporation of $CO_2$ have been made resulting in the production of various valuable chemicals such as linear or cyclic carbonates, quinazoline-2,4(1*H*,3*H*)-diones, alkylidene cyclic carbonates, and amino acids.

Although great progresses have been made on chemical transformation of $CO_2$ by transition metal-free catalysts, $CO_2$ incorporation at milder reaction conditions and more efficient catalysts are still highly desired. Especially, it is highly wishful to perform $CO_2$ conversion at low pressure ($<1$ MPa), even at 1 atm $CO_2$ pressure. Therefore, more efficient transition metal-free catalysts on the basis of activation of $CO_2$ or substrates should be further designed to improve the catalytic efficiency. We hope this presentation will stimulate further interest in the development of more effective transition metal-free catalysts for chemical transformation of $CO_2$ in academic research and industrial utilization.

**Acknowledgments** We are grateful to the National Natural Sciences Foundation of China, the Specialized Research Fund for the Doctoral Program of Higher Education (20130031110013), the MOE Innovation Team (IRT13022) of China, and the "111" Project of Ministry of Education of China (project no. B06005) for financial support.

## References

1. Parkin G (2004) Synthetic analogues relevant to the structure and function of zinc enzymes. Chem Rev 104(2):699–768
2. Darensbourg DJ, Holtcamp MW (1996) Catalysts for the reactions of epoxides and carbon dioxide. Coord Chem Rev 153:155–174
3. Leitner W (1995) Carbon dioxide as a raw material: the synthesis of formic acid and its derivatives from $CO_2$. Angew Chem Int Ed 34(20):2207–2221
4. Herrmann WA (2002) *N*-Heterocyclic carbenes: a new concept in organometallic catalysis. Angew Chem Int Ed 41:1290–1309

5. Crabtree RH (2007) Recent developments in the organometallic chemistry of N-heterocyclic carbenes. Coord Chem Rev 251(5–6):595
6. Hahn FE, Jahnke MC (2008) Heterocyclic carbenes: synthesis and coordination chemistry. Angew Chem Int Ed 47(17):3122–3172
7. Shen Y, Duan W, Shi M (2003) Chemical fixation of carbon dioxide catalyzed by binaphthyldiamino Zn, Cu, and Co salen-type complexes. J Org Chem 68:1559–1562
8. Duong HA, Tekavec TN, Arif AM, Louie J (2004) Reversible carboxylation of N-heterocyclic carbenes. Chem Commun 1:112–113
9. Zhou H, Zhang W-Z, Liu C-H, Qu J-P, Lu X-B (2008) $CO_2$ adducts of N-heterocyclic carbenes: thermal stability and catalytic activity toward the coupling of $CO_2$ with epoxides. J Org Chem 73(20):8039–8044
10. Kayaki Y, Yamamoto M, Ikariya T (2009) N-heterocyclic carbenes as efficient organocatalysts for $CO_2$ fixation reactions. Angew Chem Int Ed 48(23):4194–4197
11. Tommasi I, Sorrentino F (2009) 1,3-Dialkylimidazolium-2-carboxylates as versatile N-heterocyclic carbene–$CO_2$ adducts employed in the synthesis of carboxylates and α-alkylidene cyclic carbonates. Tetrahedron Lett 50(1):104–107
12. Zhou H, Wang Y-M, Zhang W-Z, Qu J-P, Lu X-B (2011) N-Heterocyclic carbene functionalized MCM-41 as an efficient catalyst for chemical fixation of carbon dioxide. Green Chem 13(3):644–650
13. Wang YB, Wang YM, Zhang WZ, Lu XB (2013) Fast $CO_2$ sequestration, activation, and catalytic transformation using N-heterocyclic olefins. J Am Chem Soc 135(32):11996–12003
14. Hooker JM, Reibel AT, Hill SM, Schueller MJ, Fowler JS (2009) One-pot, direct incorporation of [11C]$CO_2$ into carbamates. Angew Chem Int Ed 48(19):3482–3485
15. Zhang X, Zhao N, Wei W, Sun Y (2006) Chemical fixation of carbon dioxide to propylene carbonate over amine-functionalized silica catalysts. Catal Today 115(1–4):102–106
16. Barbarini A, Maggi R, Mazzacani A, Mori G, Sartori G, Sartorio R (2003) Cycloaddition of $CO_2$ to epoxides over both homogeneous and silica-supported guanidine catalysts. Tetrahedron Lett 44(14):2931–2934
17. Zhang X, Jia Y-B, Lu X-B, Li B, Wang H, Sun L-C (2008) Intramolecularly two-centered cooperation catalysis for the synthesis of cyclic carbonates from $CO_2$ and epoxides. Tetrahedron Lett 49(46):6589–6592
18. Ma J, Zhang X, Zhao N, Al-Arifi ASN, Aouak T, Al-Othman ZA, Xiao F, Wei W, Sun Y (2010) Theoretical study of TBD-catalyzed carboxylation of propylene glycol with $CO_2$. J Mol Catal A Chem 315(1):76–81
19. Pérez E-R, Santos RHA, Gambardella MTP, de Macedo LGM, Rodrigues-Filho UP, Launay J-C, Franco DW (2004) Activation of carbon dioxide by bicyclic amidines. J Org Chem 69:8005–8011
20. Pereira FS, deAzevedo ER, da Silva EF, Bonagamba TJ, da Silva Agostíni DL, Magalhães A, Job AE, Pérez González ER (2008) Study of the carbon dioxide chemical fixation—activation by guanidines. Tetrahedron 64(43):10097–10106
21. Heldebrant DJ, Jessop PG, Thomas CA, Eckert CA, Liotta CL (2005) The reaction of 1,8-diazabicyclo[5.4.0]undec-7-ene (DBU) with carbon dioxide. J Org Chem 70(13): 5335–5338
22. Villiers C, Dognon JP, Pollet R, Thuery P, Ephritikhine M (2010) An isolated $CO_2$ adduct of a nitrogen base: crystal and electronic structures. Angew Chem Int Ed 49(20):3465–3468
23. Gao J, He L-N, Miao C-X, Chanfreau S (2010) Chemical fixation of $CO_2$: efficient synthesis of quinazoline-2,4(1H, 3H)-diones catalyzed by guanidines under solvent-free conditions. Tetrahedron 66(23):4063–4067
24. Mizuno T, Ishino Y (2002) Highly efficient synthesis of 1H-quinazoline-2,4-diones using carbon dioxide in the presence of catalytic amount of DBU. Tetrahedron 58:3155–3158
25. Costa M, Chiusoli GP, Rizzardi M (1996) Base-catalysed direct introduction of carbon dioxide into acetylenic amines. Chem Commun 14:1699–1700

26. Ca ND, Gabriele B, Ruffolo G, Veltri L, Zanetta T, Costa M (2011) Effective guanidine-catalyzed synthesis of carbonate and carbamate derivatives from propargyl alcohols in supercritical carbon dioxide. Adv Synth Catal 353(1):133–146
27. Stephan DW, Erker G (2010) Frustrated Lewis pairs: metal-free hydrogen activation and more. Angew Chem Int Ed 49(1):46–76
28. Caputo CB, Zhu K, Vukotic VN, Loeb SJ, Stephan DW (2013) Heterolytic activation of $H_2$ using a mechanically interlocked molecule as a frustrated Lewis base. Angew Chem Int Ed 52 (3):960–963
29. Hounjet LJ, Caputo CB, Stephan DW (2012) Phosphorus as a Lewis acid: $CO_2$ sequestration with amidophosphoranes. Angew Chem Int Ed 51(19):4714–4717
30. Menard G, Stephan DW (2010) Room temperature reduction of $CO_2$ to methanol by Al-based frustrated Lewis pairs and ammonia borane. J Am Chem Soc 132:1796–1797
31. Mömming CM, Otten E, Kehr G, Fröhlich R, Grimme S, Stephan DW, Erker G (2009) Reversible metal-free carbon dioxide binding by frustrated Lewis pairs. Angew Chem Int Ed 48(36):6643–6646
32. Ménard G, Stephan DW (2011) Stoichiometric reduction of $CO_2$ to CO by aluminum-based frustrated Lewis pairs. Angew Chem Int Ed 50(36):8396–8399
33. Ashley AE, Thompson AL, O'Hare D (2009) Non-metal-mediated homogeneous hydrogenation of $CO_2$ to $CH_3OH$. Angew Chem Int Ed 48(52):9839–9843
34. Berkefeld A, Piers WE, Parvez M (2010) Tandem frustrated Lewis pair/tris (pentafluorophenyl)borane-catalyzed deoxygenative hydrosilylation of carbon dioxide. J Am Chem Soc 132:10660–10661
35. Vasile I, Parvulescu CH (2007) Catalysis in ionic liquids. Chem Rev 107:2615–2665
36. Hallett JP, Welton T (2011) Room-temperature ionic liquids: solvents for synthesis and catalysis. 2. Chem Rev 111(5):3508–3576
37. Zhang Z, Xie Y, Li W, Hu S, Song J, Jiang T, Han B (2008) Hydrogenation of carbon dioxide is promoted by a task-specific ionic liquid. Angew Chem Int Ed 47(6):1127–1129
38. Yang Z-Z, He L-N, Peng S-Y, Liu A-H (2010) Lewis basic ionic liquids-catalyzed synthesis of 5-aryl-2-oxazolidinones from aziridines and $CO_2$ under solvent-free conditions. Green Chem 12(10):1850–1854
39. Jiang T, Ma X, Zhou Y, Liang S, Zhang J, Han B (2008) Solvent-free synthesis of substituted ureas from $CO_2$ and amines with a functional ionic liquid as the catalyst. Green Chem 10(4): 465–469
40. Tundo P, Perosa A (2002) Green organic syntheses: organic carbonates as methylating agents. Chem Rec 2(1):13–23
41. Jessop PG (1999) Homogeneous catalysis in supercritical fluids. Chem Rev 99:475–493
42. Zhang S, Chen Y, Li F, Lu X, Dai W, Mori R (2006) Fixation and conversion of $CO_2$ using ionic liquids. Catal Today 115(1–4):61–69
43. Caló V, Nacci A, Monopoli A, Fanizzi A (2002) Cyclic carbonate formation from carbon dioxide and oxiranes in tetrabutylammonium halides as solvents and catalysts. Org Lett 4(15):2561–2563
44. Kawanami H, Sasaki A, Matsui K, Ikushima Y (2003) A rapid and effective synthesis of propylene carbonate using a supercritical $CO_2$-ionic liquid system. Chem Commun 2003 (7):896–897
45. Yang Z-Z, He L-N, Miao C-X, Chanfreau S (2010) Lewis basic ionic liquids-catalyzed conversion of carbon dioxide to cyclic carbonates. Adv Synth Catal 352(13):2233–2240
46. Sun J, Zhang S, Cheng W, Ren J (2008) Hydroxyl-functionalized ionic liquid: a novel efficient catalyst for chemical fixation of $CO_2$ to cyclic carbonate. Tetrahedron Lett 49(22): 3588–3591
47. Wang J-Q, Cheng W-G, Sun J, Shi T-Y, Zhang X-P, Zhang S-J (2014) Efficient fixation of $CO_2$ into organic carbonates catalyzed by 2-hydroxymethyl-functionalized ionic liquids. RSC Adv 4(5):2360

48. Zhou Y, Hu S, Ma X, Liang S, Jiang T, Han B (2008) Synthesis of cyclic carbonates from carbon dioxide and epoxides over betaine-based catalysts. J Mol Catal A Chem 284(1–2): 52–57
49. Roshan KR, Jose T, Kim D, Cherian KA, Park DW (2014) Microwave-assisted one pot-synthesis of amino acid ionic liquids in water: simple catalysts for styrene carbonate synthesis under atmospheric pressure of $CO_2$. Catal Sci Technol 4(4):963–970
50. Gong Q, Luo H, Cao J, Shang Y, Zhang H, Wang W, Zhou X (2012) Synthesis of cyclic carbonate from carbon dioxide and epoxide using amino acid ionic liquid under 1 atm pressure. Aust J Chem 65:381–386
51. Sun J, Ren J, Zhang S, Cheng W (2009) Water as an efficient medium for the synthesis of cyclic carbonate. Tetrahedron Lett 50(4):423–426
52. Chen J, Spear SK, Huddleston JG, Rogers RD (2005) Polyethylene glycol and solutions of polyethylene glycol as green reaction media. Green Chem 7(2):64–82
53. Du Y, Wang J-Q, Chen J-Y, Cai F, Tian J-S, Kong D-L, He L-N (2006) A poly(ethylene glycol)-supported quaternary ammonium salt for highly efficient and environmentally friendly chemical fixation of $CO_2$ with epoxides under supercritical conditions. Tetrahedron Lett 47(8):1271–1275
54. Du Y, Wu Y, Liu A-H, He L-N (2008) Quaternary ammonium bromide functionalized polyethylene glycol: a highly efficient and recyclable catalyst for selective synthesis of 5-aryl-2-oxazolidinones from carbon dioxide and aziridines under solvent-free conditions. J Org Chem 73(12):4709–4712
55. Tian J-S, Miao C-X, Wang J-Q, Cai F, Du Y, Zhao Y, He L-N (2007) Efficient synthesis of dimethyl carbonate from methanol, propylene oxide and $CO_2$ catalyzed by recyclable inorganic base/phosphonium halide-functionalized polyethylene glycol. Green Chem 9(6): 566–571
56. He L-N, Dou X-Y, Wang J-Q, Du Y, Wang E (2007) Guanidinium salt functionalized PEG: an effective and recyclable homo-geneous catalyst for the synthesis of cyclic carbonates from $CO_2$ and epoxides under solvent-free conditions. Synlett 2007(19):3058–3062
57. Yang Z-Z, Zhao Y-N, He L-N, Gao J, Yin Z-S (2012) Highly efficient conversion of carbon dioxide catalyzed by polyethylene glycol-functionalized basic ionic liquids. Green Chem 14(2):519–527
58. He L-N, Yasuda H, Sakakura T (2003) New procedure for recycling homogeneous catalyst: propylene carbonate synthesis under supercritical $CO_2$ conditions. Green Chem 5(1):92–94
59. Yang Z-Z, Zhao Y, Ji G, Zhang H, Yu B, Gao X, Liu Z (2014) Fluoro-functionalized polymeric ionic liquids: highly efficient catalysts for $CO_2$ cycloaddition to cyclic carbonates under mild conditions. Green Chem 16(8):3724
60. Song Q-W, He L-N, Wang J-Q, Yasuda H, Sakakura T (2013) Catalytic fixation of $CO_2$ to cyclic carbonates by phosphonium chlorides immobilized on fluorous polymer. Green Chem 15(1):110–115
61. Tsutsumi Y, Yamakawa K, Yoshida M, Ema T, Sakai T (2010) Bifunctional organocatalyst for activation of carbon dioxide and epoxide to produce cyclic carbonate: betaine as a new catalytic motif. Org Lett 12(24):5728–5731
62. Wang Y-B, Sun D-S, Zhou H, Zhang W-Z, Lu X-B (2014) Alkoxide-functionalized imidazolium betaines for $CO_2$ activation and catalytic transformation. Green Chem 16(4): 2266–2272
63. Patil YP, Tambade PJ, Deshmukh KM, Bhanage BM (2009) Synthesis of quinazoline-2,4 (1*H*,3*H*)-diones from carbon dioxide and 2-aminobenzonitriles using [Bmim]OH as a homogeneous recyclable catalyst. Catal Today 148(3–4):355–360
64. Lu W-J, Hu J-Y, Song J-L, Zhang Z-F, Yang G-Y, Han B-X (2014) Efficient synthesis of quinazoline-2,4(1*H*,3*H*)-diones from $CO_2$ using ionic liquids as dual solvent-catalyst at atmospheric pressure. Green Chem 16:221–225
65. Wang C, Luo H, Jiang DE, Li H, Dai S (2010) Carbon dioxide capture by superbase-derived protic ionic liquids. Angew Chem Int Ed 49(34):5978–5981

66. Zhao Y, Yu B, Yang Z, Zhang H, Hao L, Gao X, Liu Z (2014) A protic ionic liquid catalyzes $CO_2$ conversion at atmospheric pressure and room temperature: synthesis of quinazoline-2,4 (1H,3H)-diones. Angew Chem Int Ed 53(23):5922–5925
67. Takahashi T, Watahiki T, Kitazume S, Yasuda H, Sakakura T (2006) Synergistic hybrid catalyst for cyclic carbonate synthesis: remarkable acceleration caused by immobilization of homogeneous catalyst on silica. Chem Commun 2006(15):1664–1666
68. Sakai T, Tsutsumi Y, Ema T (2008) Highly active and robust organic–inorganic hybrid catalyst for the synthesis of cyclic carbonates from carbon dioxide and epoxides. Green Chem 10(3):337–341
69. Shim H-L, Udayakumar S, Yu J-I, Kim I, Park D-W (2009) Synthesis of cyclic carbonate from allyl glycidyl ether and carbon dioxide using ionic liquid-functionalized amorphous silica. Catal Today 148(3–4):350–354
70. Udayakumar S, Lee M, Shim H, Park S, Park D (2009) Imidazolium derivatives functionalized MCM-41 for catalytic conversion of carbon dioxide to cyclic carbonate. Catal Commun 10(5):659–664
71. Udayakumar S, Raman V, Shim H-L, Park D-W (2009) Cycloaddition of carbon dioxide for commercially-imperative cyclic carbonates using ionic liquid-functionalized porous amorphous silica. Appl Catal A Gen 368(1–2):97–104
72. Han L, Park S-W, Park D-W (2009) Silica grafted imidazolium-based ionic liquids: efficient heterogeneous catalysts for chemical fixation of $CO_2$ to a cyclic carbonate. Energy Environ Sci 2(12):1286–1292
73. Wang J-Q, Yue X-D, Cai F, He L-N (2007) Solventless synthesis of cyclic carbonates from carbon dioxide and epoxides catalyzed by silica-supported ionic liquids under supercritical conditions. Catal Commun 8(2):167–172
74. Motokura K, Itagaki S, Iwasawa Y, Miyaji A, Baba T (2009) Silica-supported aminopyridinium halides for catalytic transformations of epoxides to cyclic carbonates under atmospheric pressure of carbon dioxide. Green Chem 11(11):1876–1880
75. North M, Villuendas P, Young C (2009) A gas-phase flow reactor for ethylene carbonate synthesis from waste carbon dioxide. Chem Eur J 15(43):11454–11457
76. North M, Villuendas P (2012) Influence of support and linker parameters on the activity of silica-supported catalysts for cyclic carbonate synthesis. ChemCatChem 4(6):789–794
77. Xie H, Duan H, Li S, Zhang S (2005) The effective synthesis of propylene carbonate catalyzed by silica-supported hexaalkylguanidinium chloride. New J Chem 29(9):1199–1203
78. Cheng W, Chen X, Sun J, Wang J, Zhang S (2013) SBA-15 supported triazolium-based ionic liquids as highly efficient and recyclable catalysts for fixation of $CO_2$ with epoxides. Catal Today 200:117–124
79. Dai W-L, Chen L, Yin S-F, Luo S-L, Au C-T (2010) 3-(2-Hydroxyl-Ethyl)-1-propylimidazolium bromide immobilized on SBA-15 as efficient catalyst for the synthesis of cyclic carbonates via the coupling of carbon dioxide with epoxides. Catal Lett 135(3–4):295–304
80. Udayakumar S, Lee M-K, Shim H-L, Park D-W (2009) Functionalization of organic ions on hybrid MCM-41 for cycloaddition reaction: the effective conversion of carbon dioxide. Appl Catal A Gen 365(1):88–95
81. Udayakumar S, Park S-W, Park D-W, Choi B-S (2008) Immobilization of ionic liquid on hybrid MCM-41 system for the chemical fixation of carbon dioxide on cyclic carbonate. Catal Commun 9(7):1563–1570
82. Lu X, Wang H, He R (2002) Aluminum phthalocyanine complex covalently bonded to MCM-41 silica as heterogeneous catalyst for the synthesis of cyclic carbonates. J Mol Catal A Chem 186:33–42
83. Sun J, Cheng W, Fan W, Wang Y, Meng Z, Zhang S (2009) Reusable and efficient polymer-supported task-specific ionic liquid catalyst for cycloaddition of epoxide with $CO_2$. Catal Today 148(3–4):361–367

84. Dai W-L, Jin B, Luo S-L, Luo X-B, Tu X-M, Au C-T (2014) Polymers anchored with carboxyl-functionalized di-cation ionic liquids as efficient catalysts for the fixation of $CO_2$ into cyclic carbonates. Catal Sci Technol 4(2):556–562
85. Roshan KR, Mathai G, Kim J, Tharun J, Park G-A, Park D-W (2012) A biopolymer mediated efficient synthesis of cyclic carbonates from epoxides and carbon dioxide. Green Chem 14(10):2933–2940
86. Zhao Y, Tian J-S, Qi X-H, Han Z-N, Zhuang Y-Y, He L-N (2007) Quaternary ammonium salt-functionalized chitosan: an easily recyclable catalyst for efficient synthesis of cyclic carbonates from epoxides and carbon dioxide. J Mol Catal A Chem 271(1–2):284–289
87. Sun J, Wang J, Cheng W, Zhang J, Li X, Zhang S, She Y (2012) Chitosan functionalized ionic liquid as a recyclable biopolymer-supported catalyst for cycloaddition of $CO_2$. Green Chem 14(3):654–660
88. Patil YP, Tambade PJ, Jagtap SR, Bhanage BM (2008) Cesium carbonate catalyzed efficient synthesis of quinazoline-2,4(1*H*,3*H*)-diones using carbon dioxide and 2-aminobenzonitriles. Green Chem Lett Rev 1(2):127–132
89. Yoshida M, Hara N, Okuyama S (2000) Catalytic production of urethanes from amines and alkyl halides in supercritical carbon dioxide. Chem Commun 2:151–152
90. Salvatore RN, Shin SI, Nagle AS, Jung KW (2001) Efficient carbamate synthesis via a three-component coupling of an amine, $CO_2$, and alkyl halides in the presence of $Cs_2CO_3$ and tetrabutylammonium iodide. J Org Chem 66(3):1035–1037
91. Kawanami H, Ikushima Y (2002) Regioselectivity and selective enhancement of carbon dioxide fixation of 2-substituted aziridines to 2-oxazolidinones under supercritical conditions. Tetrahedron Lett 43(21):3841–3844
92. Yano T, Matsui H, Koike T, Ishiguro H, Fujihara H, Yoshihara M, Maeshima T (1997) Magnesium oxide-catalysed reaction of carbon dioxide with an epoxide with retention of stereochemistry. Chem Commun 12:1129–1130
93. Yamaguchi K, Ebitani K, Yoshida T, Yoshida H, Kaneda K (1999) Mg–Al mixed oxides as highly active acid–base catalysts for cycloaddition of carbon dioxide to epoxides. J Am Chem Soc 121(18):4526–4527
94. Srivastava R, Srinivas D, Ratnasamy P (2005) Zeolite-based organic–inorganic hybrid catalysts for phosgene-free and solvent-free synthesis of cyclic carbonates and carbamates at mild conditions utilizing $CO_2$. Appl Catal A Gen 289(2):128–134
95. Tu M, Davis RJ (2001) Cycloaddition of $CO_2$ to epoxides over solid base catalysts. J Catal 199(1):85–91
96. Yasuda H, He L, Takahashi T, Sakakura T (2006) Non-halogen catalysts for propylene carbonate synthesis from $CO_2$ under supercritical conditions. Appl Catal A Gen 298:177–180
97. Lu X-B, He R, Bai C-X (2002) Synthesis of ethylene carbonate from supercritical carbon dioxide/ethylene oxide mixture in the presence of bifunctional catalyst. J Mol Catal A Chem 186(1–2):1–11
98. Meléndez J, North M, Pasquale R (2007) Synthesis of cyclic carbonates from atmospheric pressure carbon dioxide using exceptionally active aluminium(salen) complexes as catalysts. Eur J Inorg Chem 2007(21):3323–3326
99. Whiteoak CJ, Kielland N, Laserna V, Escudero-Adan EC, Martin E, Kleij AW (2013) A powerful aluminum catalyst for the synthesis of highly functional organic carbonates. J Am Chem Soc 135(4):1228–1231
100. Melendez J, North M, Villuendas P, Young C (2011) One-component bimetallic aluminium (salen)-based catalysts for cyclic carbonate synthesis and their immobilization. Dalton Trans 40(15):3885–3902
101. Clegg W, Harrington RW, North M, Pasquale R (2010) Cyclic carbonate synthesis catalysed by bimetallic aluminium–salen complexes. Chem Eur J 16(23):6828–6843
102. Whiteoak CJ, Kielland N, Laserna V, Castro-Gómez F, Martin E, Escudero-Adán EC, Bo C, Kleij AW (2014) Highly active aluminium catalysts for the formation of organic carbonates from $CO_2$ and oxiranes. Chem Eur J 20(8):2264–2275

103. Mita T, Chen J, Sugawara M, Sato Y (2011) One-pot synthesis of α-amino acids from imines through $CO_2$ incorporation: an alternative method for strecker synthesis. Angew Chem Int Ed 50(6):1393–1396
104. Mita T, Higuchi Y, Sato Y (2012) One-step synthesis of racemic alpha-amino acids from aldehydes, amine components, and gaseous $CO_2$ by the aid of a bismetal reagent. Org Lett 14(24):6202–6205
105. Mita T, Higuchi Y, Sato Y (2013) One-step synthesis of racemic alpha-amino acids from aldehydes, amine components, and gaseous $CO_2$ by the aid of a bismetal reagent. Chem Eur J 19(3):1123–1128
106. Sathe AA, Hartline DR, Radosevich AT (2013) A synthesis of alpha-amino acids via direct reductive carboxylation of imines with carbon dioxide. Chem Commun 49(44):5040–5042
107. Yoshida H, Fukushima H, Ohshita J, Kunai A (2006) $CO_2$ incorporation reaction using arynes straightforward access to benzoxazinone. J Am Soc Chem 128:11040–11041
108. Kaicharla T, Thangaraj M, Biju AT (2014) Practical synthesis of phthalimides and benzamides by a multicomponent reaction involving arynes, isocyanides, and $CO_2$/$H_2O$. Org Lett 16(6):1728–1731
109. Yoshida H, Morishita T, Ohshita J (2008) Direct access to anthranilic acid derivatives via $CO_2$ incorporation reaction using arynes. Org Lett 10(17):3845–3847
110. Choi J-C, He L-N, Yasuda H, Sakakura T (2002) Selective and high yield synthesis of dimethyl carbonate directly from carbon dioxide and methanol. Green Chem 4(3):230–234
111. Fan B, Zhang J, Li R, Fan W (2008) In situ preparation of functional heterogeneous organotin catalyst tethered on SBA-15. Catal Lett 121(3–4):297–302
112. Du Y, Kong D-L, Wang H-Y, Cai F, Tian J-S, Wang J-Q, He L-N (2005) Sn-catalyzed synthesis of propylene carbonate from propylene glycol and $CO_2$ under supercritical conditions. J Mol Catal A Chem 241(1–2):233–237
113. Dandge DK, Heller JP, Wilson KV (1985) Structure solubility correlations: organic compounds and dense carbon dioxide binary systems. Ind Eng Chem Prod Res Dev 24(1): 162–166
114. Tominaga K, Sasaki Y (2002) Synthesis of 2-oxazolidinones from $CO_2$ and 1,2-aminoalcohols catalyzed by n-$Bu_2SnO$. Synlett (2):307–309
115. Choi J-C, Sakakura T, Sako T (1999) Reaction of dialkyltin methoxide with carbon dioxide relevant to the mechanism of catalytic carbonate synthesis. J Am Chem Soc 121(15): 3793–3794

Top Organomet Chem (2016) 53: 171–198
DOI: 10.1007/3418_2015_98

Published online: 14 April 2015

# $CO_2$-Mediated Formation of Chiral Fine Chemicals

**Xiao-Bing Lu**

**Abstract** The utilization of carbon dioxide as a feedstock for the synthesis of organic chemicals can contribute to a more sustainable chemical industry, since $CO_2$ is an abundant, inexpensive, and nontoxic renewable $C_1$ resource. Nevertheless, far less attention was paid to the stereochemically controlled catalytic $CO_2$ fixation/conversion processes. This review therefore aims to principally showcase the recent progress regarding $CO_2$-mediated formation of chiral fine chemicals, including enantioselective synthesis of cyclic carbonates by asymmetric ring opening of epoxides with $CO_2$, enantioselective synthesis of oxazolidinones by the coupling reaction of aziridines with $CO_2$- or base-mediated formation of oxazolidinone from ethanolamines, metal-catalyzed enantioselective synthesis of functional carboxylic acids and derivatives, and enantioselective synthesis of $CO_2$-based polycarbonates from epoxides.

**Keywords** Asymmetric catalysis · Carbon dioxide · Carboxylation · Carboxylic acid · Chiral · $CO_2$-based polycarbonate · Cyclic carbonate · Epoxide · Oxazolidinone · Polymerization catalysis

## Contents



X.-B. Lu (✉)
State Key Laboratory of Fine Chemicals, Dalian University of Technology, Dalian 116024, China
e-mail: xblu@dlut.edu.cn

## 1 Introduction

The utilization of carbon dioxide as a feedstock for the synthesis of organic chemicals can contribute to a more sustainable chemical industry, since $CO_2$ is an abundant, inexpensive, and nontoxic renewable $C_1$ resource [1–3]. More than 20 reactions concerning $CO_2$ as a starting material have been developed in recent decades, though successful industrial processes are very limited to the syntheses of urea, inorganic carbonates, methanol, salicylic acid, and organic carbonates [4–6]. It is apparent that the quantity of $CO_2$ consumed in these processes is likely always to be a very small fraction of the total $CO_2$ generated from the emission-based human activity. However, this strategy potentially provides access to the more environmentally benign routes to producing useful chemicals otherwise made from the reagents detrimental to the environment.

Indeed, the majority of reactions using $CO_2$ as a feedstock concern the preparation of relatively simple achiral chemicals, with an emphasis on $CO_2$ incorporation efficiency, while far less attention was paid to the stereochemically controlled catalytic $CO_2$ fixation/conversion processes [7, 8]. This review is intended to provide a thorough accounting of the literatures involving $CO_2$-mediated formation of chiral fine chemicals.

## 2 Enantioselective Synthesis of Cyclic Carbonates

In the early contributions, optically pure cyclic carbonates were reported to be prepared by several methods, including the cyclization of chiral diols with triphosgene [9], metal complex-catalyzed insertion of $CO_2$ into chiral epoxides [10], enzyme-mediated enantioselective hydrolysis of *racemic* cyclic carbonates [11, 12], and asymmetric hydrogenation of 5-methylene-1,3-dioxolan-2-ones catalyzed by chiral ruthenium complexes [13, 14]. Among them, the enantioselective coupling reaction of $CO_2$ and chiral terminal epoxides is the simplest route to afford enantiopure cyclic carbonates in high efficiency (Scheme 1). In this reaction process, the regioselective ring opening of a terminal epoxide at methylene C–O bond is a precondition for obtaining high enantioselectivity, since the ring opening at methine C–O bond probably results in a change in stereochemistry with configuration inversion at methine carbon (Scheme 2). Although the nucleophilic ring opening of terminal epoxides seems to typically occur at the least hindered methylene carbon, the cleavage is normally observed at both C–O bonds in the coupling reaction [15]. The regioselectivity for epoxide ring opening depends on the employed epoxide, reaction temperature, and catalyst system. Being different from propylene oxide, the nucleophilic ring opening of the terminal epoxides with an electron-withdrawing group such as styrene oxide predominantly occurs at the methine $C_\alpha$–O bond rather than the methylene $C_\beta$–O bond, thereby easily causing a change in stereochemistry at the methine carbon with inversion.

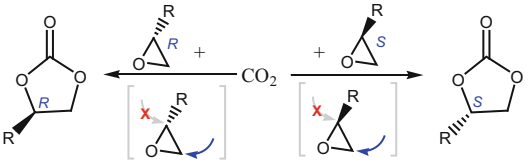

**Scheme 1** Enantioselective coupling reaction of $CO_2$ and chiral terminal epoxides

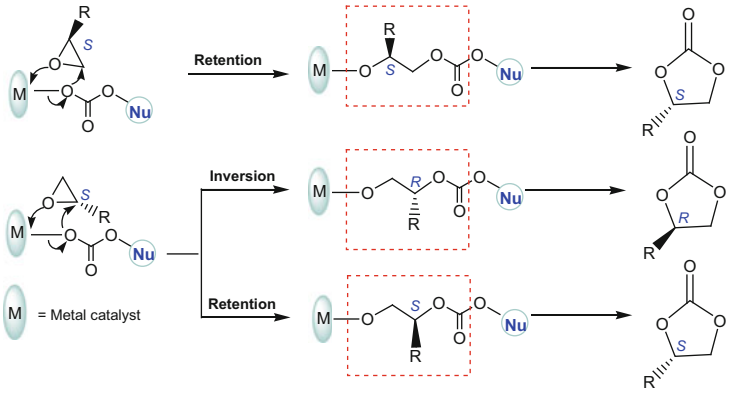


**Scheme 2** The preferential stereochemistry involved in the metal complex-mediated formation of cyclic carbonate from (*S*)-epoxide and $CO_2$

In 2003, Aresta and coworkers disclosed that in the use of $Nb_2O_5$ as catalyst for the carboxylation of (*R*) or (*S*)-configured epoxides (propylene oxide or styrene oxide) with $CO_2$, the resultant cyclic carbonates remained the configuration of chiral epoxide at methine carbon (>98% *ee*), while an obvious decrease in enantioselectivity (82–87% *ee*) was observed in the absence of $Nb_2O_5$ [16]. The high enantioselectivity was ascribed to the simultaneous interaction of the O atom of the epoxide with the Nb center, and the attack at the asymmetric carbon by the carbonate moiety formed over $Nb_2O_5$ might prevent any inversion at the chiral carbon of the epoxide to occur. Also, the use of DMF as a solvent played an important role for enantioselective ring opening of epoxide, in which the solvent could assist the carboxylation through a back attack at the more substituted carbon that might contribute in preventing any change of configuration at the chiral center. Recently, Lu et al. reported that an intramolecularly two-centered chromium complex **1a** bearing a sterically hindered nucleophilic center on the ligand could catalyze the reaction of $CO_2$ with (*S*)-propylene oxide at 80°C, giving (*S*)-propylene carbonate in 96% *ee* with retention of stereochemistry [17]. More recently, the same group demonstrated that salenAlCl bearing two appended quaternary ammonium salts **2** exhibited excellent activity (TOF, 400–5,250 $h^{-1}$) and unprecedented selectivity (≥99% *ee*) for catalyzing enantioselective coupling of $CO_2$ with various chiral epoxides in a very low catalyst loading of 0.01 mol% [18]. It was found that even performed at 120°C, the resultant cyclic carbonates from chiral

epoxides with an electron-donating group (such as propylene oxide, 1,2-butene oxide, 1,2-hexene oxide, or phenyl glycidyl ether) all had more than 99% enantioselectivity, while a significant decrease in product enantioselectivity was observed in the systems of styrene oxide or epichlorohydrin, indicating high reaction temperatures that caused the decrease in regioselective ring opening at the methylene carbon.

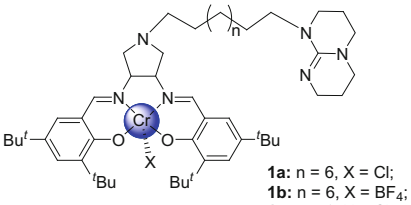


1

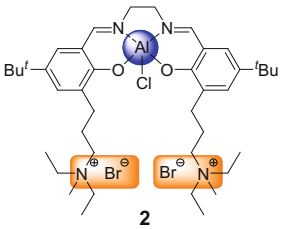

2

The most ambitious study is the enantioselective synthesis of cyclic carbonates by asymmetric ring opening of *racemic* epoxides with $CO_2$ via a catalytic kinetic resolution (Scheme 3). The key is to find highly efficient catalyst systems for selectively complexing and activating one enantiomer of the *racemic* epoxides. The first attempt was reported by Dibenedetto and Aresta, using homogeneous Nb (V)-catalysts based on chelating chiral ligands such as (*4S*, *5S*)-4,5-bis(diphenylphosphino-methyl)-2,2-dimethyl-1,3-dioxolane (DIOP) and 2,2-methylene-bis (*4S*)-phenyl-oxazoline (MBPO) for the coupling reaction of $CO_2$ with *racemic* epoxides. The highest enantioselectivity of 22% *ee* was obtained in the reaction $CO_2$ with racemic styrene oxide, while the same catalyst systems are inferior to the coupling with *racemic* propylene oxide [16].

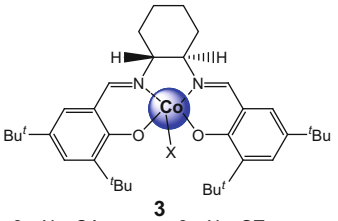

3

**3a**: X = OAc;
**3b**: X = $O_2CCCl_3$;
**3c**: X = $O_2CCF_3$;
**3d**: X = Cl;
**3e**: X = OTs;
**3f**: X = $BF_4$;
**3g**: X = $PF_6$;
**3h**: X = *p*-nitrobenzoate

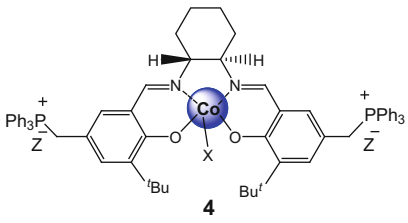

4

X = OAc, $CCl_3CO_2$, Cl, OTs, *p*-$NO_2C_6H_4CO_2$;
Z = F, Cl, Br, I

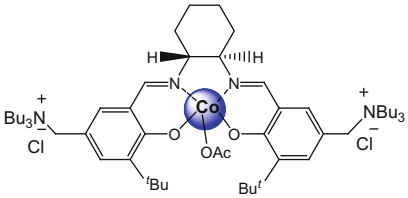

5

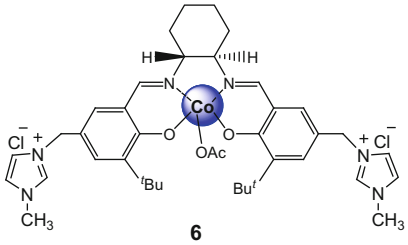

6

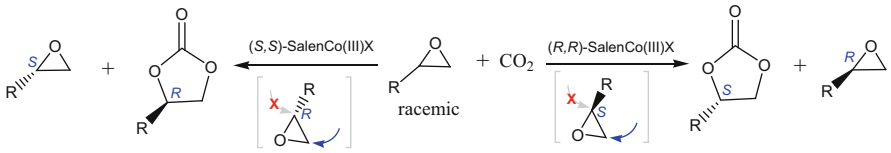


**Scheme 3** Synthesis of optically active cyclic carbonate from asymmetric coupling of $CO_2$ and *racemic* epoxides via a catalytic kinetic resolution process

In the nucleophilic ring opening of epoxides promoted by (salen)M complexes, there is ample evidence that the epoxide is beforehand activated by the coordination to the Lewis acidic (salen)M complex [19]. Based on the possible mechanisms of epoxide ring opening catalyzed by Lewis acidic (salen)M complex and nucleophilic cocatalysts, Lu and coworkers designed a binary catalyst system for producing optically active cyclic carbonates from *racemic* epoxides [20]. Using Jacobsen's chiral (salen)Co(III) catalyst **3** in conjunction with tetrabutylammonium halides ($^n$Bu$_4$NX), the authors succeeded in preparing enantioenriched propylene carbonate from *racemic* propylene oxide through a convenient solvent-free kinetic resolution with a high rate of 245 $h^{-1}$ under ambient temperature. It was found that both the axial X-counterion of chiral salenCo(III)X and the anion of the quaternary ammonium cocatalyst had significant effects on propylene carbonate enantiomeric purity. Although the $k_{rel}$ (kinetic resolution coefficient) values measured in the epoxide resolution with $CO_2$ are below what is generally considered useful, this investigation is important because it addresses the feasibility of using $CO_2$ as a $C_1$ source in asymmetric catalysis. Almost simultaneously, Paddock and Nguyen also explored the kinetic resolution of *racemic* propylene oxide with $CO_2$ as reagent using chiral salenCo(III)X **3** in combination with a Lewis base [21]. The best result (with a $k_{rel}$ of 5.6 and a TOF of 10 $h^{-1}$) was obtained using (*R*)-(+)-4-dimethylaminopyridinyl(pentaphenylcyclopentadienyl)iron as cocatalyst. Subsequently, Berkessel and Brandenburg investigated bis-(triphenylphosphoranylidene) ammonium halide (PPNY, Y = F, Cl) as cocatalyst in combination with chiral salenCo(III)X **3** for the production of enantiomerically enriched propylene carbonate [22]. The best selectivity with 83% *ee* for the resultant propylene carbonate, corresponding to a $k_{rel}$ of 19, was achieved at a low temperature of −20°C.

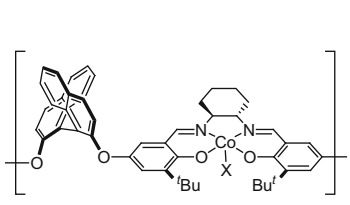

**7**

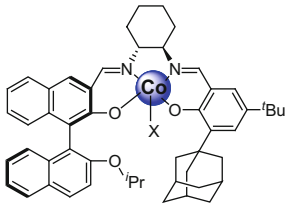

**8**

**8a**: X = 2,4-dinitrophenoxy
**8b**: X = $BF_4$

Based on the strategy of using a combination of chiral salenCo(III) complex and a nucleophilic cocatalyst for the asymmetric coupling of $CO_2$ and *racemic* epoxides, Jing and coworkers developed a series of bifunctional chiral catalysts **4–6**, in which a salenCo(III) complex and two quaternary ammonium or phosphonium salts are incorporated into a molecule, for the kinetic resolution of terminal epoxides with $CO_2$ as agent to afford optically active cyclic carbonates [23–27]. Unfortunately, no obvious improvement in product enantioselectivity and significant decrease in activity were observed. In order to improve the chiral induction environment of the catalyst, the same group designed novel polymeric binol-based cobalt(III) complex **7** bearing an auxiliary chiral site for the asymmetric coupling of $CO_2$ and *racemic* propylene oxide [28]. The (*R*/*S*)-polymer and (*S*/*R*)-polymer catalyst exhibited better enantioselectivity than the (*R*/*R*)-polymer and (*S*/*S*)-polymer catalyst. Nevertheless, the improvement in enantioselectivity is very limited, and the highest $k_{rel}$ of 10.2 was achieved at 0°C. The significant progress came with the use of multichiral [(*R*,*R*,*R*)-configured] salenCo(III) complex **8** in combination with excess PPN-DNP {2,4-dinitrophenolate salt of bis-(triphenylphosphoranylidene) ammonium} cocatalyst [29]. It was found that an ammonium salt consisting of an anion with poor leaving ability and a bulky cation benefited for improving the enantioselectivity. The highest enantioselectivity of 97.1% *ee* (a $k_{rel}$ of 75.8) was achieved for optically active propylene carbonate from *racemic* propylene oxide at –25°C. This catalyst system was found to be effective for the asymmetric coupling of $CO_2$ with other terminal epoxides including epichlorohydrin and glycidyl phenyl ether with $k_{rel}$ values between 10.7 and 31.5 at 0°C.

Interestingly, in the presence of appropriate cocatalyst or additive, chiral Co(II)-salen complexes **9** and **10** could efficiently catalyze the coupling reaction of $CO_2$ and *racemic* terminal epoxides to afford the corresponding cyclic carbonates with moderate enantioselectivity [30, 31], comparable to the previously mentioned binary catalyst systems based on chiral salenCo(III)X **3**. For example, Yamada et al. discovered that chiral salenCo(II) **10** in combination with $Et_2NSiMe_3$ cocatalyst was efficient in catalyzing $CO_2$ and *racemic* *N*,*N*′-diphenyl-aminomethyloxirane to the corresponding cyclic carbonate [31]. The best $k_{rel}$ of 32 was observed in the optimization conditions, in which after 49% conversion, the *ee* values of the resultant cyclic carbonate and unreacted epoxide are 86 and 87%, respectively. The high enantioselectivity should ascribe to the interaction between the cobalt atom and the oxygen atom in the epoxide as well as the heteroatom adjacent to the oxirane during the approach of the substrate to the cobalt (II) complex.

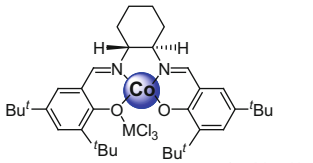


**9a**: M = Al
**9b**: M = Ga
**9c**: M = In

**9**

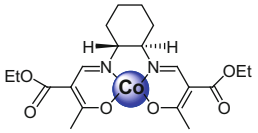


**10**

Recently, Yamada and coworkers reported a novel route for the synthesis of enantiopure functionalized cyclic carbonates via the asymmetric $CO_2$ incorporation into bispropargylic alcohols with desymmetrization catalyzed by silver acetate with a chiral Schiff base ligand (Scheme 4) [32]. Bispropargylic alcohols with various substituted groups were also good substrates that afforded the corresponding cyclic carbonates in excellent yields with good-to-high enantiomeric excesses (80–93% *ee*) regardless of the electron-donating and electron-withdrawing substituents.

## 3 Enantioselective Synthesis of Oxazolidinones

Oxazolidinones, a class of heterocyclic compounds, have attracted considerable attention in medicinal chemistry as a result of their some interesting pharmacological activity, suitable for antibacterials, immunosuppressants, or monoamine oxidase inhibitors [33]. In addition, oxazolidinone heterocycles have been widely used as chiral auxiliaries in various reactions directed to the stereoselective synthesis of natural products, antibiotics, and pharmaceuticals [34]. Oxazolidinones are mainly manufactured by phosgenation of $\beta$-amino alcohols. However, the use of phosgene precludes widespread application in laboratory and industry due to phosgene's toxicity and significantly detrimental to the environment. Replacement of phosgene with $CO_2$ is an ideal alternative. There are four routes regarding $CO_2$ as a starting material for oxazolidinone synthesis, including the coupling reaction of aziridines with $CO_2$, base-mediated formation of oxazolidinone from ethanolamines, $PPh_3$-mediated synthesis of oxazolidinone from 1,2-azido alcohols, and the reaction of propargylic amines with $CO_2$. Among them, the former two methods were also utilized for the synthesis of enantiopure oxazolidinone by the use of chiral starting material.

In contrast with the sole product resulted from the cycloaddition of epoxides and $CO_2$, the coupling reaction of aziridines with $CO_2$ usually affords two regioisomers: 5-substituted and 4-substituted oxazolidinones. The isomeric ratio is dependent on the substituents of the aziridine and the reaction temperature. He et al. reported that polyethylene glycol-supported quaternary ammonium bromide was active for the reaction of enantiopure 1-butyl-2-phenylaziridine with $CO_2$ to afford the corresponding oxazolidinone with high enantioselectivity [35]. More recently, Ren and coworkers found that salenAlCl bearing appended quaternary

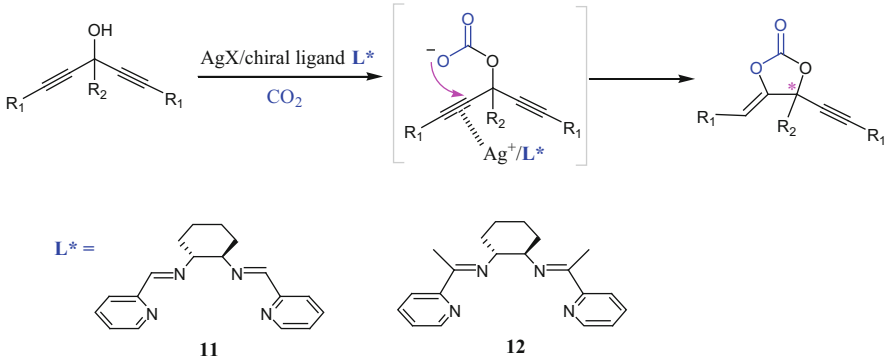


**Scheme 4** Enantioselective chemical incorporation of $CO_2$ into bispropargylic alcohols

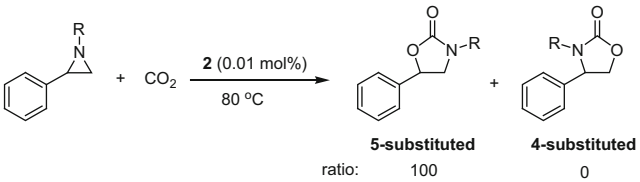


**Scheme 5** The coupling reaction of aziridines with $CO_2$

ammonium salts **2** could catalyze the coupling reaction of $CO_2$ with (*R*)-1-benzyl-2-phenylaziridine or (*R*)-1-butyl-2-phenylaziridine at 80°C could afford (*R*)-5-substituted oxazolidinones with high enantiopurity up to 99% *ee* (Scheme 5). A possible mechanism involving two consecutive $SN_2$ processes at the same carbon was suggested (Scheme 6) [18]. The nucleophilic ring opening of *N*-substituted aziridine at methine C–N bond leads to the complete configuration inversion of the methine carbon. This is followed by the backbiting with regard to the attack of the carbamate species at methine carbon after the insertion of $CO_2$. This process also results in a complete inversion of the methine carbon stereochemistry. As a result, the configuration of the methine carbon of 5-substituted oxazolidinones is the same as that of the employed *N*-substituted aziridines due to double inversion. Chai et al. also illuminated that the use of an enantiopure *N*-tosyl aziridine bearing two alkyl groups in its positions 2 and 3 resulted in the selective formation of chiral oxazolidinone product with retention of configuration [36].

Classical syntheses of chiral oxazolidin-2-ones from chiral 1,2-amino alcohols or their derivatives require toxic and hazardous phosgene or its derivatives and/or drastic conditions (strong base or very high temperature). The study regarding replacement of phosgene with $CO_2$ was widely carried out, but usually suffered from catalyst deactivation caused by the coproduced water and limited conversion due to the thermodynamic reasons (Scheme 7) [37]. In order to overcome these drawbacks, many attempts have been made to shift the equilibrium to the product side. The most straightforward way is to use a dehydrating agent to trap the

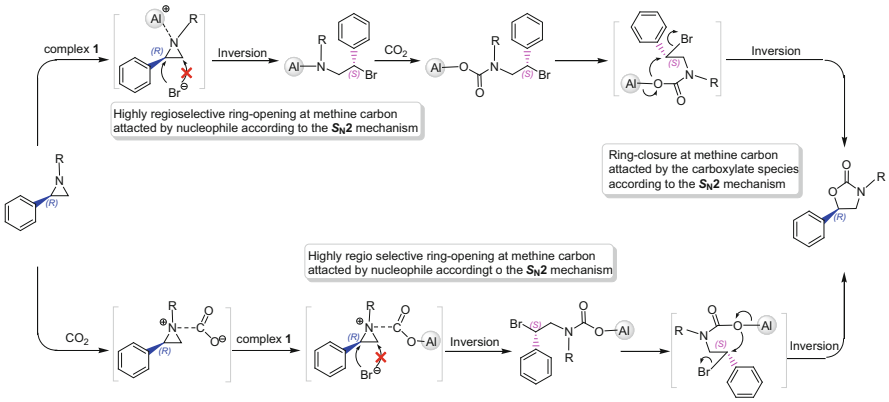


**Scheme 6** Possible mechanism for the complex **2**-mediated formation of (*R*)-5-substituted oxazolidinone from the coupling reaction of $CO_2$ with (*R*)-1-alkyl-2-phenylaziridine

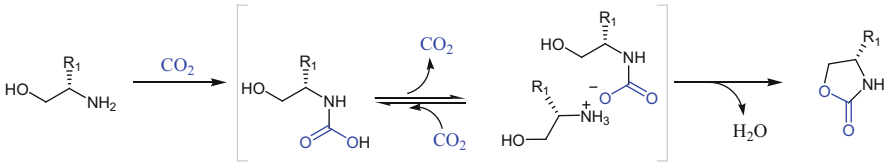


**Scheme 7** Synthesis of oxazolidinone from $CO_2$ under atmosphere pressure

coproduced water. The significant progress came from the contribution of Feroci and Inesi laboratory [38], which involved the use of 2-pyrrolidone electrogenerated base for the synthesis of chiral oxazolidin-2-ones from *β*-amino alcohols by the reaction with $CO_2$ (Scheme 8), achieving the retention of the absolute configuration of all chiral atoms.

Recently, Saito and coworkers reported a chiral oxazolidinone synthesis via the incorporation of $CO_2$ into *β*-amino alcohols using alkali metal carbonates such as $Cs_2CO_3$ as catalyst (Scheme 9) [39]. It is noteworthy that 1 atm of $CO_2$ is enough for the reaction to proceed and no special dehydrating agent is required in this system. The preliminary mechanistic study revealed that the OH of amino alcohol acts as nucleophile and the OH at carbamic acid moiety is liberated during the cyclization process (Scheme 10). Prior to this study, Muñoz realized the preparation of various chiral oxazolidinones from *β*-amino alcohols and $CO_2$ in the presence of tetramethylphenylguanidine (PhTMG) as a base and a variety of phosphorus electrophiles under mild conditions [40]. Notably, the steric hindrance or the electron deficiency/richness of the substituents did not have a deleterious effect on the carbonylation reaction.

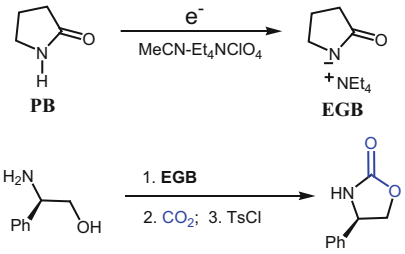


**Scheme 8** Synthesis of oxazolidin-2-one from amino alcohol according to the general procedure

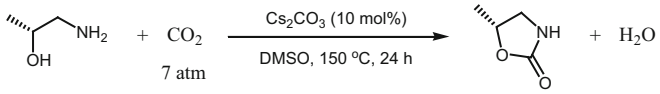


**Scheme 9** Reaction of $CO_2$ with (*R*)-1-aminopropan-2-ol

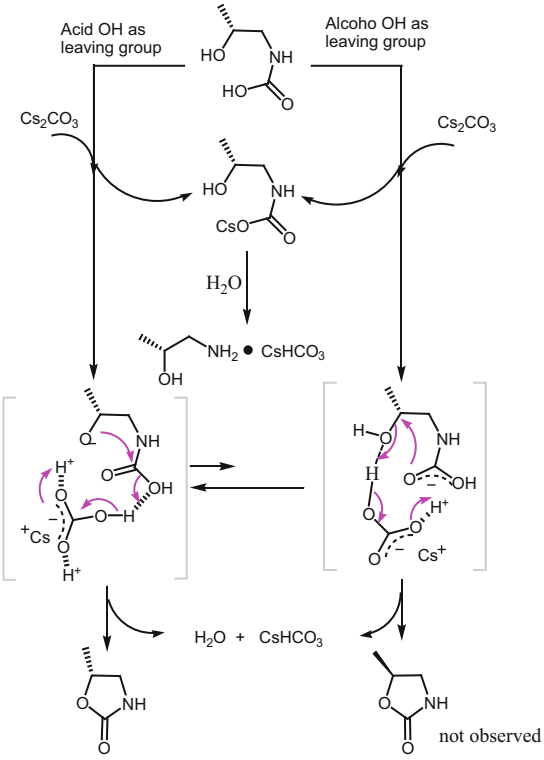


**Scheme 10** Possible routes in the reaction of $CO_2$ with (*R*)-1-aminopropan-2-ol

## 4 Enantioselective Synthesis of Functional Carboxylic Acids and Derivatives

It is highly challenging to develop efficient catalytic protocols that enable carbon–carbon bond formation between $CO_2$ and substrates in an enantioselective manner, since the limited number of available catalytic carbon–carbon bond-forming $CO_2$ incorporation reactions that can be efficiently carried out under mild conditions. In a recent study, Lu and coworkers described a novel method for asymmetric electrocarboxylation of prochiral and inexpensive available acetophenone and $CO_2$ to provide optically active 2-hydroxy-2-phenylpropionic acid [41]. Under the optimized condition, the highest enantiomeric excess could achieve 29.8% on stainless steel cathodes by the induction of the alkaloid. Although the product enantioselectivity is not satisfactory due to the difficulty in selective fixation of the small molecule of carbon dioxide via enantioselective electron transfer, it is the first time to demonstrate asymmetric electrochemical carboxylation with $CO_2$ as a reagent. A plausible mechanism concerning the selective proton transfer from the chiral proton-donating alkaloid to the ketyl radical anion was proposed (Scheme 11) [42]. The crucial chiral proton-donating species was initially formed after the alkaloid obtained a proton from the cocatalyst of butanol or directly from the reaction media. Both the cinchonidine and butanol played an important role in the asymmetric electrosynthesis process for the optically active atrolactic acid. In a more recent contribution, the enantiomeric excess of 2-hydroxy-2-arylpropionic acids was further improved to 48.6% *ee* using electrocarboxylation in $CO_2$-saturated MeCN in the presence of cinchona alkaloids with the addition of phenol.

The exciting results were obtained by Mori group [43, 44], who developed a nickel-catalyzed highly enantioselective carbon–carbon bond-forming $CO_2$ incorporation reaction based on this carboxylative cyclization from bis-1,3-dienes (Scheme 12). The remarkable feature of this reaction is that the reaction proceeds under very mild conditions in a highly regio- and stereoselective manner (90–96% *ee*). Not only aromatic but also aliphatic terminal alkynes gave unsaturated carboxylic acid in high yields. The reaction was suggested to start with oxidative cycloaddition of bis-diene **1a** to a Ni(0) complex to produce bis-π-allylnickel complex **4** (Scheme 13), and subsequent insertion of $CO_2$ into the nickel–carbon bond afforded carboxylate **5**. The role of $Et_2Zn$ in this reaction is probably regeneration of a Ni(0) complex via a transmetalation process. Thus, complex **5** reacted with $Et_2Zn$ to provide complex **6**, which can then easily undergo β-hydrogen elimination to produce complex **7**. Reductive elimination from **7** reproduced the Ni(0) complex and provided carboxylate **8**, which corresponds to ester **2a**.

More recently, Zhao and coworkers developed an iridium complex-mediated enantioselective domino reaction of $CO_2$, amines and linear allyl chlorides, or allyl carbonate to provide the branched allyl carbamates in good yields with high regioselectivity (up to 98:2) and good to excellent levels of enantioselectivity (up to 99% *ee*) (Scheme 14) [45, 46]. The mechanistic study suggested that the

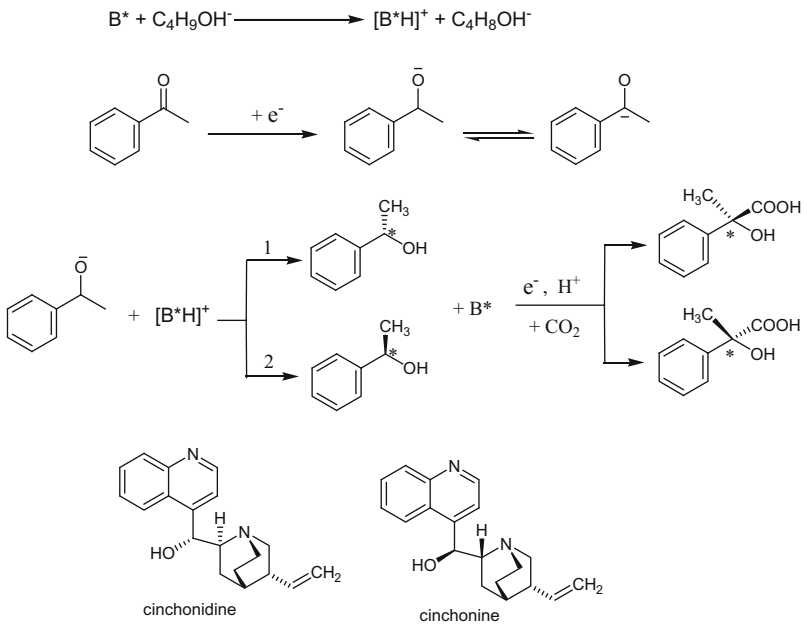


**Scheme 11** Mechanism for the asymmetric electrochemical carboxylation of acetophenone by the alkaloid

reaction started by insertion of iridium into the allyl–oxygen bond to liberate an ionized π-allyl–Ir complex **A**, methoxide, and $CO_2$. Subsequently, an amidation reaction between $CO_2$ and an amine occurs to form a carbamate ion, which in turn attacks intermediate **A** to yield an allyl carbamate **B** and regenerating the catalyst. In the absence of $K_3PO_4$, complex **A** is directly attacked by the amine to give an extrusion product, allylamine **C** (Scheme 14).

More recently, Mita and Sato reported a Cu-secondary diamine complex-catalyzed enantioselective silylation of *N-tert*-butylsulfonylimines and followed stereoretentive carboxylation under a $CO_2$ atmosphere (1 atm), affording the corresponding α-amino acids in a stereoretentive manner [47]. This two-step sequence provides a new synthetic protocol for optically active α-amino acids from gaseous $CO_2$ and imines in the presence of a catalytic amount of a chiral source.

## 5 Enantioselective Synthesis of $CO_2$-Based Polycarbonates

The alternating copolymerization of $CO_2$ with epoxides to afford degradable polycarbonates represents a green polymerization process for potential large-scale utilization of $CO_2$ in chemical synthesis. Although this polymerization was first demonstrated by Inoue in 1969 using $ZnEt_2/H_2O$ heterogeneously catalyzed

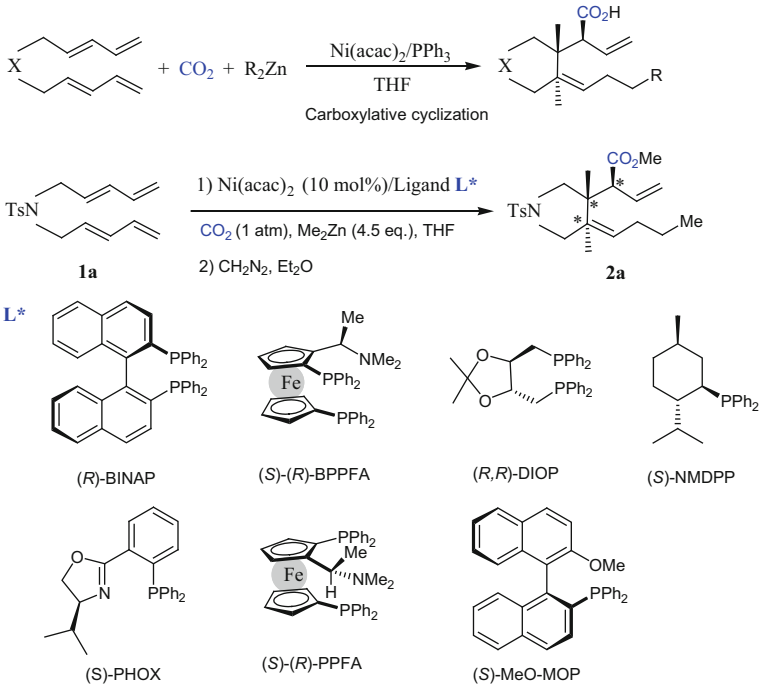


**Scheme 12** Nickel-catalyzed enantioselective carboxylative cyclization of bis-1,3-dienes

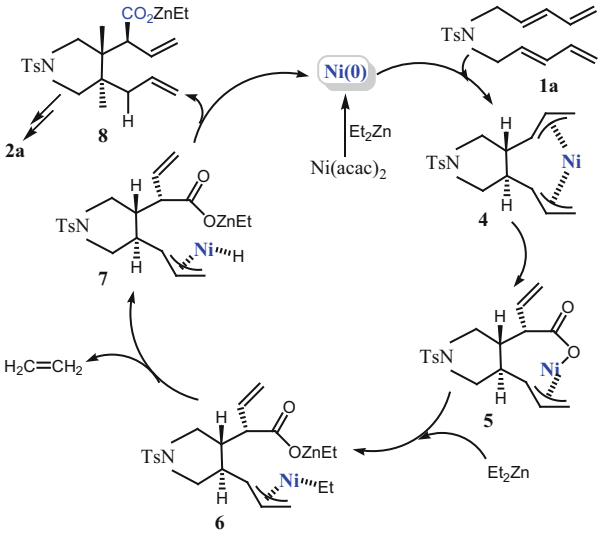


**Scheme 13** Possible mechanism of Ni(0)-catalyzed enantioselective carboxylative cyclization of bis-1,3-dienes

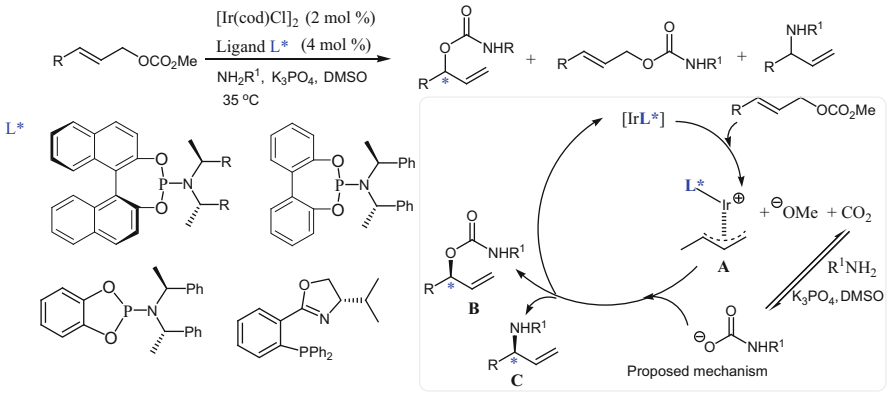


**Scheme 14** Iridium complex-mediated enantioselective domino reaction

copolymerization of $CO_2$ and propylene oxide to give poly(propylene carbonate) with a very low reaction rate (TOF, 0.12 $h^{-1}$) [48], it was not until the recent decade that significant advancements were achieved by the discoveries of several highly active catalyst systems [49, 50]. Nevertheless, these atactic $CO_2$-based polycarbonates have limited applications because of poor physical properties. A promising approach to improving their thermal and mechanical properties is to introduce stereoregularity into the polymer main chain by enantioselective polymerization catalysis. The first attempt appeared in 2003, when Coates and coworkers reported the use of salenCo(III) complexes in selective preparation of poly(propylene carbonate) from the copolymerization of $CO_2$ and propylene oxide at high catalyst loadings (epoxide/catalyst = 200–500/1, molar ratio) and a very high $CO_2$ pressure of 5.5 MPa [51]. The resulting polymers are regioregular and highly alternating. With *racemic* propylene oxide, catalyst **3a** exhibits a $k_{rel}$ of 2.8 and preferentially consumed (*S*)-propylene oxide via a kinetic resolution process (Scheme 15). Turnover frequencies (TOFs) extended over a range of 17–81 $h^{-1}$, dependent on reaction conditions and the substituent groups on the salen ligand. Surprisingly, increasing reaction temperature or reducing $CO_2$ pressure results in a significant loss in catalyst activity. However, soon after Lu and Wang found that the addition of a nucleophilic cocatalyst such as quaternary ammonium halide significantly enhanced the activity of (salen)Co(III)X, even at low $CO_2$ pressures and/or elevated temperatures, affording copolymers with >99% carbonate unit content and an increased stereochemistry control (~95% head-to-tail linkage) [52]. Systematic studies indicated that many aspects of the catalyst, including chiral diamine backbone, substituent groups on the salen ligand, and axial counterion of (salen)Co(III)X, as well as nucleophilicity, leaving ability, and coordination ability of the cocatalyst, significantly affected the catalytic activity, polymer selectivity, and enantioselectivity [53]. Binary (*R*,*R*)-(salen)Co(III)X/PPNCl (X = pentafluorobenzoate) catalyst system demonstrated a $k_{rel}$ of 9.7 for the

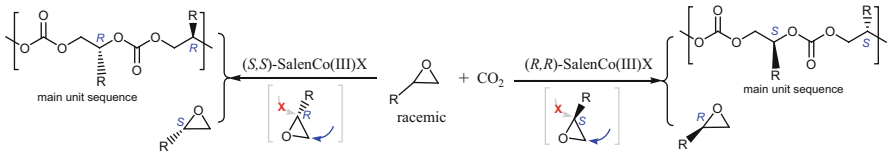


**Scheme 15** Synthesis of optically active polycarbonates from asymmetric copolymerization of $CO_2$ and racemic epoxides via a catalytic kinetic resolution process

enchainment of (*S*)- over (*R*)-propylene oxide when the copolymerization was carried out at –20°C. The following study suggested that the nucleophilic cocatalyst played both initiator for polymer chain growth and stabilizer for preventing the active Co(III) species against decomposition to inactive Co(II) [54].

Recently, Lu and coworkers prepared multichiral (*S,S,S*)-Co(III) catalysts **8a** and **13** [55, 56]. Both the (*1S,2S*)-1,2-diaminocyclohexane backbone and S-configured 2′-isopropyloxy-1,10-binaphthyl of the ligand cooperatively provide chiral environments around the central metal ion. With complex **13c** as catalyst, the highest $k_{rel}$ of 24.3 was obtained at −20°C [55]. Notably, epoxide ring opening occurred preferentially at the methylene carbon, resulting in the copolymer with >99% head-to-tail content. Interestingly, complex **14** with (*S,S*)-1,2-diaminocyclohexane backbone and R-configured 2′-isopropyloxy-1,1′-binaphthyl also exhibited excellent regioselectivity for epoxide ring opening with the polymeric product having 99% head-to-tail content, but the $k_{rel}$ of only 1.4 resulted in a low copolymer enantioselectivity.

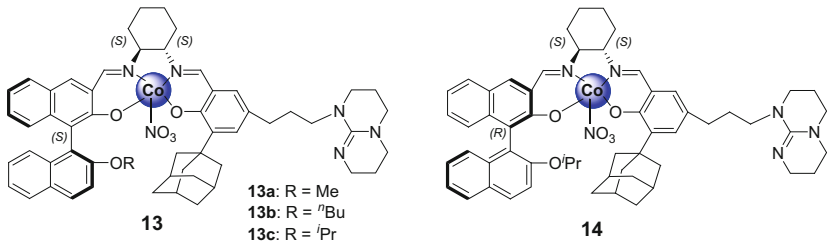


Far different from the highly regioselective ring opening of epoxides with an electron-donating group such as propylene oxide during the copolymerization with $CO_2$, binary catalyst systems based on salenCo(III)X **3** for epoxides with an electron-withdrawing group afforded regio-irregular copolymer, e.g., for styrene oxide case with a head-to-tail content of 51%, indicating that epoxide ring opening occurs almost equally at both $C_\alpha$–O and $C_\beta$–O bonds [57]. When enantiopure (*1S,2S*)-**3** (X = 2,4-dinitrophenoxide) was used to the copolymerization of $CO_2$ and *racemic* styrene oxide, a kinetic resolution was observed with a $k_{rel}$ of 1.6 at ambient temperature. The catalyst preferentially consumed (*R*)-styrene oxide over its (*S*)-configuration. Surprisingly, in comparison with the low $k_{rel}$ value, an enhanced enantioselectivity for (*R*)-configuration carbonate unit with a selective factor of 4.3 was found in the resulting copolymer [58]. Because of the low $k_{rel}$, a

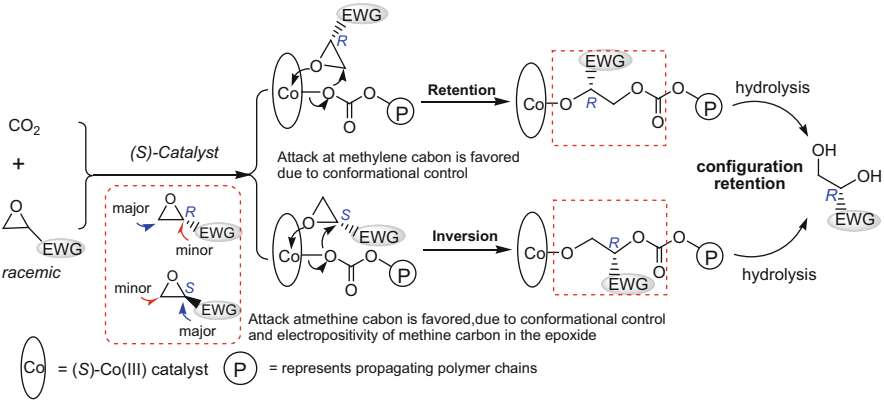


**Scheme 16** Formation of optically active polycarbonates from *racemic* epoxides with a withdrawing group and $CO_2$ by a catalytic kinetic resolution process concerning regioselective ring opening

significant amount of (*S*)-styrene oxide should be incorporated into the polycarbonate. Therefore, the increase in poly(styrene carbonate) enantioselectivity for (*R*)-configuration was ascribed to the preferential configuration inversion occurred at the methine carbon of (*S*)-styrene oxide caused by chiral induction of (*1S,2S*)-3 (Scheme 16). To confirm this assumption, the authors also performed the chiral (*S*)-styrene oxide/$CO_2$ copolymerization in the presence of the same binary catalyst. The resultant copolymer has an enantioselectivity of 32% with (*R*)-configuration excess, implying that the reaction proceeded with 66% inversion at the benzyl carbon. It was found that the chiral environment around the central metal ion significantly influences the regioselectivity of epoxide ring opening. With complex (*S,S,S*)-**8a** as catalyst, a $k_{rel}$ of 3.3 was observed in the asymmetric copolymerization of $CO_2$ and *racemic* styrene oxide. Upon replacing with (*R*)-styrene oxide, the resultant copolymer has an enantioselectivity of 92% with (*R*)-configuration excess, indicative of retaining 96% of the stereochemistry at the methine carbon of (*R*)-styrene oxide incorporated into the polycarbonate.

In a recent contribution, the same group reported the use of an enantiopure salenCo(III) complex **15** bearing an adamantine group and an appended bulky dicyclohexyl ionic ammonium salt as catalyst for the copolymerization of $CO_2$ and epichlorohydrin; a highly regioregular ring-opening step was observed with a concomitant 97% retention of configuration at the methine carbon center [59]. The resultant isotactic poly(chloropropylene carbonate) is a typical semicrystalline polymer with an enhanced $T_g$ of 42°C and a $T_m$ of 108°C [60]. The test of mechanical properties shows that the yield strength and tensile strength of the crystalline copolymer are about 10 and 30 times that of its amorphous counterpart, respectively.

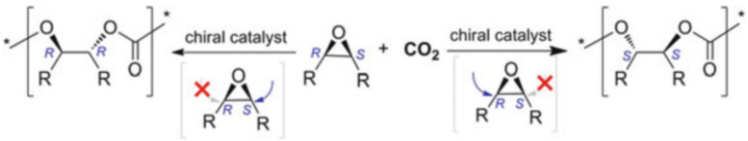


**Scheme 17** Asymmetric copolymerization of $CO_2$ and *meso*-epoxides

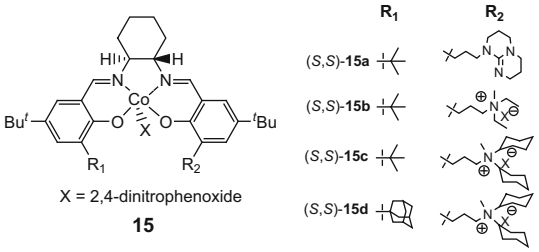


It is worthwhile noting here parenthetically that salenCo(III)X **15a** bearing an appended 1,5,7-triabicyclo[4,4,0] dec-5-ene (designated as TBD, a sterically hindered organic base) is an excellent catalyst for highly regioselective ring opening of both benzyl glycidyl ether and phenyl glycidyl ether during the copolymerization with $CO_2$, affording the corresponding polycarbonates with >99% carbonate unit content and >99% head-to-tail linkages [61, 62]. Deprotection of the resultant copolymers from benzyl glycidyl ether afforded poly(1,2-glycerol carbonate)s with a functionalizable pendant primary hydroxyl group. Poly(1,2-glycerol carbonate) showed a remarkable increase in degradation rate compared to poly (1,3-glycerol carbonate) with a $t_{1/2} = 2$–3 days. These polymers fulfill an unmet need for a readily degradable biocompatible polycarbonate. Particularly, the isotactic $CO_2$-based polycarbonate from chiral phenyl glycidyl ether is a typical semicrystalline thermoplastic, which possesses a melting point of 75°C.

Indeed, in comparison with stereoregular $CO_2$-based polycarbonates from terminal epoxides, isotactic polycarbonates from *meso*-epoxides are easy to crystallize and usually show higher melting temperatures. It is generally known that the desymmetrization nucleophilic ring opening of *meso*-epoxides with chiral catalysts or reagents is regarded as a valuable strategy for the synthesis of enantiomerically enriched products with two contiguous stereogenic centers [63]. When such a powerful synthetic strategy is used to the alternating copolymerization of $CO_2$ with *meso*-epoxides, optically active polycarbonates with main-chain chirality can be produced from optically inactive *meso*-monomers (Scheme 17). Because the ring opening of a *meso*-epoxide proceeds with inversion at one of the two chiral centers, a successful asymmetric ring opening by a chiral catalyst will produce optically active polycarbonates with an (*R,R*)- or (*S,S*)-*trans*-1,2-diol unit. The first attempt of asymmetric copolymerization of $CO_2$ with *meso*-epoxides was disclosed by Nozaki et al. using a 1:1 $Et_2Zn$/(*S*)-α,α-diphenyl(pyrrolidin-2-yl)methanol mixture as catalyst, producing the corresponding polycarbonates with moderate enantioselectivity [64]. Further mechanistic studies suggested that a dimeric zinc

complex might be the active species [65]. Soon thereafter, the Coates research group reported the use of chiral hybrid imineoxazoline zinc-based catalysts for this reaction, which showed similar enantioselectivity but higher activity and controlled molecular weight [66]. Notably, they first noted the existence of the melting temperature of the resultant isotactic-enriched poly(cyclohexene carbonate), though the authors did not provide the DSC thermogram of the sample. Based on the mechanistic understanding that dimeric zinc complex was involved in the transition state of epoxide ring-opening event during $CO_2$/cyclohexene oxide copolymerization, Ding and coworkers described a chiral dinuclear metal catalyst **18** [67], coordinated with Trost's multidentate ligand, which exhibited moderate activity and very low enantioselectivity (8–18% *ee*) for this copolymerization. Interestingly, in a recent contribution, Wang et al. discovered that a dinuclear zinc complex of chiral ligand **19** with more rigid azetidine 4-membered ring compared with pyrrolidine cycle was efficient in catalyzing $CO_2$/cyclohexene oxide copolymerization at mild conditions, affording completely alternating polycarbonates in up to 93.8% *ee* [68]. It was suggested that the intramolecular dinuclear zinc structure of the catalytically active species containing azetidine ring was more rigid than pyrrolidine, which was responsible for the great improvement of the enantioselectivity. Almost simultaneously, Coates group optimized their enantioselective zinc $\beta$-diiminate (BDI) catalyst for $CO_2$/cyclohexene oxide copolymerization [69]. Iterative catalyst optimization yielded catalysts **20a–20c**, which show TOFs up to 190 $h^{-1}$ at 22°C and produce polymers with repeat units of >90% *ee*. The maximum *ee* at 22°C was 92% *ee* using catalyst **20c**, and polymer with repeat units of 94% *ee* and a PDI of 1.3 was obtained using **20c** at 0°C. The presence of a bulky enantiopure ether substituent improves both the enantioselectivity and activity. Recently, Du and Abbina described the use of chiral zinc complex **21** with $C_1$-symmetric amido-oxazolinate ligands as catalyst for $CO_2$/cyclohexene oxide copolymerization [70]. Unfortunately, the asymmetric induction is generally low, with up to 71% *SS* unit in the main chain of the produced poly(cyclohexene carbonate)s. Prior to this study, optically active dinuclear aluminum complexes of $\beta$-ketoiminate or aminoalkoxide **22** [71], in conjunction with a bulky Lewis base as catalyst activator, were applied to the copolymerization of $CO_2$ with *meso*-epoxides, affording the corresponding polycarbonates with a moderate enantioselectivity (60–80% *ee*).

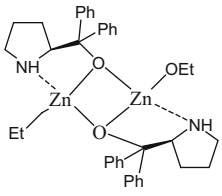


**16**

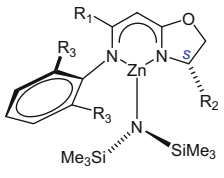


**17**

$R_1$ = Me, $CF_3$, $^i$Pr
$R_2$ = (*R*)-Ph, (*S*)-$^i$Pr, (*S*)-$^t$Bu
$R_3$ = Et, $^i$Pr

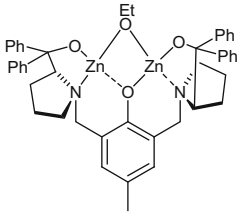

18

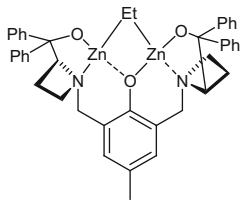

19

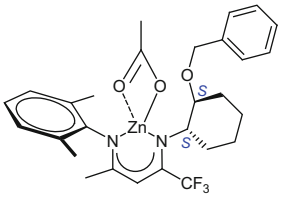

20a

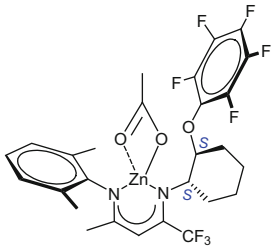

20b

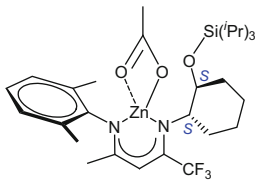

20c

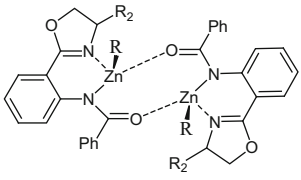

21

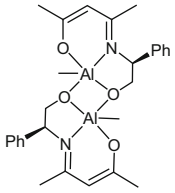

22

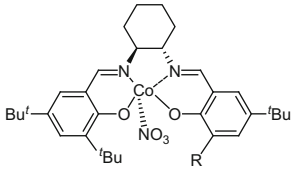

23 (*1S,2S*)-**23a**: R= $CMe_2Ph$
(*1S,2S*)-**23b**: R= $SiMe_2{}^tBu$
(*1S,2S*)-**23c**: R= adamyl

Stimulated by the success with chiral salenCo(III)-catalyzed asymmetric alternating copolymerization of *racemic* terminal epoxides and $CO_2$ [72], Lu and coworkers also applied these systems to the asymmetric copolymerization of cyclohexene oxide and $CO_2$ under mild conditions [73]. With binary catalyst system of enantiopure complex (*1R,2R*)-**3b** (trichloroacetate as the axial anion) and equimolar bis(triphenylphosphine)iminium chloride (PPNCl), copolymerization reaction at ambient temperature and 1.5 MPa $CO_2$ pressure provided isotactic-enriched poly(cyclohexene carbonate)s with a relatively low enantioselectivity of 38% *ee* for (*S,S*)-configuration. This catalyst is less selective, with an *ee* of 28%, but more active when the temperature and pressure are increased to 80°C and 2.5 MPa $CO_2$, respectively. The great progress came with the report from the same group. In 2012,

they reported a series of $C_1$-symmetric catalysts that are highly stereoselective for copolymerization of cyclohexene oxide with $CO_2$ [74]. Improved enantioselectivity is achieved by increasing the steric bulk of the ortho-substituent on one side of the ligand from a *tert*-butyl group to an adamantyl group. The highest selectivity (96% *ee*) is achieved by performing the polymerization with complex **23c** at −25°C in a 1:3 mixture of cyclohexene oxide and (*S*)-2-methyltetrahydrofuran as chiral induction agent. This resultant copolymer has a low $M_n$ of 9.2 kDa and a PDI of 1.14. More importantly, they observed the isotacticity of poly(cyclohexene carbonate) has the critical influence on its crystallinity. It was found that the poly(cyclohexene carbonate)s with less than 80% isotacticity did not show any crystallization. A $T_g$ of 122°C and a very small melting endothermic peak at 207°C with the melting enthalpy of (ΔHm) 3.92 J/g, indicating a very low degree of crystallinity, were observed in the sample (*R*)-PCHC-92 (*RR*:*SS* ratio in the polycarbonate is 92:8) (Fig. 1), while a sharp and high crystallization endothermic peak that appears at 216°C with ΔHm = 22.50 J/g was found in the highly isotactic polymer (*R*)-PCHC-98 (*RR*:*SS* = 98:2). Surprisingly, the crystallization endothermic peak of the (*R*)-PCHC-98/(*S*)-PCHC-98 (*RR*:*SS* = 2:98) blend (1/1 mass ratio) increased to 227°C with ΔHm = 29.70 J/g using the same crystallization conditions [75], indicating that the blend with two opposing configurations forms a stereocomplex with a new and distinct crystalline structure. Both WAXD (wide-angle X-ray diffraction) and AFM (atomic force microscopy) studies confirmed the formation of a stereocomplex from (*R*)-PCHC-98/(*S*)-PCHC-98 (*RR*:*SS* = 2:98) blend (1/1 mass ratio). For (*R*)-PCHC-98 sample, sharp diffraction peaks were observed at 2θ values of 12.2, 17.9, 19.0, and 20.4° (Fig. 2), while the blend of (*S*)-PCHC-98/(*R*)-PCHC-98 (1/1 mass ratio) has different diffraction peaks appearing at 2θ equal to 8.6, 17.9, and 21.5°, indicating that the stereocomplex possesses a new crystalline structure, being different from that of the sole configuration polymer. AFM observations also revealed the unique crystallization behavior. The lamellae or lamellar in (*S*)-PCHC-98 sample aggregates preferentially bend anticlockwise, while a clockwise-rotated spherulite can be clearly observed in (*R*)-PCHC-98 sample. Surprisingly, the morphological feature of the stereocomplex of (*S*)-PCHC-98/(*R*)-PCHC-98 (1/1mass ratio) changes dramatically and presents a lath-like dendritic crystal, which is very different from the bending features observed for its parent polymers (Fig. 3).

Although the binary catalyst system based on unsymmetrical chiral salenCo(III) complex **23c** exhibited the high enantioselectivity, the rigorous reaction conditions, such as a low temperature of −25°C and the use of a large amount of chiral induction agent, were prerequisites for obtaining optically active copolymer with low molecular weight in a very low rate (less than 3 $h^{-1}$). Additionally, this binary catalyst system was found to be inactive for the coupling of $CO_2$ with cyclopentene oxide (a less reactive epoxide). More recently, Lu and coworkers developed a chiral catalyst system based on enantiopure dinuclear Co(III) complexes **24** with a rigid bridging biphenyl linker, which exhibits excellent activity, unprecedented enantioselectivity, and molecular-weight control for the alternating copolymerization of $CO_2$ with *meso*-epoxides (both cyclopentene oxide and cyclohexene oxide) under

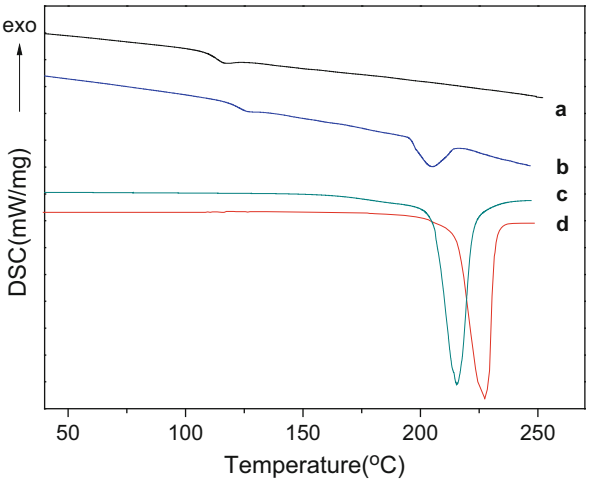


**Fig. 1** DSC thermograms of various poly (cyclohexene carbonate)s. (**a**) Atactic PCHC; (**b**) (*R*)-PCHC-92; (**c**) (*R*)-PCHC-98; (**d**) (*R*)-PCHC-98/(*S*)-PCHC-98 blend, 1/1 mass ratio

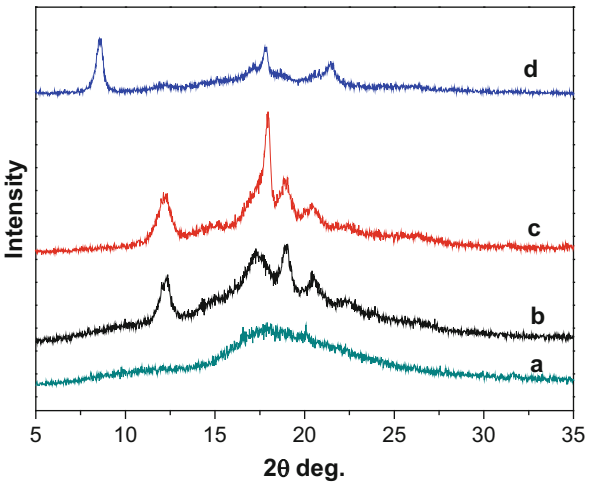


**Fig. 2** WAXD profiles of various poly(cyclohexene carbonate) samples. (**a**) Atactic PCHC; (**b**) (*R*)-PCHC-92; (**c**) (*R*)-PCHC-98; (**d**) (*R*)-PCHC-98/(*S*)-PCHC-98 blend, 1/1 mass ratio

mild reaction conditions [76]. The combination of (*S*,*S*,*S*,*S*)-**24b** with a methyl group or (*S*,*S*,*S*,*S*)-**24c** without any substituents in the phenolate ortho-positions and a nucleophilic cocatalyst PPNX (X = 2,4-dinitrophenoxide) was found to be more efficient in catalyzing this asymmetric reaction, providing the copolymer with >99% carbonate linkages and an enantioselectivity of up to 99% for *S*,*S*-configuration. Notably, the biphenol-linked dinuclear Co(III) complex is a rare privileged chiral catalyst for copolymerizing $CO_2$ with various *meso*-epoxides, including the simplest *meso*-epoxide, *cis*-2,3-epoxybutane, showing both high reactivity and enantioselectivity for producing the corresponding polycarbonates with complete alternating structure and 99% *ee*. (Fig. 4) [77]. The TOFs are in the range of

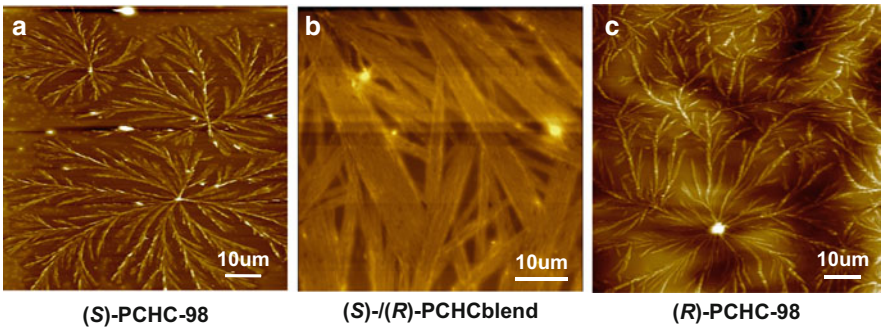


**Fig. 3** AFM height images of (**a**) (*S*)-PCHC-98; (**b**) (*R*)-PCHC-98/(*S*)-PCHC-98 blend (1/1 mass ratio); (**c**) (*R*)-PCHC-98

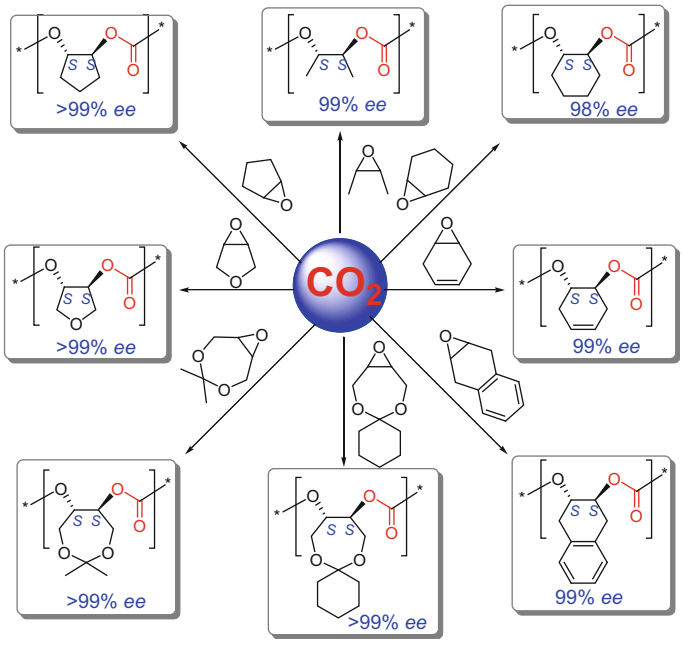


**Fig. 4** Enantioselective copolymerization of $CO_2$ and various *meso*-epoxides mediated by dinuclear Co(III) complex (*S*,*S*,*S*,*S*)-**1b** or **1c** in combination with PPN-DNP (DNP = 2,4-dinitrophenoxide)

120–1,400 $h^{-1}$, dependant on the structure of *meso*-epoxides. Among them, six isotactic $CO_2$-based polycarbonates are crystalline, possessing $T_m$s of 179–257°C [78, 79].

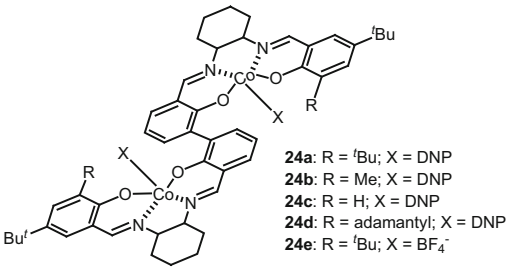


**24**

DFT calculations suggested that in the two diastereoisomers, (*S*,*S*,*S*,*S*,*S*)-conformer is more effective in catalyzing $CO_2$/CPO copolymerization than the corresponding (*S*,*S*,*R*,*S*,*S*)-conformer (Fig. 5) [77]. The calculations also showed that the dinuclear Co(III) catalyst with a *S*,*S*,*S*,*S*,*S*-configuration predominantly resulted in the formation of polycarbonates with *S*,*S*-configuration (TS-1), which was in agreement with the experimental findings. Furthermore, on the basis of kinetic study and DFT calculations, the authors gave a comprehensive mechanism understanding on (*S*,*S*,*S*,*S*)-**24**-mediated enantioselective copolymerization of $CO_2$ and *meso*-epoxides. The biphenol-linked Co(III) complexes (*S*,*S*,*S*,*S*)-**24** are the mixture of two diastereoisomers with *R*- or *S*-biphenol stereochemistry, (*S*,*S*,*R*,*S*,*S*) and (*S*,*S*,*S*,*S*,*S*)-conformers, though they originate from an achiral biphenol linker. The matched configuration of (*S*,*S*,*S*,*S*,*S*) was more effective than (*S*,*S*,*R*,*S*,*S*) for enantioselectively catalyzing this asymmetric copolymerization. The initiation is triggered by one of the two nucleophilic anions of the bimetallic cobalt catalyst from the inside cleft, and chain-growth step predominantly involves an intramolecular bimetallic cooperation mechanism, wherein alternating chain growth and dissociation of propagating carboxylate species take turn between two Co(III) ions from the inside cleft of dinuclear Co(III) catalysts by the nucleophilic attack of the growing carboxylate species at one metal center toward the activated epoxide at the other (Scheme 18). Both the absolute stereochemistry of the biphenol linker and cyclohexyl diamine skeletons determine the enantiomer preference in the copolymerization. Another path for initiation and chain growth concerns a monometallic mechanism or intermolecular bimetallic mechanism that occurred in the outside cleft of the catalyst. This is similar with the mononuclear Co(III) catalyst **4a**, in which the cyclohexyl diamine skeleton determines the enantiomer preference, providing the copolymers with the opposite configuration. Since the former is predominantly responsible for the copolymer formation and the inside cleft is the more enantioselective site, it determines the product configuration and enantioselectivity.

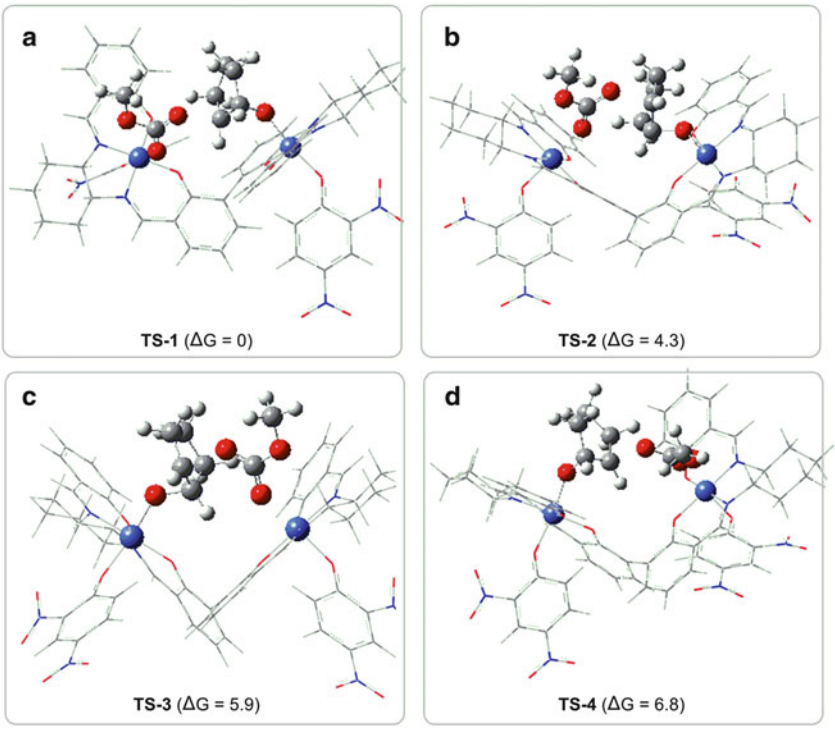


**Fig. 5** Four possible transition states for the ring opening of a cyclopentene oxide (CPO) molecule by an adjacent cobalt bound carbonate group. (**a**) TS-1, ring opening at the (*R*)-C–O bond of CPO activated by (*S*,*S*,*S*,*S*,*S*)-**1f**; (**b**) TS-2, ring opening at the (*S*)-C–O bond of CPO activated by (*S*,*S*,*S*,*S*,*S*)-**1f**; (**c**) TS-3, ring opening at the (*R*)-C–O bond of CPO activated by (*S*,*S*,*R*, *S*,*S*)-**1f**; (**d**) TS-4, ring opening at the (*S*)-C–O bond of CPO activated by (*S*,*S*,*R*,*S*,*S*)-**1f**. The energy was given in kcal/mol and toluene was employed as a solvent

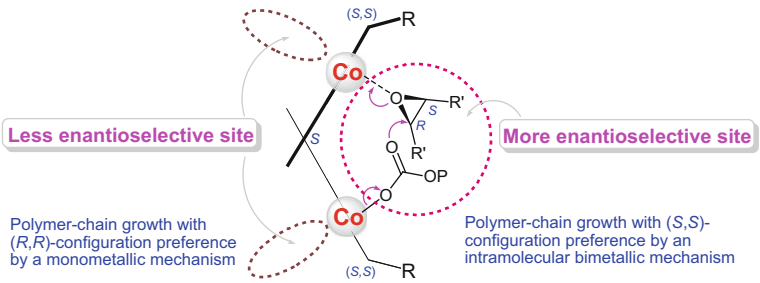


**Scheme 18** Dinuclear Co(III) complex-mediated enantioselective polymer chain growth routes

## 6 Summary and Concluding Remarks

This review therefore aims to principally showcase the recent progress regarding $CO_2$-mediated formation of chiral fine chemicals. Although these mentioned reactions suffered from some problems, e.g., the $k_{rel}$ values measured in the epoxide resolution with $CO_2$ are below what is generally considered useful, these investigations are important because they address the feasibility of using $CO_2$ as a $C_1$ source in asymmetric catalysis. To our delightsome, the discovery of the enantiopure dinuclear Co(III) catalysts for highly enantioselective copolymerization of $CO_2$ with various *meso*-epoxides to afford $CO_2$-based polycarbonates with more than 99% enantioselectivity makes this stereoselective catalysis become truly competitive. Potential applications for these isotactic semicrystalline polymers are expectant. It is hoped that further catalyst development will lead to high $k_{rel}$ values for epoxide resolution with $CO_2$, deserving of significant commercial application. Clearly, it is highly desired to develop new enantioselective catalysis focusing on amplification of the organic structures one can derive from $CO_2$ as a molecular synthon.

Computational chemistry has contributed to our understanding of the mechanistic aspects of some organic reactions. It is anticipated that this approach will play an increasingly important role in understanding the features that account for the $CO_2$-mediated formation of chiral fine chemicals and thus aid in developing new privileged catalysts.

**Acknowledgments** This work is supported by the National Natural Science Foundation of China (NSFC, Grant 21134002) and Program for Changjiang Scholars and Innovative Research Team in University (IRT13008). X. B. Lu gratefully acknowledges the Changjiang Scholars Program (T2011056) from the Ministry of Education of China.

## References

1. Sakakura T, Choi JC, Yasuda H (2007) Chem Rev 107:2365
2. Darensbourg DJ (2010) Inorg Chem 49:10765
3. Cokoja M, Bruckmeier C, Rieger B, Herrmann WA, Kühn FE (2011) Angew Chem Int Ed 50: 8510
4. He MY, Sun YH, Han BX (2013) Angew Chem Int Ed 52:9620
5. Aresta M, Dibenedetto A (2007) Dalton Trans 28:2975
6. Lu XB, Darensbourg DJ (2012) Chem Soc Rev 41:1462
7. Kielland N, Whiteoak CJ, Kleij AW (2013) Adv Synth Catal 355:2115
8. Ian Childers M, Longo JM, Van Zee NJ, LaPointe AM, Coates GW (2014) Chem Rev 114: 8129
9. Burk RM, Roof MB (1993) Tetrahedron Lett 34:395
10. Hisch H, Millini R, Wang IJ (1986) Chem Ber 119:1090
11. Matsumoto K, Fuwa S, Kitajima H (1995) Tetrahedron Lett 36:6499
12. Shimojo M, Matsumoto K, Hatanaka M (2000) Tetrahedron 56:9281
13. Trost BM, Angle SR (1985) J Am Chem Soc 107:6123

14. Gendre PL, Braun T, Bruneau C, Dixneuf PH (1996) J Org Chem 61:8453
15. Li B, Wu GP, Ren WM, Wang YM, Lu XB (2008) J Polym Sci A Polym Chem 46:6102
16. Aresta M, Dibenedetto A, Gianfrate L, Pastore C (2003) Appl Catal A Gen 255:5
17. Zhang X, Jia YB, Lu XB, Li B, Wang H, Sun LC (2008) Tetrahedron Lett 49:6589
18. Ren WM, Liu Y, Lu XB (2014) J Org Chem 79:9771
19. Jacobsen EN (2000) Acc Chem Res 33:421
20. Lu XB, Liang B, Zhang YJ, Tian YZ, Wang YM, Bai CX, Wang H, Zhang R (2004) J Am Chem Soc 126:3732
21. Paddock RL, Nguyen ST (2004) Chem Commun 1622
22. Berkessel A, Brandenburg M (2006) Org Lett 8:4401
23. Chang T, Jing HW, Jin L, Qiu WY (2007) J Mol Catal A Chem 264:241
24. Chang T, Jin L, Jing HW (2009) ChemCatChem 1:379
25. Jin L, Huang Y, Jing HW, Chang T, Yan P (2008) Tetrahedron Asymmetry 19:1947
26. Zhang S, Song Y, Jing HW, Yan P, Cai Q (2009) Chin J Catal 30:1255
27. Zhang S, Huang Y, Jing HW, Yao W, Yan P (2009) Green Chem 11:935
28. Yan P, Jing HW (2009) Adv Synth Catal 351:13
29. Ren WM, Wu GP, Lin F, Jian JY, Liu C, Luo Y, Lu XB (2012) Chem Sci 3:2094
30. Chen SW, Kawthekar RB, Kim GJ (2007) Tetrahedron Lett 48:297
31. Tanaka H, Kitaichi Y, Sato M, Ikeno T, Yamada T (2004) Chem Lett 676
32. Yoshida S, Fukui K, Kikuchi S, Yamada T (2010) J Am Chem Soc 132:4072
33. Wouters J (1998) Curr Med Chem 5:137
34. Evans DA, Kim AS (1999) In: Coates RM, Denmark SE (eds) Handbook of reagents for organic synthesis: reagents, auxiliaries and catalysts for C–C bonds. Wiley, New York, pp 91–101
35. Du Y, Wu Y, Liu AH, He LN (2008) J Org Chem 73:4709
36. Seayad J, Seayad AM, Ng JKP, Chai CLL (2012) ChemCatChem 4:774
37. Feroci M, Gennaro A, Inesi A, Orsini M, Palombi L (2002) Tetrahedron Lett 43:5863
38. Casadei MA, Feroci M, Inesi A, Rossi L, Sotgiu G (2000) J Org Chem 65:4759
39. Foo SW, Takada Y, Yamazaki Y, Saito S (2013) Tetrahedron Lett 54:4717
40. Paz J, Pérez-Balado C, Iglesias B, Muñoz L (2009) Synlett 3:395
41. Zhang K, Wang H, Zhao SF, Niu DF, Lu JX (2009) J Electroanal Chem 630:35
42. Chen BL, Tu ZY, Zhu HW, Sun WW, Wang H, Lu JX (2014) Electrochim Acta 116:475
43. Takimoto M, Mori M (2002) J Am Chem Soc 124:10008
44. Takimoto M, Nakamura Y, Kimura K, Mori M (2004) J Am Chem Soc 126:5956
45. Zheng SC, Zhang M, Zhao XM (2014) Eur Chem J 20:7216
46. Zhang M, Zhao XM, Zheng SC (2014) Chem Commun 50:4455
47. Mita T, Sugawara M, Saito K, Sato Y (2014) Org Lett 16:3028
48. Inoue S, Koinuma H, Tsuruta T (1969) J Polym Sci B Polym Lett 7:287
49. Darensbourg DJ (2007) Chem Rev 107:2388
50. Coates GW, Moore DR (2004) Angew Chem Int Ed 43:6618
51. Qin ZQ, Thomas CM, Lee S, Coates GW (2003) Angew Chem Int Ed 42:5484
52. Lu XB, Wang Y (2004) Angew Chem Int Ed 43:3574
53. Lu XB, Shi L, Wang YM, Zhang R, Zhang YJ, Peng XJ, Zhang ZC, Li B (2006) J Am Chem Soc 128:1664
54. Ren WM, Liu ZW, Wen YQ, Zhang R, Lu XB (2009) J Am Chem Soc 131:11509
55. Ren WM, Zhang WZ, Lu XB (2010) Sci Chin Chem 53:1646
56. Ren WM, Liu Y, Wu GP, Liu J, Lu XB (2011) J Polym Sci A Polym Lett 49:4894
57. Wu GP, Wei SH, Lu XB, Ren WM, Darensbourg DJ (2010) Macromolecules 43:9202
58. Wu GP, Wei SH, Ren WM, Lu XB, Li B, Zu YP, Darensbourg DJ (2011) Energy Environ Sci 4:5084
59. Wu GP, Wei SH, Ren WM, Lu XB, Xu TQ, Darensbourg DJ (2011) J Am Chem Soc 133: 15191

60. Wu GP, Xu PX, Lu XB, Zu YP, Wei SH, Ren WM, Darensbourg DJ (2013) Macromolecules 46:2128
61. Zhang H, Grinstaff MW (2013) J Am Chem Soc 135:6806
62. Ren WM, Liang MW, Xu YC, Lu XB (2013) Polym Chem 4:4425
63. Jacobsen EN, Wu MH (1999) In: Jacobsen EN, Pfaltz A, Yamamoto H (eds) Comprehensive asymmetric catalysis, vol I–III. Springer, Berlin, pp 1309–1312
64. Nozaki K, Nakano K, Hiyama T (1999) J Am Chem Soc 121:11008
65. Nakano K, Nozaki K, Hiyama T (2003) J Am Chem Soc 125:5501
66. Cheng M, Darling NA, Lobkovsky EB, Coates GW (2000) Chem Commun 2007
67. Xiao Y, Wang Z, Ding K (2005) Chem Eur J 11:3668
68. Hua YZ, Lu LJ, Huang PJ, Wei DH, Tang MS, Wang MC, Chang JB (2014) Chem Eur J 20: 12394
69. Ellis WC, Jung Y, Mulzer M, Di Girolamo R, Lobkovsky EB, Coates GW (2014) Chem Sci 5: 4004
70. Abbina S, Du GD (2012) Organometallics 31:7394
71. Nishioka K, Goto H, Sugimoto H (2012) Macromolecules 45:8172
72. Lu XB, Ren WM, Wu GP (2012) Acc Chem Res 45:1721
73. Shi L, Lu XB, Zhang R, Peng XJ, Zhang CQ, Li JF, Peng XM (2006) Macromolecules 39:5679
74. Wu GP, Ren WM, Luo Y, Li B, Zhang WZ, Lu XB (2012) J Am Chem Soc 134:5682
75. Wu GP, Jiang SD, Lu XB, Ren WM, Yan SK (2012) Chin J Polym Sci 30:487
76. Liu Y, Ren WM, Liu J, Lu XB (2013) Angew Chem Int Ed 52:11594
77. Liu Y, Ren WM, Liu C, Fu S, Wang M, He KK, Li RR, Zhang R, Lu XB (2014) Macromolecules 47:7775
78. Liu Y, Ren WM, He KK, Lu XB (2014) Nat Commun 5:5687
79. Liu Y, Wang M, Ren WM, He KK, Xu YC, Liu J, Lu XB (2014) Macromolecules 47:1269

Top Organomet Chem (2016) 53: 199–224
DOI: 10.1007/3418_2015_111

Published online: 22 April 2015

# Ni-Catalyzed Synthesis of Acrylic Acid Derivatives from $CO_2$ and Ethylene

**Sebastian Kraus and Bernhard Rieger**

**Abstract** The story of nickelalactones finally ends well. Over three decades after their discovery, catalytic processes have been successfully established to synthesize acrylate derivatives from ethylene and abundantly available carbon dioxide. The performed research during this time in the $CO_2$ utilization via C–C bond formation with olefins is presented within this review. It gives detailed insights starting from the initial milestones in the 1980s up to modern strategies through cleavage auxiliaries. Different approaches are examined from an experimental and theoretical point of view as the choice of cleavage agent and the corresponding ligand is crucial for the reaction control and suppression of undesired pathways. Methylation of the lactone species led to a first successful liberation of methyl acrylate in stoichiometric amounts. These results led to a vast progress in research with auxiliaries afterward. Upon addition of Lewis acids or strong sodium bases, finally the first two different catalytic routes have been established which are discussed in detail.

**Keywords** Acrylate · C1 olefin · Nickelalactone · Oxidative coupling

## Contents



S. Kraus and B. Rieger (✉)
Technische Universität München, Wacker-Lehrstuhl für Makromolekulare Chemie, Lichtenbergstraße 4, 85747 Garching bei München, Germany
e-mail: rieger@tum.de

## Abbreviations

| | |
|---|---|
| $Ar^F$ | 3,5-Bis(trifluoromethyl)phenyl |
| bpy | 2,2′-Bipyridine |
| BenzP* | (*R*,*R*)-(+)-1,2-Bis(*tert*-butylmethylposphino)benzene |
| BTPP | (*tert*-Butylimino)tris(pyrrolidino)phosphorane |
| cdt | 1,5,9-Cyclododecatriene |
| cod | 1,5-Cyclooctadiene |
| Cy | Cyclohexyl |
| dcpe | 1,2-Bis(dicyclohexylphosphino)ethane |
| dcpp | 1,3-Bis(dicyclohexylphosphino)propane |
| d*i*ppf | 1,1′-Bis(di-*iso*-propylphosphanyl)ferrocene |
| dppb | 1,4-Bis(diphenylphosphino)butane |
| dppe | 1,2-Bis(diphenylphosphino)ethane |
| dppf | 1,1′-Bis(diphenylphosphanyl)ferrocene |
| dppm | Bis(diphenylphosphino)methane |
| dppp | 1,3-Bis(diphenylphosphino)propane |
| d*t*bpe | 1,2-Bis(di-*tert*-butylphosphino)ethane |
| d*t*bpm | Bis(di-*tert*-butylphosphino)methane |
| d*t*bpp | 1,3-Bis(di-*tert*-butylphosphino)propane |
| DBU | 1,8-Diazabicyclo[5.4.0]undec-7-ene |
| DFT | Density functional theory |
| D*I*PEA | *N*,*N*-Di-*iso*-propylethylamine |
| IR | Infrared |
| L | Ligand |
| Lac | 2-Oxacyclopentan-3-one |
| MMA | Methyl methacrylate |
| NMR | Nuclear magnetic resonance |
| p.a. | Per year |
| PAA | Poly(acrylic acid) |
| PANa | Sodium poly(acrylate) |
| PMMA | Poly(methyl methacrylate) |
| rt | Room temperature |
| thf | Tetrahydrofuran |
| tmeda | *N*,*N*,*N*′,*N*′-Tetramethylethylenediamine |
| TOF | Turnover frequency |
| TON | Turnover number |

## 1 Introduction

Acrylic acid and its derivatives, i.e., organic esters and alkali salts, are widely used as monomers for the synthesis of polymeric materials (Fig. 1). One of the most famous examples is poly(acrylic acid) (PAA) with its unique properties as a superabsorber [1]. Depending on the degree of neutralization to sodium poly (acrylate) (PANa), this polymer is able to absorb water up to 300 times of its own mass. Besides the application in modern diapers, a huge variety of household and daycare products in cosmetics contain PAA as thickener or film-forming substance, adhesives, coatings, and paints. Due to its ability to bind earth alkali elements like calcium and magnesium, it is utilized in sequestering agents. The applications become even more versatile by using blends or copolymers from a variety of poly (acrylate)s [2].

One of the most commonly used derivatives is methyl methacrylate (MMA) in its polymerized form, poly(methyl methacrylate) (PMMA). The translucency and resistance to acids and bases make it a suitable substitute to common glass materials applied mainly in construction, the automotive sector, and medical technology. Today's production volume of acrylic acid and its derivatives reach ~4 Mt p.a. with a further increase in the future, especially due to a rising demand in emerging countries. To accommodate this demand, efficient and keen production pathways are requested by the chemical industry [3].

An overview of the abandoned production processes is drawn in Fig. 2 [1]. The cyanohydrin method (i) was established first in industrial scale. Starting from ethylene oxide, the corresponding 3-hydroxypropionitrile is formed by addition of highly toxic HCN. Treatment with $H_2SO_4$ leads to acrylic acid; however, huge amounts of $NH_4HSO_4$ are formed as undesired side product. The *Reppe* synthesis (ii) was introduced in 1939 and used coal-based acetylene and CO to undergo a heterogenic nickel-catalyzed C–C bond formation. Major disadvantages of this route are the toxicity and corrosivity of the catalyst $Ni(CO)_4$ as well as the huge energy consumption of the overall process. Similar problems occur from the pyrolysis of acetic acid to the corresponding ketene (iii). Again, the high toxicity and demand of energy forced the industry to investigate new strategies toward acrylates. The first established synthesis with a C3 building block was the *Sohio* process (iv) for the synthesis of acrylonitrile via ammoxidation. Subsequent acidic hydrolysis with sulfuric acid yields the desired product. In common with the cyanohydrin route, huge amounts of $NH_4HSO_4$ waste are produced.


**Fig. 1** Typical polymerization of acrylic acid and some of its important derivatives

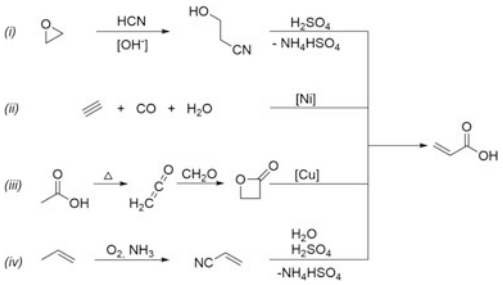


**Fig. 2** Abandoned industrial synthesis pathways to acrylic acid via (*i*) cyanohydrin, (*ii*) Reppe synthesis, (*iii*) pyrolysis, and (*iv*) Sohio process [1].

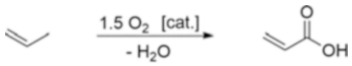


**Fig. 3** Today's industrial process for the synthesis of acrylic acid through oxidation of propylene


**Fig. 4** Ni(0)-catalyzed synthesis of acrylic acid from ethylene and $CO_2$

Today's acrylic acid is synthesized from propylene by direct oxidation with $O_2$ over molybdenum/bismuth catalysts, leading to acrolein as intermediate compound. In a subsequent second step, it is oxidized over molybdenum/vanadium catalysts to acrylic acid [2]. This process has largely replaced any other industrial method nowadays because of the increased selectivity, less undesired by-products, and hence higher profitability (Fig. **3**) [1]. However, this pathway is limited to propylene as a substrate and thus to unsubstituted acrylic acid. Additional modifications of the carboxylic group need to be performed separately.

The finiteness of oil reserves accompanied by the imbalance of supply and demand for fossil fuel leads to fluctuating market prices. Thus, novel routes to acrylic acid replace crude oil-based C3 resources with cheap, renewable, and abundantly available C2 and C1 building blocks as raw materials [4]. Besides the oxycarbonylation of ethylene with CO and water, the nickel-catalyzed direct carboxylation of ethylene with $CO_2$ (Fig. 4) represents one promising approach for industrial application [2]. The C–C coupling of $CO_2$ and ethylene with Ni (0) was discovered by Hoberg in the early 1980s [5, 6]. However transformations of nickelalactones were limited to stoichiometric reactions. Postulations about the catalytic employment of nickelalactone intermediates toward acrylic acid in 2006 [7] aroused huge attention in science leading to a dramatic increase of investigations in this topic. Within this review, we want to give an insight into the beginning

of this story 30 years ago up to the latest advances in research about the catalytic formation of acrylates from carbon dioxide and ethylene (Fig. 4).

## 2 Formation and Reactivity of Nickelalactones

### *2.1 Pioneering Work*

The initial milestones date back to the year 1980 when Yamamoto et al. published the first cyclic Ni(II) complexes with a nickelalactone motif [8]. The Ni(0) precursor $Ni(cod)_2$ was treated with acrylic acid and acrylamide in an excess of phosphine ligand. The resulting cyclic amide and ester complexes were confirmed by infrared (IR) and nuclear magnetic resonance (NMR) spectroscopy (Fig. **5**).

They postulated a pathway involving a bond rearrangement triggered by the *Michael* reaction type shift of the acidic proton to the *β*-carbon of the π-system (Fig. 6). The influence of the phosphine's steric demand and basicity on the reaction path was also revealed. While $PCy_3$ and $PEt(^tBu)_2$ favorably form the cyclic compound, a less basic P-ligand ($PEt_3$, $PPh_3$) promotes the reaction to the air-sensitive Ni(0) π-complexes.

Although the cyclic structures demand more space around the metal center, a larger cone angle of the phosphine ligand affords the lactone or lactam preferably. A bulky phosphine coordinates only via one equivalent, while less sterically crowded ligands form a nickel complex with two equivalents of phosphine. This leads to an even more occupied ligand sphere and therefore promotes the π-complex formation. An interconversion from the Ni(0) π-complex to the cyclic Ni(II) species can be observed for $(PCy_3)Ni$ by refluxing the reaction mixture in thf.

In 1982, Burkhart and Hoberg presented the first synthesis of a nickelalactone based on a C1 carbon source and an alkyne [9]. The reaction of Ni(cdt) with tmeda and $CO_2$ causes a disproportion to $Ni(CO)_4$ and $(tmeda)Ni(CO_3)$. In the presence of 2-butyne, this pathway is suppressed and affords the five-membered oxanickelacyclopentene derivative instead. Indirect proof of the structure was given upon hydrolysis or CO addition which leads to 2-methylcrotonic acid and dimethylmaleic anhydride, respectively (Fig. 7).

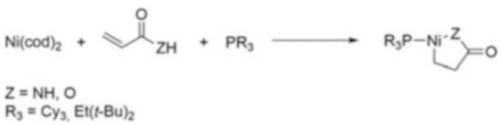


**Fig. 5** First published synthesis of nickelalactones and nickelalactams through addition of acrylic substrates by Yamamoto et al. [8]

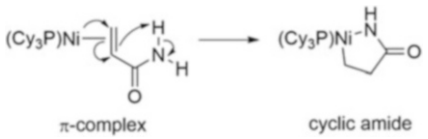


**Fig. 6** Postulated interconversion mechanism for the nickelalactam formation [8]

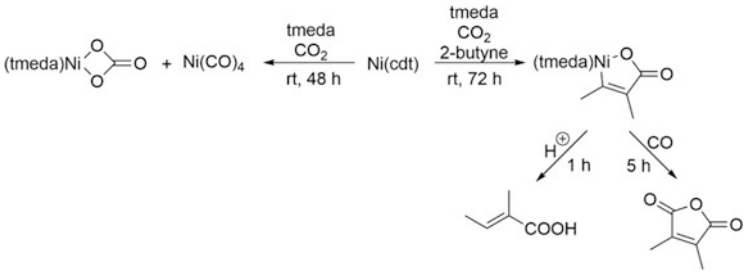


**Fig. 7** Reactivity of Ni(0) complexes toward $CO_2$ in the absence and presence of an alkyne [9]

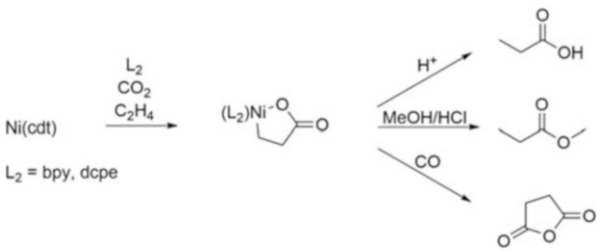


**Fig. 8** The first oxidative coupling with ethylene and $CO_2$ and subsequent conversion to organic compounds [5]

These findings were further investigated and extended to a vast variety of alkynes and subsequently to alkenes [10–13]. Activated alkenes like norbornene easily undergo a nickel-induced C–C bond formation [14]. The cyclic intermediate was not entirely characterized, but the saturated product *exo*-norbornane-2-carboxylic acid formed when HCl was added. To extend the library of utilized olefins, Hoberg employed chelating σ-donor ligands (i.e., 2,2′-bipyridine (bpy), 1,2-bis (dicyclohexylphosphino)ethane, (dcpe)) which are suitable for nonactivated alkenes like ethylene [5, 6]. In this case, the lactone formation occurs if $Ni(cod)_2$ is replaced by the more reactive $16e^-$ precursor Ni(cdt) in the absence of additional tmeda. Tmeda promotes the alternative pathway to the reductive disproportion of carbon dioxide as depicted in Fig. 7. Subsequent acidic hydrolysis of the cyclic compounds affords propionic acid and its methyl esters, whereas CO insertion liberates succinic anhydride (Fig. 8). Already in 1983, Hoberg declared these

findings as a first groundbreaking step toward nickel-catalyzed reactions of ethylene and its homologues with $CO_2$ to a huge variety of organic compounds [5].

## 2.2 *Utilization of Nickelalactones*

The research on the nickel-induced C–C coupling with $CO_2$ expanded tremendously in the following years. A wide range of linear [6] and cyclic olefins [15, 16], 1,2-dienes [13], 1,3-dienes [17–19], alkynes [10], imines, and aldehydes have been studied. Furthermore, the addition of specific promotors (electrophiles, acids, alkyl halides, CO) affords highly selective products from one nickelalactone intermediate, which makes them a versatile tool for organic compounds [20, 16]. The C–C bond formation of alkenes and its homologues affords saturated compounds; alkynes lead to products with an olefinic moiety. Depending on the auxiliary, the deactivation of the Ni complex or hydrolytic workup inhibits a catalytic approach though. Intramolecular reactions like $\beta$-H elimination and followed reductive elimination could avoid the use of promotors, but have been elusive so far. An exception is the depicted oxidative coupling of $(DBU)_2Ni(0)$, styrene, and $CO_2$ [21]. Depending on the reaction temperature, the isomers 2-phenylpropionic acid (A), 1-phenylpropionic acid (B), and additionally cinnamic acid (C) are isolated after hydrolysis. Oxidative coupling at 60°C promotes the formation of the saturated acids (A + B/C = 32/1), whereas a temperature increase to 85°C mainly yields cinnamic acid (A + B/C = 1/7). Derived from the product structure, a thermal $\beta$-H elimination is most likely initiated to afford the unsaturated alkyl species upon hydrolysis (Fig. 9). It was the first published synthesis of an α,β-unsaturated carboxylic acid from an olefin and $CO_2$. A catalysis has not been achieved as the regeneration of $(DBU)_2Ni(0)$ through reductive elimination was not observed. Hoberg assumed that H-migration to the ligand occurs and deactivates the nickel compound for recycling.

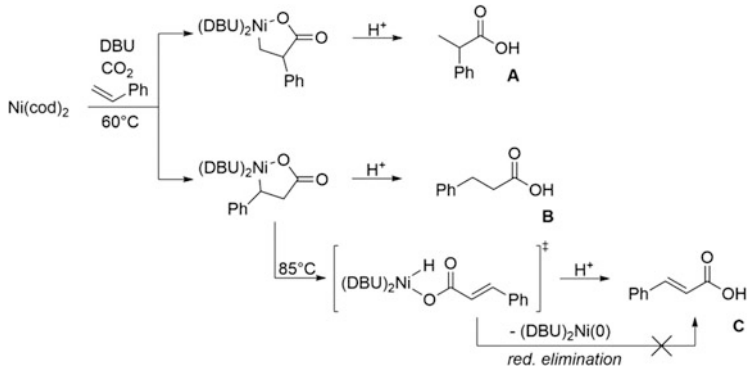


**Fig. 9** Synthesis of cinnamic acid from styrene via thermal $\beta$-H elimination by Hoberg et al. [21]

Besides the utilization of carbon dioxide, isoelectronic isocyanates have been explored, which react with C=N, C=O, or C=C double bonds in analogous manner affording imines, amides, carbamates, and ureas [22–29]. In contrast to the use of $CO_2$, catalytic conversions with isocyanates are possible.

## 2.3 Regioselectivity, Ring Contraction, and Expansion

The first mechanistic studies regarding the regioselectivity of monosubstituted alkenes in nickelalactones were reported for 1-hexene by Hoberg in 1984 [6]. The oxidative coupling for the two different occurring isomers was studied at 20 and 60°C (Fig. 10). Due to the higher stability of a metal–$C_{prim}$ bond, the lactone formation reveals a preference of product A over B. At 20°C an isomeric ratio of A/B = 4/1 is reached. With rising temperatures, the equilibrium shifts further to the thermodynamically favored product A (A/B = 25/1).

A subsequent treatment of a 4/1 mixture at 60°C affords a final ratio of A/B = 25/1, indicating that the C–C bond formation is a reversible step in the overall reaction. Various monosubstituted alkenes (e.g., propylene) reveal analogous regioselectivity, whereas specific ligands (i.e., (2-diethylaminoethyl)-dicyclohexylphosphine) are capable to invert the regioselectivity toward isomer B. Due to the electronic interactions of the precursors, the electrophilic $CO_2$ carbon favors the C–C bond formation with the nucleophilic C1 carbon of the alkene. The electronic effects play a bigger role than the thermodynamically favored formation of a M–$C_{prim}$ bond and are in good accordance with the observed regioselectivity in the coupling reaction of imines and aldehydes with $CO_2$ [30, 31]. Yamamoto et al. discovered similar M–$C_{sec}$ isomers [32] when ring contractions of six-membered nickelalactones occur (Fig. 11). The stability of six-membered nickelacycles is highly influenced by the employed auxiliary ligand.

Bulky ligands like 1,2-bis(diphenylphosphino)ethane (dppe) and its propyl-bridged homologue (dppp) cause a rapid isomerization to the methyl-substituted

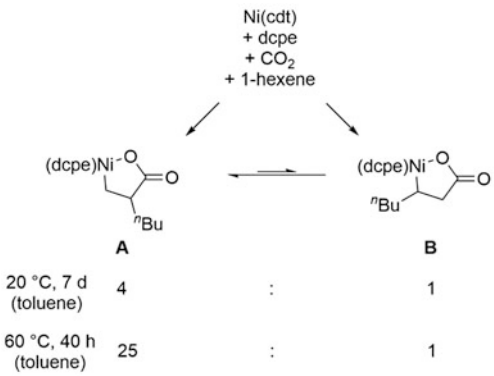


**Fig. 10** Regioselectivity and reversibility of the C–C bond formation with monosubstituted alkenes, Ni(cdt), and dcpe [6]

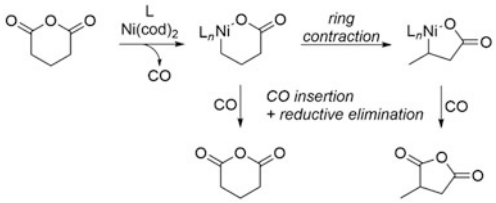


**Fig. 11** Ligand-induced ring contraction of six-membered nickelalactones [32]

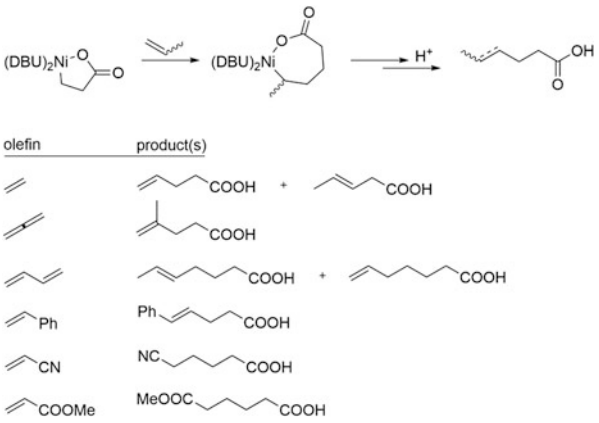


**Fig. 12** Reactions of $(DBU)_2$NiLac with C=C-containing substrates via ring expansion [34]

five-membered lactones, while less sterically demanding ligands like bpy in contrast do not induce a ring contraction. A similar trend can be observed for monodentate phosphines ($PPh_3 > PEtPh_2 > Pet_2Ph > PMePh_2 > PEt_3 > PMe_2Ph$) with regard to the Tolman's cone angle. In conclusion, a higher bulkiness of the ligand promotes the ring contraction. The degree of contraction was determined by the ratio of the respective methyl succinic anhydride and glutaric anhydride after treatment with CO. Approaches to perform the backward ring expansion were unsuccessful indicating an irreversible process due to the high stability of five-membered lactone species.

Ring expansions are accessible via insertion of olefinic compounds into the M–C bond of saturated nickelalactones bearing two 1,8-diazabicyclo[5.4.0]undec-7-ene (DBU) ligands [33, 34]. The widely used phosphines and bpy suppress this reaction pathway; respective products have not been isolated. By contrast, DBU promotes the subsequent incorporation of a second C=C double bond (Fig. 12). The five-membered lactone precursor expands to the seven-membered lactone and can be cleaved hydrolytically to obtain elongated and functionalized acids. In certain cases, $\beta$-H elimination occurs, resulting in the cleavage of the ring, formation of a Ni–H species, and regeneration of the olefinic function. The reductive elimination to the free acid and $(DBU)_2Ni(0)$ does not take place and therefore prevents a catalytic run. The same phenomenon was observed for the C–C coupling of styrene (Sect. 2.2) [21].

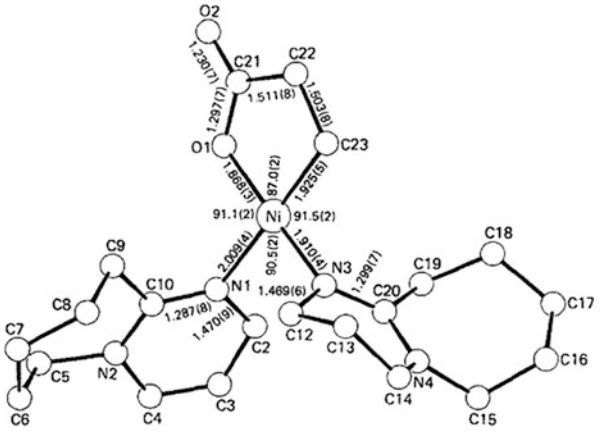


**Fig. 13** Crystal structure of $(dbu)_2$NiLac with a square-planar coordination sphere [34]

With the employment of DBU, a first successful X-ray crystal structure analysis was obtained for the five-membered nickelalactone consisting of $CO_2$ and ethylene (Fig. 13) [34]. The $16e^-$ complex revealed a square-planar coordination of the Ni atom, which is bound to the imine nitrogen of two DBU units. Due to the planar orientation, a nonbinding interaction of the metal with the hydrogen of $C_\alpha$ was excluded.

## *2.4 Preliminary Studies Toward Acrylic Acid*

The interest in the topic of nickelalactone utilization decreased in the 1990s leaving the question if a catalytic conversion for $CO_2$ could ever be realized. Despite a huge variety of synthetic methods, promotors, and ligands, each approach was limited to stoichiometric conversions at some point. Either the crucial $\beta$-H elimination or the reductive elimination did not occur. For this reason, alternative metal centers (Fe [35, 36], Pd [37, 38], Pt [39, 40], Ti [41], Zr [42], Rh [43], Mo [44, 45]) have been investigated. Nevertheless, Ni seemed to be the most versatile metal center in the C–C bond formation with olefins. In 2006, Walther et al. revived the vision of the catalytic conversion to acrylic acid. They postulated a theoretical catalytic cycle of the "dream reaction" (Fig. 14) [7]. The first step involves the oxidative coupling of a Ni(0) with ethylene and $CO_2$ and subsequent generation of an acrylate species via $\beta$-hydride elimination of the five-membered lactone. The reductive elimination of the Ni(II) center affords the π-coordinated acid which is released by ligand exchange with ethylene and hence closes the catalytic cycle.

One of the key steps in this catalytic cycle is the $\beta$-H elimination that has been elusive so far except for styrene (Sect. 2.2) [21]. Walther investigated phenyl-substituted bis(phosphine)s with different bridge lengths. They revealed that the reaction pathway upon addition of ligand to (tmeda)NiLac is strongly dependent on

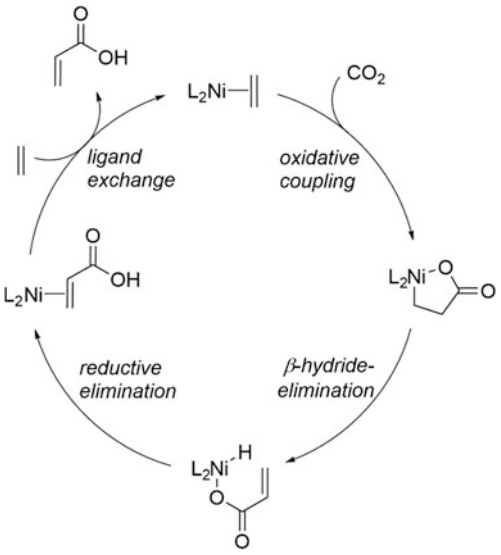


**Fig. 14** Hypothetical catalytic cycle to the formation of acrylic acid from ethylene and $CO_2$ via nickelalactone intermediates by Walther et al. [7]

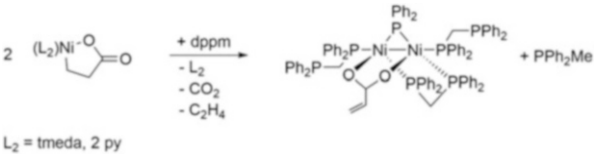


**Fig. 15** Synthesis of a bridged binuclear nickel-acrylate complex through $\beta$-H elimination [7]

the bridge length. Longer backbones either afford stable complexes (dppe), or a reductive decoupling (dppp, dppb) is induced, whereas the methylene-bridged ligand 1,1′-bis(diphenylphosphino)methane (dppm) promotes a $\beta$-H elimination and subsequent dimerization with the decoupled species $(dppm)_3Ni(0)$ to an acrylate-bridged compound (Figs. 15 and 16). However, reductive elimination from the complex to release the acrylate does not occur. Due to its stability and the sacrificial cleavage of one dppm ligand to form a phosphido bridge ($PPh2^-$), it cannot be utilized in further syntheses.

Further investigations by Walther focused on the ligand modification [46]. They obtained model compounds of the different postulated intermediates in the catalytic cycle employing rigid and bulky 1,1′-bis(di-*iso*-propylphosphanyl)ferrocene (d*i*ppf) and 1,1′-bis(diphenylphosphanyl)ferrocene (dppf) (Fig. 17). Depending on the substituents at the phosphorous atom and the synthetic strategy, a stable Ni (0) π-complex with coordinated acrylic acid, the corresponding nickelalactone, or the $Ni(0)(C_2H_4)$ π-complex is formed. Conversion of the cyclic compound to the ethylene complex was observed by $CO_2$ liberation; however, no isomerization of the lactone to the acrylic acid occurs.

Buntine et al. performed detailed computational calculations on the desired catalytic C–C coupling between $CO_2$ and ethylene mediated by the $(DBU)_2Ni$

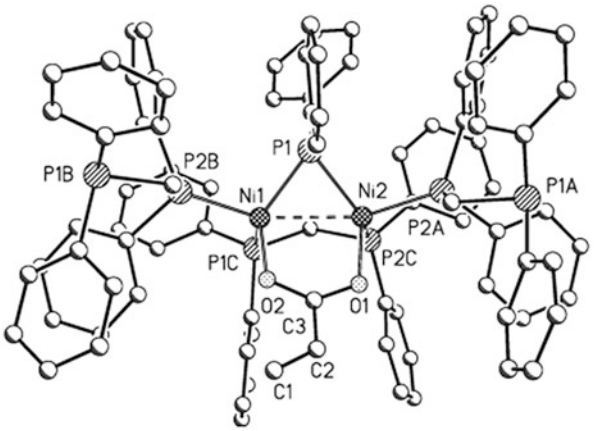


**Fig. 16** X-ray analysis of the binuclear Ni species with the acrylate-bridged ligand motif [7]

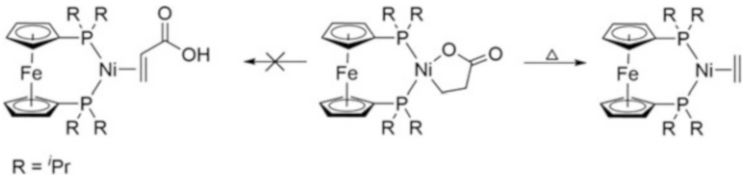


**Fig. 17** Synthesized model compounds bearing a rigid d*i*ppf ligand [46]

(0) catalyst [47]. The quantum mechanical data was elaborated using the model ligand (*m*DBU) in which the seven-membered ring was substituted by two methyl groups. It decreased the computational effort. The data reveals three main barriers in the catalytic reaction: (1) the oxidative coupling (+121.8 kJ/mol), (2) $\beta$-H elimination (+147.4 kJ/mol), and (3) the reductive elimination (+104.1 kJ/mol) through a most likely "five-center three-ligand" transition state. A transition structure for the $\beta$-H elimination in the five-membered nickelacycle proved unsuccessful due to the restricted geometry in the ring. Through an elongation of the Ni–O bond, the abstraction of the hydride may occur. With regard to the values, these barriers do not hinder the catalytic process at moderate reaction conditions; however, the overall endergonic reaction (+42.7 kJ/mol) of the catalytic cycle is most likely the biggest obstacle to overcome from a thermodynamic point of view. The deactivation pathway through H-migration of Ni–H to the N=C double bond of DBU has a moderate barrier (+150.2 kJ/mol), but the instability of the product (+102.1 kJ/mol) makes it negligible, in contrast to theories of Hoberg (Sects. 2.2 and 2.3) [34]. Prospective solutions have to improve the overall thermodynamics by removal of the acrylic acid and shift the equilibrium to the product site or modify the desired acrylic acid to improve the overall energy balance.

# 3 Liberation of Acrylates

## *3.1 Methylation of Nickelalactones*

Previous studies and DFT-based calculations lowered the expectations to realize a Ni(0)-catalyzed process to acrylic acid [47]. Therefore, novel approaches and strategies were required. In 2010, Rieger et al. reported the first liberation of an acrylate derivative via methylation of nickelalactones [48]. Upon addition of 2–100 equiv. of MeI to the reaction mixture of (dppp)NiLac in $CH_2Cl_2$, the respective methyl acrylate is obtained in yields up to 29%. Neat MeI increases the yield by 4%. The replacement of MeI with LiI yields 6% Li(acrylate) due to its low solubility and weaker interaction with the Ni–O bond. Other methylating agents like methyl triflate and trimethyloxonium tetrafluoroborate afford only traces of acrylate. Although only stoichiometric amounts of methyl acrylate were formed, a new hypothetic catalytic cycle was postulated (Fig. 18). After the oxidative coupling, the cleavage of the Ni–O moiety by MeI promotes the $\beta$-H elimination to release the desired methyl acrylate. The reductive elimination of the side product HI finally regenerates the Ni(0) catalyst.

Analogous to reactions of platina- [40] and palladalactones [49] with MeI, the methylation induces the elongation of the Ni–O bond, so that subsequent β-H elimination is promoted. Furthermore, the unfavored reductive elimination of a stable Ni–O bond is circumvented. Closure of the catalytic cycle was not achieved due to the formation of methyl propionate as by-product and unsuccessful recovery of the active species.

Limbach et al. performed deeper experimental and theoretical studies on the methylation with the d*t*bpe ligand (Fig. 19) [50]. They found out that the methylation most likely occurs at the carbonyl oxygen and proceeds via $S_N2$-type reaction with a low barrier. The methylated species equilibrates between a cationic four- and five-membered intermediate via $\beta$-H elimination. The final formation of methyl acrylate offers two possible pathways. Either a second nickelalactone deprotonates

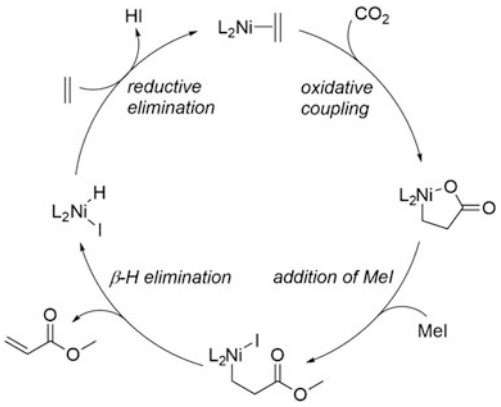


**Fig. 18** Postulated catalytic cycle for the formation of methyl acrylate from nickelalactones by Rieger et al. [48]

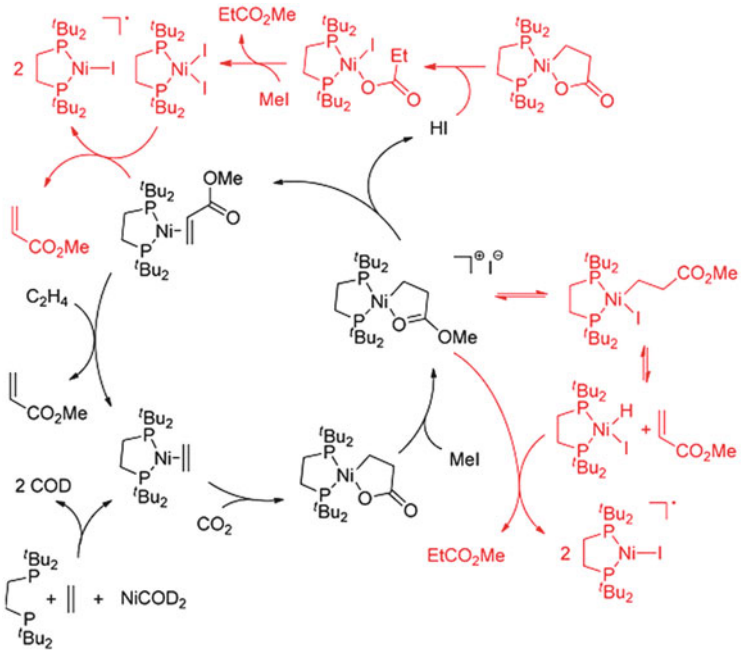


**Fig. 19** Hypothetic catalytic cycle forming methyl acrylate (*black*) and examined side reactions to methyl propionate (*red*) by Limbach et al. [50]

the cationic intermediate and affords the Ni(acrylate) π-complex, or the postulated *β*-H elimination occurs and liberates methyl acrylate from the complex. Furthermore, they identified unfavorable pathways, which inhibit a catalytic approach due to the formation of HI.

Due to the unselective reaction with MeI, a range of alternative methylating agents have been examined for various nickela- and palladalactones by Kühn [51, 52]. In contrast to results of Rieger and Limbach, methyl triflate turned out to be the most suitable cleavage agent under the chosen reaction conditions, independent of the auxiliary ligand. A fast transformation of the cyclic ester to the nickel hydride and the ring opening intermediate was observed via in situ H-NMR spectroscopy. A catalytic conversion was not performed though.

## *3.2 Lewis Acid-Induced β-H Elimination*

The spontaneous *β*-H elimination from a five-membered nickelalactone has not been observed so far, except for one styrene-based lactone [21]. However, the use of Lewis acids reveals a promoting effect on *β*-H elimination. When we take a look back, Hoberg added $BeCl_2$ to various substituted and unsubstituted nickelalactones

[53]. An immediate ring contraction occurs, most likely via $\beta$-H elimination and subsequent 2,1-insertion. Due to the ring strain and the Ni–$C_{sec}$ bond, the formed $\beta$-lactone structures exhibit a higher reactivity than their five-membered congeners and readily insert a second substrate to expand to a six-membered ring (Fig. 20). Therefore, the four-membered intermediate was not isolated. Via this route, geminal dicarboxylic acids are accessible by the addition of a second carbon dioxide. Again, the stability of the Ni–O moiety prevents a catalytic approach; hence, the acidic hydrolysis is essential to liberate the organic products.

Based on these results and observations with $Li^+$ [48], a similar strategy was published by Bernskoetter [54]. Treatment of nickelalactones, in this case (dppf) NiLac, with the strong neutral Lewis acid $B(C_6F_5)_3$ at rt promotes a rapid $\beta$-H elimination. The most likely formed nickel-acrylate hydride intermediate was not detected, but a subsequent 2,1-insertion affords the first stable four-membered $\beta$-lactone (Fig. 21). The X-ray analysis exhibits a formally zwitterionic product with the expected ring structure and the Lewis acid attached to the oxygen.

Further utilization of the $\beta$-lactone is possible via deprotonation with neutral organic bases. With DBU, unselective side reactions arise, and the Ni species partially decomposes, whereas BTPP selectively affords the deprotonated π-complex at rt after two days. From a mechanistic point of view, the source of the withdrawn proton is not identified. Most likely the deprotonation takes place from the nickel hydride intermediate. Alternative pathways like the proton abstraction from the $C_\alpha$ position in the four-membered ring or from the $CH_3$ group in $\beta$-position seem unlikely but cannot be fully excluded with regard to the $pK_a$ values of

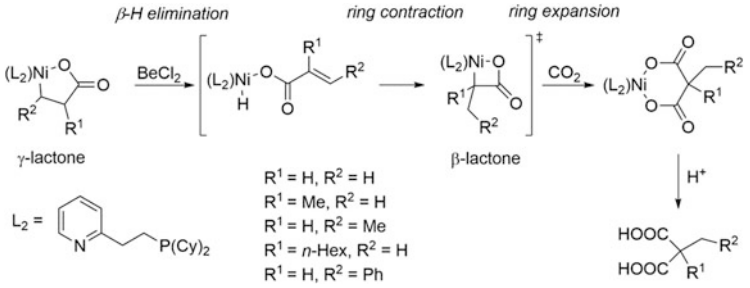


**Fig. 20** Postulated pathway to geminal dicarboxylic acids through Lewis acid-induced ring contraction by Hoberg et al. [53]

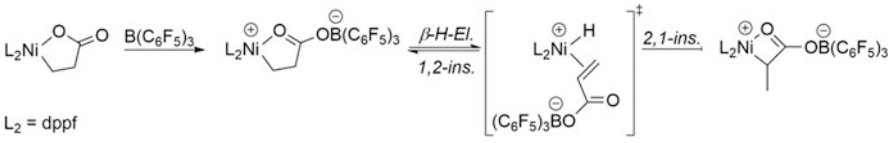


**Fig. 21** Lewis acid-induced transformation of a nickelalactone via $\beta$-H elimination and subsequent 2,1-insertion to the thermodynamically favored $\beta$-lactone [54]

the complex and the base. The subsequent ligand exchange readily occurs by addition of ethylene and expels the formed [BTPPH][($B(C_6F_5)_3$)(acrylate)]. However, the establishment of the last step of the catalytic cycle remained elusive, due to the fact that dppf does not induce an oxidative coupling with $CO_2$ under the investigated reaction conditions (Fig. 22).

Recently, Bernskoetter examined a strong influence of the chosen ligand on the lactone's reactivity [55]. Dcpm and its ethyl-bridged congener dcpe both perform the C–C bond formation of $CO_2$ and ethylene to the $\gamma$-nickelalactone in average to high yields (47% for dcpm, 88% for dcpe). Upon addition of a weak Lewis acid ($NaBAr^F{}_4$), the $Na^+$ coordinates to the carboxylic moiety. Subsequent heating to 55°C in thf induces a partial $\gamma$-to-$\beta$ isomerization ($\beta/\gamma = 1/3.5$ for dcpe, 1/8 for dcpm), verified by NMR spectroscopy and X-ray analysis. In contrast to the dcpm ligand, thf solutions of (dcpe)NiLac even isomerize in the absence of Lewis acid to an unactivated $\beta$-lactone. The unactivated species is less stable than the sodium adduct; therefore, a higher preference for the five-membered $\gamma$-lactone can be observed in equilibrium in this case (Fig. 23).

Computational analysis supports the beneficial effect of $Na^+$ on the $\gamma$-to-$\beta$ isomerization [55]. It provides a decrease of the ring strain in the formed $\beta$-lactone and stabilizes the negative charge of the carboxylic moiety in the transition state. The addition of suitable Lewis acids as cocatalysts that can bind reversibly to the carboxylic moiety to promote $\beta$-H elimination could introduce new strategies toward catalytic reactions.

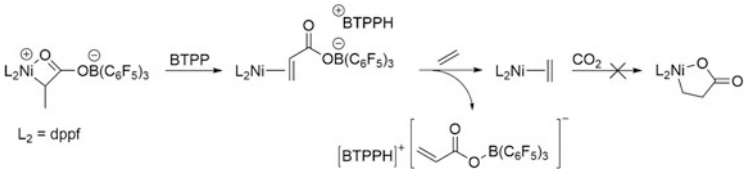


**Fig. 22** Deprotonation and subsequent release of the acrylic salt from a 2,1-insertion nickelalactone [54]

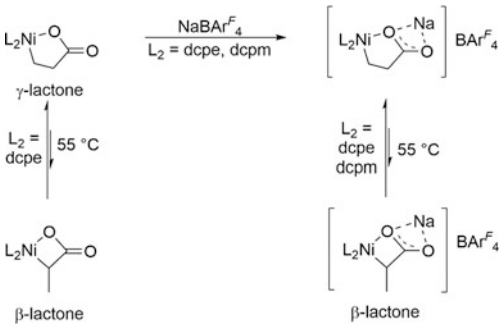


**Fig. 23** Lewis acid-assisted and Lewis acid-unactivated thermal isomerization to a $\beta$-lactone [55]

### 3.3 Catalytic Routes

The addition of cleavage auxiliaries has been broadly investigated recently. However, the employed electrophiles and Lewis acids do not lead to catalysis. Either one of the elementary steps remained elusive, or side reactions to inactive species occurred. Investigating a different approach, Limbach et al. reported in 2012 the first successful nickel-catalyzed synthesis of an acrylate, derived from carbon dioxide and ethylene (TON = 10) [3]. With the choice of a suitable ligand and the sacrificial use of a strong sodium alkoxide base, a selective catalytic reaction was established. Formation of Na(acrylate) as desired product shifts an overall endergonic reaction (for acrylic acid) [47] to a favorable exergonic process (−59 kJ/mol) (Fig 24) [56].

The initial step of the catalytic cycle represents the oxidative coupling. It reveals a strong influence by the chosen ligand. The literature-known ligands, i.e., bpy and DBU, only offer limited solubilities and stabilities; therefore, Limbach focused on *tert*-butyl and phenyl-substituted bis(phosphine)s with different bridge lengths ((–$CH_2$–)$_{1–3}$). The phenyl-substituted bis(phosphine)s rapidly form Ni(dppe)$_2$ and Ni(dppp)$_2$ upon addition of Ni(cod)$_2$, even in the presence of ethylene and $CO_2$. The use of bulky *tert*-butyl groups inhibits the deactivation by two ligands attached to one Ni(0) center. Due to their strong σ-donating properties, they rapidly form the corresponding π-ethylene complexes and subsequently induce the C–C bond formation with $CO_2$. This is in good accordance with a mechanistic point of view. The reaction is expected to occur through the C–C bond formation of an incoming $CO_2$

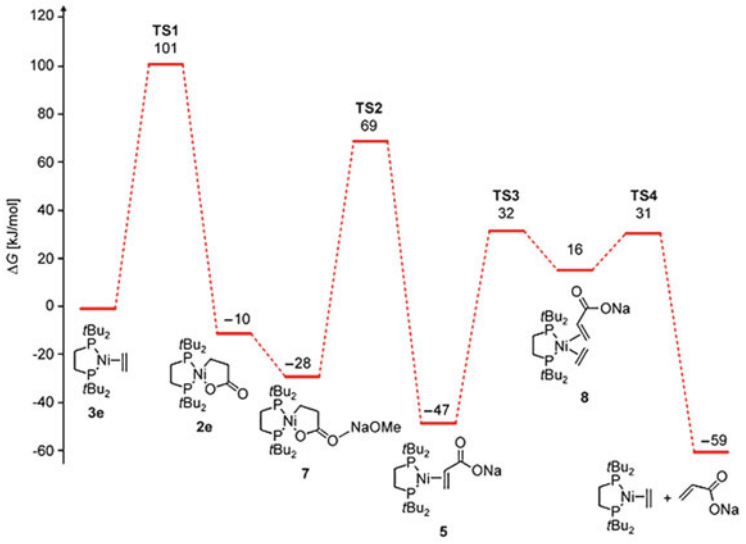


**Fig. 24** Quantum mechanical energy profile for the catalyzed synthesis of Na(acrylate) by Limbach et al. [3]

into a Ni–$C_2H_4$ bond; hence, the formation of a Ni-π-(ethylene) complex is crucial. With regard to the bridge length, only (dtbpe)NiLac forms a stable isolable compound, whereas (dtbpm)NiLac is only detectable under $CO_2$ pressure via $^{31}P$ NMR spectroscopy.

In the second step, strong sodium alkoxides induce a cleavage to the corresponding acrylate species. The role of the base has not been clearly confirmed yet since different mechanistic procedures seem possible according to the quantum mechanical calculations. This includes the deprotonation in the acidic α-position of the lactone with a subsequent rearrangement to the nickel π-acrylate species or the *β*-H elimination of an activated intermediate, as suggested for palladalactones by Aresta [38]. NaO$^t$Bu turned out to be the best suitable base under the investigated reaction conditions. Further studies have shown that the sodium cation, as well as the base, is crucial for the transformation to the acrylate. The quaternary ammonium salt $NBu_4OMe$ does not promote a lactone cleavage, whereas the supplementary addition of $NaBAr^F{}_4$ accomplishes the reaction with 47% yield. The last step requires a ligand exchange of the coordinated acrylate with ethylene to regenerate the potential catalyst. Due to a weaker π-back bonding of Na(acrylate) compared to Me(acrylate) or acrylic acid [3, 50, 56], the pressurized ethylene can release Na(acrylate) from the complex and hence close the catalytic route (Fig. 25). As a disadvantage, the presented catalysis has to be performed in two repetitive steps. Alkoxide bases irreversibly form carbonic half esters under $CO_2$ pressure, which inhibit a deprotonation. Therefore, the overall reaction is divided into a $CO_2$-rich (oxidative coupling) and $CO_2$-poor (cleavage and liberation) regime.

In further research, Limbach reported an optimized one-pot-catalysis (Fig. 26) [57]. Firstly, the sacrificial base was replaced by sodium phenoxides, due to their lower nucleophilicity. Hence, they are suitable bases under $CO_2$ pressure which do not form carbonate half esters. In correlation with the according p$K_a$ values (*ortho* < *meta* < *para*), sodium 2-fluorophenoxide reveals the highest activity of the tested substrates. NaOPh, Na(4-fluorophenoxide), and phenoxides with +I

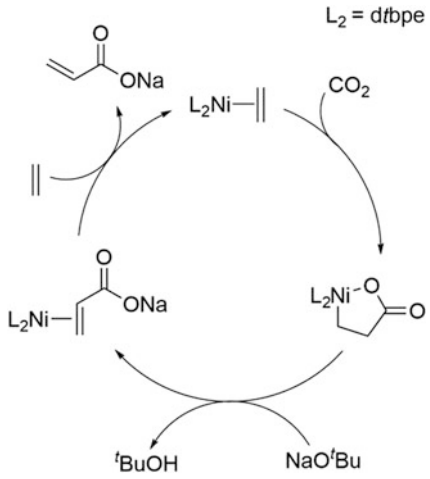


**Fig. 25** Ni(0)-catalyzed synthesis of Na(acrylate) from NaO$^t$Bu, $CO_2$, and ethylene [3]

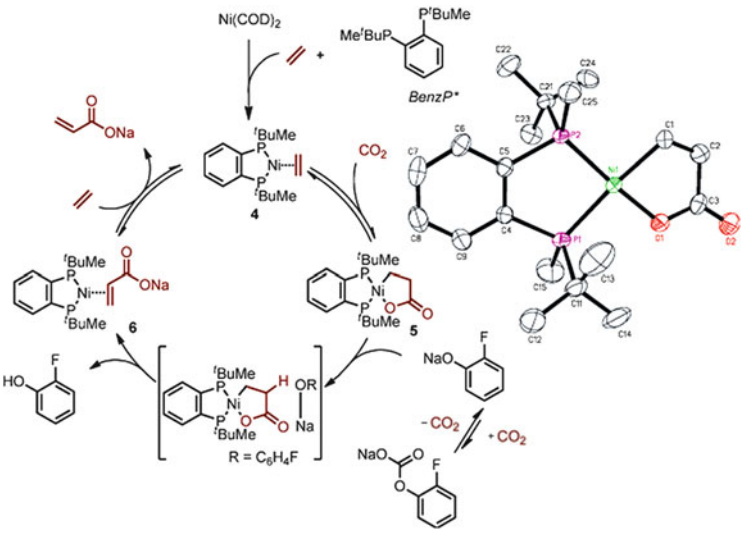


**Fig. 26** Advanced catalytic cycle with (BenzP*)Ni(0) as active species and X-ray structure of the lactone intermediate [57]

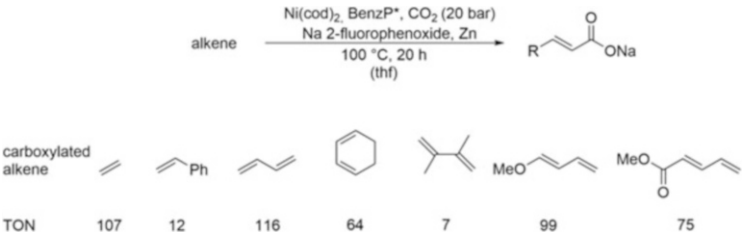


**Fig. 27** Excerpt of the carboxylated substrates via one-pot catalysis [57]

substituents exhibit significantly lower TONs. Studies on small-bite angle ligands (dtbpm, dppm), monodentate phosphines ($PPh_3$, $P^tBu_3$), and stereogenic bis(phosphine)s revealed the highest TONs for the chiral ligands (*S*)-BINAPINE, (*S*,*S*,*R*,*R*)-TangPhos, (*R*,*R*,*S*,*S*)-DuanPhos, and (*R*,*R*)-BenzP*. The addition of an excess of zinc has beneficial effects on the TON; however, the specific reason remained unclear.

Additional studies on various substrates have been performed with the BenzP* system at 100°C in thf. The direct carboxylation is applicable to a wide range of olefins including 1,3-dienes, styrenes, cycloalkenes, *Michael* acceptors, and functional group containing olefins; however, it exhibits the highest TONs for ethylene (TON = 107) and 1,3-butadiene (TON = 116) (Fig. 27). In the case of 2-vinylpyridine, styrenes, and 2,3-dimethyl butadiene, the catalytic activity dramatically decreases (TON = 2–12). Summarizing, a one-pot reaction with TONs > 100 was successfully developed, but TOF values up to 6 $h^{-1}$ still prevent this catalysis from applicability in a huge scale.

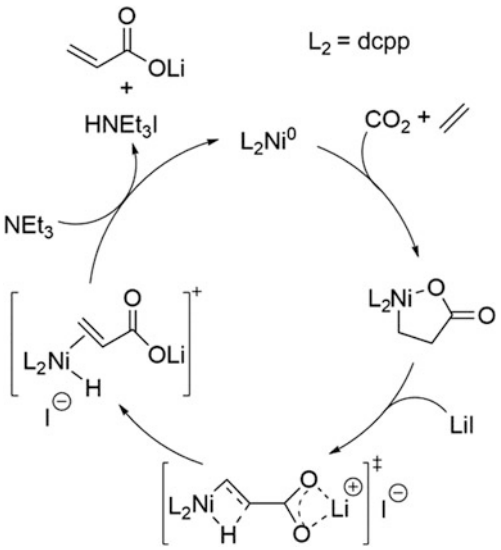


**Fig. 28** Proposed catalytic cycle for the acrylate formation upon addition of LiI by Vogt et al. [58]

Vogt et al. recently published an optimized version of Rieger's initial approach with MeI [48, 58]. They realized a catalytic formation from $CO_2$ and ethylene employing LiI as "hard" Lewis acid (Fig. 28). As examined and calculated for various Lewis acids [56, 55], the $Li^+$ cation elongates the carboxylic moiety and promotes $\beta$-H elimination. According to DFT calculations support the choice of $Li^+$ over $Na^+$, since the Gibbs free energy of the transition state (+104 kJ/mol without Lewis acid) is decreased by 20 kJ/mol for $Na^+$ and +40 kJ/mol for $Li^+$. Immediate release of the product and regeneration of the catalyst by trapping the formed HI with the base close the catalytic cycle. The role of the iodide remains unclear.

In order to suppress side reactions with the released HI (i.e., propionate), $NEt_3$ is added. D*I*PEA, $K_2CO_3$, and $Cs_2CO_3$ were less efficient. The addition of Zn dust prevented the formation of inactive $NiI_2$ species reaching a TON = 21 for dcpp after 72 h. Overall, a huge amount of sacrificial auxiliaries (base, Zn) is added to the reaction mixture, and the low TON values are far from a useful application in synthesis. But apart from Limbach's strategy involving sacrificial bases [57], the route by Vogt provides new opportunities to the formation of acrylates with Lewis acids.

## 4 Conclusion

Since the discovery of the nickel(0)-induced oxidative coupling of $CO_2$ and ethylene over three decades ago, the formed nickelalactones have been considered as potential intermediates in catalytic approaches. Initial investigations were focused on the stoichiometric conversion to useful organic compounds, e.g., saturated

carboxylic acids, esters, and anhydrides. Catalytic strategies however remained elusive. With regard to the synthesis of acrylates, the overall thermodynamics and the missing elimination reactions were pointed out as main obstacles in a catalytic formation.

After more than 25 years of research, the methylation of a nickelalactone with MeI afforded the first successful liberation of a methyl acrylate species. The methyl group elongates the Ni–O moiety and facilitates a subsequent $\beta$-H elimination to release the product. This route is accompanied by the formation of inactive Ni (II) compounds and by-products that can only be suppressed to a certain amount. Although limited to stoichiometric conversion, it was the basis for further experimental investigations and computational studies. Hence, a wide range of potential cleaving agents (i.e., electrophiles, Lewis acids) have been examined recently. Finally, two different catalytic pathways have been developed. In the presence of LiI, a catalytic conversion to Li(acrylate) with a TON = 21 was achieved. The $Li^+$ ion serves as Lewis acid and promotes the Ni–O bond dissociation. However the reaction is slow and occurring side reactions were suppressed upon stoichiometric addition of base and reducing agent. Sacrificial sodium alkoxide bases offer an alternative catalytic route via deprotonation of the lactone intermediate and subsequent transformation to sodium acrylate. By ligand modification, exploration of suitable bases, and optimization of the reaction conditions, one-pot catalysis with a TON > 100 was achieved. Further examinations will focus on the acceleration and versatility of the catalysis, since this system is not limited to ethylene only. In order to compete with the current oil-based industrial processes one day, the catalyst activities have to improve dramatically. With respect to the recent breakthrough in this field, one can be excited about prospective developments in the nickelalactone utilization. Due to the rising demand for fossil resources, novel and modern strategies like the catalytic $CO_2$-based C–C coupling with olefins to basic chemicals are highly demanded in the future.

## References

1. Behr A, Agar W, Joerissen J (2010) Einführung in die Technische Chemie. Spektrum Akademischer Verlag, Heidelberg
2. Aresta M, Dibenedetto A, Angelini A (2014) Catalysis for the valorization of exhaust carbon: from CO2 to chemicals, materials, and fuels. Technological use of $CO_2$. Chem Rev 114(3): 1709–1742. doi:10.1021/cr4002758
3. Lejkowski ML, Lindner R, Kageyama T, Bódizs GÉ, Plessow PN, Müller IB, Schäfer A, Rominger F, Hofmann P, Futter C, Schunk SA, Limbach M (2012) The first catalytic synthesis of an acrylate from CO2 and an alkene—a rational approach. Chem Eur J 18(44): 14017–14025. doi:10.1002/chem.201201757
4. Cokoja M, Bruckmeier C, Rieger B, Herrmann WA, Kühn FE (2011) Transformation of carbon dioxide with homogeneous transition-metal catalysts: a molecular solution to a global challenge? Angew Chem Int Ed 50(37):8510–8537. doi:10.1002/anie.201102010

5. Hoberg H, Schaefer D (1983) Nickel(0)-induced C-C bonding between carbon dioxide and ethylene as well as monosubstituted and disubstituted alkenes. J Organomet Chem 251(3): C51–C53. doi:10.1016/s0022-328x(00)98789-8
6. Hoberg H, Schaefer D, Burkhart G, Krüger C, Romão MJ (1984) Nickel(0)-induzierte C–C-verknüpfung zwischen kohlendioxid und alkinen sowie alkenen. J Organomet Chem 266(2): 203–224. doi:10.1016/0022-328X(84)80129-1
7. Fischer R, Langer J, Malassa A, Walther D, Gorls H, Vaughan G (2006) A key step in the formation of acrylic acid from CO2 and ethylene: the transformation of a nickelalactone into a nickel-acrylate complex. Chem Commun 23:2510–2512
8. Yamamoto T, Igarashi K, Komiya S, Yamamoto A (1980) Preparation and properties of phosphine complexes of nickel-containing cyclic amides and esters [(PR3)nNiCH2CH(R1) COZ (Z = NR2, O)]. J Am Chem Soc 102(25):7448–7456. doi:10.1021/ja00545a009
9. Burkhart G, Hoberg H (1982) Oxanickelacyclopentene derivatives from nickel(0), carbon-dioxide, and alkynes. Angew Chem Int Ed 21(1):76. doi:10.1002/anie.198200762
10. Hoberg H, Schaefer D (1982) Model complexes of nickel for the $2+2+2'$-cycloaddition of alkynes with carbon-dioxide. J Organomet Chem 238(4):383–387. doi:10.1016/s0022-328x(00)83800-0
11. Hoberg H, Apotecher B (1984) Alpha, omega-diacids from butadiene and carbon-dioxide on nickel(0). J Organomet Chem 270(1):C15–C17. doi:10.1016/0022-328x(84)80346-0
12. Hoberg H, Schaefer D (1983) Sorbic acid from piperylene and CO2 through C-C coupling on nickel. J Organomet Chem 255(1):C15–C17. doi:10.1016/0022-328x(83)80185-5
13. Hoberg H, Oster BW (1984) Nickel(0)-induced C-C bonding between 1,2-dienes and carbon-dioxide. J Organomet Chem 266(3):321–326. doi:10.1016/0022-328x(84)80145-x
14. Hoberg H, Schaefer D (1982) Nickel(0) induced C-C linkage between alkenes and carbon-dioxide. J Organomet Chem 236(1):C28–C30. doi:10.1016/s0022-328x(00)86765-0
15. Hoberg H, Ballesteros A (1991) Ni0-induzierte Herstellung cyclischer C8-Carbonsäuren aus Cyclooctenen und Kohlendioxid. J Organomet Chem 411(1–2):C11–C18. doi:10.1016/0022-328x(91)86033-m
16. Hoberg H, Ballesteros A, Sigan A, Jegat C, Milchereit A (1991) Durch (Lig)Ni(0) induzierte Herstellung von mono- und di-Carbonsäuren aus Cyclopenten und Kohlendioxid. Synthesis 1991(05):395,398. doi:10.1055/s-1991-26475
17. Hoberg H, Barhausen D (1989) Nickel(0)-induced CC coupling of CO2 with 1,3-butadiene for preparing linear C-13-acids. J Organomet Chem 379(1–2):C7–C11. doi:10.1016/0022-328x(89)80043-9
18. Hoberg H, Gross S, Milchereit A (1987) Nickel(0)-catalyzed production of a functionalized cyclopentanecarboxylic acid from 1,3-butadiene and CO2. Angew Chem Int Ed 26(6): 571–572. doi:10.1002/anie.198705711
19. Hoberg H, Schaefer D, Oster BW (1984) Diene carboxylic-acid from 1,3-dienes and CO2 through C-C bonding on nickel. J Organomet Chem 266(3):313–320. doi:10.1016/0022-328x(84)80144-8
20. Fischer R, Walther D, Braunlich G, Undeutsch B, Ludwig W, Bandmann H (1992) Nickelalactone als Synthesebausteine: Sonochemische und Bimetallaktivierung der Kreuzkopplungsreaktion mit Alkyl-halogeniden. J Organomet Chem 427(3):395–407. doi:10.1016/0022-328x(92)80077-b
21. Hoberg H, Peres Y, Milchereit A (1986) C-C coupling of alkenes with $Co_2$ in nickel(0) - production Of cinnamic acid in styrene. J Organomet Chem 307(2):C38–C40. doi:10.1016/0022-328x(86)80487-9
22. Hoberg H, Summermann K, Milchereit A (1985) CC bond formation of alkenes with isocyanates on NI-0 complexes - a new synthesis of acrylamides. Angew Chem Int Ed 24(4): 325–326
23. Hoberg H, Summermann K, Milchereit A (1985) C-C bond forming of alkenes with isocyanates on nickel(0). J Organomet Chem 288(2):237–248. doi:10.1016/0022-328x(85)87282-x

24. Hoberg H, Hernandez E (1985) Nickel(0)-catalyzed synthesis of sorbanilide from 1,3-pentadiene and phenyl isocyanate. Angew Chem Int Ed 24(11):961–962. doi:10.1002/anie.198509611
25. Hoberg H, Summermann K (1983) Diazanickelacyclopentanones synthesized from nickel(0), imines and isocyanates. J Organomet Chem 253(3):383–389. doi:10.1016/s0022-328x(00)99233-7
26. Hoberg H, Summermann K (1984) Nickel(0) catalyzed synthesis of imines from isocyanates and aldehydes. Z Naturforsch B 39(8):1032–1036
27. Hoberg H, Summermann K (1984) Nickel(0)-induced couples of benzaldehyde with isocyanates in nickel heterocycles. J Organomet Chem 264(3):379–385. doi:10.1016/0022-328x(84)85082-2
28. Hoberg H, Nohlen M (1991) Ni(O)-induced CC coupling of phenylisocyanate with cyclic 5-membered alkenes, catalytic preparation of beta, gamma-unsaturated carboxylic-acid anilides. J Organomet Chem 412(1–2):225–236. doi:10.1016/0022-328x(91)86057-w
29. Hoberg H, Hernandez E (1986) Intermolecular C-C bond-formation of azanickelacyclopentanone alpha, omega-diacid amides from alkenes and phenyl isocyanate. J Organomet Chem 311(3):307–312. doi:10.1016/0022-328x(86)80252-2
30. Kaiser J, Sieler J, Braun U, Golič L, Dinjus E, Walther D (1982) Aktivierung von Kohlendioxid an Übergangsmetallzentren: Kristall- und molekulstruktur von 2,2′-dipyridylnickela-5-methyl-2,4-dioxolan-3-on, einem Kopplungsprodukt von Kohlendioxid und Acetaldehyd am Zentralatom Nickel (0). J Organomet Chem 224(1):81–87. doi:10.1016/S0022-328X(00)82569-3
31. Walther D, Dinjus E, Sieler J, Kaiser J, Lindqvist O, Anderson L (1982) Aktivierung von kohlendioxid an übergangsmetallzentren: nickela(II)-heterocyclen aus kohlendioxid und azaolefinen am elektronenreichen nickel(0)-komplexrumpf. J Organomet Chem 240(3):289–297. doi:10.1016/S0022-328X(00)86795-9
32. Yamamoto T, Sano K, Yamamoto A (1987) Effect of ligand on ring contraction of six-membered nickel-containing cyclic esters, LnNiCH2CH2CH2COO, to their five-membered-ring isomers, LnNiCH(CH3)CH2COO. Kinetic and thermodynamic control of asymmetric induction by chiral diphosphines in the ring contraction. J Am Chem Soc 109(4):1092–1100. doi:10.1021/ja00238a017
33. Hoberg H, Peres Y, Milchereit A (1986) C-C coupling of alkenes with CO2 in nickel(0) - N-pentanoic acids in ethene. J Organomet Chem 307(2):C41–C43. doi:10.1016/0022-328x(86)80488-0
34. Hoberg H, Peres Y, Krüger C, Tsay Y-H (1987) A 1-oxa-2-nickela-5-cyclopentanone from ethene and carbon dioxide: preparation, structure, and reactivity. Angew Chem Int Ed 26(8):771–773. doi:10.1002/anie.198707711
35. Hoberg H, Jenni K, Angermund K, Krüger C (1987) C–C-linkages of ethene with CO2 on an iron(0) complex—synthesis and crystal structure analysis of [(PEt3)2Fe(C2H4)2]. Angew Chem Int Ed 26(2):153–155. doi:10.1002/anie.198701531
36. Hoberg H, Jenni K, Kruger C, Raabe E (1986) CC coupling of CO2 and butadiene on iron (0) complexes - a novel route to alpha-omega-dicarboxylic acids. Angew Chem Int Ed 25(9):810–811. doi:10.1002/anie.198608101
37. Osakada K, Doh MK, Ozawa F, Yamamoto A (1990) Catalytic and stoichiometric carbonylation of beta, gamma-unsaturated carboxylic acids to give cyclic anhydrides through intermediate palladium-containing cyclic esters. Organometallics 9(8):2197–2198. doi:10.1021/om00158a010
38. Aresta M, Pastore C, Giannoccaro P, Kovács G, Dibenedetto A, Pápai I (2007) Evidence for spontaneous release of acrylates from a transition-metal complex upon coupling ethene or propene with a carboxylic moiety or CO2. Chem Eur J 13(32):9028–9034. doi:10.1002/chem.200700532
39. Yamamoto T, Sano K, Osakada K, Komiya S, Yamamoto A, Kushi Y, Tada T (1990) Comparative studies on reactions of alpha, beta- and beta, gamma-unsaturated amides and

acids with nickel(0), palladium(0), and platinum(0) complexes. Preparation of new five- and six-membered nickel- and palladium-containing cyclic amide and ester complexes. Organometallics 9(8):2396–2403. doi:10.1021/om00158a041
40. Aye KT, Colpitts D, Ferguson G, Puddephatt RJ (1988) Activation of a.beta.-lactone by oxidative addition and the structure of a platina(IV)lactone. Organometallics 7(6): 1454–1456. doi:10.1021/om00096a039
41. Cohen SA, Bercaw JE (1985) Titanacycles derived from reductive coupling of nitriles, alkynes, acetaldehyde, and carbon dioxide with bis(pentamethylcyclopentadienyl)(ethylene) titanium(II). Organometallics 4(6):1006–1014. doi:10.1021/om00125a008
42. Burlakov VV, Arndt P, Baumann W, Spannenberg A, Rosenthal U (2006) Simple functionalizations of pentamethylcyclopentadienyl ligands by reactions of decamethylzirconocene complexes with carbon dioxide. Organometallics 25(5):1317–1320. doi:10.1021/om051063z
43. Aresta M, Quaranta E (1993) Synthesis, characterization and reactivity of [Rh(bpy)(C2H4)Cl]. A study on the reaction with C1 molecules (CH2O, CO2) and NaBPh4. J Organomet Chem 463(1–2):215–221. doi:10.1016/0022-328x(93)83420-z
44. Alvarez R, Carmona E, Cole-Hamilton DJ, Galindo A, Gutierrez-Puebla E, Monge A, Poveda ML, Ruiz C (1985) Formation of acrylic acid derivatives from the reaction of carbon dioxide with ethylene complexes of molybdenum and tungsten. J Am Chem Soc 107(19):5529–5531. doi:10.1021/ja00305a037
45. Alvarez R, Carmona E, Galindo A, Gutierrez E, Marin JM, Monge A, Poveda ML, Ruiz C, Savariault JM (1989) Formation of carboxylate complexes from the reactions of carbon dioxide with ethylene complexes of molybdenum and tungsten. X-ray and neutron diffraction studies. Organometallics 8(10):2430–2439. doi:10.1021/om00112a026
46. Langer J, Fischer R, Görls H, Walther D (2007) Low-valent nickel and palladium complexes with 1,1′-Bis(phosphanyl)ferrocenes: syntheses and structures of acrylic acid and ethylene complexes. Eur J Inorg Chem 2007(16):2257–2264. doi:10.1002/ejic.200601051
47. Graham DC, Mitchell C, Bruce MI, Metha GF, Bowie JH, Buntine MA (2007) Production of acrylic acid through nickel-mediated coupling of ethylene and carbon dioxide—a DFT study. Organometallics 26(27):6784–6792. doi:10.1021/om700592w
48. Bruckmeier C, Lehenmeier MW, Reichardt R, Vagin S, Rieger B (2010) Formation of methyl acrylate from CO2 and ethylene via methylation of nickelalactones. Organometallics 29(10): 2199–2202. doi:10.1021/om100060y
49. Kakino R, Nagayama K, Kayaki Y, Shimizu I, Yamamoto A (1999) Formation of a palladalactone complex by C–O bond cleavage of diketene promoted by a zerovalent palladium complex. Chem Lett 28(7):685–686
50. Plessow PN, Weigel L, Lindner R, Schäfer A, Rominger F, Limbach M, Hofmann P (2013) Mechanistic details of the nickel-mediated formation of acrylates from CO2, ethylene and methyl iodide. Organometallics 32(11):3327–3338. doi:10.1021/om400262b
51. Lee SYT, Cokoja M, Drees M, Li Y, Mink J, Herrmann WA, Kühn FE (2011) Transformation of nickelalactones to methyl acrylate: on the way to a catalytic conversion of carbon dioxide. ChemSusChem 4(9):1275–1279. doi:10.1002/cssc.201000445
52. Lee SYT, Ghani AA, D'Elia V, Cokoja M, Herrmann WA, Basset J-M, Kuhn FE (2013) Liberation of methyl acrylate from metallalactone complexes via M-O ring opening (M = Ni, Pd) with methylation agents. New J Chem. doi:10.1039/c3nj00693j
53. Hoberg H, Ballesteros A, Sigan A, Jégat C, Bärhausen D, Milchereit A (1991) Ligandgesteuerte Ringkontraktion von Nickela-fünf- in Vierringkomplexe—neuartige startsysteme für die präparative chemie. J Organomet Chem 407(3):C23–C29. doi:10.1016/0022-328x(91)86320-p
54. Jin D, Schmeier TJ, Williard PG, Hazari N, Bernskoetter WH (2013) Lewis acid induced β-elimination from a nickelalactone: efforts toward acrylate production from CO2 and ethylene. Organometallics 32(7):2152–2159. doi:10.1021/om400025h

55. Jin D, Williard PG, Hazari N, Bernskoetter WH (2014) Effect of sodium cation on metallacycle β-hydride elimination in CO2–ethylene coupling to acrylates. Chem Eur J 20(11):3205–3211. doi:10.1002/chem.201304196
56. Plessow PN, Schäfer A, Limbach M, Hofmann P (2014) Acrylate formation from CO2 and ethylene mediated by nickel complexes: a theoretical study. Organometallics. doi:10.1021/om500151h
57. Huguet N, Jevtovikj I, Gordillo A, Lejkowski ML, Lindner R, Bru M, Khalimon AY, Rominger F, Schunk SA, Hofmann P, Limbach M (2014) Nickel-catalyzed direct carboxylation of olefins with CO2: one-pot synthesis of α, β-unsaturated carboxylic acid salts. Chem Eur J 20(51):16858–16862. doi:10.1002/chem.201405528
58. Hendriksen C, Pidko EA, Yang G, Schäffner B, Vogt D (2014) Catalytic formation of acrylate from carbon dioxide and ethene. Chem Eur J. doi:10.1002/chem.201404082

Top Organomet Chem (2016) 53: 225–278
DOI: 10.1007/3418_2015_110

Published online: 28 May 2015

# Transition Metal-Catalyzed Carboxylation of Organic Substrates with Carbon Dioxide

**Marcel Brill, Faïma Lazreg, Catherine S.J. Cazin, and Steven P. Nolan**

**Abstract** The development of sustainable chemical processes is a long-standing challenge. Carbon dioxide represents a renewable C1 building block for organic synthesis and industrial applications as an alternative to other common feedstocks which are based on natural gas, petroleum oil, or coal. Apart from the advantages associated with the nontoxicity and abundance of $CO_2$, its utilization further enables the reduction in its atmospheric content, which contributes significantly to the greenhouse effect. Although widespread application of $CO_2$ in organic synthesis – even on an industrial scale – will not be able to fully compensate for the steadily increasing atmospheric quantities produced (mainly by the combustion of fuels), ecological and economical factors make its usage highly desirable. Therefore, tremendous efforts toward activation and utilization of $CO_2$ have been made by the scientific community over the last 30 years, and, as a result, the number of highly efficient transition metal-catalyzed $CO_2$-incorporative reactions has increased dramatically, especially within the last decade. The achievements in the development of sustainable and economic chemical processes for the carboxylation of organic molecules with $CO_2$ are presented in detail in this chapter.

**Keywords** Carbon dioxide · Carboxylation · Homogeneous catalysis · Sustainable chemistry · Transition metal

M. Brill, F. Lazreg, C.S.J. Cazin (✉), and S.P. Nolan (✉)
EaStCHEM, School of Chemistry, University of St Andrews, Purdie Building, North Haugh, St Andrews, Fife KY16 9ST, UK
e-mail: cc111@st-andrews.ac.uk; snolan@st-andrews.ac.uk

**Contents**



## 1 Introduction

The development of sustainable chemical processes is a long-standing challenge. Carbon dioxide represents a renewable C1 building block for organic synthesis and industrial applications as an alternative to other common feedstocks which are based on natural gas, petroleum oil, or coal [1]. Apart from the advantages associated with the nontoxicity and abundance of $CO_2$, its utilization further enables the reduction in its atmospheric content, which contributes significantly to the greenhouse effect. Although widespread application of $CO_2$ in organic synthesis – even on an industrial scale – will not be able to fully compensate for the steadily increasing atmospheric quantities produced (mainly by the combustion of fuels), ecological and economical factors make its usage highly desirable. Since the inherent thermodynamic and kinetic stability of $CO_2$ remains a critical challenge, sustainable and economic chemical processes are only to be realized if the development of milder reaction protocols for its conversion are achieved [2, 3]. For example, most of the few $CO_2$ transformations which have been commercialized still rely on the application of high-energy reaction partners such as epoxides [4]. Therefore, tremendous efforts toward activation and utilization of $CO_2$ have been made by the scientific community over the last 30 years, and, as a result, the number of highly efficient transition metal-catalyzed $CO_2$-incorporative reactions has increased dramatically, especially within the last decade (for a selection of recent reviews on the field: [5–8]).

This book chapter aims to provide a comprehensive summary on transition metal-catalyzed reactions involving the use of $CO_2$ in organic synthesis and its incorporation into typical organic substrates such as alkenes, alkynes, and various C–H and C–heteroatom bonds. Most topics presented in this book chapter will contain a summary of important seminal contributions to the substrate class of display, which often involve fundamental stoichiometric reactivities discovered mainly between the late 1970s and early 1980s that have been of great importance for the development of highly efficient catalytic processes.

Other exciting developments which are not strictly related to the application of $CO_2$ in classic organic synthesis are not covered within this chapter, such as the synthesis of renewable materials from polymers derived from cyclic carbonates [2, 3, 9, 10]. These heterocycles are generally accessed by the reaction between $CO_2$ and epoxides using Lewis acidic metal catalysts and have several other applications such as their use as environmentally benign polar aprotic solvents [11]. The polymers derived from cyclic carbonates can often be generated directly from starting materials in one pot.

Another very active area of research not addressed in this chapter deals with the conversion of $CO_2$ into other single carbon-containing molecules, either to access valuable building blocks for organic synthesis such as methanol and formic acid or in order to use these higher-energy compounds as renewable fuels [12, 13]. Works revolving around the recycling of $CO_2$ to methanol and its derived products have very recently been summarized by Goeppert, Prakash, and Olah and co-workers [14].

## 2 Carboxylation of Alkenes

### *2.1 Reactions with Group 11 Metals*

Group 11 transition metals have been used with preference in the carboxylation of alkyne substrates rather than alkenes, likely due to their pronounced ability to activate triple bonds (see Sect. 3.1). Therefore, the reported synthetic procedures for alkene carboxylation reactions are comprised of stepwise reaction sequences in which the alkene moiety is firstly transformed into a more reactive organoboron reagent which then undergoes a Cu(I)-catalyzed carboxylation of the C–B bond (see Sect. 4.1.1 for other C–B bond carboxylation reactions).

In 2011, the groups of Hou and independently Ohmiya, Sawamura, and co-workers developed the regioselective carboxylation of alkenes via a hydroboration/carboxylation sequence. In Ohmiya and Sawamura's methodology, mostly terminal alkynes were hydroborated by the 9-borabicyclo[3.3.1]nonane dimer ((9-BBN-H)$_2$) and then carboxylated using a mixture of CuOAc/phenanthroline catalyst (10 mol%) and KO*t*-Bu (1 equiv.) as base under an atmospheric pressure of $CO_2$ in toluene at 100°C [15]. The use of other diamines (2,2′-bipyridyine, TMEDA) and phosphine ligands ($PPh_3$, DPPE) or the defined complex [Cu(IPr)Cl](IPr = 1,3-bis(di-*iso*-propylphenyl)imidazol-5-ylidene) led to much lower conversions. A crucial parameter of the reaction conditions remained the temperature: at over 100°C (oil bath temperature), significant amounts of non-carboxylated but fully hydrogenated product were detected. The substrate scope demonstrated good functional group compatibility, tolerating, for example, silyl ether, ester, and amide moieties. Regarding the catalytic cycle (Fig. 1), a pathway proceeding via transmetalation from borate salt **A** (pathway I) rather than a stepwise mechanism proceeding via copper *tert*-butoxide complex **B** was believed to be operative (pathway II), since the coexistence of alkylborane and KO*t*-Bu as in pathway II was deemed improbable.

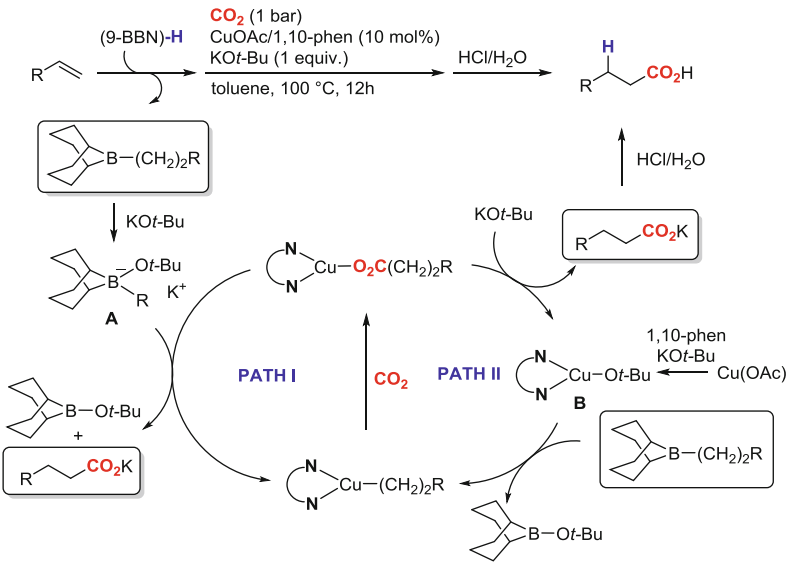


**Fig. 1** Copper-catalyzed hydroboration/carboxylation sequence (Ohmiya, Sawamura, and co-workers [15])

Hou and co-workers' methodology was based on the application of NHC–copper complexes [16]. In accordance with Sawamura's report, [Cu(IPr)Cl] was found to be only poorly effective in the hydrocarboxylation of the model substrate *p*-OMe-allylbenzene (35% isolated yield). However, using a less bulky alkoxide base such as M(OMe) (M = Na, Li) led to much higher yields. Thus, the efficacy of the process could be improved, requiring only 3 mol% copper catalyst and a lower reaction temperature of 70°C in comparison to the Sawamura procedure. Notably, the less sterically hindered complex [Cu(IMes)Cl] gave a much lower yield (41%). A wide variety of substrates bearing reactive functional groups such as alkyl halides or carbonyls were cleanly converted under atmospheric pressure of $CO_2$.

Stoichiometric reactions provided valuable insights into the possible reaction mechanism, which contrasted the mechanistic proposal of Sawamura's diamine-based system. The reaction of [Cu(IPr)OMe] with alkyl-(9-BBN) was shown to form a B–O adduct, which was characterized by X-ray diffraction analysis. This complex was converted to the corresponding alkylcarboxylate [Cu(IPr)$O_2$C-R] under $CO_2$ atmosphere at 70°C, suggesting that the transmetalation to generate [Cu(IPr)$(CH_2)_2$R] takes place in a similar fashion to pathway B, via a copper alkoxide (Fig. 1, phenanthroline ligand needs to be replaced by IPr in this case), which was found less likely to occur in Sawamura's system. It can be reasoned that since the use of the smaller lithium base leads to such a great difference in reactivity between the two protocols, the operative mechanism might also be different in each case. A pathway proceeding via adduct formation between the copper alkoxide and the alkylborane as suggested by Hou should indeed be favored by the use of a smaller base. It is also possible that the presence of a monodentate rather than bidentate ligand is in favor of such a pathway.

## 2.2 *Reactions with Group 10 Metals*

In 1976 Inoue and co-workers were the first to report a catalytic coupling reaction between butadiene and $CO_2$ using palladium(0) complexes such as $[Pd(dppe)_2]$ (dppe = bis(diphenylphosphino)ethane) and $[Pd(PPh_3)_4]$ (Fig. 2) [23]. Although the selectivity toward the $CO_2$-incorporated product, *E*-2-ethylidene-6-heptene-5-olide (in the following referred to as "δ-lactone"), was low (<13%, next to butadiene oligomers), an important foundation for future $CO_2$ insertion reactions into C–C multiple bonds was established. Mechanistically, the reaction was proposed to proceed via oxidative coupling of two butadiene molecules to form the bis-π-allyl complex **1**, followed by $CO_2$ insertion into one of the internal Pd–C bonds of the allyl fragments. The π-allyl palladacycle **2** can follow several pathways to give isomers of long-chain carboxylic acid esters or γ-lactones, but it is the cyclization reaction to give the δ-lactone intermediate **3** that proceeded with some preference. Shortly after, Musco was able to obtain significantly increased yields of carboxylated products, albeit still as a mixture of butadiene-derived octadienyl esters and δ- and γ-lactones (see Fig. 2) [19, 20]. However, certain bulky, monodentate phosphines used in a four- to sixfold excess to $[Pd(\eta^3\text{-methylallyl})(OAc)_2]$ (1.2 mol%) were able to control the product distribution to some extent, thus generating the δ-lactone as the main product in up to 28% yield (80–100 bar $CO_2$, 70°C) [20].

These discoveries led to profound interest in the selective synthesis of the **δ**-lactone. Thus, several works from the laboratories of Behr [21, 22, 24], Dinjus [25, 26], and Braunstein [27] were aimed at obtaining a deeper understanding of the operative mechanism for this and related coupling reactions in order to control the selectivities of these processes. These approaches have mainly remained focused on the application of bulky phosphine ligands.

In 1997, an interesting improvement concerning the design of new ligands for this reaction was made by Pitter and Dinjus [28], who, in a previous report, had

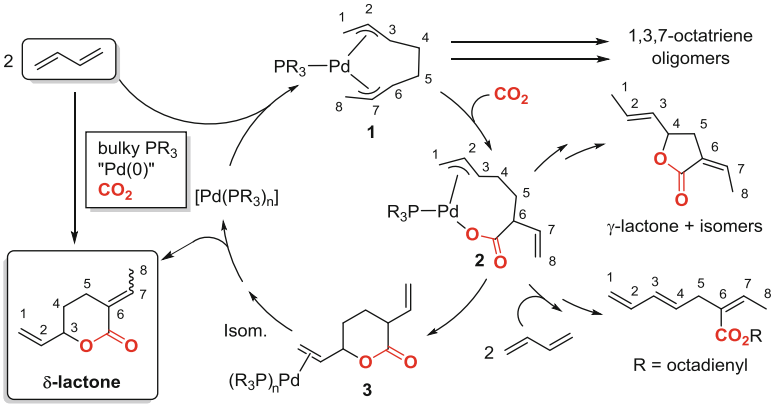


**Fig. 2** Catalytic synthesis of a δ-lactone from butadiene and $CO_2$ (adapted from seminal works by the groups of Inoue [17, 18], Musco [19, 20], and Behr [21, 22])

pointed out the beneficial effect of using a coordinating solvent, such as MeCN. Based on this knowledge, the phosphine ligand was modified into a hemilabile P, N-donor system. By placing an alkyl chain tethered cyano donor group next to a bulky $PR_2$ unit (e.g., in $(i\text{-Pr})_2\text{P-}(CH_2)_6CN$), the reaction maintained its high selectivity toward the δ-lactone, while enabling it to perform the reaction under solvent-free conditions, which is very desirable from a technical perspective. Notably, Behr and co-workers reported the design of various miniplant-scale setups [29–31].

Due to its particular relevance for a potential industrial $CO_2$ application (butadiene is a large-scale industrial $C_4$ building block), the δ-lactone was studied further in reactions aiming at its conversion into other value-added products (e.g., hydrogenation, epoxidation, and others) [32] and was investigated in polymerization reactions as a monomer building block [33–35]. In particular, radical polymerizations involving the δ-lactone have very recently rekindled interest in the palladium-catalyzed telomerization of butadiene and $CO_2$ [34]. Nozaki and co-workers have been able to combine the telomerization and polymerization steps into a one-pot copolymerization process. The polymer obtained thereby showed an overall $CO_2$ incorporation of 33% and a molecular weight of up to 85,000 [35].

Catalytic nickel-mediated coupling reactions of alkenes and $CO_2$ appeared much later, after a period of extensive research on the stoichiometric reactivity of Ni (0) metal centers toward unsaturated substrates. During the first half of the 1980s, Hoberg and co-workers were able – among others – to demonstrate various oxidative couplings between $CO_2$ and alkenes [36, 37], dienes [38, 39], alkynes [40–42], and allenes [43], leading to a deeper understanding of the elementary steps involved in these processes. For example, it was revealed that a very common pathway of $CO_2$ activation at Ni(0) metal centers proceeds via the formation of five-membered-ring nickelalactones. These compounds have been isolated and characterized via X-ray diffraction analysis in various studies [37, 44]. This enabled the possibility to study their reactivity toward further insertion reactions separately. For example, the double carboxylation of butadiene or the sequential coupling of $CO_2$ with two different monoolefins could thus be investigated in a stepwise fashion (Fig. 3) [37, 39].

Hoberg's works further led to the identification of a range of privileged ligands for the generation of stable congeners of these compounds such as the basic amines, TMEDA, and DBU (tetramethylethylenediamine and 1,8-diazabicyclo[5.4.0] undec-7-ene, respectively) which would be used with some preference in $CO_2$-incorporative nickel-mediated reactions in the following years. However, also phosphine ligands and more recently *N*-heterocyclic carbene (NHC) ligands have found application in several occasions (see next section).

Based on these stoichiometric studies and Inoue's seminal palladium-catalyzed reactions, Hoberg and co-workers were able to demonstrate in 1987 that similar reactivity patterns also apply for catalytic C–C couplings between alkene double bonds and $CO_2$ at Ni(0) metal centers [45]. A procedure was developed in which butadiene and $CO_2$ were converted into a cyclopentanoic acid derivative with high selectivity (Fig. 4), unlike Inoue's palladium-catalyzed reaction, which preferably

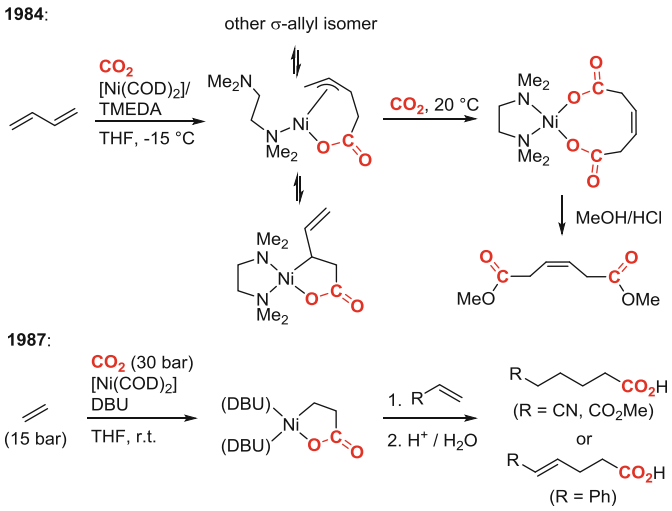


**Fig. 3** Selected examples of nickelalactone formation via oxidative coupling reactions between $CO_2$ and alkenes at Ni(0) metal centers and their further reactivity (Hoberg and co-workers [37, 39])

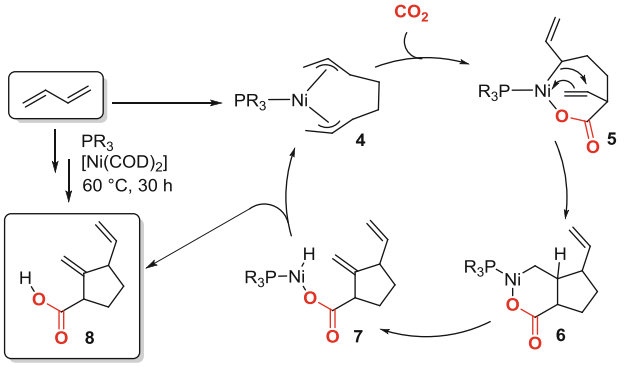


**Fig. 4** Nickel-catalyzed synthesis of a cyclopentanoic carboxylic acid from butadiene and $CO_2$ (Hoberg et al. [45])

gives the δ-lactone under certain reaction conditions (see above). Again, a bis-π-allyl complex (**4**) known from butadiene telomerization reactions [46] was proposed to form prior to the insertion of $CO_2$. In this process, the lactone intermediate **5** was proposed to rearrange to the bicyclic nickelalactone **6**, which then undergoes β-hydride elimination followed by reductive elimination to release the carboxylic acid **8** under reformation of Ni(0). The selectivity of the process was increased dramatically in favor of the cyclopentanoic acid by using P(O-*i*Pr)$_3$ in place of $PPh_3$. Notably, this was not the first $CO_2$-incorporating nickel-catalyzed process which proceeded with high selectivity. Walther and co-workers had discovered shortly before that the formal [2 + 2 + 2] cycloaddition of alkynes and $CO_2$

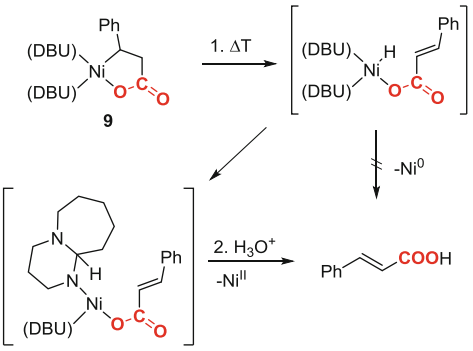


**Fig. 5** Formation of cinnamic acid from nickelalactone **9** at elevated temperatures (adapted from works of Hoberg and co-workers [36, 37, 45])

can selectively be catalyzed at Ni(0) metal centers bearing $PEt_3$ as ligand (see Sect. 3.2) [47].

To this day, the carboxylation of monoolefins, in the absence of external reductants, remains one of the biggest challenges for catalytic nickel chemistry. Unlike the previously discussed coupling between butadienes and $CO_2$, for which catalytic processes are made possible due to the formation of larger metallacyclic structures which possess the appropriate geometries for reductive elimination pathways, the reformation of Ni(0) from five-membered-ring nickelalactones is not trivial due to geometric constraints.

However, Hoberg and co-workers were able to show early on that the nickelalactone **9** (Fig. 5) could deliver cinnamic acid at elevated temperatures (and after acidic workup), yet the reaction could not be converted into a catalytic process [36]. The reason for this was explained by the non-innocent behavior of the ligand: the amidine double bond inserts into the Ni–H bond which forms via β-hydride elimination from the nickelalactone. Therefore, reductive elimination of the cinnamic acid cannot take place in the presence of this ligand system, and thus, the Ni(0) species required for catalysis to take place is not reformed. Considerable efforts have therefore been made to understand and overcome these downfalls by rational ligand design and by computational means (see Sect. 2.2.1).

### 2.2.1 Nickel-Catalyzed Reactions

**Dienes** Since the pioneering works of Hoberg, reports on catalytic $CO_2$ transformations involving alkenes and group 10 metals have strongly focused on the use of nickel precatalysts.

In 2002, the group of Mori expanded the ring-closing/carboxylation methodology to bis-1,3-dienes as substrates [48]. This work was based on previously gained insights into the stoichiometric reactivity of oxo-π-allyl nickel complexes (obtained from butadienes and $CO_2$) toward organozinc reagents (Fig. 6) [49]. While in the presence of $Ph_2Zn$ the reaction yielded isomers of monocarboxylic acids with a phenyl group incorporated into the products, the analogous reaction involving $Me_2Zn$ yielded a dicarboxylated product without methyl group incorporation.

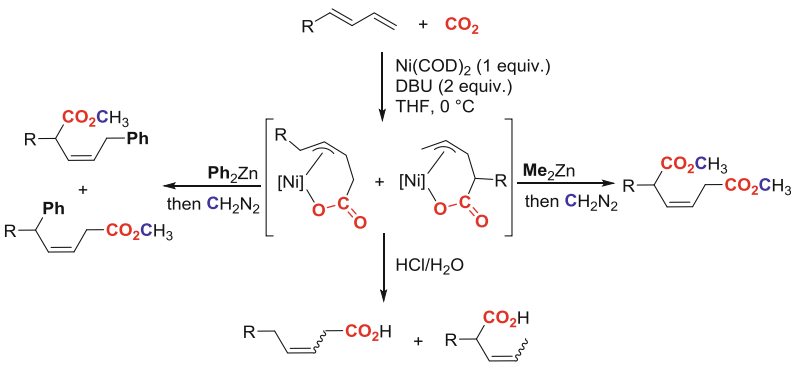


**Fig. 6** Stoichiometric reactivity of oxo-π-allyl nickel complexes (Mori and co-workers 2001 [49])

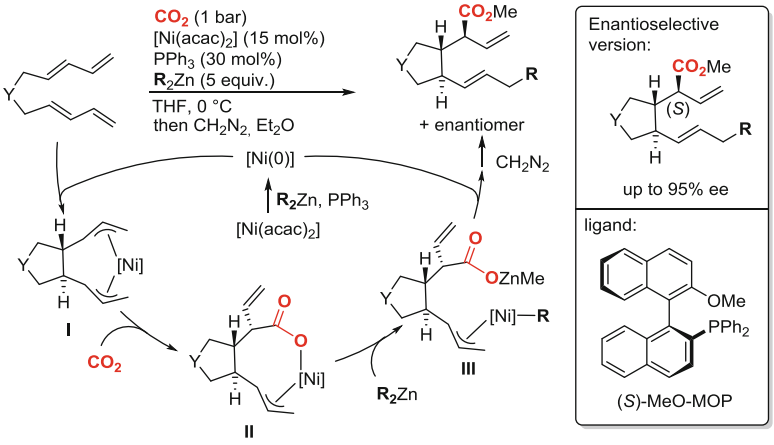


**Fig. 7** Carboxylative cyclization of 1,3-bis-butadienes (Mori and co-workers, 2003–2004 [48, 50])

The carboxylative cyclization of bis-1,3-butadienes followed 1 year later and proceeded in a highly regio- and stereoselective fashion. At atmospheric $CO_2$ pressure, using catalytic amounts [Ni(acac)$_2$] (15 mol%) and $PPh_3$ in a 1:2 ratio and an excess of stoichiometric reductant $R_2Zn$, the reaction afforded *anti*-disubstituted cyclopentane derivatives with the former methyl or phenyl moiety of the organozinc reagent attached to the terminal position of a 1-butenyl chain (Fig. 7). Mechanistically, the reaction was proposed to proceed most likely, once again, via initial formation of a bis-π-allyl system **I** at an in situ-generated Ni(0) metal center, which is accompanied by ring closure due to the linked nature of the two butadiene fragments. The following $CO_2$ insertion proceeds, as in previously discovered processes, regioselectively with preference for an internal σ-allyl C–Ni bond (not specifically shown in Fig. 7). The carboxylato–π-allyl nickelacycle **II** is then ring-opened by reaction with the organozinc reagent and the product released via reductive elimination, which proceeds regioselectively to the terminal position of the π-allyl system. The same group managed to develop the enantioselective

version of this process. By using an axially chiral phosphine in place of $PPh_3$ delivered the product with (*S*)-configuration at the C-2 position in generally high enantioselectivities and yields [50]. Most importantly, this methodology represents the first enantioselective nickel-catalyzed reaction proceeding under C–C bond formation with $CO_2$.

**Allenes** An interesting reaction type was discovered by Mori and co-workers while studying the carboxylation of allenes using their protocol consisting of $[Ni(COD)_2]$ and excess amounts of DBU and organozinc reagent ($Me_2Zn$) [51]. Surprisingly, a double carboxylation of TMS-substituted allenes was achieved under mild conditions (r.t./1 bar $CO_2$) (Fig. 8) as had been previously observed in the stoichiometric double carboxylation of butadienes with the same reagent [49]. Therefore, $Me_2Zn$ solely took on the role of reducing agent for the regeneration of the zero-valent nickel catalyst. Not even trace amounts of a product with incorporation of the organozinc's methyl group were detected in this reaction (Fig. 8).

**Monoalkenes** In the presence of an excess of a stoichiometric reductant such as $Et_2Zn$ (2.5 equiv.), the carboxylation of styrene derivatives was shown to proceed under mild conditions by Rovis and co-workers [52]. Using $[Ni(COD)_2]$ (10 mol%) in the presence of different N- and P-based ligands (20 mol%), it was discovered that only very basic amine ligands like DBU and pyridine proved effective in the carboxylation of *p*-$CO_2$Me-styrene at atmospheric $CO_2$ pressure, suggesting a pH-driven process rather than a ligand effect. This prompted the authors to screen simple inorganic bases as well. Thus, in the carboxylation of the less reactive unsubstituted styrene, $Cs_2CO_3$ was found to be even more effective than DBU and KHMDS. Additionally, it was discovered that the air-stable Ni(II) salt ($[Ni(acac)_2]$) promoted the reaction just as efficiently as the Ni(0) compound. Various styrene derivatives, bearing different functional groups such as carbonyls, esters, nitriles, and halides, were carboxylated in moderate to high yields and perfect regioselectivities. However, electron-donating substituents were only tolerated in the *meta*-position of the aryl moiety. Interestingly, the reaction was proposed to proceed via hydronickelation of the alkene followed by carboxylation rather than a pathway involving nickelalactones. The necessary nickel hydride species for this process is generated by the initial transmetalation reaction between $Et_2Zn$ and the nickel salt, followed by β-hydride elimination and ethane release.

A recent DFT study found support for the nickel hydride mechanism being slightly preferred over an oxidative coupling mechanism [53]. However, in this case, spectator ligands such as DBU were used in the calculations (Fig. 9).

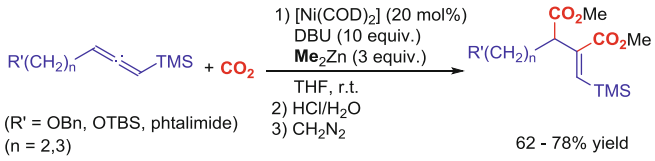


**Fig. 8** Double Carboxylation of Trimethylsilylallene (Mori and co-workers [51])

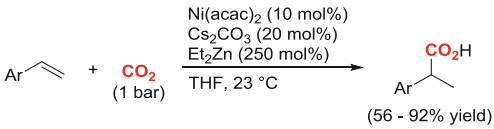


**Fig. 9** Reductive carboxylation of styrene derivatives (Rovis et al. [52])

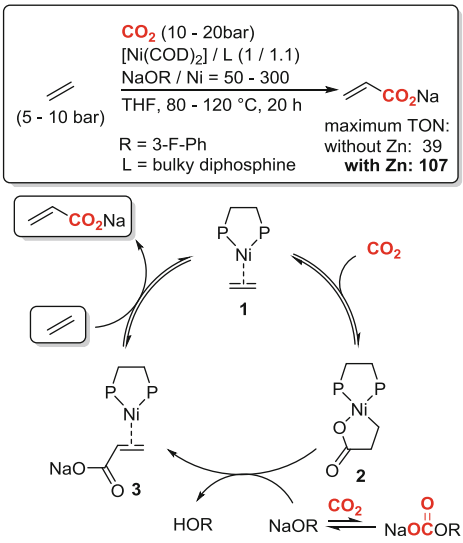


**Fig. 10** First catalytic synthesis of sodium acrylate (adapted from reports by Limbach and co-workers [62, 66])

On the other hand, in the absence of a stoichiometric reductant, the catalytic carboxylation of monoolefins to give acrylic acid derivatives is not straightforward due to the challenging β-hydride elimination step from nickelalactone intermediates as shown initially by Hoberg in the 1980s. However, later considerations revealed that the release of acrylic acid is also thermodynamically unfavored [54, 55]. As a result, the cleavage of nickelalactones by various electrophiles such as alkyl halides (see, e.g., [56–58]), protons (see, e.g., [59, 60]), and Lewis acids (see, e.g., [60, 61]) has been studied, but a catalytic process could not be established until a recent report by Limbach and co-workers [62].

The first catalytic synthesis of sodium acrylate was achieved in a two-step protocol and is based on the use of a strong sodium alkoxide base which, firstly, facilitates the kinetically challenging nickelalactone cleavage via α-deprotonation. Secondly, concerning the overall reaction, this procedure leads to the exergonic formation of an acrylate rather than acrylic acid, which is endergonic [63]. Using the bulky bisphosphine dtbpe (di-*tert*-butylphosphinoethane) and $[Ni(COD)_2]$, the initial coupling of ethylene and $CO_2$ gave the corresponding nickelalactone **1** (Fig. 10). The second part of the protocol involves the cleavage of the nickelalactone by sodium *tert*-butoxide to give the Ni(0) sodium acrylate complex **2**, which required the absence of $CO_2$ due to a competing irreversible formation of the corresponding carbonic half ester (see Fig. 10). In the final step sodium acrylate is liberated by ligand exchange with ethylene. By repeating these steps a TON of

greater than 10 was achieved, which marked an important step in possibly turning this so-called dream reaction into a viable process. Within a short period of time, several theoretical and mechanistic studies were carried out based on the findings of this exciting process and the role of alkaline metal cations in the cleavage of the lactone, which demonstrate the significant interest this report has created [63–65].

Limbach and co-workers have recently been able to introduce a refined catalytic system based on the application of 2-fluorophenoxide as base which enabled the reaction to be carried out as a one-pot process [66]. This base is of reasonably poor nucleophilicity to avoid its trapping by $CO_2$ but is sufficiently basic to allow deprotonation of the nickelalactone. Further, the efficiency of the process could be improved to a TON of up to 39 by the use of other five-membered-ring diphosphine chelating ligands and even up to 107 in the presence of zinc metal. Notably, the procedure was demonstrated to be applicable to styrenes and 1,3-dienes, giving the α,β-unsaturated carboxylic acids in high selectivity for the linear products with TONs of up to 116 (butadiene carboxylation).

Independently, Vogt and co-workers were also able to develop a simple one-pot catalytic procedure for the synthesis of lithium acrylate [67]. Key to success was the discovery that an excess of lithium iodide promotes the cleavage of diphosphine nickelalactones in the presence of $Et_3N$ as the base. A TON of up to 21 was achieved in the presence of Zn metal using dcpp (bis-(dicyclohexylphosphino) propane) as spectator ligand.

### 2.2.2 Palladium-Catalyzed Reactions

Considering the pioneering role of palladium-based catalysts in the carboxylation of dienes, the number of reports on novel methodologies has remained small in comparison to those based on nickel. After their seminal report, Inoue and co-workers were able to demonstrate in 1979 that methylenecyclopropanes, containing highly reactive double bonds, can be converted into five-membered lactones in a catalytic fashion using a system comprised of $[Pd(dba)_2]$ and $PPh_3$ (4:1) under forcing conditions (40 bar $CO_2$, 130°C) [17]. Based on earlier reports on the reaction of methylenecyclopropanes and alkenes [68], the reaction was proposed to proceed similarly via intermediate trimethylenemethane–palladium complexes which react with $CO_2$ in a [3 + 2] cycloaddition.

Recently, Takaya and Iwasawa reported the regioselective hydrocarboxylation of terminal allenes at the internal, substituted carbon atom (Fig. 11) [69]. The transformation was catalyzed by a palladium PSiP-pincer complex in DMF under mild conditions (1 bar $CO_2$, r.t. – 50°C) in the presence of $AlEt_3$ as the hydride source. The regioselectivity was proposed to arise from the fact that the insertion of the allene system into the in situ-generated Pd–H bond (of **1**) preferably gives the allyl intermediate **2** due to steric reasons. A following nucleophilic addition of the σ-allyl fragment to the $CO_2$ molecule is enforced at the γ-position due to the electron-rich and strained nature of the pincer ligand to give the carboxylato complex **3**. The product is released in the form of an aluminum salt by a

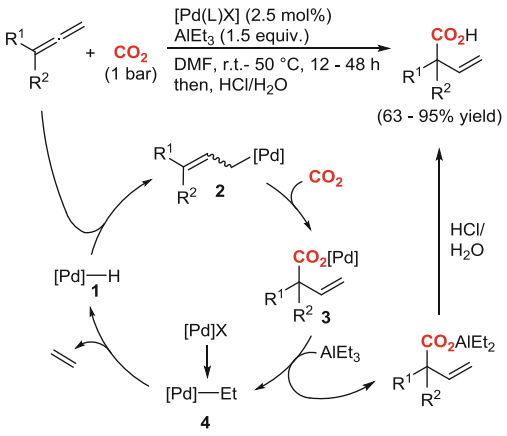


**Fig. 11** Carboxylation of allenes catalyzed by a palladium PSiP-pincer complex (Iwasawa and co-workers [69])

transmetalation/β-hydride elimination sequence. Generally high yields were obtained for the carboxylation of 1,1-disubstituted allenes bearing pendant functional groups such as silyl ethers, trisubstituted double bonds, carbonyls, and ethers.

The methodology was later transferred to 1,3-diene systems as substrates which, in the case of 1,1-disubstituted butadienes, were also regioselectively carboxylated at the higher substituted carbon atoms [70].

## 2.3 *Reactions with Miscellaneous Transition Metals*

Although efficient catalytic carboxylations of alkenes using metals other than those from group 10 or 11 have only very recently been discovered, the methodologies reported already present very useful protocols and will surely be of significant importance for the scientific community in the years to come. Thomas and co-workers were able to show that simple Fe(II) salts, which – besides their low toxicity and abundancy – are highly attractive from a cost perspective, can be used for the carboxylation of styrene derivatives, albeit in a stepwise protocol involving the use of Grignard reagents as stoichiometric reductants [71]. Two other novel methodologies have focused on an alternative approach to carboxylation reactions in general. Here, $CO_2$ is converted in situ to the more reactive CO molecule by rhodium or ruthenium catalysts, which is then suggested to undergo typical CO insertion-type chemistry [72, 73]. Due to safety concerns and environmental issues for the use of CO gas as chemical reagent, this approach is highly desirable. Moreover, with respect to atom efficiency and cost, $CO_2$ is a highly attractive alternative source of CO compared to other reagents which have been used for this purpose such as aldehydes [74], cinnamyl alcohol [75], and other higher alcohols [76].

**Rhodium** Leitner and co-workers have recently reported the hydrocarboxylation of olefins by $H_2$ and $CO_2$ catalyzed by a system consisting of $[Rh(\mu\text{-}Cl)(CO)_2]_2$ (2.5 mol%) and excess of $PPh_3$ ligand (25 mol%) in AcOH as solvent (Fig. 12) [72]. Notably, as the authors have stated, the methodology had already been disclosed for the hydrocarboxylation of ethylene as early as 1978 under very harsh reaction conditions (700 bar, 180°C) using heterogeneous palladium or rhodium catalysts or $[Rh(PPh_3)_3Cl]$ in the presence of HBr, but without further discussion of the details of this interesting reaction [77]. In Leitner's procedure, the presence of the promoter *n*-hexyl iodide, an acidic additive such as TsOH, and high reaction temperature (180°C) was required for the conversion of various terminal and internal olefins into the corresponding carboxylic acids in good yields. However, the partial pressures of $CO_2$ and $H_2$ could be lowered to just 60 and 10 bar, respectively, in comparison to the seminal report. It was shown that the reaction actually proceeds via hydrocarbonylation, followed by hydrolysis of a metal acyl species with water (a formal hydrohydroxycarbonylation), stemming from its in situ generation by the reverse water–gas shift reaction (rWGSR), which is also the source of the CO molecule.

**Ruthenium** Similarly to Leitner's hydrocarboxylation of alkenes, Beller and co-workers reported an alternative ruthenium-catalyzed strategy for the use of $CO_2$ as carbonylation reagent. Using $[Ru_3(CO)_{12}]$ (1 mol%) as precatalyst, a

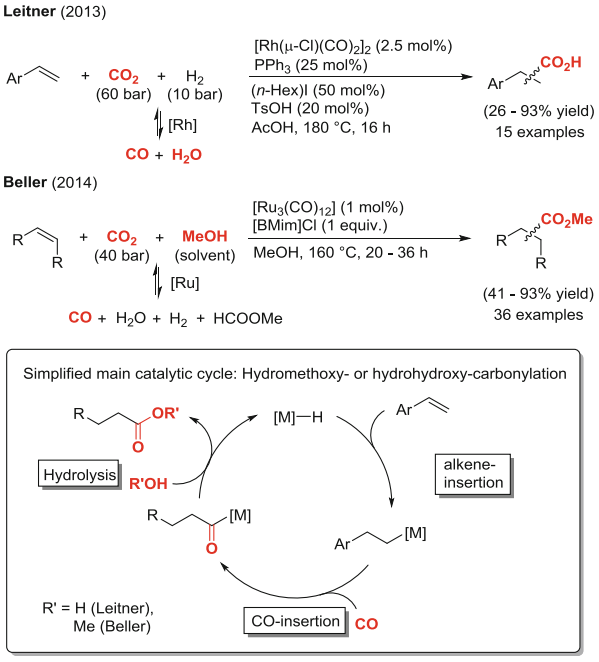


**Fig. 12** Hydrocarboxylation of alkenes by in situ carbonylation methodologies (mechanism adapted from works by Leitner [72], Beller [73], and García [78])

mixture of $CO_2$ and MeOH can be used for the methoxycarbonylation of alkenes giving the corresponding carboxylic acid methyl esters due to hydrolysis of the in situ-generated metal acyl species with MeOH. In this case, the CO molecule, needed for the carbonylation step, is generated from the reaction of MeOH and $CO_2$. Therefore, MeOH takes on the role of reductant and esterification agent. The $CO_2$ molecule was identified as the main carbonyl source as deducted from $^{13}C$ labeling experiments. However, these experiments also showed that other pathways also contribute to the formation of CO to a lower degree, as, for example, alcohol dehydrogenation. Notably, this methodology ($CO_2$ + MeOH) had been reported previously on nickel-based catalysts by García and co-workers, albeit in lower efficiency [78]. Bisphosphine nickel dimers of the type $[(P\text{^}P)Ni(\mu\text{-}H)]_2$ (20 mol%) catalyzed the hydroesterification of styrene derivatives with both electron-poor- and electron-rich-substituted aryl moieties in low to good yields. A mechanistic proposal consisting of sequential alkene insertion into a metal hydride fragment, CO insertion, and hydrolysis was proposed in a similar fashion to the rhodium- and ruthenium-catalyzed reactions (Fig. 12).

**Iron** For several years iron compounds had not been considered as suitable mediators of $CO_2$ transformations. Greenhalgh and Thomas were able to circumvent the intrinsically low reactivity of organoiron compounds in C–C bond formation reactions with $CO_2$ by using an iron(II) precatalyst consisting of $FeCl_2$ and a tridentate NNN pincer ligand (1 mol%) for an initial hydromagnesiation reaction of styrene derivatives [79]. A new Grignard reagent is formed in situ with high regioselectivity toward the α-magnesiated species, which is carboxylated at atmospheric $CO_2$ pressures. Thereby, a range of 2-aryl propionic acids were obtained with high to nearly perfect regioselectivities and in good to high yields. This methodology was also applied in a short synthesis of ibuprofen comprising of only iron-catalyzed reaction steps (Fig. 13) [79].

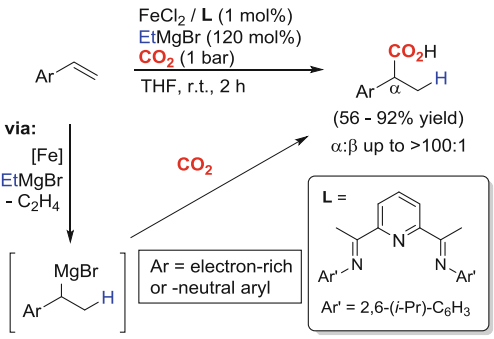


**Fig. 13** Carboxylation of styrene derivatives via an iron-catalyzed hydromagnesiation/carboxylation sequence (Thomas and co-workers [71])

# 3 Carboxylation of Alkynes

## *3.1 Reactions with Group 11 Metals*

In 1974 Saegusa and co-workers reported the first important breakthrough concerning the carboxylation of terminal alkynes with $CO_2$, which did not rely on the use of strongly basic organolithium reagents [80]. Stoichiometric reactions between copper or silver phenylacetylides generated from CuO*t*-Bu or AgO*t*-Bu and phenylacetylene were shown to undergo insertion of $CO_2$ into the metal–carbon bonds. Subsequent reaction of the carboxylato complexes with methyl iodide yielded methyl propiolic esters (Fig. 14). A substantial ligand effect on the performance of the reaction was experienced, showing weak donors such as $P(OMe)_3$ and pyridine to be ineffective in this type of transformation, whereas stronger donor ligands such as $P(n\text{-Bu})_3$ and *t*-BuNC gave the product in 50–71% isolated yields.

Due to the historical importance of terminal alkyne C–H bond carboxylation for coinage metal-catalyzed carboxylation processes of alkynes in general, these reactions will be presented in this section and not within Sect. 4.1.1 on other direct C–Y bond carboxylation reactions.

Following these initial findings, the acetylide complex [{$(n\text{-Bu})_3$P}Cu–C≡CPh] was used in a further study on the reversibility of the $CO_2$ insertion [81]. It was discovered that copper(I) phenylpropiolate underwent an irreversible decarboxylation at 35°C, forming the acetylide derivative. However, in the presence of an excess of phosphine ligand, the reaction was reversible and did not reach completion. In accordance with the results of the previously reported carboxylation reaction, a correlation between an equilibrium shift toward the carboxylated species and the strength of σ-donating ligands was observed ($P(n\text{-Bu})_3 > PPh_3 > P(OMe)_3$).

Despite these encouraging results, the first catalytic version was only reported 20 years later [82]. Using simple copper(I) and silver(I) halide or nitrate salts (4 mol %), Inoue and co-workers achieved the carboxylation of 1-alkynes at atmospheric $CO_2$ pressure in the presence of mild bases ($K_2CO_3$, $K_3PO_4$). A copper(II) salt like $CuBr_2$ proved to be less efficient. The equilibrium was again shifted toward the carboxylation product by the use of an in situ alkylation agent such as 1-bromohexane, yielding hexyl propiolic esters. Most importantly, the presence of a polar aprotic solvent such as DMF or DMAc was essential for the success of the reaction. Aromatic and aliphatic alkynes (phenylacetylene, *p*-tolylacetylene, 1-octyne) could thereby be converted to the corresponding esters in good yields.

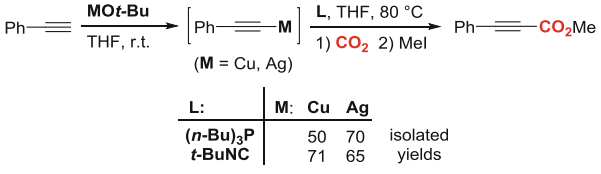


**Fig. 14** Stoichiometric carboxylation of phenylacetylene (Saegusa and co-workers [80])

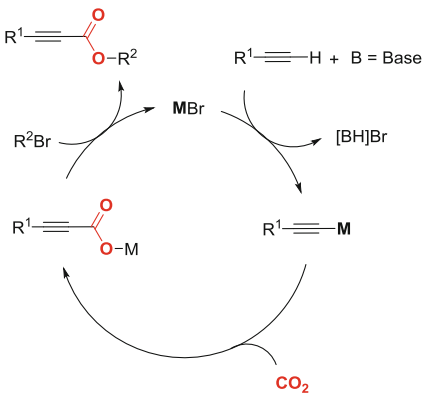


**Fig. 15** Plausible mechanism for the catalytic carboxylation of terminal alkynes (according to Inoue and co-workers, 1994 [82])

The mechanistic proposal was based on the previous stoichiometric investigations by Saegusa [80]. This involved the formation of a metal acetylide species from the metal salt, the alkyne, and the base, followed by the insertion of $CO_2$ into the metal–carbon bond. The product is released by reaction of the resulting metal carboxylate with the alkyl halide under regeneration of the metal halide catalyst. Since this report, several contributions have significantly improved on this useful reaction. Recently, the results in this area have been highlighted by Gooßen [83]. These and other rapid developments in copper-based catalysis opened new perspectives for reaction methodologies involving the catalytic $CO_2$ incorporation by copper complexes in organic synthesis (Fig. 15) [84].

### 3.1.1 Copper-Catalyzed Reactions

**Terminal Alkynes** In 2010, Gooßen and co-workers reported a copper precatalyst system for the efficient carboxylation of terminal alkynes, which did not rely on the use of alkyl halides as trapping agents for the carboxylated intermediates [85]. Previously, the group had demonstrated that copper–phenanthroline complexes efficiently enabled the extrusion of $CO_2$ from propiolic acid derivatives, which suggested their application in the reverse reaction [86]. Thus, mixed phenanthroline/phosphine copper(I) nitrate complexes (1 mol%), in the presence of $Cs_2CO_3$, allowed the carboxylation of 1-octyne under mild conditions (50°C, 1 bar $CO_2$). Obtaining satisfactory yields for the carboxylation of phenylacetylene derivatives required lower temperatures (35°C), higher $CO_2$ pressure (5 bar), and a particular ligand combination within the copper(I) precatalyst system ((4,7-diphenyl-1,10-phenanthroline)[bis(tris(4-fluorophenyl)phosphine]copper (I) nitrate (**A**)). The reaction proved general, delivering a wide substrate scope, with moderate to excellent yields for a range of alkyl- and aryl-substituted 1-alkynes.

Within the same year, Zhang disclosed an alternative methodology for the transformation of terminal alkynes under milder conditions (ambient temperature and $CO_2$ pressure) (Fig. 16) [87, 88]. Their catalyst system, based on CuCl (2 mol%)

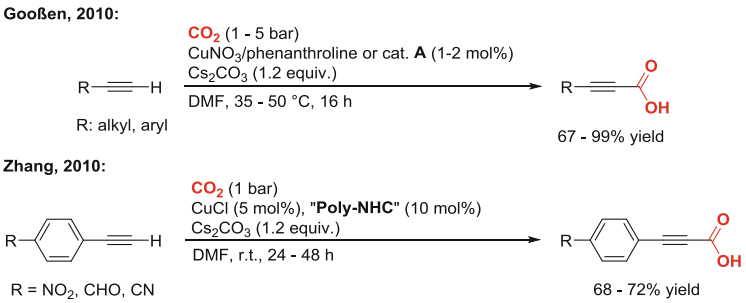


**Fig. 16** Highly efficient copper-catalyzed carboxylation of terminal alkynes (Gooßen [85] and Zhang and co-workers [87, 88])

and TMEDA (1.5 mol%), efficiently promoted the formation of a variety of phenylpropiolic acids in generally good yields in the presence of $K_2CO_3$ as base. Notably, alkyl-substituted alkynes required the use of $Cs_2CO_3$ in order to reach high yields, presumably due to its increased basicity. However, the presence of electron-withdrawing groups (EWGs) on the phenyl ring of the aryl alkyne did not lead to the corresponding acids, even in the presence of a strong base such as KO*t*-Bu. To overcome this limitation an extensive ligand screening was conducted, including multidentate pyridine and NHC ligands. A peculiar polytopic *N*-heterocyclic carbene ligand (named "poly-NHC" or "PNHC") was found to be quite effective for this purpose (Fig. 17). Thus, with 10 mol% of PNHC ligand and 5 mol% of CuCl, using $Cs_2CO_3$ as base, even highly electron-deficient arylacetylenes bearing, e.g., *p*-$NO_2$, *p*-CHO, or *p*-CN groups were carboxylated in decent yields (68–72%). The efficiency of the system was rationalized by a mechanistic proposal based on a dual activating role of the PNHC ligand. In this regard, one of the ligand's NHC functionalities was believed to coordinate to a copper acetylide species, while another remotely attached free NHC moiety activates $CO_2$ by adduct formation. Carboxylation of the acetylide was therefore believed to be facilitated in the following $CO_2$ transfer step. Regeneration of the copper–acetylide intermediate takes place via deprotonation of the substrate by the copper carboxylate species.

Very recently, a methodology based on supercritical $CO_2$ as solvent and reactant for the carboxylation of terminal aryl alkynes has been reported by Suo, Han, and co-workers [89]. Interestingly, the commonly used carbonate bases were efficiently replaced by DBU, showing an improvement in the conversions with 2 mol% of CuI as copper source at a mild temperature (50°C). The copper-free reaction, catalyzed only by DBU, requires higher temperatures (80°C) and $CO_2$ pressure (120 bar) to achieve a comparably high yield. Adding a catalytic amount of CuI under these conditions significantly reduced the yields as the reverse reaction is favored.

In parallel to the direct carboxylation reports, Zhang, Lu, and co-workers reported a catalytic carboxylative alkylation methodology in resemblance to Inoue's seminal work (see Sect. 3.1) [90]. Using 10 mol% of a well-defined NHC-based catalyst [Cu(IPr)Cl] and $K_2CO_3$ as the base in DMF at 60°C, the model substrate, phenylacetylene, was carboxylated under 15 bar $CO_2$ pressure (Fig. 18). The intermediately formed carboxylate was directly converted to the

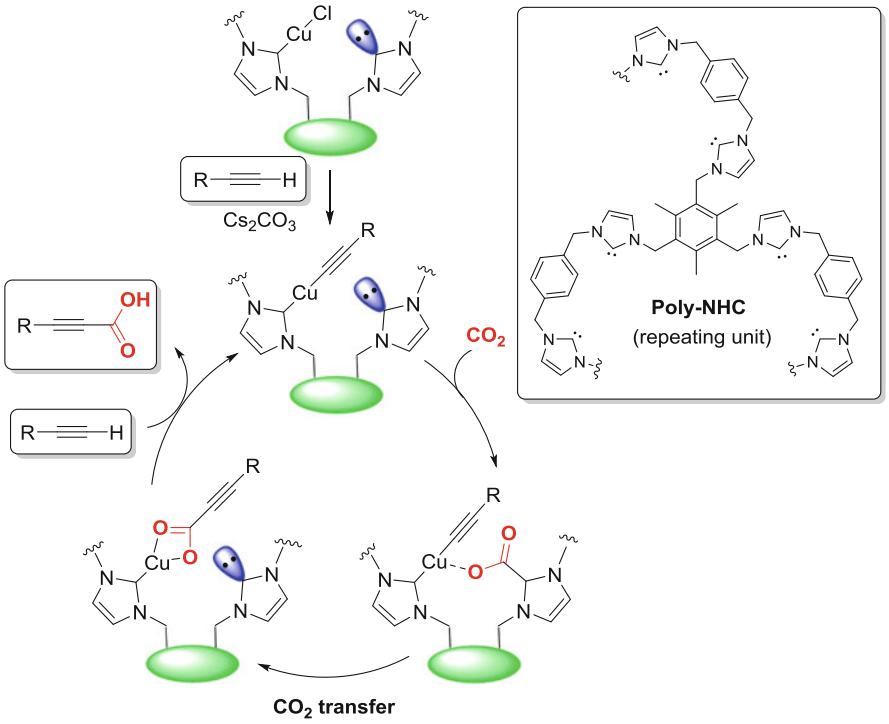


**Fig. 17** Mechanistic proposal for the carboxylation of terminal alkynes using polydentate NHC ligands (Zhang and co-workers [87])

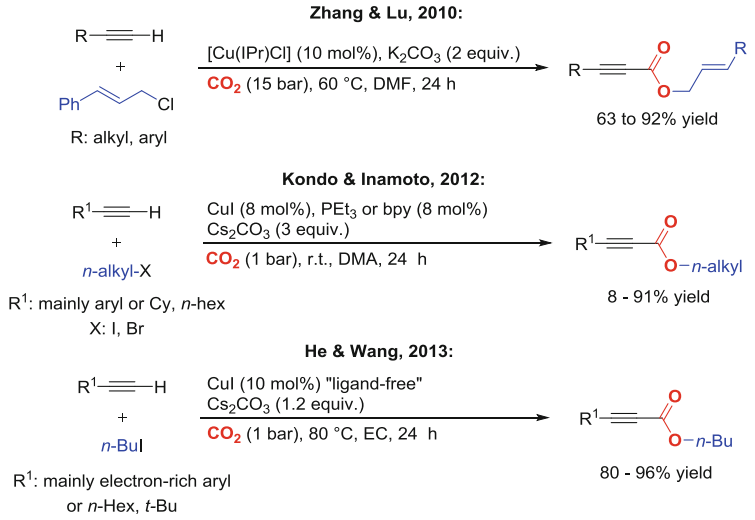


**Fig. 18** Copper-catalyzed carboxylative alkylations of terminal alkynes (Literature references from top to bottom: [90, 92, 93])

corresponding cinnamyl ester due to the presence of cinnamyl chloride as alkylation agent. Cu(I) halide salts without additional ligand or CuCl in the presence of other NHC- or nitrogen-based ligands (IMes = 1,3-bis(2,4,6-trimethylphenyl) imidazol-5-ylidene, TMEDA = tetramethylethylenediamine, bpy = 2,2-′-bipyridine) gave much lower isolated yields (24–68%) than the IPr-based precatalyst (91%). The relatively high $CO_2$ pressure ensured sufficiently fast carboxylation in order to suppress the direct coupling between the copper acetylide species and the allylic halide, as well as an increase of the overall reaction rate. The ligand screening further revealed that NHC-based catalysts seemed to significantly reduce the formation of direct coupling products (to trace amounts) in comparison to other ligands, therefore hinting toward a faster $CO_2$ insertion promoted by NHCs compared to other ligands. A variety of alkyl- and aryl-substituted terminal alkynes were converted to cinnamyl esters in moderate to excellent yields. The use of a few other allylic and propargylic chlorides as well as α-chlorocarbonyl electrophiles also proved to be effective coupling partners. Notably, the precatalyst could be recovered in generally good yields. Very recently, the mechanism of this transformation was investigated computationally by Yuan and Lin [91].

In 2012, Kondo and co-workers reported another protocol for the carboxylative alkylation of terminal alkynes [92]. Using 8 mol% of CuI as precatalyst, 80°C was needed for the coupling of phenylacetylene, $CO_2$ (1 atm), and 1 equiv. of *n*-butyl iodide in DMF. By addition of NHC, phosphine, or 2,2′-bipyridine ligands to the reaction mixture, the reaction proceeded at room temperature. Interestingly, NHC ligands performed poorly in comparison to the phosphines, among which the highly electron-rich $PEt_3$ gave the highest yield (90%). Reactions involving aryl alkynes with EDGs (EDG = electron-donating group) proceeded in high yields, whereas a range of other substrates such as EWG-substituted (EWG = electron-withdrawing group) aryl alkynes or alkyl alkynes required the exchange of the ligand to 2,2-′-bipyridine in order to maintain good yields. However, this was not the case for all electron-poor substrates (*p*-$CO_2$Me and *p*-$NO_2$ gave 32 and 8% yield, respectively). Regarding the alkylation reagent, alkyl bromides were also identified as suitable reaction partners, while chloride and triflate analogs remained unreactive. In the absence of the halide, the carboxylic acid could be isolated in good yield. The authors pointed out that the exclusion of water was critical for the success of the reaction.

Recently, Wang reported a ligand-free alternative to this methodology [93]. This was achieved by the use of organic carbonates as solvent, which improve the solubility of $CO_2$ and potentially stabilize reactive intermediates. Furthermore, they are less harmful than other polar aprotic solvents, such as DMF or DMA, which are often the solvents of choice for these transformations (see above). Once again, among a series of tested organic and inorganic bases, carbonates such as $K_2CO_3$ and especially $Cs_2CO_3$ proved most effective in the model coupling of phenylacetylene, $CO_2$, and *n*-butyl iodide in ethylene carbonate (EC) as solvent at 80°C. Cyclic carbonates (PC = propylene carbonate, EC) led to higher catalytic activity than acyclic derivatives such as diethyl and dimethyl carbonate. Regarding the activity of the copper precatalyst, a clear trend was observed in the following

decreasing order: CuI > CuBr > CuCl. Good to excellent yields were achieved for a wide range of alkynes; however, mainly electron-rich aryl alkynes were investigated in this study. DFT calculations in the gas phase highlighted that by using EC as solvent, the barrier for the $CO_2$ insertion step is significantly reduced in comparison to the solvent-free reaction, as the transition state is stabilized by coordination of the carbonyl oxygen of EC.

**Internal Alkynes** Over the last 5 years, carboxylative transformations of alkyne triple bonds have evolved into powerful synthetic tools to access α,β-unsaturated carboxylic acid derivatives. The first to disclose such a methodology were Tsuji and co-workers in the hydrocarboxylation of alkynes using NHC–copper complexes [94]. [Cu(IMes)F] at 1 mol% loading gave the highest GC yield in the hydrocarboxylation of the model substrate, diphenylacetylene, using triethoxysilane as reductant at ambient pressure of $CO_2$ in 1,4-dioxane at 100°C. Interestingly, PMHS, a cheap hydrosilane source, could also be applied successfully, showing only a slight decrease in conversion (86 to 80%). Regarding the stereoselectivity of the reaction, only *E*-alkenes were formed from symmetrically diaryl-substituted alkyne substrates. With unsymmetrically substituted substrates the precatalyst needed to be altered to the complex bearing the backbone chlorinated NHC ligand $IPr^{Cl}$ (4,5-dichloro-1,3-bis(2,6-di-*iso*-propylphenyl)-1H-imidazol-2-ylidene). This enabled the successful carboxylation of various 1-aryl-2-alkyl alkynes at 2.5 mol % catalyst loading in moderate to good regioselectivity. All elementary steps of the proposed mechanism could be investigated by stoichiometric reactions, leading to a plausible mechanistic cycle (Fig. 19). In the initial step, the precatalyst is transformed by the silane into the corresponding copper hydride. This species reacts with the alkyne toward the formation of a copper alkenyl complex via a *syn*-hydrocupration. The subsequent $CO_2$ insertion leads to the corresponding carboxylato complex, which presented the only step among the stoichiometrically

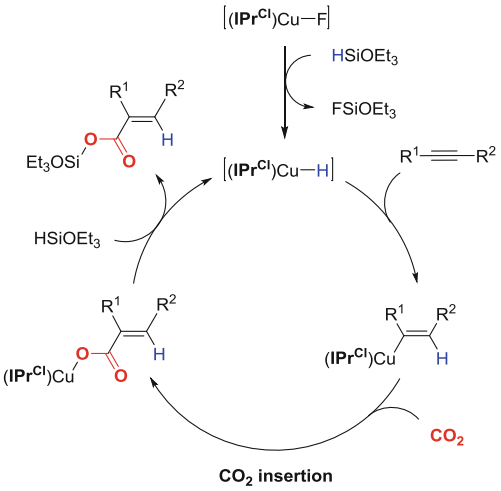


**Fig. 19** Plausible mechanism for the hydrocarboxylation of alkynes (Tsuji and co-workers [94])

investigated reactions that needed higher temperatures (65 °C), thus suggesting its possible role as rate-determining step. By reaction of this complex with the silane, the catalyst is regenerated, and the product is released as a silyl ester. The corresponding acid is obtained from acidic workup.

Following this report, other systems have been disclosed, combining functionalization and carboxylation methodologies. In 2012, Tsuji presented the catalytic silacarboxylation of internal alkynes (Fig. 20) [95]. The reaction of 1-phenyl-1-propyne with $CO_2$ and $Me_2PhSi$-B(pin) as silicon source led to the formation of a silalactone in the presence of a strong base (12 mol% NaO*t*Bu) and copper(I) chloride precatalysts (2.5–3 mol%) bearing electron-rich and bulky phosphine ligands such as P(*t*Bu)$_3$ and PCy$_3$ or the NHC ligand IMes. The increase in steric bulk associated with using IPr as ligand led to a dramatic decrease in catalytic activity. The most important advantage of using the phosphine-based catalysts was a substantially higher regioselectivity (96:4), which is in favor of the isomer containing the bulky silane group attached to the methyl-bound carbon atom. An important factor associated with the choice of silane reagent is that only $Me_2PhSi$-B(pin) efficiently gave silalactone products, while, for example, $Et_3Si$-B(pin) predominantly gave a mixture of regioisomeric β-silyl-α,β-unsaturated carboxylic acids and other by-products. Disilanes as silicon source such as $PhMe_2Si$–$SiPhMe_2$ showed no reactivity whatsoever. Mechanistically, the initial hypothesis was that the silacarboxylation would proceed stepwise through sequential reactions known from the literature: silaboration of the alkyne (see, e.g., [96, 97]) followed by carboxylation of the resulting boronic ester functionality (see Sect. 4.1.1). However, this pathway was excluded on the basis of control experiments attempting the carboxylation of the separately prepared β-silyl-vinylboronic ester intermediate, which did not occur. In contrast, the reaction was proposed to proceed via silacupration of the alkyne (after initial transmetalation of the silyl fragment from $Me_2PhSi$-B(pin) to [Cu(L)(O*t*-Bu)]), affording the alkenyl copper intermediate **II** (Fig. 20). After $CO_2$ insertion into the Cu–C bond, the carboxylato complex **III**

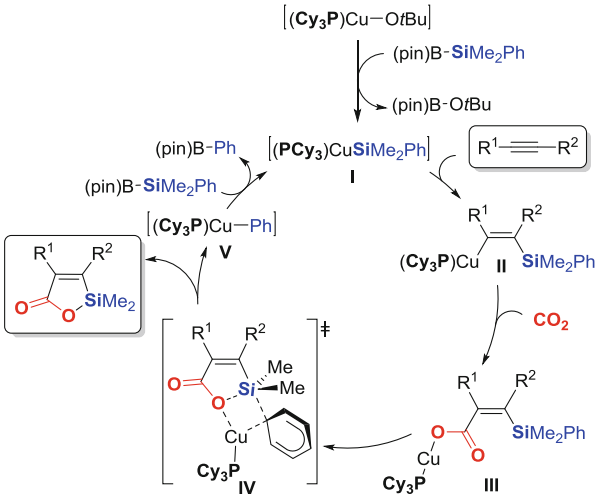


**Fig. 20** Silacarboxylation of internal alkynes (Tsuji and co-workers [95])

undergoes a cyclization via C–O bond formation and a concerted transfer of the phenyl substituent to the cationic Cu(I) fragment to afford the silalactone and [Cu(L)Ph] (**V**). The stabilizing influence of the Si–phenyl moiety on the transition state **IV** seems to be a prerequisite for the cyclization to occur, which presumably also accounts for the narrow scope of silaboranes that can be used in this transformation.

In the same year, Hou and co-workers reported the combination of borylation and carboxylation of internal alkynes catalyzed by NHC–copper complexes and $B_2(pin)_2$ as boron source, ultimately yielding boralactones (Fig. 21) [98]. Again, more bulky NHC–copper complexes like [Cu(IPr)Cl] (5 mol%) in the presence of 1.1 equiv. of Li*O*t-Bu showed low conversion of the model substrate diphenylacetylene, whereas precatalysts bearing the less sterically demanding congeners IMes and SIMes showed a significant increase in isolated yields from trace amounts to 73 and 81%, respectively (THF, 80°C, 14 h). Symmetrical aryl alkynes bearing both EWGs and EDGs were both converted in moderate to high yields. Among these, functional groups such as esters or halides were tolerated. In the case of unsymmetrical alkynes bearing alkyl groups (Me, Et) adjacent to phenyl moieties, the boryl group ends up regioselectively at the alkyl-substituted carbon atom. This is presumably due to sterics, as also shown by Tsuji in the silacarboxylation reaction [95]. Notably, the terminal alkyne phenylacetylene also gave the cyclic boralactone (and not phenyl propiolic acid) in very high regioselectivity – in accordance with the strongly differing substituent sizes.

Mechanistically, a similar catalytic cycle to the one proposed by Tsuji for the silacarboxylation reaction was depicted. After in situ formation of the *tert*-butoxide copper catalyst, transmetalation of B(pin) from $B_{2(}pin)_2$ generates [Cu(SIMes)(Bpin)]. This is followed by alkyne insertion into the Cu–B bond in a *syn*-fashion to give a boraalkenyl copper species (**VI**, Fig. 21). The trapping of the formed alkenyl copper species with $CO_2$ generates the cyclic lactone **VII**, which contains the Cu(SIMes) fragment coordinated to the boryl ester oxygen atom. Notably, this complex could be characterized by X-ray diffraction analysis.

Shortly thereafter, in 2013, Hou reported an extensive study on controlling the regio- and stereospecificity of methylative and hydrogenative carboxylations of various alkynes using a sequence of methyl- or hydroalumination followed by carboxylation of the in situ-generated alkenylaluminum reagent by NHC–copper catalysts (Fig. 22) [99]. Interestingly, and in contrast to all formerly presented

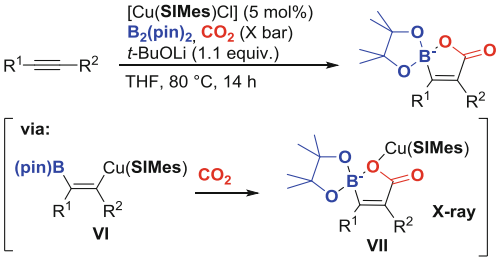


**Fig. 21** Boracarboxylation/lactonization sequence of internal alkynes (Hou and co-workers [98])

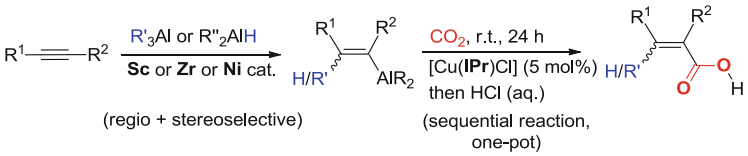


**Fig. 22** Regio- and stereoselective hydro- and methylcarboxylation of internal alkynes (Hou and co-workers [99])

reactions, the optimization of the reaction conditions identified [Cu(IPr)Cl] (5 mol %) as the most active precatalyst for the formation of the corresponding carboxylic acids at ambient temperature and atmospheric pressure of $CO_2$. Higher temperatures (70°C) led to a significant drop in isolated yield (from quantitative to 86%). In these types of reactions, the copper(I) catalyst solely takes on the role of carboxylation mediator, while the methylation or hydrogenation step is carried out beforehand using a system comprised of an aluminum reagent (1.5 equiv.) and an alumination catalyst based on scandium ($[Cp^*ScR_2]/[Ph_3C][B(C_6F_5)_4]$) or zirconium ($[(Cp)_2ZrCl_2]$/MAO, MAO = methylaluminoxane).

In the first investigated reaction, the alkenylaluminum species, formed under *syn*-methylalumination using 1.5 equiv. of $Me_3Al$ and the scandium catalyst system (5 mol%), was carboxylated under an atmosphere of $CO_2$ at room temperature by the addition of a solution of the copper catalyst directly to the reaction mixture. An additional base was not needed, in contrast to the previously reported carboxylation procedures. It is important to note that the authors checked that the alkenylaluminum species alone does not insert $CO_2$, even at 70°C. The regioselectivity of the alumination step was controlled by using substrates bearing ether functionalities (both alkyl and silyl ethers) in the γ-position to the internal triple bond. The chelation to aluminum ensures that the carboxylation takes place at the proximal position and the methylation at the distal position of the triple bond in relation to the alkyl ether group. Most interestingly, both regio- and stereoselectivity of the reaction were inverted for substrates bearing one TMS group attached to the triple bond, regardless of the presence of ether directing groups as the other substituent of the alkyne. Although the authors did not present a rational explanation for this observation, it was pointed out that this anti-specific methylalumination was the first of its kind.

The methodology was next transferred to the regio- and stereoselective methylcarboxylation of terminal alkynes by carrying out the alumination step under zirconium catalysis (10 mol%). For a formal hydrogenative carboxylation of the same substrate class, *i*-$Bu_2AlH$ was used in combination with $[NiCl_2(PPh_3)_2]$ (5 mol%) as catalyst. In both reactions, carbo- or hydrometalation proceeded in a *syn*-fashion, and the carboxylation occurred at the terminal position of the triple bond. Notably, the regioselectivity of the hydrocarboxylation reaction could be inverted by changing the nickel precatalyst to $[(dppp)NiCl_2]$ (dppp = 1,3-bis (diphenylphosphino)propane).

### 3.1.2 Silver-Catalyzed Reactions

**Terminal Alkynes** Less work has been dedicated to silver-catalyzed processes, although it has been known since the seminal work of Saegusa that silver also represents a potent mediator for carboxylation reactions [80]. In 2008, Anastas reported a methodology for the formation of lactones via a reaction sequence comprised of carboxylative alkylation and cyclization [100]. Using propargylic bromides as alkylation agents, the coupling with a terminal alkyne and $CO_2$ creates a 1,6-diyne system which further cyclizes under [2 + 2 + 2] cycloaddition (for reviews on [2 + 2 + 2] cycloadditions (Fig. 23), see [101, 102]). It was found that AgI afforded the coupling of phenylacetylene, 3-phenyl-propargyl bromide, and $CO_2$ (1 atm) at 100°C within 2 h. The following cyclization reaction proceeded within 6 h, and it was confirmed that it also proceeded in the absence of metal catalyst, demonstrating that the second step of the multicomponent reaction represents a purely thermal process. Interestingly, copper salts failed to deliver the desired product. A small range of substituted arylacetylenes were thus transformed into mixtures of the regioisomeric lactones in low to moderate yields. Notably, from a green chemistry perspective, the process has proven superior to traditional multistep synthetic procedures.

In 2011, Lu and co-workers reported the ligand-free carboxylation of terminal alkynes catalyzed by AgI (1 mol%) under mild conditions (50°C, 2 bar $CO_2$) using $Cs_2CO_3$ as base in DMF [103]. Previously, the group had developed the copper-catalyzed carboxylative alkylation between terminal alkynes, allylic chlorides, and $CO_2$ [90]. Interestingly, silver salts proved more efficient than their copper analogs in the non-alkylative process. Silver salts other than AgI, such as $AgPF_6$ and $AgBF_4$, also displayed high activity; however, their hygroscopic properties made the simple halide salt the catalyst of choice. Regarding the efficiency of the methodology, aryl- and alkyl-substituted terminal alkynes were converted with moderate to high yields, tolerating various functional groups such as aryl-Br, aryl-Cl, aryl-F, aryl-$CF_3$, aryl-OH, and aryl-OMe. EWGs attached to the phenyl

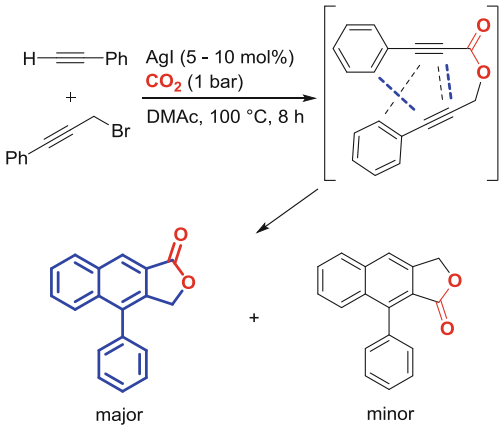


**Fig. 23** Carboxylative alkylation/cyclization sequence of terminal alkynes (Anastas and co-workers, 2008 [100])

rings of arylpropiolic acids decreased the yields slightly in comparison to electron-rich substrates.

The process was extended to the carboxylative alkylation methodology using alkyl chlorides and the same catalyst at low loading (0.1 mol%) [104]. In comparison to the previous carboxylation procedure, an increase of the $CO_2$ pressure to 15 bar was required. Silver salts other than AgI were effective promoters (in the case of $AgBF_4$ even slightly better) of the model coupling of phenyl acetylene, cinnamyl chloride, and $CO_2$, but again, AgI was used due to more convenient handling procedures. A broad range of functional groups attached to the aryl moieties of arylacetylenes and the cinnamyl chloride were tolerated. Terminal alkyl alkynes were also found to be suitable substrates.

In parallel, Zhang and Yu reported a carboxylation based on a polymer-supported silver nanoparticle catalyst system [105]. The PNHC ligand system, which was previously introduced into copper-catalyzed carboxylation of terminal alkynes by the same group (see Sect. 3.1.1), was grafted on silver nanoparticles by reaction of the precursor imidazolium salt of the ligand with $AgNO_3$ in hot DMSO. Confirmation of poly-NHC formation and determination of the silver content (6.8 wt%) in the resulting nanocomposite were determined by FT-IR and solid-state NMR spectroscopy. The nanoparticles allowed the transformation of mostly arylacetylenes under very mild conditions (r.t., 1 atm of $CO_2$) into the corresponding propiolic acid derivatives in high yields (92–96%). It was shown that the catalyst's recyclability was high, showing almost no loss in reactivity after five runs at 0.3 mol% catalyst loading. Concerning the mechanism, the same activating role of a free NHC group toward $CO_2$ was suggested as previously for the copper-catalyzed reaction.

Shortly after Zhang and Lu had disclosed the carboxylation of terminal alkynes using AgI, Gooßen was able to improve on this procedure significantly by simply using DMSO as solvent [106]. Thus, at very low catalyst loading of Ag(I) sources such as $AgBF_4$ or $Ag_2O$ (500 ppm) and 1 bar of $CO_2$, various 1-alkynes were converted to propiolic acids in very high yields, with only a few exceptions. It was reasoned that the high catalytic activity of this system might be due to the higher solubility of $CO_2$ than in other solvents. The formation of silver nanoparticles, as reported for heating of silver salts in DMSO, could not safely be ruled out.

**Internal Alkynes** Reports on silver-catalyzed carboxylation procedures involving internal alkynes have remained scarce, in spite of some impressive reports in copper catalysis (see Sect 3.1.1). In 2007, Yamada and co-workers reported the rearrangement of propargylic alcohols to α,β-unsaturated ketones ("Meyer–Schuster rearrangement") catalyzed by AgOMs (10 mol%, OMs = $O_3S$-$CH_3$) and mediated by $CO_2$ at 1–10 bar pressure (Fig. 24) [107]. DBU was found to be a suitable base for this process. During optimization of the reaction conditions, the formation of cyclic carbonate **A** was also observed. Interestingly, via the right choice of solvent, the selectivity toward either product could be controlled with good to high yields. Other $CO_2$-incorporative protocols which make use of the intramolecular reaction between an intermediately formed carboxylato group and

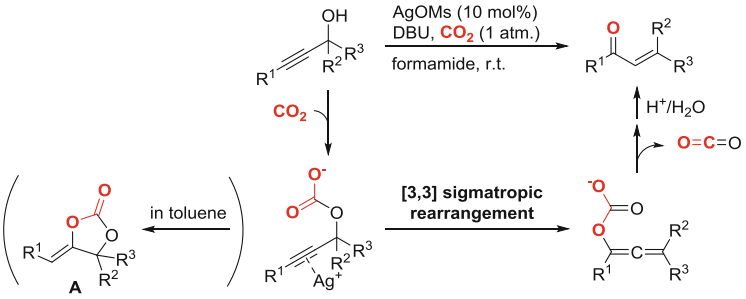


**Fig. 24** Silver(I)-catalyzed, $CO_2$-mediated Meyer–Schuster rearrangement (Yamada and co-workers [107])

an alkyne moiety are presented in Sect. 4.1.1, as they involve the carboxylation of C–H bonds.

The oxygen atom in the rearranged product was shown to originate from the $CO_2$ molecule by $^{18}O$ labeling experiments. While toluene selectively led to the cyclic carbonate, the enone was obtained predominantly when formamide was used as solvent. A range of secondary and tertiary propargylic alcohols were shown to be converted to the corresponding enones in moderate to very high yields under the optimized conditions at 10 bar $CO_2$ pressure, although *E*/*Z* selectivity was found to be an issue for chiral alcohol substrates ($R^2 \neq R^3$).

## *3.2 Reactions with Group 10 Metals*

Alkyne trimerization in a formal [2 + 2 + 2] cycloaddition is a common coupling process mediated by Ni(0) metal centers [108]. Walther and co-workers reported on a variant of this process which was initially discovered by Inoue and co-workers [18] involving the formal [2 + 2 + 2] cycloaddition of two 3-hexyne molecules and one $CO_2$ molecule, thus generating tetraethyl-2-pyrone [47]. A catalytic system consisting of trialkylphosphine and [Ni(COD)$_2$] in acetonitrile as solvent was able to deliver the product in up to 96% selectivity and high yield, which was unprecedented for 3d transition metal-catalyzed C–C coupling reactions between unsaturated substrates and $CO_2$ at the time. Generally, polar solvents were most suited for this reaction; however, the presence of acetonitrile in various solvent mixtures was found crucial for obtaining quantitative conversion and high selectivity. Thus, acetonitrile was proposed to be involved in the operative mechanism by *N*-coordination to the metal center in the presumed active species of type [($Et_3P$)(κ-*N*-MeCN)Ni($\eta^2$-alkyne)]. This complex was proposed to give the corresponding nickelalactone via oxidative coupling with $CO_2$, followed by insertion of a second molecule of the alkyne into the Ni–C bond and then reductive elimination to liberate the pyrone (Fig. 25).

Important contributions to the development of protocols for the catalytic carboxylation of alkynes with $CO_2$ to give *non-cyclized* carboxylic acid derivatives were

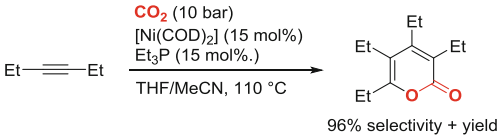


**Fig. 25** Catalytic, selective synthesis of tetraethyl-2-pyrone (Walther and co-workers, 1987 [47])

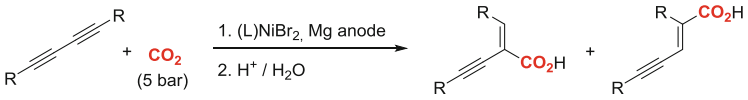


**Fig. 26** Catalytic electroreductive carboxylation of diynes (Duñach and co-workers, 1987 [111])

reported by the group of Duñach in the late 1980s and early 1990s [109, 110]. These reports are based on electroreductive methods which enable the regeneration of the active Ni(0) species bearing bidentate N-donor ligands typically used at the time for oxidative cyclization at these metal centers such as bipyridine or ligands similar to TMEDA. Mechanistically, the reactions were generally proposed to proceed similarly to the pathways discovered for non-electrochemical procedures via intermediate nickelalactone formation. Notably, high regio- and stereoselectivities were obtained in the monocarboxylation of diynes to yield (*E*)-2-vinylidene-3-yne carboxylic acids Fig. 26; a precatalyst comprised of 2 equiv. of pentamethyldiethylenetriamine (PMDTA) in relation to $NiBr_2$ was employed [111, 112]. The group later successfully extended the methodology to 1,3-enynes [113] as well as nonconjugated diynes and enynes as substrates (Fig. 26) [114].

An important study on stoichiometric alkyne carboxylation reactions was conducted by Yamamoto and Saito [115] in 1999, which led to the development of a series of related stoichiometric and catalytic carboxylation reactions. They reported a highly chemo- and regioselective procedure for the carboxylation of alkynes, enynes, and diynes using stoichiometric amounts of Hoberg's DBU/$Ni(COD)_2$ system (Fig. 27) [115]. This combination was identified as the only active system for the carboxylation of terminal alkynes among various other ligands tested. All terminal alkyne functionalities in these substrate classes were chemoselectively carboxylated under mild conditions (1 bar $CO_2$, 0°C) with high regioselectivity toward $CO_2$ incorporation at the terminal position. In comparison to the electrochemical procedure reported by Duñach's and co-workers the opposite regioselectivity was obtained, which was rationalized by the assumption that the nickelalactone formation proceeds under kinetic control via the approach of the $CO_2$ molecule to the less hindered carbon atom. Symmetrical 1,3-diyne systems were regioselectively carboxylated at one of the terminal carbon atoms, while for their unsymmetrically substituted congeners, the selectivity for thus two competing positions (1- or 4-position) was found to be in favor of the less bulky substituted carbon atom.

Nickel-mediated carboxylation reactions of alkynes have been investigated computationally by Buntine and co-workers with a focus on unsymmetrical substrates in order to explain the experimentally observed regioselectivities [116]. Indeed, it was

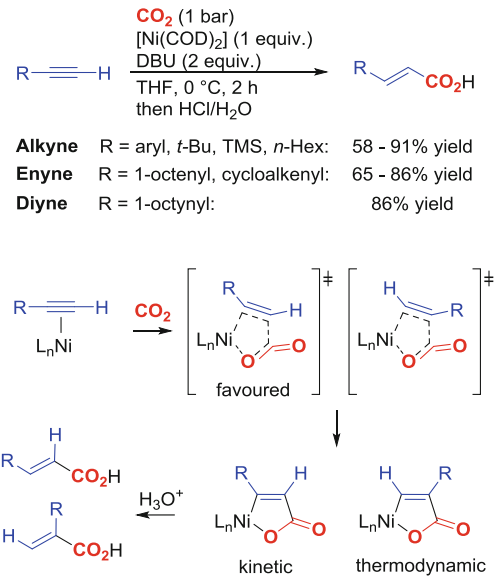


**Fig. 27** Regio- and chemoselective stoichiometric carboxylation of terminal alkynes, enynes, and diynes (Yamamoto and Saito et al. [115], mechanism adapted from Buntine and co-workers [116])

found that 3-substituted oxanickelacyclopentenes are thermodynamically favored over 2-substituted congeners and that the latter present the kinetic products.

A few years later, Iwasawa and co-workers reported similar conditions for the carboxylation of arylacetylenes and 1-aryl-1-propynes using a series of bis (amidine) ligands (1 equiv.) in place of DBU. They were able to show that these ligands can switch regioselectivities to some degree, in favor of the unpredicted regioisomer (especially for arylacetylenes as substrates) [117].

### 3.2.1 Nickel-Catalyzed Reactions

**Monoalkynes** Mori and co-workers developed a procedure for the catalytic alkylative or arylative carboxylation of alkynes with various organozinc reagents and $CO_2$ (Fig. 28) [118]. A few years earlier, the same group had disclosed a stoichiometric study on this reaction mediated by Hoberg's DBU/[Ni(COD)$_2$] system (Fig. 28) [119]. In this report, terminal aryl and alkyl alkynes were carboxylated highly regio- and stereoselectively to give β,β′-disubstituted unsaturated carboxylic acids. A good selection of aryl- and alkylzinc reagents was effectively employed as nucleophiles. Using $Et_2Zn$ as alkylation agent gave the desired product in only 9% yield, which was due to a fast β-hydride elimination pathway, leading to the corresponding hydrogenative carboxylation product.

In 2005, the group discovered that in order to perform the reaction in a catalytic fashion, DBU had to be used in excess (Fig. 28). Thus, an activating role of DBU toward the organozinc reagent was hypothesized due to adduct formation (generating [$Me_2Zn(DBU)_2$]). For TMS-substituted alkynes the regioselectivity of the process was found to be in favor of the isomer bearing the carboxylate group at the

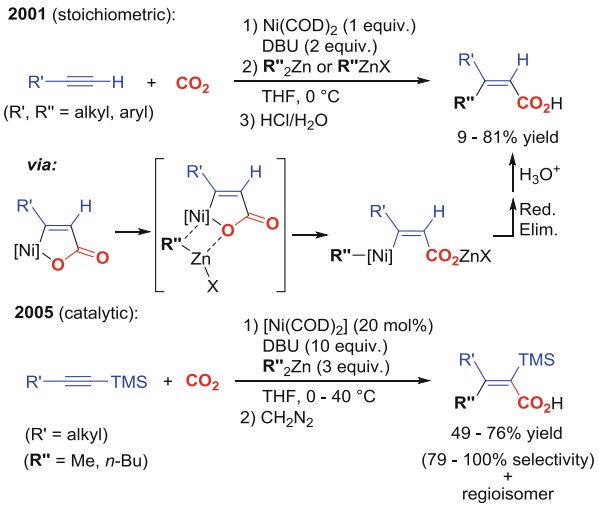


**Fig. 28** Highly regio- and stereoselective arylative or alkylative carboxylations of alkynes (Mori and co-workers [118, 119])

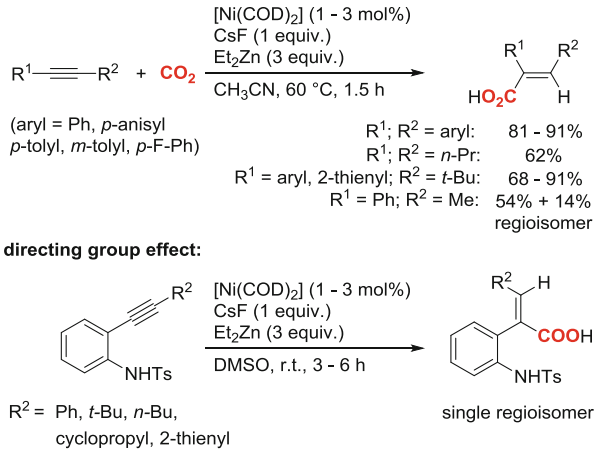


**Fig. 29** *Syn*-selective hydrocarboxylation of alkynes (Ma and co-workers [121])

carbon atom connected to the silyl group, while alkynes bearing an *n*-alkyl and a bulky group such as an aryl or *t*-Bu substituent led to the reversed selectivity with the carboxylate group attached to the less hindered carbon atom. Shortly after, the methodology was applied successfully in the synthesis of tamoxifen, a drug used in the treatment of breast cancer [120], and extended to the regio- and stereoselective double carboxylation of TMS–allene (see Sect. 2.2.1) [51].

Ma and co-workers reported the *syn*-stereoselective hydrocarboxylation of alkynes with high to perfect regioselectivity using $Et_2Zn$ as reductant at ambient $CO_2$ pressure (Fig. 29) [121]. Interestingly, the procedure did not require the use of

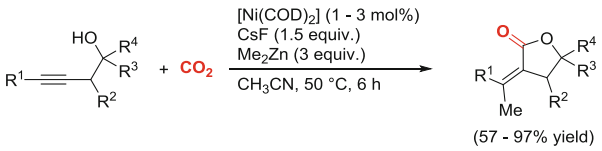


**Fig. 30** Synthesis of α-alkylidene-γ-butyrolactones from propargylic alcohols and $CO_2$ (Ma and co-workers, 2011 [121])

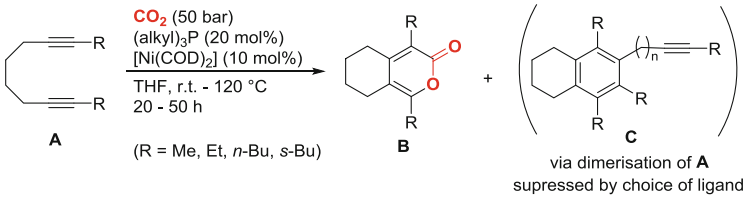


**Fig. 31** α-Pyrone synthesis from diynes and $CO_2$ catalyzed by trialkylphosphine Ni(0) complexes (Tsuda, Saegusa, and co-workers [123])

an additional ligand to the typical Ni(0) precatalyst [Ni(COD)$_2$]. Instead, a stoichiometric amount of CsF (1 equiv.) was needed in order to hydrocarboxylate the model substrate diphenylacetylene in high yields, giving (*E*)-2,3-diphenylacrylic acid via a formal *syn*-hydrocarboxylation. Symmetrical diarylacetylenes were carboxylated in high yields, whereas the carboxylation of 4-octyne was significantly less efficient (62% yield). Unsymmetrical substrates such as mixed aryl- and *t*-Bu-substituted alkynes were converted with perfect selectivity and good to high yields into the products bearing the carboxylate group at the aryl-substituted carbon atom. For 1-phenyl-1-propyne on the other hand, regioselectivity dropped to roughly a 4:1 ratio in favor of the cinnamic acid derivative (carboxylate group at the methyl-bound carbon atom).

This CsF-based protocol was also suitable for the synthesis of α-alkylidene-γ-butyrolactones from the reaction of propargylic alcohols and $CO_2$ [122]. The reaction proceeded with incorporation of the stoichiometric reductants methyl group ($ZnMe_2$) (Fig. 30).

**Diynes** Tsuda, Saegusa, and co-workers reported the cycloaddition of diynes and $CO_2$ to yield bicyclic α-pyrones using Ni(0) precatalysts generated in situ from electron-rich trialkyl phosphines and [Ni(COD)$_2$] (Fig. 31) [123]. In accordance with the results from Pitter and Dinjus on the intermolecular variant of this reaction (see Sect. 3.2.1) [47], the $CO_2$-incorporated [2 + 2 + 2] cycloaddition product, pyrone **B**, was obtained with preference over the arene **C**, in the presence of the appropriate bulky monodentate phosphine. For different substitution patterns at the terminal alkyne position, the choice of ligand also strongly affected the yield of the reaction. Thus, the ideal ligand had to be screened for each substrate separately.

A major improvement on the synthesis of α-pyrones from diynes and $CO_2$ was disclosed by Louie and co-workers (Fig. 32) [124]. In comparison to the previous

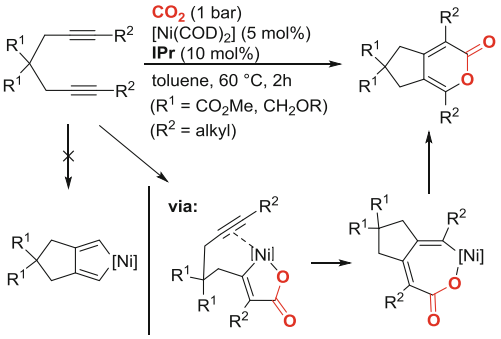


**Fig. 32** α-Pyrone synthesis from diynes and $CO_2$ (Louie and co-workers [124])

procedure [123], an in situ-generated NHC-based catalyst comprised of IPr and [Ni(COD)$_2$] in a 2:1 ratio was employed and was able to reduce the catalyst loading to 5 mol% for the reaction of alkyl-substituted diynes and $CO_2$ under mild reaction conditions (1 bar $CO_2$, 60°C). It was found that by using the previously reported, isolated complex [Ni(IPr)$_2$] [125], the catalyst loading could be reduced further to 1 mol%. However, the "in situ catalyst" was preferred due to practical reasons. The reaction was proposed to proceed via initial [2 + 2] cycloaddition of $CO_2$ and one alkyne moiety followed by insertion of the second alkynyl unit and reductive elimination under C–O bond formation. A pathway starting with initial nickelole formation was excluded on the basis of stoichiometric experiments conducted in the absence of $CO_2$. For unsymmetrical substrates bearing different ending groups at the alkyne moieties (e.g., $R^2$ = Me and TMS), a perfect regioselectivity was observed toward the product in which the bulky TMS group is attached to the oxygen atom of the ester functionality (3-position of the pyrone ring). This reactivity was later investigated in greater detail for a range of unsymmetrical substrates, and it was discovered that the regioselectivity of the process is strongly dependent on the size of the terminal groups of the diyne and also the NHC ligand used (IPr generally outperformed IMes) [126].

Mori and co-workers investigated this reaction type on enyne substrates [127, 128] and were able to apply the new methodology to the synthesis of natural products [129]. Notably, the cyclization of 1,6-enynes proceeded selectively via seven-membered-ring nickelalactones which formed via a formal carboxylation of the terminal position of the double bond part followed by cyclization. Thus, the hydrolysis of these lactones yielded cyclohexanes functionalized with a carboxymethyl group and an exocyclic double bond [129].

## 4 Carboxylation of C–Y Bonds (Y = H, B, O, Halogen)

Organometallic compounds possessing polarized M–C bonds have long been established as valuable tools for the synthesis of carboxylic acids by their reaction with $CO_2$. Common methodologies usually require the use of highly reactive

Grignard or organolithium reagents. Apart from being potentially hazardous procedures, another major drawback is their general low functional group tolerance. Therefore, the application of less reactive sources of carbon nucleophiles has been investigated in various transition metal-catalyzed processes. Recent developments include not only the use of alternative carbon nucleophiles such as organotin [130, 131], organozinc [132, 133], and organoboron reagents [134, 135] but also of certain substrates for direct C–H activation/carboxylation sequences. Other important developments are based on the carboxylation of organic halides or pivalates by reductive methods, which have been investigated most commonly using nickel precatalysts [136]. Some palladium- [137] and copper-catalyzed processes have also been developed [138].

## *4.1 Reactions with Group 11 Metals*

### 4.1.1 Copper-Catalyzed Reactions

**C–B Bonds** Organocopper compounds have shown versatility and functional group tolerance in various organic transformations due to the low polarity of the Cu–C bond. The carboxylation of in situ-generated C($sp^3$)–B bonds was previously discussed in Sect. 2.1 as part of the sequential, reductive carboxylation strategies of alkenes by the groups of Hou and Sawamura [15, 16].

Previous to these reports, the groups of Iwasawa [134] and Hou [135] had independently developed protocols for the carboxylation of C($sp^2$)–B bonds of aryl boronates, which showed a broader substrate scope and functional group tolerance than the established rhodium-catalyzed variant of this reaction (see Sect. 4.3) [139]. In Hou and co-workers' protocol, [Cu(IPr)Cl] was employed at 1 mol% loading in the presence of stoichiometric amount of KO*t*-Bu in refluxing THF and atmospheric $CO_2$ pressure. A very broad range of 4-substituted aryl boronates were converted to carboxylic acids in generally high yields. Heteroaryl and alkenyl boronates were also shown to be efficiently coupled with $CO_2$.

Iwasawa's slightly less efficient methodology involves the use of CuI (5 mol%) and a rigid bisoxazoline ligand (6 mol%) which was identified as the most efficient among a series of P- and N-donor ligands. In the presence of an excess of CsF (3 equiv.), a series of aryl and heteroaryl boronates were carboxylated at 90°C in DMF. A particular superiority of this system over the rhodium-catalyzed procedure was evident for substrates bearing additional double or triple bonds or for certain alkenyl boronates, which in the case of the rhodium-mediated process do not show any conversion into carboxylic acids.

A recent extension of Hou's methodology reported by Duong and co-workers involves the carboxylation of C($sp^3$)–B bonds of allylic boronates, which required the increase of the catalyst loading to 5 mol% (Fig. 33) [140]. In the case of the conversion of tertiary C($sp^3$)–B bonds, up to 15 mol% catalyst loading was required to obtain decent yields. Most interestingly, the reaction proceeded in most cases with high regioselectivity toward β,γ-unsaturated, tertiary carboxylic acid products.

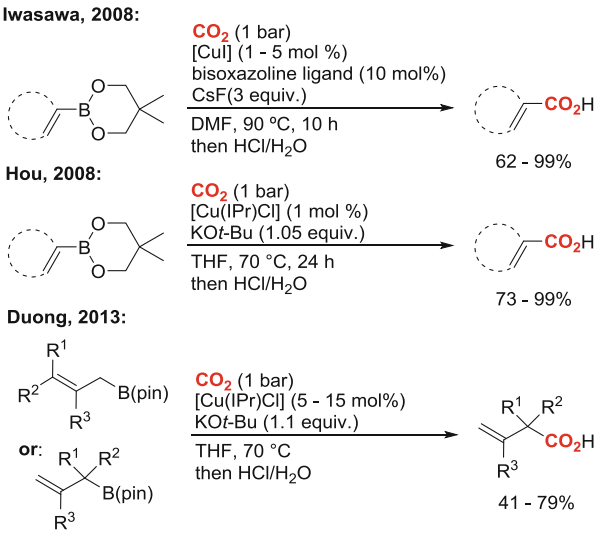


**Fig. 33** Protocols used in the carboxylation of C($sp^2$)– and C($sp^3$)–B bonds (Literature references from top to bottom: [134, 135, 140])

**Cu–I Bonds** A recent report by Daugulis and co-workers has shown that Cu(I) can also be a potent catalyst for the reductive carboxylation of aryl iodides under atmospheric pressure of $CO_2$ using $Et_2Zn$ as stoichiometric reductant [138]. An initial ligand screening with CuI as the precatalyst revealed that bidentate, nitrogen-based ligands were superior to mono- and bidentate phosphines. Under the optimized conditions CuI was used at 3 mol% loading with equimolar amounts of either TMEDA (*N*,*N*,*N*′,*N*′-tetramethylethylenediamine) or DMEDA (*N*,*N*′-dimethylethylenediamine) for the carboxylation of a series of electron-rich and electron-poor aryl iodides under mild conditions (1 bar $CO_2$, 25–70°C) in moderate to good yields. Other aryl-halide bonds were well tolerated under the reaction conditions. Notably, an *ortho*-dimethyl-substituted aryl iodide was also carboxylated in a decent yield (61%). A mechanism was proposed, involving an oxidative addition of the aryl iodide to an in situ-generated Cu(0) species, followed by $CO_2$ insertion and Cu(0) regeneration via $L_nCuEt$, which is generated from the reaction of a copper carboxylate with $Et_2Zn$.

**C–H Bonds** Aside from the carboxylation of terminal alkyne C–H bonds catalyzed by coinage metals (see Sect. 3.1), significant progress has been made for analogous reactions involving aryl and heteroaryl C–H bonds, which has recently been highlighted by Ackermann [141]. In 2010, Fortman and Nolan synthesized the first NHC–copper hydroxide complex, which was found to be a powerful tool for C–H activation of suitably acidic aryl C–H bonds, allowing for the formation of a wide range of [Cu(IPr)R] complexes [142]. These results laid the groundwork for the application of the copper hydroxide synthon as precatalyst for the carboxylation of aryl and heterocyclic C–H bonds (Fig. 34) [143].

Carboxylation was achieved at slightly elevated $CO_2$ pressure and temperature (1.5 bar, 40–65°C) in the presence of 3 mol% precatalyst and CsOH as base, which

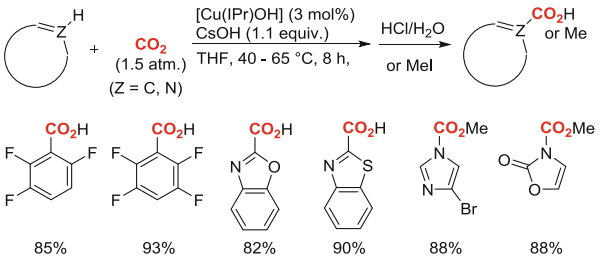


**Fig. 34** Selected examples of copper-catalyzed N–H and C–H carboxylation of aromatic and heteroaromatic substrates (Cazin, Nolan, and co-workers [143])

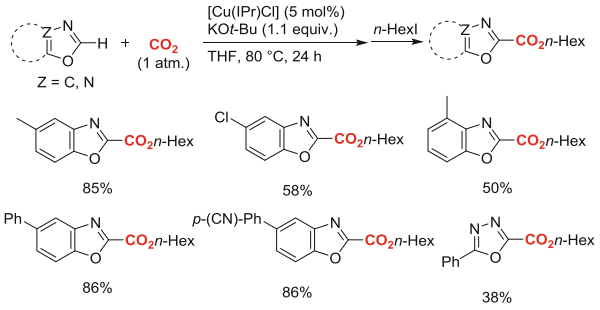


**Fig. 35** Selected examples of the carboxylation of aromatic *N*-heterocycles (Hou and co-workers [144])

regenerates the copper hydroxide species after carboxylation of the in situ-formed aryl or heteroaryl complex [Cu(IPr)R]. A series of aryl carboxylic acids were prepared from aromatics bearing C–H bonds (tri- and tetra-fluorinated benzenes, oxazoles) and N–H bonds (imidazoles, pyrazoles) with $pK_{a(DMSO)}$ values up to 27.7. *N*-Carboxylated products were isolated as the corresponding methyl esters by reaction of the crude reaction mixtures with MeI. Interestingly, the copper complex bearing the saturated NHC ligand SIPr performed significantly less efficiently, as did the less bulky IMes- and SIMes-containing analogs.

In parallel to this work, Hou and co-workers used [Cu(IPr)Cl] in combination with KO*t*-Bu as base to perform the carboxylation of mostly benzoxazole derivatives, which were isolated as the corresponding *n*-hexyl esters by conversion of the crude mixture with *n*-hexyl iodide (Fig. 35) [144]. In comparison to the procedure reported by Cazin and Nolan, a slightly higher catalyst loading of 5 mol% and an increased reaction temperature of 80°C were required. Valuable mechanistic insights were gained by stoichiometric reactions which enabled the identification of key reaction intermediates (Fig. 36). The C2-metalated benzoxazole complex generated from [Cu(IPr)Cl], KO*t*-Bu, and benzoxazole was carboxylated smoothly with $CO_2$ at room temperature, giving the corresponding carboxylato complex in high yield. X-ray diffraction analysis revealed a five-membered-ring chelate structure formed by one carboxylate oxygen atom and the benzoxazole nitrogen atom coordinated to the $[Cu(IPr)]^+$ fragment. Liberation of the benzoxazole carboxylate was achieved in the subsequent reaction of the complex with KO*t*-Bu, thus regenerating the active species of the catalytic cycle.

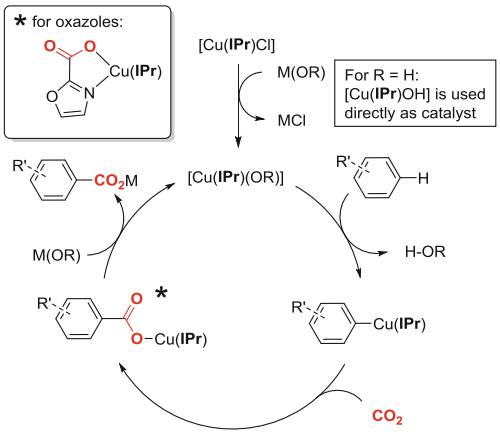


**Fig. 36** Proposed mechanism of copper-catalyzed carboxylation of aromatic C–H bonds (adapted from reports of the Groups of Cazin, Nolan, and Hou [143, 144])

Ariafard and Yates and co-workers have studied the reaction mechanism via DFT calculations and proposed that the carboxylation step proceeds via a metal-stabilized carbene intermediate, which represents an isomeric form of the C2-metalated oxazole intermediate mentioned above [145]. The nucleophilic attack of the carbene lone pair on the $CO_2$ molecule proceeds with a low barrier to yield the five-membered-ring carboxylato complex.

Shortly after these reports, the Fukuzawa group demonstrated that 1,2,3-triazol-5-ylidene ligands bearing the same diaryl substitution pattern as IPr (called "TPr" = 1,4-bis(di*iso*propylphenyl)-1,2,3-triazol-5-ylidene) perform slightly better under conditions identical to Hou's protocol [146].

### 4.1.2 Silver-Catalyzed Reactions

**C–H Bonds** Yamada and co-workers reported the formation of β-ketolactones via C–C bond formation between α-propargyl-substituted carbonyl compounds and $CO_2$ at room temperature (Fig. 37) [147]. A key feature of the methodology is that the inherently unstable β-ketocarboxylates formed in situ are trapped by the intramolecular reaction between the carboxylate group and the alkyne moiety, which is activated by lewis-acidic silver (I) species. Therefore, silver(I) takes on the role of carboxylation and cyclization mediator. Among the polar aprotic solvents tested, DMF led to the best yields in the presence of silver benzoate as catalyst (20 mol%). MTBD (7-Methyl-1,5,7-triazabicyclo(4.4.0)dec-5-ene) was shown to be the most effective base among similarly strong, sterically hindered amines. Functional groups attached to the aryl rings of either the ketone ($R^1$) or the alkyne ($R^3$) moiety of the substrate led to strongly varying reaction times ranging from 2 to 10 days. Aliphatic ketone derivatives ($R^1 = n$-alkyl) required higher $CO_2$ pressure (20 bar) and gave low to moderate yields (31–59%). The geometry of the

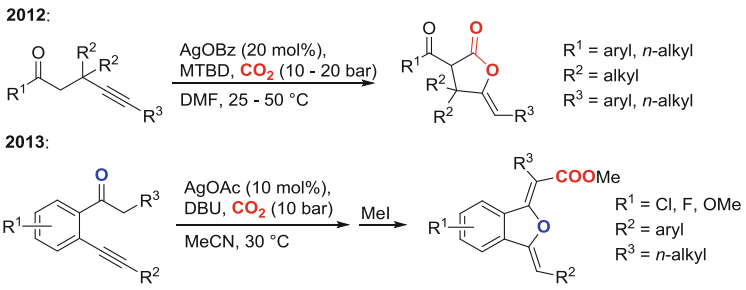


**Fig. 37** Silver(I)-catalyzed sequential carboxylation/cyclization procedures (Yamada and co-workers [147, 148])

exocyclic double bond was confirmed to be of *Z*-configuration by X-ray and NOE NMR analysis.

Recently, the same group has transferred this methodology to *o*-alkynylacetophenones as substrates [148]. In contrast to the previously reported reaction, the intermediately formed β-ketocarboxylic acid does not cyclize via the attack of the newly formed carboxylate moiety on the triple bond, but instead via the carbonyl oxygen atom to produce dihydrobenzofuran derivatives (Fig. 37). In this case AgOAc (10 mol%) in the presence of DBU as base was found to be the most suitable system to achieve the 5-exo-dig cyclization under 10 bar of $CO_2$ pressure in acetonitrile solvent.

Shortly after this report, Zhang, Lu, and co-workers disclosed a significant improvement on this methodology by showing that the catalyst loading can be reduced to 2 mol% using $AgBF_4$ and MTBD as base under otherwise similar conditions (r.t., $CO_2$ balloon) [149]. Notably, the addition of 2 mol% of $PPh_3$ led to a drastic decrease in conversion of the model substrate *o*-(phenylethynyl) acetophenone (95 to 51%). This study also included deuterium labeling experiments and DFT calculations, providing evidence for an operative mechanism involving a 1,5-hydrogen shift and explaining the high selectivity of the process toward the 5-exo oxygen cyclization product. On the basis of these studies, two plausible catalytic cycles were proposed (Fig. 38). The preferred pathway involves the tautomerization of the β-ketocarboxylate, followed by nucleophilic attack of the enol oxygen atom on the silver(I) π-acetylide (pathway I). The second passes through the direct attack of the carbonyl oxygen atom on the silver(I) π-acetylide and requires a subsequent 1,5-hydride shift to form the benzofuran **A** (pathway II). This pathway was believed to be less operative due to a low degree of deuteration at the former alkyne functionality and on the basis of DFT-calculated barriers for cyclization steps **I** and **II**.

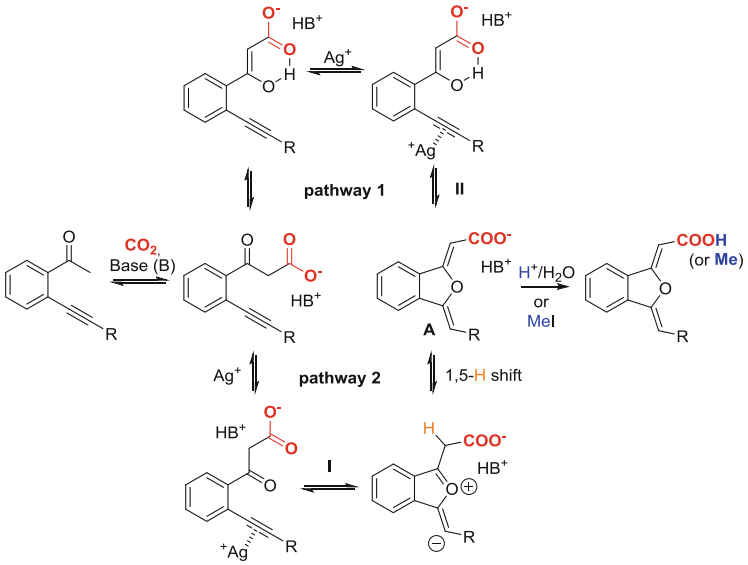


**Fig. 38** Mechanistic pathways in the silver(I)-catalyzed carboxylation/cyclization of *o*-alkynylacetophenones to dihydrobenzofuran derivatives (Zhang, Lu, and co-workers [149])

### 4.1.3 Gold-Catalyzed Reactions

While copper and silver have been widely used in carboxylation reactions, examples based on gold remained almost undiscovered. In 2010 an important discovery concerning the use of NHC–gold complexes was made by Nolan and co-workers [150]. In analogy to their previously introduced copper catalyst system, [Au(IPr)(OH)] ($pK_{a(DMSO)} = 30.3$) was used to regioselectively carboxylate the most acidic C–H bond of carbo- and heterocycles with $pK_{a(DMSO)}$ values lower than 30.3. Initial optimization on oxazole revealed that the complex performed very well even at low loadings (1.5 mol%) and under mild conditions (r.t., 1 bar $CO_2$). Reactions run at 45°C required higher catalyst loading (3 mol%) which was attributed to the lower solubility of $CO_2$ at this temperature. Forming the gold hydroxide catalyst in situ by employing [Au(IPr)Cl] as precatalyst gave slightly reduced yields in comparison to the defined gold hydroxide catalyst (88 vs. 94%, respectively, at 45°C, 3 mol% loading). This was explained by the identification of an induction period preceding the catalytic reaction of the "in situ catalyst." Interestingly, the system showed high recyclability after six runs (98% activity retention per cycle). The scope of the reaction was evaluated on aromatic heterocycles, such as oxazoles, thiazoles and their corresponding benzannulated congeners, and di-, tri-, and tetra-halogenated arenes (F, Cl). Notably, thiazole as substrate gave regioisomeric C2- and C5-carboxylated compounds due to similar $pK_{a(DMSO)}$ values of the respective C–H bonds, and substrates with $pK_{a(DMSO)}$ values slightly above 30.3 were carboxylated with the more basic [Au(I*t*Bu)OH] precatalyst ($pK_{aDMSO} = 32.4(2)$).

A mechanistic proposal similar to the copper-catalyzed reaction was presented, based on similar stoichiometric experiments (see Fig. 36).

## 4.2 Reactions with Group 10 Metals

### 4.2.1 Nickel-Catalyzed Reactions

**C–M Bonds (M = Zn, B)** Yorimitsu and Oshima and co-workers discovered that various primary alkylzinc iodide reagents bearing pendant functional groups such as double bonds, ethers, esters, and aromatic C–Cl bonds are carboxylated by $CO_2$ at atmospheric pressure using catalytic amounts of [Ni(acac)$_2$] in the presence of 2 equiv. of $PCy_3$ per nickel complex [131]. Other electron-rich phosphines or *N*-donors such as DBU and dtbpy performed less efficiently in the model coupling of *n*-hexylzinc iodide–lithium chloride complex with $CO_2$. Notably, the absence of lithium chloride led to a dramatically reduced yield (Fig. 39).

In parallel to this work, Yeung and Dong reported a procedure for the carboxylation of organozinc bromides using Ni(0) and Pd(II) precatalysts [133]. The reactions also required the use of electron-rich phosphines, suggesting the mechanism to proceed via initial oxidative addition of the $CO_2$ molecule, followed by transmetalation of the organozinc reagent and reductive elimination, thus resembling the Negishi cross-coupling reaction in which the organohalide is replaced by $CO_2$ as the electrophile coupling partner (Fig. 40). Defined Ni(0) complexes such as Aresta's complex [Ni($PCy_3$)$_2$($\eta^2$-$CO_2$)] or [Ni($PCy_3$)$_2$($N_2$)], at 5 mol% loading, performed slightly better than an "in situ catalyst" comprised of [Ni(COD)]$_2$ and $PCy_3$ in a 1:2 ratio. A range of linear alkylzinc reagents bearing pending ester and halide functionalities as well as phenylzinc bromide were carboxylated at 0°C and atmospheric $CO_2$ pressure with good to high yields.

The first nickel-catalyzed carboxylation of organoboron reagents was very recently reported by Nolan and co-workers [151]. Air-stable, well-defined nickel allyl complexes of the type [Ni(NHC)($\eta^3$-allyl)Cl] bearing bulky and flexible NHCs of the IPr ligand family were investigated in the model carboxylation of *p*-anisylboronic acid neopentylglycol ester (Fig. 41). Only the complexes of the very bulky IPr* subclass of these ligands (IPr* = 1,3-bis(2,6-diphenylmethyl-4-methylphenyl)imidazol-2-ylidene) showed quantitative conversion of the substrate at 100°C in toluene and at atmospheric $CO_2$ pressure. Under the optimized

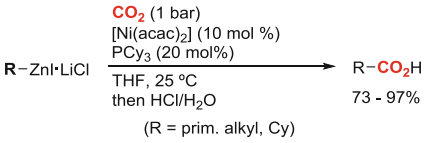


**Fig. 39** Carboxylation of organozinc reagents using Ni(II) and Ni(0) precatalysts (Yorimitsu, Oshima, and co-workers [132])

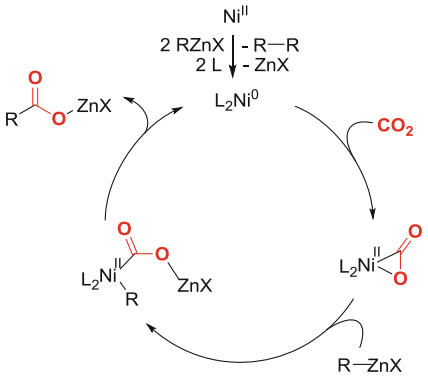


**Fig. 40** Mechanistic proposal for the carboxylation of organozinc reagents (Yeung, Dong, and co-workers [133])

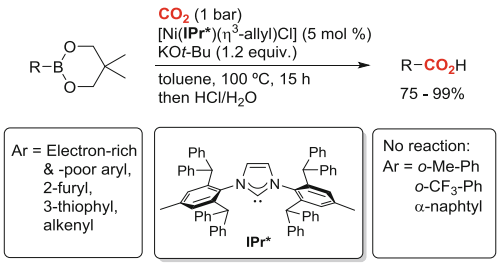


**Fig. 41** NHC nickel-catalyzed carboxylation of aryl and alkenyl boronates (Nolan and co-workers [151])

conditions a range of electron-deficient and electron-rich aryl boronates were converted into the corresponding benzoic acid derivatives with generally high yields. While *ortho*-substitution did not seem to be tolerated well in this reaction (*o*-Me and *o*-$CF_3$, no conversions), a few alkenyl and heteroaryl boronates were shown to be efficiently carboxylated in comparable yields. A preliminary mechanistic study hinted that the active transmetalation agent in this reaction might be an aryltrialkoxyborate salt generated from the alkoxide base and the boron reagent, which was isolated and characterized by X-ray diffraction analysis.

**C–X Bonds (X = Cl, O)** While the first catalytic one-pot reductive carboxylation strategy of arene C–X bonds was reported with palladium (see following section) [137], most protocols which have been developed are nickel-based processes and typically proceed at ambient conditions. Generally, these reports involve the use of phosphine or bipyridine Ni(II) dihalide salts as precatalysts (5–10 mol%) in the presence of manganese or zinc metal (1–5 equiv.) as stoichiometric reductants in polar aprotic solvents such as DMF, DMA, or DMI (dimethylformamide, dimethylacetamide, 1,3-dimethyl-2-imidazolidinone, respectively) (Fig. 42). Often, the presence of halide additives such as $Et_4NI$, *n*-$Bu_4NI$, or $MgCl_2$ is required in order to efficiently promote these reactions.

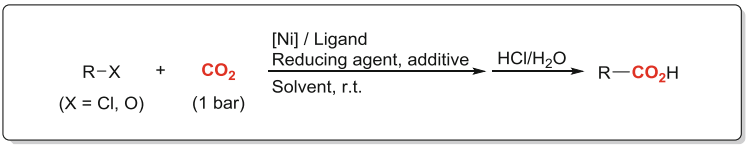


| | R | [Ni] / L | Reductant | Additive | Solvent | Time | Yield |
|---|---|---|---|---|---|---|---|
| (A) | 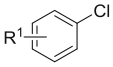 | $[Ni(PPh_3)_2Cl_2]$ / $PPh_3$ (5 mol% / 10 mol%) | Mn (3 equiv.) | $Et_4NI$ (10 mol%.) | DMI | 20 h | 51 - 90% |
| (B) |  | $[Ni(bpy)_2Br_2]$ / bpy (5 mol% / 15 mol%) | Mn (3 equiv.) | $Et_4NI$ (10 mol%.) | DMI | 20 h | 52 - 77% |
| (C) | 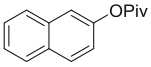 | $[Ni(dppf)Cl_2]$ / dppf (7 mol% / 20 mol%) | Mn (1 equiv.) | - | DMA | 48h (80 °C) | 47 - 78% |
| (D) | 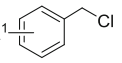 | $[Ni(glyme)_2Cl_2]$ / $PCp_3HBF_4$ (10 mol% / 20 mol%) | Zn (5 equiv.) | $MgCl_2$ (200 mol%.) | DMF | o.n. | 49 - 79% |
| (E) | 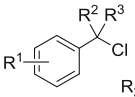 | $[Ni(PCy_3)_2Cl_2]$ (10 mol%) | Zn (5 equiv.) | TBAI (20 mol%.) | DMA | o.n. | 47 - 61% |
| (F) | 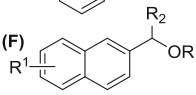 | $[Ni(PMe_3)_2Cl_2]$ (7 mol%) | Mn (2 equiv.) | - | DMF | 24h | 46 - 83% |

**Fig. 42** Nickel-catalyzed carboxylation of aryl, alkenyl, or benzyl C–Cl and C–O bonds in the presence of stoichiometric reductants (works by the groups of Tsuji and Martin)

The first carboxylation of C–Cl bonds by $CO_2$ was reported by Tsuji and co-workers in 2012 [136]. A range of electron-rich and electron-poor aryl chlorides bearing various functionalities such as ester, acetoxy, boronate, and $CF_3$ groups in *para*- or *meta*-position to the chloride substituent were carboxylated with good to high yields with $[Ni(PPh_3)_2Cl_2]$ (5 mol%) as precatalyst in the presence of additional $PPh_3$ ligand (Fig. 42a). A few alkenyl chlorides were also shown to be converted to the corresponding acrylic acid derivatives in moderate to good yields using $[Ni(bpy)Br_2]$ (5 mol%) in the presence of a threefold excess of the bpy ligand (Fig. 42b). Interestingly, a mechanistic proposal involving Ni(I) was given due to insights gained, for example, from the stoichiometric carboxylation of $[Ni(PPh_3)_2(Ph)Cl]$ with $CO_2$, which only proceeded in the presence of Mn, suggesting a reduction of Ni(II) to Ni(I) prior to $CO_2$ insertion (Fig. 43).

The carboxylation of $C(sp^3)$–halide bonds was achieved shortly after by the group of Martin in a similar protocol using zinc metal in place of manganese as reductant and nickel(II) complexes containing more electron-rich P-donors such as $PCy_3$ (Cy = cyclohexyl) and $PCp_3$ (Cp = cyclopentyl) [152]. While an in situ precatalyst system comprised of $[Ni(glyme)Cl_2]$ and $PCp_3 \cdot HBF_4$ promoted the carboxylation of primary benzylic chlorides in the presence of $MgCl_2$ (2 equiv.) (Fig. 42d), secondary and tertiary congeners were converted to carboxylic acids using $[Ni(PCy_3)_2Cl_2]$ (10 mol%) (Fig. 42e). In both cases modest yields were achieved. Very notably, the reaction proceeded with high selectivity even in the

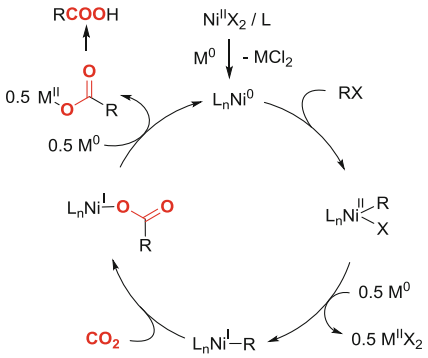


**Fig. 43** Proposed mechanism for nickel-catalyzed carboxylation of aromatic C–Cl bonds (Tsuji and co-workers [136])

presence of aromatic C–Cl bonds. A mechanism comprised of the same principal elementary steps to the one proposed by Tsuji and co-workers was presented, again supported by a stoichiometric experiment: the conversion of [Ni(PCp$_3$)($\eta^3$-benzyl)Cl] with $CO_2$ proceeded only in the presence of Zn dust (and the additive $MgCl_2$, while its role remained speculative).

Martin and co-workers have been able to extend these methodologies to the carboxylation of C–O bonds using pivalic acid benzyl esters and aromatic pivalates as substrates (Fig. 42f, c, respectively) [153] and very recently to unactivated primary alkyl bromides and sulfonates [154]. In the latter case a catalyst system of [Ni(glyme)Cl$_2$] (10 mol%) and phenanthroline ligands (22 mol%) was employed, while manganese metal was again used in excess as reducing agent (2.2–2.4 equiv.). Thereby, various long-chain alkyl bromides and sulfonates (OTs, OMs, $O_2CCF_3$) bearing – among others – pendant ether, ester, nitrile, keto, and aryl-Cl moieties were converted with moderate to good yields to the corresponding carboxylic acids.

### 4.2.2 Palladium-Catalyzed Reactions

**C–M Bonds (M = Sn, Zn, B)** In 1997 Nicholas and co-workers reported the first catalytic carboxylation of organometallic reagents with less polarized C–M bonds than the typically used organolithium and Grignard reagents [130]. Allylstannanes were converted to a mixture of 3-butenoic and 2-butenoic acid stannyl esters in a 9:1 mixture at elevated temperature and $CO_2$ pressure (70°C, 33 bar) using [Pd(PPh$_3$)$_4$] (8 mol%) as precatalyst (Fig. 44). Based on these results, the same group developed a Stille-type carboxylative cross-coupling reaction between allylstannanes and allyl chlorides under a relatively high $CO_2$ pressure (50 bar) [155]. Very notably, also platinum complexes were investigated in this report, which displayed a rare example for the activity of homogeneous platinum compounds in $CO_2$-incorporative catalysis.

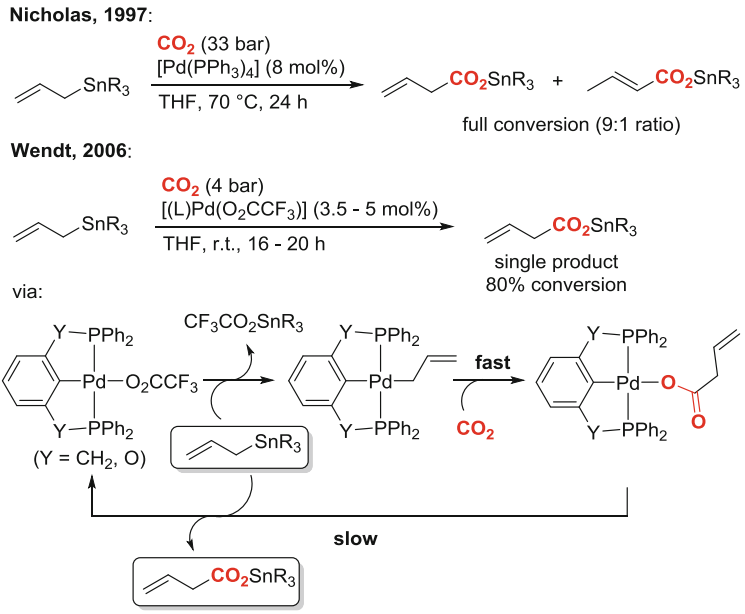


**Fig. 44** Carboxylation of allylstannane with $CO_2$ (works from the groups of Nicholas [130] and Wendt [131])

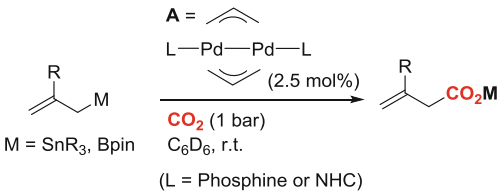


**Fig. 45** Carboxylation of allylstannanes and allylboranes catalyzed by Pd(I) allyl dimers (Hazari and co-workers [156])

Wendt and co-workers were able to achieve milder reaction conditions and a dramatically enhanced selectivity in the carboxylation of allylstannanes toward the 3-butenoic acid ester by using a PCP pincer palladium(II) complex (Fig. 44), albeit never reaching full conversion of the allylstannane reagent (up to 80%) [131]. The ligand's role was considered crucial for the observed reactivity due to an enhancement of the nucleophilicity of an intermediate σ-allyl complex formed after transmetalation of allylstannane to the Pd(II) metal center (Fig. 44).

Another concept for exploiting the nucleophilic rather than electrophilic reactivity of allyl palladium systems toward the $CO_2$ molecule was realized by Hazari and co-workers [156]. Since this nucleophilic behavior was found to be exhibited by bridging $\eta^3$-allyl ligands in stoichiometric carboxylation reactions of Pd(I) dimers such as **A** (Fig. 45), this complex was used as a precatalyst in the

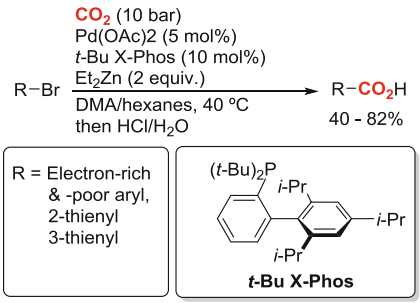


**Fig. 46** Palladium-catalyzed reductive carboxylation of aryl bromides (Martin and co-workers [137])

catalytic carboxylation of allylstannanes and allylboranes. The same group also discovered that a family of well-defined complexes of the type [Pd(L)($\eta^3$-allyl)(carboxylate)] (L = $PR_3$ or NHC), which are accessible from the reaction of complexes such as [Pd(L)($\eta^3$-allyl)($\eta^1$-allyl)] with $CO_2$, are also potent catalysts for these transformations under mild conditions (1 bar $CO_2$, r.t.) [157].

**C–X Bonds (X = Br, O)** The carboxylation of aromatic halides has been intensively investigated by electrochemical methods since the late 1980s and early 1990s (see, e.g., Amatore et al. [158] and references therein). However, the palladium-catalyzed reductive carboxylation of aryl bromides using $ZnEt_2$ as stoichiometric reductant was first achieved by Martin and co-workers [137] with a precatalyst system comprised of [$Pd(OAc)_2$] (5 mol%) and a very bulky phosphine of the Buchwald ligand family such as ***t*-Bu-X-Phos** (10 mol%) (Fig. 46) [159]. Compared to a series of other monodentate phosphines and NHCs, this ligand showed a remarkably higher selectivity toward the carboxylated product in the model reaction between $CO_2$ (10 bar) and *p*-*n*-butylphenylbromide in DMA at 40°C. The by-products arising from simple reduction or cross-coupling with the dialkylzinc reagent accompanied this reaction. Modest yields were obtained for the carboxylation of a wide range of electron-rich and electron-poor aryl bromides bearing functionalities such as carbonyl, epoxide, arene, C–Cl, or ester groups.

The stoichiometric carboxylation of group 10 metal allyl complexes has been reported in a number of reports [160], but the development of a catalytic transformation involving allyl intermediates has remained limited apart from Inoue's carboxylation of methylenecyclopropanes, which is believed to proceed via trimethylenemethane–palladium complexes (see Sect. 2.2.2). Recently, Greco and co-workers reported that these types of compounds can be used in isolated form as the precatalysts in the carboxylation of a formal methylenecyclopropane equivalent: 2-(acetoxymethyl)-3-(trimethylsilyl)propene [161]. Thus, similarly to Inoue's report, γ-butyrolactones were obtained via a [3 + 2] cycloaddition, but under much milder reaction conditions (1 bar, 75°C, 30 min).

**C–H Bonds** A seminal report from 1984 on the carboxylation of aromatic C–H bonds from Fujiwara and co-workers involves the use of simple palladium salts under forcing conditions (150°C, 30 bar $CO_2$) [162]. Thereby, a few arenes and

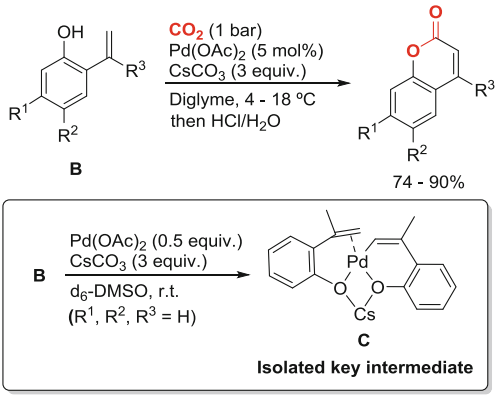


**Fig. 47** Direct carboxylation of alkenyl C–H bonds with $CO_2$ (Iwasawa and co-workers [163])

heteroarenes were converted to carboxylic acids with stoichiometric amounts of either $Pd(OAc)_2$ or $Pd(NO_3)_2$ in low (thiophene, furan) to high yields (anisole, benzene) with respect to the palladium complex. Notably the use of *t*-BuOOH increased the yields significantly.

A recent, interesting strategy for the carboxylation of C–H bonds was introduced by the group of Iwasawa for the synthesis of coumarin derivatives from *ortho*-hydroxystyrenes using $Pd(OAc)_2$ (5 mol%) in diglyme (diglyme = bis (2-methoxyethyl) ether) at 100°C under atmospheric $CO_2$ pressure [163]. The presence of an excess of base ($Cs_2CO_3$) was required for the activation of the alkenyl C–H bond, presumably to enhance the coordinating properties of the hydroxy directing group. A range of substrates bearing electron-donating and electron-withdrawing substituents at the arene ring were converted to the coumarin products in moderate to high yields. A key intermediate of the reaction could easily be synthesized and characterized by X-ray diffraction analysis. The alkenyl palladium complex **C**, bearing two substrate molecules, was accessed by the reaction of substrate **B** with $Pd(OAc)_2$ (0.5 equiv.) and $Cs_2CO_3$ (3 equiv.) in the absence of $CO_2$ (Fig. 47). Both alkoxide donors are bridged by a $Cs^+$ ion, which itself was found to be ligated by another 3 oxygen atoms stemming from diglyme in the crystal structure.

## *4.3 Reactions with Miscellaneous Transition Metals*

**C–B Bonds** The first transition metal-catalyzed carboxylation of organoboron reagents was reported by Iwasawa and co-workers in 2006 [139]. Based on seminal works of the 1970s and 1980s from the groups of Vol'pin, Aresta, and Darensbourg who reported the stoichiometric carboxylation of different phenylrhodium species [164–166], the first catalytic rhodium-catalyzed carboxylation process was developed using aryl boronic esters as the nucleophilic reaction partner of $CO_2$ (Fig. 48). It was found that the precatalyst $[Rh(COD)(\mu\text{-}OH)]_2$ (3 mol%) most efficiently

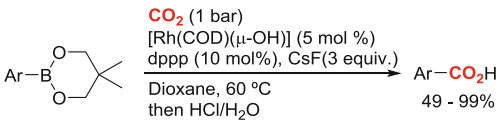


**Fig. 48** Carboxylation of aryl boronates by a Rh(I) diphosphine catalyst system (Iwasawa and co-workers [139])

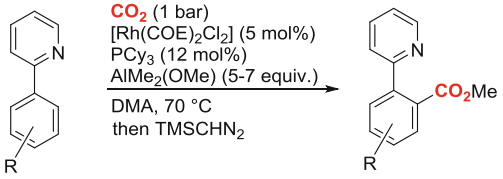


**Fig. 49** Rhodium-catalyzed direct carboxylation of arenes (Iwasawa and co-workers [167])

catalyzed the reaction in the presence of CsF (3 equiv.) and bidentate phosphine ligands such as dppp (bis-(diphenylphosphino)propane) (7 mol%) with preference over a series of other typically used inorganic bases and monodentate phosphines, respectively. Under the optimized conditions, this catalyst combination permitted the carboxylation of a series of *para*-substituted aryl boronates in dioxane under mild conditions (1 bar $CO_2$, 60°C) yielding the products in moderate to high yields. *Ortho*- and *meta*-substituted substrates and heteroaryl boronic esters produced lower yields. Notably, the carboxylation of a few alkenyl boronates proceeded in good yields at a slightly higher catalyst loading (5 mol%) and did not further undergo a 1,4-addition reaction between the produced acrylic acid derivative and the organoboronate, which is typical for rhodium catalysis.

**C–H Bonds** The well-known ability of Rh(I) complexes to act as catalysts in transformations involving C–H activations inspired Iwasawa and co-workers to investigate if this reactivity could be exploited in a sequential carboxylation of the Rh–C bond (Fig. 49) [167]. Typical substrates containing N-donor atoms for directed C–H activation processes were investigated such as 2-phenylpyridines and 1-phenylpyrazoles. At atmospheric $CO_2$ pressure, the precatalyst $[Rh(COE)_2(\text{-}\mu\text{-}Cl)]_2$ (5 mol%) permitted the *ortho*-carboxylation of a series of differently substituted phenylpyridines in the presence of a bulky phosphine ligand ($PCy_3$, 12 mol%) and a methylaluminum reagent (2 equiv.). Moderate to good yields were obtained for these substrates, whereas phenylpyrazoles were generally carboxylated less efficiently. The products were isolated as the corresponding methyl esters generated from the treatment of the reaction mixtures with TMS-$CHN_2$. The C–H activation required for this process was proposed to proceed at a Rh(I)-methyl species, which forms in situ by the reaction of the methylaluminum reagent and the rhodium precursor. A Rh(III) intermediate is then generated via cyclometalation of the phenylpyridine, followed by reductive elimination of methane and then $CO_2$ insertion into the Rh(I)–aryl bond to give a Rh(I) carboxylate. The subsequent

transmetalation reaction with the methyl aluminum reagent liberates the product as an aluminum carboxylate and regenerates the active Rh(I)-methyl species.

Mita, Sato, and co-workers have recently disclosed the challenging carboxylation of benzylic $C(sp^3)$–H bonds in sequential, one-pot protocols [168]. These ligand-free protocols involve the use of either Ir(I) or Ru(0) complexes such as $[Ir(COD)_2Cl]_2$ and $Ru_3(CO)_{12}$ in the presence of $Et_3SiH$ to enable an initial silylation of both $C(sp^2)$–H and $C(sp^3)$–H bonds of a tolyl ring system containing a pyridyl directing group. The following CsF-mediated carboxylation of the double silated intermediate proceeded only at the $C(sp^3)$–Si bond and gave the products in up to 90% yield.

## References


1. Behr A (1987) Use of carbon dioxide in industrial organic syntheses. Chem Eng Technol 10: 16–27
2. Mikkelsen M, Jorgensen M, Krebs FC (2010) The teraton challenge. A review of fixation and transformation of carbon dioxide. Energy Environ Sci 3:43–81
3. Arakawa H et al (2001) Catalysis research of relevance to carbon management: progress, challenges, and opportunities. Chem Rev 101:953–996
4. Sakakura T, Kohno K (2009) The synthesis of organic carbonates from carbon dioxide. Chem Commun 11:1312–1330
5. Omae I (2012) Recent developments in carbon dioxide utilization for the production of organic chemicals. Coord Chem Rev 256:1384–1405
6. Tsuji Y, Fujihara T (2012) Carbon dioxide as a carbon source in organic transformation: carbon–carbon bond forming reactions by transition-metal catalysts. Chem Commun 48: 9956–9964
7. Huang K, Sun C-L, Shi Z-J (2011) Transition-metal-catalyzed C–C bond formation through the fixation of carbon dioxide. Chem Soc Rev 40:2435–2452
8. Sakakura T, Choi J-C, Yasuda H (2007) Transformation of carbon dioxide. Chem Rev 107: 2365–2387
9. Martin R, Kleij AW (2011) Myth or reality? Fixation of carbon dioxide into complex organic matter under mild conditions. ChemSusChem 4:1259–1263
10. Coates GW, Moore DR (2004) Discrete metal-based catalysts for the copolymerization of $CO_2$ and epoxides: discovery, reactivity, optimization, and mechanism. Angew Chem Int Ed 43:6618–6639
11. Shaikh A-AG, Sivaram S (1996) Organic carbonates. Chem Rev 96:951–976
12. Federsel C, Jackstell R, Beller M (2010) State-of-the-art catalysts for hydrogenation of carbon dioxide. Angew Chem Int Ed 49:6254–6257
13. Wang W, Wang S, Ma X, Gong J (2011) Recent advances in catalytic hydrogenation of carbon dioxide. Chem Soc Rev 40:3703–3727
14. Goeppert A, Czaun M, Jones J-P, Prakash GKS, Olah GA (2014) Recycling of carbon dioxide to methanol and derived products – closing the loop. Chem Soc Rev 43:7995–8048
15. Ohmiya H, Tanabe M, Sawamura M (2011) Copper-catalyzed carboxylation of alkylboranes with carbon dioxide: formal reductive carboxylation of terminal alkenes. Org Lett 13: 1086–1088
16. Ohishi T, Zhang L, Nishiura M, Hou Z (2011) Carboxylation of alkylboranes by N-heterocyclic carbene copper catalysts: synthesis of carboxylic acids from terminal alkenes and carbon dioxide. Angew Chem Int Ed 50:8114–8117

17. Inoue Y, Hisi T, Satake M, Hashimoto H (1979) Reaction of methylenecyclopropanes with carbon dioxide catalysed by palladium(0) complexes. Synthesis of five-membered lactones. J Chem Soc Chem Commun 982
18. Inoue Y, Itoh Y, Hashimoto H (1978) Oligomerization of 3-hexyne by nickel(0) complexes under $CO_2$. Incorporation of $CO_2$ and novel cyclotrimerization. Chem Lett 633–634
19. Musco A, Perego C, Tartiari V (1978) Telomerization reactions of butadiene and $CO_2$ catalyzed by phosphine pd(0) complexes: (*E*)-2-ethylidenehept-6-en-5-olide and octadienyl esters of 2-ethylidenehepta-4,6-dienoic acid. Inorg Chim Acta 28:L147–L148
20. Musco A (1980) Co-oligomerization of butadiene and carbon dioxide catalysed by tertiary phosphine–palladium complexes. J Chem Soc Perkin Trans 1:693–698
21. Behr A, Juszak K-D (1983) Palladium-catalyzed reaction of butadiene and carbon dioxide. J Organomet Chem 255:263–268
22. Behr A, Juszak A-D, Keim W (1983) Synthese von 2-ethyliden-6-hepten-5-olid. Synthesis 574
23. Sasaki Y, Inoue Y, Hashimoto H (1976) Reaction of carbon dioxide with butadiene catalysed by palladium complexes. Synthesis of 2-ethylidenehept-5-en-4-olide. J Chem Soc Chem Commun 605–606
24. Behr A, He R, Juszak K-D, Krüger C, Tsay Y-H (1986) Steuerungsmöglichkeiten bei der Übergangsmetall-katalysierten Umsetzung von 1,3-Dienen mit Kohlendioxid. Chem Ber 119:991–1015
25. Dinjus E, Leitner W (1995) New insights into the palladium-catalysed synthesis of δ-lactones from 1,3-dienes and carbon dioxide. Appl Organomet Chem 9:43–50
26. Pitter S, Dinjus E (1997) Phosphinoalkyl nitriles as hemilabile ligands: new aspects in the homogeneous catalytic coupling of $CO_2$ and 1,3-butadiene. J Mol Catal A 125:39–45
27. Braunstein P, Matt D, Nobel D (1988) Carbon dioxide activation and catalytic lactone synthesis by telomerization of butadiene and carbon dioxide. J Am Chem Soc 110:3207–3212
28. Pitter S, Dinjus E (1997) Phosphinoalkyl nitriles as hemilabile ligands: new aspects in the homogeneous catalytic coupling of $CO_2$ and 1,3-butadiene. J Mol Catal A Chem 125:39–45
29. Behr A, Heite M (2000) Telomerisation von Kohlendioxid und 1,3-Butadien: Verfahrensentwicklung via Miniplant-Technik. Chem Ing Technol 72:58–61
30. Behr A, Bahke P, Becker M (2004) Palladium-katalysierte Telomerisation von Kohlendioxid mit Butadien im Labor- und Miniplantmaßstab. Chem Ing Technol 76:1828–1832
31. Behr A, Becker M (2006) The telomerisation of 1,3-butadiene and carbon dioxide: process development and optimisation in a continuous miniplant. Dalton Trans 4607–4613
32. Behr A, Henze G (2011) Use of carbon dioxide in chemical syntheses via a lactone intermediate. Green Chem 13:25–39
33. Haack V, Dinjus E, Pitter S (1998) Synthesis of polymers with an intact lactone ring structure in the main chain. Die Angew Makromol Chem 257:19–22
34. Fiorani G, Kleij AW (2014) Preparation of $CO_2$/diene copolymers: advancing carbon dioxide based materials. Angew Chem Int Ed 53:2–5
35. Nakano R, Ito S, Nozaki K (2014) Copolymerization of carbon dioxide and butadiene via a lactone intermediate. Nat Chem 6:325–331
36. Hoberg H, Peres Y, Milchereit A (1986) C–C-Verknüpfung von Alkenen mit $CO_2$ an Nickel (0); Herstellung von Zimtsäure aus Styrol. J Organomet Chem 307:C38–C40
37. Hoberg H, Peres Y, Krüger C, Tsay Y-H (1987) A 1-Oxa-2-Nickela-5-cyclopentanone from ethene and carbon dioxide: preparation, structure, and reactivity. Angew Chem Int Ed Engl 26:771–773
38. Walther D, Dinjus E, Sieler J, Thanh NN, Schade W, Leban I (1983) Aktivierung von $CO_2$ an Übergangsmetallzentren: Struktur und Reaktivität eines C–C-Kopplungsproduktes von $CO_2$ und 2,3-Dimethylbutadien am elektronenreichen Nickel(0). Z Naturforsch B 23:237
39. Hoberg H, Apotecher B (1984) α, β-Disäuren aus Butadien und Kohlendioxid an Nickel(0). J Organomet Chem 270:C15–C17

40. Hoberg H, Schaefer D, Burkhart G (1982) Oxanickelacyclopenten-Derivate, ein neuer Typ vielseitig verwendbarer Synthone. J Organomet Chem 228:C21–C24
41. Burkhart G, Hoberg H (1982) Oxanickelacyclopentene derivatives from nickel(0), carbon dioxide, and alkynes. Angew Chem Int Ed Engl 21:76
42. Hoberg H, Schaefer G, Burkhart G, Krüger C, Romão MJ (1984) Nickel(0)-induzierte C–C-Verknüpfung zwischen Kohlendioxid und Alkinen sowie Alkenen. J Organomet Chem 266: 203–224
43. Hoberg H, Oster BW (1984) Nickel(0)-induzierte C–C zwischen 1,2-Dienen und Kohlendioxid. J Organomet Chem 266:321–326
44. Walther D, Dinjus E, Sieler J, Andersen L, Lindqvist O (1984) Aktivierung von Kohlendioxid an Übergangsmetallzentren: Metallaringschluss mit Dicyclopentadien am elektronenreichen Nickel(0)-Komplexrumpf als topo- und stereoselektive Reaktion. J Organomet Chem 276: 99–107
45. Hoberg H, Gross S, Milchereit A (1987) Nickel(0)-catalyzed production of a functionalized cyclopentanecarboxylic acid from 1,3-butadiene and $CO_2$. Angew Chem Int Ed Engl 26: 571–572
46. Büssemeier B, Jolly PW, Wilke G (1974) A model for the nickel-catalyzed cooligomerization of butadiene with substituted alkynes. J Am Chem Soc 96:4726–4727
47. Walther D, Schönberg H, Dinjus E (1987) Aktivierung von Kohlendioxid an Übergangsmetallzentren: Selektive Cooligomerisation mit Hexin(−3) durch das Katalysatorsystem Acetonitril/Trialkylphosphan/Nickel(0) und Struktur eines Nickel(0)-Komplexes mit Side-on gebundenem Acetonitril. J Organomet Chem 334:377–388
48. Takimoto M, Mori M (2003) Novel catalytic $CO_2$ incorporation reaction: nickel-catalyzed region- and stereoselective ring-closing carboxylation of bis-1,3-dienes. J Am Chem Soc 124: 10008–10009
49. Taimoto M, Mori M (2001) Cross-coupling reaction of oxo-π-allylnickel complex generated from 1,3-diene under an atmosphere of carbon dioxide. J Am Chem Soc 123:2895–2896
50. Takimoto M, Nakamura Y, Kimura K, Mori M (2004) Highly enantioselective catalytic carbon dioxide incorporation reaction: nickel-catalyzed asymmetric carboxylative cyclization of bis-1,3-dienes. J Am Chem Soc 126:5956–5957
51. Takimoto M, Kawamura M, Mori M, Sato Y (2005) Nickel-catalyzed regio- and stereoselective double carboxylation of trimethylsilylallene under an atmosphere of carbon dioxide and its application to the synthesis of chaetomellic acid A anhydride. Synlett 13:2019–2022
52. Williams CM, Johnson JB, Rovis T (2008) Nickel-catalyzed reductive carboxylation of styrenes using $CO_2$. J Am Chem Soc 130:14936–14937
53. Yuan R, Lin Z (2014) Computational insight into the mechanism of nickel-catalyzed reductive carboxylation of styrenes using $CO_2$. Organometallics 33:7147–7156
54. Graham DC, Mitchell C, Bruce MI, Metha GF, Bowie JH, Buntine MA (2007) Production of acrylic acid through nickel-mediated coupling of ethylene and carbon dioxide – a dft study. Organometallics 26:6784–6792
55. Lee SYT, Cokoja M, Drees M, Li Y, Mink J, Herrmann WA, Kühn FE (2011) Transformation of nickelalactones to methyl acrylate: on the way to a catalytic conversion of carbon dioxide. ChemSusChem 4:1275–1279
56. Lee SYT, Ghani AA, D'Elia V, Cokoja M, Herrmann WA, Basset J-M, Kühn FE (2013) Liberation of methyl acrylate from metallalactone complexes via M − O ring opening (M = Ni, Pd) with methylation agents. New J Chem 37:3512–3517
57. Plessow PN, Weigel L, Lindner R, Schäfer A, Rominger F, Limbach M, Hofmann P (2013) Mechanistic details of the nickel-mediated formation of acrylates from $CO_2$, ethylene and methyl iodide. Organometallics 32:3327–3338
58. Bruckmeier C, Lehenmeier MW, Reichardt R, Vagin S, Rieger B (2010) Formation of methyl acrylate from $CO_2$ and ethylene via methylation of nickelalactones. Organometallics 29:2199–2202

59. Hoberg H, Ballesteros A, Sigan A, Jegat C, Milchereit A (1991) Durch (Lig)Ni(0) induzierte Herstellung von mono- und di-Carbonsäuren aus Cyclopenten und Kohlendioxid. Synthesis 5:395–398
60. Hoberg H, Ballesteros A, Sigan A (1991) Ein neuartiger Ligandentyp zur CC-verknüpfung von Cycloalkenen mit $CO_2$ am (Lig)$Ni^0$-System, folgereaktionen. J Organomet Chem 403: C19–C22
61. Jin D, Schmeier TJ, Williard PG, Hazari N, Bernskoetter WH (2013) Lewis acid induced β-elimination from a nickelalactone: efforts toward acrylate production from $CO_2$ and ethylene. Organometallics 32:2152–2159
62. Lejkowski ML, Lindner R, Kageyama T, Bódizs GE, Plessow PN, Müller IB, Schäfer A, Rominger F, Hofmann P, Futter C, Schunk SA, Limbach M (2012) The first catalytic synthesis of an acrylate from CO2 and an alkene – a rational approach. Chem Eur J 18: 14017–14025
63. Plessow PN, Schäfer A, Limbach M, Hofmann P (2014) Acrylate formation from $CO_2$ and ethylene mediated by nickel complexes: a theoretical study. Organometallics 33:3657–3668
64. Yang G, Schäffner B, Blug M, Hensen EJM, Pidko EA (2014) A mechanistic study of ni-catalyzed carbon dioxide coupling with ethylene towards the manufacture of acrylic acid. ChemCatChem 6:800–807
65. Jin D, Williard PG, Hazari N, Bernskoetter WH (2014) Effect of sodium cation on metallacycle β-hydride elimination in $CO_2$-ethylene coupling to acrylates. Chem Eur J 20: 3205–3211
66. Huguet N, Jevtovikj I, Gordillo A, Lejkowski M, Lindner R, Bru M, Khalimon AY, Rominger F, Schunk SA, Hofmann P, Limbach M (2014) Nickel-catalyzed direct carboxylation of olefins with CO2: one-pot synthesis of α, β-unsaturated carboxylic acid salts. Chem Eur J 20:16858–16862
67. Hendriksen H, Pidko EA, Yang G, Schaeffner B, Vogt D (2014) Catalytic formation of acrylate from carbon dioxide and ethene. Chem Eur J 20:12037–12040
68. Binger F, Schuchardt U (1977) Palladium(0)-catalyzed $[2\sigma + 2\pi]$ cycloadditions methylenecyclopropane to alkenes. Angew Chem Int Ed Engl 16:249–250
69. Takaya J, Iwasawa N (2008) Hydrocarboxylation of allenes with $CO_2$ catalyzed by silyl pincer-type palladium complex. J Am Chem Soc 130:15254–15255
70. Takaya J, Sasano K, Iwasawa N (2011) Efficient one-to-one coupling of easily available 1,3-dienes with carbon dioxide. Org Lett 13:1698–1701
71. Greenhalgh MD, Thomas SP (2012) Iron-catalyzed, highly regioselective synthesis of α-aryl carboxylic acids from styrene derivatives and $CO_2$. J Am Chem Soc 134:11900–11903
72. Ostapowicz TG, Schmitz M, Krystof M, Klankermayer J, Leitner W (2013) Carbon dioxide as a C1 building block for the formation of carboxylic acids by formal catalytic hydrocarboxylation. Angew Chem Int Ed 52:12119–12123
73. Wu L, Liu Q, Fleischer I, Jackstell R, Beller M (2014) Ruthenium-catalysed alkoxycarbonylation of alkenes with carbon dioxide. Nat Commun 5:3091
74. Morimoto T, Fuji K, Tsutsumi K, Kakiuchi K (2002) CO-Transfer carbonylation reactions. a catalytic Pauson-Khand-Type reaction of enynes with aldehydes as a source of carbon monoxide. J Am Chem Soc 124:3806–3807
75. Park JH, Cho Y, Chung YK (2010) Rhodium-catalyzed Pauson–Khand-type reaction using alcohol as a source of carbon monoxide. Angew Chem Int Ed 49:5138–5141
76. Verendel JJ, Nordlund M, Andersson PG (2013) Selective metal-catalyzed transfer of $H_2$ and CO from polyols to alkenes. ChemSusChem 6:426–429
77. Lapidus AL, Pirozhkov SD, Koryakin AA (1978) Catalytic synthesis of propionic acid by carboxylation of ethylene with carbon dioxide. Bull Acad Sci USSR Div Chem Sci 27: 2513–2515
78. González-Sebastián L, Flores-Alamo M, García JJ (2012) Nickel-catalyzed reductive hydroesterification of styrenes using $CO_2$ and MeOH. Organometallics 31:8200–8207

79. Greenhalgh MD, Kolodziej A, Sinclair F, Thomas SP (2014) Iron-catalyzed hydromagnesiation: synthesis and characterization of benzylic Grignard reagent intermediate and application in the synthesis of Ibuprofen. Organometallics 33:5811–5819
80. Tsuda T, Ueda K, Saegusa T (1974) Carbon dioxide insertion into organocopper and organosilver compounds. J Chem Soc Chem Commun 380–381
81. Tsuda T, Chujo Y, Saegusa T (1975) Reversible carbon dioxide fixation by organocopper complexes. J Chem Soc Chem Commun 963–964
82. Fukue Y, Oi S, Inoue Y (1994) Direct synthesis of alkyl 2-alkynoates from alk-1-ynes, $CO_2$, and bromoalkanes catalysed by copper(I) or silver(I) salt. J Chem Soc Chem Commun 2091
83. Manjolinho F, Arndt M, Gooßen K, Gooßen LJ (2012) Catalytic C–H carboxylation of terminal alkynes with carbon dioxide. ACS Catal 2:2014–2021
84. Zhang L, Hou Z (2013) N-heterocyclic carbene (NHC)-copper-catalysed transformations of carbon dioxide. Chem Sci 4:3395–3403
85. Gooßen LJ, Rodríguez N, Manjolinho F, Lange PP (2010) Synthesis of propiolic acids *via* copper-catalyzed insertion of carbon dioxide into the C–H bond of terminal alkynes. Adv Synth Catal 352:2913–2917
86. Gooßen LJ, Thiel WR, Rodríguez N, Linder C, Melzer B (2007) Copper-catalyzed protodecarboxylation of aromatic carboxylic acids. Adv Synth Catal 349:2241–2246
87. Yu D, Zhang Y (2010) Copper- and copper-*N*-heterocyclic carbene-catalyzed C─H activating carboxylation of terminal alkynes with $CO_2$ at ambient conditions. Proc Natl Acad Sci 107:20184–20189
88. Yu D, Zhang Y (2011) The direct carboxylation of terminal alkynes with carbon dioxide. Green Chem 13:1275–1279
89. Li F-W, Suo Q-L, Hong H-L, Zhu N, Wang Y-Q, Han L-M (2014) DBU and copper (I) mediated carboxylation of terminal alkynes using supercritical $CO_2$ as a reactant and solvent. Tetrahedron Lett 55:3878–3880
90. Zhang W-Z, Li W-J, Zhang X, Zhou H, Lu X-B (2010) Cu(I)-catalyzed carboxylative coupling of terminal alkynes, allylic chlorides, and $CO_2$. Org Lett 12:4748–4751
91. Yuan R, Lin Z (2014) Mechanism for the carboxylative coupling reaction of a terminal alkyne, $CO_2$, and an allylic chloride catalyzed by the Cu(I) complex: a DFT study. ACS Catal 4:4466–4473
92. Inamoto K, Asano N, Kobayashi K, Yonemoto M, Kondo Y (2012) A copper-based catalytic system for carboxylation of terminal alkynes: synthesis of alkyl 2-alkynoates. Org Biomol Chem 10:1514–1516
93. Yu B, Diao Z-F, Guo C-X, Zhong C-L, He L-N, Zhao Y-N, Song Q-W, Liu A-H, Wang J-Q (2013) Carboxylation of terminal alkynes at ambient CO2 pressure in ethylene carbonate. Green Chem 15:2401–2407
94. Fujihara T, Xu T, Semba K, Terao J, Tsuji Y (2011) Copper-catalyzed hydrocarboxylation of alkynes using carbon dioxide and hydrosilanes. Angew Chem Int Ed 50:523–527
95. Fujihara T, Tani Y, Semba K, Terao J, Tsuji Y (2012) Copper-catalyzed silacarboxylation of internal alkynes by employing carbon dioxide and silylboranes. Angew Chem Int Ed 51: 11487–11490
96. Suginome M, Matsuda T, Nakamura H, Ito Y (1999) Regio- and stereoselective of (*Z*)-β-silylalkenylboranes by silaboration of alkynes catalyzed by palladium and platinum complexes. Tetrahedron 55:8787–8800
97. Ohmura T, Oshima K, Suginome M (2008) Palladium-catalysed *cis*- and *trans*-silaboration of terminal alkynes: complementary access to stereo-defined trisubstituted alkenes. Chem Commun 1416–1418
98. Zhang L, Cheng J, Carry B, Hou Z (2012) Catalytic Boracarboxylation of alkynes with diborane and carbon dioxide by an N-heterocyclic carbene copper catalyst. J Am Chem Soc 134:14314–14317

99. Takimoto M, Hou Z (2013) Cu-catalyzed formal methylative and hydrogenative carboxylation of alkynes with carbon dioxide: efficient synthesis of α, β-unsaturated carboxylic acids. Chem Eur J 19:11439–11445
100. Eghbali N, Eddy J, Anastas PT (2008) Silver-catalyzed one-pot synthesis of arylnaphtalene lactones. J Org Chem 73:6932–6935
101. Chopade PR, Louie J (2006) [2 + 2 + 2] Cycloaddition reactions catalyzed by transition metal complexes. Adv Synth Catal 348:2307–2327
102. Kotha S, Brahmachary E, Lahiri K (2005) Transition metal catalyzed [2+2+2] cycloaddition and application in organic synthesis. Eur J Org Chem 4741–4767
103. Zhang X, Zhang W-Z, Ren X, Zhang L-L, Lu X-B (2011) Ligand-free Ag(I)-catalyzed carboxylation of terminal alkynes with $CO_2$. Org Lett 13:2402–2405
104. Zhang X, Zhang W-Z, Shi L-L, Zhu C, Jiang J-L, Lu X-B (2012) Ligand-free Ag(I)-catalyzed carboxylative coupling of terminal alkynes, chloride compounds, and $CO_2$. Tetrahedron 68:9085–9089
105. Yu D, Tan MX, Zhang Y (2012) Carboxylation of terminal alkynes with carbon dioxide catalyzed by poly(N-heterocyclic carbene)-supported silver nanoparticles. Adv Synth Catal 354:969–974
106. Arndt M, Risto E, Krause T, Gooßen LJ (2012) C–H carboxylation of terminal alkynes catalyzed by low loadings of silver(I)/DMSO at ambient $CO_2$ pressure. ChemCatChem 4: 484–487
107. Sugawara Y, Yamada W, Yoshida S, Ikeno T, Yamada T (2007) Carbon dioxide-mediated catalytic rearrangement of propargyl alcohols into α, β-unsaturated ketones. J Am Chem Soc 129:12902–12903
108. Reppe W, Schweckendiek W (1948) Cyclisierende Polymerisation von Acetylen. III Benzol, Benzolderivate und hydroaromatische Verbindungen. Liebigs Ann Chem 560:104–116
109. Duñach E, Périchon J (1988) Electrochemical carboxylation of terminal alkynes catalyzed by nickel complexes: unusual reactivity. J Organomet Chem 353:239–246
110. Duñach E, Périchon J (1989) Nickel-catalyzed reductive electrocarboxylation of disubstituted alkynes. J Organomet Chem 364:C33–C36
111. Dérien S, Clinet J-C, Duñach E, Périchon J (1991) First example of direct carbon dioxide incorporation into 1,3-diynes: a highly regio-and stereo-selective nickel-catalysed electrochemical reaction. J Chem Soc Chem Commun 549–550
112. Dérien S, Duñach E, Périchon J (1991) From stoichiometry to catalysis: electroreductive coupling of alkynes and carbon dioxide with nickel-bipyridine complexes. Magnesium ions as the key for catalysis. J Am Chem Soc 113:8447–8454
113. Dérien S, Clinet J-C, Duñach E, Périchon J (1992) New C–C bond formation through the nickel-catalysed electrochemical coupling of 1,3-enynes and carbon dioxide. J Organomet Chem 424:213–224
114. Dérien S, Clinet J-C, Duñach E, Périchon J (1992) Activation of carbon dioxide: nickel-catalyzed electrochemical carboxylation of diynes. J Org Chem 58:2578–2588
115. Saito S, Nakagawa S, Koizumi T, Hirayama K, Yamamoto Y (1999) Nickel-mediated regio- and chemoselective carboxylation of alkynes in the presence of carbon dioxide. J Org Chem 64:3975–3978
116. Graham DC, Bruce MI, Metha GF, Bowie JH, Buntine MA (2008) Regioselective control of the nickel-mediated coupling of acetylene and carbon dioxide – a dft study. J Organomet Chem 693:2703–2710
117. Aoki M, Kaneko M, Izumi S, Ukai K, Iwasawa N (2004) Bidentate amidine ligands for nickel (0)-mediated coupling of carbon dioxide with unsaturated hydrocarbons. Chem Commun 2568–2569
118. Shimizu K, Takimoto M, Sato Y, Mori M (2005) Nickel-catalyzed regioselective synthesis of tetrasubstituted alkene using alkylative carboxylation of disubstituted alkyne. Org Lett 7: 195–197

119. Takimoto M, Shimizu K, Mori M (2001) Nickel-promoted alkylative or arylative carboxylation of alkynes. Org Lett 3:3345–3347
120. Shimizu K, Takimoto, M, Mori M, Sato, Y (2006) Effective synthesis of tamoxifen using nickel-catalyzed arylative carboxylation. Synlett 3182–3184
121. Li S, Yuan W, Ma S (2011) Highly regio- and stereoselective three-component nickel-catalyzed *syn*-hydrocarboxylation of alkynes with diethyl zinc and carbon dioxide. Angew Chem Int Ed 50:2578–2582
122. Li S, Ma S (2011) Highly selective nickel-catalyzed methyl-carboxylation of homopropargylic alcohols for α-alkylidene-γ-butyrolactones. Org Lett 13:6046–6049
123. Tsuda T, Morikawa S, Sumiya R, Saegusa T (1988) Nickel(0)-catalyzed cycloaddition of diynes and carbon dioxide to bicyclic α-pyrones. J Org Chem 53:3140–3145
124. Louie J, Gibby EG, Farnworth MV, Tekavec TN (2002) Efficient nickel-catalyzed [2 + 2 + 2] cycloaddition of $CO_2$ and diynes. J Am Chem Soc 124:15188–15189
125. Böhm VPW, Gstöttmayr CWK, Weskamp T, Herrmann WA (2001) Catalytic C–C bond formation through selective activation of C–F bonds. Angew Chem Int Ed 40:3387–3389
126. Tekavec TN, Arif AM, Louie J (2004) Regioselectivity in nickel(0) catalyzed cycloadditions of carbon dioxide with diynes. Tetrahedron 60:7431–7437
127. Takimoto M, Mizuno T, Sato Y, Mori M (2005) Nickel-mediated carboxylative cyclization of enynes. Tetrahedron Lett 46:5173–5176
128. Takimoto M, Mizuno T, Mori M, Sato Y (2006) Nickel-mediated cyclization of enynes under an atmosphere of carbon dioxide. Tetrahedron 62:7589–7597
129. Mizuno T, Oonishi Y, Takimoto M, Sato Y (2011) Total synthesis of (−)-Corynantheidine by nickel-catalyzed carboxylative cyclization of enynes. Eur J Org Chem 2606–2609
130. Shi M, Nicholas KM (1997) Palladium-catalyzed carboxylation of allyl stannanes. J Am Chem Soc 119:5057
131. Johansson R, Wendt O F (2006) Insertion of $CO_2$ into a palladium allyl bond and a Pd(II) catalysed carboxylation of allyl stannanes. Dalton Trans 488–492
132. Ochiai H, Jang M, Hirano K, Yorimitsu H, Oshima K (2008) Nickel-catalyzed carboxylation of organozinc reagents with $CO_2$. Org Lett 10:2681–2683
133. Yeung CS, Dong VM (2008) Beyond aresta's complex: Ni- and Pd-catalyzed organozinc coupling with $CO_2$. J Am Chem Soc 130:7826–7827
134. Takaya J, Tadami S, Ukai K, Iwasawa N (2008) Copper(I)-catalyzed carboxylation of aryl- and alkenylboronic esters. Org Lett 10:2697–2700
135. Ohishi T, Nishiura M, Hou Z (2008) Carboxylation of organoboronic esters catalyzed by N-heterocyclic carbene copper(I) complexes. Angew Chem Int Ed Engl 47:5792–5795
136. Fujihara T, Nogi K, Xu T, Terao J, Tsuji Y (2012) Nickel-catalyzed carboxylation of aryl and vinyl chlorides employing carbon dioxide. J Am Chem Soc 134:9106–9109
137. Correa A, Martín R (2009) Palladium-catalyzed direct carboxylation of aryl bromides with carbon dioxide. J Am Chem Soc 131:15974–15975
138. Tran-Vu H, Daugulis O (2013) Copper-catalyzed carboxylation of aryl iodides with carbon dioxide. ACS Catal 3:2414–2420
139. Ukai K, Aoki M, Takaya J, Iwasawa N (2006) Rhodium(I)-catalyzed carboxylation of aryl- and alkenylboronic esters with $CO_2$. J Am Chem Soc 128:8706–8707
140. Duong HA, Huleatt PB, Tan Q-W, Shuying EL (2013) Regioselective copper-catalyzed carboxylation of allylboronates with carbon dioxide. Org Lett 15:4034–4037
141. Ackermann L (2011) Transition-metal-catalyzed carboxylation of C–H bonds. Angew Chem Int Ed 50:3842–3844
142. Forman GC, Slawin AMZ, Nolan SP (2010) A versatile cuprous synthon: [Cu(IPr)(OH)] (IPr = 1,3-bis(diisopropylphenyl)imidazol-2-ylidene). Organometallics 29:3966–3972
143. Boogaerts IIF, Fortman GC, Furst MRL, Cazin CSJ, Nolan SP (2010) Carboxylation of N–H/C–H bonds using N-heterocyclic carbene copper(I) complexes. Angew Chem Int Ed 49: 8674–8677

144. Zhang L, Cheng J, Ohishi T, Hou Z (2010) Copper-catalyzed direct carboxylation of C–H bonds with carbon dioxide. Angew Chem Int Ed 49:8670–8673
145. Ariafard A, Zarkoob F, Batebi H, Stranger R, Yates BF (2011) DFT studies on the carboxylation of the C–H bond of heteroarenes by copper(I) complexes. Organometallics 30: 6218–6224
146. Inomata H, Ogata K, Fukuzawa S, Hou Z (2012) Direct C–H carboxylation with carbon dioxide using 1,2,3-triazol-5-ylidene copper(I) complexes. Org Lett 14:3986–3989
147. Kikuchi S, Sekine K, Ishida T, Yamada T (2012) C–C bond formation with carbon dioxide promoted by a silver catalyst. Angew Chem Int Ed 51:6989–6992
148. Sekine K, Takayanagi A, Kikuchi S, Yamada T (2013) Silver-catalyzed C–C bond formation with carbon dioxide: significant synthesis of dihydroisobenzofurans. Chem Commun 49: 11320–11322
149. Zhang W-Z, Shi L-L, Liu C, Yang X-T, Wang Y-B, Luo Y, Lu X-B (2014) Sequential carboxylation/intramolecular cyclization reaction of *o*-alkynyl acetophenone with $CO_2$. Org Chem Front 1:275–283
150. Boogaerts IIF, Nolan SP (2010) Carboxylation of C–H bonds using *N*-heterocyclic carbene gold(I) complexes. J Am Chem Soc 132:8858–8859
151. Makida Y, Marelli E, Slawin AMZ, Nolan SP (2014) Nickel-catalysed carboxylation of organoboronates. Chem Commun 50:8010–8013
152. León T, Correa A, Martin R (2013) Ni-catalyzed direct carboxylation of benzyl halides with $CO_2$. J Am Chem Soc 135:1221–1224
153. Correa A, León T, Martín R (2013) Ni-catalyzed carboxylation of C($sp^2$)- and C($sp^3$)-O bonds with $CO_2$. J Am Chem Soc 136:1062–1069
154. Liu Y, Cornella J, Martin R (2014) Ni-catalyzed carboxylation of unactivated primary alkyl bromides and sulfonates with $CO_2$. J Am Chem Soc 136:11212–11215
155. Franks RJ, Nicholas KM (2000) Palladium-catalyzed carboxylative coupling of allylstannanes and allyl halides. Organometallics 2000:1458–1460
156. Hruszkewycz DP, Wu J, Hazari N, Incarvito CD (2011) Palladium(I)-bridging allyl dimers for the catalytic functionalization of $CO_2$. J Am Chem Soc 133:3280–3282
157. Wu J, Hazari N (2011) Palladium catalyzed carboxylation of allylstannanes and boranes using $CO_2$. Chem Commun 47:1069–1071
158. Amatore C, Jutand A, Khalil F, Nielsen M (1992) Carbon dioxide as a $C_1$ building block. Mechanism of palladium-catalyzed carboxylation of aromatic halides. J Am Chem Soc 114: 7076–7085
159. Surry DS, Buchwald SL (2011) Dialkylbiaryl phosphines in Pd-catalyzed amination: a user's guide. Chem Sci 2:27–50
160. Jolly PW, Stobbe S, Wilke G, Goddard C, Krüger JC, Sekutowski JC, Tsay Y-H (1978) Reactions of carbon dioxide with allylnickel compounds. Angew Chem Int Ed Engl 17: 124–125
161. Greco GE, Gleason BL, Lowery TA, Kier MJ, Hollander LB, Gibbs SA, Worthy AD (2007) Palladium-catalyzed [3 + 2] cycloaddition of carbon dioxide and trimethylenemethane under mild conditions. Org Lett 9:3817–3820
162. Sugimoto H, Kawata I, Taniguchi H, Fujiwara Y (1984) Palladium-catalyzed carboxylation of aromatic compounds with carbon dioxide. J Organomet Chem 266:C44–C46
163. Sasano K, Takaya J, Iwasawa N (2013) Palladium(II)-catalyzed direct carboxylation of alkenyl C-H bonds with $CO_2$. J Am Chem Soc 135:10954–10957
164. Kolomnikov IS, Gusev AO, Belopotapova TS, Grigoryan MK, Lysyak TV, Struchkov YT, Vol'Pin ME (1974) J Organomet Chem 69:C10
165. Albano P, Aresta M, Manassero M (1980) Inorg Chem 19:1069
166. Darensbourg DJ, Grötsch G, Wiegreffe P, Rheingold AL (1987) Inorg Chem 26:3827
167. Mizuno H, Takaya J, Iwasawa N (2011) Rhodium(I)-catalyzed direct carboxylation of arenes with $CO_2$ via chelation-assisted C–H bond activation. J Am Chem Soc 133:1251–1253
168. Mita T, Michigami K, Sato Y (2012) Sequential protocol for C(sp3)-H carboxylation with $CO_2$: transition-metal-catalyzed benzylic C–H silylation and fluoride-mediated carboxylation. Org Lett 14:3462–3465

Top Organomet Chem (2016) 53: 279–304
DOI: 10.1007/3418_2015_109

Published online: 26 June 2015

# Recent Progress in Carbon Dioxide Reduction Using Homogeneous Catalysts

**Lipeng Wu, Qiang Liu, Ralf Jackstell, and Matthias Beller**

**Abstract** Efficient chemical transformations of carbon dioxide into value-added chemicals are of growing importance in academic and industrial laboratories. In this respect, the reduction of carbon dioxide to formic acid, methanol etc., offers interesting possibilities. Herein, we describe the recent developments in carbon dioxide reductions mainly focusing on the use of defined organometallic catalysts and in some cases organocatalysts are also included.

**Keywords** Carbon dioxide · Homogeneous catalysis · Organometallics · Reduction

## Contents



L. Wu, Q. Liu, R. Jackstell, and M. Beller (✉)
Leibniz-Institut für Katalyse an der Universität Rostock, Albert-Einstein-Street 29a, 18059 Rostock, Germany
e-mail: matthias.beller@catalysis.de

# 1 Introduction

Since the beginning of the industrial revolution, the concentration of carbon dioxide in the atmosphere has been significantly increased because of burning fossil resources to generate energy supply. This increase is generally considered to be the main reason for global warming [1]. Although the chemical use of carbon dioxide cannot solve the problem of global warming alone, it's utilization in synthesis offers interesting opportunities for the chemical industry and organic synthesis [2]. In general, carbon dioxide is a favourable C1 feedstock due to its abundance, availability, low toxicity and recyclability. Recent advances in organometallic catalysis provide effective means for the chemical transformation of $CO_2$ and its incorporation into valuable organic compounds [3–8]. Notably, a variety of products including urea, cyclic carbonates and salicylic acid are produced already on industrial scale. In addition, direct carboxylation of Ar–X (X = Cl, Br, OPiv, $B(OR)_2$ or H) and hydrocarboxylation of carbon–carbon multiple bonds offer interesting opportunities although these areas are still far away from practical applications.

While in biological systems the reduction of carbon dioxide is associated with photosynthesis, artificial reductions ideally make use of hydrogen. Several excellent reviews in this area have been published by Jessop and Leitner in 1995 [9, 10] and 2004 [11] and recently in 2011 by Gong [12]. Mechanistic perspectives and applications using homogeneous (Jessop and Leitner) and heterogeneous (Gong) catalysts were covered. Thus, the main subject of this review will be on advancements, which have been made since then.

# 2 Products from $CO_2$ Reduction

## *2.1 From Carbon Dioxide to Formic Acid and Its Derivatives*

### 2.1.1 Using Hydrogen as Reductant

The first homogeneously catalysed hydrogenation of carbon dioxide to formic acid was reported in 1976 [13]. Since then, especially in the last two decades, intensive studies followed. Normally, bases were added to thermodynamically drive the reaction from carbon dioxide to formic acid because the gas phase reaction has a positive $\Delta G$ value (Scheme 1). In the presence of inorganic base, formates are produced as final products, while in the presence of primary and secondary amine

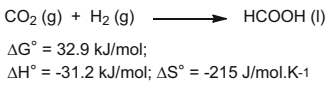


**Scheme 1** Hydrogenation of carbon dioxide to formic acid: thermodynamics

bases, formamides are obtained. Nowadays, tertiary amines are often used and proved to be the most active additive. In the presence of tertiary amines, an acid/amine ratio (AAR) normally in the range of 1.3 to 2.7 is obtained. On the other hand, the reduction of carbon dioxide into formates in aqueous solution is more favourable, in which case $HCO_3^-$ or $CO_3^{2-}$ are the actual substrates.

Initial investigations of carbon dioxide reduction revealed ruthenium complexes to be most active. For example, Hashimoto and Inoue found that $H_2Ru(PPh_3)_4$ gave the best yield for the carbon dioxide reduction among different transition metal complexes [9]. Further improvement was disclosed by Noyori and co-workers who used $Ru^{II}$ catalysts ($RuCl_2[P(CH_3)_3]_4$) in supercritical $CO_2$ ($scCO_2$) in the presence of triethylamine ($NEt_3$) to give a TON of 7,200 [14, 15]. The increased catalyst efficiency was believed to be a result of the higher miscibility of $H_2$ in $scCO_2$ compared with other previously used solvents. This strategy was further improved, and catalyst TON values up to 28,500 and TOF 95,000 $h^{-1}$ by using [RuCl(OAc)$(P(CH_3)_3)_4$] were reported [16]. In this latter work, Jessop was also able to obtain methyl formate with a TON of 3,500 and dimethylformamide (DMF) with 420,000, respectively. In 2007, Himeda and co-workers [17] reported the use of [$Ir^{III}$Cp*] as efficient catalyst for the hydrogenation of carbon dioxide; formic acid was obtained with a TON of 222,000. In 2009, Nozaki and co-workers [18] used a defined iridium–pincer trihydride complex [$Ir^{III}$PNP] **1** for the hydrogenation of carbon dioxide (Scheme 2) and reported the highest TON value of 3,500,000 and TOF of 150,000 $h^{-1}$ in aqueous KOH generating potassium formate as the final product.

It is also worth mentioning that in 2010 the group of Fachinetti [19] reported the production of $HCOOH/NEt_3$ adducts by $CO_2$ hydrogenation using $[RuCl_2(P(CH_3)_3)_4]$ precursor at 40°C and 120 bar pressure in neat

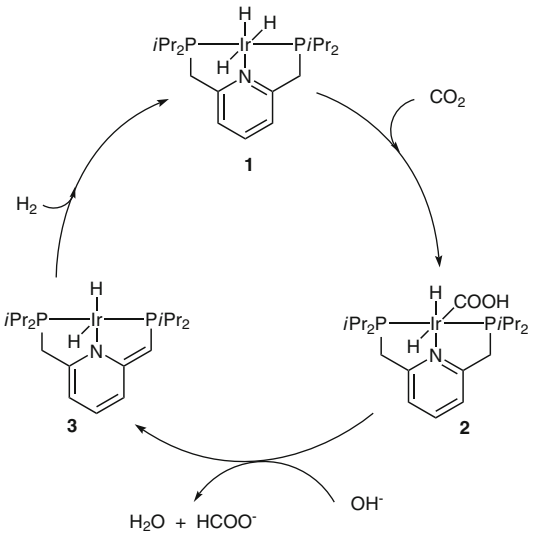


**Scheme 2** Mechanism for [$Ir^{III}$PNP]-catalysed formic acid generation

trimethylamine. In their work, the goal was to prevent HCOOH decomposition and to use the resulting adducts as hydrogen transfer reagents.

From all these examples, we can conclude that still today second- and third-row transition metals of groups eight through ten constitute metals of choice for carbon dioxide hydrogenation under mild conditions.

Besides hydrogenation of $CO_2$, the biologically relevant reduction of carbonates and bicarbonates to formates constitutes interesting reactions (Scheme 3). However, relatively less work has been reported on such transformations. Notably, in 2003 Joó and co-workers reported $[RuCl_2(mTPPMS)_{22}]$ as active catalyst (TON = 108) using an aqueous bicarbonate solution [20]. Later on, our group published an improved system based on $[RuCl_2(benzene)]_2$ and dppm for the hydrogenation of bicarbonates in water [21]. By applying dppm as ligand, a TON of 2,473 and a yield of 55% could be achieved. At that time, this constituted the highest TON recorded for the hydrogenation of bicarbonates without the addition of $CO_2$.

In 2013, novel acyl-phosphine ligands such as **4** (Fig. 1) were designed and used in the presence of Ru(Me-allyl)$_2$(COD). Using this system, the TON for the Ru-catalysed hydrogenation of bicarbonates was improved to 9,128 [22].

The hydrogenation of bicarbonates to formates offers the possibility to reversibly store hydrogen. In such a "hydrogen battery", the hydrogen can be released on demand in the presence of suitable catalyst under mild conditions. Performing several hydrogenation/dehydrogenation cycles, this concept was demonstrated by our group in early 2011 by using the previously investigated $Ru^{II}$/dppm catalyst (Scheme 4) [23]. Notably, the group of Laurency developed a similar concept and used $[RuCl_2(mTPPMS)_2]_2$ as catalyst for hydrogenation/dehydrogenation. Their system showed good stability and no significant drop of activity was observed after several cycles [24].

Another $H_2$-storage system was also developed by our group using $HCO_2H$ as the storage material (Scheme 5) [25]. In this respect, the work of Himeda and co-workers describing the hydrogenation of carbon dioxide and decomposition of formic acid using half-sandwich iridium complex-4.4′-dihydroxy-2,2′-bipyridine (DHBP) **5** is of interest, too (Fig. 2) [26]. In this latter case, the hydroxyl group of

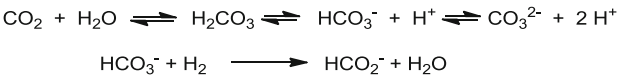


**Scheme 3** Equilibrium of aqueous carbon dioxide solution and reduction of bicarbonate to formate

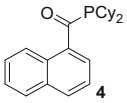


**Fig. 1** Acyl-phosphine ligand (dicyclohexyl 1-naphthoyl phosphine) for the hydrogenation of bicarbonates and carbon dioxide

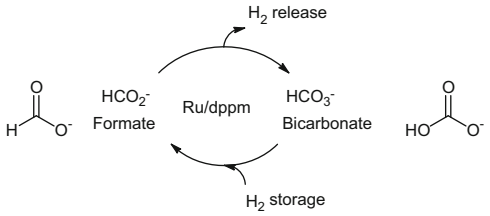


**Scheme 4** Hydrogen uptake and release in the bicarbonate/formate system

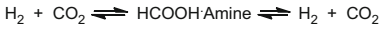


**Scheme 5** Hydrogen storage system based on the hydrogenation of carbon dioxide to formic acid

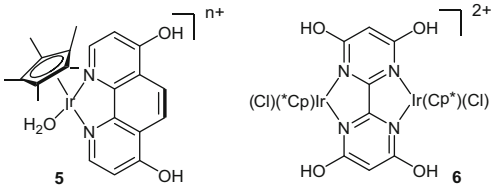


**Fig. 2** Structure of half-sandwich iridium complex and dinuclear [Cp*Ir]

the ligand is crucial for the high activity. The same positive ligand effect was also observed later in the ruthenium and rhodium analogues [27, 28]. More recently, Himeda and Fujita were able to synthesize a dinuclear [Cp*Ir] **6** catalyst for the $CO_2$ hydrogenation. A TOF of 70 $h^{-1}$ was achieved under very mild conditions (25°C and 1 bar).

So far, all the shown bicarbonate reductions are performed in the presence of precious metal complexes. However, also nonnoble metal-catalysed reactions have been discovered in recent years. For example, applying an iron catalyst [29], formates are obtained from bicarbonate in yield up to 88% with a TON of 610. Here, $[FeH(PP_3)]BF_4$ ($PP_3$ = tris[(2-diphenylphosphino)ethyl]phosphine) was used as the defined catalyst. Besides, the reduction of carbon dioxide was also realized; thus, methyl formate was obtained by hydrogenation of $CO_2$ in the presence of $NEt_3$ and methanol with a TON = 585 and 56% yield. For the production of DMF, 75% yield and TON = 727 were obtained. In 2012, we were able to improve the productivity and activity of this iron system (TON = 7,500 and TOF = 750) via the modification of ligand structure [30].

Soon after our first report using an iron catalyst, the group of Milstein used the iron (II) pincer complex *trans*-[(*t*Bu-PNP)Fe$(H)_2(CO)$] **7** in the hydrogenation of carbon dioxide and sodium bicarbonate [31]. The reactions were run at a relatively low temperature (80°C) and pressure (6–10 bar) with TON up to 788 and TOF up to 156 $h^{-1}$. Based on mechanistic studies, the reaction cycle shown in Scheme 6 was

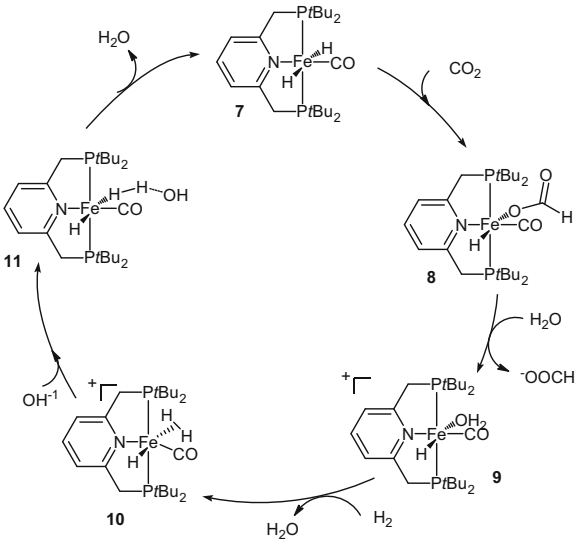


**Scheme 6** Proposed mechanism for the hydrogenation of $CO_2$ catalysed by Fe(II) pincer complex

proposed. Firstly, insertion of carbon dioxide into the Fe–H bond leads to the oxygen-bound formate complex **8**; the formate ligand is easily replaced by a water molecule to give the cationic complex **9**. Then, in the presence of hydrogen, the dihydrogen-coordinated species **10** is formed which after heterolytic cleavage of the $H_2$ regenerates the iron complex **7**.

Regarding nonnoble metal catalysts, in 2012 our group reported a well-defined cobalt dihydrogen complex prepared from $Co(BF_4)_2{\cdot}6H_2O$ and tetraphos ($PP_3$ = tris [(2-diphenylphosphino)ethyl]phosphine) for the hydrogenation of sodium bicarbonate and carbon dioxide. For the sodium formate formation, TON up to 3,877 was obtained [32]. In addition, Linehan and co-workers reported in 2013 an active cobalt system containing $Co(dmpe)_2H$ **12** (dmpe = 1,2-bis(dimethylphosphino)ethane) and Verkade's base (2,8,9-triisopropyl-2,5,8,9-tetraaza-1-phosphabicyclo[3.3.3]undecane) for the hydrogenation of carbon dioxide at ambient conditions. TOF of 3,400 $h^{-1}$ at room temperature and 1 bar of 1:1 $CO_2$ and $H_2$ were achieved. At higher pressure 20 bar, the TOF was improved to 74,000 $h^{-1}$ [33]. The key to their success was the choice of a suitable base to match the pKa of the cobalt dihydrogen intermediate $[Co(dmpe)_2(H)_2]^+$ **14**, so the deprotonation can occur easily to form the mono-hydride active species **12** for carbon dioxide insertion (Scheme 7) [34].

Though numerous catalysts for the hydrogenation of carbon dioxide to formic acid have been investigated, for practical applications, improvements regarding the recycling of the catalysts and separation of formic acid from the resulting salts are still problematic. In this context, it is noteworthy that researchers from BASF reported the use of trihexylamine as amine additive and polar diol as solvent [35]. The key point of their finding is that the resulting formic acid trihexylamine salts are not miscible with the free amine and can be easily cleaved thermally to

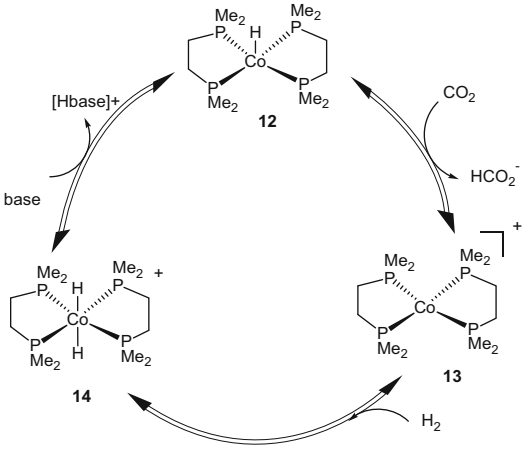


**Scheme 7** Proposed catalytic cycle for $CO_2$ hydrogenation using Co $(dmpe)_2H$

formic acid and amine under mild condition. The respective ammonium salts are soluble in diols, while the amine is not. Thus, a two-phase system is formed, and most of the active ruthenium species can be recycled from the amine phase. Interestingly, they also found that ruthenium carbonyl species were formed in the carbon dioxide hydrogenation reactions.

Most of the active carbon dioxide hydrogenation catalysts require basic additives [36], which inevitably produce the formate salts as final products. In order to avoid the tedious separation of formic acid from the salt mixture, one solution is to run the reaction under acidic conditions. In this respect, the work of Ogo and Fukuzumi is interesting, who firstly reported the reduction of $CO_2$ to formic acid under acidic conditions using a water-soluble ruthenium catalyst [37, 38]. Very recently, Laurenczy and his colleagues were also able to run the direct hydrogenation of carbon dioxide into formic acid in acid buffer system (pH 2.7), which prevents the formation of formate salts in aqueous solution. In the presence of a water-soluble ruthenium catalyst $[RuCl_2(PTA)_4]$ (PTA = 1,3,5-triaza-7-phosphaadamantane), 0.2 M formic acid was obtained [39]. Moreover, it was demonstrated that this catalyst can be reused multiple times.

Another way to separate formic acid from the reaction solution is to heterogenize the catalyst. Although a number of heterogeneous catalysts are known for the hydrogenation of carbon dioxide, in this review, the immobilization of molecular-defined complexes will be addressed. In this respect, Han [40] described a process using an immobilized ruthenium catalyst together with an ionic liquid (IL) containing a tertiary amino group as non-volatile base. After reaction, simple filtration and distillation lead to formic acid. Though the catalyst "Si"-$(CH_2)_3NH(CSCH_3)$-$RuCl_3$-$PPh_3$ is heterogenized, at the micro level, it is homogeneous. Similar strategies were also used by Nakahara [41] and Leitner [42] independently.

### 2.1.2 Transfer Hydrogenation of Carbon Dioxide

Though phosphine-based catalysts were extensively investigated for carbon dioxide reduction, the use of related NHC (*N*-heterocyclic carbene) complexes received less attention. In 2010, Peris reported the carbon dioxide reduction to formate in the presence of several iridium NHC complexes (Scheme 8) [43].

Among the different complexes investigated, **16** performed best with a TON up to 1,800 at 80°C in the presence of 60 bars of carbon dioxide and hydrogen (1:1). Because these NHC complexes were also active in the transfer hydrogenation of C=O bonds, the transfer hydrogenation of carbon dioxide using isopropanol as hydrogen source was investigated, too. Indeed, they achieved catalyst TON up to 150. Besides, the use of other secondary alcohols such as cyclohexanol and 1-phenylethanol was also possible even though the activity was somewhat lower. Later on, the same group synthesized ruthenium complexes ($\eta^6$-arene)Ru(bis-NHC) for the reduction of $CO_2$ with hydrogen and isopropanol. At higher temperature (200°C), a maximum TON 874 was achieved for the transfer hydrogenation of carbon dioxide to formate [44]. Moreover, water-soluble carbenes (Fig. 3) were used, which led to improved catalyst TON [45]. Using the transfer hydrogenation concept, Dibenedetto and Aresta reported in 2011 the $[RuCl_2(PPh_3)_3]$-catalysed reduction of carbon dioxide using aqueous glycerol. Though the TON was low, this concept is very interesting [46].

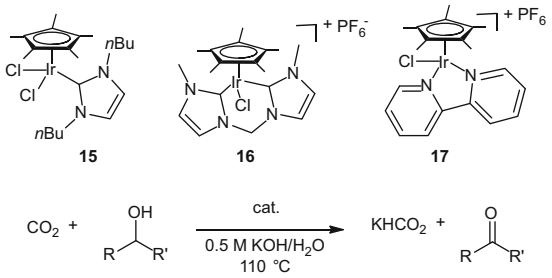


**Scheme 8** Iridium complexes tested in the transfer hydrogenation reaction of carbon dioxide

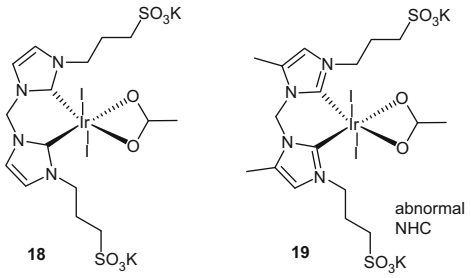


**Fig. 3** Water-soluble Ir NHC catalysts for transfer hydrogenation of carbon dioxide

### 2.1.3 Using Hydrosilanes

Apart from hydrogen and alcohols, some hydrosilanes constitute interesting reductants which are easy to handle and readily available. Thus, the reduction of carbon dioxide to formic acid using hydrosilanes was investigated in several studies. In 2010, Baba reported the copper-catalysed formation of formic acid from carbon dioxide. Here, silyl formate is formed initially, which is then hydrolysed to formic acid (Scheme 9) [47]. At 1 bar of carbon dioxide, formic acid was obtained in 95% yield with a TON of 8,100. Interestingly, the copper catalyst performed better compared to other transition metal catalysts, e.g. ruthenium [48] and iridium. Later on, Nozaki and her colleagues also reported a similar transformation using Cu/NHC as catalyst [49]. In 2013, García reported that $[(dippe)Ni(\mu\text{-}H)]_2$ catalysed such reaction and also showed the possibility of transfer of the silyl formate to alkyl formates or formamides (Scheme 9) [50].

Using metal-free conditions, Cantat and co-workers demonstrated elegantly that simply base [51] or carbene [52] catalysed the formation of formamide from $CO_2$ and hydrosilane. Here, the base TBD (1,5,7-triazabicyclo[4.4.0]dec-5-ene) performed best in the reduction of $CO_2$ (Scheme 10).

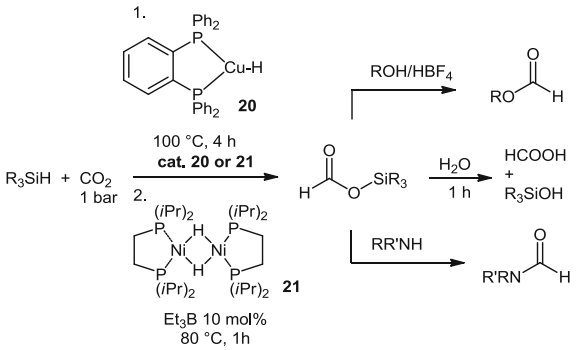


**Scheme 9** Copper- and nickel-catalysed hydrosilylation of carbon dioxide to formic acid and it's derivatives

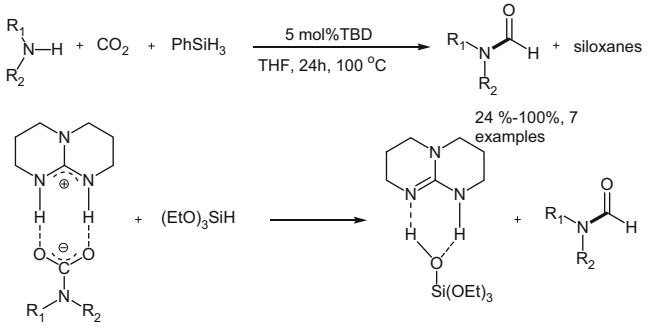


**Scheme 10** TBD-catalysed formylation of amine using $CO_2$ and hydrosilane

## 2.2 *From Carbon Dioxide to Carbon Monoxide*

### 2.2.1 Hydrogen as Reductant

The hydrogenation of $CO_2$ to CO, the so-called reverse-water–gas-shift reaction, is equivalent to the hydrogenation of $CO_2$ to formic acid and subsequent dehydration (Scheme 11). Indeed, Khan [53] reported the carbon dioxide reduction to formic acid which was decomposed to CO and hydrogen. However, it should be noted that formic acid is not always the reaction intermediate for CO production.

In 1993, Sasaki and Tominaga reported the hydrogenation of $CO_2$ to CO using $Ru_3(CO)_{12}$ as catalyst. In the presence of KI as additive, methanol and methane were also observed as products [54]. The latter two products are assumed to arise from the hydrogenation of in situ formed CO. Soon after, the same group improved this reaction by using [PPN]Cl (bis(triphenylphosphine)iminium chloride) as additive. Here, improved catalyst TON of 80 was achieved at 160°C after 5 h [55]. The formation of formic acid as intermediate was ruled out by mechanistic studies. Instead, a chloride-assisted deprotonation of ruthenium hydride species was proposed as shown in Scheme 12.

Interestingly, 20 years after the original work, the same group reported the synthesis of a series of mononuclear Ru halogen carbonyl complexes, [PPN][$RuX_3(CO)_3$] ($X = Cl^-$, $Br^-$, and $I^-$), which showed similar productivity in the RWGS reactions [56].

In order to drive the reaction more towards CO, strategies to remove/use the CO or water generated from the reaction system have been developed. In this respect, Sasaki's group reported that in the presence of ethylene oxide (which absorbs the

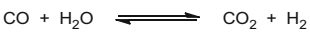


**Scheme 11** Water–gas-shift equilibrium

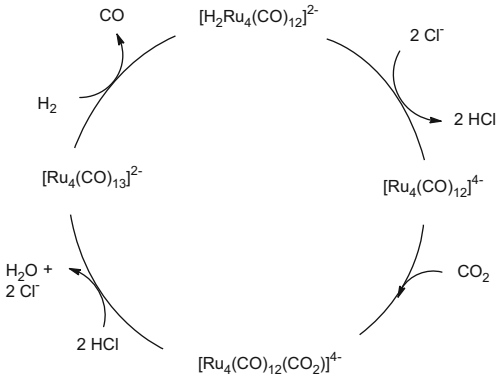


**Scheme 12** $Cl^-$-assisted reverse-water–gas-shift reaction

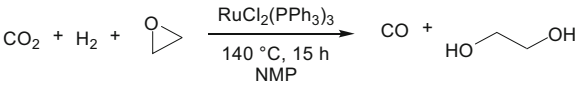


**Scheme 13** Ethylene oxide-accelerated reduction of $CO_2$ to CO

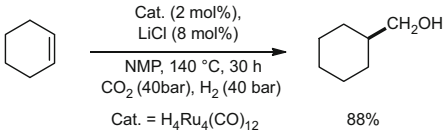


**Scheme 14** Ruthenium-catalysed hydroformylation/reduction of cyclohexene with carbon dioxide

water to give ethylene glycol), $CO_2$ is readily hydrogenated to CO in 71% yield (Scheme 13) [57].

Here, ethylene oxide simply acts as dehydration agent to remove the water in the RWGS equilibrium. Moreover, the subsequent use of CO to produce value-added chemicals has been investigated as well [58]. Thus, in 2000, Tominaga and Sasaki combined carbon dioxide reduction and alkene carbonylation in a one-pot manner to produce alcohols from $CO_2$, hydrogen and alkenes [59]. At 140°C, cyclohexylmethanol is obtained in 88% yield directly from cyclohexene in the presence of LiCl and $H_4Ru_4(CO)_{12}$ (Scheme 14). Four years later, the same group reported a detailed study on the above-mentioned reaction. They found that the catalytic activity of ruthenium complex is strongly affected by the anionic species of the added salts. The reaction rate increased in the order of $I^- < Br^- < Cl^-$, which is also the order of their proton affinities [60]. In order to improve the selectivity, more recently, additives like [Bmim][X] (Bmim:1-butyl-3-methylimidazolium) as well as different ruthenium clusters [61] such as $H_4Ru_4(CO)_{12}$ and $Ru_3(CO)_{12}$, $[Ru(CO)_3Cl_2]_2$ and ligands were added to the reaction. Interestingly, improved results (higher TON and selectivity) were obtained when bulky monodentate phosphite ligands were used [62].

### 2.2.2 Reductants Other than $H_2$

Based on our experience in hydrogen-borrowing reactions, we further developed the transfer hydrogenation of carbon dioxide to CO using alcohols and its direct use in alkene carbonylation reactions (Scheme 15) [63]. In such carbonylations which make use of RWGS reactions, water is produced as a side product and is not involved in the following alkene carbonylation reactions. Notably, Leitner and co-workers reported a related rhodium-catalysed hydrocarboxylation of alkenes with carbon dioxide and hydrogen to produce carboxylic acids [64].

Besides dihydrogen and alcohols, there are also other reductants reported for the reduction of carbon dioxide to CO. For example, in 2005, Sadighi reported the use of diboron compounds as $CO_2$ deoxygenation reagents. More specifically,

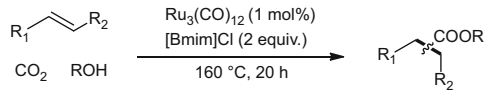


**Scheme 15** Reduction of $CO_2$ to CO using alcohols and subsequent carbonylation reactions

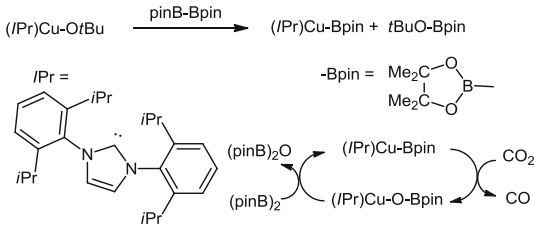


**Scheme 16** Copper-catalysed reduction of $CO_2$ to CO

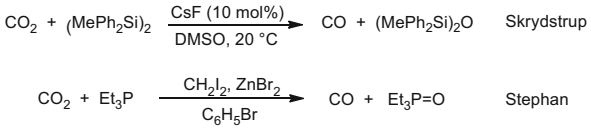


**Scheme 17** Reduction of $CO_2$ to CO

organocopper (I) complexes stabilized by NHC ligands reacted with pinB–pinB (bis(pinacolato)-diboron) to form the (IPr)Cu(Bpin) which reacted with $CO_2$ under atmospheric pressure to produce the (IPr)Cu(OBpin) and release CO at the same time. The active species can be regenerated by reaction of (IPr)Cu(OBpin) with pinB–pinB (Scheme 16) [65].

In 2014, Lindhardt and Skrydstrup reported the mild and selective reduction of $CO_2$ to CO using disilane as deoxygenation reagent in the presence of catalytic amount of CsF at room temperature (Scheme 17). In this context also the work of Stephan and co-workers is noteworthy, which demonstrated the catalytic reduction of $CO_2$ to CO with phosphine as reductant through an in situ generated carbodiphosphorane and zinc (II) [66].

### 2.2.3 Photocatalysed $CO_2$ Reduction to CO

Inspired by plants' efficiency in converting carbon dioxide to carbohydrates and other organic matter through photosynthesis, chemists have explored the possibilities of directly reducing $CO_2$ to CO by photocatalytic means [67]. Because $CO_2$ does not absorb either visible or UV radiation in the wavelengths of 200–700 nm, this process normally requires a suitable photocatalyst (PS: photosensitizer) to absorb UV–vis radiation and then transfer an electron to $CO_2$. Hence, the reduction process begins with excitation of the photosensitizer (PS). In the case of

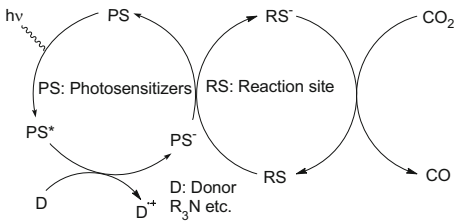


**Scheme 18** General reaction scheme for photocatalytic $CO_2$ reduction to CO

organometallic PS in general, a transfer of an electron from the metal centre onto the coordinated ligands takes place. Back-electron transfer from the ligands to the metal after the charge transfer is prevented by including an electron-donating species to quench the exciting state of the photocatalyst, thus forming the one electron-reduced (OER) intermediate for further $CO_2$ reduction processes.

Already in 1982, seminal work by Lehn and co-workers led to the development of the first photocatalytic $CO_2$ reductions. Here, $CoCl_2$ was used as the catalytic site for $CO_2$ reduction with $[Ru(bpy)_3]Cl_2$ as photosensitizer (Scheme 18) [68]. Apart from CO, hydrogen was produced as a side product via proton reduction. Though the turnover number of $(CO + H_2)$ was comparably low (32) based on $[Ru(bpy)_3]Cl_2$, the simultaneous reduction of $CO_2$ and $H_2O$ produces syngas, which is of interest, too. Clearly, this work represents an early step in the development of chemical systems capable of artificial photosynthesis and solar energy conversion. Later on, the same research group found that rhenium-based complexes $[Re(bipy)(CO)_3X]$ ($X = Cl^-$, $Br^-$) acting as both photosensitizer and catalyst are more efficient and selective catalysts for $CO_2$ reduction [69]. It was proposed that the dissociation of the ligand $X^-$ from the unstable 19-electron complex by OER is a key step in the photocatalysed reduction of $CO_2$.

Additionally, Fujita and co-workers identified the binuclear [Re-C(O)O-Re] moiety as a key intermediate of the two-electron reduction process from $CO_2$ to CO [70]. In 2008, an efficient photocatalytic system was successfully developed by the group of Ishitani using mixed catalysts with *fac*-$[Re(bpy)(CO)_3(CH_3CN)]^+$ and *fac*-$[Re\text{-}4,4'\text{-}(MeO)_2bpy(CO)_3P(OEt)_3]^+$ as photocatalysts [71]. Despite the improved activity of rhenium poly-pyridine complexes, a major problem with these photocatalysts is the lack of an extended absorption into the visible region. To solve this problem, Ishitani, Bian and co-workers presented the use of covalently linked hetero-nuclear Ru and Re multimetallic complexes in the photocatalytic reduction of $CO_2$. The enhancement of the photocatalytic response to light in the visible region was achieved due to intramolecular electron transfer from the OER Ru species to the Re moiety. The binuclear complex Ru–Re, tri-nuclear complex $RuRe_2$ and tetra-nuclear complex $RuRe_3$ all furnished higher TON for the reduction of $CO_2$ to CO (Fig. 4) [72, 73].

In recent years, the synthesis of new Re complexes for $CO_2$ reduction to CO continued to attract attention. As an example, Hadadzadeh [74] reported the synthesis of a dinuclear Re(I) complex in 2014 (Fig. 5), $[ReCl(CO)_3(l\text{-}tptzH)Re(CO)_3]$ **24**, (tptzH = 2,4,6-tri(pyridine-2-yl)-2H-1,3,5-triazine-1-ide), for the $CO_2$ reduction with a TON of 17.

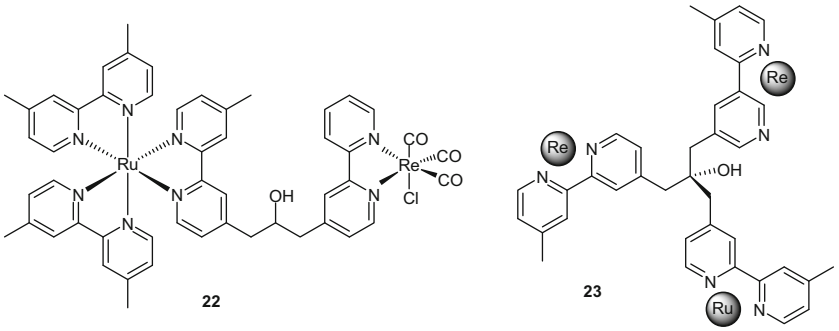


**Fig. 4** Structure of hetero-nuclear Ru and Re multimetallic complexes

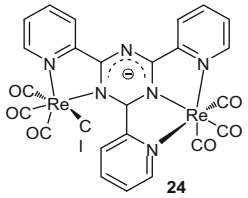


**Fig. 5** Structure of dinuclear Re(I) complex for $CO_2$ reduction

Apart from Re and Re–Ru dinuclear complexes, in 2013, Sato and Ishitani [75] developed the mononuclear iridium (III) complex $[Ir(tpy)(ppy)Cl]^+$ **25** for the selective reduction of $CO_2$ to CO under visible light at 480 nm. Interestingly, there was no extra photosensitizer needed. Here, tri-ethanolamine was used as an artificial electron donor and the proposed mechanism is shown in Scheme 19.

As shown in Fig. 6, ruthenium complexes alone also showed activity in the photocatalytic $CO_2$ reduction. For example, in 2014 Ishida [76] reported the use of $[Ru(bpy)_2(CO)_2](PF_6)_2$ (bpy = 2,2′-bipyridine) **28** as catalyst and $[Ru(bpy)_3](PF_6)_2$ **29** as photosensitizer in the presence of 1-benzyl-1,4-dihydronicotinamide (BNAH) as an electron donor for the $CO_2$ reduction to CO. Interestingly, the iron-based complex **32** was also reported as active catalyst by Bonin and Robert using $Ir(ppy)_3$ or 9-CNA (9-cyanoanthracene) as photosensitizers. Here, TON up to 140 was obtained (Fig. 7) [77].

## *2.3 From Carbon Dioxide to Formaldehyde*

Though formaldehyde was proposed as intermediate in several $CO_2$ reduction reactions, HCHO had not been isolated or even observed until 2013 when Bontemps and Sabo-Etienne reported the evidence for formaldehyde formation through NMR studies in the course of $CO_2$ reduction using HBpin [78]. Later on, they used

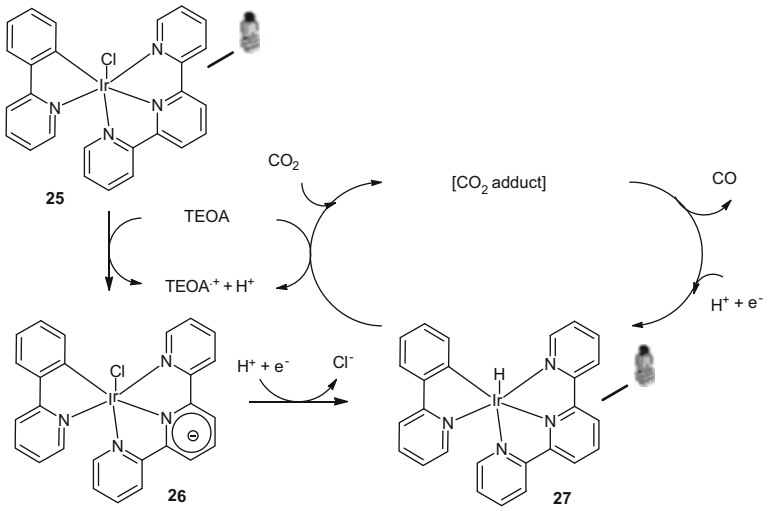


**Scheme 19** Proposed mechanism for photocatalytic reduction of $CO_2$ in the presence of iridium complex **25**

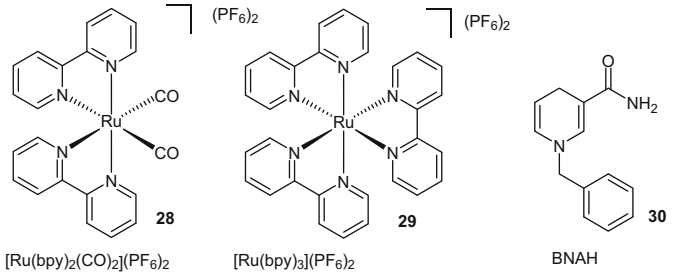


**Fig. 6** Structure of ruthenium complexes in the photoreduction of $CO_2$

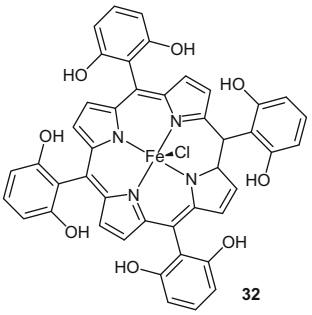


**Fig. 7** Iron-based catalyst for photocatalysed carbon dioxide reduction

**Scheme 20** Formation of formaldehyde from carbon dioxide

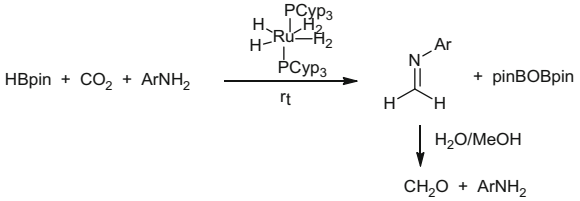


amine to trap the formaldehyde to form the corresponding imine. After hydrolysis, they obtained a formalin solution, which demonstrated for the first time the production of formaldehyde from $CO_2$ (Scheme 20) [79].

Most recently, Oestreich reported the use of tethered Ru–S complexes for the catalytic hydrosilylation of carbon dioxide to formaldehyde bis(silyl)acetal or silylated methanol [80].

## *2.4 From Carbon Dioxide to Methanol*

The conversion of atmospheric carbon dioxide to methanol is a potential technology for the production of fuel alternatives based on renewable energy [81, 82]. Besides, methanol is used as starting material for the synthesis of various bulk chemicals, for example, ethylene and propylene [83]. In this respect, the "George Olah Carbon Dioxide to Renewable Methanol Plant" represents a demonstration plant in Iceland using a heterogeneous copper–zinc oxide–alumina catalyst for the hydrogenation of carbon dioxide [84]. Meanwhile, homogeneous catalysts able to reduce $CO_2$ at low(er) temperature received increasing attention.

### 2.4.1 Using Hydrogen as Reductant

In 2011, Sanford and colleagues reported the sequential hydrogenation of $CO_2$ to methanol using a combination of a Ru–Pincer **33** and a ruthenium–phosphine **34** pre-catalyst in the presence of Lewis acid $Sc(OTf)_3$. The catalytic sequence involves (a) hydrogenation of carbon dioxide to formic acid by **34**, (b) acid esterification to formate and (c) hydrogenation of ester to methanol by **33** (Scheme 21). The incompatibility of **33** and $Sc(OTf)_3$ was solved by physically separating the catalysts using a vial in the autoclave. Thus, an overall catalyst turnover number of 21 was achieved.

More recently, the reduction of carbon dioxide to methanol using one single ruthenium–phosphine complex was achieved by Klankermayer and Leitner. The combination of the tridentate ligand triphos (1,1,1-tris(diphenylphosphinomethyl) ethane) and $[Ru(acac)_3]$ in the presence of MSA (methanesulfonic acid) in situ formed an active catalyst to produce methanol with a TON of 221 at 140°C, 60 bar

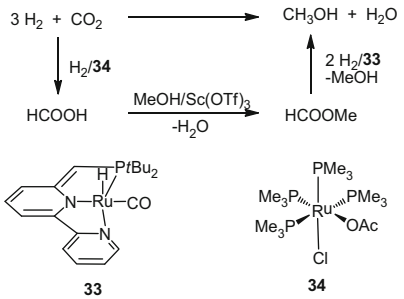


**Scheme 21** Cascade reduction of $CO_2$ to methanol

hydrogen and 20 bar $CO_2$ (Scheme 22) [85]. The same authors reported in 2015 a detailed mechanism via DFT study on this reduction process. Moreover, a biphasic reaction system involving $H_2O$ and 2-MTHF was developed, in which case methanol is extracted into the aqueous phase.

In addition, Milstein and co-workers reported in early 2011 an alternative route to methanol from carbon dioxide using organic carbonates or formats as substrates in the presence of Ru–pincer catalysts. Turnover number as high as 4,700 was achieved [86]. Though the process is an "efficient" way from carbon dioxide to methanol, the economic viability is problematic due to the price of the starting materials. In this respect, the work of the group of Ding is interesting, who used cyclic carbonates as starting material for the production of methanol. Excellent TON of 87,000 and TOF of up to 1,200 $h^{-1}$ were accomplished [87].

### 2.4.2 Using Other Reductants for the Production of Methanol

The reduction of $CO_2$-derived formic acid was studied by Miller and Goldberg [88]. Here, formic acid acted as hydrogen source and carbon substrate. The iridium complex $[Cp^*Ir(bpy)(H_2O)]$ $(OTf)_2$ **35** ($Cp^*$ = pentamethylcyclopentadienyl, bpy = 2,2-bipyridine, OTf = trifluoromethanesulfonate) which is known as an active transfer hydrogenation catalyst proved to be the most active catalyst (Scheme 23). Methanol and methyl formate were observed in the solution with 2% yield of methanol. Based on isotope labelling experiments, the author proposed that the formic acid was first reduced to formaldehyde by the in situ formed [Ir–H] and the formaldehyde was further reduced to methanol. The low product yield and expensive iridium catalyst encouraged Cantat and colleagues to further develop this method. In fact, using $[Ru(methylallyl)_2COD]$ in the presence of triphos and MSA improved the yield to 50% at 150°C [89].

Interestingly, in 2014 Hong [90] from Seoul reported the transfer hydrogenation method using isopropanol hydrogen source to produce methanol indirectly from carbon dioxide (cyclic carbonates). Again, PNP–Ru(II)-type complexes were the

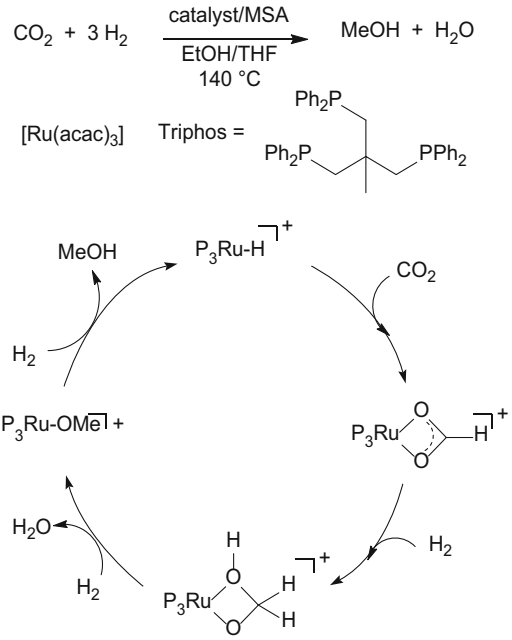


**Scheme 22** Single ruthenium–phosphine complex-catalysed methanol formation from $CO_2$

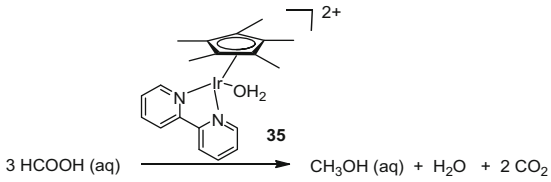


**Scheme 23** Iridium-catalysed disproportionation of formic acid to methanol

most active catalysts. In the presence of inorganic base, TON up to 16,600 was achieved (Scheme 24).

The hydrosilylation of $CO_2$ to methoxysilyl species is already known since 1989 using Ir(CN)(CO)(dppe) (dppe = 1,2-bis(diphenylphosphino)ethane) at 40°C though with low TON [91]. In 2010, Guan was able to demonstrate that in the presence of nickel–pincer hydride, the catalytic hydroboration of $CO_2$ to methoxyboryl species was feasible using borane at room temperature [92]. The nickel hydride complex **36** was isolated and a mechanism was proposed (Scheme 25) [93]. Firstly, $CO_2$ inserts into the Ni–H bond; then the subsequent cleavage of Ni–O bond with HBcat (catecholborane) releases HCOOBcat, which is reduced to formaldehyde by another HBcat. Finally, hydroboration of formaldehyde gives the product $CH_3OBcat$.

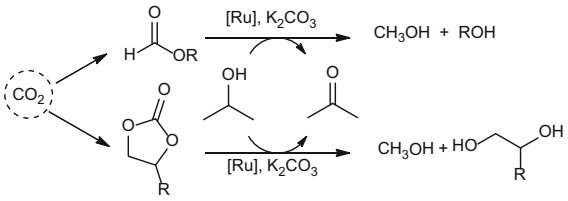


**Scheme 24** Transfer hydrogenation of formates and cyclic carbonates to methanol

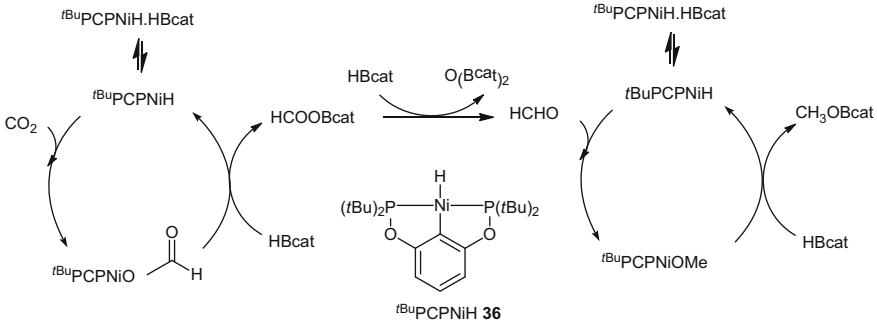


**Scheme 25** Ni-catalysed reduction of carbon dioxide with borane

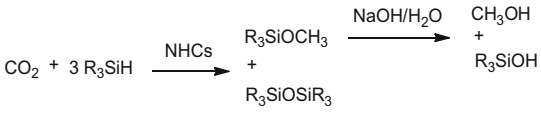


**Scheme 26** Reduction of carbon dioxide to methanol with silanes

It is well known that nucleophilic NHC (*N*-heterocyclic carbene) activates $CO_2$ to form imidazolium carboxylates. Based on this work, in 2009 Zhang and Ying [94] reported the reduction of carbon dioxide with silane to silylmethoxide [95] which after hydrolysis produced methanol under ambient conditions (Scheme 26). Regarding transition metal-free reduction systems [96–99] for methanol production, the work from O'Hare and Stephan is noteworthy, who have used FLPs (frustrated Lewis pairs) as catalyst. The activation of $CO_2$ by FLPs forms bridging carboxylate species which are reduced with ammonia borane [100] or by low pressure of hydrogen [101]. Finally, hydrolysis of $CH_3O$–LA (LA = $BX_3$ or $AlX_3$) led to methanol [102].

## 2.5 From Carbon Dioxide to Ethanol

It is known that ethanol can be produced via CO hydrogenation using Co-, Ru- and Rh-based catalysts. However, the homogeneous hydrogenation of $CO_2$ to ethanol is barely known. In their studies on the hydrogenation of carbon dioxide to CO, Sasaki and Tominaga found that a small amount of EtOH was formed, too. Notably, they further improved the yield of ethanol by using $Co_2(CO)_8$ as cocatalyst in the $Ru_3(CO)_{12}$/KI system. Mechanistic studies revealed that the ruthenium was responsible for the production of MeOH, while cobalt species catalysed methanol homologation with CO [103].

## 2.6 From Carbon Dioxide to Methylamines

In 2014, the market value of methylamines such as $MeNH_2$, $Me_2NH$ and $Me_3N$ exceeded 4,000 Euro/ton. Therefore, the reductive methylation of amines with $CO_2$ can create additional value. The methylation of amines via six-electron reduction of $CO_2$ remained unknown until 2013 when Cantat and his colleagues reported a zinc catalyst for the methylation of amines with $CO_2$ and hydrosilanes at low pressure [104]. Furthermore, the selective reduction of urea was possible under similar reaction conditions. Meanwhile, our group developed a Ru/phosphine catalyst system that was able to convert carbon dioxide and amines into various kinds of *N*-methylated products in the presence of hydrosilanes ($PhSiH_3$). Notably, diverse functional groups were well tolerated under these conditions (Scheme 27) [105]. Very recently, Cantat also showed the possibility of using iron catalysts for this transformation albeit high catalyst loading was needed [106].

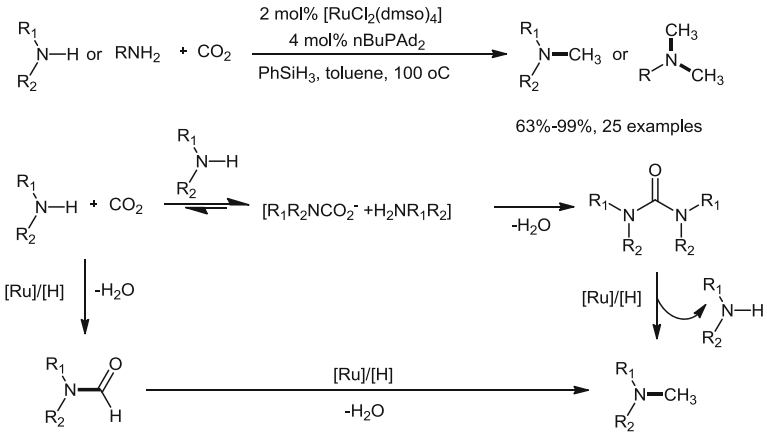


**Scheme 27** Ruthenium-catalysed methylation of amine using hydrosilane as reductant

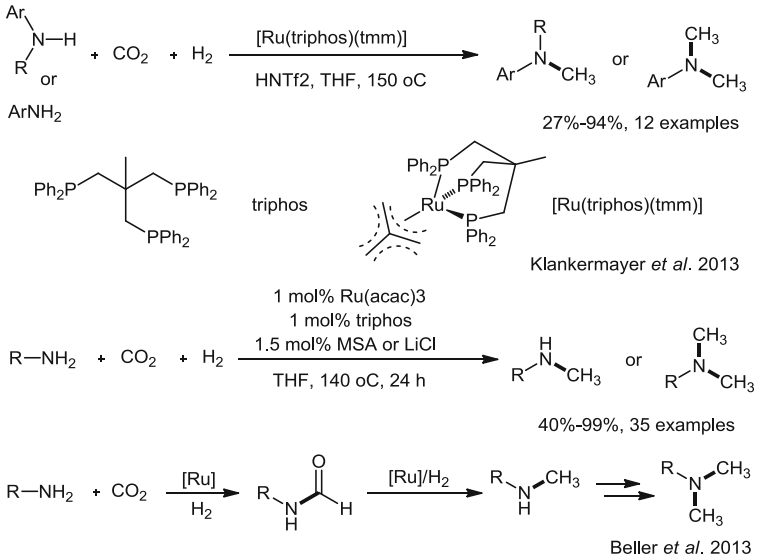


**Scheme 28** Ruthenium-catalysed methylation of amines using $CO_2$ and hydrogen

Although some silanes are considered to be waste products from the silicone industry, all these methodologies are limited by the accessibility of the hydrosilanes and an additional workup step to remove siloxane by-products. Obviously, catalytic methylations using $CO_2$ and $H_2$ represent a greener method with $H_2O$ as the only by-product. In this respect, it is noteworthy to mention the work from Klankermayer [107] and Beller [108] who simultaneously reported the conversion of amines into methylamines in the presence of $CO_2$ and $H_2$. On the one hand, Klankermayer et al. presented the use of a molecularly defined ruthenium complex [Ru(triphos)(tmm)] together with readily available organic acids as cocatalysts to afford the methylation of aryl amines in good yields. On the other hand, our group demonstrated the *N*-methylation of both aromatic and aliphatic amines using $CO_2$/$H_2$. Applying an in situ combination of $Ru(acac)_3$, triphos and either acid additives or LiCl, the desired methylated amines were obtained (Scheme 28). Most recently, our group also developed the methylation of C–H bonds using the same system; thus, indoles, pyrroles and electron-rich arenes react with $CO_2$ and $H_2$ to give the corresponding methylated products [109].

## 2.7 *From Carbon Dioxide to Methane*

The reduction of carbon dioxide to methane (Scheme 29) is of substantial industrial importance; however, synthetic systems capable of reducing carbon dioxide to methane have been elusive, though carbon dioxide can be reduced to all kinds of

$$CO_2 + 4\,H_2 \longrightarrow CH_4 + 2\,H_2O$$

**Scheme 29** Methanation process

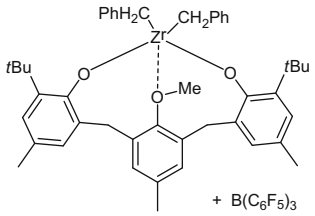


**Fig. 8** Structure of zirconium complex and borane for methane production from $CO_2$

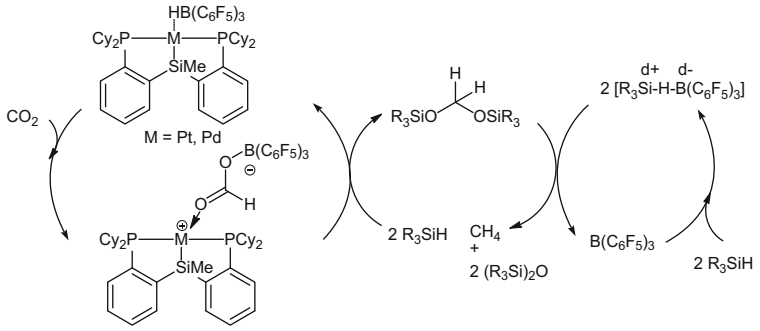


**Scheme 30** Proposed mechanism for methane formation from $CO_2$

other chemicals as mentioned above. In 1989, Vaska showed the possibility of producing methane from carbon dioxide and hydrogen in the presence of ammonia using $[Ir(Cl)(CO)(PPh_3)_2]$ as catalyst; formamide was found to be the intermediate [110]. In 2006, Matsuo and Kawaguchi reported the reduction of carbon dioxide to methane with hydrosilanes as the reductant [111]. In this case, in situ formed zirconium–borane complexes were used as the catalyst. The reaction was run in an NMR tube and TON up to 225 was achieved. The structure of zirconium is shown in Fig. 8.

In 2012, Brookhart [112] reported a more efficient iridium catalyst with general structure $(POCOP)Ir(H)(HSiR_3)$ for the hydrosilylation of $CO_2$ to methane. More specifically, they found that less bulky silanes like $Me_2EtSiH$ gave more selectively methane. TON up to 8,300 was achieved. Meanwhile, Turculet [113] reported similar reactions using platinum and palladium silyl pincer complexes. The formation of a formate ester as intermediate was observed, which was further reduced to $R_3SiOCH_2OSiR_3$ and $R_3SiOCH_3$ and finally to $R_3SiOSiR_3$ and $CH_4$ (Scheme 30).

Notably, Piers et al. discovered that frustrated Lewis pairs also act as catalysts for the reduction of $CO_2$ to methane using boranes. Here, the key step is the activation of $CO_2$ by FLPs (frustrated Lewis pairs) which is further reduced

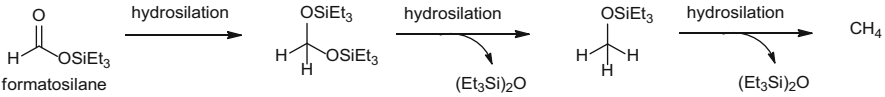


**Scheme 31** Pathway for hydrosilation of $CO_2$ to methane

(Scheme 31) [114]. Besides, strong Lewis acid such as $[Et_2Al]^+$ and even $[R_3Si]^+$ showed activity in the methane production from $CO_2$ [115, 116].

Finally, it is worth mentioning that the photoreduction of $CO_2$ to $CH_4$ was reported, as early as 1986. In this respect, Willner and co-workers [117] reported the use of $Ru(bpz)_3^{2+}$ (bpz = tri(bipyrazine)) as photosensitizer and ruthenium metal as catalyst for the process.

## 3 Concluding Remarks

In the last two decades, significant developments were achieved in the area of carbon dioxide reduction. Important basic discoveries, e.g. metal-free reductions, as well as significant improvements of more practical processes took place. As an example, after several years of research work, homogeneously catalysed reduction of carbon dioxide to formic acid derivatives has become a promising tool even for industrial applications. Particularly, the production of formic acid can be achieved using iridium and ruthenium complexes with very high catalyst turnover numbers or nonnoble metal catalysts such as iron. Notably, in these cases, catalyst efficiency does not represent today the limiting factor for commercial realizations. Here, feedstock prices and process engineering technologies are crucial. In the next years, similar efficient catalytic processes are expected for methanol and methane generation. Apart from hydrogenations, most reductions using silanes or boranes constitute interesting basic studies, but will be very difficult to realize on a larger scale. In these works, the basic understanding of the individual elementary steps of the catalytic cycles is most important. In contrast, the "simple" optimization of catalyst turnover numbers using boranes or silanes is less interesting. In the future, challenging work for carbon dioxide valorization will include easily available feedstocks such as $CO_2$ streams directly from power plants. Besides, the efficient production of C–C bonds via (photo)catalytic means constitutes a major goal for basic science.

## References

1. Aresta M (2010) *Carbon Dioxide as Chemical Feedstock*
2. Cokoja M, Bruckmeier C, Rieger B, Herrmann WA, Kühn FE (2011) Angew Chem Int Ed 50:8510–8537

3. Behr A (1988) Angew Chem 100:681–698
4. Maeda C, Miyazaki Y, Ema T (2014) Catal Sci Technol 4:1482–1497
5. Huang K, Sun C-L, Shi Z-J (2011) Chem Soc Rev 40:2435–2452
6. Mikkelsen M, Jorgensen M, Krebs FC (2010) Energy Environ Sci 3:43–81
7. Sakakura T, Choi J-C, Yasuda H (2007) Chem Rev 107:2365–2387
8. Liu Q, Wu L, Jackstell R, Beller M (2015) Nat Commun 6:5933
9. Jessop PG, Ikariya T, Noyori R (1995) Chem Rev 95:259–272
10. Leitner W (1995) Angew Chem Int Ed 34:2207–2221
11. Jessop PG, Joó F, Tai C-C (2004) Coord Chem Rev 248:2425–2442
12. Wang W, Wang S, Ma X, Gong J (2011) Chem Soc Rev 40:3703–3727
13. Inoue Y, Izumida H, Sasaki Y, Hashimoto H (1976) Chem Lett 863–864
14. Jessop PG, Hsiao Y, Ikariya T, Noyori R (1996) J Am Chem Soc 118:344–355
15. Jessop PG, Ikariya T, Noyori R (1994) Nature 368:231–233
16. Munshi P, Main AD, Linehan JC, Tai C-C, Jessop PG (2002) J Am Chem Soc 124:7963–7971
17. Himeda Y, Onozawa-Komatsuzaki N, Sugihara H, Kasuga K (2007) Organometallics 26: 702–712
18. Tanaka R, Yamashita M, Nozaki K (2009) J Am Chem Soc 131:14168–14169
19. Preti D, Squarcialupi S, Fachinetti G (2010) Angew Chem Int Ed 49:2581–2584
20. Elek J, Nádasdi L, Papp G, Laurenczy G, Joó F (2003) Appl Catal A 255:59–67
21. Federsel C, Jackstell R, Boddien A, Laurenczy G, Beller M (2010) ChemSusChem 3: 1048–1050
22. Gowrisankar S, Federsel C, Neumann H, Ziebart C, Jackstell R, Spannenberg A, Beller M (2013) ChemSusChem 6:85–91
23. Boddien A, Gärtner F, Federsel C, Sponholz P, Mellmann D, Jackstell R, Junge H, Beller M (2011) Angew Chem Int Ed 50:6411–6414
24. Papp G, Csorba J, Laurenczy G, Joó F (2011) Angew Chem Int Ed 50:10433–10435
25. Boddien A, Federsel C, Sponholz P, Mellmann D, Jackstell R, Junge H, Laurenczy G, Beller M (2012) Energy Environ Sci 5:8907–8911
26. Yuichiro H (2010) J Am Chem Soc 1056:141–153
27. Himeda Y, Miyazawa S, Hirose T (2011) ChemSusChem 4:487–493
28. Hou C, Jiang J, Zhang S, Wang G, Zhang Z, Ke Z, Zhao C (2014) ACS Catal 4:2990–2997
29. Federsel C, Boddien A, Jackstell R, Jennerjahn R, Dyson PJ, Scopelliti R, Laurenczy G, Beller M (2010) Angew Chem Int Ed 49:9777–9780
30. Ziebart C, Federsel C, Anbarasan P, Jackstell R, Baumann W, Spannenberg A, Beller M (2012) J Am Chem Soc 134:20701–20704
31. Langer R, Diskin-Posner Y, Leitus G, Shimon LJW, Ben-David Y, Milstein D (2011) Angew Chem Int Ed 50:9948–9952
32. Federsel C, Ziebart C, Jackstell R, Baumann W, Beller M (2012) Chem Eur J 18:72–75
33. Jeletic MS, Mock MT, Appel AM, Linehan JC (2013) J Am Chem Soc 135:11533–11536
34. Jeletic MS, Helm ML, Hulley EB, Mock MT, Appel AM, Linehan JC (2014) ACS Catal 4: 3755–3762
35. Schaub T, Paciello RA (2011) Angew Chem Int Ed 50:7278–7282
36. Drake JL, Manna CM, Byers JA (2013) Organometallics 32:6891–6894
37. Hayashi H, Ogo S, Fukuzumi S (2004) Chem Commun 2714–2715
38. Ogo S, Kabe R, Hayashi H, Harada R, Fukuzumi S (2006) Dalton Trans 4657–4663
39. Moret S, Dyson PJ, Laurenczy G (2014) Nat Commun 5. doi:10.1038/ncomms5017
40. Zhang Z, Xie Y, Li W, Hu S, Song J, Jiang T, Han B (2008) Angew Chem Int Ed 47: 1127–1129
41. Yasaka Y, Wakai C, Matubayasi N, Nakahara M (2010) J Phys Chem C 114:3510–3515
42. Wesselbaum S, Hintermair U, Leitner W (2012) Angew Chem Int Ed 51:8585–8588
43. Sanz S, Benítez M, Peris E (2009) Organometallics 29:275–277
44. Sanz S, Azua A, Peris E (2010) Dalton Trans 39:6339–6343
45. Azua A, Sanz S, Peris E (2011) Chem Eur J 17:3963–3967

46. Dibenedetto A, Stufano P, Nocito F, Aresta M (2011) ChemSusChem 4:1311–1315
47. Motokura K, Kashiwame D, Miyaji A, Baba T (2012) Org Lett 14:2642–2645
48. Jansen A, Pitter S (2004) J Mol Catal A Chem 217:41–45
49. Shintani R, Nozaki K (2013) Organometallics 32:2459–2462
50. González-Sebastián L, Flores-Alamo M, García JJ (2013) Organometallics 32:7186–7194
51. Das Neves Gomes C, Jacquet O, Villiers C, Thuéry P, Ephritikhine M, Cantat T (2012) Angew Chem Int Ed 51:187–190
52. Jacquet O, Das Neves Gomes C, Ephritikhine M, Cantat T (2012) J Am Chem Soc 134: 2934–2937
53. Khan MMT, Halligudi SB, Shukla S (1989) J Mol Catal 57:47–60
54. Tominaga K-I, Sasaki Y, Kawai M, Watanabe T, Saito M (1993) J Chem Soc Chem 629–631
55. Tominaga K-I, Sasaki Y, Hagihara K, Watanabe T, Saito M (1994) Chem Lett 23:1391–1394
56. Tsuchiya K, Huang J-D, Tominaga K-I (2013) ACS Catal 3:2865–2868
57. Tominaga K-I, Sasaki Y, Watanabe T, Saito M (1997) Energy 22:169–176
58. Wu L, Liu Q, Jackstell R, Beller M (2014) Angew Chem Int Ed 53:6310–6320
59. Tominaga K-I, Sasaki Y (2000) Catal Commun 1:1–3
60. Tominaga K-I, Sasaki Y (2004) J Mol Catal A Chem 220:159–165
61. Jääskeläinen S, Haukka M (2003) Appl Catal A 247:95–100
62. Liu Q, Wu L, Fleischer I, Selent D, Franke R, Jackstell R, Beller M (2014) Chem Eur J 20:6809
63. Wu L, Liu Q, Fleischer I, Jackstell R, Beller M (2014) Nat Commun 5:3091
64. Ostapowicz TG, Schmitz M, Krystof M, Klankermayer J, Leitner W (2013) Angew Chem Int Ed 52:12119–12123
65. Laitar DS, Müller P, Sadighi JP (2005) J Am Chem Soc 127:17196–17197
66. Dobrovetsky R, Stephan DW (2013) Angew Chem Int Ed 52:2516–2519
67. Takeda H, Ishitani O (2010) Coord Chem Rev 254:346–354
68. Lehn J-M, Ziessel R (1982) Proc Natl Acad Sci 79:701–704
69. Hawecker J, Lehn J-M, Ziessel R (1983) Chem Commun 536–538
70. Hayashi Y, Kita S, Brunschwig BS, Fujita E (2003) J Am Chem Soc 125:11976–11987
71. Takeda H, Koike K, Inoue H, Ishitani O (2008) J Am Chem Soc 130:2023–2031
72. Bian Z-Y, Sumi K, Furue M, Sato S, Koike K, Ishitani O (2008) Inorg Chem 47:10801–10803
73. Gholamkhass B, Mametsuka H, Koike K, Tanabe T, Furue M, Ishitani O (2005) Inorg Chem 44:2326–2336
74. Shakeri J, Hadadzadeh H, Tavakol H (2014) Polyhedron 78:112–122
75. Sato S, Morikawa T, Kajino T, Ishitani O (2013) Angew Chem Int Ed 52:988–992
76. Kuramochi Y, Kamiya M, Ishida H (2014) Inorg Chem 53:3326–3332
77. Bonin J, Robert M, Routier MS (2014) J Am Chem Soc 136:16768–16771
78. Bontemps S, Sabo-Etienne S (2013) Angew Chem Int Ed 52:10253–10255
79. Bontemps S, Vendier L, Sabo-Etienne S (2014) J Am Chem Soc 136:4419–4425
80. Metsänen TT, Oestreich M (2015) Organometallics 34:543–546
81. Goeppert A, Czaun M, Jones J-P, Surya Prakash GK, Olah GA (2014) Chem Soc Rev 43: 7995–8048
82. Ganesh I (2014) Renew Sust Energ Rev 31:221–257
83. Cui Z-M, Liu Q, Song W-G, Wan L-J (2006) Angew Chem Int Ed 45:6512–6515
84. Olah GA (2013) Angew Chem Int Ed 52:104–107
85. Wesselbaum S, vom Stein T, Klankermayer J, Leitner W (2012) Angew Chem Int Ed 51: 7499–7502
86. Balaraman E, Gunanathan C, Zhang J, Shimon LJW, Milstein D (2011) Nat Chem 3:609–614
87. Han Z, Rong L, Wu J, Zhang L, Wang Z, Ding K (2012) Angew Chem Int Ed 51: 13041–13045
88. Miller AJM, Heinekey DM, Mayer JM, Goldberg KI (2013) Angew Chem Int Ed 52: 3981–3984

89. Savourey S, Lefèvre G, Berthet J-C, Thuéry P, Genre C, Cantat T (2014) Angew Chem Int Ed 53:10466–10470
90. Kim SH, Hong SH (2014) ACS Catal 4:3630–3636
91. Eisenschmid TC, Eisenberg R (1989) Organometallics 8:1822–1824
92. Chakraborty S, Zhang J, Krause JA, Guan H (2010) J Am Chem Soc 132:8872–8873
93. Chakraborty S, Patel YJ, Krause JA, Guan H (2012) Polyhedron 32:30–34
94. Riduan SN, Zhang Y, Ying JY (2009) Angew Chem Int Ed 48:3322–3325
95. Huang F, Lu G, Zhao L, Li H, Wang Z-X (2010) J Am Chem Soc 132:12388–12396
96. Das Neves Gomes C, Blondiaux E, Thuéry P, Cantat T (2014) Chem Eur J 20:7098–7106
97. Anker MD, Arrowsmith M, Bellham P, Hill MS, Kociok-Kohn G, Liptrot DJ, Mahon MF, Weetman C (2014) Chem Sci 5:2826–2830
98. Zhang L, Cheng J, Hou Z (2013) Chem Commun 49:4782–4784
99. Courtemanche M-A, Légaré M-A, Maron L, Fontaine F-G (2013) J Am Chem Soc 135: 9326–9329
100. Ménard G, Stephan DW (2010) J Am Chem Soc 132:1796–1797
101. Ashley AE, Thompson AL, O'Hare D (2009) Angew Chem Int Ed 48:9839–9843
102. Courtemanche M-A, Légaré M-A, Maron L, Fontaine F-G (2014) J Am Chem Soc 136: 10708–10717
103. Tominaga K-I, Sasaki Y, Saito M, Hagihara K, Watanabe T (1994) J Mol Catal 89:51–55
104. Jacquet O, Frogneux X, Das Neves Gomes C, Cantat T (2013) Chem Sci 4:2127–2131
105. Li Y, Fang X, Junge K, Beller M (2013) Angew Chem Int Ed 52:9568–9571
106. Frogneux X, Jacquet O, Cantat T (2014) Catal Sci Technol 4:1529–1533
107. Beydoun K, vom Stein T, Klankermayer J, Leitner W (2013) Angew Chem Int Ed 52: 9554–9557
108. Li Y, Sorribes I, Yan T, Junge K, Beller M (2013) Angew Chem Int Ed 52:12156–12160
109. Li Y, Yan T, Junge K, Beller M (2014) Angew Chem Int Ed 53:10476–10480
110. Vaska L, Schreiner S, Felty RA, Yu JY (1989) J Mol Catal 52:L11–L16
111. Matsuo T, Kawaguchi H (2006) J Am Chem Soc 128:12362–12363
112. Park S, Bézier D, Brookhart M (2012) J Am Chem Soc 134:11404–11407
113. Mitton SJ, Turculet L (2012) Chem Eur J 18:15258–15262
114. Berkefeld A, Piers WE, Parvez M (2010) J Am Chem Soc 132:10660–10661
115. Khandelwal M, Wehmschulte RJ (2012) Angew Chem Int Ed 51:7323–7326
116. Wen M, Huang F, Lu G, Wang Z-X (2013) Inorg Chem 52:12098–12107
117. Maidan R, Willner I (1986) J Am Chem Soc 108:8100–8101

# Index